frontiers | Research Topics

Biology of mesenchymal stromal cells -emerging new concepts to improve function and scalability

Edited by
Tokiko Nagamura-Inoue, Willem Fibbe and Keiya Ozawa

Published in
Frontiers in Cell and Developmental Biology
Frontiers in Genetics

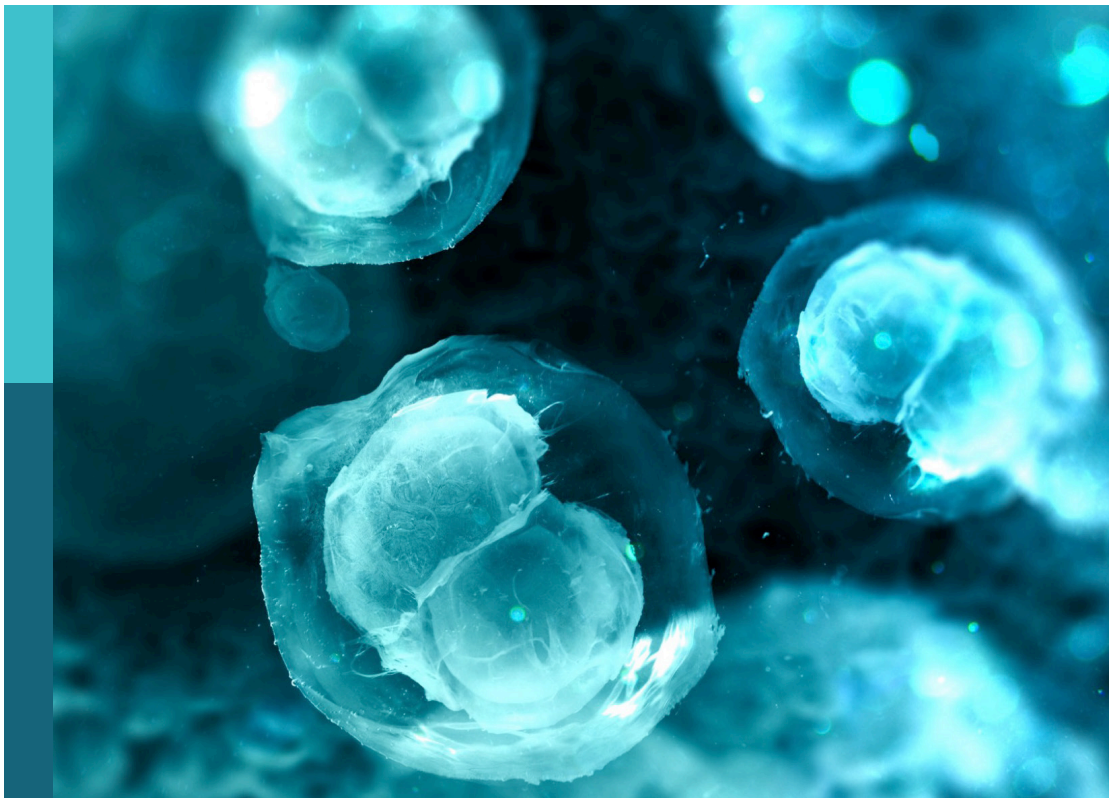

ISSN 1664-8714
ISBN 978-2-8325-5587-3
DOI 10.3389/978-2-8325-5587-3

About Frontiers

Frontiers is more than just an open access publisher of scholarly articles: it is a pioneering approach to the world of academia, radically improving the way scholarly research is managed. The grand vision of Frontiers is a world where all people have an equal opportunity to seek, share and generate knowledge. Frontiers provides immediate and permanent online open access to all its publications, but this alone is not enough to realize our grand goals.

Frontiers journal series

The Frontiers journal series is a multi-tier and interdisciplinary set of open-access, online journals, promising a paradigm shift from the current review, selection and dissemination processes in academic publishing. All Frontiers journals are driven by researchers for researchers; therefore, they constitute a service to the scholarly community. At the same time, the *Frontiers journal series* operates on a revolutionary invention, the tiered publishing system, initially addressing specific communities of scholars, and gradually climbing up to broader public understanding, thus serving the interests of the lay society, too.

Dedication to quality

Each Frontiers article is a landmark of the highest quality, thanks to genuinely collaborative interactions between authors and review editors, who include some of the world's best academicians. Research must be certified by peers before entering a stream of knowledge that may eventually reach the public - and shape society; therefore, Frontiers only applies the most rigorous and unbiased reviews. Frontiers revolutionizes research publishing by freely delivering the most outstanding research, evaluated with no bias from both the academic and social point of view. By applying the most advanced information technologies, Frontiers is catapulting scholarly publishing into a new generation.

What are Frontiers Research Topics?

Frontiers Research Topics are very popular trademarks of the *Frontiers journals series*: they are collections of at least ten articles, all centered on a particular subject. With their unique mix of varied contributions from Original Research to Review Articles, Frontiers Research Topics unify the most influential researchers, the latest key findings and historical advances in a hot research area.

Find out more on how to host your own Frontiers Research Topic or contribute to one as an author by contacting the Frontiers editorial office: frontiersin.org/about/contact

Biology of mesenchymal stromal cells -emerging new concepts to improve function and scalability

Topic editors

Tokiko Nagamura-Inoue — The University of Tokyo, Japan

Willem Fibbe — Leiden University Medical Center (LUMC), Netherlands

Keiya Ozawa — Jichi Medical University, Japan

Citation

Nagamura-Inoue, T., Fibbe, W., Ozawa, K., eds. (2024). *Biology of mesenchymal stromal cells -emerging new concepts to improve function and scalability*. Lausanne: Frontiers Media SA. doi: 10.3389/978-2-8325-5587-3

Table of contents

frontiers | Frontiers in Cell and Developmental Biology

TYPE Review
PUBLISHED 21 September 2023
DOI 10.3389/fcell.2023.1220694

OPEN ACCESS

EDITED BY
Willem Fibbe,
Leiden University Medical Center (LUMC), Netherlands

REVIEWED BY
Marcio Alvarez-Silva,
Federal University of Santa Catarina, Brazil
Mariaceleste Aragona,
University of Copenhagen, Denmark

*CORRESPONDENCE
Ruoshi Xu,
xurs@scu.edu.cn

RECEIVED 11 May 2023
ACCEPTED 11 September 2023
PUBLISHED 21 September 2023

CITATION
Luo X, Liu Z and Xu R (2023), Adult tissue-specific stem cell interaction: novel technologies and research advances. *Front. Cell Dev. Biol.* 11:1220694. doi: 10.3389/fcell.2023.1220694

Adult tissue-specific stem cell interaction: novel technologies and research advances

Xutao Luo, Ziyi Liu and Ruoshi Xu*

State Key Laboratory of Oral Diseases, National Center for Stomatology, National Clinical Research Center for Oral Diseases, Department of Cariology and Endodontics, West China Hospital of Stomatology, Sichuan University, Chengdu, China

Adult tissue-specific stem cells play a dominant role in tissue homeostasis and regeneration. Various *in vivo* markers of adult tissue-specific stem cells have been increasingly reported by lineage tracing in genetic mouse models, indicating that marked cells differentiation is crucial during homeostasis and regeneration. How adult tissue-specific stem cells with indicated markers contact the adjacent lineage with indicated markers is of significance to be studied. Novel methods bring future findings. Recent advances in lineage tracing, synthetic receptor systems, proximity labeling, and transcriptomics have enabled easier and more accurate cell behavior visualization and qualitative and quantitative analysis of cell-cell interactions than ever before. These technological innovations have prompted researchers to re-evaluate previous experimental results, providing increasingly compelling experimental results for understanding the mechanisms of cell-cell interactions. This review aimed to describe the recent methodological advances of dual enzyme lineage tracing system, the synthetic receptor system, proximity labeling, single-cell RNA sequencing and spatial transcriptomics in the study of adult tissue-specific stem cells interactions. An enhanced understanding of the mechanisms of adult tissue-specific stem cells interaction is important for tissue regeneration and maintenance of homeostasis in organisms.

KEYWORDS

stem cell interactions, dual lineage tracing, synthetic receptor, transcriptomics, proximity labeling

1 Introduction

Adult tissue-specific stem cells interactions can be viewed as communication modalities that play a central role in regulating cell behavior and function (Xin et al., 2016).

In this paper, we first discuss the methods for studying adult tissue-specific stem cells interactions in two directions: bioinformatics analysis and visualization analysis. Specifically, these techniques or methods include lineage tracing, synthetic receptor systems, proximity labeling, and transcriptome analysis. In addition, there are few systematic descriptions of the mechanisms of stem cell interactions. Therefore, this paper also combs the biological understanding of adult tissue-specific stem cells interactions. We do not provide a summary assessment of all relevant literature, and references throughout the text tend to be more illuminating examples. Based on the latest literatures, stems cells referred in this review focus on adult tissue-specific stem cells.

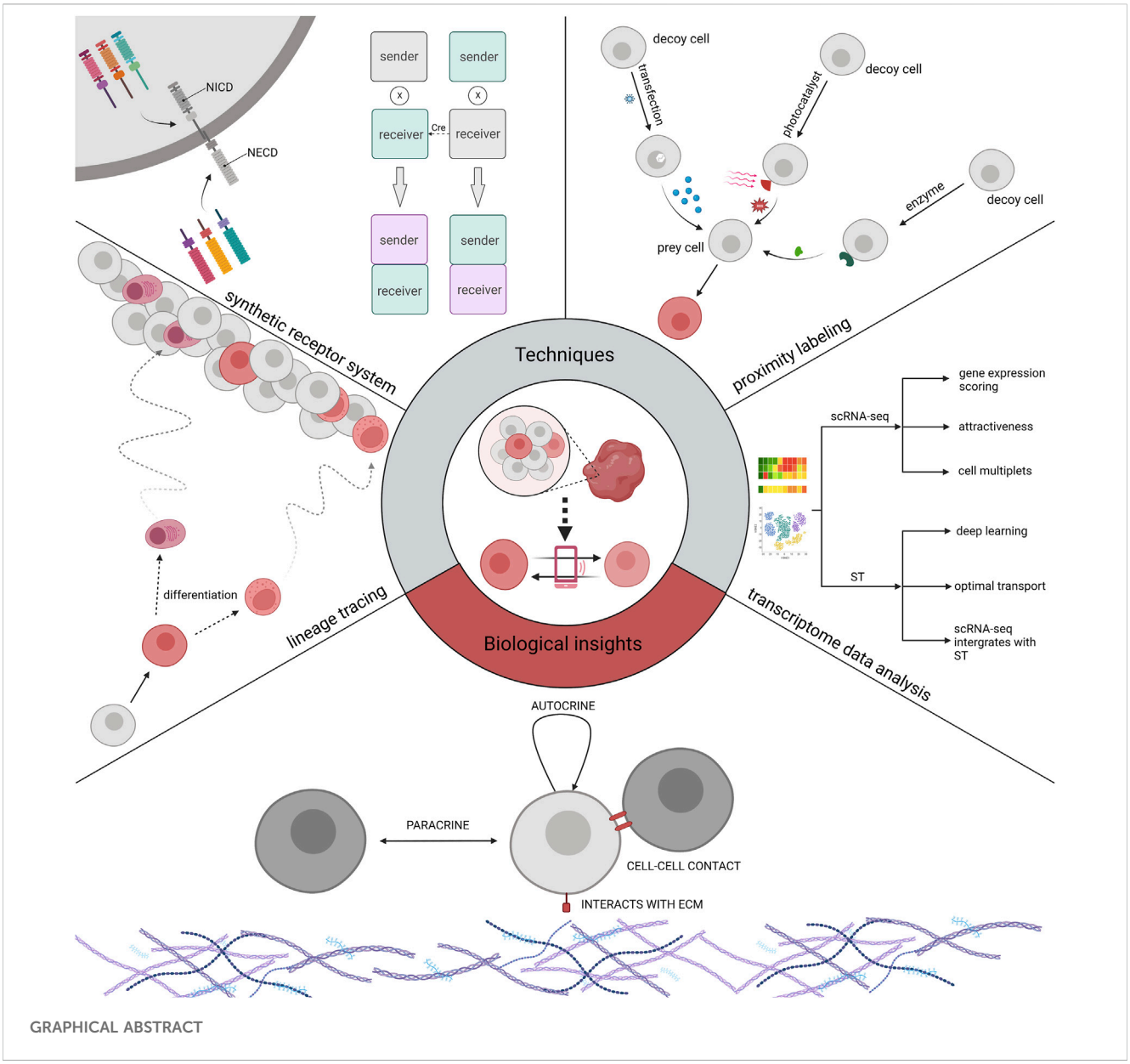

2 Tracking the targets all the way: lineage tracing

Lineage tracing is a powerful means of monitoring cells in various physiological and pathological processes, resulting in many valuable biological discoveries (Kumar et al., 2014; He et al., 2017a; Wu et al., 2021; Hou et al., 2022). Cell lineage tracing techniques have used classical fluorescent protein markers combined with microscopy to identify a few cell clones and to introduce heritable DNA barcodes into single cells to track larger numbers of more complex cell clones, the latter including Cre-mediated recombination and CRISPR-Cas9-mediated editing (Meinke et al., 2016; Baron and van Oudenaarden, 2019). Optogenetic engineering has been developed to some extent. It has been used for detailed *in vivo* single-cell analysis because of its efficiency and spatiotemporal specificity (Yao et al., 2020; Li et al., 2022a; Geiller et al., 2022). Here, we describe the advances in cell lineage tracing technology, with a focus on Cre/LoxP recombinase systems (Figure 1).

2.1 Genetic lineage tracing has entered the era of the recombinase system

The Cre/LoxP recombinase system is widely used for *in vivo* tracking of stem or progenitor cell lines. Its main working principle can be briefly summarised as follows: Cre mediates the removal of transcription termination DNA sequences on the LoxP side, whereupon predesigned reporter genes are expressed in cells expressing Cre (Meinke et al., 2016). Coupled with the fact that this genetic marker can be passed on to progeny cells, this feature allows researchers to elucidate cell lineages as well as track cell fate decisions in stem or progenitor cell lines (van Berlo et al., 2014; Liu et al., 2016; Zhu et al., 2016). However, many controversies have

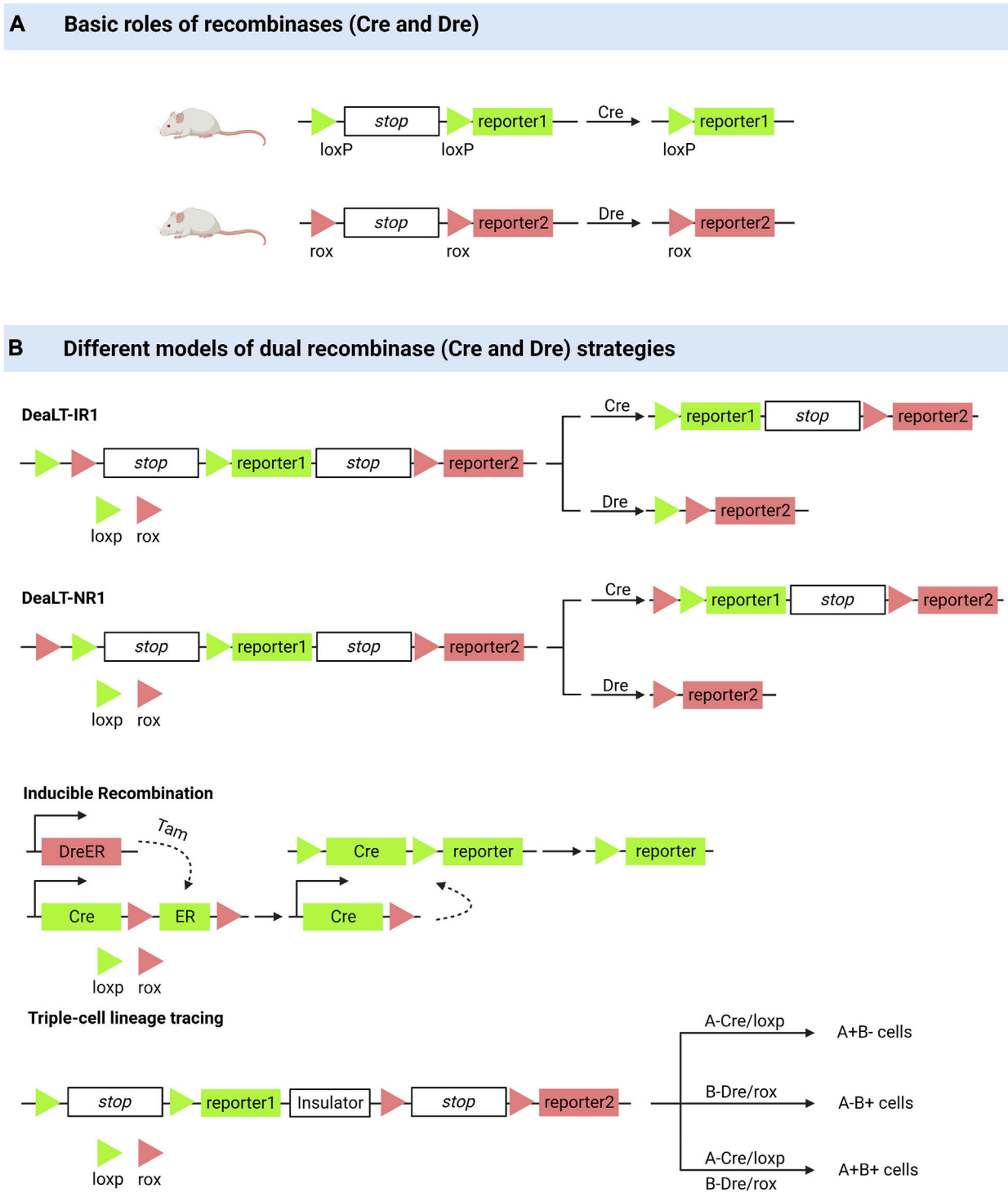

FIGURE 1
Dual enzyme lineage tracing system. **(A)** Cre or Dre recombinases can knock out sequences between loxP or between rox. **(B)** DeaLT-IR: the loxp and rox sites are arranged alternately in a sequence. DeaLT-NR: two sites of loxp are contained within two sites of rox. Inducible Recombination: the DreER was activated with the inducer tamoxifen to produce a Dre recombinase to remove the sequence between the two rox sites. Triple-cell lineage tracing (an example): On a sequence, two sites of loxp and their corresponding reporters were distributed on either side of an insulating sequence, and cells expressing different recombinant enzymes (Cre, Dre, Cre and Dre) showed three reported results.

arisen regarding the drawbacks of the Cre/LLoxP system (Liu et al., 2016). Single-spectrum tracing has been criticized for a long history (van Berlo et al., 2014). The complexity of Cre transgene expression patterns and the toxicity generated to activate Cre are of concern, and in some cases, the data obtained by applying the Cre/LoxP knock-in system have been proven incorrect (Zhu et al., 2016; Pu

et al., 2018). He et al. (2017a) pioneered the Cre: Dre dual-recombinase reporter system. This system combines the Cre/LoxP system with the Dre/rox system, where the Dre/rox recombination system releases Cre from the CreER and allows Cre targeting of the LoxP allele. Determining Cre activity using two different gene promoters provides a higher gene targeting precision than was previously possible with a single gene promoter controlling Cre. Besides being used for cell lineage tracing, it can also be used to query the functions of cell subpopulations *in vivo* (Pu et al., 2018).

2.1.1 Improved spatial resolution

The ability of bronchioalveolar stem cells (BASCs) to regenerate the bronchoalveolar junction region after an injury has been demonstrated using dual-recombinase-activated lineage tracing (DeaLT) system, reiterating previous findings (Salwig et al., 2019; Liu et al., 2020a). Applying the same technique, one demonstrated the dominance of self-renewal of pancreatic β-cells in pancreatic β-cell regeneration (Zhao et al., 2021). The idea that pancreatic progenitor cells give rise to pancreatic β-cells was challenged. DeaLT has also been applied to bone tissues. The division of labor between chondrocytes and Lepr^{+} bone marrow stem cells (BMSCs) during long bone formation is clearly illustrated (Shu et al., 2021). It has also been revealed that a subpopulation of Krt14+ Ctsk+ cells involved in maxillary bone regeneration has both epithelial and mesenchymal properties (Weng et al., 2022). In lung and liver injury, it was previously thought that macrophages that are non-vascularly recruited to reach the viscera via CD44 and ATP directly promote the repair and regeneration of the injured viscera (Wang and Kubes, 2016; Deniset et al., 2019). Updated techniques have helped re-evaluate this idea, and the results of the experiments do not support the scientific validity of the idea (Jin et al., 2021a).

2.1.2 The time continuity of lineage tracing is realized

Based on the Cre: Dre dual recombinase reporter system, Lingjuan He et al. (2021) developed a cell proliferation tracer model, called "ProTracer." Specifically, DreER-rox recombination removes the estrogen receptor DNA on the rox side, whereupon the sequence encoding CrexER is converted into constitutively active Cre gene sequences, resulting in cells of Ki67-Cre genotype. In these cells, the expression of constitutively active Cre gene sequences is triggered by the Ki67 promoter, and the transcriptional activity of Ki67 is continuously recorded by the R26-GFP reporter gene activation. This model allows the tracing of Ki67+ cells at any moment and the recording of cell proliferation over time. ProTracer combines dual recombinases to continuously document the proliferation of whole cell populations in multiple tissues and organs, thereby eliminating potential selectivity bias. The use of ProTracer allows for the sequential recording of the initial tamoxifen-triggered DreER-rox recombination initiating the Ki67- Cre gene, thus overcoming the technical dilemma of using Cre/LoxP alone, which requires prolonged CreER activation with tamoxifen (He et al., 2021). ProTracer records circulating cardiomyocytes in both dividing and non-dividing cardiomyocytes. Most circulating cardiomyocytes and dividing cardiomyocytes (approximately 13% of tracer cardiomyocytes) are highly confined to the subendocardial muscle of the left ventricle of the adult heart (Liu et al., 2021). They also assessed postnatal cardiomyocyte proliferation using ProTracer, which showed a rapid and sustained decline in the number of circulating cardiomyocytes from birth to adolescence. These results support the claim that prepubertal cardiac proliferation shows a burst (Pu et al., 2022).

2.2 Optogenetics has a promising future in genetic lineage tracing

We also note the contribution of optogenetic genetic engineering to the content of our work, which is widely used to study and control cells and has been previously described (Tan et al., 2022). Optogenetics regulates cell physiology by combining light with genetic engineering. The advantages of high spatiotemporal accuracy and single-cell resolution offered by optogenetic tools have made it a powerful technique for the precise detection of signaling and intercellular interactions (Leopold et al., 2018; Uroz et al., 2018; Gagliardi et al., 2021; Zhang et al., 2021; Kim and Schnitzer, 2022). Felker et al. (2018) described the formation of zebrafish ventricles by progenitor cells using optogenetic techniques for lineage tracing. The combination of optogenetic genetic engineering with Cre/LoxP systems has also been experimentally implemented (Taslimi et al., 2016; Morikawa et al., 2020); however, its limitations are related to the lack of specificity of the Cre/LoxP system itself (Tan et al., 2022). Optogenetic tools provide a tunable platform for studying the dose- and intensity-dependent signaling between sending cells and receiving cells (Tan et al., 2022). Moreover, current research models in optogenetics are not sufficiently rich, and we suggest that optogenetic genetic engineering can be applied to study the function of adult tissue-specific stem cells in homeostasis and regeneration. A combination of dual recombinant enzyme lineage tracer strategies and optogenetic engineering can be widely applied.

3 Customized cell signaling: synthetic receptor systems

Inspired by the natural cell-signaling paradigm, researchers have implemented artificially designed synthetic receptor systems to manipulate signal translation to control cellular functions, including artificially tunable cellular sensing and subsequent transcriptional responses (Zhu et al., 2022; Roybal et al., 2016; Morsut et al., 2016; Hernandez-Lopez et al., 2021). The development of synthetic receptor systems has gradually evolved from initial modest modifications of natural proteins to the holistic design of modular technologies that increasingly approach the engineering of customized cellular functions (Manhas et al., 2022). Artificial effects on cellular activity through synthetic receptors include but are not limited to, control of pluripotent stem cells differentiation (Lee et al., 2023). And if the endpoint of intracellular signaling is set to the expression of fluorescent genes, we can clearly distinguish which cells receive the influence of the sender cells (Figure 2).

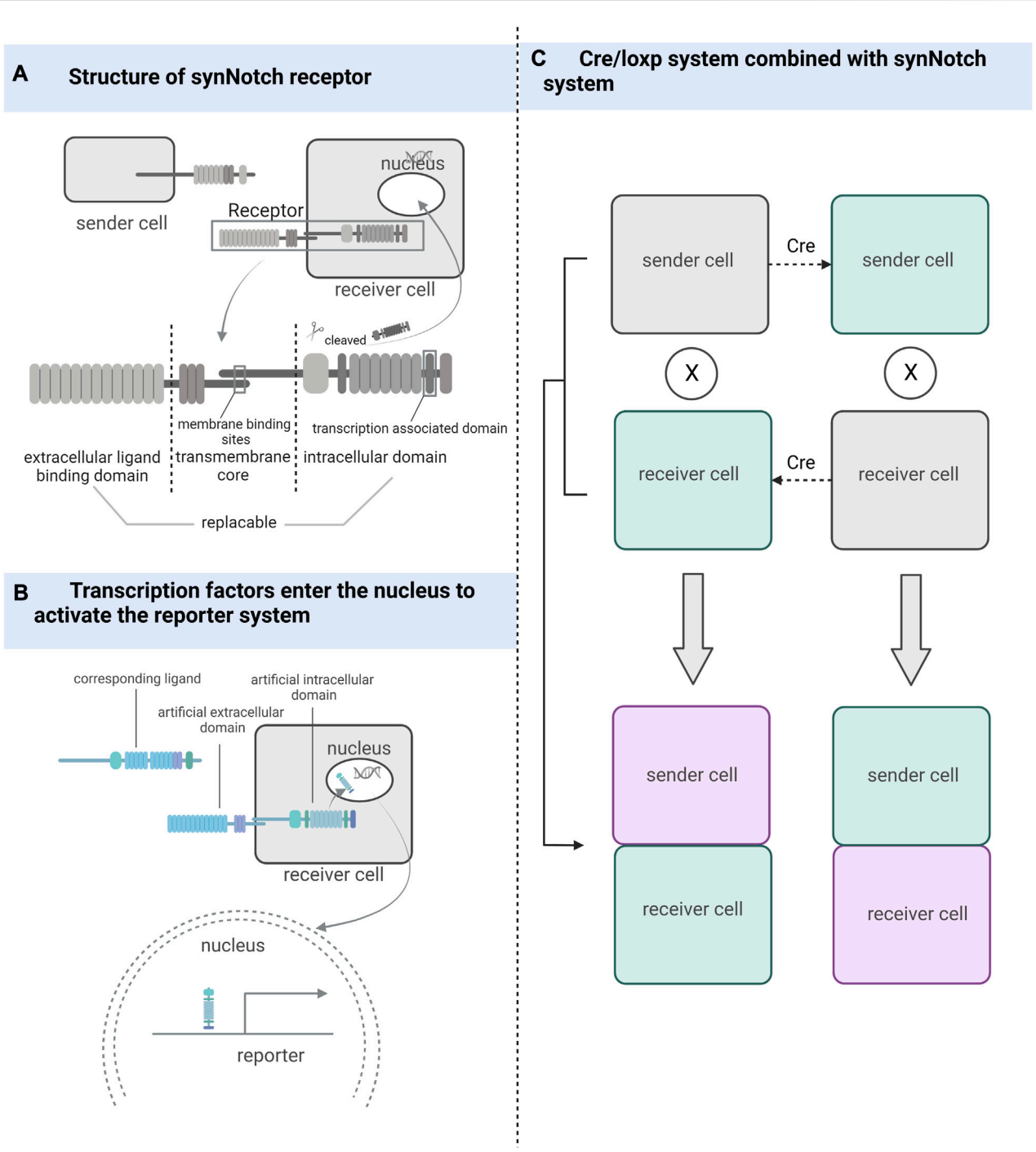

FIGURE 2
The working mechanism of the synthetic receptor system. **(A)** synNotch receptor consists of an extracellular ligand-binding domain, a native Notch receptor transmembrane core, and an intracellular domain linked to the transcriptional factor-associated intracellular domain. **(B)** After the ligand binds to the synthetic receptor, transcription factors located in the intracellular segment are cleaved and take effect in the nucleus. **(C)** Combining the Cre/loxP system with the synthetic receptor system can also be used to detect and track cells that have undergone cell-cell contact, whether sending or receiving cells.

3.1 Monitoring cell-cell contacts

The synNotch receptor system, which detects cell-cell contact, was developed during the development of synthetic receptor systems (Morsut et al., 2016). The synNotch receptor is described as a receptor that signals through intramembrane protein hydrolysis and contains an extracellular ligand-binding domain, a native Notch receptor transmembrane core, and an intracellular domain linked to transcriptional factor-associated intracellular domain (Toda et al., 2018). Both the extracellular and intracellular domains of the Notch receptor are artificially substitutable so that highly diverse cell-cell interactions can be artificially

engineered (Struhl and Adachi, 1998; Gordon et al., 2015). The synNotch receptor system can potentially become a powerful tool for studying cell-cell contact by being designed in a rational way that exploits the precise spatial control of synNotch pathway activation dependent on direct cell-cell contact (Morsut et al., 2016).

3.2 Combination of synNotch with different reporting systems

Firstly, Huang et al. used different enhancers to drive synNotch ligands and receptors to monitor neuronal and glial cell interactions and achieve long-term genetic modifications in a *Drosophila* model (Huang et al., 2016). He et al. (2017b) improved this idea by combining the synNotch receptor with a transcriptional stop signal and flip-flopping enzyme (FLP) recombination target sites on either side. These sequences were placed before the GFP ligand and controlled using the same promoter. The removal of gene sequences between FLP recombination target sites was achieved using FLP recombination, and the GFP ligand was expressed only in the presence of FLP, enabling the permanent labeling of cells for lineage tracing and real-time capture of intercellular contacts. This attempt led to breakthroughs in mammalian cell models, where Toda et al. (2018) used synNotch to design a modular signaling platform to enable the operation of artificial genetic programs at the tissue level. Specifically, the team used specific cell-cell contacts to induce changes in calmodulin adhesion that altered the local signals received by the cells, demonstrating the potential of artificially manipulated tissue generation. Zhang et al. (2022a) used Myc-tagged anti-GFP nanosomes (αGFP) and tetracycline (tet) trans-activator (tTA) to replace the extracellular and intracellular domains in the synNotch receptor system, respectively, and designed a genetic marker for labeling cell-cell contacts using tetO-LacZ as a reporter allele and membrane-bolted green fluorescent protein (mGFP) as a ligand. The contact of the sending cell containing the ligand with the cell containing the corresponding synNotch receptor triggers cleavage of the Notch transmembrane structural domain, releasing tTA into the nucleus, which in turn activates the reporter allele (Zhang et al., 2022a). If the Cre/LoxP system is used instead of the tetO-LacZ reporter system, it is not only possible to determine whether cell contact has occurred but also to permanently track cells that have made cell-cell contact and their progeny. SynNotch, combined with the Cre/LoxP system, can be used as a tool for genetic tracing of cell-cell contact (Zhang et al., 2022a).

4 Proximity labeling

Many proximity labeling systems have been developed to analyze protein-protein interactions, but relatively few have been applied to study cell-cell interactions (Liu et al., 2020b). Substances with catalytic effects (enzymes or photocatalysts) are bound to membrane proteins of the target cell for the production of intermediates (Ge et al., 2019; Liu et al., 2022a). The added substrate is attached by the intermediate to the cell that interacts with the target cell. This process is called proximity labeling. In certain aspects, proximity labeling offers many advantages over other techniques for studying cellular interactions. The proximity labeling approach is closer to the natural environment than synthetic receptors. The data provided by bioinformatics functions primarily as a reference, and predictions made about cellular interactions require further validation. Techniques based on imaging to study cellular interactions do not provide molecular information about cellular interactions and do not isolate the cells of interest for subsequent analysis. According to our objectives, the limitation of the present proximity labeling method is that the cells studied are mostly immune cells and tumor cells, while few descriptions involving adult tissue-specific stem cells are available. We need to further validate whether proximity labeling is applicable to stem cell studies. Proximity labeling techniques commonly used for cellular interaction studies currently include both enzyme-based and photocatalyst-based types (Figure 3).

4.1 Enzymatic labeling

4.1.1 Genetic manipulation

This class of proximity labeling protocols uses genetic engineering to make decoy cells express the enzymes used for proximity labeling and transfer label to prey cells. The main types of proximity marker technologies used to study cellular interactions are LIPSTIC, EXCELL and PUP-IT.

LIPSTIC uses sortase A (SrtA) genetically engineered to be expressed in decoy cells to transfer the markers to prey cells (Pasqual et al., 2018). This label can only be transferred when the cells are close enough to each other for the ligand receptor to bind to each other. This scheme provides information on the cells where the interaction occurs and quantifies this interaction. However, prior glycine placement of cells is required for the application of LIPSTIC. Recently the team described a modified version of LIPSTIC, uLIPSTIC, which is expected to enable the detection and analysis of CCIs across multiple organs (Nakandakari-Higa, 2023).In the EXCELL protocol, SrtA was improved to a variant mgSrtA, which has advantages in terms of cell labeling efficiency and signal-to-noise ratio. Compared to LIPSTIC, EXCELL does not require prepositioned glycine and also has the ability to discover unknown cell-cell interactions (Ge et al., 2019).The innovative feature of PUP-IT versus other neighboring labeling protocols is that both enzyme and substrate are proteins, and thus have better selectivity in genetic fusion strategies (Liu et al., 2018). PUP-IT2 is characterized by the minimization of fusion proteins and the virtual absence of self-labeling of enzyme (Yue et al., 2022). The relatively low labeling efficiency of the PUP-IT protocol has been reported in the literature and may not be suitable for studying cell-cell interactions (Ge et al., 2019).

4.1.2 Non-genetic manipulation

The FucoID protocol installs the glycosyltransferase directly onto the decoy cell without gene expression on the cell membrane (Liu et al., 2020b). This enzyme allows the transfer of GDP-Fuc-GF-Biotin substrate to the prey cell, thus enabling proximity labeling. The development team used FucoID to detect and isolate T cells interacting with dentritic cells in a pancreatic tumor model with new bystander T cells, driving personalized

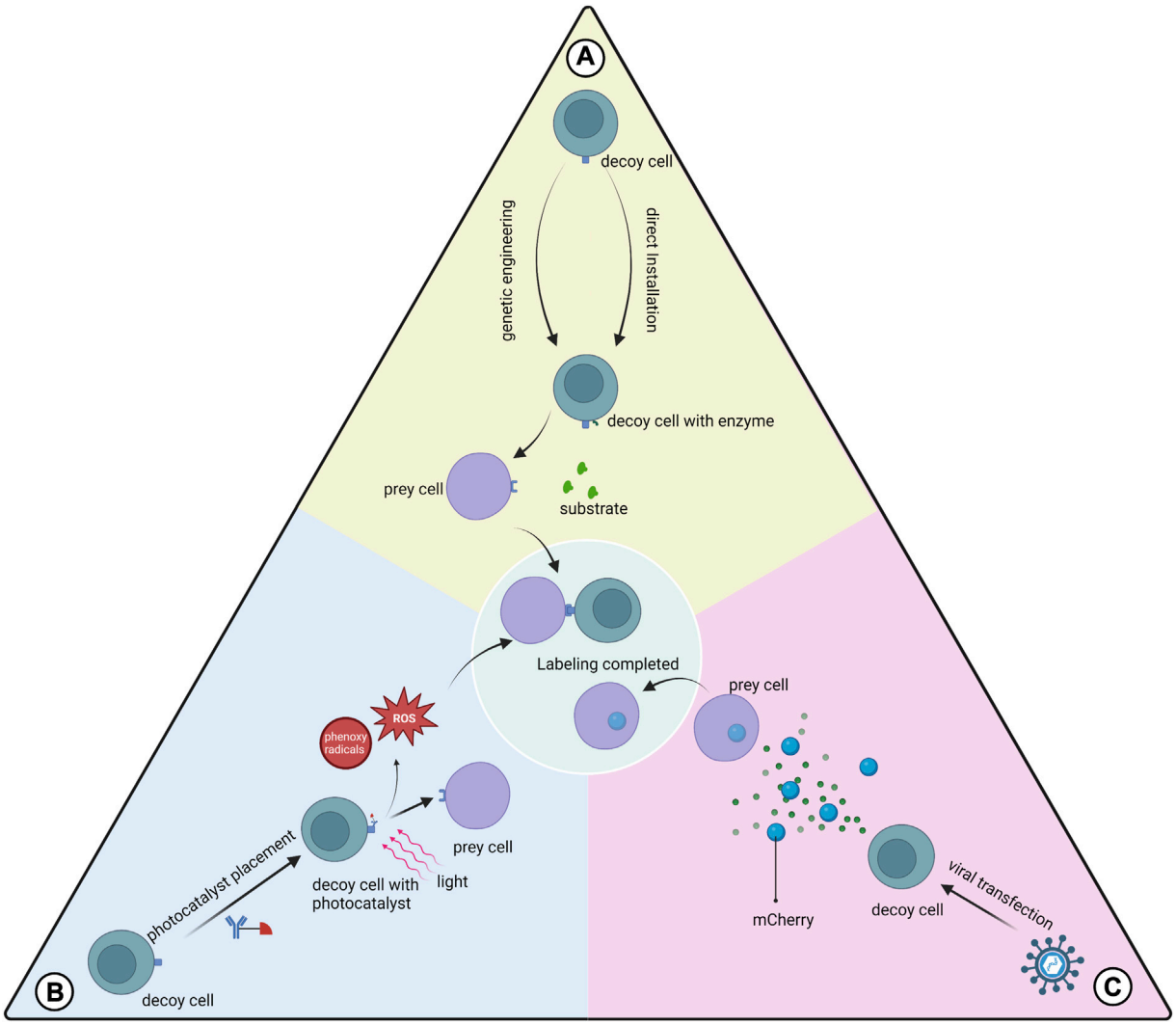

FIGURE 3
Three types of proximity labeling. **(A)** Enzymes are expressed on the cell membrane of the decoy cell by genetic engineering or are installed on the decoy cell by mediation such as antibodies to catalyze substrate labeling of the prey cell; **(B)** Photocatalysts pre-installed on the decoy cell are activated using light of a certain wavelength to generate free radicals at the interaction interface, which mediates the labeling; **(C)** Decoy cells transfected with viruses express and secrete markers that can be absorbed by the prey cell.

cancer therapy. The team updated the tool library of the FucoID protocol and proposed two probes, cell-sFT and Ab-sFT (Qiu et al., 2022). The former requires pre-placement of fucosyltransferase (FT) on decoy cells, while the latter does not, thus it can be applied in cases where decoy cells are difficult to isolate.

4.2 Photocatalytic labeling

Protocols using photocatalysts have greater temporal control and remote manipulation than enzymatic proximity-labeling systems (Liu et al., 2022a). These protocols typically generate reaction intermediates such as free radicals at the cell-cell interaction interface to label prey cells.

PhoXCELL is an update of the EXCELL protocol (Liu et al., 2022a). PhoXCELL introduces Dibromofluorescein as a photocatalyst that mediates the transfer of cellular labeling using singlet oxygen (radicals). The diffusion radius of oxygen radicals is smaller compared to other radicals, reducing the possibility of false positive assay results. The PhoTag protocol uses phenoxy radicals to label neighboring cells (Oslund et al., 2022). This protocol recognizes and couples to decoy cell membrane proteins via an antibody-mediated photocatalyst and is primarily used to analyze physical interactions. This study also describes the combination of PhoTag with multi-omics single-cell sequencing to provide more information about the cells involved in the interaction. μMap uses carbene as a reaction intermediate, which has a shorter half-life compared to phenoxy radicals, which contributes to the resolution (Geri et al., 2020). μMap-red uses longer wavelength red light combined with a photocatalyst to generate from aryl azides nitrogen-containing radicals, which is suitable for *in situ* studies of cellular interactions in animal models (Buksh et al., 2022).

4.3 Direct labeling

We also focused on the mCherry-niche labeling system (Ombrato et al., 2021). This is a labeling method for detecting cells in the tumor microenvironment that receive secreted proteins from tumor cells (O et al., 2019). Through viral transfection, tumor cells stably express mCherry, and the stronger the tumor cell secretion capacity, the more mCherry is secreted. mCherry is readily taken up by other cell types and labels the cells. Further validation of the contribution of the mCherry-niche system to the study of the paracrine secretome of MSCs is needed.

4.4 Engineered virus labeling

Engineered viral labeling in fact goes beyond the definition of proximity labeling that we presented at the beginning of this section. However, the brief logic of engineered virus labeling is applying the ligand of interest to discover the receptor that interacts with it, which is consistent with the core idea of proximity labeling to discover prey cells that interact with decoy cells. Specifically, engineered viral labeling uses lentiviruses with artificially defined ligands to engage in ligand-receptor interactions with cells that have the corresponding receptors (Yu et al., 2022a). The interacting cells endocytose the corresponding engineered viruses. Cells are labeled by the barcode of the virus, thus allowing the identification of cells interact with that ligand. In addition, when multiple engineered viruses with different ligands with barcodes are used to mix with cells of interest, it is also possible to identify which ligands the cells interact with (Yu et al., 2022a).

5 Integration and systematization of transcriptomics analysis

Stem cell interactions and their consequences include processes such as signal transmission and transduction, the response of genetic systems, and changes in stem cell behavior, which are recorded in high-resolution omics data. To date, many tools have been developed to infer cellular interactions (Nitzan et al., 2019; Browaeys et al., 2020; Cang and Nie, 2020; Efremova et al., 2020; Ren et al., 2020; Jin et al., 2021b; Dries et al., 2021; Fang et al., 2022; Li and Yang, 2022; Shao et al., 2022; Sun et al., 2022; Cang et al., 2023; Fischer et al., 2023; Tang et al., 2023). They are mainly based on scRNA-seq and spatial transcriptome data (Figure 4; Table 1).

5.1 Single-cell RNA sequencing (scRNA-seq)

scRNA-seq is a mighty method for analyzing information regarding intra- and extracellular interactions using whole transcriptional profiling (Travaglini et al., 2020; Wang et al., 2020; Wang et al., 2021a). scRNA-seq is mainly used to identify different cell types and map the developmental trajectory of cells (Paik et al., 2020). In addition, scRNA-seq can be used to predict cell interactions. scRNA-seq data are used to perform computer modeling to build tissue-level models to predict intercellular interactions through ligand-receptor pairs (Del Sol and Jung, 2021).

To systematically use transcriptome data to infer cell-cell interactions and generate potential cell-cell communication networks, many analytical tools have been developed, including NicheNet, CellPhoneDB and CellChat (Vento-Tormo et al., 2018; Browaeys et al., 2020; Centonze et al., 2020; Efremova et al., 2020; Jin et al., 2021b). These considerations have been updated using newer technologies from only one ligand-receptor gene pair used to the integrated consideration of different subunit states in receptors as multi-subunit complexes (Efremova et al., 2020). Moreover, more complete data on cellular interactions were compiled (Jin et al., 2021b). Important signaling cofactors and cellular spatial locations have also been considered (Efremova et al., 2020; Saviano et al., 2020; Jin et al., 2021b). Compared to CellPhoneDB, NicheNet can also analyze the gene expression of receiver cells (Browaeys et al., 2020). CellChat performs better in predicting strong intercellular interactions (Jin et al., 2021b). Furthermore, the developers of CellChat described the application of the tool in the pseudotime analysis of continuous cell states. But the systematic description of the application of the pseudotime analysis in improving intercellular interactions was not reflected until the development of TraSig (Li et al., 2022b). TraSig focuses on the temporal heterogeneity of gene expression in homogeneous clusters of cells by including ligand-receptor genes that are expressed at similar rates in the pseudotime in the prediction criteria for positive ligand-receptor pair interactions.

Table 1 compares in detail the differences between tools for analyzing cell-to-cell interactions using transcriptome data, including tools mentioned above. There are concerns that distant endocrine signals are difficult to capture owing to the technical limitations of scRNA-seq (Liu et al., 2022b; Dimitrov et al., 2022). CCI mediators have also been studied in a relatively homogeneous manner, and attempts have been made to investigate mediators other than proteins (Dimitrov et al., 2022).

5.2 Spatial transcriptomics (ST)

ST technologies discussed in this paper refer to technologies aimed at preserving spatial information and obtaining transcriptome information (Ståhl et al., 2016). ST provides spatial information and is used to study cell-cell contact. The technical shortcomings of ST are reflected in the lack of resolution and transcriptome coverage, but these shortcomings are being rapidly filled (Longo et al., 2021; Rao et al., 2021; Dimitrov et al., 2022; Tian et al., 2022). The ability of spatial transcriptomics to reveal the identity, extent, and spatial location of expressed genes (Kobayashi et al., 2020) links tissue biology to transcriptomics and is a powerful means of exploring the local representation of spatial patterns of cellular gene expression. For example, based on single-cell analysis of ST, Kadur Lakshminarasimha Murthy et al. (2022) revealed the fate trajectory of a bipotent progenitor cell population in the lungs during lung regeneration. This is different from the process that occurs in the lungs of mice (Choi et al., 2020; Kobayashi et al., 2020). Visual analysis based on ST has depicted the entire process from human pluripotent stem cells to hematopoietic stem cells (Calvanese et al., 2022), validating and gaining a deeper understanding of previous studies (Zhou et al., 2016). The current description of *in situ* cellular interactions can be achieved by sorting physically

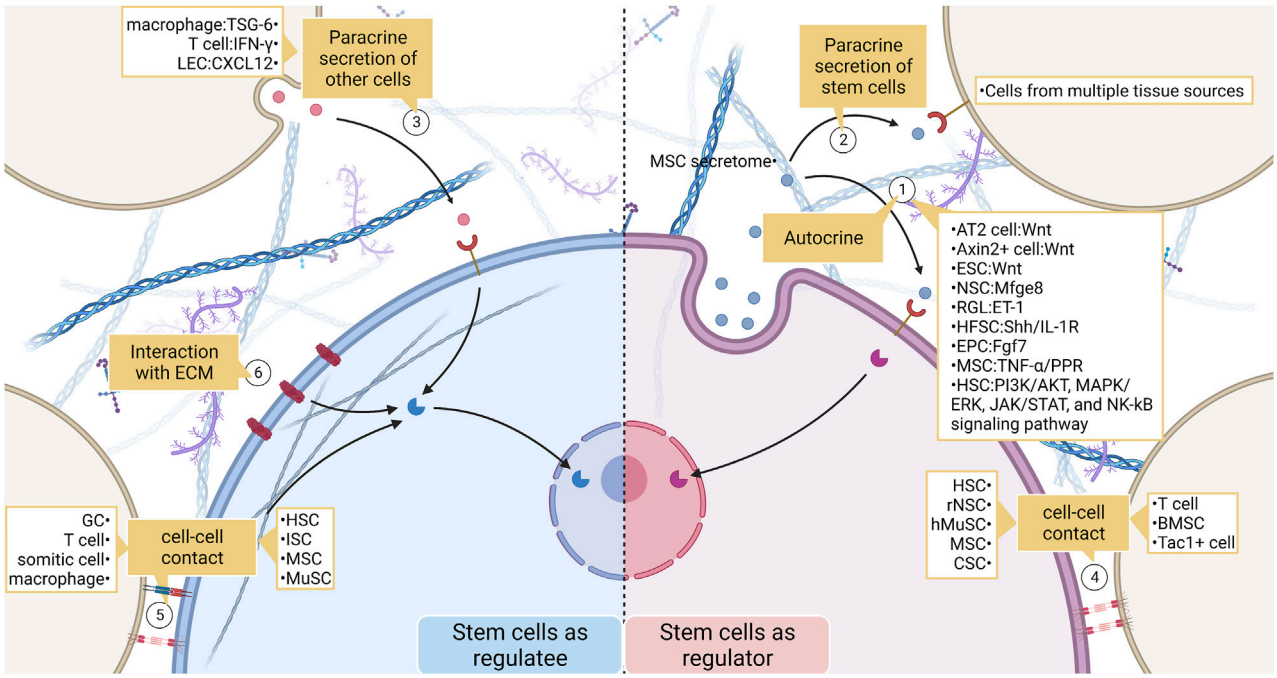

FIGURE 4
The broad landscape of stem cell interactions. (1) Stem cells act as signal senders and regulate their behavior. Effects include recruiting stem cells, maintaining the normal fate of stem cells, and influencing stem cell proliferation and differentiation. (2) (3) Stem cells communicate with non-stem cells by secreting chemicals. (4) (5) Stem cells and non-stem cells transmit mechanical or biochemical information to each other through cell-cell contact. (6) Stem cells also communicate closely with ECM. ECM regulates stem cell behavior by enriching ligands as well as by their physical properties. LEC, lymphatic endothelial cell; MSC, mesenchymal stem cell; ESC, embryonic stem cell; NSC, neural stem cell; RGL, radial glial-like neural stem cell; HFSC, hair follicle stem cell; EPC, epithelial progenitor cell; HSC, hemopoietic stem cell; hMuSC, human Muscle Stem cell; CSC, cancer stem cell; BMSC, bone marrow stromal cell; ISC, intestinal stem cell; GC, granule cell.

interacting cell groups using scRNA-seq (Giladi et al., 2020). This technique overcomes the limitation of missing spatial information when using scRNA-seq alone to analyze the expression of intercellular contact-dependent genes (Kim et al., 2023). An application has also been developed for the analysis of physical interactions in complex tissues, using unsupervised and high-throughput multiplex sequencing techniques that can reconstruct the spatial structure of the interactome (Andrews et al., 2021). Furthermore, the identification and labeling of intercellular contacts and ligand-receptor signaling from massively parallel single-cell sequencing data have been achieved (Ghaddar and De, 2022). Quantification of cell-cell interactions can be achieved using *in situ* molecular colocalization. Its advantage over chromatin immunoprecipitation sequencing or ribosome analysis is the ability to perform *in situ* analyses (Tian et al., 2022). Moreover, a technique has been proposed for human clinical samples without the use of genetic modification strategies, which provides sample transcript information and long-term, stable tracking of cytodynamics. It can be used as a complement to spatial omics and typical single-cell sequencing (Genshaft et al., 2021). The use of cell space maps has been proposed to improve the accuracy of inference of intercellular communication (Fischer et al., 2023). Mathematical models are developed centered on nodes to simulate ligand-receptor interactions to explain intercellular interactions and reduce the rate of misinterpretation of intercellular dependence. A recent technique based on collective optimal transport, COMMOT, was proposed for inferring and visualizing intercellular communication (Cang et al., 2023). However, the authors pointed out the possibility of false positives in the results generated by applying this technique. In addition, Zhu et al. (2023) developed a platform for simulating real ST data, which provides an efficient and low-cost data source for evaluating different spatially resolved transcriptomics techniques.

6 Update on the stem cell interaction mechanism theory

Adult tissue-specific stem cells receive biochemical or mechanical signals from cellular or non-cellular components of the niche, generating a series of intracellular signal transduction pathways, which in turn undergo structural or functional changes (Pinho and Frenette, 2019; Brunet et al., 2023). Biochemical signaling between cells may occur in three forms: 1) free diffusion of ligands, which includes both autocrine and paracrine mechanisms; 2) ligands are secreted and present in the extracellular matrix (ECM), and receptors bind to these ligands when cells come into contact with the ECM; 3) ligands are expressed on the cell surface, and cells expressing surface receptors and cells expressing surface ligands are transmitted through direct binding of ligand-receptor signals. In contrast, mechanical information transmission

TABLE 1 Tools for studying cellular interactions.

Tool	Input	Method	Roles and limitations	References
NicheNet	Gene expression data	Weighted interaction network; calculate interaction potential scores; infer signaling pathways based on scores	Analysis of target gene expression as influenced by CCC; Intracellular signaling was considered; No mention of the multisubunit structure of the ligand and receptor	Browaeys et al. (2020)
CellPhoneDB v2.0	scRNA-seq	Calculate the mean gene expression of ligand and receptor; screen for LRPs showing cell-state specificity	Subunit structures of ligands and receptors are considered; Cannot reason completely about all interactions between cells; does not take into account the spatial proximity between cells	Efremova et al. (2020)
CellChat	scRNA-seq	Identify differentially expressed signaling genes; calculate CCC probabilities; identify major signals	More suitable for predicting stronger interactions; Predicting fewer interactions	Jin et al. (2021b)
Trasig	scRNA-seq	Sort each cell of different cell clusters in proposed time and analyze their gene expression; analyze the change of gene expression with proposed time; calculate the correlation of possible ligand-receptors	Reduced false positives in CCC prediction using pseudotime analysis	Li et al. (2022b)
PAGA	scRNA-seq	Cell clustering; calculation of connectivity between cell clusters to obtain PAGA graphs; integration of PAGA graphs with databases of CCC	Based on known CCC databases	Wolf et al. (2019)
icellnet	scRNA-seq	Calculate LRP scores; visualize LRP scores	Describes how the integration of downstream signaling pathways and target gene expression profiles into CCC analysis may lead to false positive or false negative results	Noël et al. (2021)
SingleCellSignalR	scRNA-seq	LRP scoring; output LR interaction; link upstream and downstream for analysis	Based on known LRP database; based on regularized product score; ignores the spatial relationships between interacting cells	Cabello-Aguilar et al. (2020)
CellCall	scRNA-seq	Calculate communication scores and predict interactions using ligand-receptor expression and downstream TF activity	Integrates signals from inside and outside the cell; ignoring non-gene expression factors; non-protein ligand-receptor data urgently need to be supplemented	Zhang et al. (2021)
RNA-Magnet	scRNA-seq/ST	Rate the attractiveness of each cell based on the ligand-receptor expression pattern; provide the orientation of the attractor cells	the predicted attractor cell population is specific and may not be applicable to the prediction of other CCC	Baccin et al. (2020)
NATMI	scRNA-seq	Extract the expression of various ligands or receptors from different cell types; predict the interaction of cell types expressing ligands with cell types expressing homologous receptors	Ignoring information other than gene expression levels; relying on the completeness of the LRP database	Hou et al. (2020)
SoptSC	scRNA-seq	Predict the probability of signaling by the degree of ligand-receptor expression and the activity of target genes	Ignores unknown intercellular communication; not suitable for dynamic intercellular communication; analyzed intercellular communication is unidirectional	Wang et al. (2019)
PIC-seq	scRNA-seq	sequences PIC to obtain scRNA-seq data, combined with single-cell sequencing data to deconvolute the PIC complex into several single cells	Identify intracellular physical interactions; based on cell multiplets	Giladi et al. (2020)
Neighbor-seq	scRNA-seq	Creating artificial multiplets; machine learning to distinguish between different combinations of multiplets; evaluating multiplet enrichment; calculating enrichment scores for CCI; constructing CCI networks	based on cell multiplets	Ghaddar and De (2022)
CIM-seq	scRNA-seq	Retention of cell multiplets in single cell suspensions for RNA sequencing; deconvolution of transcriptome data to break up cell multiplets; differential gene expression analysis		Andrews et al. (2021)

(Continued on following page)

TABLE 1 (*Continued*) Tools for studying cellular interactions.

Tool	Input	Method	Roles and limitations	References
Tools based on ST				
COMMOT	ST and scRNA-seq	Optimal transport strategies were used to analyze the direction and strength of CCC	Visualizing CCC, annotating CCC direction, and analyzing CCC downstream effect; The possibility of a false positive of CCC; Neglect of *in situ* space proximity	Cang et al. (2023)
NCEM	scRNA-seq; MERFISH data	The results of ST data analysis were used as input information to train NCEM to predict the spatial specificity of cellular gene expression	Based on GNN; Reasoning about intercellular communication and simulating ecological niche effects	Fischer et al. (2023)
SpaOTsc	scST/scRNA-seq with corresponding spatial data	The scRNA-seq data were corroborated with spatial transcriptome data; structured optimal transport strategy was used	Reconstructing intercellular communication and estimating the spatial characteristics of intercellular signals; the judgment of cell interactions is based on the spatial distance between cells, and may not be suitable for all types of cell interactions	Cang and Nie (2020)
SpaCI	scST	Projecting cell spatial location and gene expression patterns into the same latent space; using a triplet loss training model to determine whether an LRP interacts with each other	Revealing the relationship between TFs and ligands and the ligand-receptor pair	Tang et al. (2023)
STRIDE	scRNA-seq; ST	Decomposition of spatial transcriptome data into components containing spatial information and other components, and integration with scRNA seq data	Inferring intercellular interactions; A high match of spatial data with scRNA-seq data is required; Insufficient ability to discriminate between similar cell types within the same lineage	Sun et al. (2022)
SpaTalk	single-cell and spot-based ST	GNN learning is used to calculate LRI probabilities; the most likely cellular interactions are filtered by combining LRI probabilities with spatial distances	Inferring cellular communication and signaling pathways; Deficiencies in inferring cellular telecommunications; the LRP database maybe incomplete	Shao et al. (2022)
Giotto	10X Genomics Vissium data	Cell clustering; Genes with spatial differential expression or correlation were searched	visualizing spatial histology data; Interactions between cell types rather than between cells are analyzed	Dries et al. (2021)
DeepLinc	Deep learning from cell interactions and ST	Cell interactions are directly learned from scST data using VGAE, skipping cell clustering	Discovery of new cell types; Reconstruct a complete cell interaction landscape; Inferring cellular telecommunications; Only single cell spatial transcriptome data can be used and dynamic cellular interactions, such as cell differentiation, cannot be analyzed	Li and Yang (2022)

ST, spatial transcriptomics; scST, single cell spatial transcriptomics; TF, transcription factor; LRTF, ligand-receptor-TF axis; LRI, ligand-receptor interaction; LRP, ligand-receptor pairs; LRT, ligand-receptor-target; CCC, cell-cell communication; FDC, follicular dendritic cell; CAF, cancer-associated fibroblast; GNN, graph neural network; NCEM, node-centric expression model; PIC, physically interacting cells; VGAE, variational graph autoencoder.

between cells is mainly related to intercellular connections and the ECM nature and structure (Humphrey et al., 2014).

6.1 Free diffusion

6.1.1 Autocrine

Initially, cellular autocrine was more often studied using cancer cells as a model, and this mechanism was found to control the growth of various cells, especially to stimulate cell proliferation (Adkins et al., 1984; Huang et al., 1984; Lang et al., 1985; Sporn and Roberts, 1985). The ability of the autocrine mechanism to stimulate cell proliferation has also been demonstrated in normal tissues under physiological conditions as well as in stem cells (Gaudio et al., 2006; Abdel-Malak et al., 2008; Gallipoli et al., 2013; Pardo-Saganta et al., 2015). Autocrine signaling, an important stem cell communication mechanism, has been studied extensively. Pathways closely related to stem cell autocrine such as TGF-β, VEGF, mTOR, SHH, and Wnt signaling pathways have been revealed (Lim et al., 2013; Chen et al., 2014; Hsu et al., 2014; Nabhan et al., 2018; Yeh et al., 2018; Zhou et al., 2018; Morinaga et al., 2021).

In the lung, alveolar type 2 cells (AT2) act as alveolar adult tissue-specific stem cells in response to injury (Nabhan et al., 2018; Zacharias et al., 2018). AT2 cells secrete Wnt to recruit more AT2 cells and prevent daughter cells from undergoing transdifferentiation. Axin2+ cells in the skin contribute significantly to wound healing, and its proliferation requires Wnt/β-catenin signaling activation (Lim et al., 2013). In turn, Axin2+ cells themselves can secrete Wnt and self-renew through an autocrine mechanism. Sustained neurogenesis in adult neural stem cells requires autocrine Mfge8 signaling (Zhou et al., 2018). Zhou et al. (2018) used single-cell transcriptome analysis to identify Mfge8 transcripts in resting radial glial-like neural stem cells (RGL). Mechanistically, Mfge8 enrichment inhibited mTOR1 signaling and prevented RGL overactivation and depletion. Additionally, RGL can autocrinologically produce endothelin-1 to promote their proliferation and maintenance (Adams et al., 2020). It has been demonstrated that maintaining transit-expanded cell populations requires autocrine SHH production, which is also necessary for the proliferation of hair follicle stem cells (Hsu et al., 2014). Morinaga et al. (2021) found that autocrine/paracrine IL-1R resulting from a

high-fat diet was associated with NK-kB activation and SHH inhibition, depleting hair follicle stem cells and macroscopically accelerating hair loss. Temporal heterogeneity of thymic epithelial types was revealed by scRNA-seq, which was combined with CRISPR-Cas9 technology to characterize the changes in the thymic epithelium over time in more detail (Nusser et al., 2022). This experiment also showed that autocrine secretion of Fgf7 continues to stimulate massive proliferation of the thymic epithelium, but the pool of epithelial progenitor cells is not depleted, and the characteristics of the thymic epithelium remain unchanged (Nusser et al., 2022). In bone tissue models, the production of tumor necrosis factor (TNF-α) released by MSCs is thought to be a key factor in the maintenance of self-renewal and differentiation of MSCs and their involvement in maintaining bone homeostasis (Yu et al., 2021). Similar results were observed for jawbones. The expression and secretion of PPR by PTHrP+ MSCs in dental follicles are necessary for maintaining a normal cell fate (Takahashi et al., 2019). During embryogenesis, embryonic stem cells (ESCs) produce a cytokine-containing Wnt receptor that allows ESCs to distinguish between niche signals (Junyent et al., 2020). ESCs actively select Wnt ligands secreted by trophectodermal stem cells to promote self-renewal and synthesize more cytokines, thereby participating in accelerated embryogenesis. Post-hematopoietic stem/progenitor cells also benefit from autocrine signaling, and the mechanisms involved are the PI3K/AKT, MAPK/ERK, JAK/STAT, and NK-kB signaling pathways, which have been sorted out (Hurwitz et al., 2020; Stone et al., 2022).

6.1.2 Paracrine

Most paracrine studies on stem cells focus on the secretome of MSCs (Chang et al., 2021). This regenerative medicine branch does not focus on directly exploiting the proliferative and differentiation capacity of stem cells but rather on the regenerative and immunomodulatory potential of MSCs secretions (Kumar et al., 2019). It is worth clarifying that mesenchymal stem cell (MSC) is recently not considered a "stem cell" precisely because they lack multipotency *in vivo* (Caplan, 2017). The use of medicinal signaling cells as the true meaning of MSCs has gained some acceptance (de Windt et al., 2017).

Proteomics-based analyses have shown that stem cell secretomes from different ecological niches have different functions (Kumar et al., 2019). For different application contexts, we can use different tailored secretomes or even factors such as biomaterials to control efficacy (Chang et al., 2021). Given that in recent years there has been dedicated literature to identify various MSC secretome delivery options, this paper will not repeat them in this section (Chang et al., 2021; Han et al., 2022).

Chemical molecules secreted by non-stem cells have powerful and multi-effect regulatory effects on the biological behavior of stem cells. T cells in the brains of older individuals inhibit neural stem cell proliferation by secreting interferon γ (Dulken et al., 2019).

6.2 Proximity communication between cells

Interactions between cells nearby may occur by passing certain cellular substances or ligand-receptor binding. In this subsection, intercellular connections transmit biochemical signals, which are distinguished from mechanical signals in the next section.

6.2.1 Embryonic developmental stage

During embryonic development, a positive feedback loop exists between the length of intercellular contacts and the nodal signaling pathway (Barone et al., 2017). This positive feedback loop controls decisions regarding the fate of the developing embryos. Furthermore, intercellular contacts between posterior lateral plate mesodermal cells and somitic cells expressing Notch ligands allow the former to acquire the identity of a hematopoietic stem cell precursor, that is, blood-derived endothelium (Rho et al., 2019).

6.2.2 Nervous system

Experimental nervous system models illustrate that ephrin-B3 downregulation on the cell membrane of excited hippocampal dentate granule cells (GCs) triggers EphB2 signaling attenuation in adjacent radial neural stem cells (rNSCs) through direct cell contact, leading to rNSC activation and the generation of new neurons (Dong et al., 2019). Conversely, when enhanced EphB2-ephrin-B3 signaling contributes to the maintenance of the quiescent state of rNSCs. In contrast, intercellular contacts affect gene expression and fate determination in human-induced pluripotent neural stem/progenitor cells cultured *in vitro* (McIntyre et al., 2022). Transcriptome analysis identified the differential expression of Notch and Wnt, further suggesting that Notch and Wnt are responsible for the neurogenic cell fate of neural stem/progenitor cells.

6.2.3 Immune system

6.2.3.1 The biological behavior of stem cells is modulated

Interactions between immune cells and stem cells have also been reported. The fate of intestinal stem cells (ISC) is regulated by adhesion signals from immune cells (Chen et al., 2021). Binding of integrin αEβ7 expressed by T cells to E-cadherin on ISC cell membranes triggers Wnt signaling promotion and inhibition of Notch signaling, thus maintaining normal ISC differentiation. Biton et al. detected MHC II enrichment in Lgr5 ISC using scRNA-seq, revealing the influence of the interactions between Th cells and Lgr5 ISC on stem cell renewal and differentiation. Pro-inflammatory signals can promote intestinal stem cell differentiation (Biton et al., 2018). The mechanism of aplastic anemia is also related to the interaction between T cells and hematopoietic stem/progenitor cells, leading to their destruction (Zhu et al., 2021).

The paracrine effects of stem cells are also influenced by the cell-cell contact between stem cells and other cells. For example, the immunomodulatory effects of MSCs are enhanced upon contact with pro-inflammatory macrophages (Li et al., 2019). Additionally, macrophages can direct muscle stem cells to repair skeletal muscles by secreting stem cell niche signals (Ratnayake et al., 2021). Vascular cells and lymphatic vessel cells can be considered as components of stem cell niche (Kusumbe et al., 2014; Itkin et al., 2016; Biswas et al., 2023). Lymphatic vessels influence the proliferation and differentiation of hemopoietic stem cells and bone progenitor cells through the secretion of CXCL12.

6.2.3.2 The biological behavior of cells in contact with stem cells is modulated

Moreover, immune cell function is affected by intercellular contact between stem cells and immune cells. This may be due to the secretion of cytokines that affect stem cells (Alunno et al., 2018). There are other cases; for example, the transfer of active

mitochondrial and plasma membrane fragments to Tregs occurs during intercellular contact between MSCs and Treg cells dependent on HLA, allowing for enhanced Treg immunosuppression (Piekarska et al., 2022). MSCs enhance Treg immunosuppression through contact-dependent interactions that are partly mediated by MSC-expressed CD80 (Mittal et al., 2022). Myogenic hMuStem cells suppress T cell activity and promote Treg production through paracrine or intercellular contacts (Charrier et al., 2022). Thus, hMuStem cells are potent immunomodulators. Particularly, cancer-initiation stem cells expressing CD4 inhibit the activity of cytotoxic T cells through direct contact with the latter (Miao et al., 2019).

Stem cells can also regulate immune cell functions through paracrine and intercellular contacts (Lynch et al., 2020). TGF-β MSC enhanced immune suppression is Smad2/3 dependent as well as intercellular contact-dependent. In contrast, TGF-β MSC promotes Treg expansion and T cell activation through paracrine secretion when PGE2 is the main mediator.

6.2.4 Bone

In bone marrow tissue, bone marrow regeneration after radiation clearance is inseparable from the transfer of mitochondria from hematopoietic stem cells to bone marrow mesenchymal stromal cells through intercellular contacts (Golan et al., 2020). Hematopoietic stem/progenitor cells are extensively polarised after contact with bone marrow stromal cells specifically via SDF1 (Bessy et al., 2021). Specific interactions between developing neutrophils and megakaryocytes are also observed in the bone marrow (Boisset et al., 2018). Their interaction is enhanced under certain pathological conditions because neutrophils can survive inside megakaryocytes. This study also revealed an interaction between Lgr5+ stem cells and Tac1+ enteroendocrine cells. The experiment leaves room for improvement in judging whether the interaction occurs or not, as the authors mention that "the expected interaction needs to be verified *in situ*."

6.3 Mechanical regulation

6.3.1 Perception and transmission of mechanical information by stem cells

Mechanical signals include both the structure and properties of the ECM and forces generated by the cell through various connections (Humphrey et al., 2014). This information is translated through mechanotransduction into information that affects gene expression, linking upstream and downstream biological responses (Zanconato et al., 2016; Panciera et al., 2017). Mechanotransduction initiation is associated with the recognition of external mechanical information by various membrane proteins, such as cell-expressed adhesion molecules, and the feedback of mechanical forces by the cytoskeletal structure within the cell (Totaro et al., 2018). Recent studies revealed the contribution of transcription factors Yes-associated protein (YAP) and transcriptional coactivator with PDZ-binding motif (TAZ) to mechanical information input (Meng et al., 2018; Totaro et al., 2018; Zanconato et al., 2019). The work of Totaro et al. (2018) showed that the ECM-integrin-, F-actin-, Hippo-, Wnt-, and G protein-coupled receptor-YAP/TAZ pathways, providing essential information on how YAP/TAZ acts as a transcription factor in response to upstream signals and regulates downstream pathways. Mechanoreceptive information via focal adhesions is the main source of information received by YAP/TAZ (Vining and Mooney, 2017). Wang et al. (2021b) identified cerebral cavernous malformation 3 (CCM3), an upstream molecule that regulates YAP/TAZ, and demonstrated that MSC differentiation is influenced by this pathway. CCM3 is localized at focal adhesion sites in cancer-associated fibroblasts and MSCs and controls mechanotransduction and YAP/TAZ activity. Meng et al. (2018) identified another upstream molecule of the Hippo pathway, Ras-related GTPase 2(RAP2), which mediates the ECM rigidity-YAP/TAZ-nucleus signaling pathway. RAP2 specifically transmits ECM rigidity signals and inhibits YAP/TAZ through a series of reactions after activation under low-rigidity conditions. Chang et al. (2018) complemented the inhibitory effect of the SWI/SNF complex on YAP/TAZ and proposed that increased nuclear YAP/TAZ accumulation and SWI/SNF complex inhibition were two necessary conditions for obtaining a YAP/TAZ response. In addition, two actin cytoskeleton regulators upstream of YAP1 have been reported (Aragona et al., 2020). Changes in gap junctions in the human papilla stem can also mediate stem cell interactions with the external physical microenvironment (Zhou et al., 2020). Primary cilia are also involved in the mechanical regulation of human tissues and can play a role in promoting the differentiation of different stem cell populations (Chen et al., 2016; Li et al., 2022c; Palla et al., 2022).

6.3.2 Mechanically informed stem cell self-renewal regulation and proliferation

Mechanically gated Piezo1 channels are expressed in both neural stem cells and astrocytes and regulate adult neurogenesis (Pathak et al., 2014; Chi et al., 2022). In *Drosophila*, the proliferation and differentiation of all stem cells that ectopically express Piezo are promoted by a mechanism that is inseparable from calcium signaling (He et al., 2018). Piezo1 is also expressed in muscle stem cells (MuSCs), where it transmits mechanical signals that help maintain MuSC quiescence and prevent senescence (Peng et al., 2022). Furthermore, Piezo1 mediates changes in MuSC status, which promotes skeletal muscle regeneration (Ma et al., 2022). During increased muscle loading, MSCs promote muscle stem cell proliferation through the Yap1/Taz-Thbs1-CD47 pathway (Kaneshige et al., 2022). When there is muscle sclerosis due to injury, etc., this change in physical information is transmitted to the nucleus via YAP/TAZ to maintain muscle stem cell activation and proliferation (Silver et al., 2021). Adult muscle stem cells maintain quiescence through the interaction of calcitonin receptors with secreted collagen (Baghdadi et al., 2018). The Notch–collagen V-calcitonin receptor signaling cascade may play similar roles in different stem cell populations.

Wnt and Src-YAP signaling cooperate to drive intestinal regeneration (Guillermin et al., 2021). Additionally, intracellular crowding due to compressive mechanical information enhances Wnt/β-catenin signaling and promotes ISC self-renewal (Li et al., 2021).

6.3.3 Mechanical information regulates the fate decision of stem cells

Physical signaling with tunable properties that act immediately and locally is an object of interest to regulate the differentiation of

stem cells into specific lineages (Kong et al., 2021). The ECM-integrin α5-F-actin-YAP1-Notch signaling way regulates the fate decisions of bipotent pancreatic progenitor cells, especially the first half, i.e., the integrity of extracellular matrix-integrin α5 promotes ductal lineage fate and *vice versa* in favor of endocrine cell fate (Mamidi et al., 2018). MSCs are often used in bone regeneration engineering. The mechanical signal of reduced collagen alignment in the ECM is captured by MSCs, causing MSCs to prefer the adipose to osteogenic fate (Huber et al., 2020). Smaller differences in mechanical force information can determine whether MSCs choose an osteogenic or lipogenic fate via the myosin II, Rac1, Src, FAK, YAP, and TAZ signaling pathways (Han et al., 2019). The integrin/N-calmucin-cofilin-actin-YAP pathway leads to the osteogenic differentiation of human MSCs (Zhang et al., 2022b). Moreover, osteogenic differentiation of periodontal ligament stem cells can be promoted by enhanced Tet2/HDAC1/E-calmodulin/β-linked protein signaling (Yu et al., 2022b). The intercalated disc-mediated mechanosensory pathway between cardiac myocytes eventually activates the ectopic adipogenic program, which partly explains why cardiac adipocytes share a common precursor with some cardiac myocytes (Dorn et al., 2018).

Indeed, numerous researchers have shed a light on how mechanical information affects cell behavior. Chaudhuri et al. (2020) previously focused on the effects of the ECM on cell behavior, providing insights. Kong et al. (2021) elucidated the mechanisms by which nanomaterials applied in stem cell research transmit physical signals that affect the fate of stem cells. Valet et al. (2022) focused on the vertebrate embryogenesis stage and described how mechanical signaling regulates key developmental processes during this period. A recent study systematically organized the mechanisms by which biomechanics regulate cell fate, with a focus on mechanical transduction, intracellular signaling, and cell surface mechanics (De Belly et al., 2022). Methods and tools with higher spatial and temporal resolutions are still required.

7 Overview and perspectives

We are currently studying the mechanisms underlying stem cell interactions to improve the application of stem cells in regenerative medicine. To systematically and precisely elucidate these mechanisms, technologies with higher spatial and temporal resolutions, more realistic simulations of the stem cell microenvironment, and more specific stem cell population differentiation and tracing are required. This demand has led to many powerful technologies that elucidate the mechanisms of stem cell interactions. We discuss how lineage tracing, synthetic receptors, proximity labeling and transcriptome data analysis tools can be applied in the study of CCI. The techniques presented in this paper include but are not limited to using stem cells as research models, and using non-stem cells as research models has complementary and reference significance. In addition, we note some other techniques. For example, SPEAC-seq based on CRISPR-Cas9 with microfluidic microarrays to identify cell signaling pathways (Wheeler et al., 2023). It provides a demonstration of CRISPR-Cas9 applied to CCI studies.

The study of stem cell interactions is in a rapidly evolving stage, especially in the context of rapid iterative updates in biotechnology. Although, the biological understanding of stem cell interactions sorted out in this paper is not sufficient to elaborate a comprehensive picture of stem cell behavior during mammalian development or injury repair, it contributes to a complete description of stem cell interaction mechanisms in the future.

Author contributions

XL, ZL, and RX contributed to conception and design of this study. XL and ZL contributed to the literature searching and analysis. XL, ZL, and RX organized and draw the figures. XL, ZL, and RX wrote the draft of the manuscript. All authors contributed to the article and approved the submitted version.

Funding

This work was supported by the National Natural Science Foundation of China (82001001), National Postdoctoral Program for Innovation Talents (BX20190224), Natural Science Foundation of Sichuan Province (2022NSFSC1431), Postdoctoral Foundation of Sichuan University (2020SCU12018), Research Funding of West China Hospital of Stomatology (RD-02-202101 and RCDWJS 2023-18), and National College Students' innovation and entrepreneurship training program (202310611508, 202310611492). The schematics were created using Biorender.

Conflict of interest

The authors declare that the research was conducted in the absence of any commercial or financial relationships that could be construed as a potential conflict of interest.

Publisher's note

References

Abdel-Malak, N. A., Srikant, C. B., Kristof, A. S., Magder, S. A., Di Battista, J. A., and Hussain, S. N. A. (2008). Angiopoietin-1 promotes endothelial cell proliferation and migration through AP-1-dependent autocrine production of interleukin-8. *Blood* 111 (8), 4145–4154. doi:10.1182/blood-2007-08-110338

Adams, K. L., Riparini, G., Banerjee, P., Breur, M., Bugiani, M., and Gallo, V. (2020). Endothelin-1 signaling maintains glial progenitor proliferation in the postnatal subventricular zone. *Nat. Commun.* 11 (1), 2138. doi:10.1038/s41467-020-16028-8

Adkins, B., Leutz, A., and Graf, T. (1984). Autocrine growth induced by src-related oncogenes in transformed chicken myeloid cells. *Cell* 39 (2), 439–445. doi:10.1016/0092-8674(84)90451-3

Alunno, A., Bistoni, O., Montanucci, P., Basta, G., Calafiore, R., and Gerli, R. (2018). Umbilical cord mesenchymal stem cells for the treatment of autoimmune diseases: beware of cell-to-cell contact. *Ann. Rheum. Dis.* 77 (3), e14. doi:10.1136/annrheumdis-2017-211790

Andrews, N., Serviss, J. T., Geyer, N., Andersson, A. B., Dzwonkowska, E., Šutevski, I., et al. (2021). An unsupervised method for physical cell interaction profiling of complex tissues. *Nat. Methods* 18 (8), 912–920. doi:10.1038/s41592-021-01196-2

Aragona, M., Sifrim, A., Malfait, M., Song, Y., Van Herck, J., Dekoninck, S., et al. (2020). Mechanisms of stretch-mediated skin expansion at single-cell resolution. *Nature* 584 (7820), 268–273. doi:10.1038/s41586-020-2555-7

Baccin, C., Al-Sabah, J., Velten, L., Helbling, P. M., Grünschläger, F., Hernández-Malmierca, P., et al. (2020). Combined single-cell and spatial transcriptomics reveal the molecular, cellular and spatial bone marrow niche organization. *Nat. Cell Biol.* 22 (1), 38–48. doi:10.1038/s41556-019-0439-6

Baghdadi, M. B., Castel, D., Machado, L., Fukada, S. I., Birk, D. E., Relaix, F., et al. (2018). Reciprocal signalling by Notch-Collagen V-CALCR retains muscle stem cells in their niche. *Nature* 557 (7707), 714–718. doi:10.1038/s41586-018-0144-9

Baron, C. S., and van Oudenaarden, A. (2019). Unravelling cellular relationships during development and regeneration using genetic lineage tracing. *Nat. Rev. Mol. Cell Biol.* 20 (12), 753–765. doi:10.1038/s41580-019-0186-3

Barone, V., Lang, M., Krens, S. F. G., Pradhan, S. J., Shamipour, S., Sako, K., et al. (2017). An effective feedback loop between cell-cell contact duration and morphogen signaling determines cell fate. *Dev. Cell* 43 (2), 198–211. doi:10.1016/j.devcel.2017.09.014

Bessy, T., Candelas, A., Souquet, B., Saadallah, K., Schaeffer, A., Vianay, B., et al. (2021). Hematopoietic progenitors polarize in contact with bone marrow stromal cells in response to SDF1. *J. Cell Biol.* 220 (11), e202005085. doi:10.1083/jcb.202005085

Biswas, L., Chen, J., De Angelis, J., Singh, A., Owen-Woods, C., Ding, Z., et al. (2023). Lymphatic vessels in bone support regeneration after injury. *Cell* 186 (2), 382–397.e24. doi:10.1016/j.cell.2022.12.031

Biton, M., Haber, A. L., Rogel, N., Burgin, G., Beyaz, S., Schnell, A., et al. (2018). T helper cell cytokines modulate intestinal stem cell renewal and differentiation. *Cell* 175 (5), 1307–1320. doi:10.1016/j.cell.2018.10.008

Boisset, J. C., Vivié, J., Grün, D., Muraro, M. J., Lyubimova, A., and van Oudenaarden, A. (2018). Mapping the physical network of cellular interactions. *Nat. Methods* 15 (7), 547–553. doi:10.1038/s41592-018-0009-z

Browaeys, R., Saelens, W., and Saeys, Y. (2020). NicheNet: modeling intercellular communication by linking ligands to target genes. *Nat. Methods* 17 (2), 159–162. doi:10.1038/s41592-019-0667-5

Brunet, A., Goodell, M. A., and Rando, T. A. (2023). Ageing and rejuvenation of tissue stem cells and their niches. *Nat. Rev. Mol. Cell Biol.* 24 (1), 45–62. doi:10.1038/s41580-022-00510-w

Buksh, B. F., Knutson, S. D., Oakley, J. V., Bissonnette, N. B., Oblinsky, D. G., Schwoerer, M. P., et al. (2022). μMap-red: proximity labeling by red light photocatalysis. *J. Am. Chem. Soc.* 144 (14), 6154–6162. doi:10.1021/jacs.2c01384

Cabello-Aguilar, S., Alame, M., Kon-Sun-Tack, F., Fau, C., Lacroix, M., and Colinge, J. (2020). SingleCellSignalR: inference of intercellular networks from single-cell transcriptomics. *Nucleic Acids Res.* 48 (10), e55. doi:10.1093/nar/gkaa183

Calvanese, V., Capellera-Garcia, S., Ma, F., Fares, I., Liebscher, S., Ng, E. S., et al. (2022). Mapping human haematopoietic stem cells from haemogenic endothelium to birth. *Nature* 604 (7906), 534–540. doi:10.1038/s41586-022-04571-x

Cang, Z., and Nie, Q. (2020). Inferring spatial and signaling relationships between cells from single cell transcriptomic data. *Nat. Commun.* 11 (1), 2084. doi:10.1038/s41467-020-15968-5

Cang, Z., Zhao, Y., Almet, A. A., Stabell, A., Ramos, R., Plikus, M. V., et al. (2023). Screening cell-cell communication in spatial transcriptomics via collective optimal transport. *Nat. Methods* 20 (2), 218–228. doi:10.1038/s41592-022-01728-4

Caplan, A. I. (2017). Mesenchymal stem cells: time to change the name!. *Stem Cells Transl. Med.* 6 (6), 1445–1451. doi:10.1002/sctm.17-0051

Centonze, A., Lin, S., Tika, E., Sifrim, A., Fioramonti, M., Malfait, M., et al. (2020). Heterotypic cell-cell communication regulates glandular stem cell multipotency. *Nature* 584 (7822), 608–613. doi:10.1038/s41586-020-2632-y

Chang, C., Yan, J., Yao, Z., Zhang, C., Li, X., and Mao, H. Q. (2021). Effects of mesenchymal stem cell-derived paracrine signals and their delivery strategies. *Adv. Healthc. Mater* 10 (7), e2001689. doi:10.1002/adhm.202001689

Chang, L., Azzolin, L., Di Biagio, D., Zanconato, F., Battilana, G., Lucon Xiccato, R., et al. (2018). The SWI/SNF complex is a mechanoregulated inhibitor of YAP and TAZ. *Nature* 563 (7730), 265–269. doi:10.1038/s41586-018-0658-1

Charrier, M., Lorant, J., Contreras-Lopez, R., Téjédor, G., Blanquart, C., Lieubeau, B., et al. (2022). Human MuStem cells repress T-cell proliferation and cytotoxicity through both paracrine and contact-dependent pathways. *Stem Cell Res. Ther.* 13 (1), 7. doi:10.1186/s13287-021-02681-3

Chaudhuri, O., Cooper-White, J., Janmey, P. A., Mooney, D. J., and Shenoy, V. B. (2020). Effects of extracellular matrix viscoelasticity on cellular behaviour. *Nature* 584 (7822), 535–546. doi:10.1038/s41586-020-2612-2

Chen, G., Xu, X., Zhang, L., Fu, Y., Wang, M., Gu, H., et al. (2014). Blocking autocrine VEGF signaling by sunitinib, an anti-cancer drug, promotes embryonic stem cell self-renewal and somatic cell reprogramming. *Cell Res.* 24 (9), 1121–1136. doi:10.1038/cr.2014.112

Chen, J. C., Hoey, D. A., Chua, M., Bellon, R., and Jacobs, C. R. (2016). Mechanical signals promote osteogenic fate through a primary cilia-mediated mechanism. *Faseb J.* 30 (4), 1504–1511. doi:10.1096/fj.15-276402

Chen, S., Zheng, Y., Ran, X., Du, H., Feng, H., Yang, L., et al. (2021). Integrin αEβ7(+) T cells direct intestinal stem cell fate decisions via adhesion signaling. *Cell Res.* 31 (12), 1291–1307. doi:10.1038/s41422-021-00561-2

Chi, S., Cui, Y., Wang, H., Jiang, J., Zhang, T., Sun, S., et al. (2022). Astrocytic Piezo1-mediated mechanotransduction determines adult neurogenesis and cognitive functions. *Neuron* 110 (18), 2984–2999.e8. doi:10.1016/j.neuron.2022.07.010

Choi, J., Park, J. E., Tsagkogeorga, G., Yanagita, M., Koo, B. K., Han, N., et al. (2020). Inflammatory signals induce AT2 cell-derived damage-associated transient progenitors that mediate alveolar regeneration. *Cell Stem Cell* 27 (3), 366–382. doi:10.1016/j.stem.2020.06.020

De Belly, H., Paluch, E. K., and Chalut, K. J. (2022). Interplay between mechanics and signalling in regulating cell fate. *Nat. Rev. Mol. Cell Biol.* 23 (7), 465–480. doi:10.1038/s41580-022-00472-z

de Windt, T. S., Vonk, L. A., and Saris, D. B. F. (2017). Response to: mesenchymal stem cells: time to change the name!. *Stem Cells Transl. Med.* 6 (8), 1747–1748. doi:10.1002/sctm.17-0120

Del Sol, A., and Jung, S. (2021). The importance of computational modeling in stem cell research. *Trends Biotechnol.* 39 (2), 126–136. doi:10.1016/j.tibtech.2020.07.006

Deniset, J. F., Belke, D., Lee, W. Y., Jorch, S. K., Deppermann, C., Hassanabad, A. F., et al. (2019). Gata6(+) pericardial cavity macrophages relocate to the injured heart and prevent cardiac fibrosis. *Immunity* 51 (1), 131–140. doi:10.1016/j.immuni.2019.06.010

Dimitrov, D., Türei, D., Garrido-Rodriguez, M., Burmedi, P. L., Nagai, J. S., Boys, C., et al. (2022). Comparison of methods and resources for cell-cell communication inference from single-cell RNA-Seq data. *Nat. Commun.* 13 (1), 3224. doi:10.1038/s41467-022-30755-0

Dong, J., Pan, Y. B., Wu, X. R., He, L. N., Liu, X. D., Feng, D. F., et al. (2019). A neuronal molecular switch through cell-cell contact that regulates quiescent neural stem cells. *Sci. Adv.* 5 (2), eaav4416. doi:10.1126/sciadv.aav4416

Dorn, T., Kornherr, J., Parrotta, E. I., Zawada, D., Ayetey, H., Santamaria, G., et al. (2018). Interplay of cell-cell contacts and RhoA/MRTF-A signaling regulates cardiomyocyte identity. *Embo J.* 37 (12), e98133. doi:10.15252/embj.201798133

Dries, R., Zhu, Q., Dong, R., Eng, C. H. L., Li, H., Liu, K., et al. (2021). Giotto: a toolbox for integrative analysis and visualization of spatial expression data. *Genome Biol.* 22 (1), 78. doi:10.1186/s13059-021-02286-2

Dulken, B. W., Buckley, M. T., Navarro Negredo, P., Saligrama, N., Cayrol, R., Leeman, D. S., et al. (2019). Single-cell analysis reveals T cell infiltration in old neurogenic niches. *Nature* 571 (7764), 205–210. doi:10.1038/s41586-019-1362-5

Efremova, M., Vento-Tormo, M., Teichmann, S. A., and Vento-Tormo, R. (2020). CellPhoneDB: inferring cell-cell communication from combined expression of multi-subunit ligand-receptor complexes. *Nat. Protoc.* 15 (4), 1484–1506. doi:10.1038/s41596-020-0292-x

Fang, R., Xia, C., Close, J. L., Zhang, M., He, J., Huang, Z., et al. (2022). Conservation and divergence of cortical cell organization in human and mouse revealed by MERFISH. *Science* 377 (6601), 56–62. doi:10.1126/science.abm1741

Felker, A., Prummel, K. D., Merks, A. M., Mickoleit, M., Brombacher, E. C., Huisken, J., et al. (2018). Continuous addition of progenitors forms the cardiac ventricle in zebrafish. *Nat. Commun.* 9 (1), 2001. doi:10.1038/s41467-018-04402-6

Fischer, D. S., Schaar, A. C., and Theis, F. J. (2023). Modeling intercellular communication in tissues using spatial graphs of cells. *Nat. Biotechnol.* 41 (3), 332–336. doi:10.1038/s41587-022-01467-z

Gagliardi, P. A., Dobrzyński, M., Jacques, M. A., Dessauges, C., Ender, P., Blum, Y., et al. (2021). Collective ERK/Akt activity waves orchestrate epithelial homeostasis by driving apoptosis-induced survival. *Dev. Cell* 56 (12), 1712–1726.e6. doi:10.1016/j.devcel.2021.05.007

Gallipoli, P., Pellicano, F., Morrison, H., Laidlaw, K., Allan, E. K., Bhatia, R., et al. (2013). Autocrine TNF-α production supports CML stem and progenitor cell survival and enhances their proliferation. *Blood* 122 (19), 3335–3339. doi:10.1182/blood-2013-02-485607

Gaudio, E., Barbaro, B., Alvaro, D., Glaser, S., Francis, H., Ueno, Y., et al. (2006). Vascular endothelial growth factor stimulates rat cholangiocyte proliferation via an

autocrine mechanism. *Gastroenterology* 130 (4), 1270–1282. doi:10.1053/j.gastro.2005.12.034

Ge, Y., Chen, L., Liu, S., Zhao, J., Zhang, H., and Chen, P. R. (2019). Enzyme-mediated intercellular proximity labeling for detecting cell-cell interactions. *J. Am. Chem. Soc.* 141 (5), 1833–1837. doi:10.1021/jacs.8b10286

Geiller, T., Sadeh, S., Rolotti, S. V., Blockus, H., Vancura, B., Negrean, A., et al. (2022). Local circuit amplification of spatial selectivity in the hippocampus. *Nature* 601 (7891), 105–109. doi:10.1038/s41586-021-04169-9

Genshaft, A. S., Ziegler, C. G. K., Tzouanas, C. N., Mead, B. E., Jaeger, A. M., Navia, A. W., et al. (2021). Live cell tagging tracking and isolation for spatial transcriptomics using photoactivatable cell dyes. *Nat. Commun.* 12 (1), 4995. doi:10.1038/s41467-021-25279-y

Geri, J. B., Oakley, J. V., Reyes-Robles, T., Wang, T., McCarver, S. J., White, C. H., et al. (2020). Microenvironment mapping via Dexter energy transfer on immune cells. *Science* 367 (6482), 1091–1097. doi:10.1126/science.aay4106

Ghaddar, B., and De, S. (2022). Reconstructing physical cell interaction networks from single-cell data using Neighbor-seq. *Nucleic Acids Res.* 50 (14), e82. doi:10.1093/nar/gkac333

Giladi, A., Cohen, M., Medaglia, C., Baran, Y., Li, B., Zada, M., et al. (2020). Dissecting cellular crosstalk by sequencing physically interacting cells. *Nat. Biotechnol.* 38 (5), 629–637. doi:10.1038/s41587-020-0442-2

Golan, K., Singh, A. K., Kollet, O., Bertagna, M., Althoff, M. J., Khatib-Massalha, E., et al. (2020). Bone marrow regeneration requires mitochondrial transfer from donor Cx43-expressing hematopoietic progenitors to stroma. *Blood* 136 (23), 2607–2619. doi:10.1182/blood.2020005399

Gordon, W. R., Zimmerman, B., He, L., Miles, L. J., Huang, J., Tiyanont, K., et al. (2015). Mechanical allostery: evidence for a force requirement in the proteolytic activation of notch. *Dev. Cell* 33 (6), 729–736. doi:10.1016/j.devcel.2015.05.004

Guillermin, O., Angelis, N., Sidor, C. M., Ridgway, R., Baulies, A., Kucharska, A., et al. (2021). Wnt and Src signals converge on YAP-TEAD to drive intestinal regeneration. *Embo J.* 40 (13), e105770. doi:10.15252/embj.2020105770

Han, P., Frith, J. E., Gomez, G. A., Yap, A. S., O'Neill, G. M., and Cooper-White, J. J. (2019). Five piconewtons: the difference between osteogenic and adipogenic fate choice in human mesenchymal stem cells. *ACS Nano* 13 (10), 11129–11143. doi:10.1021/acsnano.9b03914

Han, Y., Yang, J., Fang, J., Zhou, Y., Candi, E., Wang, J., et al. (2022). The secretion profile of mesenchymal stem cells and potential applications in treating human diseases. *Signal Transduct. Target Ther.* 7 (1), 92. doi:10.1038/s41392-022-00932-0

He, L., Huang, J., and Perrimon, N. (2017b). Development of an optimized synthetic Notch receptor as an *in vivo* cell-cell contact sensor. *Proc. Natl. Acad. Sci. U. S. A.* 114 (21), 5467–5472. doi:10.1073/pnas.1703205114

He, L., Li, Y., Li, Y., Pu, W., Huang, X., Tian, X., et al. (2017a). Enhancing the precision of genetic lineage tracing using dual recombinases. *Nat. Med.* 23 (12), 1488–1498. doi:10.1038/nm.4437

He, L., Pu, W., Liu, X., Zhang, Z., Han, M., Li, Y., et al. (2021). Proliferation tracing reveals regional hepatocyte generation in liver homeostasis and repair. *Science* 371 (6532), 371. doi:10.1126/science.abc4346

He, L., Si, G., Huang, J., Samuel, A. D. T., and Perrimon, N. (2018). Mechanical regulation of stem-cell differentiation by the stretch-activated Piezo channel. *Nature* 555 (7694), 103–106. doi:10.1038/nature25744

Hernandez-Lopez, R. A., Yu, W., Cabral, K. A., Creasey, O. A., Lopez Pazmino, M. D. P., Tonai, Y., et al. (2021). T cell circuits that sense antigen density with an ultrasensitive threshold. *Science* 371 (6534), 1166–1171. doi:10.1126/science.abc1855

Hou, R., Denisenko, E., Ong, H. T., Ramilowski, J. A., and Forrest, A. R. R. (2020). Predicting cell-to-cell communication networks using NATMI. *Nat. Commun.* 11 (1), 5011. doi:10.1038/s41467-020-18873-z

Hou, S., Dong, J., Gao, Y., Chang, Z., and Ding, X. (2022). Heterogeneity in endothelial cells and widespread venous arterialization during early vascular development in mammals. *Cell Res.* 32 (4), 333–348. doi:10.1038/s41422-022-00615-z

Hsu, Y. C., Li, L., and Fuchs, E. (2014). Transit-amplifying cells orchestrate stem cell activity and tissue regeneration. *Cell* 157 (4), 935–949. doi:10.1016/j.cell.2014.02.057

Huang, J. S., Huang, S. S., and Deuel, T. F. (1984). Transforming protein of simian sarcoma virus stimulates autocrine growth of SSV-transformed cells through PDGF cell-surface receptors. *Cell* 39 (1), 79–87. doi:10.1016/0092-8674(84)90193-4

Huang, T. H., Velho, T., and Lois, C. (2016). Monitoring cell-cell contacts *in vivo* in transgenic animals. *Development* 143 (21), 4073–4084. doi:10.1242/dev.142406

Huber, A. K., Patel, N., Pagani, C. A., Marini, S., Padmanabhan, K. R., Matera, D. L., et al. (2020). Immobilization after injury alters extracellular matrix and stem cell fate. *J. Clin. Invest.* 130 (10), 5444–5460. doi:10.1172/JCI136142

Humphrey, J. D., Dufresne, E. R., and Schwartz, M. A. (2014). Mechanotransduction and extracellular matrix homeostasis. *Nat. Rev. Mol. Cell Biol.* 15 (12), 802–812. doi:10.1038/nrm3896

Hurwitz, S. N., Jung, S. K., and Kurre, P. (2020). Hematopoietic stem and progenitor cell signaling in the niche. *Leukemia* 34 (12), 3136–3148. doi:10.1038/s41375-020-01062-8

Itkin, T., Gur-Cohen, S., Spencer, J. A., Schajnovitz, A., Ramasamy, S. K., Kusumbe, A. P., et al. (2016). Distinct bone marrow blood vessels differentially regulate haematopoiesis. *Nature* 532 (7599), 323–328. doi:10.1038/nature17624

Jin, H., Liu, K., Tang, J., Huang, X., Wang, H., Zhang, Q., et al. (2021a). Genetic fate-mapping reveals surface accumulation but not deep organ invasion of pleural and peritoneal cavity macrophages following injury. *Nat. Commun.* 12 (1), 2863. doi:10.1038/s41467-021-23197-7

Jin, S., Guerrero-Juarez, C. F., Zhang, L., Chang, I., Ramos, R., Kuan, C. H., et al. (2021b). Inference and analysis of cell-cell communication using CellChat. *Nat. Commun.* 12 (1), 1088. doi:10.1038/s41467-021-21246-9

Junyent, S., Garcin, C. L., Szczerkowski, J. L. A., Trieu, T. J., Reeves, J., and Habib, S. J. (2020). Specialized cytonemes induce self-organization of stem cells. *Proc. Natl. Acad. Sci. U. S. A.* 117 (13), 7236–7244. doi:10.1073/pnas.1920837117

Kadur Lakshminarasimha Murthy, P., Sontake, V., Tata, A., Kobayashi, Y., Macadlo, L., Okuda, K., et al. (2022). Human distal lung maps and lineage hierarchies reveal a bipotent progenitor. *Nature* 604 (7904), 111–119. doi:10.1038/s41586-022-04541-3

Kaneshige, A., Kaji, T., Zhang, L., Saito, H., Nakamura, A., Kurosawa, T., et al. (2022). Relayed signaling between mesenchymal progenitors and muscle stem cells ensures adaptive stem cell response to increased mechanical load. *Cell Stem Cell* 29 (2), 265–280.e6. doi:10.1016/j.stem.2021.11.003

Kim, J., Rothová, M. M., Madan, E., Rhee, S., Weng, G., Palma, A. M., et al. (2023). Neighbor-specific gene expression revealed from physically interacting cells during mouse embryonic development. *Proc. Natl. Acad. Sci. U. S. A.* 120 (2), e2205371120. doi:10.1073/pnas.2205371120

Kim, T. H., and Schnitzer, M. J. (2022). Fluorescence imaging of large-scale neural ensemble dynamics. *Cell* 185 (1), 9–41. doi:10.1016/j.cell.2021.12.007

Kobayashi, Y., Tata, A., Konkimalla, A., Katsura, H., Lee, R. F., Ou, J., et al. (2020). Persistence of a regeneration-associated, transitional alveolar epithelial cell state in pulmonary fibrosis. *Nat. Cell Biol.* 22 (8), 934–946. doi:10.1038/s41556-020-0542-8

Kong, Y., Duan, J., Liu, F., Han, L., Li, G., Sun, C., et al. (2021). Regulation of stem cell fate using nanostructure-mediated physical signals. *Chem. Soc. Rev.* 50 (22), 12828–12872. doi:10.1039/d1cs00572c

Kumar, M. E., Bogard, P. E., Espinoza, F. H., Menke, D. B., Kingsley, D. M., and Krasnow, M. A. (2014). Mesenchymal cells. Defining a mesenchymal progenitor niche at single-cell resolution. *Science* 346 (6211), 1258810. doi:10.1126/science.1258810

Kumar, P., Kandoi, S., Misra, R., S, V., K, R., and Verma, R. S. (2019). The mesenchymal stem cell secretome: A new paradigm towards cell-free therapeutic mode in regenerative medicine. *Cytokine Growth Factor Rev.* 46, 1–9. doi:10.1016/j.cytogfr.2019.04.002

Kusumbe, A. P., Ramasamy, S. K., and Adams, R. H. (2014). Coupling of angiogenesis and osteogenesis by a specific vessel subtype in bone. *Nature* 507 (7492), 323–328. doi:10.1038/nature13145

Lang, R. A., Metcalf, D., Gough, N. M., Dunn, A. R., and Gonda, T. J. (1985). Expression of a hemopoietic growth factor cDNA in a factor-dependent cell line results in autonomous growth and tumorigenicity. *Cell* 43 (1), 531–542. doi:10.1016/0092-8674(85)90182-5

Lee, J. C., Brien, H. J., Walton, B. L., Eidman, Z. M., Toda, S., Lim, W. A., et al. (2023). Instructional materials that control cellular activity through synthetic Notch receptors. *Biomaterials* 297, 122099. doi:10.1016/j.biomaterials.2023.122099

Leopold, A. V., Chernov, K. G., and Verkhusha, V. V. (2018). Optogenetically controlled protein kinases for regulation of cellular signaling. *Chem. Soc. Rev.* 47 (7), 2454–2484. doi:10.1039/c7cs00404d

Li, D., Velazquez, J. J., Ding, J., Hislop, J., Ebrahimkhani, M. R., and Bar-Joseph, Z. (2022b). TraSig: inferring cell-cell interactions from pseudotime ordering of scRNA-seq data. *Genome Biol.* 23 (1), 73. doi:10.1186/s13059-022-02629-7

Li, H., Wu, Y., Qiu, Y., Li, X., Guan, Y., Cao, X., et al. (2022a). Stable transgenic mouse strain with enhanced photoactivatable Cre recombinase for spatiotemporal genome manipulation. *Adv. Sci. (Weinh)* 9 (34), e2201352. doi:10.1002/advs.202201352

Li, R., and Yang, X. (2022). De novo reconstruction of cell interaction landscapes from single-cell spatial transcriptome data with DeepLinc. *Genome Biol.* 23 (1), 124. doi:10.1186/s13059-022-02692-0

Li, W., Zhu, Z., He, K., Ma, X., Pignolo, R. J., Sieck, G. C., et al. (2022c). Primary cilia in satellite cells are the mechanical sensors for muscle hypertrophy. *Proc. Natl. Acad. Sci. U. S. A.* 119 (24), e2103615119. doi:10.1073/pnas.2103615119

Li, Y., Chen, M., Hu, J., Sheng, R., Lin, Q., He, X., et al. (2021). Volumetric compression induces intracellular crowding to control intestinal organoid growth via wnt/β-catenin signaling. *Cell Stem Cell* 28 (1), 170–172. doi:10.1016/j.stem.2020.12.003

Li, Y., Zhang, D., Xu, L., Dong, L., Zheng, J., Lin, Y., et al. (2019). Cell-cell contact with proinflammatory macrophages enhances the immunotherapeutic effect of mesenchymal stem cells in two abortion models. *Cell Mol. Immunol.* 16 (12), 908–920. doi:10.1038/s41423-019-0204-6

Lim, X., Tan, S. H., Koh, W. L. C., Chau, R. M. W., Yan, K. S., Kuo, C. J., et al. (2013). Interfollicular epidermal stem cells self-renew via autocrine Wnt signaling. *Science* 342 (6163), 1226–1230. doi:10.1126/science.1239730

Liu, H., Luo, H., Xue, Q., Qin, S., Qiu, S., Liu, S., et al. (2022a). Antigen-specific T cell detection via photocatalytic proximity cell labeling (PhoXCELL). *J. Am. Chem. Soc.* 144 (12), 5517–5526. doi:10.1021/jacs.2c00159

Liu, K., Tang, M., Jin, H., Liu, Q., and Zhu, H. (2020a). Triple-cell lineage tracing by a dual reporter on a single allele. *J. Biol. Chem.* 295 (3), 690–700. doi:10.1074/jbc.RA119.011349

Liu, Q., Yang, R., Huang, X., Zhang, H., He, L., Zhang, L., et al. (2016). Genetic lineage tracing identifies *in situ* Kit-expressing cardiomyocytes. *Cell Res.* 26 (1), 119–130. doi:10.1038/cr.2015.143

Liu, Q., Zheng, J., Sun, W., Huo, Y., Zhang, L., Hao, P., et al. (2018). A proximity-tagging system to identify membrane protein-protein interactions. *Nat. Methods* 15 (9), 715–722. doi:10.1038/s41592-018-0100-5

Liu, X., Pu, W., He, L., Li, Y., Zhao, H., Li, Y., et al. (2021). Cell proliferation fate mapping reveals regional cardiomyocyte cell-cycle activity in subendocardial muscle of left ventricle. *Nat. Commun.* 12 (1), 5784. doi:10.1038/s41467-021-25933-5

Liu, Z., Li, J. P., Chen, M., Wu, M., Shi, Y., Li, W., et al. (2020b). Detecting tumor antigen-specific T cells via interaction-dependent fucosyl-biotinylation. *Cell* 183 (4), 1117–1133. doi:10.1016/j.cell.2020.09.048

Liu, Z., Sun, D., and Wang, C. (2022b). Evaluation of cell-cell interaction methods by integrating single-cell RNA sequencing data with spatial information. *Genome Biol.* 23 (1), 218. doi:10.1186/s13059-022-02783-y

Longo, S. K., Guo, M. G., Ji, A. L., and Khavari, P. A. (2021). Integrating single-cell and spatial transcriptomics to elucidate intercellular tissue dynamics. *Nat. Rev. Genet.* 22 (10), 627–644. doi:10.1038/s41576-021-00370-8

Lynch, K., Treacy, O., Chen, X., Murphy, N., Lohan, P., Islam, M. N., et al. (2020). TGF-β1-Licensed murine MSCs show superior therapeutic efficacy in modulating corneal allograft immune rejection *in vivo*. *Mol. Ther.* 28 (9), 2023–2043. doi:10.1016/j.ymthe.2020.05.023

Ma, N., Chen, D., Lee, J. H., Kuri, P., Hernandez, E. B., Kocan, J., et al. (2022). Piezo1 regulates the regenerative capacity of skeletal muscles via orchestration of stem cell morphological states. *Sci. Adv.* 8 (11), eabn0485. doi:10.1126/sciadv.abn0485

Mamidi, A., Prawiro, C., Seymour, P. A., de Lichtenberg, K. H., Jackson, A., Serup, P., et al. (2018). Mechanosignalling via integrins directs fate decisions of pancreatic progenitors. *Nature* 564 (7734), 114–118. doi:10.1038/s41586-018-0762-2

Manhas, J., Edelstein, H. I., Leonard, J. N., and Morsut, L. (2022). The evolution of synthetic receptor systems. *Nat. Chem. Biol.* 18 (3), 244–255. doi:10.1038/s41589-021-00926-z

McIntyre, W. B., Karimzadeh, M., Riazalhosseini, Y., Khazaei, M., and Fehlings, M. G. (2022). Cell-cell contact mediates gene expression and fate choice of human neural stem/progenitor cells. *Cells* 11 (11), 1741. doi:10.3390/cells11111741

Meinke, G., Bohm, A., Hauber, J., Pisabarro, M. T., and Buchholz, F. (2016). Cre recombinase and other tyrosine recombinases. *Chem. Rev.* 116 (20), 12785–12820. doi:10.1021/acs.chemrev.6b00077

Meng, Z., Qiu, Y., Lin, K. C., Kumar, A., Placone, J. K., Fang, C., et al. (2018). RAP2 mediates mechanoresponses of the Hippo pathway. *Nature* 560 (7720), 655–660. doi:10.1038/s41586-018-0444-0

Miao, Y., Yang, H., Levorse, J., Yuan, S., Polak, L., Sribour, M., et al. (2019). Adaptive immune resistance emerges from tumor-initiating stem cells. *Cell* 177 (5), 1172–1186. doi:10.1016/j.cell.2019.03.025

Mittal, S. K., Cho, W., Elbasiony, E., Guan, Y., Foulsham, W., and Chauhan, S. K. (2022). Mesenchymal stem cells augment regulatory T cell function via CD80-mediated interactions and promote allograft survival. *Am. J. Transpl.* 22 (6), 1564–1577. doi:10.1111/ajt.17001

Morikawa, K., Furuhashi, K., de Sena-Tomas, C., Garcia-Garcia, A. L., Bekdash, R., Klein, A. D., et al. (2020). Photoactivatable Cre recombinase 3.0 for *in vivo* mouse applications. *Nat. Commun.* 11 (1), 2141. doi:10.1038/s41467-020-16030-0

Morinaga, H., Mohri, Y., Grachtchouk, M., Asakawa, K., Matsumura, H., Oshima, M., et al. (2021). Obesity accelerates hair thinning by stem cell-centric converging mechanisms. *Nature* 595 (7866), 266–271. doi:10.1038/s41586-021-03624-x

Morsut, L., Roybal, K. T., Xiong, X., Gordley, R. M., Coyle, S. M., Thomson, M., et al. (2016). Engineering customized cell sensing and response behaviors using synthetic notch receptors. *Cell* 164 (4), 780–791. doi:10.1016/j.cell.2016.01.012

Nabhan, A. N., Brownfield, D. G., Harbury, P. B., Krasnow, M. A., and Desai, T. J. (2018). Single-cell Wnt signaling niches maintain stemness of alveolar type 2 cells. *Science* 359 (6380), 1118–1123. doi:10.1126/science.aam6603

Nakandakari-Higa, S. (2023). *Universal recording of cell-cell contacts* in vivo *for interaction-based transcriptomics*. bioRxiv.

Nitzan, M., Karaiskos, N., Friedman, N., and Rajewsky, N. (2019). Gene expression cartography. *Nature* 576 (7785), 132–137. doi:10.1038/s41586-019-1773-3

Noël, F., Massenet-Regad, L., Carmi-Levy, I., Cappuccio, A., Grandclaudon, M., Trichot, C., et al. (2021). Dissection of intercellular communication using the transcriptome-based framework ICELLNET. *Nat. Commun.* 12 (1), 1089. doi:10.1038/s41467-021-21244-x

Nusser, A., Sagar, Swann, J. B., Krauth, B., Diekhoff, D., Calderon, L., et al. (2022). Developmental dynamics of two bipotent thymic epithelial progenitor types. *Nature* 606 (7912), 165–171. doi:10.1038/s41586-022-04752-8

Ombrato, L., Nolan, E., Kurelac, I., Mavousian, A., Bridgeman, V. L., Heinze, I., et al. (2019). Metastatic-niche labelling reveals parenchymal cells with stem features. *Nature* 572 (7771), 603–608. doi:10.1038/s41586-019-1487-6

Ombrato, L., Nolan, E., Passaro, D., Kurelac, I., Bridgeman, V. L., Waclawiczek, A., et al. (2021). Generation of neighbor-labeling cells to study intercellular interactions *in vivo*. *Nat. Protoc.* 16 (2), 872–892. doi:10.1038/s41596-020-00438-5

Oslund, R. C., Reyes-Robles, T., White, C. H., Tomlinson, J. H., Crotty, K. A., Bowman, E. P., et al. (2022). Detection of cell-cell interactions via photocatalytic cell tagging. *Nat. Chem. Biol.* 18 (8), 850–858. doi:10.1038/s41589-022-01044-0

Paik, D. T., Cho, S., Tian, L., Chang, H. Y., and Wu, J. C. (2020). Single-cell RNA sequencing in cardiovascular development, disease and medicine. *Nat. Rev. Cardiol.* 17 (8), 457–473. doi:10.1038/s41569-020-0359-y

Palla, A. R., Hilgendorf, K. I., Yang, A. V., Kerr, J. P., Hinken, A. C., Demeter, J., et al. (2022). Primary cilia on muscle stem cells are critical to maintain regenerative capacity and are lost during aging. *Nat. Commun.* 13 (1), 1439. doi:10.1038/s41467-022-29150-6

Panciera, T., Azzolin, L., Cordenonsi, M., and Piccolo, S. (2017). Mechanobiology of YAP and TAZ in physiology and disease. *Nat. Rev. Mol. Cell Biol.* 18 (12), 758–770. doi:10.1038/nrm.2017.87

Pardo-Saganta, A., Tata, P. R., Law, B. M., Saez, B., Chow, R. D. W., Prabhu, M., et al. (2015). Parent stem cells can serve as niches for their daughter cells. *Nature* 523 (7562), 597–601. doi:10.1038/nature14553

Pasqual, G., Chudnovskiy, A., Tas, J. M. J., Agudelo, M., Schweitzer, L. D., Cui, A., et al. (2018). Monitoring T cell-dendritic cell interactions *in vivo* by intercellular enzymatic labelling. *Nature* 553 (7689), 496–500. doi:10.1038/nature25442

Pathak, M. M., Nourse, J. L., Tran, T., Hwe, J., Arulmoli, J., Le, D. T. T., et al. (2014). Stretch-activated ion channel Piezo1 directs lineage choice in human neural stem cells. *Proc. Natl. Acad. Sci. U. S. A.* 111 (45), 16148–16153. doi:10.1073/pnas.1409802111

Peng, Y., Du, J., Günther, S., Guo, X., Wang, S., Schneider, A., et al. (2022). Mechano-signaling via Piezo1 prevents activation and p53-mediated senescence of muscle stem cells. *Redox Biol.* 52, 102309. doi:10.1016/j.redox.2022.102309

Piekarska, K., Urban-Wójciuk, Z., Kurkowiak, M., Pelikant-Małecka, I., Schumacher, A., Sakowska, J., et al. (2022). Mesenchymal stem cells transfer mitochondria to allogeneic Tregs in an HLA-dependent manner improving their immunosuppressive activity. *Nat. Commun.* 13 (1), 856. doi:10.1038/s41467-022-28338-0

Pinho, S., and Frenette, P. S. (2019). Haematopoietic stem cell activity and interactions with the niche. *Nat. Rev. Mol. Cell Biol.* 20 (5), 303–320. doi:10.1038/s41580-019-0103-9

Pu, W., He, L., Han, X., Tian, X., Li, Y., Zhang, H., et al. (2018). Genetic targeting of organ-specific blood vessels. *Circ. Res.* 123 (1), 86–99. doi:10.1161/CIRCRESAHA.118.312981

Pu, W., Zhang, M., Liu, X., He, L., Li, J., Han, X., et al. (2022). Genetic proliferation tracing reveals a rapid cell cycle withdrawal in preadolescent cardiomyocytes. *Circulation* 145 (5), 410–412. doi:10.1161/CIRCULATIONAHA.121.057019

Qiu, S., Zhao, Z., Wu, M., Xue, Q., Yang, Y., Ouyang, S., et al. (2022). Use of intercellular proximity labeling to quantify and decipher cell-cell interactions directed by diversified molecular pairs. *Sci. Adv.* 8 (51), eadd2337. doi:10.1126/sciadv.add2337

Rao, A., Barkley, D., França, G. S., and Yanai, I. (2021). Exploring tissue architecture using spatial transcriptomics. *Nature* 596 (7871), 211–220. doi:10.1038/s41586-021-03634-9

Ratnayake, D., Nguyen, P. D., Rossello, F. J., Wimmer, V. C., Tan, J. L., Galvis, L. A., et al. (2021). Macrophages provide a transient muscle stem cell niche via NAMPT secretion. *Nature* 591 (7849), 281–287. doi:10.1038/s41586-021-03199-7

Ren, X., Zhong, G., Zhang, Q., Zhang, L., Sun, Y., and Zhang, Z. (2020). Reconstruction of cell spatial organization from single-cell RNA sequencing data based on ligand-receptor mediated self-assembly. *Cell Res.* 30 (9), 763–778. doi:10.1038/s41422-020-0353-2

Rho, S. S., Kobayashi, I., Oguri-Nakamura, E., Ando, K., Fujiwara, M., Kamimura, N., et al. (2019). Rap1b promotes notch-signal-mediated hematopoietic stem cell development by enhancing integrin-mediated cell adhesion. *Dev. Cell* 49 (5), 681–696. doi:10.1016/j.devcel.2019.03.023

Roybal, K. T., Williams, J. Z., Morsut, L., Rupp, L. J., Kolinko, I., Choe, J. H., et al. (2016). Engineering T cells with customized therapeutic response programs using synthetic notch receptors. *Cell* 167 (2), 419–432. doi:10.1016/j.cell.2016.09.011

Salwig, I., Spitznagel, B., Vazquez-Armendariz, A. I., Khalooghi, K., Guenther, S., Herold, S., et al. (2019). Bronchioalveolar stem cells are a main source for regeneration of distal lung epithelia *in vivo*. *Embo J.* 38 (12), e102099. doi:10.15252/embj.2019102099

Saviano, A., Henderson, N. C., and Baumert, T. F. (2020). Single-cell genomics and spatial transcriptomics: discovery of novel cell states and cellular interactions in liver physiology and disease biology. *J. Hepatol.* 73 (5), 1219–1230. doi:10.1016/j.jhep.2020.06.004

Shao, X., Li, C., Yang, H., Lu, X., Liao, J., Qian, J., et al. (2022). Knowledge-graph-based cell-cell communication inference for spatially resolved transcriptomic data with SpaTalk. *Nat. Commun.* 13 (1), 4429. doi:10.1038/s41467-022-32111-8

Shu, H. S., Liu, Y. L., Tang, X. T., Zhang, X. S., Zhou, B., Zou, W., et al. (2021). Tracing the skeletal progenitor transition during postnatal bone formation. *Cell Stem Cell* 28 (12), 2122–2136.e3. doi:10.1016/j.stem.2021.08.010

Silver, J. S., Günay, K. A., Cutler, A. A., Vogler, T. O., Brown, T. E., Pawlikowski, B. T., et al. (2021). Injury-mediated stiffening persistently activates muscle stem cells through YAP and TAZ mechanotransduction. *Sci. Adv.* 7 (11), eabe4501. doi:10.1126/sciadv.abe4501

Sporn, M. B., and Roberts, A. B. (1985). Autocrine growth factors and cancer. *Nature* 313 (6005), 745–747. doi:10.1038/313745a0

Ståhl, P. L., Salmén, F., Vickovic, S., Lundmark, A., Navarro, J. F., Magnusson, J., et al. (2016). Visualization and analysis of gene expression in tissue sections by spatial transcriptomics. *Science* 353 (6294), 78–82. doi:10.1126/science.aaf2403

Stone, A. P., Nascimento, T. F., and Barrachina, M. N. (2022). The bone marrow niche from the inside out: how megakaryocytes are shaped by and shape hematopoiesis. *Blood* 139 (4), 483–491. doi:10.1182/blood.2021012827

Struhl, G., and Adachi, A. (1998). Nuclear access and action of notch *in vivo*. *Cell* 93 (4), 649–660. doi:10.1016/s0092-8674(00)81193-9

Sun, D., Liu, Z., Li, T., Wu, Q., and Wang, C. (2022). STRIDE: accurately decomposing and integrating spatial transcriptomics using single-cell RNA sequencing. *Nucleic Acids Res.* 50 (7), e42. doi:10.1093/nar/gkac150

Takahashi, A., Nagata, M., Gupta, A., Matsushita, Y., Yamaguchi, T., Mizuhashi, K., et al. (2019). Autocrine regulation of mesenchymal progenitor cell fates orchestrates tooth eruption. *Proc. Natl. Acad. Sci. U. S. A.* 116 (2), 575–580. doi:10.1073/pnas.1810200115

Tan, P., He, L., Huang, Y., and Zhou, Y. (2022). Optophysiology: illuminating cell physiology with optogenetics. *Physiol. Rev.* 102 (3), 1263–1325. doi:10.1152/physrev.00021.2021

Tang, Z., Zhang, T., Yang, B., Su, J., and Song, Q. (2023). spaCI: deciphering spatial cellular communications through adaptive graph model. *Brief. Bioinform* 24 (1), bbac563. doi:10.1093/bib/bbac563

Taslimi, A., Zoltowski, B., Miranda, J. G., Pathak, G. P., Hughes, R. M., and Tucker, C. L. (2016). Optimized second-generation CRY2-CIB dimerizers and photoactivatable Cre recombinase. *Nat. Chem. Biol.* 12 (6), 425–430. doi:10.1038/nchembio.2063

Tian, L., Chen, F., and Macosko, E. Z. (2022). The expanding vistas of spatial transcriptomics. *Nat. Biotechnol.* 41, 773–782. doi:10.1038/s41587-022-01448-2

Toda, S., Blauch, L. R., Tang, S. K. Y., Morsut, L., and Lim, W. A. (2018). Programming self-organizing multicellular structures with synthetic cell-cell signaling. *Science* 361 (6398), 156–162. doi:10.1126/science.aat0271

Totaro, A., Panciera, T., and Piccolo, S. (2018). YAP/TAZ upstream signals and downstream responses. *Nat. Cell Biol.* 20 (8), 888–899. doi:10.1038/s41556-018-0142-z

Travaglini, K. J., Nabhan, A. N., Penland, L., Sinha, R., Gillich, A., Sit, R. V., et al. (2020). A molecular cell atlas of the human lung from single-cell RNA sequencing. *Nature* 587 (7835), 619–625. doi:10.1038/s41586-020-2922-4

Uroz, M., Wistorf, S., Serra-Picamal, X., Conte, V., Sales-Pardo, M., Roca-Cusachs, P., et al. (2018). Regulation of cell cycle progression by cell-cell and cell-matrix forces. *Nat. Cell Biol.* 20 (6), 646–654. doi:10.1038/s41556-018-0107-2

Valet, M., Siggia, E. D., and Brivanlou, A. H. (2022). Mechanical regulation of early vertebrate embryogenesis. *Nat. Rev. Mol. Cell Biol.* 23 (3), 169–184. doi:10.1038/s41580-021-00424-z

van Berlo, J. H., Kanisicak, O., Maillet, M., Vagnozzi, R. J., Karch, J., Lin, S. C. J., et al. (2014). c-kit+ cells minimally contribute cardiomyocytes to the heart. *Nature* 509 (7500), 337–341. doi:10.1038/nature13309

Vento-Tormo, R., Efremova, M., Botting, R. A., Turco, M. Y., Vento-Tormo, M., Meyer, K. B., et al. (2018). Single-cell reconstruction of the early maternal-fetal interface in humans. *Nature* 563 (7731), 347–353. doi:10.1038/s41586-018-0698-6

Vining, K. H., and Mooney, D. J. (2017). Mechanical forces direct stem cell behaviour in development and regeneration. *Nat. Rev. Mol. Cell Biol.* 18 (12), 728–742. doi:10.1038/nrm.2017.108

Wang, J., and Kubes, P. (2016). A reservoir of mature cavity macrophages that can rapidly invade visceral organs to affect tissue repair. *Cell* 165 (3), 668–678. doi:10.1016/j.cell.2016.03.009

Wang, S., Drummond, M. L., Guerrero-Juarez, C. F., Tarapore, E., MacLean, A. L., Stabell, A. R., et al. (2020). Single cell transcriptomics of human epidermis identifies basal stem cell transition states. *Nat. Commun.* 11 (1), 4239. doi:10.1038/s41467-020-18075-7

Wang, S., Englund, E., Kjellman, P., Li, Z., Ahnlide, J. K., Rodriguez-Cupello, C., et al. (2021b). CCM3 is a gatekeeper in focal adhesions regulating mechanotransduction and YAP/TAZ signalling. *Nat. Cell Biol.* 23 (7), 758–770. doi:10.1038/s41556-021-00702-0

Wang, S., Karikomi, M., MacLean, A. L., and Nie, Q. (2019). Cell lineage and communication network inference via optimization for single-cell transcriptomics. *Nucleic Acids Res.* 47 (11), e66. doi:10.1093/nar/gkz204

Wang, Y., Wang, J. Y., Schnieke, A., and Fischer, K. (2021a). Advances in single-cell sequencing: insights from organ transplantation. *Mil. Med. Res.* 8 (1), 45. doi:10.1186/s40779-021-00336-1

Weng, Y., Wang, H., Wu, D., Xu, S., Chen, X., Huang, J., et al. (2022). A novel lineage of osteoprogenitor cells with dual epithelial and mesenchymal properties govern maxillofacial bone homeostasis and regeneration after MSFL. *Cell Res.* 32 (9), 814–830. doi:10.1038/s41422-022-00687-x

Wheeler, M. A., Clark, I. C., Lee, H. G., Li, Z., Linnerbauer, M., Rone, J. M., et al. (2023). Droplet-based forward genetic screening of astrocyte-microglia cross-talk. *Science* 379 (6636), 1023–1030. doi:10.1126/science.abq4822

Wolf, F. A., Hamey, F. K., Plass, M., Solana, J., Dahlin, J. S., Göttgens, B., et al. (2019). PAGA: graph abstraction reconciles clustering with trajectory inference through a topology preserving map of single cells. *Genome Biol.* 20 (1), 59. doi:10.1186/s13059-019-1663-x

Wu, Y., Zhou, L., Liu, H., Duan, R., Zhou, H., Zhang, F., et al. (2021). LRP6 downregulation promotes cardiomyocyte proliferation and heart regeneration. *Cell Res.* 31 (4), 450–462. doi:10.1038/s41422-020-00411-7

Xin, T., Greco, V., and Myung, P. (2016). Hardwiring stem cell communication through tissue structure. *Cell* 164 (6), 1212–1225. doi:10.1016/j.cell.2016.02.041

Yao, S., Yuan, P., Ouellette, B., Zhou, T., Mortrud, M., Balaram, P., et al. (2020). RecV recombinase system for *in vivo* targeted optogenomic modifications of single cells or cell populations. *Nat. Methods* 17 (4), 422–429. doi:10.1038/s41592-020-0774-3

Yeh, H. W., Hsu, E. C., Lee, S. S., Lang, Y. D., Lin, Y. C., Chang, C. Y., et al. (2018). PSPC1 mediates TGF-β1 autocrine signalling and Smad2/3 target switching to promote EMT, stemness and metastasis. *Nat. Cell Biol.* 20 (4), 479–491. doi:10.1038/s41556-018-0062-y

Yu, B., Shi, Q., Belk, J. A., Yost, K. E., Parker, K. R., et al. (2022a). Engineered cell entry links receptor biology with single-cell genomics. *Cell* 185 (26), 4904–4920.e22. doi:10.1016/j.cell.2022.11.016

Yu, T., Zhang, L., Dou, X., Bai, R., Wang, H., Deng, J., et al. (2022b). Mechanically robust hydrogels facilitating bone regeneration through epigenetic modulation. *Adv. Sci. (Weinh)* 9 (32), e2203734. doi:10.1002/advs.202203734

Yu, W., Chen, C., Kou, X., Sui, B., Yu, T., Liu, D., et al. (2021). Mechanical force-driven TNFα endocytosis governs stem cell homeostasis. *Bone Res.* 8 (1), 44. doi:10.1038/s41413-020-00117-x

Yue, S., Xu, P., Cao, Z., and Zhuang, M. (2022). PUP-IT2 as an alternative strategy for PUP-IT proximity labeling. *Front. Mol. Biosci.* 9, 1007720. doi:10.3389/fmolb.2022.1007720

Zhang, Y., Liu, T., Hu, X., Wang, M., Wang, J., Zou, B., et al. (2021b). CellCall: integrating paired ligand-receptor and transcription factor activities for cell-cell communication. *Nucleic Acids Res.* 49 (15), 8520–8534. doi:10.1093/nar/gkab638

Zacharias, W. J., Frank, D. B., Zepp, J. A., Morley, M. P., Alkhaleel, F. A., Kong, J., et al. (2018). Regeneration of the lung alveolus by an evolutionarily conserved epithelial progenitor. *Nature* 555 (7695), 251–255. doi:10.1038/nature25786

Zanconato, F., Cordenonsi, M., and Piccolo, S. (2019). YAP and TAZ: a signalling hub of the tumour microenvironment. *Nat. Rev. Cancer* 19 (8), 454–464. doi:10.1038/s41568-019-0168-y

Zanconato, F., Cordenonsi, M., and Piccolo, S. (2016). YAP/TAZ at the roots of cancer. *Cancer Cell* 29 (6), 783–803. doi:10.1016/j.ccell.2016.05.005

Zhang, S., Zhao, H., Liu, Z., Liu, K., Zhu, H., Pu, W., et al. (2022a). Monitoring of cell-cell communication and contact history in mammals. *Science* 378 (6623), eabo5503. doi:10.1126/science.abo5503

Zhang, Z., Denans, N., Liu, Y., Zhulyn, O., Rosenblatt, H. D., Wernig, M., et al. (2021a). Optogenetic manipulation of cellular communication using engineered myosin motors. *Nat. Cell Biol.* 23 (2), 198–208. doi:10.1038/s41556-020-00625-2

Zhang, Z., Sha, B., Zhao, L., Zhang, H., Feng, J., Zhang, C., et al. (2022b). Programmable integrin and N-cadherin adhesive interactions modulate mechanosensing of mesenchymal stem cells by cofilin phosphorylation. *Nat. Commun.* 13 (1), 6854. doi:10.1038/s41467-022-34424-0

Zhao, H., Huang, X., Liu, Z., Pu, W., Lv, Z., He, L., et al. (2021). Pre-existing beta cells but not progenitors contribute to new beta cells in the adult pancreas. *Nat. Metab.* 3 (3), 352–365. doi:10.1038/s42255-021-00364-0

Zhou, C., Zhang, D., Du, W., Zou, J., Li, X., and Xie, J. (2020). Substrate mechanics dictate cell-cell communication by gap junctions in stem cells from human apical papilla. *Acta Biomater.* 107, 178–193. doi:10.1016/j.actbio.2020.02.032

Zhou, F., Li, X., Wang, W., Zhu, P., Zhou, J., He, W., et al. (2016). Tracing haematopoietic stem cell formation at single-cell resolution. *Nature* 533 (7604), 487–492. doi:10.1038/nature17997

Zhou, Y., Bond, A. M., Shade, J. E., Zhu, Y., Davis, C. H. O., Wang, X., et al. (2018). Autocrine Mfge8 signaling prevents developmental exhaustion of the adult neural stem cell pool. *Cell Stem Cell* 23 (3), 444–452. doi:10.1016/j.stem.2018.08.005

Zhu, C., Lian, Y., Wang, C., Wu, P., Li, X., Gao, Y., et al. (2021). Single-cell transcriptomics dissects hematopoietic cell destruction and T-cell engagement in aplastic anemia. *Blood* 138 (1), 23–33. doi:10.1182/blood.2020008966

Zhu, I., Liu, R., Garcia, J. M., Hyrenius-Wittsten, A., Piraner, D. I., Alavi, J., et al. (2022). Modular design of synthetic receptors for programmed gene regulation in cell therapies. *Cell* 185 (8), 1431–1443.e16. doi:10.1016/j.cell.2022.03.023

Zhu, J., Shang, L., and Zhou, X. (2023). SRTsim: spatial pattern preserving simulations for spatially resolved transcriptomics. *Genome Biol.* 24 (1), 39. doi:10.1186/s13059-023-02879-z

Zhu, L., Finkelstein, D., Gao, C., Shi, L., Wang, Y., López-Terrada, D., et al. (2016). Multi-organ mapping of cancer risk. *Cell* 166 (5), 1132–1146. doi:10.1016/j.cell.2016.07.045

frontiers | Frontiers in Cell and Developmental Biology

TYPE Original Research
PUBLISHED 22 November 2023
DOI 10.3389/fcell.2023.1145421

OPEN ACCESS

EDITED BY
Tokiko Nagamura-Inoue,
The University of Tokyo, Japan

REVIEWED BY
Takeo Mukai,
The University of Tokyo, Japan
Dean Philip John Kavanagh,
University of Birmingham,
United Kingdom
Tingting Sun,
Zaozhuang University, China

*CORRESPONDENCE
Marxa L. Figueiredo,
mlfiguei@purdue.edu

RECEIVED 01 September 2023
ACCEPTED 02 November 2023
PUBLISHED 22 November 2023

CITATION
Rivera-Cruz CM, Kumar S and Figueiredo ML (2023), Poly I:C-priming of adipose-derived mesenchymal stromal cells promotes a pro-tumorigenic phenotype in an immunocompetent mouse model of prostate cancer. *Front. Cell Dev. Biol.* 11:1145421. doi: 10.3389/fcell.2023.1145421

Poly I:C-priming of adipose-derived mesenchymal stromal cells promotes a pro-tumorigenic phenotype in an immunocompetent mouse model of prostate cancer

Cosette M. Rivera-Cruz, Shreya Kumar and Marxa L. Figueiredo*

Department of Basic Medical Sciences, Purdue University, West Lafayette, IN, United States

Introduction: Mesenchymal stromal cells (MSC) are envisioned as a potential cellular vehicle for targeted cancer therapies due to their tumor tropism and immune permissiveness. An obstacle in their use is the duality in their interactions within tumors, rendering them pro-tumorigenic or anti-tumorigenic, in a context dependent manner. MSC preconditioning, or priming, has been proposed as a strategy for directing the effector properties of MSC at tumor sites.

Methods: We primed human MSC derived from adipose tissues (ASC), a clinically advantageous MSC source, utilizing toll-like receptor agonists. Subsequently, we explored the consequences in tumor progression and transcriptome upon the interaction of tumor cells with primed or unprimed ASC in an *in vivo* model of prostate cancer, the second most common cancer and second leading cause of cancer related death in men in the USA.

Results and discussion: In the studied model, poly I:C-primed ASC were found to significantly accelerate tumor growth progression. And while unprimed and LPS-primed ASC did not exert a significant effect on tumor growth at the macroscopic level, gene expression analyses suggested that all treatments promoted distinct modulatory effects in the tumor microenvironment, including altered modulation of angiogenesis, and immune response processes. However, the effects resulting from the collective interaction across these processes must be sufficiently skewed in a pro-tumorigenic or anti-tumorigenic direction for evidence of tumor progression modulation to be detectable at the macroscopic level. Our study highlights potential MSC-tumor microenvironment interactions that may be leveraged and should be considered in the development of cancer therapeutics utilizing MSC.

KEYWORDS

mesenchymal stromal cells, adipose-derived mesenchymal stromal cells, priming, polarization, toll-like receptors, prostate cancer

1 Introduction

Prostate cancer (PrCa) is the most common cancer and second leading cause of cancer related death in men in the United States of America (USA), expected to have accounted for 29% of new cancer cases and 11% of cancer deaths in men in the USA in 2023 (Siegel et al., 2023). Similarly to other cancers, despite many advances in treatments, a significant challenge to efficiently treat this disease is encountered once PrCa presents at an advanced stage, i.e., invasive adenocarcinoma, where the disease has started to spread outside of the prostate. For these cases, the traditional treatment course initially includes androgen deprivation therapy (ADT). Unfortunately, ADT can result in the selection of tumor cell clones that are no longer dependent on normal levels of androgens and can continue growing despite ADT. This transition is estimated to occur in 10%–20% of patients within approximately 5 years of follow-up (Kirby et al., 2011). PrCa that has progressed to this stage is termed castration resistant prostate cancer (CRPC), and the mean survival for patients with this stage of disease is 14 months. Challenges to therapeutic modalities outside of ADT often involve targeting inefficiency and limited dose tolerance due to toxicity, thus further exploration and development of therapeutics is needed, with an interest in the field on multimodal therapeutics and development of new targeting strategies for more efficient and less toxic therapeutic delivery (Chang et al., 2014; Terlizzi and Bossi, 2022).

Mesenchymal stromal cells (MSC) have been proposed as a potential cellular vehicles for targeted cancer therapies (Nowakowski et al., 2016). This is owing to an inherent tropism for the cells towards tumors and for their immune permissive phenotype, characteristics that are considered promising for enhancing therapeutic delivery while avoiding potential side effects. Also, rapid clearance can be avoided relative to other therapeutics such as triggered by chemotherapies and oncolytic viruses (e.g. an immune response) when administered systemically in the absence of a carrier. Further, MSC can interact with the tumor microenvironment (TME) by means of immunomodulation, modulation of metabolic processes, angiogenesis and extracellular matrix (ECM) deposition, thus having the potential of acting as effector cells beyond their roles as treatment delivery platforms. However, a duality in the interaction of MSC with tumors might render them pro-tumorigenic or anti-tumorigenic, in a context dependent manner (Norozi et al., 2016). These observations thus have raised interest in the development of strategies to enhance and/or consistently 'guide' MSC towards an anti-tumorigenic potential (Vicinanza et al., 2022). In 2010, a paradigm to MSC activation was proposed by which priming of BM-MSC with ligands of TLR4 or TLR3 yielded opposite cellular functional phenotypes (Waterman et al., 2010). More specifically, TLR4 stimulation by lipopolyssacharide (LPS) yielded a pro-inflammatory MSC phenotype, whereas TLR3 priming with polyinosinic:polycytidylic acid (polyI:C) rendered these cells immunosuppressive. These distinct phenotypes were evaluated in the context of an ovarian cancer *in vivo* model and the different TLR agonists were reported to exert anti-tumorigenic (LPS-primed) or pro-tumorigenic (poly I:C-primed) roles, respectively (Waterman et al., 2012).

While BM-MSC remain the most commonly studied MSC subtype, and were the focus of the MSC polarization paradigm reports, MSC derived from other tissues may provide advantages for clinical use such as higher relative abundance and differential functional potential (Strioga et al., 2012). In our previous work (Rivera-Cruz and Figueiredo, 2023), we had identified phenotypical and functional consequences of TLR priming on ASC that partially resembled those previously reported for BM-MSC (Waterman et al., 2010). In our assessment, LPS-priming of ASC rendered them immunostimulatory in immune killing assay coculture assays in the presence of human prostate adenocarcinoma cells and stimulated peripheral blood mononuclear cells. Understanding that tumorigenesis is a complex process involving many other TME components and other supportive tissues, we aimed to evaluate the consequences of TLR-priming in an immunocompetent model of androgen independent prostate cancer by assessing changes in tumor progression, gene expression and immune composition of tumors treated with TLR-primed ASC.

2 Materials and methods

2.1 Cell culture

Human ASC from a male Caucasian donor were obtained from Obatala. Cells were obtained from the vendor after characterization (e.g., surface marker expression profile, differentiation potential) and de-identification (Supplementary File S1). ASC were cultured on fibronectin-coated plasticware in modified media (ASC media) (Shearer et al., 2016). At passage 4, cells were transduced with a lentivirus to express renilla luciferase (LV-Rluc-Puro; G&P Bioscience, Santa Clara, CA) at MOI 2, using a ViraDuctin Lentivirus Transduction Kit (Cell BioLabs, San Diego, CA). Selection for transduced cells was performed for 2 weeks by supplementing growth media with 1 μg/mL of puromycin (Sigma-Aldrich). Mouse TRAMP-C2 (TC2) cells are advanced prostate adenocarcinoma cells (ATCC, CRL-2731), derived from a primary tumor in the prostate of Probasin-SV40-T antigen (TRAMP) adult C57/BL6 male mouse (Foster et al., 1997). Our group has further transduced TC2 with a lentivirus to express activated H-ras G12V and mouse androgen receptor (TC2R) (Zolochevska et al., 2013), observing significantly more rapid growth of these cells relative to the parental TC2 (Umbaugh et al., 2017). The TC2R cells serve as a model of aggressive PrCa to be examined in C57/BL6 immunocompetent mice. These cells were maintained in DMEM-F12 supplemented with 10% FBS and 1% Antibiotic-Antimycotic (Anti-Anti, Gibco).

2.2 ASC TLR priming

ASC were thawed and expanded as described above. After expansion, cells were seeded in 6-well tissue culture plates (not coated with fibronectin) at a density of 3 x 10^5 cells/well and allowed to attach overnight in ASC media. ASC were primed *ex vivo* for 1 h in assay media containing DMEM-F12 (Corning) supplemented with 16.5% FBS (ATCC), 1% Anti-Anti. Unprimed MSC, incubated in base assay media, were used as control. TLR agonists were added to the base assay media as follows: Poly I:C 1 μg/mL (1:1 mix of high molecular weight (HMW) and low molecular weight (LMW) poly I:C, Invivogen, San Diego, CA), or LPS 10 ng/mL (Millipore-Sigma, Urbana, IL) (Waterman et al., 2010). After the completion of the

hour, cell cultures were washed twice with 1x Dulbecco's Phosphate Buffered Saline (Gibco), lifted by trypsinization and comixed with PrCa cells as described below for administration into the mice.

2.3 *In vivo* assessment of tumor progression

Animal care and procedures were performed in accordance with the Purdue Animal Care and Use Committee Institutional Review Board and the Laboratory Animal Program (LAP). All mice utilized in these experiments were housed in the Purdue LAP Facilities, where overall changes in mice health and behavior were monitored daily by facility technicians and veterinary staff. Tumors were induced in 10-week-old C57BL/6J male mice (Envigo) by subcutaneous injection of 1.25 x 10^5 TC2R cells +1.25 x 10^3 TLR-primed (or unprimed) ASC in sterile saline into their flanks (dorsolateral) while under isoflurane anesthesia. Mice injected only with TC2R cells were utilized as controls. Mice were randomly assigned to groups (n = 11; between two independent experiments), with at least one representative of each group per cage. The tumor growth was monitored over time utilizing vernier caliper measurements, in a blinded fashion. Tumor volume was calculated utilizing the following equation:

$$Tumor\ volume\,(mm^3) = \frac{\pi}{6} \times (\text{larger diameter}\,(\text{mm})) \times (smaller\ diameter\,(mm))^2$$

The experimental endpoint (19–21 days) was selected based on when at least one mouse reached the maximum allowable tumor burden in the study (tumor length of 20 mm).

2.4 Tissue collection

Mice were humanely euthanized by CO_2 in several cohorts (through day 21) when the largest tumors within the experiment reached 20 mm in its their largest diameter. Tumor segments were collected in 10% buffered formalin and RNAlater (ThermoFisher, Mt Prospect, IL) and stored according to manufacturer's protocols for later evaluation.

2.5 RNA isolation

Total RNA was isolated from timepoint-matched (day 20) tumors (n = 3 per treatment group) that had been preserved in 1 mL RNAlater, following manufacturer's protocols, then RNAlater removed and dried tissues kept at −80°C. Briefly, tumors were immersed in 600 µL of RLT buffer +10 µL of β-Mercaptoethanol, and homogenized with a PRO200 homogenizer (MidSci, ValleyPark, MO, United States) in three brief pulses of 10–15 s each at a mid-power. Lysates were then processed using a Qiagen RNAeasy kit (Qiagen).

2.6 RNA-seq analysis

Sample processing for RNA sequencing was performed by LC Sciences (Houston, TX, United States), with analysis support. Briefly, a poly (A) RNA sequencing library was prepared following Illumina's TruSeq-stranded-mRNA protocol. RNA integrity was checked with Agilent Technologies 2100 Bioanalyzer. Poly (A) tail-containing mRNAs were purified using oligo- (dT) magnetic beads with two rounds of purification. After purification, poly (A) RNA was fragmented using divalent cation buffer in elevated temperature. Quality control analysis and quantification of the sequencing library were performed using Agilent Technologies 2100 Bioanalyzer High Sensitivity DNA Chip. Paired-ended sequencing was performed on Illumina's NovaSeq 6000 sequencing system. For transcripts assembly, cutadapt (Martin, 2011) and perl scripts in house were used to remove the reads that contained adaptor contamination, low quality bases and undetermined bases. Sequence quality was verified using FastQC (http://www.bioinformatics.babraham.ac.uk/projects/fastqc/), and HISAT2 (Kim et al., 2015) was used to map reads to the *Mus musculus* genome (ftp://ftp.ensembl.org/pub/release-101/fasta/mus_musculus/dna/). Reads were assembled using StringTie (Pertea et al., 2015), then transcriptomes were merged to reconstruct a comprehensive transcriptome using perl scripts and gffcompare. StringTie and ballgown (http://www.bioconductor.org/packages/release/bioc/html/ballgown.html) were used to estimate transcript expression levels. StringTie and ballgown (http://www.bioconductor.org/packages/release/bioc/html/ballgown.html) were used to estimate levels of expression of all transcripts. StringTie (Pertea et al., 2015) was used to perform expression level for mRNAs by calculating FPKM. Pearson correlation analysis was utilized to determine outliers within treatment groups, with R < 0.9 considered an outlier. mRNAs differential expression analysis was performed by R package DESeq2 (Love et al., 2014) between two different groups (and by R package edgeR (Robinson et al., 2010) between two samples). The mRNAs with the parameter of *p*-value below 0.05 and absolute fold change ≥1.5 were considered differentially expressed mRNAs. Metascape (Zhou et al., 2019) the Express Analysis was utilized to identify by ontology assessment potential cellular processes and pathways associated with the differential gene expression observations. Metascape identifies all statistically enriched terms and calculates accumulative hypergeometric *p*-values and enrichment factors used for filtering. The remaining significant terms are hierarchically clustered into a tree based on Kappa-statistical similarities among their gene memberships and a 0.3 kappa score is applied as the threshold to cast the tree into term clusters.

2.7 Immune cell profiling analysis using RNA-seq data

For a general analysis of the immune landscape, we utilized ImmuCellAI (Immune cell abundance identifier) (Miao et al., 2021) and TIMER2.0 (Li et al., 2020) to obtain estimated immune cell profiles, as well as broad microenvironment, immune, stromal, or infiltration scores. ImmuCell AI estimates the abundance of several immune cell (sub) types utilizing gene expression data and based on reference expression profiles and marker gene sets curated from pure immune cell types, using a ssGSEA enrichment score for the expression deviation profile for each cell type. TIMER2.0 uses the immunedeconv package (Sturm et al., 2019) to estimate immune cell abundance using six algorithms described in Li et al. (2020), also taking tissue-type specific information into account (PRAD,

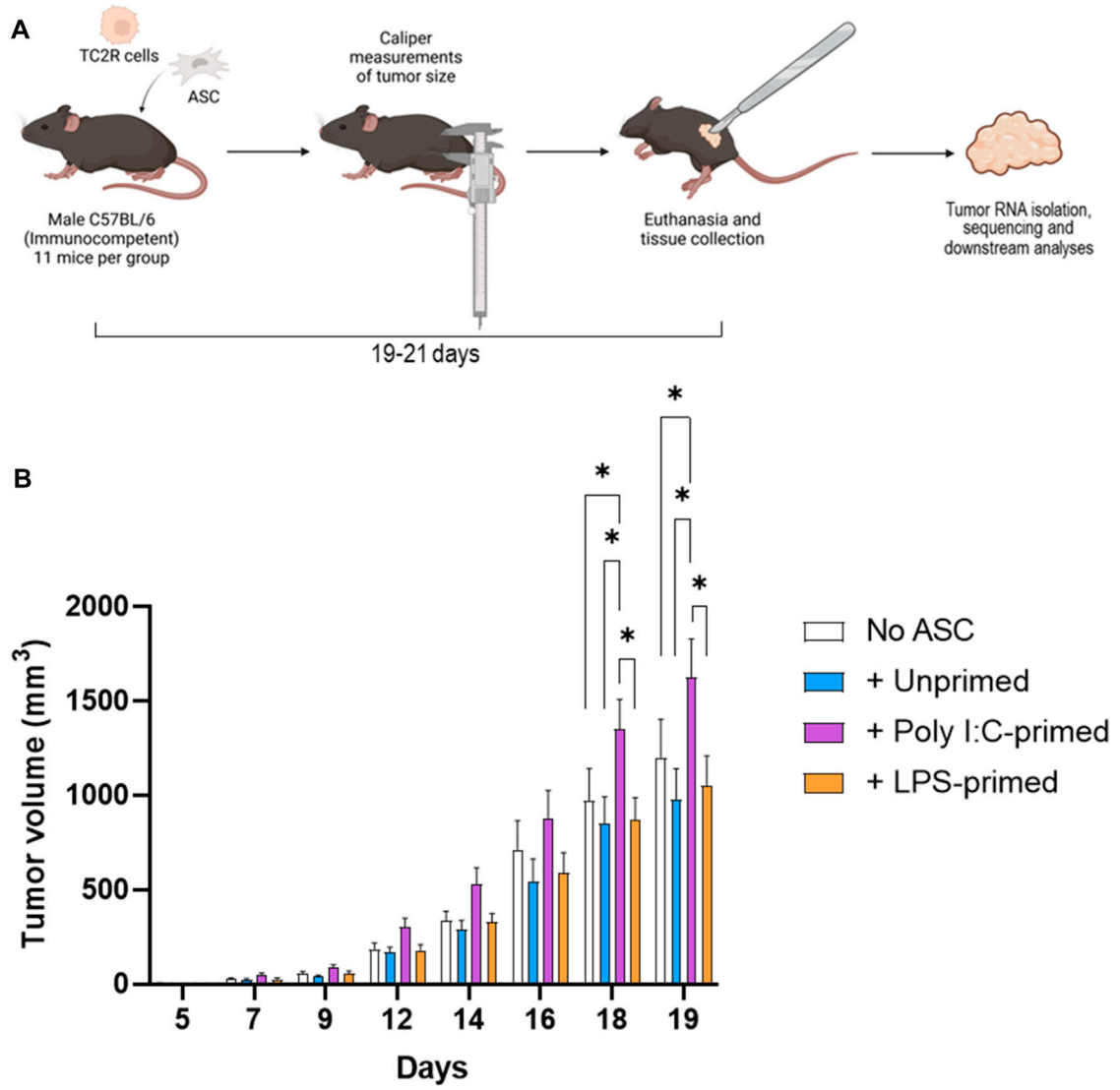

FIGURE 1
Tumor induction and monitoring. **(A)**. Diagram depicting the experimental workflow. Prostate cancer tumors (TC2R) were induced *via* co-injection of TLR-primed ASC and tumor progression was followed *via* caliper measurements over time. At day 19–21, mice were euthanized, and tumors were excised and processed for RNA sequencing as described in the methods section. **(B)**. Tumor volume time course. Data is presented as mean (n = 11, from two independent experiments) ± SEM. Groups included: No ASC (white bars), +Unprimed ASC (blue bars), +PolyI:C-primed ASC (purple bars), and +LPS-primed ASC (orange bars). Analysis was performed by a two-way ANOVA between treatment groups, and a *p*-value of <0.05 was considered significant (*).

prostate adenocarcinoma, for example) in order to improve the estimation accuracy. In combination, these tools provide a detailed immune cell profiling (>100 (sub) cell types), utilizing preprocessing and visualization of all the estimations together from recently characterized algorithms (including EPIC, quanTIseq and TIMER) in the comprehensive platform (Li et al., 2020).

2.8 IPA analysis

Ingenuity Pathways Analysis (IPA) (Qiagen) Core Analysis was utilized to investigate mechanistic networks, upstream regulators, and functions of differentially expressed genes identified by RNA-seq analysis for each treatment group comparison to the untreated (No ASC) control group. The IPA analyses performed included i) Graphical Summary, and ii) Mechanistic Networks. The Graphical Summary integrates significant upstream regulators, diseases, functions, and pathways while reducing redundancy. It includes the most significant Canonical Pathways by *p*-value, regardless of their z-score strength. Upstream regulators include genes, mRNAs, and proteins, with consideration of the differential gene expression magnitude. This summary is based on precomputed relationships between molecules, functions, diseases, and pathways obtained through a machine learning algorithm. The networks are created using a heuristic graph algorithm and content-based machine learning (Krämer et al., 2022). The Mechanistic Networks analysis connects upstream regulators that can work together to elicit the gene expression changes observed in a dataset, with cutoff $p < 0.05$ and activation z-score > 2.0 or < -2.0.

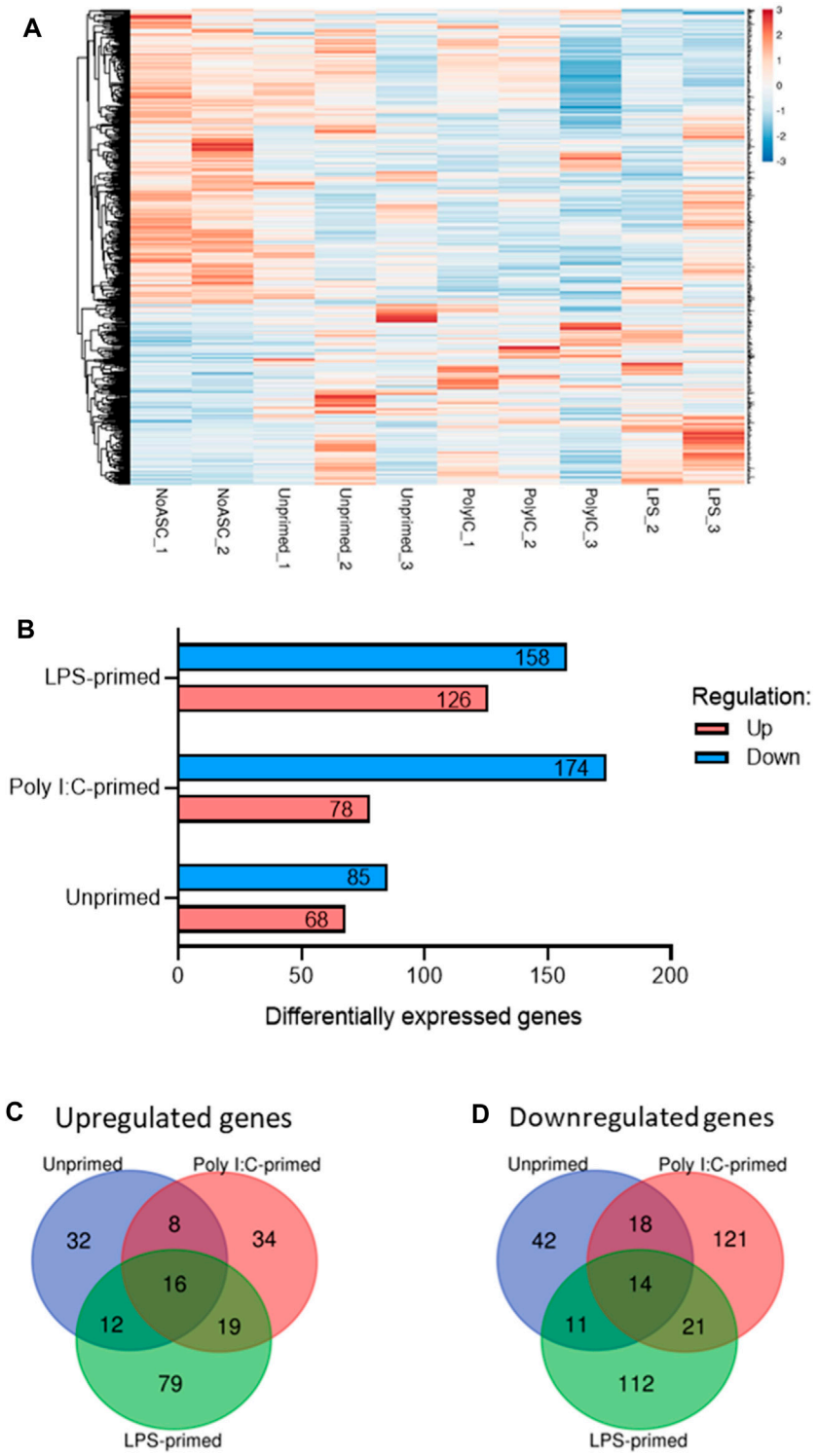

FIGURE 2
Summary of differentially expressed genes identified *via* RNA-seq of tumors. **(A)**. Heatmap of differentially expressed genes in one or more treatment group relative to No ASC controls generated *via* ClustVis (Metsalu and Vilo, 2015). Rows are centered and clustered using Euclidean distance and average linkage. Unit variance scaling was applied to rows from RPKM input values and values were plotted, with red representing higher relative expression and blue representing lower relative expression. **(B)**. Summary of up- (red) and downregulated (blue) genes for each treatment group relative to the untreated control tumors. Summary of overlap in genes upregulated **(C)** and downregulated **(D)** across treatment groups using Venn diagrams generated using the Van de Peer Lab Venn diagram tool (http://bioinformatics.psb.ugent.be/webtools/Venn/). Genes were considered differentially expressed if FC ≥ 1.5 or ≤ −1.5 and *p*-value <0.05 as determined by DESeq2 analysis (Love et al., 2014).

2.9 Statistical analysis

Statistical analysis of RNA-seq data was performed *via* R package DESeq2. For other analyses, GraphPad Prism version 9.3.0 for Windows (GraphPad Software, San Diego, California United States, www.graphpad.com) was used to calculate statistically significant differences among groups, using multiple *t*-test or ANOVA with *p*-value <0.05 considered significant. Statistical test or package used for each dataset is described in the corresponding figure legends.

3 Results

3.1 Poly I:C-primed, but not unprimed nor LPS-primed ASC promote prostate cancer tumor progression

To assess the effects of TLR-priming on ASC-mediated modulation of tumor progression, we evaluated the effect of the presence of these ASC in the prostate tumor growth rates in a murine model. For this purpose, syngeneic TC2R tumors were induced in immunocompetent mice, accompanied by a dose of either *ex vivo* TLR-primed ASC, unprimed ASC, or no ASC. Tumor sizes were monitored *via* caliper measurements for ~3 weeks (Figure 1, Supplementary File S2). For these experiments, mice injected with tumor cells only (no ASC) were selected as a control group. While no significant differences in tumor growth were observed in unprimed ASC and LPS-primed ASC compared to the untreated controls, a significant increase in tumor growth relative to all other experimental groups was observed in mice that received poly I:C-primed ASC (Figure 1). At day 19 after tumor induction, this represented a 35% increase in tumor size in the poly I:C-primed ASC-treated relative to the untreated control (no ASC) group. No sporadic mouse deaths occurred in the duration of the described experiments. At day 19, five mice met our end-point tumor burden criteria (Treatment groups: one No ASC, one + LPS-primed ASC, and three + Poly I:C-primed ASC). These mice were euthanized on day 19 and the remaining mice were euthanized between days 19–21, following euthanasia guidelines based on tumor burden. The tumor growth dynamics observed suggested that administering unprimed or LPS-primed cells at these low ratios (1% ASC relative to starting tumor cell count), although physiologically significant in the context of a prostate tumor (Brennen et al., 2013), were not sufficient to induce a significant pro-tumorigenic nor anti-tumorigenic response in the studied model. On the other hand, poly I:C-primed ASC acted in a pro-tumorigenic manner, significantly worsening disease progression.

3.2 Differential gene expression in the tumors

Having observed significant differences in tumor growth rates across treatment groups, we sought to investigate potential modes of action mediating these effects. For this purpose, RNA-seq analysis was performed in representative timepoint-matched tumor samples (n = 3) as described in section 3.2.6. RNA-seq analysis identified a total of 541 genes differentially expressed (Fold Change (FC) ≥ 1.5 or ≤ −1.5 and *p*-value <0.05) across one or more treatment groups relative to the No ASC control tumors (Figure 2). Changes in expression of 420 (77.6%) of these genes were found to be unique to a single treatment group, whereas 30 genes (5.5%) were found to be regulated in the same direction across all treatment groups relative to the No ASC controls (Figures 2C, D). No genes were regulated with opposite directionality across our treatment groups.

MSC are capable of interacting with tumor cells and components of the TME through various mechanisms, including immunomodulation *via* cytokine secretion and cell-to-cell contact (Rivera-Cruz et al., 2017), ECM deposition (Hass, 2020), and metabolic reprogramming (Pers et al., 2021). To gain some understanding of the consequences of the differential expression of genes observed across our samples in the context of cellular processes and pathways, we performed ontology enrichment analysis *via* Metascape for genes differentially expressed relative to the untreated tumor controls, within each treatment group (Figures 3, 4, Supplementary File S3). As expected, based on the overlap in the differentially expressed genes observed across samples (Figures 2B, C), regulation of some processes was shared across two or more treatment groups. Among these were processes associated with cell migration and chemotaxis, and immunity.

While no significant differences in tumor progression rate were noted in tumors treated with unprimed or LPS-primed ASC relative to the untreated controls (Figure 1), our RNA-seq data suggests that there were several significantly altered processes in these tumors (Figures 3, 4). The presence of unprimed ASC in TC2R tumors was found to upregulate genes associated with enrichment in nervous system processes such as migration and gliogenesis, and immune related processes such as the positive regulation of leukocyte migration (Figure 3A). On the other hand, terms enriched within downregulated genes included Class A/1 (Rhodopsin-like receptors) and processes related to cell secretion, among other neural and immunity related processes (Figure 3B).

The analysis using the genes upregulated in the LPS-primed ASC treated tumors relative to control (no ASC) TC2R tumors produced several enriched terms, with the most significant hits aligning with processes associated with vasculature and cGMP-mediated signaling (Figure 4A). Downregulated genes for this treatment group were primarily enriched in terms related to inflammatory and immune processes (Figure 4B).

Since poly I:C ASC presence in tumors promoted their growth rate, this may suggest that alterations to the TME effected by the administered primed ASC collaborate with the already tumor permissive environment that develops at these tumor sites. The analysis using the genes upregulated in the Poly I:C-primed ASC group relative to control (no ASC) tumors indicated, for the upregulated genes, an enrichment of terms related to ECM-receptor interactions, sprouting angiogenesis and pathways in cancer, among others (Figure 5A). On the other hand, the genes downregulated in this treatment group relative to control were enriched in several immune-related and cell adhesion or ECM-related processes, among others (Figure 5B).

When evaluating ontologies relevant to differential gene expression between TLR-primed and unprimed treated samples (Supplementary File S4), processes involving regulation of cell migration, cytokine production and immunomodulation emerged

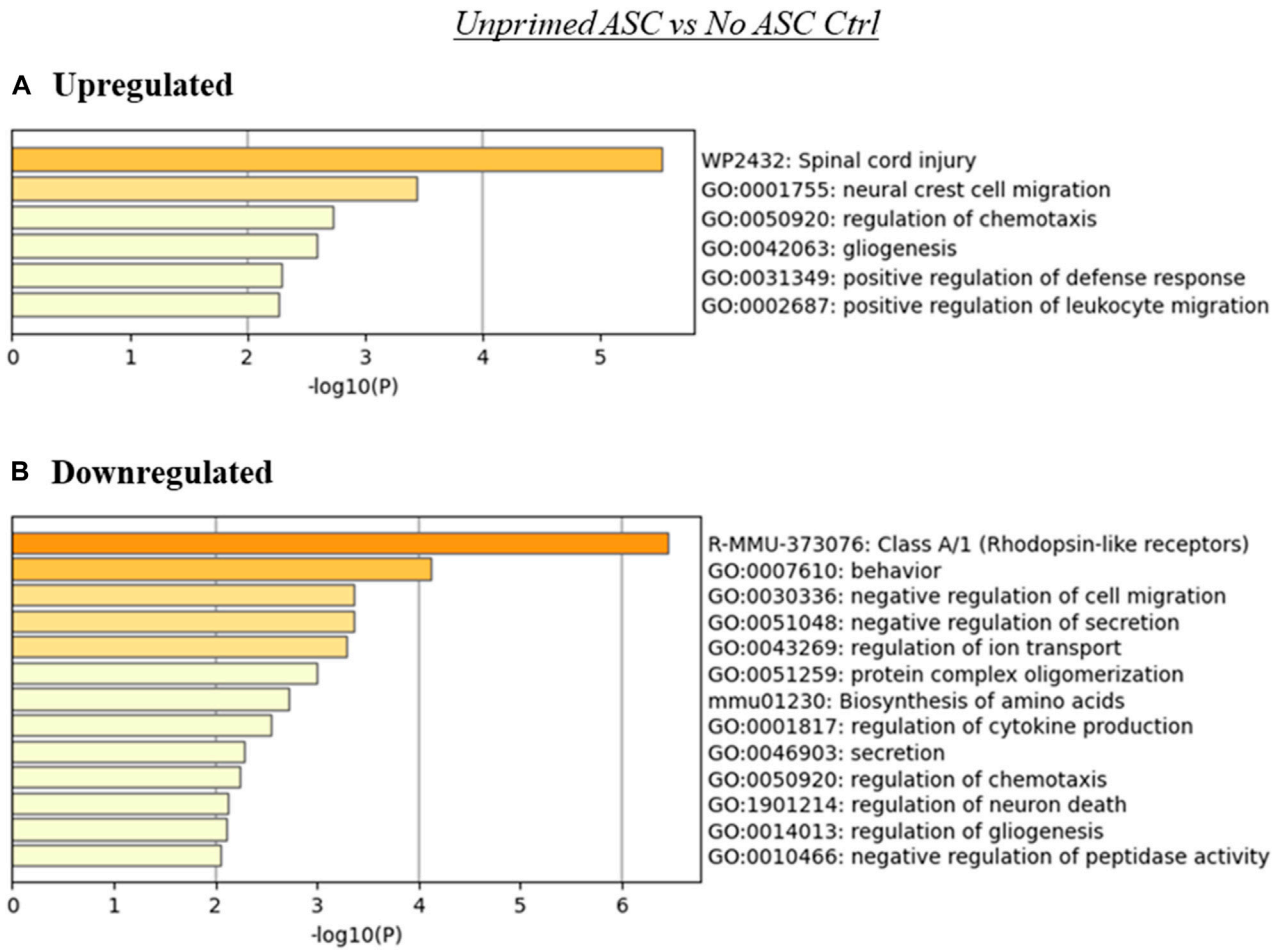

FIGURE 3
Summary of enriched terms identified in unprimed ASC treated tumors relative to untreated controls. Genes differentially expressed in unprimed ASC treated samples relative to untreated tumor controls were evaluated *via* Metascape enrichment analysis. Separate analyses were conducted for genes based on their regulation [**(A)** upregulated, **(B)** downregulated)]. Figures depict statistically significant enriched terms (-log10(p)) in a bar plot format, obtained from hierarchical clustering of processes based on Kappa-statistical similarities among their gene memberships.

as the most significantly enriched. Collectively, these findings suggested that administering ASC in either a primed or unprimed status can significantly modulate processes within tumors relating to the communication between tumor cells with the microenvironment, as well as with the immune system. A common target of this modulation are immune processes, although the nature of these changes may diverge across different groups depending on the ASC priming modality. These modulated processes likely act in conjunction, and the interplay among the many molecular processes influence the overall effects detected at the macroscopic level in altered tumor progression.

3.3 Estimation of altered immune composition in the tumors

Given that several immune processes were shown to be enriched within our treatment groups relative to the untreated tumor controls, and that some of these changes diverged across ASC treatment groups, we sought to evaluate potential differences in immune composition across these groups. For this purpose, we utilized two web-based tools with algorithms that permit the estimation of immune components within samples based on bulk RNA-seq analysis, ImmuCell AI and TIMER2.0.

Through these analyses, we identified significant changes in several cell populations relevant to immune response in tumors (Figure 6). Namely, tumors treated with unprimed ASC showed significantly lower cancer associated fibroblasts and stromal scores relative to control (no ASC) tumors. Poly I:C-primed ASC treated tumors displayed a significant increase in B1 cells, NK cells and Tregs, whereas neutrophils, macrophages, T helper cells, cancer associated fibroblasts, resting mast cells, and stroma score values were decreased in these tumors relative to controls (no ASC). In the case of the LPS-primed ASC treated group, significantly higher abundance scores were obtained for NK, endothelial, and lymphoid cells, yet pDC, macrophage, and immune scores were lower relative to the control tumors (no ASC). Together this data suggested that administration of ASC into tumors even at low percentages (1% of initial tumor cell count) can significantly alter the tumor immune composition, regardless of their priming status. These immune changes by unprimed or LPS-primed ASC, however, were

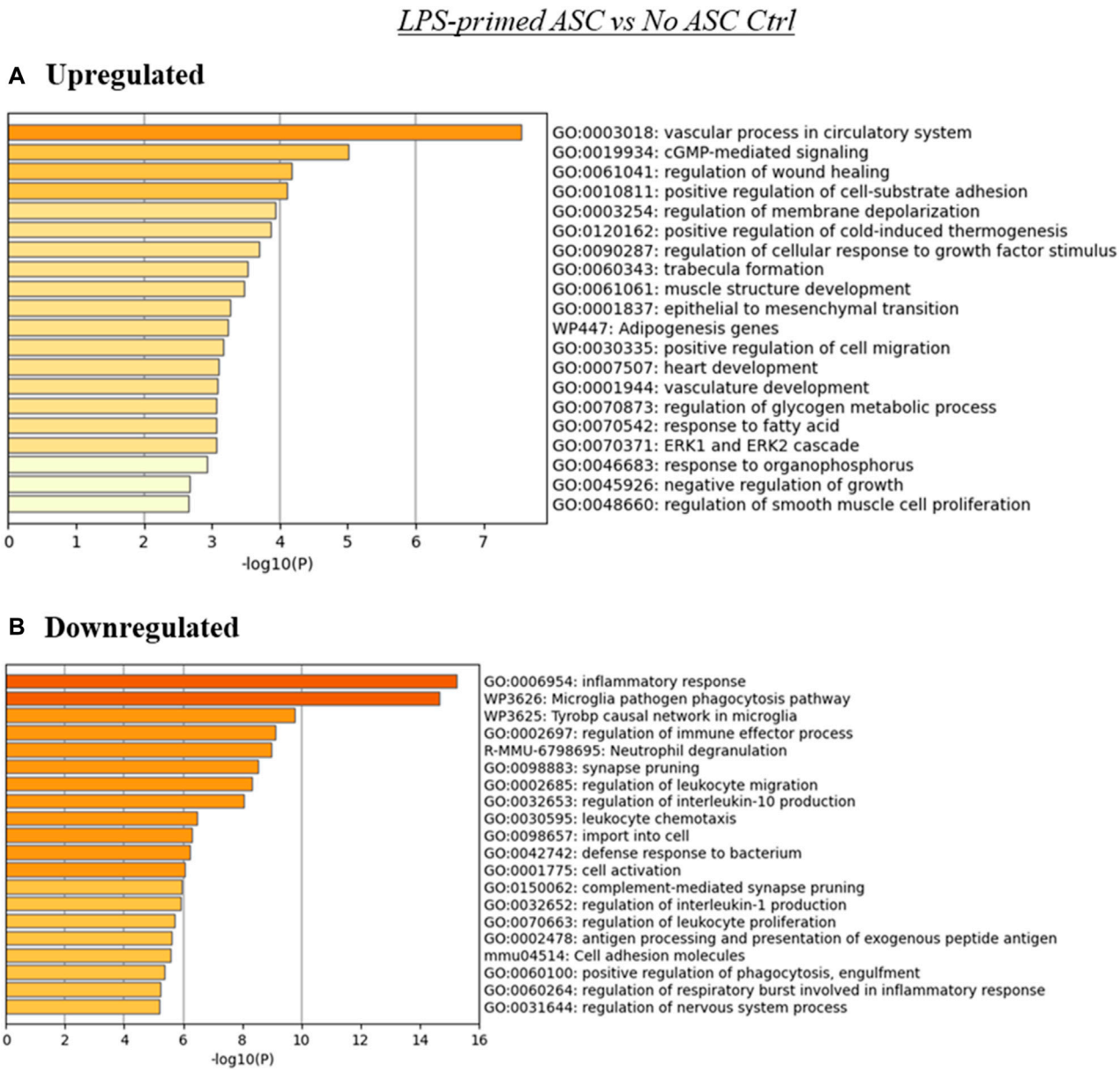

FIGURE 4
Summary of enriched terms identified in LPS-primed ASC treated tumors relative to untreated controls. Genes differentially expressed in LPS-primed ASC treated samples relative to untreated tumor controls were evaluated *via* Metascape enrichment analysis. Separate analyses were conducted for genes based on their regulation [**(A)** upregulated, **(B)** downregulated)]. Figures depict statistically significant enriched terms (-log10(p)) in a bar plot format, obtained from hierarchical clustering of processes based on Kappa-statistical similarities among their gene memberships.

insufficient to tilt the TME to either a pro-tumorigenic or an anti-tumorigenic phenotype. In the case of poly I:C-primed ASC treated tumors, it is likely that the differences in tumor immune composition may have contributed to the increased tumor growth rate observed.

3.4 Regulatory networks by Ingenuity pathway analysis (IPA)

A set of additional analyses was performed using IPA to obtain some insight into the potential mechanisms underlying the observed differences in tumor growth rate by the differently primed ASC populations relative to the no ASC control. The graphical summary analysis provided an overview of the major biological themes emerging from the most significant entities detected in the datasets to help illustrate how these themes connected to each other. For the LPS-primed group, several processes and molecules were predicted as inhibited, in particular, upstream regulators CD40LG (CD40 ligand), colony stimulating factor (CSF)1, Hbb (hemoglobin subunit beta)-b1/b2, and interleukin (IL)-27, with connecting effects of reduced response from phagocytes and other myeloid cells. Interestingly, NOTCH (notch receptor) related molecules were

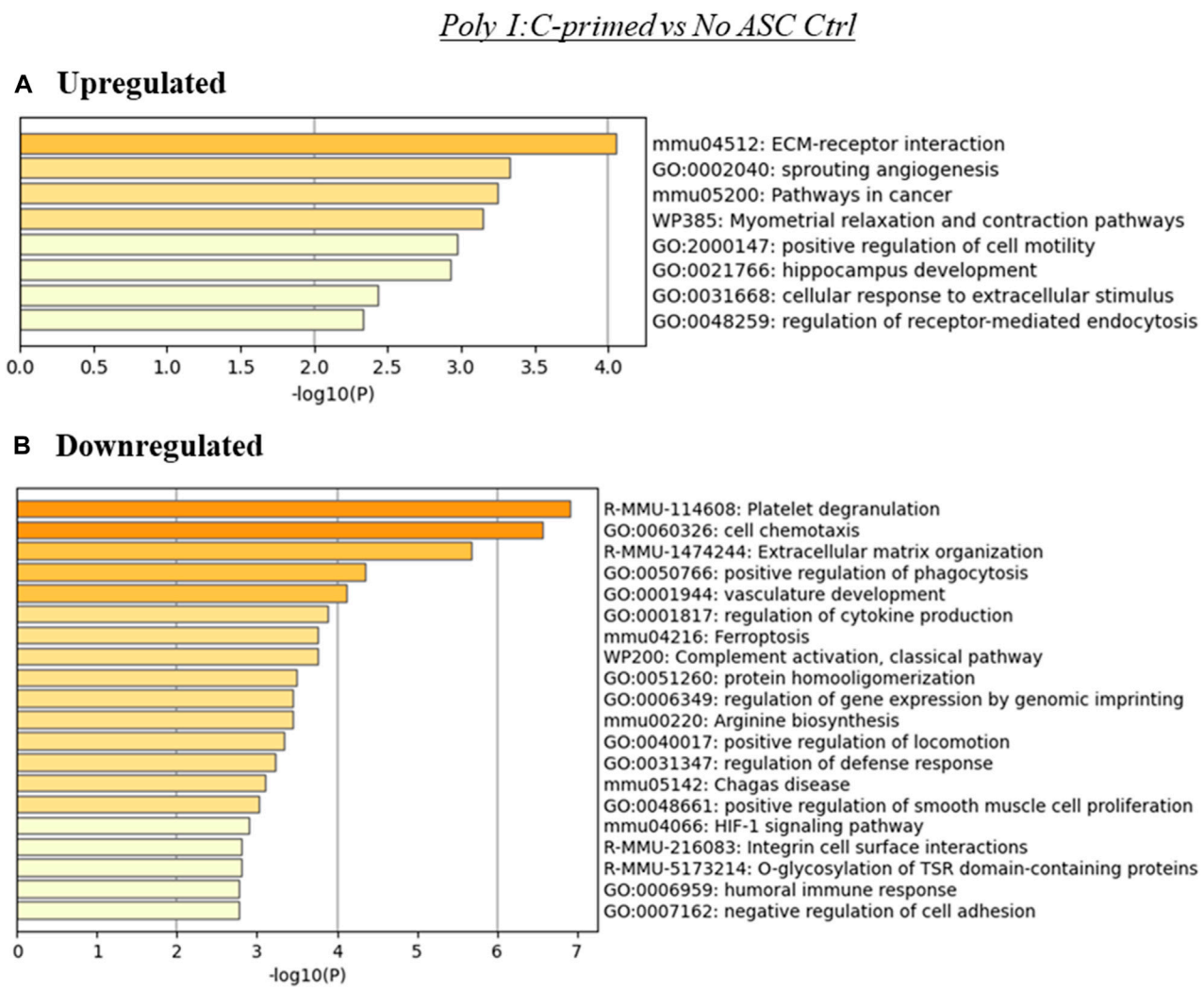

FIGURE 5
Summary of enriched terms identified in poly I:C-primed ASC treated tumors relative to untreated controls. Genes differentially expressed in poly I:C-primed ASC treated samples relative to untreated tumor controls were evaluated *via* Metascape enrichment analysis. Separate analyses were conducted for genes based on their regulation [**(A)** upregulated, **(B)** downregulated). Figures depict statistically significant enriched terms (-log10(p)) in a bar plot format, obtained from hierarchical clustering of processes based on Kappa-statistical similarities among their gene memberships.

predicted as activated regulators, connecting at least to the engulfment of myeloid cells function (Figure 7A). The poly I:C-primed ASC group showed a strong influence of inhibition of IL-1B (and IL-1A), epidermal growth factor (EGF), IL-17A, CSF2, IL-6, and TLR3, connecting to predicted reductions in the immune response of phagocytes and leucocytes, and APC binding. The activated regulators included MEF2C (myocyte enhancer factor 2C), through BHLHE40 (basic helix-loop-helix family member E40) inhibition and from MYOCD (myocylin) activation, and also activation of SRF (serum response factor) and HAND2 (heart and neural crest derivatives expressed 2) (Figure 7B).

Finally, the unprimed ASC population did not have enough connectable entities with sufficiently high or low z-scores to meet the cutoffs. Yet, the unprimed ASC treated tumors had VCAN (Versican) as an activated upstream regulator with a z-score of 1.4 and an inhibited regulator JUN protooncogene with a z-score of −1.5, both with significant values for the multiple testing corrected *p*-value (B-H or Benjamin-Hochberg). For the unprimed ASC group, JUN inhibition along with VCAN activation connect to the potentially anti-tumorigenic mechanisms of reduced matrix metallopeptidase (MMP) 12 activation, and a decrease in C-C Motif Chemokine Ligand (CCL) 2, NOTCH3, and other nodes of interest that can be pursued in future studies (Figure 8A). For the LPS primed ASC group, Signal Transducer And Activator Of Transcription (STAT) 3 was ultimately inhibited, and this could represent a mechanism of anti-tumorigenesis (Figure 8B). For the poly I:C-primed ASC group, an interesting mechanistic network differed from the LPS group in a predicted inhibition of Mitogen-Activated Protein Kinase 3/1 (ERK1/2), and in a stronger predicted inhibition of JUN, along with a predicted activation of Tumor Protein 53 (TP53), a key tumor-suppressor gene (Figure 8C).

10.3389/fcell.2023.1145421

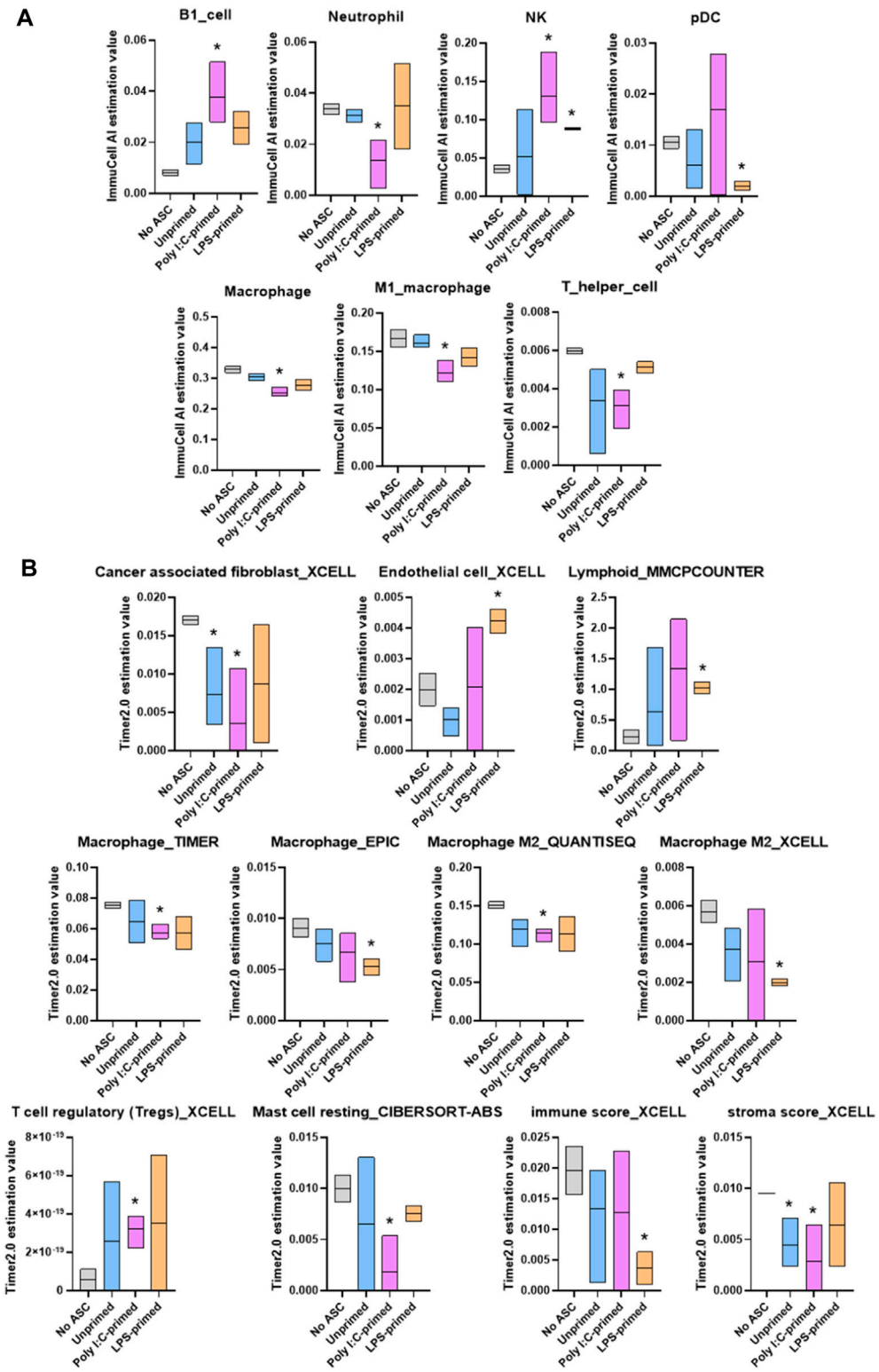

FIGURE 6
Summary of significant differences in immune cell abundance between treatment groups. Immune cell abundance in tumor samples were estimated from bulk RNA-seq data using ImmuCell AI **(A)** and TIMER 2.0 **(B)** algorithms. Cell populations with significant differences in abundance relative to untreated controls in at least one treatment group are included in the figure. Data presented as abundance estimation value in min-to-max box plots with line representing the mean. Analysis was performed by multiple t-tests, comparing each treatment group to the No ASC controls, p-value <0.05 was considered significant (*).

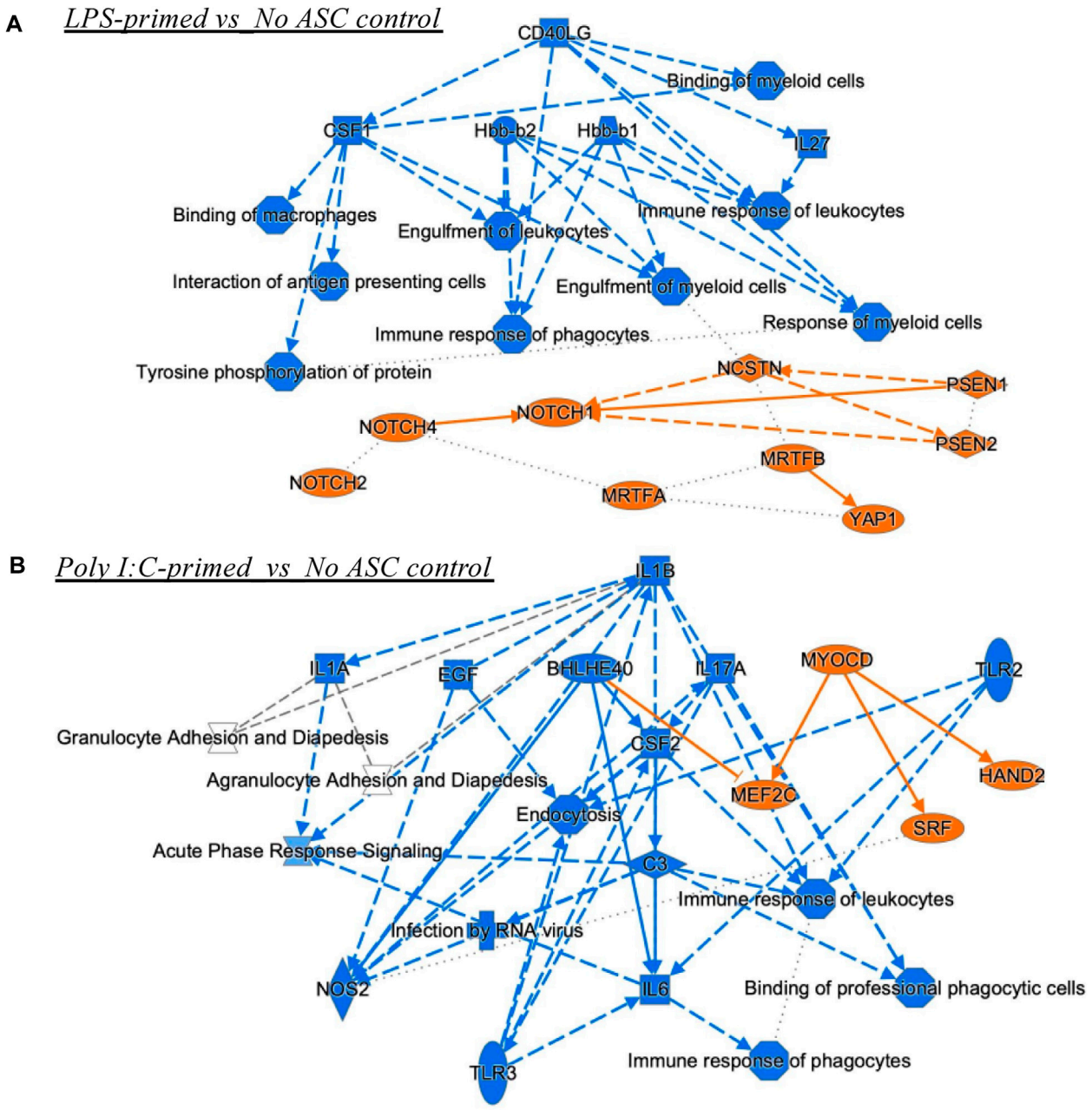

FIGURE 7
Graphical summary of IPA analyses. These include Upstream Regulators and Diseases and Functions analyses for comparisons LPS-primed versus No ASC control **(A)**, and Poly I:C-primed versus No ASC control **(B)** that had significant z-scores (lowest B-H corrected *p* values). The unprimed ASC group did not have enough upstream regulators or diseases and functions for connectivity in the graphical summary analysis. Orange, predicted activation, Blue, predicted inhibition. Solid lines, direct relationship or interaction; Dotted lines, inferred relationship, or indirect interaction.

4 Discussion

With the emergence of an interest in the use of mesenchymal stromal cells for anti-cancer therapeutics, there is an increased need to better understand the mechanisms by which MSC may be regulated to exert anti-tumorigenic functions and prevent their pro-tumorigenic activities. Among these strategies, pre-conditioning by *ex vivo* stimulation with TLR ligands has been proposed to promote polarized pro- or anti-inflammatory MSC phenotypes with pro- or anti-tumorigenic properties, respectively. This phenomenon, however, has remained largely unexplored in MSC from alternative tissue sources beyond BM-MSC, for example, ASC, which may provide clinical advantages because of culture characteristics that allow a faster acquisition of clinically relevant doses in reduced time.

In our previous work (Rivera-Cruz and Figueiredo, 2023), we identified similarities to the polarization phenotype occurring in ASC in response to TLR priming. However, our work was limited in that, in the functional evaluation of TLR-primed ASC within this study, we studied interactions between primed ASC, immune cells,

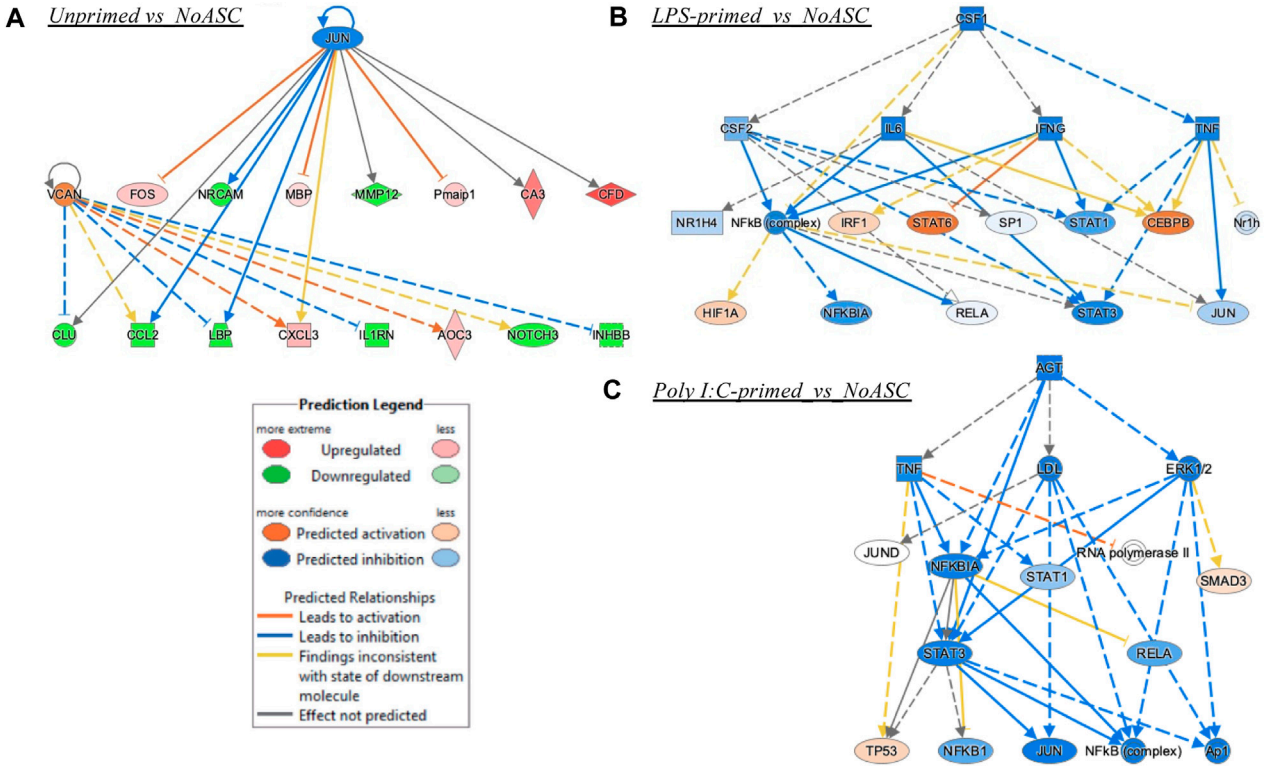

FIGURE 8
Mechanistic networks formed by each treatment group. **(A)** Unprimed ASC vs. No ASC control treatment of TC2R tumors, **(B)** LPS-primed ASC vs. No ASC control; **(C)** Poly I:C-primed ASC vs. No ASC control. Prediction Legend indicates the directionality of predicted activation of inhibition, whereas the relationships among the nodes are illustrated by a variety of color lines.

and cancer cells in isolation. Tumorigenesis and tumor immunity are also influenced by more complex processes, such as angiogenesis, interactions with the tumor stroma, among others. To further our understanding of the consequences of TLR-priming in modulating the effect of ASC administration in prostate cancer tumors, we evaluated tumor growth rates and mRNA signatures of tumors treated with ASC of different priming statuses and compared them to those of untreated tumors.

By monitoring tumor size over time in our model, we identified a significant increase in the growth rate of tumors treated with poly I:C-primed ASC relative to all other treatment groups. These observations were consistent across two independent experiments for which pooled results are summarized in Figure 1. No significant differences were observed relative to the untreated control group, in the unprimed ASC nor the LPS-primed ASC treatment groups. These findings are interesting in that they partially recapitulate the effects of MSC-tumor interactions observed in the initial polarization reports, in that poly I:C induced a pro-tumorigenic action by the BM-MSC treatments (Waterman et al., 2012). Yet, the potentially anti-tumorigenic effects of LPS-primed cells reported by this group and suggested in our ASC *in vitro* experiments (Rivera-Cruz and Figueiredo, 2023) were not evident in these *in vivo* experiments. There are many potential reasons for these observed differences. When compared to the reports by Waterman *et al.*, potential contributors to these differences may include a distinct MSC tissue source, differences in cell administration route and dosing, and ultimately distinctions in the tumor models assessed, including tumor location and tumor type. To better understand potential mechanisms mediating these observed differences, we performed RNA-seq analysis on representative tumor samples from each treatment group. Interestingly, while no significant differences had been observed at the macroscopic level in unprimed ASC nor LPS-primed ASC treated tumors (Figure 1), significant differences were observed between these groups and the untreated controls at the level of gene expression (Figure 2). While our heatmap displayed variability across samples within the same ASC-treated groups, indicating that a degree of heterogeneity may be maintained in the ASC population despite priming, many of the differentially expressed genes were uniquely identified in their respective treatment groups (Figures 2C, D). This suggests that the administration of these cells might induce treatment-specific differences in the tumors. However, these differences may not always be sufficient to potentiate altered tumor growth rates detectable at the macroscopic level.

For the unprimed and LPS-primed ASC treatment groups, among the enriched terms found by the Metascape ontology assessment based on differentially expressed genes were terms related to nervous system, cell migration, and immune system related processes, among others (Figures 3, 4). Intriguingly, enrichment of terms related to these categories was identified to some extent in both the upregulated and downregulated genes for these groups, suggesting that there is not a clear directionality of

these changes. This, however, matches our observation in that no evident (nor significant) effects were observed in tumor development over time. These enriched categories are however interesting in that they encompass a variety of potential mechanisms for tumor progression modulation relevant to prostate cancer. For example, in the case of nervous system related processes, in prostate cancer and other cancer types, neurogenesis and axon genesis associated with tumors and subsequent nerve-cancer crosstalk is understood to drive carcinogenesis (Silverman et al., 2021). Further, although prostate adenocarcinomas are of epithelial origin, neuroendocrine differentiation can occur following treatment, and it is understood to contribute to mechanisms of ADT resistance and worsening prognosis in prostate cancer (Kaarijärvi et al., 2021). These neuroendocrine cells are typically independent of androgens and have been shown to support the growth of androgen-sensitive adenocarcinoma even under androgen ablation (Jin et al., 2004). Potential roles on the induction of neuroendocrine differentiation have been attributed to cancer associated fibroblasts (CAF), a cell population that is believed to be able to originate from MSC (Kato et al., 2019). In the case of processes associated with cell migration, these processes may affect recruitment of other cell populations, such as immune cells, to the TME. In conjunction with other immune system related processes, these changes may contribute to differences in immune infiltration and response to the tumors. MSC are known to exert functions in immune recruitment and immunomodulation *via* cell-cell contact and soluble factors, and the nature of these interactions may be pro- or anti-tumorigenic depending on the context (Rivera-Cruz et al., 2017).

In the poly I:C-primed ASC treatment group, similarly to the other ASC-treated groups, several overarching categories of processes were modulated, some of which were enriched in both the upregulated and downregulated gene lists (Figure 5). Some examples included ECM-receptor interactions, angiogenesis, and cell motility-related processes. Since we detected significantly different effects in the tumor growth rate for the poly I:C ASC-treated group, this may suggest that any specific TME-related processes were sufficient to induce a more pro-tumorigenic phenotype in this group. ECM-related processes could be implicated, as these were among the terms enriched in both upregulated and downregulated genes. Dysregulation of ECM-related proteins, such as integrins, is implicated in modulation of tumor progression by roles in cell proliferation, cell adhesion, migration and angiogenesis (Venning et al., 2015). Development of new vasculature, or angiogenesis, is commonly considered a hallmark of cancer progression as the new vasculature provides access to a higher blood supply, enabling tumor cell proliferation (Hanahan, 2022). While targeting angiogenesis is of interest in the field of cancer therapeutics, this is a difficult task as angiogenesis signaling is highly redundant (Melegh and Oltean, 2019). While MSC have been reported to be able to have anti-angiogenic roles (Pan et al., 2019), more often they have been reported to exert pro-angiogenic properties within tumors, for example, through the secretion of angiogenic factors (i.e., VEGF) (Beckermann et al., 2008).

A few functional processes were differentially enriched in poly I:C-treated samples, which may have "tilted the balance" towards the more rapid tumor growth detected in our *in vivo* experiments. Among these, several immune processes were enriched in the list of downregulated genes in this treatment group. Examples of these processes included phagocytosis and humoral response. Interestingly, when evaluating the relative abundance of immune cell populations in these tumors (Figure 6), the poly I:C-primed ASC treated samples were found to contain significantly reduced phagocytic populations such as neutrophils and macrophages. We did, however, also detect a significant increase in B1 cells, which was unexpected in the context of the suppression of humoral response. Further supporting a more tumorigenic phenotype following the poly I:C ASC treatment, we also observed an increase in the abundance of regulatory T cells. While the effect of decreases in resting mast cells, stromal scores and CAFs, and increases in NK cell abundance might potentially promote an opposite immunomodulatory effect, for the latter, this would depend on the activation state, which is not assessed in this estimation. Interestingly, in a study looking at immune infiltration in prostate tumors comparing 190 normal prostate tissues to 537 PrCa samples (Wu et al., 2020), NK cells were found more abundantly in tumor tissues, with the majority of these cells found at a resting stage. Further, this group also found that PrCa tumors have a lower abundance of resting mast cells compared to normal tissues. These observations are concordant with our observations in immune cell estimates in poly I:C for these cell subsets and these at least in part may be correlated with disease progression. However, observations in regard to macrophage and neutrophil infiltrates by Wu et al. (2020) were dissimilar to our observations of decreased amounts in these populations within our tumor samples relative to control (no ASC).

The reduced response from phagocytes and other myeloid cells in the LPS primed group detected by IPA was consistent with detection of lower macrophages in the immune profiling data. Interestingly, NOTCH activation is associated with the promotion of macrophage activation towards an anti-tumor (M1) phenotype (Wang et al., 2010). This further supports the notion of potentially counteracting mechanisms being at play nullifying each other and somewhat maintaining a balance where a distinct pro-tumorigenic/anti-tumorigenic role cannot be clearly observed. Future studies can explore dosage changes or alterations to the priming protocol to further potentiate the roles of NOTCH signaling and other anti-tumorigenic consequences of LPS-primed ASC on tumor growth. The poly I:C group, paradoxically, showed a reduction in many regulators that are pro-inflammatory, yet impacted myeloid cell populations, consistent with the immune cell profiling data of reduced M1 macrophage abundance in tumors. The M1 macrophage is tumoricidal and as such, the reduction in that population through several potential mechanisms (CSF2 reduction may be one (Sielska et al., 2020)) can impact tumorigenesis. Some of the regulators affected by this treatment however could be implicated in anti-tumorigenic activities (*i.e.*, IL-6 (Jiang et al., 2011)), yet modulation identified in other regulators are potentially implicated in prostate cancer tumorigenesis, such as BHLHE40 (Dmitriev et al., 2015), and SRF (Prencipe et al., 2018). This once again suggests that modulatory effects of these treatments result in a tug-of-war of pro- and anti-tumorigenic actions yet poly I:C-primed ASC treatments used in these experiments were capable of "tilting the

balance" of these interactions to a more pro-tumorigenic environment as suggested by the effects observed on tumor progression *in vivo*.

In addition to the mechanisms described earlier, it remains possible that the pro-tumorigenic potential of poly I:C-primed ASC may also be mediated by an increased abundance or survival of ASC at the tumor site. Although we did not assess ASC survival/abundance in the studied tumors, previous data from our group and others suggest that ASC are non-tumorigenic (Zolochevska et al., 2012) and that TLR-primed MSC are capable of modulating tumor growth without significantly inducing MSC colony formation or tumor formation potential (Waterman et al., 2012). However, the question of whether TLR-priming affects ASC survival and tumor-forming potential *in vivo* remains unanswered and may be the focus of future investigations. Furthermore, additional work is needed to functionally validate the mechanisms proposed in this study and to explore how various preconditioning parameters, dosages, and routes of administration can affect the complex balance of MSC-tumor interactions (Otsu et al., 2009; Zheng et al., 2016). While our study provides a solid foundation for informing subsequent investigations of MSC-tumor interactions, it is important to note that, in this study, primed-ASC were co-administered with cancer cells. This co-administration may not closely resemble the clinical use of these cells. Therefore, we should in future studies explore other contexts that more closely resemble clinical settings, such as systemic administration to tumor-bearing mice.

5 Conclusion

Taken together our data suggest that TLR-priming of MSC may differentially affect the tumor progression modulation roles of ASC. Mediating these roles are likely processes involving angiogenesis, immunomodulation, and others such as nervous system-related processes and chemotaxis, with roles that may influence pro- or anti-tumorigenic actions. However, the effects resulting from the collective interaction across these processes must be sufficiently skewed in one of these directions for evidence of tumor progression modulation to be detectable at the macroscopic level. An example was the observation made from the analyses of the tumors treated with poly I:C-primed ASC in our experiments, where this treatment resulted in a significant increase in tumor progression compared to all other treatment groups evaluated.

Data availability statement

The data presented in the study are deposited in the NCBI GEO Datasets repository, accession number GSE245489.

Ethics statement

Ethical approval was not required for the studies on humans in accordance with the local legislation and institutional requirements because only commercially available established cell lines were used. The animal study was approved by PACUC: Purdue University IACUC. The study was conducted in accordance with the local legislation and institutional requirements.

Author contributions

CR-C: conceptualization, experimental design and execution, data analysis, and writing of original draft. SK: Experimental execution. MLF: conceptualization, experimental design, writing, reviewing, editing, and supervision. All authors contributed to the article and approved the submitted version.

Funding

The author(s) declare financial support was received for the research, authorship, and/or publication of this article. This work was supported by the Basic Medical Sciences at Purdue University, the Purdue Research Foundation 60000025, the Purdue Doctoral Fellowship (CR-C), and NIH R21CA153165 and in part R01CA196947 (MLF) and analysis assistance from the Bioinformatics Core from the Institute for Cancer Research, NIH grant P30 CA023168.

Acknowledgments

We acknowledge support from the Basic Medical Sciences at Purdue University, and the Purdue Imaging Facility.

Conflict of interest

The authors declare that the research was conducted in the absence of any commercial or financial relationships that could be construed as a potential conflict of interest.

Publisher's note

Supplementary material

The Supplementary Material for this article can be found online at: https://www.frontiersin.org/articles/10.3389/fcell.2023.1145421/full#supplementary-material

References

Beckermann, B. M., Kallifatidis, G., Groth, A., Frommhold, D., Apel, A., Mattern, J., et al. (2008). VEGF expression by mesenchymal stem cells contributes to angiogenesis in pancreatic carcinoma. *Br. J. Cancer* 99, 622–631. doi:10.1038/sj.bjc.6604508

Brennen, W. N., Chen, S., Denmeade, S. R., and Isaacs, J. T. (2013). Quantification of Mesenchymal Stem Cells (MSCs) at sites of human prostate cancer. *Oncotarget* 4 (1), 106–17. doi:10.18632/oncotarget.805

Chang, A. J., Autio, K. A., Roach, M., and Scher, H. I. (2014). High-risk prostate cancer-classification and therapy. *Nat. Rev. Clin. Oncol.* 11, 308–323. doi:10.1038/nrclinonc.2014.68

Dmitriev, A. A., Rosenberg, E. E., Krasnov, G. S., Gerashchenko, G. V., Gordiyuk, V. V., Pavlova, T. V., et al. (2015). Identification of novel epigenetic markers of prostate cancer by NotI-microarray analysis. *Dis. Markers* 2015, 241301. doi:10.1155/2015/241301

Foster, B. A., Gingrich, J. R., Kwon, E. D., Madias, C., and Greenberg, N. M. (1997). Characterization of prostatic epithelial cell lines derived from transgenic adenocarcinoma of the mouse prostate (TRAMP) model. *Cancer Res.* 57, 3325–3330.

Hanahan, D. (2022). Hallmarks of cancer: new dimensions. *Cancer Discov.* 12, 31–46. doi:10.1158/2159-8290.CD-21-1059

Hass, R. (2020). Role of MSC in the tumor microenvironment. *Cancers* 12, 2107. doi:10.3390/cancers12082107

Jiang, X. P., Yang, D. C., Elliott, R. L., and Head, J. F. (2011). Down-regulation of expression of interleukin-6 and its receptor results in growth inhibition of MCF-7 breast cancer cells. *Anticancer Res.* 31, 2899–2906.

Jin, R. J., Wang, Y., Masumori, N., Ishii, K., Tsukamoto, T., Shappell, S. B., et al. (2004). NE-10 neuroendocrine cancer promotes the LNCaP xenograft growth in castrated mice. *Cancer Res.* 64, 5489–5495. doi:10.1158/0008-5472.CAN-03-3117

Kaarijärvi, R., Kaljunen, H., and Ketola, K. (2021). Molecular and functional links between neurodevelopmental processes and treatment-induced neuroendocrine plasticity in prostate cancer progression. *Cancers (Basel)* 13, 692. doi:10.3390/cancers13040692

Kato, M., Placencio-Hickok, V. R., Madhav, A., Haldar, S., Tripathi, M., Billet, S., et al. (2019). Heterogeneous cancer-associated fibroblast population potentiates neuroendocrine differentiation and castrate resistance in a CD105-dependent manner. *Oncogene* 38, 716–730. doi:10.1038/s41388-018-0461-3

Kim, D., Langmead, B., and Salzberg, S. L. (2015). HISAT: a fast spliced aligner with low memory requirements. *Nat. Methods* 12, 357–360. doi:10.1038/nmeth.3317

Kirby, M., Hirst, C., and Crawford, E. D. (2011). Characterising the castration-resistant prostate cancer population: a systematic review. *Int. J. Clin. Pract.* 65, 1180–1192. doi:10.1111/j.1742-1241.2011.02799.x

Krämer, A., Green, J., Billaud, J. N., Pasare, N. A., Jones, M., and Tugendreich, S. (2022). Mining hidden knowledge: embedding models of cause-effect relationships curated from the biomedical literature. *Bioinform Adv.* 2, vbac022. vbac022. doi:10.1093/bioadv/vbac022

Li, T., Fu, J., Zeng, Z., Cohen, D., Li, J., Chen, Q., et al. (2020). TIMER2.0 for analysis of tumor-infiltrating immune cells. *Nucleic Acids Res.* 48, W509–W514. doi:10.1093/nar/gkaa407

Love, M. I., Huber, W., and Anders, S. (2014). Moderated estimation of fold change and dispersion for RNA-seq data with DESeq2. *Genome Biol.* 15, 550. doi:10.1186/s13059-014-0550-8

Martin, M. (2011). Cutadapt removes adapter sequences from high-throughput sequencing reads. *EMBnet. J.* 17, 10–12. doi:10.14806/ej.17.1.200

Melegh, Z., and Oltean, S. (2019). Targeting angiogenesis in prostate cancer. *Int. J. Mol. Sci.* 20, 2676. doi:10.3390/ijms20112676

Metsalu, T., and Vilo, J. (2015). ClustVis: a web tool for visualizing clustering of multivariate data using Principal Component Analysis and heatmap. *Nucleic Acids Res.* 43, W566–W570. doi:10.1093/nar/gkv468

Miao, Y.-R., Xia, M., Luo, M., Luo, T., Yang, M., and Guo, A.-Y. (2021). ImmuCellAI-mouse: a tool for comprehensive prediction of mouse immune cell abundance and immune microenvironment depiction. *Bioinformatics* 38, 785–791. doi:10.1093/bioinformatics/btab711

Norozi, F., Ahmadzadeh, A., Shahrabi, S., Vosoughi, T., and Saki, N. (2016). Mesenchymal stem cells as a double-edged sword in suppression or progression of solid tumor cells. *Tumour Biol.* 37, 11679–11689. doi:10.1007/s13277-016-5187-7

Nowakowski, A., Drela, K., Rozycka, J., Janowski, M., and Lukomska, B. (2016). Engineered mesenchymal stem cells as an anti-cancer trojan horse. *Stem Cells Dev.* 25, 1513–1531. doi:10.1089/scd.2016.0120

Otsu, K., Das, S., Houser, S. D., Quadri, S. K., Bhattacharya, S., and Bhattacharya, J. (2009). Concentration-dependent inhibition of angiogenesis by mesenchymal stem cells. *Blood* 113, 4197–4205. doi:10.1182/blood-2008-09-176198

Pan, J., Wang, X., Li, D., Li, J., and Jiang, Z. (2019). MSCs inhibits the angiogenesis of HUVECs through the miR-211/Prox1 pathway. *J. Biochem.* 166, 107–113. doi:10.1093/jb/mvz038

Pers, Y.-M., Jorgensen, C., and Khoury, M. (2021). Editorial: the role of metabolism in MSC-mediated immunomodulation. *Front. Immunol.* 12, 751865. doi:10.3389/fimmu.2021.751865

Pertea, M., Pertea, G. M., Antonescu, C. M., Chang, T.-C., Mendell, J. T., and Salzberg, S. L. (2015). StringTie enables improved reconstruction of a transcriptome from RNA-seq reads. *Nat. Biotechnol.* 33, 290–295. doi:10.1038/nbt.3122

Prencipe, M., Fabre, A., Murphy, T. B., Vargyas, E., O'Neill, A., Bjartell, A., et al. (2018). Role of serum response factor expression in prostate cancer biochemical recurrence. *Prostate* 78, 724–730. doi:10.1002/pros.23516

Rivera-Cruz, C. M., and Figueiredo, M. L. (2023). Evaluation of human adipose-derived mesenchymal stromal cell Toll-like receptor priming and effects on interaction with prostate cancer cells. *Cytotherapy* 25 (1), 33–45. doi:10.1016/j.jcyt.2022.09.009

Rivera-Cruz, C. M., Shearer, J. J., Figueiredo Neto, M., and Figueiredo, M. L. (2017). The immunomodulatory effects of mesenchymal stem cell polarization within the tumor microenvironment niche. *Stem Cells Int.* 2017, 4015039. doi:10.1155/2017/4015039

Robinson, M. D., Mccarthy, D. J., and Smyth, G. K. (2010). edgeR: a Bioconductor package for differential expression analysis of digital gene expression data. *Bioinformatics* 26, 139–140. doi:10.1093/bioinformatics/btp616

Shearer, J. J., Wold, E. A., Umbaugh, C. S., Lichti, C. F., Nilsson, C. L., and Figueiredo, M. L. (2016). Inorganic arsenic-related changes in the stromal tumor microenvironment in a prostate cancer cell-conditioned media model. *Environ. Health Perspect.* 124, 1009–1015. doi:10.1289/ehp.1510090

Siegel, R. L., Miller, K. D., Sandeep Wagle, N., and Jemal, A. (2023). Cancer statistics, 2023. *CA Cancer J. Clin.* 73, 17–48. doi:10.3322/caac.21763

Sielska, M., Przanowski, P., Pasierbińska, M., Wojnicki, K., Poleszak, K., Wojtas, B., et al. (2020). Tumour-derived CSF2/granulocyte macrophage colony stimulating factor controls myeloid cell accumulation and progression of gliomas. *Br. J. Cancer* 123, 438–448. doi:10.1038/s41416-020-0862-2

Silverman, D. A., Martinez, V. K., Dougherty, P. M., Myers, J. N., Calin, G. A., and Amit, M. (2021). Cancer-associated neurogenesis and nerve-cancer cross-talk. *Cancer Res.* 81, 1431–1440. doi:10.1158/0008-5472.CAN-20-2793

Strioga, M., Viswanathan, S., Darinskas, A., Slaby, O., and Michalek, J. (2012). Same or not the same? Comparison of adipose tissue-derived versus bone marrow-derived mesenchymal stem and stromal cells. *Stem Cells Dev.* 21, 2724–2752. doi:10.1089/scd.2011.0722

Sturm, G., Finotello, F., Petitprez, F., Zhang, J. D., Baumbach, J., Fridman, W. H., et al. (2019). Comprehensive evaluation of transcriptome-based cell-type quantification methods for immuno-oncology. *Bioinformatics* 35, i436–i445. doi:10.1093/bioinformatics/btz363

Terlizzi, M., and Bossi, A. (2022). High-risk locally advanced prostate cancer: multimodal treatment is the key. *Eur. Urol. Open Sci.* 38, 14–16. doi:10.1016/j.euros.2021.07.010

Umbaugh, C. S., Diaz-Quiñones, A., Neto, M. F., Shearer, J. J., and Figueiredo, M. L. (2017). A dock derived compound against laminin receptor (37 LR) exhibits anti-cancer properties in a prostate cancer cell line model. *Oncotarget* 9 (5), 5958–5978. doi:10.18632/oncotarget.23236

Venning, F. A., Wullkopf, L., and Erler, J. T. (2015). Targeting ECM disrupts cancer progression. *Front. Oncol.* 5, 224. doi:10.3389/fonc.2015.00224

Vicinanza, C., Lombardi, E., Da Ros, F., Marangon, M., Durante, C., Mazzucato, M., et al. (2022). Modified mesenchymal stem cells in cancer therapy: a smart weapon requiring upgrades for wider clinical applications. *World J. Stem Cells* 14, 54–75. doi:10.4252/wjsc.v14.i1.54

Wang, Y. C., He, F., Feng, F., Liu, X. W., Dong, G. Y., Qin, H. Y., et al. (2010). Notch signaling determines the M1 versus M2 polarization of macrophages in antitumor immune responses. *Cancer Res.* 70, 4840–4849. doi:10.1158/0008-5472.CAN-10-0269

Waterman, R. S., Henkle, S. L., and Betancourt, A. M. (2012). Mesenchymal stem cell 1 (MSC1)-based therapy attenuates tumor growth whereas MSC2-treatment promotes tumor growth and metastasis. *PLoS One* 7, e45590. doi:10.1371/journal.pone.0045590

Waterman, R. S., Tomchuck, S. L., Henkle, S. L., and Betancourt, A. M. (2010). A new mesenchymal stem cell (MSC) paradigm: polarization into a pro-inflammatory MSC1 or an Immunosuppressive MSC2 phenotype. *PLoS One* 5, e10088. doi:10.1371/journal.pone.0010088

Wu, Z., Chen, H., Luo, W., Zhang, H., Li, G., Zeng, F., et al. (2020). The landscape of immune cells infiltrating in prostate cancer. *Front. Oncol.* 10, 517637. doi:10.3389/fonc.2020.517637

Zheng, H., Zou, W., Shen, J., Xu, L., Wang, S., Fu, Y. X., et al. (2016). Opposite effects of coinjection and distant injection of mesenchymal stem cells on breast tumor cell growth. *Stem Cells Transl. Med.* 5, 1216–1228. doi:10.5966/sctm.2015-0300

Zhou, Y., Zhou, B., Pache, L., Chang, M., Khodabakhshi, A. H., Tanaseichuk, O., et al. (2019). Metascape provides a biologist-oriented resource for the analysis of systems-level datasets. *Nat. Commun.* 10, 1523. doi:10.1038/s41467-019-09234-6

Zolochevska, O., Ellis, J., Parelkar, S., Chan-Seng, D., Emrick, T., Wei, J., et al. (2013). Interleukin-27 gene delivery for modifying malignant interactions between prostate tumor and bone. *Hum. Gene Ther.* 24, 970–981. doi:10.1089/hum.2013.091

Zolochevska, O., Yu, G., Gimble, J. M., and Figueiredo, M. L. (2012). Pigment epithelial-derived factor and melanoma differentiation associated gene-7 cytokine gene therapies delivered by adipose-derived stromal/mesenchymal stem cells are effective in reducing prostate cancer cell growth. *Stem Cells Dev.* 21, 1112–1123. doi:10.1089/scd.2011.0247

frontiers | Frontiers in Cell and Developmental Biology

TYPE Original Research
PUBLISHED 11 March 2024
DOI 10.3389/fcell.2024.1329218

OPEN ACCESS

EDITED BY
Simone Pacini,
University of Pisa, Italy

REVIEWED BY
Yuyao Tian,
Massachusetts General Hospital, Harvard Medical School, United States
Ajoy Aloysius,
University of Kentucky, United States

*CORRESPONDENCE
Tokiko Nagamura-Inoue,
tokikoni@g.ecc.u-tokyo.ac.jp

RECEIVED 28 October 2023
ACCEPTED 29 February 2024
PUBLISHED 11 March 2024

CITATION
Hori A, Takahashi A, Miharu Y, Yamaguchi S, Sugita M, Mukai T, Nagamura F and Nagamura-Inoue T (2024), Superior migration ability of umbilical cord-derived mesenchymal stromal cells (MSCs) toward activated lymphocytes in comparison with those of bone marrow and adipose-derived MSCs.
Front. Cell Dev. Biol. 12:1329218.
doi: 10.3389/fcell.2024.1329218

Superior migration ability of umbilical cord-derived mesenchymal stromal cells (MSCs) toward activated lymphocytes in comparison with those of bone marrow and adipose-derived MSCs

Akiko Hori[1,2,3], Atsuko Takahashi[1,2,3], Yuta Miharu[1,2,3], Satoru Yamaguchi[4], Masatoshi Sugita[5], Takeo Mukai[2], Fumitaka Nagamura[6] and Tokiko Nagamura-Inoue[1,2,3]*

[1]Department of Cell Processing and Transfusion, Research Hospital, The Institute of Medical Science, The University of Tokyo, Tokyo, Japan, [2]IMSUT CORD, Research Hospital, The Institute of Medical Science, The University of Tokyo, Tokyo, Japan, [3]Division of Somatic Stem Cell Research, Center for Stem Cell Biology and Regenerative Medicine, The Institute of Medical Science, The University of Tokyo, Tokyo, Japan, [4]Department of Obstetrics, Yamaguchi Hospital, Chiba, Japan, [5]Department of Obstetrics, NTT Medical Center Tokyo Hospital, Tokyo, Japan, [6]Division of Advanced Medicine Promotion, The Advanced Clinical Center, The Institute of Medical Science, The University of Tokyo, Tokyo, Japan

Introduction: Mesenchymal stromal cells (MSCs) are activated upon inflammation and/or tissue damage and migrate to suppress inflammation and repair tissues. Migration is the first important step for MSCs to become functional; however, the migration potency of umbilical cord-derived MSCs (UC-MSCs) remains poorly understood. Thus, we aimed to assess the migration potency of UC-MSCs in comparison with those of bone marrow-derived MSCs (BM-MSCs) and adipose tissue-derived MSCs (AD-MSCs) and investigate the influence of chemotactic factors on the migration of these cells.

Methods: We compared the migration potencies of UC-, BM-, and AD-MSCs toward allogeneic stimulated mononuclear cells (MNCs) in mixed lymphocyte reaction (MLR). The number of MSCs in the upper chamber that migrated toward the MLR in the lower chamber was counted using transwell migration assay.

Results and discussion: UC-MSCs showed significantly faster and higher proliferation potencies and higher migration potency toward unstimulated MNCs and MLR than BM- and AD-MSCs, although the migration potencies of the three types of MSCs were comparable when cultured in the presence of fetal bovine serum. The amounts of CCL2, CCL7, and CXCL2 in the supernatants were significantly higher in UC-MSCs co-cultured with MLR than in MLR alone and in BM- and AD-MSCs co-cultured with MLR, although they did not induce the autologous migration of UC-MSCs. The amount of CCL8 was higher in BM- and AD-MSCs than in UC-MSCs, and the amount of IP-10 was higher in AD-MSCs co-cultured with MLR than in UC- and BM-MSCs. The migration of UC-MSCs toward the MLR was partially attenuated by platelet-derived growth factor, insulin-like

growth factor 1, and matrix metalloproteinase inhibitors in a dose-dependent manner. Conclusion: UC-MSCs showed faster proliferation and higher migration potency toward activated or non-activated lymphocytes than BM- and AD-MSCs. The functional chemotactic factors may vary among MSCs derived from different tissue sources, although the roles of specific chemokines in the different sources of MSCs remain to be resolved.

KEYWORDS

mesenchymal stromal cells, umbilical cord, migration, mixed lymphocyte reaction, bone marrow, adipose tissue, chemokines, cytokine

1 Introduction

Mesenchymal stromal cells (MSCs) can be obtained from several sources, including the bone marrow (BM), adipose tissue (AD), and umbilical cord (UC) (Gnecchi and Melo, 2009; Gruber et al., 2010). MSCs are activated upon inflammation and/or tissue damage and migrate to suppress inflammation and repair tissues. Insulin-like growth factor (IGF-1) and platelet-derived growth factor receptor (PDGF) are the most potent chemotactic factors of BM-MSCs (Ponte et al., 2007) and AD-MSCs (Baek et al., 2011). Fetal bovine serum (FBS) containing these growth factors promotes the migration potencies of BM-MSCs (Mishima and Lotz, 2008) and AD-MSCs (Baek et al., 2011), although reports about the chemotaxis of whole UC-MSCs in the presence of FBS are lacking. The migration potencies of BM-MSCs and AD-MSCs are promoted by pre-incubating with tumour necrosis factor (TNF)-α (Ponte et al., 2007; Ponte et al., 2007; Baek et al., 2011; Baek et al., 2011). The migration potency of BM-MSCs toward injured tissues has been associated with the expression of chemokines, including stromal-derived factor-1 (SDF-1) and CXCR4 (Liesveld et al., 2020). BM-MSCs attract hematopoietic stem cells (HSCs) and provide a favorable environment for hematopoiesis. Tondreau et al. demonstrated that inflammatory cytokines promote the migratory capacity of BM-MSCs according to the expression of interleukin (IL)-6, PDGF, IGF-1, and SDF-1 receptors. The production of matrix metalloproteinases (MMP1, MMP2, and MMP13) and tissue inhibitor of metalloproteinase (TIMP1/2) also promotes migration through the extracellular matrix (Tondreau et al., 2009).

BM-MSCs and UC-MSCs have been used clinically in immunotherapy and regenerative medicine to treat acute graft-versus-host disease (GVHD) after allogeneic HSC transplantation (Le Blanc and Davies, 2015; Murata et al., 2021; Nagamura-Inoue et al., 2022), COVID-19-related acute respiratory distress syndrome (Dilogo et al., 2021; Lanzoni et al., 2021), and other inflammatory diseases. The mixed lymphocyte reaction (MLR) assay, in which lymphocyte activation is induced by the co-culture of allogeneic cells such as dendritic cells, mimics acute GVHD *in vitro*. We previously demonstrated that responder T cell proliferation triggered by allogeneic dendritic cells can be efficiently inhibited by UC-derived MSCs (UC-MSCs) from a third-party donor (He et al., 2015; He et al., 2021; Kurogi et al., 2021). We also found that UC-MSCs actively migrate toward injured cells, that is, glucose-depleted SH-SY5Y human neuroblastoma cells, *in vitro* (Mukai et al., 2016). Furthermore, we demonstrated that UC-MSCs administered intravenously into an intraventricular hemorrhage mouse model become trapped in the lungs and then accumulate in the brain, although the injected UC-MSCs could not be detected in the mice after 3 weeks (Mukai et al., 2017). However, the migration potency of UC-MSCs toward inflammatory cells in response to allogeneic stimuli remains poorly understood.

Thus, we aimed to assess the migration potency of UC-MSCs toward inflammatory cells in comparison with those of BM-MSCs and AD-MSCs. This study is the first to report the superior migration ability of UC-MSCs toward inflammatory cells in comparison with those of BM-MSCs and AD-MSCs.

2 Materials and methods

2.1 Isolation and culture of MSCs

This study was approved by the Ethics Committee of the Institute of Medical Science, University of Tokyo (IMSUT) (No. 2021-108). UC-MSCs were provided by the IMSUT Hospital Cord Blood and Cord Bank (IMSUT CORD), Japan. IMSUT CORD activity was reviewed and approved by the IRB (No. 35-2). UC-MSCs were isolated from three donors using previously reported methods (Mori et al., 2015; Shimazu et al., 2015). Briefly, frozen-thawed UC tissues were minced into 2 mm fragments and subjected to an improved explant culture procedure. Tissue fragments were placed in complete α-minimal essential medium (αMEM; Wako Pure Chemical Industries, Ltd., Japan) supplemented with 10% FBS (SERANA, Germany) and antibiotics–antimycotics (Antibiotic-Antimycotic, 100X; Life Technologies, United States) at 37°C with 5% CO_2. Cells migrating from the UC tissue fragments were harvested using TrypLE Select (Life Technologies) and denoted as passage 1 (P1) UC-MSCs. P1 cells were frozen in StemCell Banker (Zenogen pharma Co., Ltd., Japan) (Mori et al., 2015). The 2.5×10^5 frozen-thawed cells suspended in culture medium were seeded in a 10 cm culture dish and further expanded until 80%–90% confluency and passaged every 5 days with the medium refreshed every 2 days. P4 cells were used in subsequent experiments. UC-MSCs were cryopreserved in StemCell Banker and thawed before use.

Human BM mononuclear cells (BM-MNCs) (Lonza, United States) and human AD-MSCs (Lonza, United States) were purchased from LONZA KK. BM-MNCs were cultured in αMEM

supplemented with 10% FBS, and the initial cells obtained were denoted as P1 BM-MSCs. BM-MSCs and AD-MSCs were cultured until P4 and used for further experiments.

2.2 Cell proliferation assay

The proliferation abilities of P2 UC-, BM-, and AD-MSCs were compared in αMEM supplemented with 10% FBS. In brief, 2.5×10^5 cells were suspended in complete medium and plated in a 10 cm-diameter dish (n = 3 in each MSC type). The number of cells was counted using trypan blue staining under a microscope. The cumulative population doubling level (PDL) was then calculated. The PDLs of the cells at each passage were calculated using the formula 2n = Nx/N0, where Nx is the cell number after culture and N0 is the cell number before culture (Kurogi et al., 2021).

2.3 Analysis of surface markers in MSCs

Flow cytometry was performed as described previously (Kurogi et al., 2021; Nagamura-Inoue et al., 2022). The cells were labeled with monoclonal antibodies, which are listed in Supplementary Table S1. The cells were acquired using BD™FACSCanto II flow cytometer (BD) and analyzed using FlowJo software (BD).

2.4 Adipogenic, osteogenic, and chondrogenic differentiation assays

The MSCs were plated at a density of 5×10^4 cells/well in 12-well plates and induced to differentiate into adipocytes with culture medium supplemented with 100 μM indomethacin (Sigma-Aldrich Co. LLC, United States), 1 μM dexamethasone (FUJIFILM Wako Pure Chemical Corporation, Japan), 0.5 μM IBMX (Sigma-Aldrich), and 10 μg/mL insulin (Sigma-Aldrich) for 2 weeks. Then, the cells were stained with Oil Red O (Sigma-Aldrich) (He et al., 2014). UC-MSCs were cultured for 4 weeks using a StemPro osteogenesis differentiation kit (Thermo Fisher Scientific Inc., United States) in accordance with the manufacturer's instructions, and their osteogenic differentiation was evaluated. The cells were stained with alizarin red (Sigma-Aldrich). In the chondrogenic differentiation assay, we used a pellet culture system using Stem MACS™ Chondro Diff Media (Miltenyi Biotec GmbH; Germany) at 2.5×10^5 in 15 mL conical tubes for 3 weeks. The cells were fixed with 4% formaldehyde and stained with toluidine blue (Sigma-Aldrich).

2.5 MLR

An allogeneic MLR assay was conducted as previously described (He et al., 2015; Kurogi et al., 2021; Nagamura-Inoue et al., 2022). Peripheral blood MNCs were used as the responder (R). PMDC05 cells were provided by Dr. Narita at the Faculty of Medicine, Niigata University (Narita et al., 2008; Narita et al., 2009). PMDC05 cells were irradiated and used as the stimulator (S). On the day of the MLR, R (4×10^5) and S (4×10^4) cells were mixed in 24-well plates at an R:S ratio of 10:1 in the presence of 0.625 ng/mL anti-human CD3 antibody (Lymactin-T; Cell Science & Technology Inc., Japan) (Nagamura-Inoue et al., 2022). The inhibition of the allogeneic MLR by MSC co-culture for 4 days in the presence of 10% FBS was investigated as previously described (Nagamura-Inoue et al., 2022) (Supplementary Figure S1).

2.6 Migration assays

The migratory abilities of MSCs were evaluated using a 24-well transwell chamber (Corning, United States) inserted with an 8 μm filter membrane. On the day of the migration assay, the MLR ratio described above was set in the lower chamber, and MSCs were plated at 5×10^3 cells/well in the upper transwell chamber and co-cultured at 37°C with 5% CO_2 overnight. The MSCs migrated toward the opposite side of the transwell chamber in response to the stimuli, including αMEM with 10% FBS (Montemurro et al., 2011), 4×10^4 MNCs with or without MLR, primed MNCs with reagents in the lower chamber of 24-well plates, and other indicated reagents described below. Appropriate MNC number was assessed by different concentrations of cells (from 4×10 to 4×10^5/lower chamber). Then, MSCs at the opposite filter side of the upper transwell chamber were fixed with 10% paraformaldehyde for 10 min, washed once with phosphate-buffered saline (Nissui Pharmaceutical Co., Ltd., Japan), and stained with 1 μg/mL 4′,6-diamidino-2-phenylindole, dihydrochloride (Cellstain®-DAPI, DoJin, Japan). The number of cells trapped on the opposite filter side was counted in all fields under the fluorescent microscope (×200; Niko Ti-S30-EDF-Ph-S, Nikon, Japan).

To evaluate the migration potency in response to chemokines, 1 ng/mL CCL2 (recombinant human MCP-1, Fujifilm-Wako chemicals Cor., Japan), 100 ng/mL CCL7 (Human CHO-expressed MSCP-3/CCL7, Genscript, United States), and 1 ng/mL CXCL2 (human CXCL2 protein, Acro) were added in the lower chamber of the migration assay system, after dose-dependency experiments (Data not shown).

To assess the inflammatory MNCs on the migration of UC-MSCs, MNCs primed with 10 μg/mL phytohemagglutinin-L (PHA-L, Roche, Germany), 1 μg/mL lipopolysaccharide (LPS, Fujifilm-Wako Chemicals Cor., Japan), and 10 ng/mL recombinant human TNF-α (Peprotech, United States) were incubated overnight, washed once, and then transferred to the new lower chamber of the migration assay system. The migrating cells were counted on the next day (17 h incubation). Then, the UC-MSCs were plated in the upper chamber and cultured overnight followed by counting the migrating cells as described above.

Various inhibitory factors were added to the migration assay to identify which of them induce migration. These factors included AG1296 for platelet-derived growth factor receptor (Cayman Chemical Company, United States) (Fiedler et al., 2004; Nazari et al., 2016), picropodophyllin (PPP) for insulin-like growth factor 1 receptor (IGF-1R; Merck, Deutschland) (Wang et al., 2019), and GM6001 for MMPs (Cayman Chemical Company) (Kasper et al., 2007). 5×10^3 cells/well of MSCs were plated in the upper transwell chamber in the presence of 10% FBS with indicated concentration of AG1296 and PPP. For GM6001 inhibition assay, 5×10^3 cells/well of UC-MSCs and 1.5×10^3 cells/well of BM- and AD-MSCs were plated

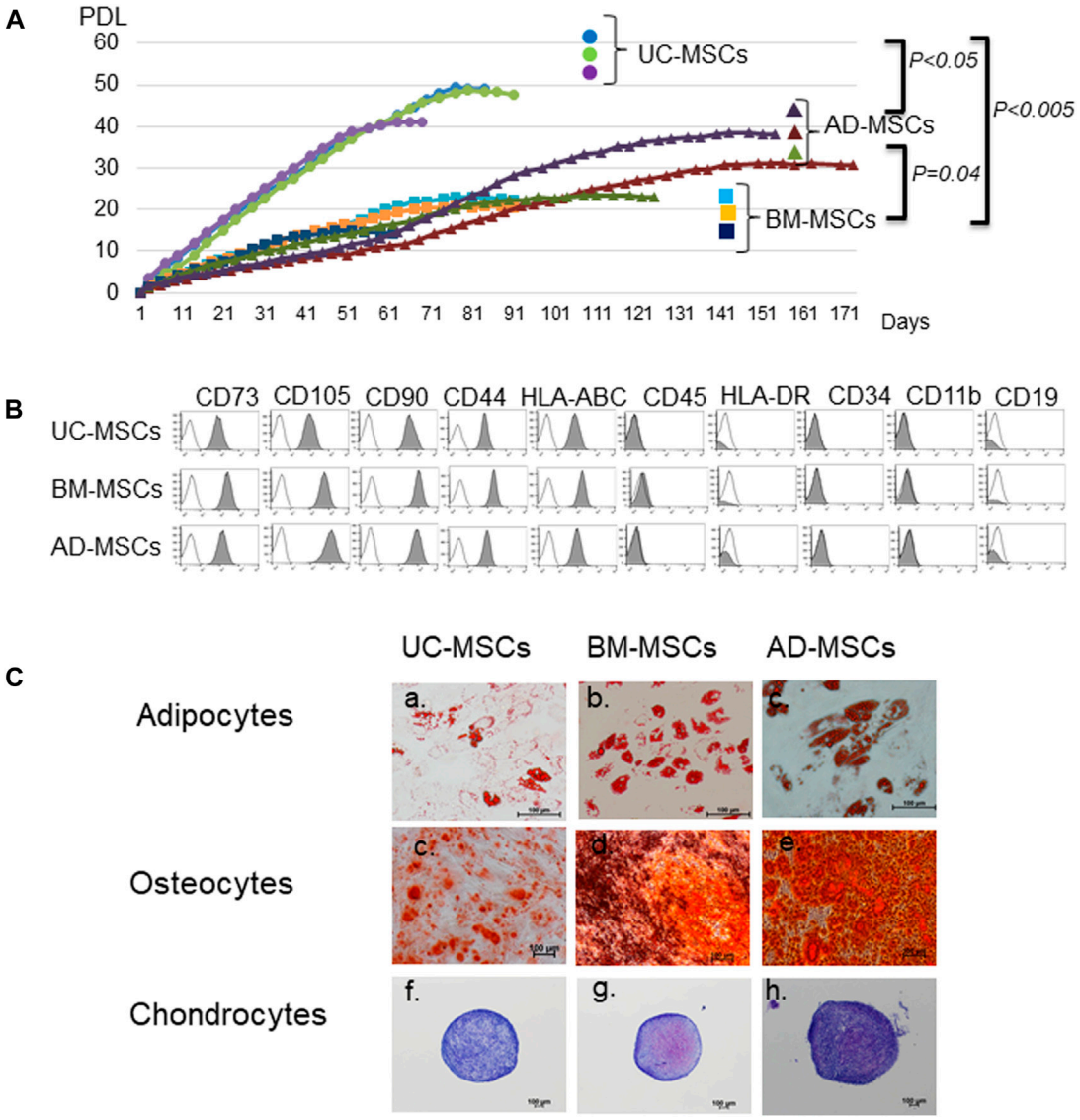

FIGURE 1
Characteristics of mesenchymal stromal cells (MSCs) from different tissue sources. **(A)** Proliferation of MSCs derived from umbilical cord (UC), bone marrow (BM), and adipose tissues (AD). Data are representative of three independent experiments and shown as mean ± SD of triplicate experiments, respectively. **(B)** Surface markers of UC-, BM-, and AD-MSCs. **(C)** Differentiation potencies of UC-, BM-, and AD-MSCs. Adipocytes are stained with oil red O, osteocytes with alizarin red, and chondrocytes with toluidine blue. UC-MSCs: umbilical cord-derived mesenchymal stromal cells, BM-MSC: bone marrow-derived MSCs, AD-MSC: adipose tissue-derived MSCs. Data are shown as mean ± SD calculated from those of three individual donors.

in the upper transwell chamber in the presence of 10% FBS., respectively.

Analysis of chemokines concentrations in the supernatant of allogeneic MLR co-cultured with UC-MSCs.

The concentrations of chemokines in the supernatant, including chemokine (C-C motif) ligand (CCL) 1, CCL2, CCL5, CCL7, CCL8, CCL11, CCL13, CCL18, CCL22, CXCL2, CXCL8, CXCL9, CXCL10, and SDF-1 content were measured using cytokine beads assay, a Human Proinflammatory Chemokine Panel (13-plex; BioLegend, United States) and Human proinflammatory chemokine Panel 2 (12-plex; BioLegend, United States) analyzed using LEGENDplex version 8.0 software (BioLegend, United States). Bead fluorescence readings were acquired using a FACSCanto II flow cytometer (BD) in accordance with the manufacturer's instructions. All samples were analyzed in triplicate.

2.7 qRT-PCR analysis

Quantitative reverse transcription polymerase chain reaction (qRT-PCR) was carried out to determine the chemokine receptors and secretion of chemokines (Korbecki et al., 2020) and MMP of the MSCs. Total RNA was extracted from MSCs using Nucleospin RNA (Invitrogen Corp, Carlsbad, CA, United States). RT-PCR was performed using PrimeScript™ RT reagent kit (Takara, Shiga, Japan) in accordance with the manufacturer's instructions. The

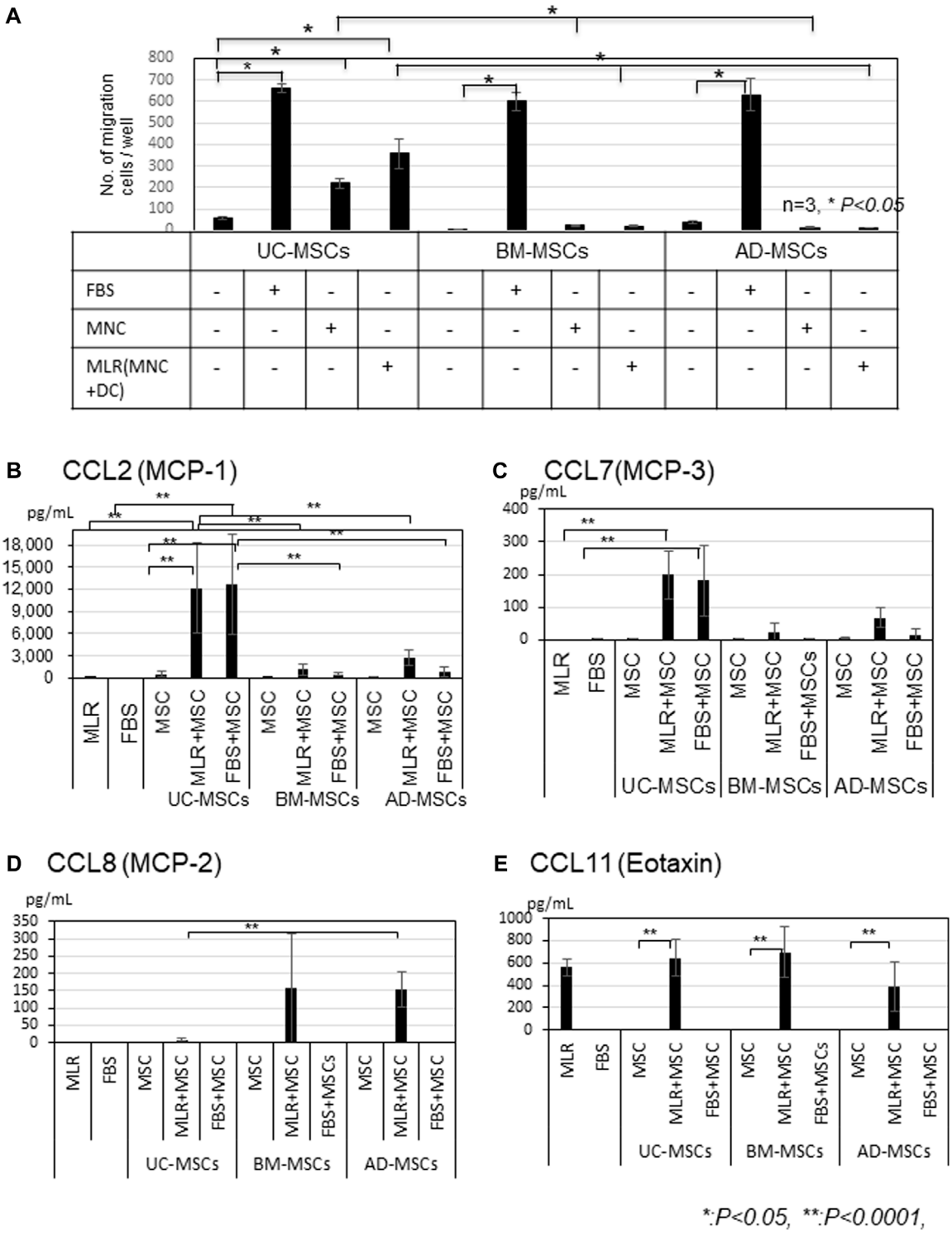

FIGURE 2
(Continued).

PCR program was as follows: initial incubation at 95°C for 30 s, followed by 40 cycles of 95°C for 5 s and 60°C for 30 s. Melting curves were generated by monitoring the fluorescence of TB green signal from 95°C to 60°C, decreasing by 0.5°C for each cycle. The data were analyzed in the BioRad CFX96 real-time PCR system (BioRad, Japan). Primer sets are shown in Supplementary Table S2.

2.8 Statistical analysis

JMP 17.0.0 software (SAS Institute, Cary, NC, United States) was used for statistical analyses. One-way or two-way analysis of variance with Tukey's multiple comparison test was conducted to compare differences between samples. Measurement data were

10.3389/fcell.2024.1329218

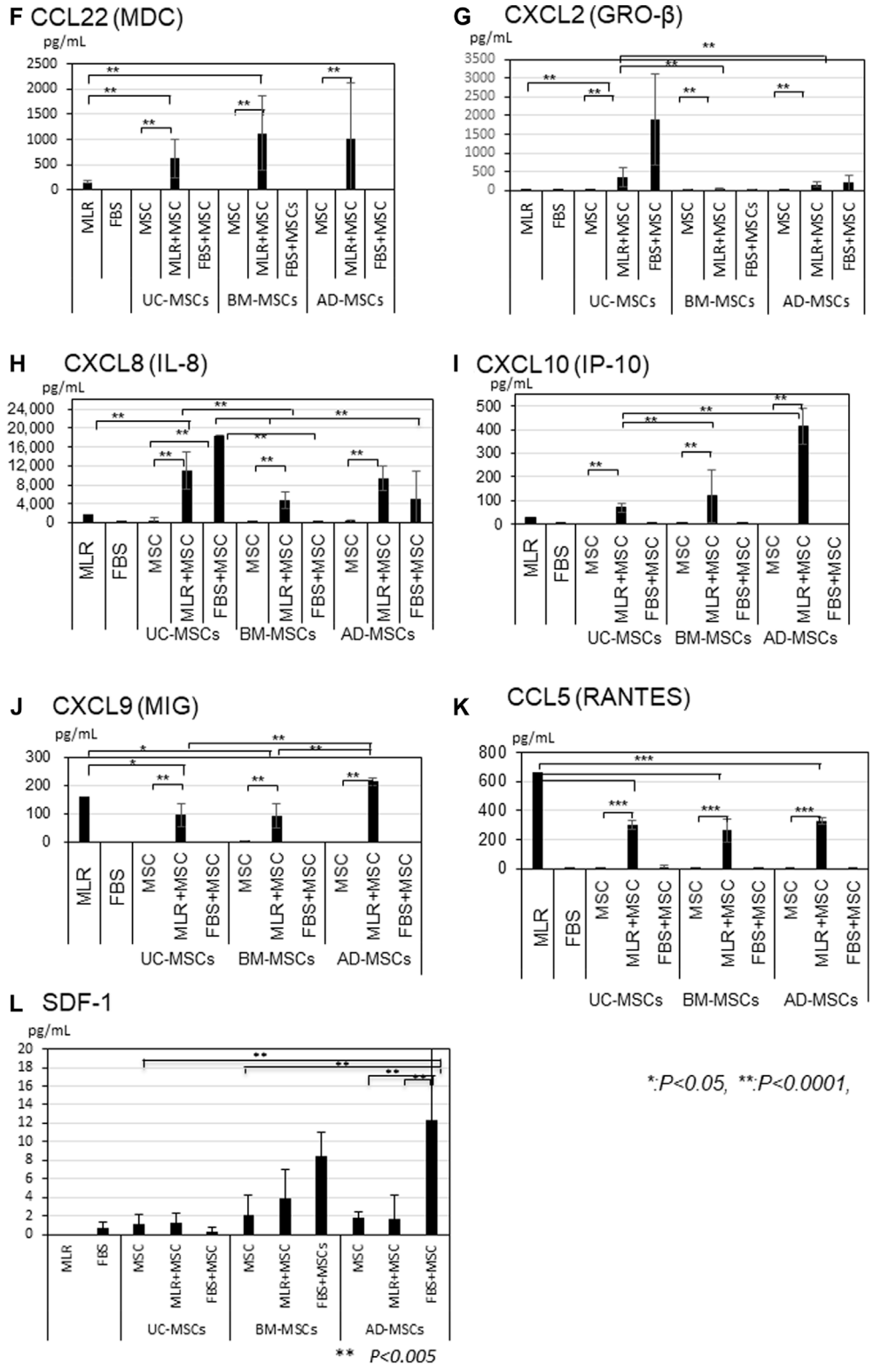

FIGURE 2
(Continued). Comparison of migration potencies of UC-, BM, and AD-MSCs toward MLR and chemokine levels in the supernatant. **(A)** Migrated cell counts of UC-, BM, and AD-MSCs in the upper chamber in the presence of FBS and co-culture with MLR. Data are representative of three independent experiments and shown as mean ± SD of triplicate experiments, respectively. **(B–K)** Supernatant of MSCs in the presence or absence of FBS and co-culture with MLR, respectively. **(B)** CCL2 (MCP-1), **(C)** CCL7, **(D)** CCL8 (MCP-2), **(E)** CCL11 (Eotaxin), **(F)** CCL22 (MDC), **(G)** CXCL2 (GRO-β), **(H)** CXCL8 (IL-8), **(I)** CXCL10 (IP10), **(J)** CXCL9 (MIG), **(K)** CCL5(RANTES), and **(L)** SDF-1. Data are shown as mean ± SD calculated from those of three individual donors.

expressed as mean ± SD, and $p < 0.05$ was considered statistically significant.

3 Results

3.1 Characteristics of UC-, BM-, and AD-MSCs

We compared the basic characteristics of UC-, BM, and AD-MSCs. The proliferation potencies of UC-, BM-, and AD-MSCs were compared. UC-MSCs demonstrated higher proliferation ability and speed than BM-MSCs and AD-MSCs. The proliferation limit was 46.3 ± 4.5 PDL in UC-MSCs (n = 3), 19.3 ± 4.5 in BM-MSCs (n = 3), and 31.1 ± 7.5 in AD-MSCs (n = 3; UC-MSCs vs. BM-MSCs; $p < 0.005$, UC-MSCs vs. AD-MSCs; $p = 0.041$, AD-MSCs vs. BM-MSCs; $p < 0.05$; Figure 1A). The mean ± SD of the days to reach PDL 10 was 14.8 ± 1.5 days in UC-MSCs, 28.0 ± 0 days in BM-MSCs, and 45.0 ± 11.5 days in AD-MSCs (UC-MSCs vs. BM-MSCs; $p = 0.049$, UC-MSCs vs. AD-MSCs; $p < 0.005$, AD-MSCs vs. BM-MSCs; P = not significant).

In accordance with the criteria of MSCs defined by the International Society of Cell & Gene Therapy (ISCT) (Dominici et al., 2006), UC-, BM-, and AD-MSCs were equally spindle-shaped, plastic-adherent cells positive for CD73, CD105, CD90, HLA-ABC, and CD44 and negative for CD45, HLA-DR, CD34, CD11b, and CD19 (Figure 1B). We also compared the abilities of UC-, BM-, and AD-MSCs to differentiate into adipocytes, osteoblasts, and chondrocytes (Figure 1C). Adipocytes stained with oil red O showed red droplets in the cells, and osteocytes with calcium deposits exhibited red particles. The pellet culture system was applied to analyze chondrogenic differentiation, and elastic firm pellets were observed. Toluidine blue staining revealed extracellular matrix formation in the cells grown in chondrogenic induction medium. Metachromasia occurred less frequently in UC-MSCs than in BM-MSCs and AD-MSCs. After immunochemical staining with alizarin red for osteogenic differentiation, UC-MSCs showed fewer calcium deposits than BM-MSCs and AD-MSCs.

3.2 Migration ability

We compared the migration abilities of UC-, BM-, and AD-MSCs toward allogeneic MLR or FBS by using transwell migration assays (Figure 2A). FBS significantly induced migration compared with no FBS (control) in all MSCs ($p < 0.05$). The number of migrating UC-MSCs significantly increased in response to unstimulated MNCs or allogeneic stimulated MNC (MLR; $p < 0.05$), whereas the number of migrating BM- and AD-MSCs did not increase in response to both of them. UC-MSCs showed a significantly higher migration ability toward unstimulated or allogeneic stimulated MNCs than BM- and AD-MSCs ($p < 0.05$). Furthermore, the number of migrating UC-MSCs co-cultured with allogeneic MLR tended to be greater than that of unstimulated MNCs. Direct or indirect co-culture of UC-, BM-, and AD-MSCs showed no significantly different inhibitory effects on allogeneic MLR, although MLR assay was conducted in the medium supplemented with FBS (Supplementary Figure S1).

3.3 Chemokines in the supernatant of migration assay

CCL2, CCL7, CCL22, IL-8, and IP-10 amounts were higher in the co-cultures of UC-, BM-, and AD-MSCs with MLR than in MLR alone (Figure 2B, C, F, H, I). CCL2 and CCL7 levels were significantly higher in the supernatant of UC-MSCs co-cultured with MLR or in the presence of FBS than in that of BM- and AD-MSCs (Figure 2B, C, $p < 0.0001$), whereas CCL8 level was higher in BM- and AD-MSCs than in UC-MSCs (Figure 2D). The amounts of IL-8 were also significantly higher in UC-MSCs co-cultured with MLR than in BM-MSCs, but the difference between UC-MSCs and AD-MSCs was not significant (MLR + UC-MSCs vs. MLR + BM-MSCs; $p < 0.05$, MLR + UC-MSCs vs. MLR + AD-MSCs; not significant; Figure 2H).

IP-10 levels were induced by the co-culture with MLR and significantly higher in AD-MSCs co-cultured with MLR than in BM- and UC-MSCs (Figure 2I). CCL11, CXCL9 and CCL5 levels increased in MLR, but co-culture with MSCs did not further increase these levels (Figure 2E, J, K). Meanwhile, CCL1, CCL13, and CCL18 levels were not elevated in any type of MSCs (Supplementary Figure S2A–C). A small amount of SDF-1 was induced in the culture of BM-MSCs and AD-MSCs with FBS but not in that of UC-MSCs (Figure 2L).

3.4 Influence of chemokines and inflammations on the migration of MSCs

To determine whether the chemokines elevated in the supernatant of UC-MSCs co-cultured with MLR can increase the migration potency of UC-MSCs in an autocrine manner, we directly added CCL2 (n = 3), CCL7 (n = 3), and CXCL2 (n = 3) in the MSCs and evaluated the induction of migration. Even when large amounts of CCL2, CCL7, and CXCL2 were secreted by UC-MSCs co-cultured with MLR, they did not increase the migration potency of UC-MSCs. CCL2, CCL7, and CXCL2 also did not increase the migration potencies of BM- and AD-MSC. The major CCL2 receptor, CCR2 was not expressed on UC-, BM-, and AD-MSCs. CCL2 receptors (CCR1, CCR2, CCR3, CCR4, and CCR5) and CCL7 receptors (CCR1, CCR2, CCR3, and CCR5) cross interfere for several ligands. Quantitative qRT-PCR and flow cytometry analysis results showed that UC-, BM, and AD-MSCs tested weak positive for CCR1 and less weak for CCR4 but not for CCR2, CCR3, and CCR5 with or without 10% FBS supplementation (Supplementary Figure S4A–E). qRT-PCR data also showed that the CXCL2 receptor CXCR2 was not expressed at all in the MSCs (Supplementary Figure S4F).

Considering that UC-MSCs seemed sensitive to migrate toward MNCs, we first assessed the influence of MNC dose on the migration potency of UC-MSCs to identify whether the inflammatory MNCs can increase the migration potency of UC-MSCs. UC-MSCs migrated toward MNCs in a dose-dependent manner at the range of 4×10–4×10^4 in the lower chamber of 24-well plates; however, interestingly, the excess confluency at 4×10^5 suppressed the migration (Figure 3B).

Thus, we used the lower dose of MNCs for proliferation in the chamber. We primed MNCs with inflammatory reagents, such as

10.3389/fcell.2024.1329218

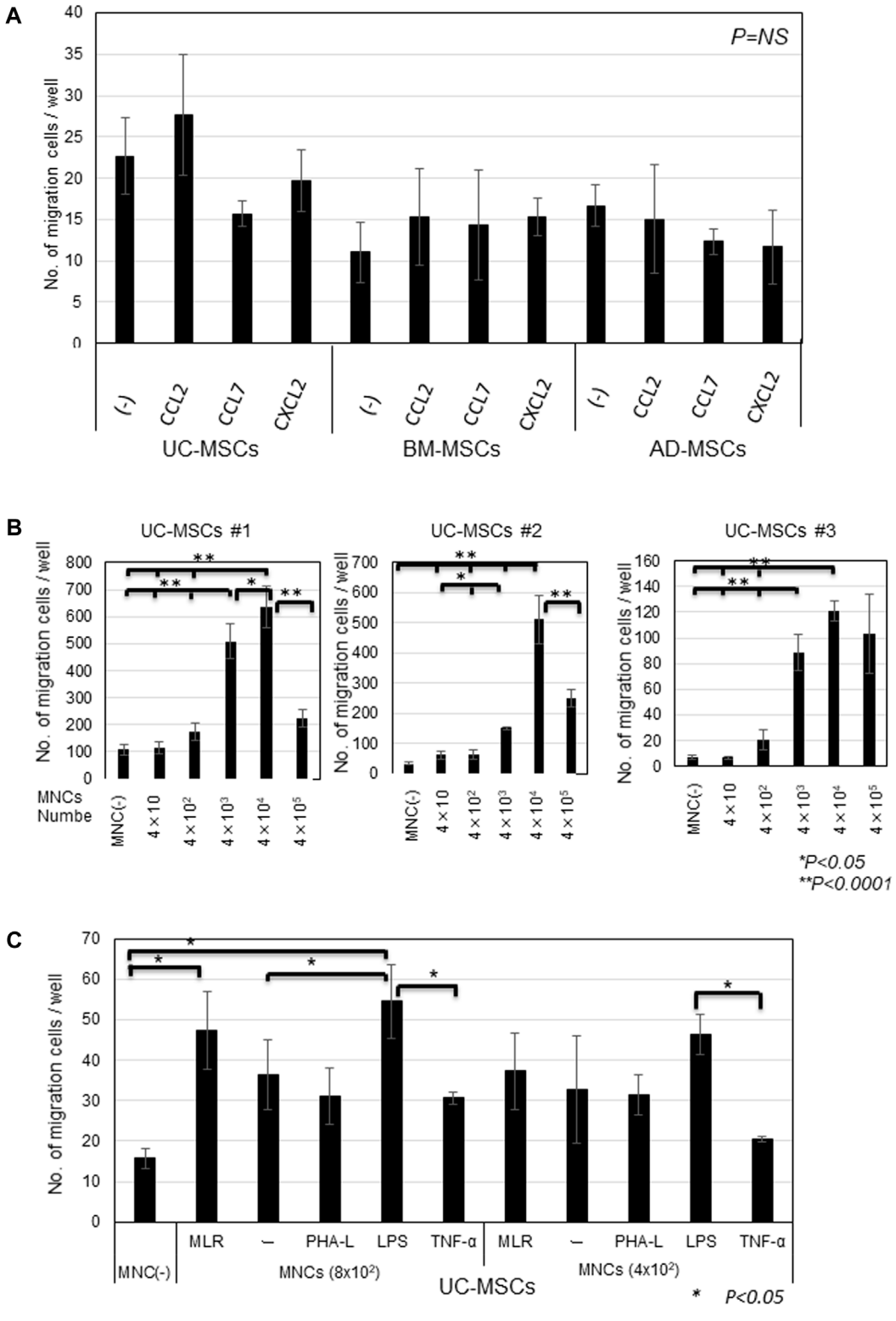

FIGURE 3
Migration of MSCs in response to CCL2, CCL7, and CXCL2 and MNCs stimulated by inflammatory factors **(A)** Migrated cell counts of UC-, BM-, and AD-MSCs in response to CCL2, CCL7, and CXCL2. 1 ng/mL CCL2, 100 ng/mL CCL7, and 1 ng/mL CXCL2 (human CXCL2 protein, Acro) were added in the lower chamber of the migration assay system. Representative data are shown as MSCs from three donors, respectively. **(B)** Migrating cell counts of UC-MSCs toward different doses of MNCs. Data are shown as three individual experiments of UC-MSCs derived from three donors. *$p < 0.05$, **$p < 0.0001$. **(C)** Migrated cell counts of UC-MSCS in response to MLR and MNCs primed with PHA-L, LPS, and TNF-α, respectively. Different MNC numbers in the lower chambers before stimulation are shown. Representative data of three independent experiments with mean ± SD are shown. *$p < 0.05$.

10.3389/fcell.2024.1329218

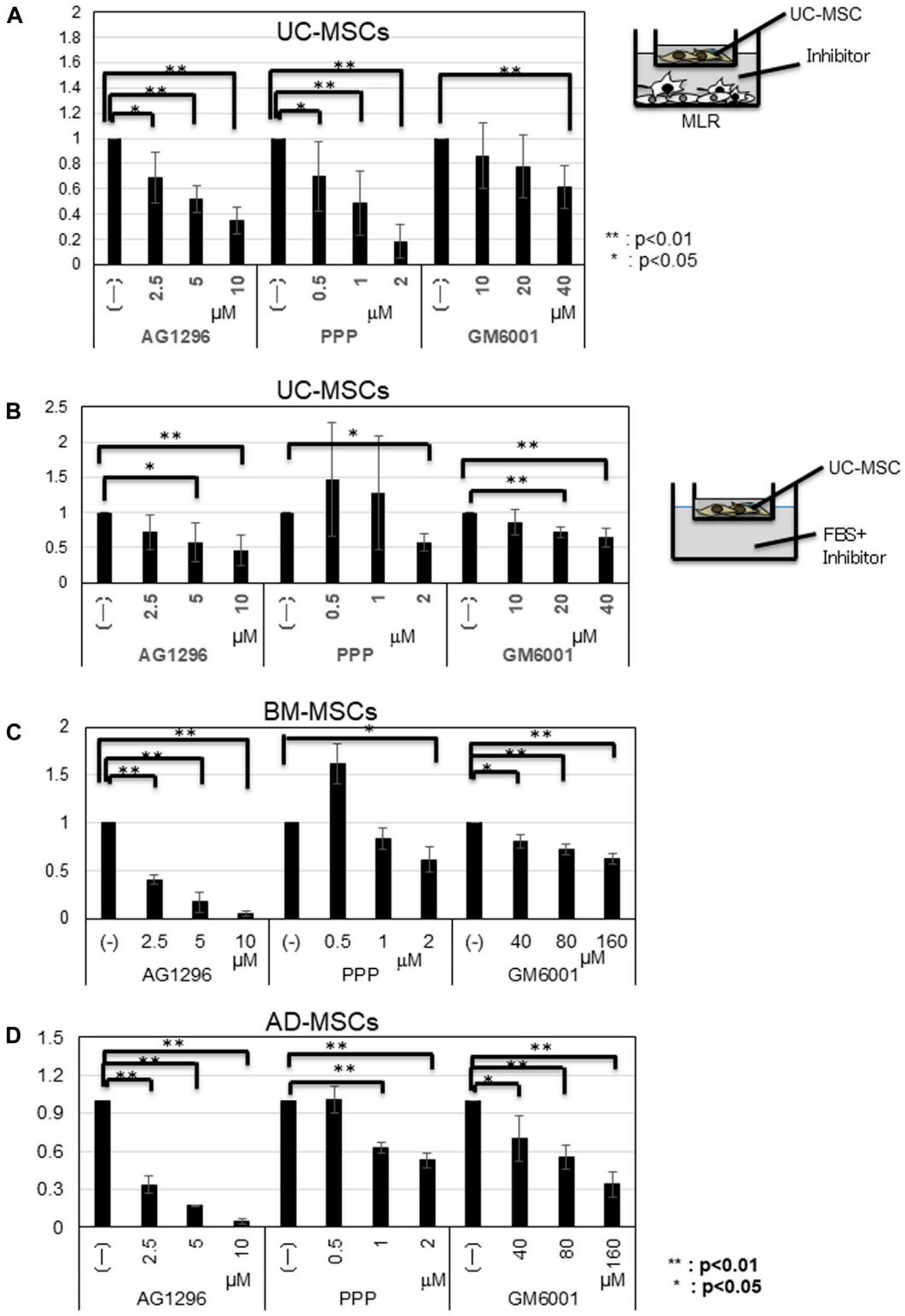

FIGURE 4
Influence of inhibitors on the migration of MSCs toward MLR. **(A)** Migrated cell counts of UC-MSCs in response to MLR with indicated inhibitors. AG1296; PDGF (platelet-derived growth factor) inhibitor; PPP; IGF-1 (insulin-like growth factor-1) inhibitor, and GM6001; MMP (matrix metalloproteinases) inhibitor. **(B)** UC-MSCs; **(C)** BM-MSCs; **(D)** AD-MSCs in the presence of FBS and inhibitors. Data are shown as mean ± SD calculated from migrated cell numbers of three individual donors, relative to the control (MSCs alone). 5×10^3 cells/well of MSCs were plated in the upper transwell chamber with indicated concentration of AG1296 and PPP. For GM6001 inhibition assay, 5×10^3 cells/well of UC-MSCs and 1.5×10^3 cells/well of BM- and AD-MSCs were plated in the upper transwell chamber, respectively. *$p < 0.05$, **$p < 0.01$.

PHA-L, LPS, and TNF-α. MNCs primed with LPS increased the migration of UC-MSCs compared with MNCs alone at 8 × 10^2 MNCs/well, but the influence of LPS-primed MNCs on the migration was observed less at the lower amount of MNCs (4 × 10^2; Figure 3C). Conversely, the migration of UC-MSCs toward MNCs primed with PHA-L and TNF-α was attenuated rather than accelerated.

3.5 Influence of inhibitors on the migration of MSCs

The amounts of CCL2, CCL7, and CXCL2 were elevated in UC-MSCs co-cultured with MLR, but these chemokines did not increase the migration potency of UC-MSCs. We then studied the influence of PDGF, IGF-1, and MMPs, which are well-known migration growth factors, on the migration of MSCs. Considering that these factors have several subtypes, we used inhibitors for PDGFA/B, IGF-1, and MMPs (MMP2, MMP9, and MMP14). We added AG1296 for PDGF, PPP for IGF-1, and GM6001 for MMPs, into the migration system of UC-MSCs toward the MLR. The migration of UC-MSCs toward the MLR was inhibited by the PDGF, IGF-1, and MMPs inhibitors in a dose-dependent manner (Figure 4A).

Supplementation with 10% FBS increased the migration potency of all types of MSCs. Thus, we conducted an inhibition assay using inhibitors for PDGFA/B, IGF-1, and MMPs. In the presence of FBS, the migration of all types of MSCs was inhibited by AG1296, PPP, and GM6001 in a dose-dependent manner. The migration of BM- and AD-MSCs required a higher GM6001 dose (Figure 4B–D). qRT-PCR results demonstrated that the amounts of MMP2, MMP9, and MMP14 increased more in BM- and AD-MSCs than those in UC-MSCs (Supplementary Figure S4C–E).

4 Discussion

UC-MSCs grow faster and have a higher maximal proliferation limit than BM-and AD-MSCs. Rapid proliferation increases the number of cells in a limited period and reduces the culture cost. UC-MSCs could proliferate up to more than 40 PDL, AD-MSCs approximately 30 PDL, and BM-MSCs less than approximately 20 PDL. UC, BM, and AD-MSCs expressed the same surface markers as those defined by ISCT. However, UC-MSCs showed less potency for differentiating into osteocytes than BM- and AD-MSCs, which is consistent with the finding of a previous study (Drela et al., 2016; Calcat et al., 2023). Hsieh et al. (2010) demonstrated that WJ-MSCs (UC-MSCs without vessels before culture) express more angiogenesis- and growth-related genes, including epidermal growth factor and FLT1, whereas BM-MSCs express more osteogenic genes, such as RUNX2, DLX5, and NPR3 (Hsieh et al., 2010). The gene expression pattern of BM-MSCs is more similar to that of osteoblasts than WJ-MSCs, suggesting a better osteogenic potential. By contrast, WJ-MSCs are more primitive because they share more common genes with embryonic stem cells and can less differentiate into osteocytes. We also demonstrated through PCR that UC-MSCs express Oct4, Nanog, and SSEA3/4 (He et al., 2014). Drela et al. (2016) reported that Wharton's jelly-MSCs (UC-MSCs without vessels) exhibit a higher proliferation rate than BM-MSCs, representing an example of immature-type "pre-MSC," which is largely composed of embryonic-like, pluripotent cells with the default neural-like differentiation.

Migration is the first important step for MSCs to become functional. Compared with BM- and AD- MSCs, UC-MSCs showed significantly higher migration potency toward unstimulated MNCs and allogenic MLR. In corresponding to higher migration, the CCL2, CCL7, and CXCL2 levels were significantly higher in UC-MSCs co-cultured with MLR than in MLR, FBS, MNCs, and MSCs alone and in BM- and AD-MSCs co-cultured with MLR. Specifically, their levels were more than 10-fold greater in MLR with UC-MSCs than in MLR with BM- and AD-MSCs, suggesting a unique response of UC-MSCs to FBS and inflammation. These chemokines were not elevated in MLR or MLR with BM-, AD-MSCs, such as CCL11, MIG, and RANTES. We hypothesized that UC-MSCs increase the migration potency in response to the self-secreted CCL2, CCL7, and CXCL2 by an autocrine mechanism. However, none of these chemokines could significantly induce the migration of UC-MSCs. To prove these results, we studied the possible receptors for CCL2, such as CCR1, CCR2, CCR3, CCR4, and CCR5 (She et al., 2022). Flow cytometry results showed negative expression of CCR2, CCR3, and CCR5; moreover, CCR1 and CCR4 had low mRNA levels in UC-MSCs (Supplementary Figure S3A–E), although the expression levels of BM- and AD-MSCs are controversial (Ponte et al., 2007; Baek et al., 2011; She et al., 2022). Ponte et al. reported BM-MSCs did not migrate towards CCL2 (MCP-1), although low-positive for CCR2, positive for CCR3, CCR4, and CCR5. UC-MSCs did not respond to these chemokines, suggesting that these chemokines may educate or recruit the other cells in response to MNC in MLR rather than induce chemotaxis of UC-MSCs.

CCL2, CCL7, and CXCL2 are potent chemotactic factors that cause the accumulation of monocytes polarized from M1 to M2 macrophages (Sierra-Filardi et al., 2014; Bao et al., 2022; Wu et al., 2022). Recently, CCL2 has attracted attention as a target in cancer therapy because of its immunosuppression in cancer extensions (Fei et al., 2021; Fei et al., 2021). Sierra-Filardi et al. (2014) (Sierra-Filardi et al., 2014) found that CCL2 determines the extent of macrophage polarization from M1 to M2, whereas CCL2-CCR2 blockade by CCR2 upregulates the expression of M1 polarization-associated genes and cytokines and downregulates the expression of M2-associated markers in human macrophages (Wu et al., 2022). CCL2 recruits not only monocytes but also regulatory T cells, neural progenitor cells, microglia, hepatic stellate cells, and several tumor cells, which express CCR2. CCL2 knockout causes abnormal monocyte recruitment in mice and several inflammatory models *in vivo* and influences the expression of cytokines related to T helper responses (Lu et al., 1998). Zhang et al. (2021) (Zhang et al., 2021) reported that human BM-MSCs enhance the chemotaxis of T cells activated by IL-2 and inhibit their proliferation through the CCL2–CCR2 axis. Furthermore, Cao et al. (2021) (Cao et al., 2021) demonstrated that CCL2 plays an important role in the treatment of idiopathic pneumonia syndrome (IPS) in an acute GVHD mouse model. In an IPS mouse model, the application of mouse BM-MSCs prolongs survival and reduces pathological damage and T cell infiltration into the lung tissue, whereas the administration of CCR2 or

CCL2 antagonists in MSC-treated mice significantly attenuates the prophylactic effect of MSCs on IPS. Although these previous studies demonstrated that the CCL2-CCR2 axis is related to BM-MSCs, UC-MSCs secreting higher levels of CCL2 and CCL7 than BM-MSCs may have some advantages over BM-MSCs in treating IPS as a complication of HSC transplantation. Wu et al. (Wu et al., 2022) found through lung metastasis analysis that CCL7 is highly expressed in lung adenocarcinoma and that its knockdown suppresses chemotaxis and M2 skewing in macrophages. Bao et al. (2022) (Bao et al., 2022) reported that CXCL2 is highly expressed in the lung metastasis of colorectal cancer and induces the activation and attraction of M2 macrophages. Taken together, our results suggest that inflammation induces UC-MSCs to secrete CCL2, CCL7, and CXCL2, which may not activate the migration of UC-MSCs, but may accumulate and recruit macrophages to polarize into the M2 phenotype to control inflammation. The mechanisms and functions of these chemokines in immune systems have not been fully understood, and the effects of CCL2, CCL7, and CXCL2 secreted by UC-MSCs on the immune cells remained to be elucidated. Thus, further studies should focus on the migration of MNCs toward UC-MSCs and/or the direct influence of UC-MSCs co-cultured with MLR on the immune cells to elucidate the function of MSCs.

With regard the other cytokines in UC-MSCs, IL-8 was also significantly induced in UC-MSCs co-cultured with MLR or in the presence of FBS, compared with that in BM-MSC co-cultured with MLR and FBS. IL-8 (CXCL8) is an inflammatory cytokine that induces neutrophil chemotaxis, phagocytosis, and angiogenesis. In the MLR suppression and regulatory T cell induction, Barcia et al. (2015) (Barcia et al., 2015) reported that UC-MSCs are less immunogenic and show higher immunosuppressive activity than BM-MSCs. UC-MSCs showed lower expression levels of HLA-DR, HO-1, IGFBP1/4/6, ILR1, IL6R, and PTGES and higher expression levels of CD200, CD273, CD274, IL1B, IL-8, LIF, and TGFB2 than BM-MSCs, although the functional role of IL-8 in the suppression of MLR remains to be elucidated. By contrast, CXCL9 (MIG), CCL5 (RANTES), and CCL11 (Eotaxin) levels were elevated in MLR, and co-culture of MSCs with MLR did not increase these levels further, suggesting that these chemokines may induce the migration of MSCs or activate the functions. The levels of inflammatory cytokine CXCL10 (IP10) were higher in AD-MSCs than in UC- and BM-MSCs. Although the role of IP-10 in AD-MSCs co-cultured with MLR was not yet clarified, the potency of AD-MSCs in suppressing activated T cells in allogenic MLR was not inferior to those of UC-MSCs and BM-MSCS *in vitro*. In the present study, SDF-1 levels were higher in BM-MSCs and AD-MSCs than in UC-MSCs. This result is theoretical because BM-MSCs support HSC expansion in the BM (Marquez-Curtis and Janowska-Wieczorek, 2013), although the high SDF-1 secretion of AD-MSCs is unexpected.

We next studied the migration potency of UC-MSCs co-cultured with MNCs stimulated by PHA-L, LPS, and TNF-α. Interestingly, the migration potency of UC-MSCs toward MNCs increased when stimulated with LPS, but MNCs stimulated by PHA-L and TNF-α failed to promote the migration of UC-MSCs. We could not exclude the direct interaction of these reagents in the study, even though we washed once before co-culture. Interestingly, UC-MSCs were sensitive to migrate toward the unstimulated MNCs in a dose-dependent manner, although packed high concentration showed the reverse results, suggesting the inhibition factors secreted by packed MNCs. We could not measure and analyze the chemokines in the study. These results suggested that UC-MSCs are sensitive to migrate toward MNCs, but excess dose or excess stimuli may suppress the migration.

Taken together with the above results, we needed to identify the key factors inducing the migration of UC-MSCs co-cultured with MNCs and MLR. Previous studies reported that PDGFA/B, IGF-1, and MMPs (MMP2, MMP9, MMP14, and TIMP1/2) are the key factors inducing the migration in the presence of FBS, a secure migration inducer (Mishima et al., 2010). Considering that these factors have several subtypes, we used the inhibitors AG1296 for PDGF, PPP for IGF-1, and GM6001 for MMPs and found that the migration of UC-MSCs was partially attenuated by the addition of these inhibitory factors in a dose-dependent manner. The results suggested that PDGFA/B, IGF-1 and MMPs play important roles even in the migration of UC-MSCs toward the MLR. We also conducted inhibition assays using UC-, BM-, and AD-MSCs supplemented with FBS as the control. As expected, the migration potencies of the three types of MSCs were attenuated by PDGF, IGF-1, and MMP inhibitors. The MMP inhibitor GM6001 was required more concentration in BM-, and AD-MSCs than UC-MSCs, possibly because of the larger amount of MMPs in these MSCs than in UC-MSCs (Supplementary Figure S4). In the present study, we did not demonstrate the influence of UC-MSCs on MNC characteristics, including polarization. To clarify the benefit of UC-MSCs, we need to identify the specific factors secreted by MLR or receptors in UC-MSCs.

This study has some limitations. In the relationship of migration/the specific elevation of chemokines in UC-MSCs and immunosuppressive potency, the three types of MSCs also showed no difference in MLR inhibitory effect (Supplementary Figure S1). Migration and MLR inhibition assays are carried out under different conditions because FBS is required in the MLR inhibition assay (Nagamura-Inoue et al., 2022). Moreover, the co-culture period differs between the migration assay (overnight) and MLR inhibition assay (4 days). Therefore, we could not conclude that the migration ability is reflected in our MLR inhibition ability. Thus, time-course experiments may be required to identify additional differences among chemokines or MSCs in the future. However, the fact that UC-MSCs may be more sensitive to migrate to the activated or non-activated lymphocytes than BM- and AD-MSCs might be one of the advantages of UC-MSCs over the two other MSC types in the clinical treatment of acute GVHD.

In conclusion, UC-MSCs showed faster proliferation and higher migration potency toward activated or non-activated MNCs than BM- and AD-MSCs. The functional chemotactic factors may vary among MSCs derived from different tissue sources, although the role of specific chemokines in the different sources of MSCs remained to be resolved.

Data availability statement

The original contributions presented in the study are included in the article/Supplementary Material, further inquiries can be directed to the corresponding author.

Ethics statement

The studies involving humans were approved by the Ethics Committee of the Institute of Medical Science, University of Tokyo (IMSUT) (No. 2021-108). UC-MSCs were provided by the IMSUT Hospital Cord Blood and Cord Bank (IMSUT CORD), Japan. IMSUT CORD activity was reviewed and approved by the IRB (No. 35-2). The studies were conducted in accordance with the local legislation and institutional requirements. Written informed consent for participation in this study was provided by the participants' legal guardians/next of kin.

Author contributions

AH: Writing–review and editing, Writing–original draft, Validation, Methodology, Investigation, Formal Analysis. AT: Writing–review and editing, Validation, Methodology, Investigation, Formal Analysis, Data curation. YM: Writing–review and editing, Methodology, Investigation. SY: Writing–review and editing, Resources. MS: Writing–review and editing, Resources. TM: Writing–review and editing, Formal Analysis. FN: Writing–review and editing, Validation, Funding acquisition. TN-I: Writing–review and editing, Writing–original draft, Validation, Supervision, Project administration, Funding acquisition, Formal Analysis, Data curation.

Funding

The author(s) declare that financial support was received for the research, authorship, and/or publication of this article. This study was supported by Grants-in-Aids for Scientific Research from the Japan Agency for Medical Research and Development (AMED) (Project Number (PJ):19bk0104070h0003/20bk01041h0001/21bk0104109h0002). AMED No. 21be0804004h0001/22be0804004h0002/23be0804004h0003 support the stable delivery of somatic stem cells to researchers and companies as cord blood and UC-MSC medical products. This study was partially supported by a joint research study of the University of Tokyo with Human Life Cord Japan Inc. on the basic study of UC-MSCs and the development of banking (September 2017). TN-I is a senior medical advisor at Human Life Cord Japan Inc.

Acknowledgments

We thank Dr. Narita at the School of Health Sciences, Faculty of Medicine, Niigata University, for providing the PMDC05 cell line. We thank Ms. Nagaya for the technical support. We would like to thank Editage (www.editage.jp) for English language editing.

Conflict of interest

The authors declare that the research was conducted in the absence of any commercial or financial relationships that could be construed as a potential conflict of interest.

The author(s) declared that they were an editorial board member of Frontiers, at the time of submission. This had no impact on the peer review process and the final decision.

Publisher's note

Supplementary material

The Supplementary Material for this article can be found online at: https://www.frontiersin.org/articles/10.3389/fcell.2024.1329218/full#supplementary-material

References

Baek, S. J., Kang, S. K., and Ra, J. C. (2011). *In vitro* migration capacity of human adipose tissue-derived mesenchymal stem cells reflects their expression of receptors for chemokines and growth factors. *Exp. Mol. Med.* 43, 596–603. doi:10.3858/emm.2011.43.10.069

Bao, Z., Zeng, W., Zhang, D., Wang, L., Deng, X., Lai, J., et al. (2022). SNAIL induces EMT and lung metastasis of tumours secreting CXCL2 to promote the invasion of M2-type immunosuppressed macrophages in colorectal cancer. *Int. J. Biol. Sci.* 18, 2867–2881. doi:10.7150/ijbs.66854

Barcia, R. N., Santos, J. M., Filipe, M., Teixeira, M., Martins, J. P., Almeida, J., et al. (2015). What makes umbilical cord tissue-derived mesenchymal stromal cells superior immunomodulators when compared to bone marrow derived mesenchymal stromal cells? *Stem Cells Int.* 2015, 583984. doi:10.1155/2015/583984

Calcat, I. C. S., Rendra, E., Scaccia, E., Amadeo, F., Hanson, V., Wilm, B., et al. (2023). Harmonised culture procedures minimise but do not eliminate mesenchymal stromal cell donor and tissue variability in a decentralised multicentre manufacturing approach. *Stem Cell Res. Ther.* 14, 120. doi:10.1186/s13287-023-03352-1

Cao, M., Liu, H., Dong, Y., Liu, W., Yu, Z., Wang, Q., et al. (2021). Mesenchymal stem cells alleviate idiopathic pneumonia syndrome by modulating T cell function through CCR2-CCL2 axis. *Stem Cell Res. Ther.* 12, 378. doi:10.1186/s13287-021-02459-7

Dilogo, I. H., Aditianingsih, D., Sugiarto, A., Burhan, E., Damayanti, T., Sitompul, P. A., et al. (2021). Umbilical cord mesenchymal stromal cells as critical COVID-19 adjuvant therapy: a randomized controlled trial. *Stem Cells Transl. Med.* 10, 1279–1287. doi:10.1002/sctm.21-0046

Dominici, M., Le Blanc, K., Mueller, I., Slaper-Cortenbach, I., Marini, F., Krause, D., et al. (2006). Minimal criteria for defining multipotent mesenchymal stromal cells. The International Society for Cellular Therapy position statement. *Cytotherapy* 8, 315–317. doi:10.1080/14653240600855905

Drela, K., Lech, W., Figiel-Dabrowska, A., Zychowicz, M., Mikula, M., Sarnowska, A., et al. (2016). Enhanced neuro-therapeutic potential of Wharton's Jelly-derived mesenchymal stem cells in comparison with bone marrow mesenchymal stem cells culture. *Cytotherapy* 18, 497–509. doi:10.1016/j.jcyt.2016.01.006

Fei, L., Ren, X., Yu, H., and Zhan, Y. (2021). Targeting the CCL2/CCR2 Axis in cancer immunotherapy: one stone, three birds? *Front. Immunol.* 12, 771210. doi:10.3389/fimmu.2021.771210

Fiedler, J., Etzel, N., and Brenner, R. E. (2004). To go or not to go: migration of human mesenchymal progenitor cells stimulated by isoforms of PDGF. *J. Cell Biochem.* 93, 990–998. doi:10.1002/jcb.20219

Gnecchi, M., and Melo, L. G. (2009). Bone marrow-derived mesenchymal stem cells: isolation, expansion, characterization, viral transduction, and production of conditioned medium. *Methods Mol. Biol.* 482, 281–294. doi:10.1007/978-1-59745-060-7_18

Gruber, H. E., Deepe, R., Hoelscher, G. L., Ingram, J. A., Norton, H. J., Scannell, B., et al. (2010). Human adipose-derived mesenchymal stem cells: direction to a phenotype sharing similarities with the disc, gene expression profiling, and coculture with human annulus cells. *Tissue Eng. Part A* 16, 2843–2860. doi:10.1089/ten.TEA.2009.0709

He, H., Nagamura-Inoue, T., Takahashi, A., Mori, Y., Yamamoto, Y., Shimazu, T., et al. (2015). Immunosuppressive properties of Wharton's jelly-derived mesenchymal stromal cells *in vitro*. *Int. J. Hematol.* 102, 368–378. doi:10.1007/s12185-015-1844-7

He, H., Nagamura-Inoue, T., Tsunoda, H., Yuzawa, M., Yamamoto, Y., Yorozu, P., et al. (2014). Stage-specific embryonic antigen 4 in Wharton's jelly-derived mesenchymal stem cells is not a marker for proliferation and multipotency. *Tissue Eng. Part A* 20, 1314–1324. doi:10.1089/ten.TEA.2013.0333

He, H., Takahashi, A., Mukai, T., Hori, A., Narita, M., Tojo, A., et al. (2021). The immunomodulatory effect of triptolide on mesenchymal stromal cells. *Front. Immunol.* 12, 686356. doi:10.3389/fimmu.2021.686356

Hsieh, J. Y., Fu, Y. S., Chang, S. J., Tsuang, Y. H., and Wang, H. W. (2010). Functional module analysis reveals differential osteogenic and stemness potentials in human mesenchymal stem cells from bone marrow and Wharton's jelly of umbilical cord. *Stem Cells Dev.* 19, 1895–1910. doi:10.1089/scd.2009.0485

Kasper, G., Glaeser, J. D., Geissler, S., Ode, A., Tuischer, J., Matziolis, G., et al. (2007). Matrix metalloprotease activity is an essential link between mechanical stimulus and mesenchymal stem cell behavior. *Stem Cells* 25, 1985–1994. doi:10.1634/stemcells.2006-0676

Korbecki, J., Kojder, K., Siminska, D., Bohatyrewicz, R., Gutowska, I., Chlubek, D., et al. (2020). CC chemokines in a tumor: a review of pro-cancer and anti-cancer properties of the ligands of receptors CCR1, CCR2, CCR3, and CCR4. *Int. J. Mol. Sci.* 21, 8412. doi:10.3390/ijms21218412

Kurogi, H., Takahashi, A., Isogai, M., Sakumoto, M., Takijiri, T., Hori, A., et al. (2021). Umbilical cord derived mesenchymal stromal cells in microcarrier based industrial scale culture sustain the immune regulatory functions. *Biotechnol. J.* 16, e2000558. doi:10.1002/biot.202000558

Lanzoni, G., Linetsky, E., Correa, D., Messinger Cayetano, S., Alvarez, R. A., Kouroupis, D., et al. (2021). Umbilical cord mesenchymal stem cells for COVID-19 acute respiratory distress syndrome: a double-blind, phase 1/2a, randomized controlled trial. *Stem Cells Transl. Med.* 10, 660–673. doi:10.1002/sctm.20-0472

Le Blanc, K., and Davies, L. C. (2015). Mesenchymal stromal cells and the innate immune response. *Immunol. Lett.* 168, 140–146. doi:10.1016/j.imlet.2015.05.004

Liesveld, J. L., Sharma, N., and Aljitawi, O. S. (2020). Stem cell homing: from physiology to therapeutics. *Stem Cells* 38, 1241–1253. doi:10.1002/stem.3242

Lu, B., Rutledge, B. J., Gu, L., Fiorillo, J., Lukacs, N. W., Kunkel, S. L., et al. (1998). Abnormalities in monocyte recruitment and cytokine expression in monocyte chemoattractant protein 1-deficient mice. *J. Exp. Med.* 187, 601–608. doi:10.1084/jem.187.4.601

Marquez-Curtis, L. A., and Janowska-Wieczorek, A. (2013). Enhancing the migration ability of mesenchymal stromal cells by targeting the SDF-1/CXCR4 axis. *Biomed. Res. Int.* 2013, 561098. doi:10.1155/2013/561098

Mishima, S., Nagai, A., Abdullah, S., Matsuda, C., Taketani, T., Kumakura, S., et al. (2010). Effective *ex vivo* expansion of hematopoietic stem cells using osteoblast-differentiated mesenchymal stem cells is CXCL12 dependent. *Eur. J. Haematol.* 84, 538–546. doi:10.1111/j.1600-0609.2010.01419.x

Mishima, Y., and Lotz, M. (2008). Chemotaxis of human articular chondrocytes and mesenchymal stem cells. *J. Orthop. Res.* 26, 1407–1412. doi:10.1002/jor.20668

Montemurro, T., Andriolo, G., Montelatici, E., Weissmann, G., Crisan, M., Colnaghi, M. R., et al. (2011). Differentiation and migration properties of human foetal umbilical cord perivascular cells: potential for lung repair. *J. Cell Mol. Med.* 15, 796–808. doi:10.1111/j.1582-4934.2010.01047.x

Mori, Y., Ohshimo, J., Shimazu, T., He, H., Takahashi, A., Yamamoto, Y., et al. (2015). Improved explant method to isolate umbilical cord-derived mesenchymal stem cells and their immunosuppressive properties. *Tissue Eng. Part C Methods* 21, 367–372. doi:10.1089/ten.TEC.2014.0385

Mukai, T., Mori, Y., Shimazu, T., Takahashi, A., Tsunoda, H., Yamaguchi, S., et al. (2017). Intravenous injection of umbilical cord-derived mesenchymal stromal cells attenuates reactive gliosis and hypomyelination in a neonatal intraventricular hemorrhage model. *Neuroscience* 355, 175–187. doi:10.1016/j.neuroscience.2017.05.006

Mukai, T., Nagamura-Inoue, T., Shimazu, T., Mori, Y., Takahashi, A., Tsunoda, H., et al. (2016). Neurosphere formation enhances the neurogenic differentiation potential and migratory ability of umbilical cord-mesenchymal stromal cells. *Cytotherapy* 18, 229–241. doi:10.1016/j.jcyt.2015.10.012

Murata, M., Terakura, S., Wake, A., Miyao, K., Ikegame, K., Uchida, N., et al. (2021). Off-the-shelf bone marrow-derived mesenchymal stem cell treatment for acute graft-versus-host disease: real-world evidence. *Bone Marrow Transpl.* 56, 2355–2366. doi:10.1038/s41409-021-01304-y

Nagamura-Inoue, T., Kato, S., Najima, Y., Isobe, M., Doki, N., Yamamoto, H., et al. (2022). Immunological influence of serum-free manufactured umbilical cord-derived mesenchymal stromal cells for steroid-resistant acute graft-versus-host disease. *Int. J. Hematol.* 116, 754–769. doi:10.1007/s12185-022-03408-7

Narita, M., Kuroha, T., Watanabe, N., Hashimoto, S., Tsuchiyama, J., Tochiki, N., et al. (2008). Plasmacytoid dendritic cell leukemia with potent antigen-presenting ability. *Acta Haematol.* 120, 91–99. doi:10.1159/000165510

Narita, M., Watanabe, N., Yamahira, A., Hashimoto, S., Tochiki, N., Saitoh, A., et al. (2009). A leukemic plasmacytoid dendritic cell line, PMDC05, with the ability to secrete IFN-alpha by stimulation via Toll-like receptors and present antigens to naive T cells. *Leuk. Res.* 33, 1224–1232. doi:10.1016/j.leukres.2009.03.047

Nazari, M., Ni, N. C., Ludke, A., Li, S. H., Guo, J., Weisel, R. D., et al. (2016). Mast cells promote proliferation and migration and inhibit differentiation of mesenchymal stem cells through PDGF. *J. Mol. Cell Cardiol.* 94, 32–42. doi:10.1016/j.yjmcc.2016.03.007

Ponte, A. L., Marais, E., Gallay, N., Langonne, A., Delorme, B., Herault, O., et al. (2007). The *in vitro* migration capacity of human bone marrow mesenchymal stem cells: comparison of chemokine and growth factor chemotactic activities. *Stem Cells* 25, 1737–1745. doi:10.1634/stemcells.2007-0054

She, S., Ren, L., Chen, P., Wang, M., Chen, D., Wang, Y., et al. (2022). Functional roles of chemokine receptor CCR2 and its ligands in liver disease. *Front. Immunol.* 13, 812431. doi:10.3389/fimmu.2022.812431

Shimazu, T., Mori, Y., Takahashi, A., Tsunoda, H., Tojo, A., and Nagamura-Inoue, T. (2015). Serum- and xeno-free cryopreservation of human umbilical cord tissue as mesenchymal stromal cell source. *Cytotherapy* 17, 593–600. doi:10.1016/j.jcyt.2015.03.604

Sierra-Filardi, E., Nieto, C., Dominguez-Soto, A., Barroso, R., Sanchez-Mateos, P., Puig-Kroger, A., et al. (2014). CCL2 shapes macrophage polarization by GM-CSF and M-CSF: identification of CCL2/CCR2-dependent gene expression profile. *J. Immunol.* 192, 3858–3867. doi:10.4049/jimmunol.1302821

Tondreau, T., Meuleman, N., Stamatopoulos, B., De Bruyn, C., Delforge, A., Dejeneffe, M., et al. (2009). *In vitro* study of matrix metalloproteinase/tissue inhibitor of metalloproteinase production by mesenchymal stromal cells in response to inflammatory cytokines: the role of their migration in injured tissues. *Cytotherapy* 11, 559–569. doi:10.1080/14653240903051541

Wang, C., Li, X., Dang, H., Liu, P., Zhang, B. O., and Xu, F. (2019). Insulin-like growth factor 2 regulates the proliferation and differentiation of rat adipose-derived stromal cells via IGF-1R and IR. *Cytotherapy* 21, 619–630. doi:10.1016/j.jcyt.2018.11.010

Wu, Z., Bai, X., Lu, Z., Liu, S., and Jiang, H. (2022). LINC01094/SPI1/CCL7 Axis promotes macrophage accumulation in lung adenocarcinoma and tumor cell dissemination. *J. Immunol. Res.* 2022, 6450721. doi:10.1155/2022/6450721

Zhang, Y. L., Qiao, S. K., Xing, L. N., Guo, X. N., and Ren, J. H. (2021). Mesenchymal stem cells enhance chemotaxis of activated T cells through the CCL2-CCR2 Axis *in vitro*. *Bull. Exp. Biol. Med.* 172, 263–269. doi:10.1007/s10517-021-05373-3

frontiers | Frontiers in Cell and Developmental Biology

TYPE Mini Review
PUBLISHED 27 March 2024
DOI 10.3389/fcell.2024.1379091

OPEN ACCESS

EDITED BY
Tokiko Nagamura-Inoue,
The University of Tokyo, Japan

REVIEWED BY
Yuyao Tian,
Massachusetts General Hospital and Harvard Medical School, United States

*CORRESPONDENCE
Virginia Egea,
Virginia.Egea@med.uni-muenchen.de

RECEIVED 30 January 2024
ACCEPTED 15 March 2024
PUBLISHED 27 March 2024

CITATION
Egea V (2024), Caught in action: how MSCs modulate atherosclerotic plaque.
Front. Cell Dev. Biol. 12:1379091.
doi: 10.3389/fcell.2024.1379091

Caught in action: how MSCs modulate atherosclerotic plaque

Virginia Egea[1,2]*

[1]Institute for Cardiovascular Prevention (IPEK), Ludwig-Maximilians-University, Munich, Germany, [2]DZHK (German Center for Cardiovascular Research), Partner Site Munich Heart Alliance, Munich, Germany

Atherosclerosis (AS) is a medical condition marked by the stiffening and constriction of the arteries. This is caused by the accumulation of plaque, a substance made up of fat, cholesterol, calcium, and other elements present in the blood. Over time, this plaque solidifies and constricts the arteries, restricting the circulation of oxygen-rich blood to the organs and other body parts. The onset and progression of AS involve a continuous inflammatory response, including the infiltration of inflammatory cells, foam cells derived from monocytes/macrophages, and inflammatory cytokines and chemokines. *Mesenchymal stromal cells* (*MSCs*), a type of multipotent stem cells originating from various body tissues, have recently been demonstrated to have a protective and regulatory role in diseases involving inflammation. Consequently, the transplantation of MSCs is being proposed as a novel therapeutic strategy for atherosclerosis treatment. This mini-review intends to provide a summary of the regulatory effects of MSCs at the plaque site to lay the groundwork for therapeutic interventions.

KEYWORDS

MSCs, atherosclerotic plaques, cell-therapy, Trojan horse approach, migration

Introduction

Atherosclerosis is a chronic inflammatory reaction of the blood vessel wall caused by dyslipidemia (Weber and Noels, 2011). Inflammation is important in all stages of atherosclerosis, from plaque formation to rupture (Libby, 2021). When the endothelium is dysfunctional, it disrupts the balance between pro-inflammatory and protective pathways, leading to the accumulation of atherogenic lipoproteins. This triggers the release of chemotactic factors that recruit immune cells and promote the formation of atherosclerotic plaques. Despite the availability of appropriate pharmacological and surgical treatment modalities, AS remains the leading cause of cardiovascular death worldwide (Vaduganathan et al., 2022). Current treatment strategies aim to stabilize plaque, suppress inflammation, and lower serum lipid levels. Interestingly, stem cells exhibit a range of effects, including the ability to regulate lipid levels, suppress inflammation, repair damaged tissues, and support hematopoiesis, offering an innovative approach to the treatment of AS (Nauta and Fibbe, 2007; Li et al., 2017). MSC are present in nearly all tissues and originate from various sources such as bone marrow, adipose tissue, and peripheral blood. These cells possess the ability to differentiate into multiple cell types belonging to the mesodermal and myogenic lineages, a process influenced by environmental stimuli (Pittenger et al., 1999). In addition, MSCs produce a wide array of chemokines, cytokines, and growth factors in response to their surroundings, bestowing upon them immunomodulatory and anti-fibrotic characteristics (Nauta and Fibbe, 2007). In the realm of cell-based therapies MSCs are considered to be exceptional

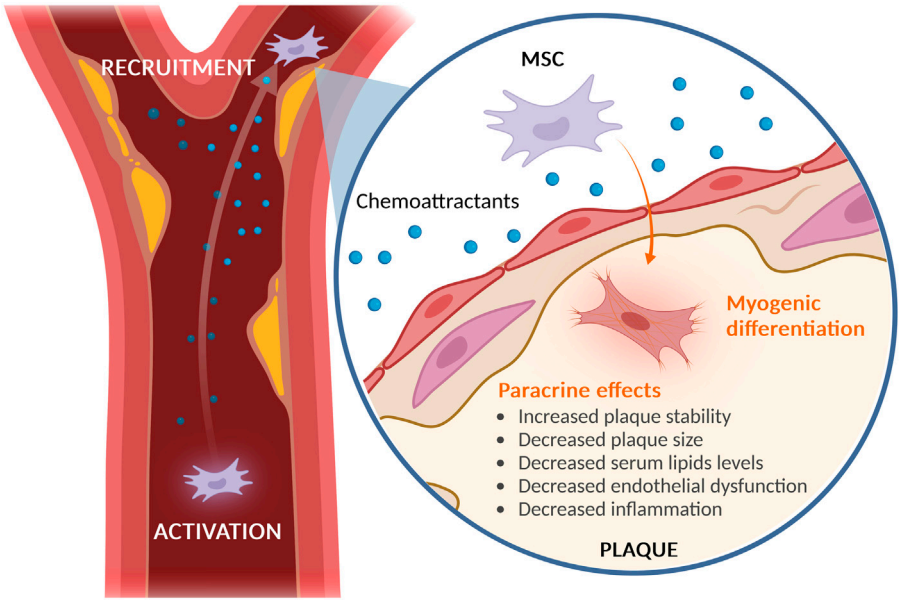

FIGURE 1
Recruitment of MSCs to Atherosclerotic Plaque. *MSCs* exhibit a natural tendency to migrate to sites of inflammation, including atherosclerotic plaques. Once at these sites, MSCs display a protective role primarily through paracrine signaling, which helps in reducing endothelial dysfunction, hyperlipidemia, and inflammation. This results in an overall increase in plaque stability and decrease in plaque size. Furthermore, studies have shown that MSCs are stimulated by the surrounding atherosclerotic plaque to differentiate into myogenic cells.[11] Created with BioRender.com.

candidates (Lalu et al., 2012; Samsonraj et al., 2017). Their capacity to differentiate into different cell types and *in vitro* expansion are well-established (Salem and Thiemermann, 2010). For therapeutic strategies, it may be feasible to manipulate MSCs *in vitro* and reinfuse them into patients, primarily mitigating risk factors linked to the onset of atherosclerosis, predominantly through a paracrine mechanism. In this scenario, the efficient recruitment of cells to the plaque site is of paramount importance.

Activation and recruitment of MSC to the atherosclerotic plaques

While the paracrine role of MSCs is increasingly acknowledged, the mechanisms of their migration from the bloodstream to targeted lesions with compromised vascular integrity are not fully understood. Our studies demonstrated that in response to chemotactic signals such as transforming growth factor-beta 1 (TGF-β1), stromal cell-derived factor 1 (SDF-1), interleukin-1 beta (IL-1β) and tumor necrosis factor-alpha (TNF-α), MSCs are able to invade through barriers of extracellular matrix (ECM) facilitated by the secretion of matrix metalloproteinases (MMPs) (Ries et al., 2007). MSCs are capable of migrating through human reconstituted basement membranes, utilizing MMP-2, membrane type 1-MMP (MT1-MMP), and tissue inhibitor of metalloproteinases TIMP-2 for this purpose. TGF-β1 has been identified to increase the levels of MMP-2 and MT1-MMP without affecting TIMP-1 or TIMP-2, indicating its significant role in MSC trafficking through the extracellular matrix (ECM) by inducing these MMPs. Additionally, IL-1β and tumor necrosis factor-alpha TNF-α, which are typically present in wounds and inflamed tissues, have been shown to significantly enhance the expression of MMP-9 and MT1-MMP, thereby promoting MSC invasion. In contrast, SDF-1 has a comparatively minor effect on MSC migration, which may be attributed to a smaller subset of MSCs expressing the C-X-C motif chemokine receptor 4 (CXCR4) receptor or to the MMP-mediated cleavage of SDF-1 (Ries et al., 2007). Nevertheless, blocking the SDF-1/CXCR4 signaling pathway markedly reduces the recruitment of transplanted stem cells to target tissues (Son et al., 2006; Wang et al., 2006). Atherosclerotic plaques, being inflammatory lesions, also generate high levels of cathelicidin antimicrobial peptide LL-37, a small peptide derived from neutrophils which is believed to contribute to disease progression (Zhang et al., 2015). LL-37 has been demonstrated to elevate early growth response factor 1 (*EGR1*) expression and stimulate mitogen-activated protein kinase (MAPK) activation, thereby augmenting MSC functions such as cell proliferation, cell motility, and paracrine activities. These regulatory effects could prove beneficial for tissue regeneration applications, particularly in the context of implantation (Yang et al., 2016). Own recently findings indicate that LL-37, known to be prevalent in the plasma and plaques of atherosclerosis patients, serves as a chemoattractant for MSCs (Egea et al., 2023). Our investigation also identified microRNA (miRNA) let-7f as a pivotal regulator in the LL-37 mediated trafficking of MSCs to inflamed tissues. LL-37 influences cells through formyl peptide receptor 2 (FPR2), a prevalent G protein-coupled receptor that triggers the expression of miRNA let-7f. This, in turn, enhances FPR2 on the cell surface in a positive feedback loop, implying an indirect regulatory function of let-7f by targeting a suppressor of FPR2 expression in these cells (Egea et al., 2023). A similar mechanism of let-7f indirectly boosting CXCR4 expression in MSCs has been previously reported by us. (Egea et al., 2021) Let-7f

not only enhances LL-37/FPR2-mediated chemotaxis towards plaques but also upregulates CXCR4, SDF-1α receptor, and induces the expression and release of ECM-degrading MMP-9, thereby improving pericellular proteolysis. This mechanism may facilitate MSCs recruitment in response to tissue injuries and inflammation under physiological conditions (Egea et al., 2021). At the molecular level, let-7f likely targets repressors of cellular susceptibility and chemotactic migration, thereby promoting MSC invasion Figure 1. In recent studies Hu et al. have also shown integrin beta 3 (ITGB3) to improve plaque-recruitment of MSCs into a mouse model of atherosclerosis (Hu et al., 2023).

Paracrine effects of MSCs in the atherosclerotic plaques

Endothelial dysfunction, the initiator of atherosclerotic plaque formation, involves a positive feedback loop (Marchio et al., 2019). Pathological stimuli such as hypertension cause endothelial damage, leading to the deposition of oxidized LDL (ox-LDL), which triggers an immune response supporting atherogenesis. Nitric oxide (NO), a crucial signaling molecule post-endothelial dysfunction, is produced by endothelial nitric oxide synthase (eNOS) and regulated by Akt-mediated phosphorylation (Fulton, 2016). In atherosclerosis, NO exhibits strong protective effects by inhibiting LDL oxidation, leukocyte adhesion, smooth muscle cell proliferation, and platelet aggregation, while also regulating vascular tone (Marchio et al., 2019).

MSCs have demonstrated the ability to restore endothelial function, thereby stopping atherogenesis (Salvolini et al., 2010). Culture medium from human skin-derived MSCs increased NO production in human aortic endothelial cells, showcasing their paracrine potential (Salvolini et al., 2010). Lin et al. showed that human MSCs prevent ox-LDL-mediated inhibition of eNOS activity in human umbilical vein endothelial cells by phosphorylating and restoring Akt/eNOS activity (Lin et al., 2015).

Furthermore, various studies highlight MSC´s ability to reduce hyperlipidemia, a condition that increases the risk of atherosclerosis, in various animal models (Hong et al., 2019; Libby, 2021). Frodermann et al. reported for instance that using bone marrow-MSCs (BM-MSCs) significantly reduced serum cholesterol levels, particularly very-low-density-lipoproteins (VLDLs), in LDLR−/− mice, 4 weeks post-administration (Frodermann et al., 2015). In a different study, Hong et al. observed that the administration of gingival-MSCs to ApoE−/− mice resulted in a decrease in total cholesterol and LDLs (Hong et al., 2019). They also recorded a reduction in the expression of sterol regulatory element-binding protein 1c (SREBP-1c), a transcription factor involved in fatty acid biosynthesis, and an increase in the expression of peroxisome proliferator-activated receptor-α (PPAR-α), a transcription factor that controls fatty acid β-oxidation. These observations suggest a unique mechanism for MSC-mediated lipid reduction. This theory was further supported by Li et al., who found that the administration of umbilical cord blood-MSCs to leptin-deficient mice resulted in a decrease in lipid levels (Lin et al., 2015). They attributed this to an increase in PPAR-α and a decrease in fatty acid synthase, an enzyme regulated by SREBP-1c, which aligns with Hong et al.'s findings. In summary, there is compelling evidence that the administration of MSCs can reduce serum lipid levels, thereby decreasing lipid accumulation in plaques. However, further research is required to fully comprehend the mechanisms involved and to confirm these results in humans.

Various risk factors such as aging, hypertension, hypercholesterolemia, diabetes, and obesity contribute to the inflammatory onset in AS by promoting the accumulation of ox-LDL, activation of NLRP3 inflammasome, and the recruitment of leukocytes into the plaque (Hoseini et al., 2018). Recent studies have highlighted the anti-inflammatory properties of MSCs, modulating the response of immune cells in the plaque (Lee and Song, 2018).

Dendritic Cells (DCs) are a type of antigen-presenting cells that significantly contribute to the activation of adaptive immunity (Gil-Pulido and Zernecke, 2017). *They play a pivotal role in atherogenesis, as they prime and activate T cells.* Research indicates that MSCs can inhibit the differentiation and maturation of DCs, impair antigen uptake, and decrease the expression of costimulatory molecules (CD80, CD86), thereby reducing T-cell activation and proliferation (Reis et al., 2018). This effect is associated with the secretion of extracellular vesicles containing miRNA-21-5p by MSCs (Roufaiel et al., 2016). *T-lymphocytes* represent another cell type influenced by MSCs. Studies have shown that BM-MSCs can reduce DC-induced $CD2^+$ T-cell proliferation in a dose-dependent manner, through the secretion of anti-inflammatory cytokines such as TGF-β (Di Nicola et al., 2002). Additionally, cell-to-cell contact has been found to enhance this inhibitory effect. However, the necessity of cell-to-cell contact in reducing T-cell proliferation remains a topic of debate.

Monocytes and macrophages are also being influenced by MSCs. Chemotaxis drives monocyte migration from the blood and adventitia into the intima, where they differentiate into macrophages. These mature macrophages can engulf LDLs and become foam cells (Libby, 2021). Several studies have demonstrated that MSCs can reduce macrophage foam cell formation *in vitro* by modulating the expression of scavenger receptors, including CD36, SRA1, and ATP-binding cassette transporter (Wang et al., 2015). Furthermore, MSCs have been shown to reduce the expression of chemokine receptors on inflammatory monocytes and promote phenotype switching to anti-inflammatory macrophages. *In vivo*, the promotion of anti-inflammatory cytokine profiles and suppression of macrophage numbers by MSCs have been used to explain the reduction in plaque size (Li et al., 2015; Zhang et al., 2018).

Differentiation of MSCs within atherosclerotic plaques

MSC have the ability to differentiate into a variety of cell types, including osteoblasts, chondrocytes, myocytes, and adipocytes (Pittenger et al., 1999). Upon recruitment to the plaque site, these MSCs are subjected to the influences of the new environment, which potentially jeopardizes their stemness and triggers differentiation. Recently, our studies provide evidence that human plaque components elicit differentiation of MSCs into smooth muscle cell-like cells (Egea et al., 2023). The role of MSCs in plaque development is complex and bidirectional. Early in plaque formation, MSCs contribute to inflammation and foam cell formation, while in later stages, they produce extracellular matrix proteins and collagen fibers, which help stabilize the plaques (Bennett et al., 2016). Interestingly, vulnerable plaques prone to

rupture are characterized by only few smooth muscle cells in a thin cap (Finn et al., 2010). Thus, myogenic differentiation of MSCs in plaque environment might confer a stabilizing effect in vulnerable plaques in later stages of AS. In fact, transplanted MSCs were shown to stabilize vulnerable plaques in an animal model of atherosclerosis by strengthening the fibrous cap (Wang et al., 2015). Consistently, we found that human plaque lysates upregulated endogenous levels of miR-335 in MSCs, a miRNA shown to promote overall plaque stability (Egea et al., 2023).

Conclusion and future perspective

Numerous research efforts have highlighted the propensity of MSCs to migrate towards atheromatous tissues, contributing to atheroprotection through the secretion of paracrine factors and their maturation into cells that stabilize plaques. The differentiation potential, paracrine effects, exosomal release, and direct-contact modulatory functions of MSCs have been the focus of extensive investigation. Each of these mechanisms plays a role in the holistic process of MSC therapy in AS. Nevertheless, the protective mechanisms of MSCs warrant further exploration. Understanding the function of MSCs in varying stages of atherosclerosis, the disparities among MSC sources, and the efficiency of MSC recruitment to the plaque are all crucial areas for further study to enhance the safety, efficacy, and outcomes of MSC-based therapy.

Author contributions

VE: Writing–original draft, Writing–review and editing.

Funding

The author(s) declare that no financial support was received for the research, authorship, and/or publication of this article.

Conflict of interest

The author declares that the research was conducted in the absence of any commercial or financial relationships that could be construed as a potential conflict of interest.

Publisher's note

All claims expressed in this article are solely those of the authors and do not necessarily represent those of their affiliated organizations, or those of the publisher, the editors and the reviewers. Any product that may be evaluated in this article, or claim that may be made by its manufacturer, is not guaranteed or endorsed by the publisher.

References

Bennett, M. R., Sinha, S., and Owens, G. K. (2016). Vascular smooth muscle cells in atherosclerosis. *Circ. Res.* 118 (4), 692–702. doi:10.1161/CIRCRESAHA.115.306361

Di Nicola, M., Carlo-Stella, C., Magni, M., Milanesi, M., Longoni, P. D., Matteucci, P., et al. (2002). Human bone marrow stromal cells suppress T-lymphocyte proliferation induced by cellular or nonspecific mitogenic stimuli. *Blood* 99 (10), 3838–3843. doi:10.1182/blood.v99.10.3838

Egea, V., Kessenbrock, K., Lawson, D., Bartelt, A., Weber, C., and Ries, C. (2021). Let-7f miRNA regulates SDF-1α- and hypoxia-promoted migration of mesenchymal stem cells and attenuates mammary tumor growth upon exosomal release. *Cell Death Dis.* 12 (6), 516. doi:10.1038/s41419-021-03789-3

Egea, V., Megens, R. T. A., Santovito, D., Wantha, S., Brandl, R., Siess, W., et al. (2023). Properties and fate of human mesenchymal stem cells upon miRNA let-7f-promoted recruitment to atherosclerotic plaques. *Cardiovasc Res.* 119 (1), 155–166. doi:10.1093/cvr/cvac022

Finn, A. V., Nakano, M., Narula, J., Kolodgie, F. D., and Virmani, R. (2010). Concept of vulnerable/unstable plaque. *Arterioscler. Thromb. Vasc. Biol.* 30 (7), 1282–1292. doi:10.1161/ATVBAHA.108.179739

Frodermann, V., van Duijn, J., van Pel, M., van Santbrink, P. J., Bot, I., Kuiper, J., et al. (2015). Mesenchymal stem cells reduce murine atherosclerosis development. *Sci. Rep.* 5, 15559. doi:10.1038/srep15559

Fulton, D. J. (2016). Transcriptional and posttranslational regulation of eNOS in the endothelium. *Adv. Pharmacol.* 77, 29–64. doi:10.1016/bs.apha.2016.04.001

Gil-Pulido, J., and Zernecke, A. (2017). Antigen-presenting dendritic cells in atherosclerosis. *Eur. J. Pharmacol.* 816, 25–31. doi:10.1016/j.ejphar.2017.08.016

Hong, R., Wang, Z., Sui, A., Liu, X., Fan, C., Lipkind, S., et al. (2019). Gingival mesenchymal stem cells attenuate pro-inflammatory macrophages stimulated with oxidized low-density lipoprotein and modulate lipid metabolism. *Arch. Oral Biol.* 98, 92–98. doi:10.1016/j.archoralbio.2018.11.007

Hoseini, Z., Sepahvand, F., Rashidi, B., Sahebkar, A., Masoudifar, A., and Mirzaei, H. (2018). NLRP3 inflammasome: its regulation and involvement in atherosclerosis. *J. Cell Physiol.* 233 (3), 2116–2132. doi:10.1002/jcp.25930

Hu, H. J., Xiao, X. R., Li, T., Liu, D. M., Geng, X., Han, M., et al. (2023). Integrin beta 3-overexpressing mesenchymal stromal cells display enhanced homing and can reduce atherosclerotic plaque. *World J. Stem Cells* 15 (9), 931–946. doi:10.4252/wjsc.v15.i9.931

Lalu, M. M., McIntyre, L., Pugliese, C., Fergusson, D., Winston, B. W., Marshall, J. C., et al. (2012). Safety of cell therapy with mesenchymal stromal cells (SafeCell): a systematic review and meta-analysis of clinical trials. *PLoS One* 7 (10), e47559. doi:10.1371/journal.pone.0047559

Lee, D. K., and Song, S. U. (2018). Immunomodulatory mechanisms of mesenchymal stem cells and their therapeutic applications. *Cell Immunol.* 326, 68–76. doi:10.1016/j.cellimm.2017.08.009

Li, F., Guo, X., and Chen, S. Y. (2017). Function and therapeutic potential of mesenchymal stem cells in atherosclerosis. *Front. Cardiovasc Med.* 4, 32. doi:10.3389/fcvm.2017.00032

Li, Q., Sun, W., Wang, X., Zhang, K., Xi, W., and Gao, P. (2015). Skin-derived mesenchymal stem cells alleviate atherosclerosis via modulating macrophage function. *Stem Cells Transl. Med.* 4 (11), 1294–1301. doi:10.5966/sctm.2015-0020

Libby, P. (2021). The changing landscape of atherosclerosis. *Nature* 592 (7855), 524–533. doi:10.1038/s41586-021-03392-8

Lin, Y. L., Yet, S. F., Hsu, Y. T., Wang, G. J., and Hung, S. C. (2015). Mesenchymal stem cells ameliorate atherosclerotic lesions via restoring endothelial function. *Stem Cells Transl. Med.* 4 (1), 44–55. doi:10.5966/sctm.2014-0091

Marchio, P., Guerra-Ojeda, S., Vila, J. M., Aldasoro, M., Victor, V. M., and Mauricio, M. D. (2019). Targeting early atherosclerosis: a focus on oxidative stress and inflammation. *Oxid. Med. Cell Longev.* 2019, 8563845. doi:10.1155/2019/8563845

Nauta, A. J., and Fibbe, W. E. (2007). Immunomodulatory properties of mesenchymal stromal cells. *Blood* 110 (10), 3499–3506. doi:10.1182/blood-2007-02-069716

Pittenger, M. F., Mackay, A. M., Beck, S. C., Jaiswal, R. K., Douglas, R., Mosca, J. D., et al. (1999). Multilineage potential of adult human mesenchymal stem cells. *Science* 284 (5411), 143–147. doi:10.1126/science.284.5411.143

Reis, M., Mavin, E., Nicholson, L., Green, K., Dickinson, A. M., and Wang, X. N. (2018). Mesenchymal stromal cell-derived extracellular vesicles attenuate dendritic cell maturation and function. *Front. Immunol.* 9, 2538. doi:10.3389/fimmu.2018.02538

Ries, C., Egea, V., Karow, M., Kolb, H., Jochum, M., and Neth, P. (2007). MMP-2, MT1-MMP, and TIMP-2 are essential for the invasive capacity of human mesenchymal stem cells: differential regulation by inflammatory cytokines. *Blood* 109 (9), 4055–4063. doi:10.1182/blood-2006-10-051060

Roufaiel, M., Gracey, E., Siu, A., Zhu, S. N., Lau, A., Ibrahim, H., et al. (2016). CCL19-CCR7-dependent reverse transendothelial migration of myeloid cells clears Chlamydia muridarum from the arterial intima. *Nat. Immunol.* 17 (11), 1263–1272. doi:10.1038/ni.3564

Salem, H. K., and Thiemermann, C. (2010). Mesenchymal stromal cells: current understanding and clinical status. *Stem Cells* 28 (3), 585–596. doi:10.1002/stem.269

Salvolini, E., Orciani, M., Vignini, A., Mattioli-Belmonte, M., Mazzanti, L., and Di Primio, R. (2010). Skin-derived mesenchymal stem cells (S-MSCs) induce endothelial cell activation by paracrine mechanisms. *Exp. Dermatol* 19 (9), 848–850. doi:10.1111/j.1600-0625.2010.01104.x

Samsonraj, R. M., Raghunath, M., Nurcombe, V., Hui, J. H., van Wijnen, A. J., and Cool, S. M. (2017). Concise review: multifaceted characterization of human mesenchymal stem cells for use in regenerative medicine. *Stem Cells Transl. Med.* 6 (12), 2173–2185. doi:10.1002/sctm.17-0129

Son, B. R., Marquez-Curtis, L. A., Kucia, M., Wysoczynski, M., Turner, A. R., Ratajczak, J., et al. (2006). Migration of bone marrow and cord blood mesenchymal stem cells *in vitro* is regulated by stromal-derived factor-1-CXCR4 and hepatocyte growth factor-c-met axes and involves matrix metalloproteinases. *Stem Cells* 24 (5), 1254–1264. doi:10.1634/stemcells.2005-0271

Vaduganathan, M., Mensah, G. A., Turco, J. V., Fuster, V., and Roth, G. A. (2022). The global burden of cardiovascular diseases and risk: a compass for future health. *J. Am. Coll. Cardiol.* 80 (25), 2361–2371. doi:10.1016/j.jacc.2022.11.005

Wang, Y., Johnsen, H. E., Mortensen, S., Bindslev, L., Ripa, R. S., Haack-Sorensen, M., et al. (2006). Changes in circulating mesenchymal stem cells, stem cell homing factor, and vascular growth factors in patients with acute ST elevation myocardial infarction treated with primary percutaneous coronary intervention. *Heart* 92 (6), 768–774. doi:10.1136/hrt.2005.069799

Wang, Z. X., Wang, C. Q., Li, X. Y., Feng, G. K., Zhu, H. L., Ding, Y., et al. (2015). Mesenchymal stem cells alleviate atherosclerosis by elevating number and function of CD4(+)CD25 (+)FOXP3 (+) regulatory T-cells and inhibiting macrophage foam cell formation. *Mol. Cell Biochem.* 400 (1-2), 163–172. doi:10.1007/s11010-014-2272-3

Weber, C., and Noels, H. (2011). Atherosclerosis: current pathogenesis and therapeutic options. *Nat. Med.* 17 (11), 1410–1422. doi:10.1038/nm.2538

Yang, Y., Choi, H., Seon, M., Cho, D., and Bang, S. I. (2016). LL-37 stimulates the functions of adipose-derived stromal/stem cells via early growth response 1 and the MAPK pathway. *Stem Cell Res. Ther.* 7 (1), 58. doi:10.1186/s13287-016-0313-4

Zhang, X., Huang, F., Li, W., Dang, J. L., Yuan, J., Wang, J., et al. (2018). Human gingiva-derived mesenchymal stem cells modulate monocytes/macrophages and alleviate atherosclerosis. *Front. Immunol.* 9, 878. doi:10.3389/fimmu.2018.00878

Zhang, Z., Meng, P., Han, Y., Shen, C., Li, B., Hakim, M. A., et al. (2015). Mitochondrial DNA-LL-37 complex promotes atherosclerosis by escaping from autophagic recognition. *Immunity* 43 (6), 1137–1147. doi:10.1016/j.immuni.2015.10.018

frontiers | Frontiers in Cell and Developmental Biology

TYPE Original Research
PUBLISHED 28 March 2024
DOI 10.3389/fcell.2024.1367242

OPEN ACCESS

EDITED BY
Tokiko Nagamura-Inoue,
The University of Tokyo, Japan

REVIEWED BY
Yuyao Tian,
Massachusetts General Hospital and Harvard Medical School, United States
Xiaolei Li,
University of Pennsylvania, United States

*CORRESPONDENCE
Zoltán Veréb,
vereb.zoltan@med.u-szeged.hu

†These authors have contributed equally to this work and share first authorship

RECEIVED 08 January 2024
ACCEPTED 15 March 2024
PUBLISHED 28 March 2024

CITATION
Szűcs D, Monostori T, Miklós V, Páhi ZG, Póliska S, Kemény L and Veréb Z (2024), Licensing effects of inflammatory factors and TLR ligands on the regenerative capacity of adipose-derived mesenchymal stem cells. *Front. Cell Dev. Biol.* 12:1367242. doi: 10.3389/fcell.2024.1367242

Licensing effects of inflammatory factors and TLR ligands on the regenerative capacity of adipose-derived mesenchymal stem cells

Diána Szűcs[1,2,3†], Tamás Monostori[1,2,3†], Vanda Miklós[4†], Zoltán G. Páhi[5,6], Szilárd Póliska[7], Lajos Kemény[1,3,8] and Zoltán Veréb[1,3,4*]

[1]Regenerative Medicine and Cellular Pharmacology Laboratory, Department of Dermatology and Allergology, University of Szeged, Szeged, Hungary, [2]Doctoral School of Clinical Medicine, University of Szeged, Szeged, Hungary, [3]Centre of Excellence for Interdisciplinary Research, Development and Innovation, University of Szeged, Szeged, Hungary, [4]Biobank, University of Szeged, Szeged, Hungary, [5]Genome Integrity and DNA Repair Core Group, Hungarian Centre of Excellence for Molecular Medicine (HCEMM), University of Szeged, Szeged, Hungary, [6]Department of Pathology, Albert Szent-Györgyi Medical School, University of Szeged, Szeged, Hungary, [7]Genomic Medicine and Bioinformatics Core Facility, Department of Biochemistry and Molecular Biology, Faculty of Medicine, University of Debrecen, Debrecen, Hungary, [8]Hungarian Centre of Excellence for Molecular Medicine-USz Skin Research Group, University of Szeged, Szeged, Hungary

Introduction: Adipose tissue-derived mesenchymal stem cells are promising contributors to regenerative medicine, exhibiting the ability to regenerate tissues and modulate the immune system, which is particularly beneficial for addressing chronic inflammatory ulcers and wounds. Despite their inherent capabilities, research suggests that pretreatment amplifies therapeutic effectiveness.

Methods: Our experimental design exposed adipose-derived mesenchymal stem cells to six inflammatory factors for 24 h. We subsequently evaluated gene expression and proteome profile alterations and observed the wound closure rate post-treatment.

Results: Specific pretreatments, such as IL-1β, notably demonstrated an accelerated wound-healing process. Analysis of gene and protein expression profiles revealed alterations in pathways associated with tissue regeneration.

Discussion: This suggests that licensed cells exhibit potentially higher therapeutic efficiency than untreated cells, shedding light on optimizing regenerative strategies using adipose tissue-derived stem cells.

KEYWORDS

adipose-derived mesenchymal stem cells, regenerative medicine, licensing, inflammation, immune system

1 Introduction

Adipose tissue is distributed throughout various anatomical sites in the human body, including subcutaneous and visceral locations, intra-articular spaces, intramuscular regions, intra-hepatic depots, and the bone marrow. Beyond an energy reservoir, adipose tissue functions as an endocrine organ, producing many bioactive molecules that modulate

metabolic and cellular processes. Among these molecules are adipokines (e.g., leptin, adiponectin, omentin, and resistin), pro- and anti-inflammatory cytokines (e.g., IL-6, TNF-α, IL-1β, IL-8, MCP-1, IL-1Ra, IL-6, IL-7, IL-8, and IL-11), growth factors (e.g., VEGF, HGF, FGF, IGF-1, and BDNF), pro-apoptotic and pro-angiogenic factors, as well as microvesicles enriched with proteins and nucleic acids. Adipose tissue can be categorized into three main types: white adipose tissue, primarily involved in energy storage but also secreting adipokines; brown adipose tissue, responsible for thermogenesis regulation while retaining some energy storage capacity; and beige adipose tissue, which contributes to thermogenesis and energy storage (Konno et al., 2013; Cao et al., 2015; Li and Hua, 2017; Mushahary et al., 2018; Qi et al., 2018; Pittenger et al., 2019; Mazini et al., 2020; Song et al., 2020; Bunnell BA, 2021).

Adipose tissue-derived mesenchymal stem cells (AD-MSCs) reside within adipose tissue, primarily within the stromal vascular fraction (SVF) accessible through minimally invasive procedures. AD-MSCs are multipotent cells characterized by self-renewal potential and the ability to differentiate into mesodermal lineage cells such as adipocytes, chondrocytes, and osteoblasts. They exhibit high proliferation rates and possess immunosuppressive properties, rendering them and their secretome valuable assets in regenerative medicine applications for diseases associated with immune-related disorders. AD-MSCs play a pivotal role in immune response regulation by engaging in direct cell–cell interactions or through the secretion of bioactive factors. These cells interact with various immune cell types, including T cells, B cells, macrophages, natural killer cells (NKs), dendritic cells (DCs), neutrophils, and mast cells (Anton et al., 2012; Konno et al., 2013; Cao et al., 2015; Li and Hua, 2017; Mushahary et al., 2018; Qi et al., 2018; Ridiandries et al., 2018; Zwick et al., 2018; Pittenger et al., 2019; Al-Ghadban and Bunnell, 2020; Mazini et al., 2020; Song et al., 2020; Bunnell BA, 2021; Szucs et al., 2023).

AD-MSCs exert their immunomodulatory influence by interacting with T cells through cell adhesion molecules and modifying the secretion of mediators such as IDO, TGFβ, IL-10, and PGE2. Additionally, T cells reciprocally affect AD-MSCs through chemokine production. Studies have demonstrated that AD-MSCs, in the presence of high pro-inflammatory cytokine levels, promote regulatory T cell (Treg) generation while inhibiting T cell proliferation, activation, and differentiation, thus suppressing immune responses. Conversely, under low pro-inflammatory cytokine exposure conditions, AD-MSCs suppress Treg generation and activate T cell proliferation, activation, and differentiation. AD-MSCs exhibit dual effects on B cells, inhibiting and promoting their proliferation, activation, and differentiation while also inducing chemotaxis and Breg induction. These cells can impede NK cell proliferation, activation, and migration while stimulating NK cell progenitor proliferation and activation.

Furthermore, AD-MSCs hinder DC differentiation, endocytosis, maturation, activation, and migration, inhibiting mast cell degranulation, inflammatory cytokine expression, and chemotaxis. Macrophage polarization is influenced by AD-MSCs, favoring the M2 phenotype and inhibiting the M1 phenotype. At the same time, AD-MSCs modulate neutrophils by inhibiting activation, recruitment, extracellular neutrophil trap formation, and protease secretion while promoting neutrophil survival and recruitment (Anton et al., 2012; Konno et al., 2013; Cao et al., 2015; Li and Hua, 2017; Carelli et al., 2018; Guasti et al., 2018; Mushahary et al., 2018; Qi et al., 2018; Ridiandries et al., 2018; Zwick et al., 2018; Pittenger et al., 2019; Al-Ghadban and Bunnell, 2020; Mazini et al., 2020; Munir et al., 2020; Song et al., 2020; Bunnell BA, 2021; Krampera and Le Blanc, 2021; Szucs et al., 2023).

Due to their immunomodulatory properties, angiogenic potential, and differentiation capacity, AD-MSCs offer a promising avenue for tissue repair (Szucs et al., 2023), regeneration, and replacement in a broad spectrum of conditions characterized by tissue damage. AD-MSCs hold significant therapeutic potential for applications such as wound healing and skin regeneration in various contexts, including diabetic and non-diabetic ulcers, non-healing wounds, extensive burns, and physicochemical skin injuries. Moreover, AD-MSCs find relevance in autoimmune disorders, hematological conditions, graft-versus-host disease, bone and cartilage repair, cardiovascular and muscular diseases, neurodegenerative disorders, and radiation-induced injuries. These versatile cells offer a means to restore tissue function effectively and safely. To ensure secure and successful application in AD-MSC-based therapies, the purity and potency of these cells must be rigorously assessed before administration (Fu et al., 2009; DelaRosa and Lombardo, 2010; Anton et al., 2012; François et al., 2012; Shohara et al., 2012; Konno et al., 2013; Cao et al., 2015; Furuta et al., 2016; Li and Hua, 2017; Carelli et al., 2018; Feldbrin et al., 2018; Guasti et al., 2018; Mushahary et al., 2018; Qi et al., 2018; Ridiandries et al., 2018; Zwick et al., 2018; Pittenger et al., 2019; Sahu et al., 2019; Al-Ghadban and Bunnell, 2020; Kuca-Warnawin et al., 2020; Kurte et al., 2020; Mazini et al., 2020; Munir et al., 2020; Song et al., 2020; Xiao et al., 2020; Bunnell BA, 2021; Krampera and Le Blanc, 2021; Nieto-Nicolau et al., 2021; Krawczenko and Klimczak, 2022; Cheng et al., 2023; Huerta et al., 2023; Szucs et al., 2023).

Adipose tissue-derived mesenchymal stem cells (AD-MSCs) hold significant clinical therapeutic promise attributed to their multifaceted attributes encompassing regenerative, anti-apoptotic, antifibrotic, antioxidant, and immunomodulatory capacities. Beyond the application of AD-MSCs themselves, harnessing their secretome has emerged as an avenue with the potential to influence disease progression positively. Emerging research underscores the dynamic nature of AD-MSC secretion profiles, which can be further tailored through strategic pretreatments, enhancing their suitability for therapeutic applications (Anton et al., 2012; François et al., 2012; Konno et al., 2013; Wu et al., 2013; Cao et al., 2015; Li and Hua, 2017; Guasti et al., 2018; Qi et al., 2018; Zwick et al., 2018; Pittenger et al., 2019; Al-Ghadban and Bunnell, 2020; Mazini et al., 2020; Song et al., 2020; Bunnell BA, 2021; Chang and Nguyen, 2021; Brembilla et al., 2023; Szucs et al., 2023).

Existing literature highlights strategies to augment the effectiveness of MSC-based therapies, focusing on mimicking inflammatory microenvironments. Pro-inflammatory cytokines and hypoxic conditions have been explored as factors capable of potentiating MSC-mediated anti-inflammatory responses. Nevertheless, in these instances, the concomitant detection of classical pro-inflammatory signals has raised questions regarding whether immunosuppressive or pro-inflammatory MSC phenotypes are primarily responsible for

the observed therapeutic effects. The complete elucidation of these indications remains a work in progress, with the precise nature of agents and their therapeutically effective concentrations yet to be definitively determined or standardized. Notably, suboptimal conditions may promote the prevalence of a pro-inflammatory MSC phenotype, while excessive concentrations can impact cell viability. In the context of Good Manufacturing Practice (GMP) for cell therapy product manufacturing, pretreatment strategies may also raise regulatory and licensing considerations. However, it is worth highlighting that licensed MSCs often represent the next Frontier in MSC-based therapies, particularly for addressing injuries associated with acute and sub-acute inflammation. Ongoing research continues to delve into the underlying biological processes and the development of safe and efficacious pretreatment approaches. Thus far, the findings have been exceedingly promising, offering significant prospects for advancing the field of regenerative medicine (Anton et al., 2012; François et al., 2012; Konno et al., 2013; Wu et al., 2013; Cao et al., 2015; Li and Hua, 2017; Guasti et al., 2018; Hu and Li, 2018; Qi et al., 2018; Zwick et al., 2018; Pittenger et al., 2019; Al-Ghadban and Bunnell, 2020; Mazini et al., 2020; Song et al., 2020; Bunnell BA, 2021; Chang and Nguyen, 2021; Brembilla et al., 2023; Szucs et al., 2023).

Our study evaluates the wound healing and skin regeneration capabilities of AD-MSCs, particularly in the context of highly inflamed environments, which can influence their expression profile. We hypothesize that the pretreatment of AD-MSCs may be vital to enhancing therapeutic efficacy. Our investigation aims to shed light on the molecular and cellular responses of AD-MSCs to inflammatory factors, specifically LPS, TNFα, IL1β, IFNγ, and PolyI:C. Our findings may contribute to developing more effective therapies where cell preconditioning is pivotal in augmenting therapeutic outcomes. Moreover, our experimental framework has the potential to assess patient-specific responses to inflammatory factors, aiding in the development of personalized therapeutic approaches.

2 Materials and methods

2.1 AD-MSC isolation

The collection of adipose tissue complied with the guidelines of the Helsinki Declaration, and it was approved by the National Public Health and Medical Officer Service (NPHMOS) and the National Medical Research Council (16821-6/2017/EÜIG, STEM-01/2017), which follows the EU Member States' Directive 2004/23/EC on presumed written consent practice for tissue collection. Abdominal adipose tissues were removed from patients (Sex:2/3 F/M, Age: 50.2 ± 11.7 years), and the isolation was performed within 1 h after plastic surgery. A detailed description of the AD-MSC isolation protocol can be found in our previous article (Szucs et al., 2023).

2.2 Differentiation of adipose-tissue-derived mesenchymal stem cells

The differentiation potential of adipose-tissue-derived mesenchymal stem cells was verified by differentiating into adipocyte, chondrocyte, and osteocyte lines. They were cultured in a 24-well plate, 5×10^4 cells/well; after 24 h of incubation, the differentiation medium was added. The commercially available Gibco's StemPro® Adipogenesis (A1007001), Osteogenesis (A1007201), and Chondrogenesis (A1007101) Differentiation Kits were applied according to the manufacturer's guidelines (Gibco, Thermo Fisher Scientific, Waltham, MA United States). After 21 days of maintenance, the cells were fixed with 4% methanol-free formaldehyde (37,308, Molar Chemicals, Hungary) for 20 min at RT. Differentiation stages of AD-MSCs were validated using different dyes. For visualization of lipid-laden particles, Nile red staining (19,123, Sigma-Aldrich, Merck KGaA, Darmstadt, Germany) was utilized, and Alizarin red staining (A5533, Sigma-Aldrich, Merck KGaA, Darmstadt, Germany) was applied to show the mineral deposits during osteogenesis. Toluidine blue staining (89640-5G, Sigma-Aldrich, Merck KGaA, Darmstadt, Germany) was wielded to label the chondrogenic mass.

2.3 Flow cytometry

The surface antigen expression pattern was characterized by three-color flow cytometry using fluorochrome-conjugated antibodies with isotype-matching controls. For the measurement of the fluorochrome signal, the BD FACSAriaTM Fusion II flow cytometer (BD Biosciences Immunocytometry Systems, Franklin Lakes, NJ, United States) was applied, and data were processed by Flowing Software (Cell Imaging Core, Turku Centre for Biotechnology, Finland).

2.4 Treatment of AD-MSC

The applied AD-MSC cells were derived from the abdominal adipose tissue of three different donors. In a T25 cm^2 flask, 2.8×10^5 cells were seeded using the upkeeping cell culture media described above, and the cells were incubated for 24 h. Next, the cell culture media was changed for treatment; cells were treated with (A) LPS [100 ng/mL] (tlrl-peklps, ultrapure, Invivogen, San Diego, CA, United States), (B) TNFα [100 ng/mL] (300-01A, Peprotech, London, United Kingdom), (C) IL-1β [10 ng/mL] (200-01B, Peprotech, London, United Kingdom), (D) IFNγ [10 ng/mL] (300-02, Peprotech, London, United Kingdom) or (E) PolyI:C [25 ng/mL] (tlrl-pic, Invivogen, San Diego, CA, United States). After adding inflammatory agents, the cells were maintained for 24 h under standard conditions (37°C, 5% CO_2, untreated cells left as control). Upon 24-h treatment, the cells were collected and processed for RNA isolation.

2.5 RNA isolation for RNA-Sequencing

In the context of RNS sequencing, three biological replicates were employed, consistent with the methodology employed in our preceding investigations. The cells were collected, and the pellet was dissolved in 1 mL TRI Reagent® (TR118/200, Genbiotech Argentina, Bueno Aries, Argentina) and kept at −80°C for 24 h. After thawing, 200 µL chloroform (83,627.320, VWR, Radnor, PA, United States) was added to samples, and they were incubated at RT for 10 min

after rigorous mixing. For phase separation, the samples were centrifuged at 13,400 g at 4°C for 20 min. The aqueous phase was measured into clean tubes, and 500 µL 2-propanol (SO-9352-B025, Molar Chemicals, Hungary) was added and mixed thoroughly. After this, the incubation and phase-separation steps were repeated. The supernatants were eliminated, and the pellets were washed with 750 µL 75% EtOH-DEPC. The samples were centrifuged at 7,500 *g* at 4°C for 5 min, then the supernatants were discarded, and the samples were dried at 45°C for 20 min. The pellets were suspended in RNase-free water and incubated at 55°C for 10 min. The concentration was measured using an IMPLEN N50 UV/Vis Nanophotometer (Implen GmbH, Munich, Germany), and RNA samples were stored at −80°C until use.

High-throughput mRNA sequencing analysis was implemented on the Illumina sequencing platform to achieve global transcriptome data. The total RNA sample quality was investigated using the Eukaryotic Total RNA Nano Kit according to the manufacturer's guidelines on Agilent BioAnalyzer. Samples with an RNA integrity number (RIN) value >7 were accepted for the library preparation. RNA-Seq libraries were prepared from total RNA using the Ultra II RNA Sample Prep kit (New England BioLabs) according to the manufacturer's protocol. In short, poly-A RNAs were captured by oligo-dT conjugated magnetic beads, and then mRNAs were eluted and fragmented at 94°C. First-strand cDNA was created by random priming reverse transcription; then, double-stranded cDNA was made in the second-strand synthesis step. After the reparation of ends, A-tailing and adapter ligation took place. The adapter-ligated fragments were amplified in enrichment PCR, and finally, sequencing libraries were produced. Sequencing runs were performed on the Illumina NextSeq 500 instrument, applying single-end 75-cycle sequencing.

2.6 Data analysis

Raw RNA-seq reads were fed into a pipeline to quantify reads mapping to each genomic feature. Quality control (QC) steps were built in at each step of the pipeline, and QC was carried out with FastQC and MultiQC. To remove low-quality bases, short reads, and adapters, Trimmomatic was used. We relied on Illumina's "Considerations for RNA Seq read length and coverage" (https://knowledge.illumina.com/library-preparation/rna-library-prep/library-preparation-rna-library-prep-reference_material-list/000001243) to determine if the reads were appropriate for further analysis. The next step consisted of aligning the reads to the human genome (GRCh38) using Bowtie2, whereas samples with an alignment percentage over 90% were accepted. This was followed by read quantification using FeatureCounts, a highly efficient general-purpose read summarization program that counts mapped reads for genomic features such as genes, exons, promoters, gene bodies, genomic bins, and chromosomal locations. The resulting count's table was used for further downstream analysis. For the methods of differential gene expression, PCA analysis, generating the heatmaps of the differentially expressed genes and the pre-selected pathways, and generating volcano plots, see previous article (Szucs et al., 2023). Pathway analysis was conducted using the ViSEAGO package (Brionne et al., 2019). The input for the analysis was a ranked gene list of the differentially expressed genes with p-value <0.05 and log2foldchange > |1|. Functional Gene Ontology enrichment was performed with the fgsea package (Korotkevich et al., 2021) using the ViSEAGOrunfgsea command with the "fgseaMultilevel" method (parameters: scoreType = "std", minSize = 5). Enrichment results were merged (Supplementary Table S1), and semantic similarity measures were made using Wang distance measures, which are based on graph topology. The clustering of the enrichment results was based on the Ward D2 method, and the dendrogram was split into 20 categories (Yu et al., 2010). The heatmap showing these results was made with the ComplexHetamap package (Gu et al., 2016).

2.7 Quanterix multi-plex ELISA

For the cytokine assay, we used the Quanterix SP-X digital biomarker analyzer (Quanterix). The system detected simultaneously 10 cytokines in a multiplex assay with Simoa Corplex Cytokine Panel 1 10-Plex Kit (REF: 85-0329, Quanterix). The assay was performed according to the manufacturer's protocol. Supernatants were thawed, centrifuged, and 4-times diluted with assay diluent. Calibration standards were prepared freshly and measured in triplicates samples in duplicates. After the measurement, results were analyzed and visualized in GraphPad.

2.8 *In vitro* scratch assay

AD-MSC cells from three donors were collected and counted using an EVE automatic cell counter (NanoEntek, Hwaseong, Republic of Korea). The *in vitro* scratch assay measures the cell proliferation and migration. The required 1.5×10^4 cells per well seeded in E-Plate WOUND 96 plates (REF: 300,600,970, Agilent/BioTek, Santa Clara, CA, United States) in maintenance media. The cells were cultured for 24 h under standard conditions (37°C, 5% CO_2), and then the protocol was separated into two different directions. (I.) Upon 24 h incubation, the scratch was created, and the media was changed immediately to media containing inflammatory agents. It is followed by 48 h of impedance measurement by xCELLigence Real-Time Cell Analyzer (RTCA) device (Agilent/BioTek, Santa Clara, CA, United States). (II.) After 24 h incubation, the media was replaced with media containing inflammatory agents, and the cells were incubated 24 h under standard conditions; then, the scratch was made, and the media was changed immediately to agents-free upkeeping media, followed by 48 h impedance measurement. The scratches were generated using the AccuWound 96 Scratch Tool (Agilent/BioTek, Santa Clara, CA, United States) wound-making device.

2.9 RNA isolation and real-time PCR

Upon inflammation-inducing treatments (described above), the Macherey-Nagel NucleoSpin RNA Mini kit (740,955.250, Dueren, Germany) was applied according to the manufacturer's instructions. All work with RNA and cDNA samples was performed in BioSan UVT-B-AR DNA/RNA UV-Cleaner box (Riga, Latvia). After RNA was extracted and their quality and quantity were verified by IMPLEN N50 UV/Vis nanophotometer, the cDNA synthesis was

performed using High-Capacity cDNA Reverse Transcription Kit (4,368,813, Applied Biosystems™, Thermo Fisher Scientific, Waltham, MA, United States) according to the protocol of the manufacturer. Analytik Jena qTOWER^3 G Touch Real-Time Thermal Cycler (Jena, Germany) was utilized for reverse transcription.

2.10 qPCR

The Xceed qPCR Probe 2x Mix No-ROX kit (NPCR10502L, Institute of Applied Biotechnologies, Prague, Czech Republic) and TaqMan probes (4,331,182, 250 rxns, FAM-MGB, Thermo Fisher Scientific, Waltham, MA, United States) were used for quantitative PCR. Three biological and three technical replicates were applied in all cases, and data were analyzed by $2^{-\Delta\Delta CT}$ method. The protocol was executed according to the manufacturer's instructions.

2.11 ELISA

For measurement of cytokine/chemokine levels in cells upon inflammation induction, the Human IL-6 ELISA set (555220), Human IL-8 ELISA set (555244), Human IP-10 ELISA set (550926), and Reagent Set B (550534) were applied from BD OptEIA™ (BD Biosciences, Franklin Lakes, NJ, United States) according to the guidelines of the manufacturer.

2.12 Cytotoxic effect of inflammatory agents on AD-MSCs

To measure the cytotoxicity of the given treatment, the Cytotoxicity Detection Kit (LDH) (REF: 11644793001, Roche, Basel, Switzerland) was applied according to the manufacturer's instructions. Cell supernatants were collected upon 24 h of inflammation induction (described above), and the colorimetric absorbance measurement was executed by Synergy HTX multiplate reader (Agilent/BioTek, Santa Clara, CA, United States) on 490 nm, reference wavelength was 620 nm.

2.13 Cell proliferation and metabolism

Effects on proliferation were measured with BrdU Cell Proliferation ELISA Kit (Ref: 11647229001, Roche, Basel, Switzerland). The thymidine analog 5-bromo-2′-deoxyuridine (BrdU) is incorporated into the DNA, thus allowing the determination of the inhibitory or stimulatory effect on the proliferation of the activator molecules. $1{,}5 \times 10^4$ cells per well were seeded into a 96-well plate. The inflammatory environment was simulated with the materials and concentrations mentioned above. The treatment lasted 24 h, and the assays were performed according to the manufacturer's protocol. Measurement was performed on Synergy HTX multiplate reader (Agilent/BioTek, Santa Clara, CA, United States) at 550 nm, with reference at 650 nm for MTT assay, on 450 nm, with reference at 690 nm.

Changes in metabolism due to an inflammatory environment were examined by Cell Proliferation Kit (MTT) (Ref: 11465007001, Roche, Basel, Switzerland) according to the manufacturer's guidelines. The bioreduction of tetrazolium salt to formazan gives information about cellular metabolism and viability. 1.5×10^4 cells per well were seeded into a 96-well plate, then the cells were incubated for 24 h under standard conditions (37°C, 5% CO_2). Next, the 24 h induction of inflammation was taken place (described above), and the colorimetric absorbance measurement was carried out by Synergy HTX multiplate reader (Agilent/BioTek, Santa Clara, CA, United States) on 550 nm, reference wavelength was 650 nm.

3 Results

3.1 Overall transcriptomic profile of treated cells

The Venn diagrams illustrate the extensive impact of the treatments on gene expression, revealing both upregulation and downregulation of numerous genes, along with significant intersections (Figure 1A). Specifically, the treatments exhibited downregulation of genes as follows: LPS (104 genes), TNF-α (87 genes), IL-1β (50 genes), IFN-γ (56 genes), and PolyI:C (83 genes), with a collective influence on 25 shared genes. Conversely, the treatments led to the upregulation of multiple genes: LPS (14 genes), TNF-α (34 genes), IL-1β (26 genes), IFN-γ (38 genes), and PolyI:C (14 genes), with a common effect observed in 109 genes. These findings underscore the intricate and multifaceted impact of the treatments on the transcriptomic profile, revealing both shared and unique regulatory responses across the treated conditions. The Volcano plot illustrates extensive alterations in gene expression induced by the treatments, encompassing up and downregulation of genes' expression (Figure 1B). Notably, among the top 10 most significantly altered genes, a majority exhibition.

3.2 ViSEAGO and clustered pathways

The heatmap generated through ViSEAGO analysis delineates treatments into two primary clusters, with PolyI:C, TNF-α, and IFN-γ forming one cluster and IL-1β and LPS constituting the other (Figure 2A). There is a difference between the two groups in defense and immune response, signal transduction, chemotaxis, cellular response to chemical stimulus, biological regulation, and T-cell activation. They have common effects on organelle organization, mitotic cell cycle, primary metabolic process, DNA repair, system development, ion transmembrane transport, lipid transport, cellular process, meiotic cell cycle, and cell cycle regulation.

The treatments exert distinct effects on multiple pathways: LPS impacts two pathways, TNFα influences eight pathways, IL-1β affects one pathway, IFN-γ modulates three pathways, and PolyI:C impacts five pathways (Figure 2B). This differential influence on various molecular pathways underscores the complexity of the treatments' interactions with cellular processes. The treatments

10.3389/fcell.2024.1367242

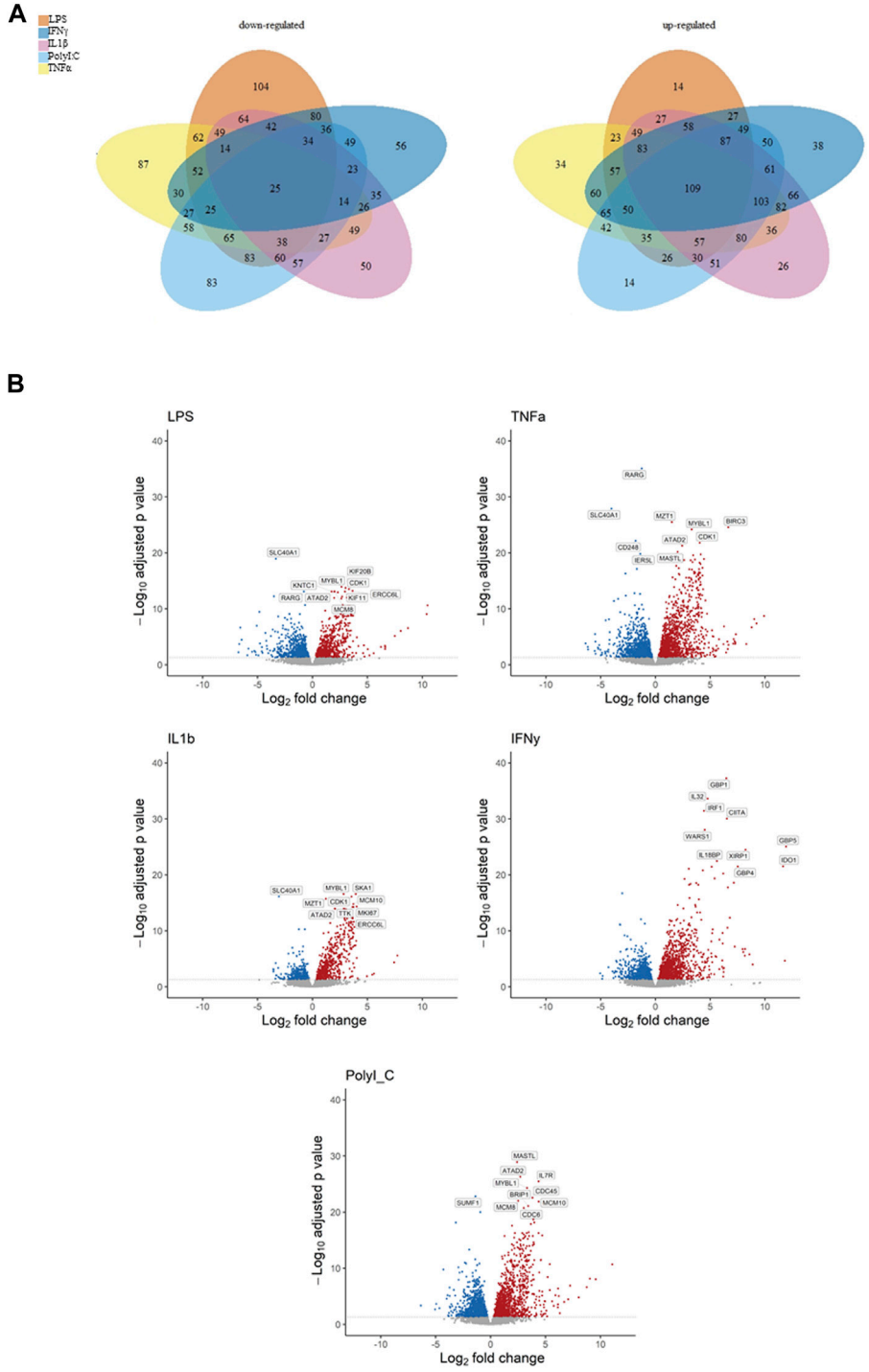

FIGURE 1
Representation of down- and upregulated DEGs after pro-inflammatory treatment compared to the control condition, **(A)** Venn diagrams illustrating overlapping gene numbers between the treatments, and Volcano plots **(B)** depicting the most significantly altered genes, where p adjusted < 0.05 are shown in red, significantly downregulated genes p adjusted < 0.05 are shown in blue.

also elicit shared alterations in multiple pathways. Specifically, LPS and TNFα affect four common pathways, while IFNγ and PolyI:C induce changes in three overlapping pathways. Additionally, LPS and IFN-γ influence one common pathway, as do LPS and PolyI:C, and TNFα and PolyI:C. Notably, the combined treatment of LPS, TNFα, and PolyI:C results in concurrent modifications in three pathways, whereas the combination of LPS, TNFα, and IL-1β influences one shared pathway. Furthermore, TNFα, IFNγ, and PolyI:C collectively impact one common pathway. Lastly, the joint influence of LPS, TNFα, IL-1β, and PolyI:C is reflected in

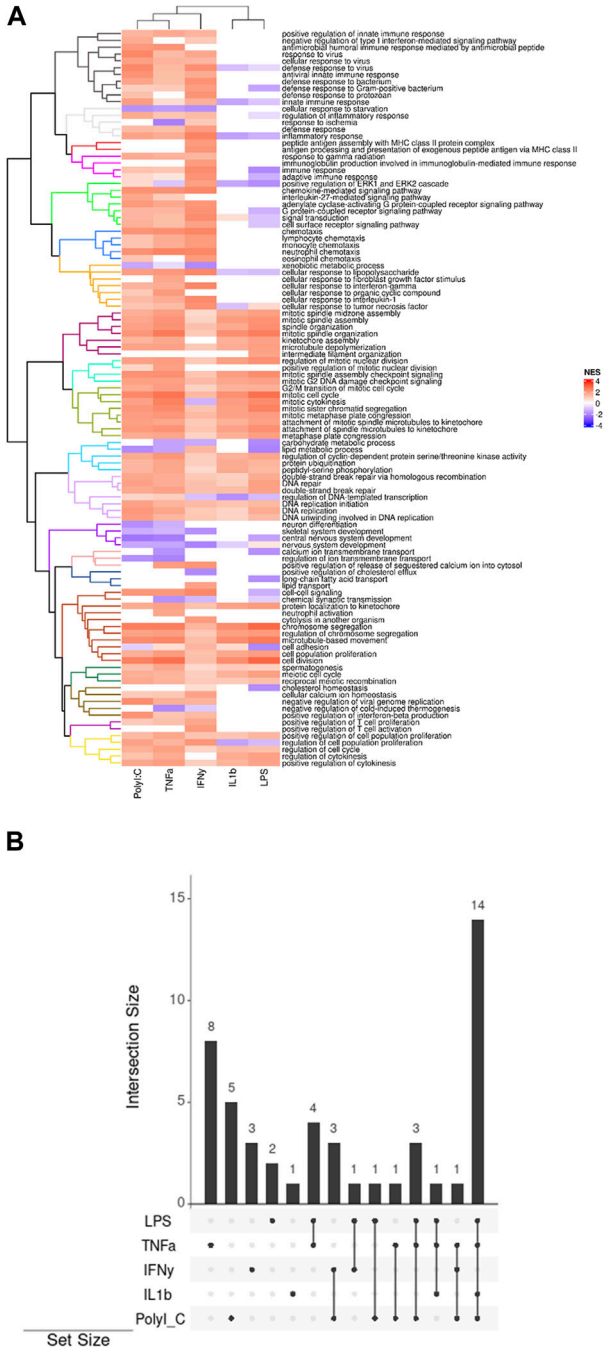

FIGURE 2
(A) Display of clustered pathways heatmap generated by ViSEAGO. The different colors represent uniform groups, including several pathways and biological processes **(B)** The UpSet plots visually represent the gene intersections within various pathways in the AD-MSC following treatment with pro-inflammatory agents. The vertical bars highlight the number of shared genes, denoting the intersection size, among specific pathway sets, indicated by bottom-filled connected circles.

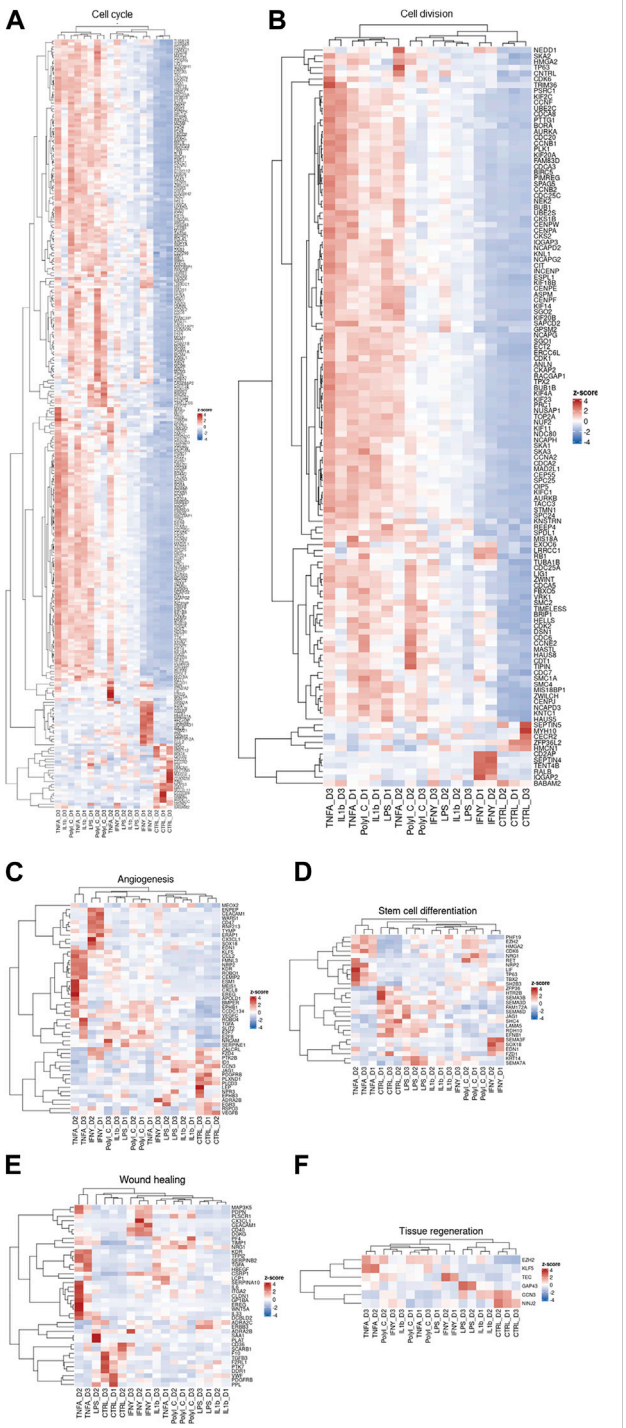

FIGURE 3
Clustered heatmaps depicting various processes: **(A)** Cell cycle, **(B)** Cell division, **(C)** Angiogenesis, **(D)** Stem cell differentiation, **(E)** Wound healing, and **(F)** Tissue regeneration. These biological processes are crucial for AD-MSC tissue regeneration, healing, and immunomodulation of the microenvironment.

alterations in 14 pathways, emphasizing the intricate interplay of these treatments in affecting cellular processes.

Our transcriptomic dataset has been visualized through a series of heatmaps, categorized based on predefined pathways (Figure 3). Across all heatmaps, the distinction is evident between the transcriptional patterns of treated and control samples, albeit with notable inter-donor variations. This dataset is an illustrative exemplar of the diverse cellular responses induced by treatments, each reflecting the unique molecular landscape of individual patients. Notably, genes

10.3389/fcell.2024.1367242

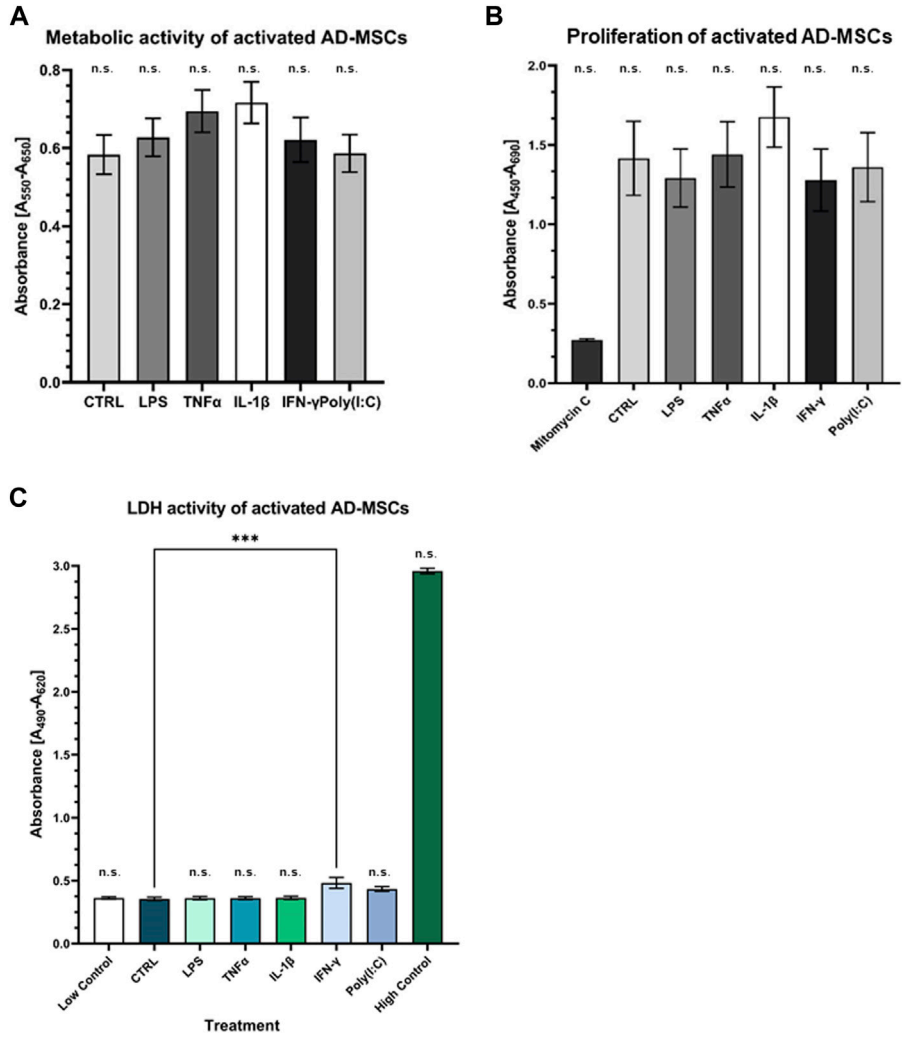

FIGURE 4
Assessment of metabolic and proliferation activity of treated AD-MSCs **(A)** The metabolic activity of the treated cells was detected by MTT assay. There is no significant change compared to the control. **(B)** BrdU incorporation indicated the proliferative capacity of cells, which was not significantly affected by treatments. **(C)** Cell viability was not affected by any treatments, indicating that our results were not caused by dead cells. (N = 3 donors, each measurement performed in triplicates).

modulated by TNF-α and IFN-γ in the angiogenesis pathway heatmap tend to cluster together. In the context of cell cycle and cell division pathways, TNF-α, IL-1β, and PolyI:C appear to share analogous effects, whereas IFN-γ delineates a distinct grouping. Regarding stem cell differentiation, the impact of LPS and IL-1β aligns closely with that of the control group. TNF-α exhibits similarity with PolyI:C and IFN-γ manifests as an independent cluster.

Furthermore, the heatmap of tissue regeneration reveals that LPS and IL-1β treatments display comparable profiles to the control group, whereas TNF-α delineates discrete gene clusters. LPS and IL-1β treatments diverge from the control group in wound healing pathways, whereas TNF-α, IFN-γ, and PolyI:C treatments segregate into distinct clusters. These observations highlight the nuanced and pathway-specific effects of the treatments on cellular responses, underlining the complexity of treatment outcomes across diverse biological contexts.

3.3 Perform cellular characterization and evaluate the safety of treatment

Primary cell cultures were maintained, and their differentiation potential was assessed. Remarkably, these cells demonstrated tri-lineage differentiation capacity, encompassing adipogenic, chondrogenic, and osteogenic lineages (Supplementary Figure S1). This differentiation was verified through microscopic examination of distinct cell type-specific features, reinforcing the suitability of these cultures as a valuable model for our study. The FACS analysis revealed crucial cell characteristics and verified their mesenchymal origin, bolstering their identity and facilitating further exploration of their unique traits and functions in our study [data not shown; see previous article by (12)]. Cytotoxicity and viability tests showed that the cells did not receive a cytotoxic amount of inflammatory agents, and their metabolism and viability were preserved during treatment, underscoring the safety and potential

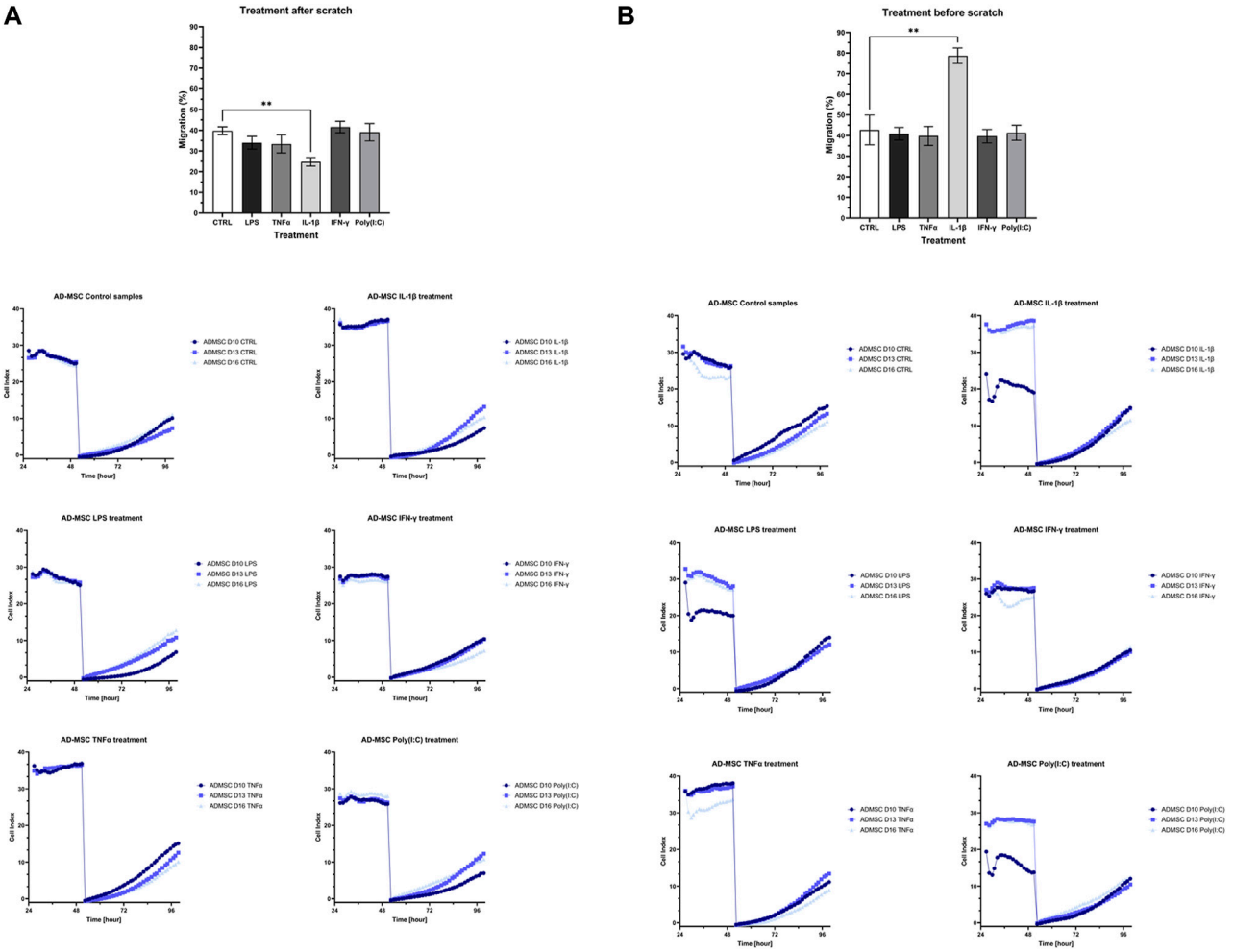

FIGURE 5
The bar charts and diagrams show the results of the cell proliferation and migration studies with two visualized layouts. The impedance-based method measured the re-population of the direct wound size. **(A)** "treatment before scratch", which is intended to model that the wound is initially in an inflammatory environment, and **(B)** "treatment after scratch", which is designed to model an infected wound. Both of these cases have a clinical manifestation in chronic non-healing wounds and, e.g., infectious wounds associated with diabetes.

therapeutic relevance of the administered agents in cellular health and function (Figure 4).

3.4 Influence of treatments on the cell proliferation and migration

The cell proliferation and migration assay utilized impedance measurements to assess the rate of cell migration during wound closure in treated samples relative to a control group after the injury. Two experimental conditions were examined: one where the wound was introduced before treatment (Figure 5A) and another where treatment preceded wound induction (Figure 5B). In both cases, distinct variations in wound closure dynamics were evident between cells subjected to IL-1β treatment and the control group. Specifically, when applied before wound initiation, IL-1β significantly hastened wound closure, whereas its post-wound application decelerated the process.

3.5 Gene and protein expression analysis by qPCR and ELISA

The quantitative polymerase chain reaction (qPCR) analysis results unveiled distinct gene expression patterns in response to various treatments (Figure 6). Notably, CXCL-8 demonstrated a robust upregulation in response to all treatments, with a marked increase following exposure to LPS, TNFα, and IL-1β. Conversely, both NAGS and STAT6 exhibited consistent downregulation across all treatment conditions. Interestingly, while TNFα treatment had no appreciable effect on IL-6 expression, the other administered treatments induced a significant reduction in IL-6 mRNA levels.

Furthermore, CXCL-10 displayed an elevated expression profile in response to TNFα treatment and a modest increase following IFNγ exposure. Conversely, ASGR1 exhibited a notable decrease in expression levels following treatment with LPS, TNFα, and IFNγ, while it demonstrated an elevation in response to IL1β and PolyI:C. In the case of ICAM1, its expression slightly increased following

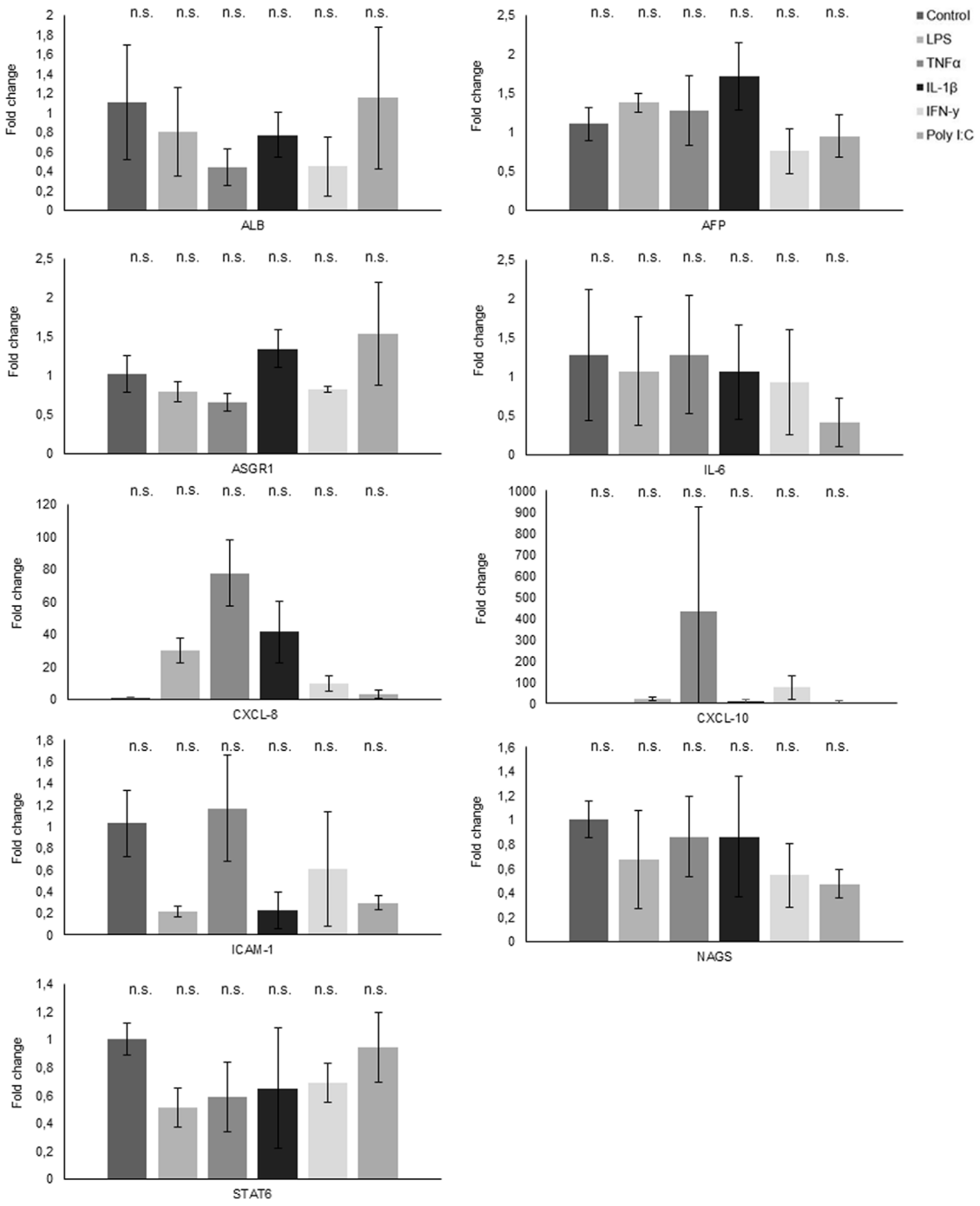

FIGURE 6
Gene expression analysis through qPCR reveals the fold change in various genes following treatments.

TNFα treatment, but conversely, it experienced a decrease when subjected to all other treatments.

At the protein level, noteworthy distinctions emerge (Figure 7A). Specifically, the treatments with LPS, TNFα, and IL-1β resulted in a notable upsurge in IL-6 levels, whereas IFNγ and Poly I:C treatments led to a discernible reduction in IL-6 protein concentrations. CXCL-8 exhibited an augmentation in response to LPS and TNFα treatments, contrasted by a diminishment observed following the remaining treatment regimens. Interestingly, CXCL-10 demonstrated an elevation in protein levels across all administered treatments, with particularly significant peaks observed following TNFα and IFNγ treatments. The multiplex ELISA findings reveal notable changes in the IFNγ, IL-5, IL-12p70, and IL-22 levels. Specifically, IL-5, IL-12p70, and IL-22 significantly increased following IL-1β treatment (Figure 7B).

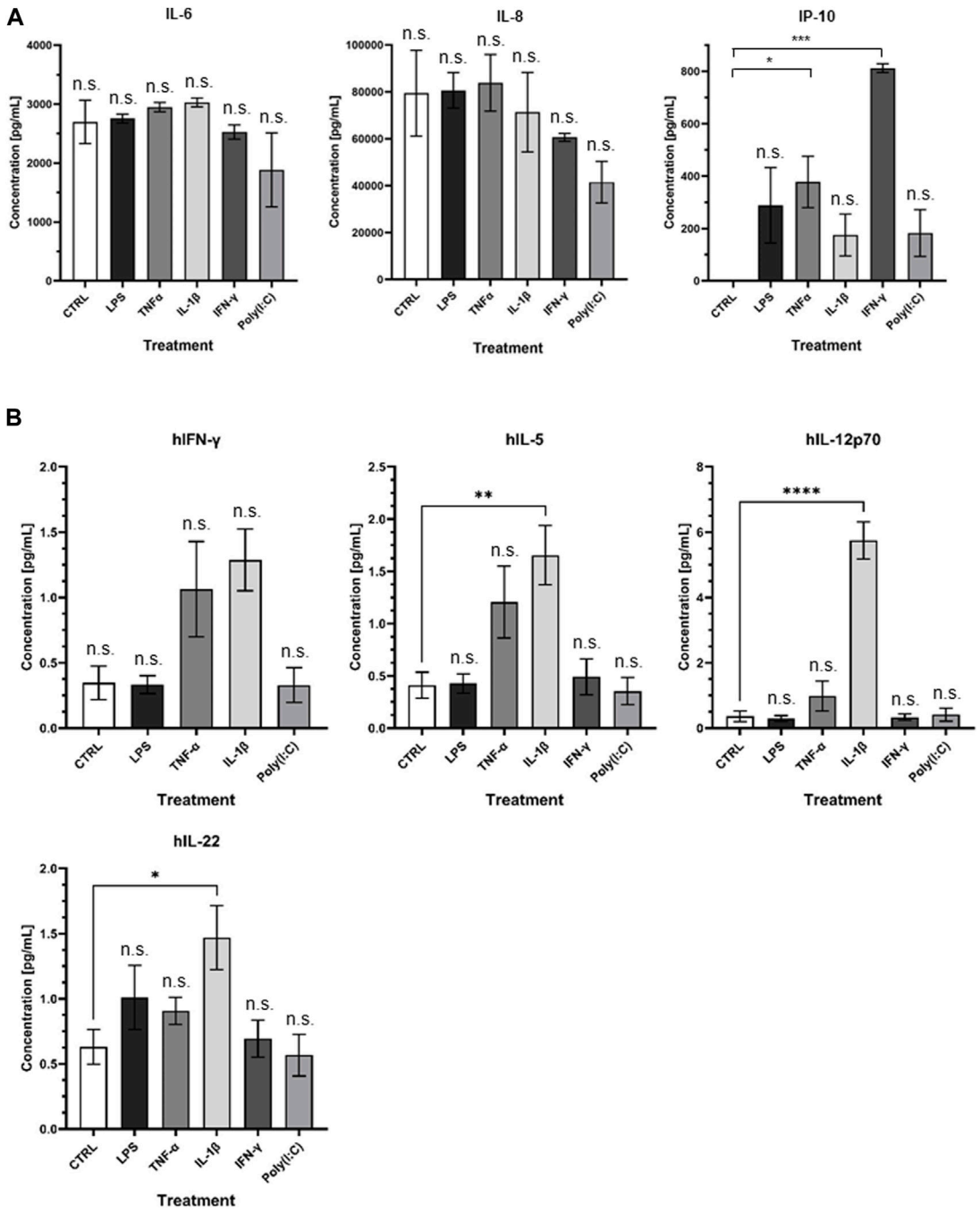

FIGURE 7
(A) Visual representation of ELISA results and **(B)** presentation of Quanterix findings.

4 Discussion

Mesenchymal stem cells (MSCs) are crucial in various immunological processes. They actively regulate their microenvironment and influence the differentiation of different cells, including immune cells, by producing cytokines and growth factors (Saparov et al., 2016). In their basal state, MSCs exhibit antiangiogenic properties. The immunomodulatory effectiveness of MSCs is contingent upon the nature and intensity of inflammatory signals received, such as interferon-γ (IFN-γ), tumor necrosis factor-α (TNF-α), and Toll-like receptor (TLR)-mediated activation. Under specific inflammatory stimuli (IFN-γ, TNF-α, TLR-mediated activation), MSCs transform, becoming antiapoptotic, proangiogenic, and immunosuppressive (Meisel et al., 2004; Krampera et al., 2006; Ghannam et al., 2010; Saparov et al., 2016; Vereb et al., 2020). They contribute to inflammation reduction through the secretion of factors like interleukin-6 (IL-6), indoleamine 2,3-dioxygenase (IDO), HLA G5 (human leukocyte antigen G5), interleukin-10 (IL-10), transforming growth factor beta-1 (TGFb1), hepatocyte growth factor (HGF), HOX-1, IL-1Ra

(IL-1 receptor antagonist), prostaglandin E2 (PGE2), and through cell-cell contact (Bartholomew et al., 2002; Meisel et al., 2004; Aggarwal SP and Pittenger, 2005; Saparov et al., 2016). The immunomodulatory potential of MSCs thus hinges on their response to specific inflammatory cues (Renner et al., 2009; Li et al., 2012). Mesenchymal stem cells (MSCs) actively produce a diverse array of chemokines and adhesion molecules, including ligands for CXC chemokine receptor 3 (CXCR3), C-C chemokine receptor type 5 (CCR5), intercellular adhesion molecule 1 (ICAM-1/CD54), and vascular cell adhesion molecule 1 (VCAM-1) (Vereb et al., 2016; Vereb et al., 2020). The pronounced expression of CXCR3 in effector and memory T cells underscores the pivotal significance of MSC-generated chemokines, particularly CXCL9 (chemokine ligand 9), CXCL10 (chemokine ligand 10), and CXCL11 (chemokine ligand 11). These chemokines play a critical role in orchestrating the recruitment of lymphocytes to the site of tissue damage, thereby ensuring optimal functionality of immunosuppression (Crop et al., 2010; Wang et al., 2014; Saparov et al., 2016). The ability of MSCs to influence the immune system and the effects are intricately tied to variables such as the tissue origin (whether from fat, bone marrow, *etc.*), the specific microenvironment they inhabit, and the nature of their interactions with other cellular partners. The role of adipose-derived mesenchymal stem cells (AD-MSCs) in wound healing is a subject of considerable significance. These cells exhibit a wide array of regenerative, anti-apoptotic, antifibrotic, anti-oxidative, and immunomodulatory properties, rendering them invaluable for therapeutic applications, particularly in wound healing (Neuss et al., 2004; Fu et al., 2009; DelaRosa and Lombardo, 2010; Trayhurn et al., 2011; Shohara et al., 2012; Konno et al., 2013; Cao et al., 2015; Ti et al., 2015; Furuta et al., 2016; Carelli et al., 2018; Feldbrin et al., 2018; Mushahary et al., 2018; Ridiandries et al., 2018; Sahu et al., 2019; Al-Ghadban and Bunnell, 2020; Kuca-Warnawin et al., 2020; Kurte et al., 2020; Munir et al., 2020; Xiao et al., 2020; Bunnell BA, 2021; Krampera and Le Blanc, 2021; Nieto-Nicolau et al., 2021; Krawczenko and Klimczak, 2022; Skibber et al., 2022; Wiese et al., 2022; Cheng et al., 2023; Huerta et al., 2023).

Moreover, the secretome of AD-MSCs, the array of substy release, has positively affected various diseases. Research has focused on the impact of priming or pre-conditioning AD-MSCs with pro-inflammatory cytokines, such as interferon-gamma (IFN-γ) and tumor necrosis factor-alpha (TNFα), on their immunomodulatory capabilities. This treatment enhances their potential to suppress the immune response by upregulating specific genes associated with signaling proteins, immune molecules, and cell surface markers (Heo et al., 2011; Konno et al., 2013; Cao et al., 2015; Saparov et al., 2016; Chinnadurai et al., 2017; Carvalho et al., 2019; Al-Ghadban and Bunnell, 2020; Bunnell BA, 2021). However, the precise balance between immunosuppressive and pro-inflammatory effects remains an area of ongoing exploration. Mesenchymal stem cell (MSC) therapy has experienced substantial growth over the last two decades, with over 1,000 trials conducted.

Nevertheless, only a tiny fraction has progressed to industry-sponsored phase III trials, primarily due to the relative novelty of this field. Challenges persist in optimizing cell quantity delivery methods and comprehending the importance of MSC localization at the injury site. Licensing AD-MSCs with IFN-γ is suggested to enhance their immunomodulatory potential, with clinical experiences showing potential for treating immune-related diseases (Waterman et al., 2010; Heo et al., 2011; Konno et al., 2013; Cao et al., 2015; Saparov et al., 2016; Chinnadurai et al., 2017; Hu and Li, 2018; Carvalho et al., 2019; Al-Ghadban and Bunnell, 2020; Bunnell BA, 2021; Lu and Qiao, 2021). Immunoglobulin kappa chains in various cancer cell types have also garnered attention in recent studies (Chen et al., 2009; Zhao et al., 2021). These investigations underscore the significance of key proteins like RAG1, RAG2, and AID, which are pivotal for immunoglobulin production and rearrangement (Zhao et al., 2021). Although emerging evidence suggests a potential role of immunoglobulin expression in promoting cancer cell growth, the functional consequences remain unclear. Given the vital roles of immunoglobulins in human physiology and disease management, in-depth research is crucial to uncover their multifaceted functions, particularly in cancer etiology and therapeutic strategies. In conclusion, these studies collectively emphasize the importance of AD-MSCs in wound healing, their licensing with pro-inflammatory cytokines, and the intriguing role of immunoglobulins in various cellular contexts, particularly in cancer. Ongoing research holds promise for further advancements in regenerative medicine and cancer biology (Chen et al., 2009; Zhao et al., 2021).

The immense potential of adipose-derived mesenchymal stem cells (AD-MSCs) in regenerative medicine is undeniable. Their regenerative, anti-apoptotic, antifibrotic, anti-oxidative, and immunomodulatory qualities offer substantial promise for clinical therapy (DelaRosa and Lombardo, 2010; Konno et al., 2013; Cao et al., 2015; Carelli et al., 2018; Qi et al., 2018; Pittenger et al., 2019; Song et al., 2020; Bunnell BA, 2021; Szucs et al., 2023). Additionally, our evolving comprehension of AD-MSCs has unveiled the dynamic role played by their secretome and the substances they release (Trayhurn et al., 2011). This secretome can be customized through specific pretreatments, enhancing its therapeutic adaptability. Investigations into the paracrine effects of AD-MSCs have yielded compelling findings. For instance, pre-conditioning AD-MSCs with tumor necrosis factor-alpha (TNFα) and applying their secretome to cutaneous wounds in rats has remarkably expedited wound healing, proliferation, angiogenesis, epithelialization, and macrophage recruitment (Heo et al., 2011; Saparov et al., 2016). Notably, pro-inflammatory cytokines like IL-6 and IL-8 have been recognized as contributors to this acceleration (Saparov et al., 2016; Heo et al., 2011) Similarly, AD-MSCs subjected to pre-treatment with lipopolysaccharides (LPS) have demonstrated their potential in promoting wound healing and angiogenesis, coupled with an increased release of growth factors associated with tissue regeneration and immune responses (Wang et al., 2022). AD-MSCs have showcased their immunomodulatory capabilities in a mouse model of atopic dermatitis, effectively suppressing B-lymphocyte proliferation and maturation (Shin et al., 2017). These promising findings underscore the diverse applications of AD-MSCs and their secretome in regenerative medicine. The varying roles of cytokines, the impact of factors such as MMP-9 and MMP-8 on wound healing, and identifying potential therapeutic targets collectively enrich the landscape of AD-MSC therapy. The intricate interplay of these elements highlights their critical significance in advancing regenerative medicine (Chang and Nguyen, 2021). Croitoru-Lamoury and others explored how the

proinflammatory cytokines TNF-α and IFN-γ influence the gene expression of chemokines and their receptors in human mesenchymal stem cells (HuMSCs). HuMSCs were exposed to TNF-α, IFN-γ, or a combination of both for up to 72 h, and gene expression was examined using RT-PCR at various time points (Croitoru-Lamoury et al., 2007). The findings revealed that TNF-α increased the expression of the receptor CXCR4, while both TNF-α and IFN-γ boosted the gene transcription of multiple chemokines (CCL2/MCP-1, CCL3/MIP-1α, CCL4/MIP-1β, CCL5/RANTES, CXCL8/IL-8, CXCL10/IP-10) and cytokines (IL-1β and IL-6). IFN-γ specifically heightened the gene expression of specific chemokines (CXCL9/MIG, CX3CL1/fractalkine) and IL-6. Notably, the combined treatment of TNF-α and IFN-γ synergistically increased the expression of several genes, including CCL3/MIP-1α, CCL4/MIP-1β, CCL5/RANTES, CXCL9/MIG, CXCL10/IP-10, CX3CL1/fractalkine, IL-1β, and IL-6 (Croitoru-Lamoury et al., 2007). One of the most important anti-inflammatory cytokines is IL-10. MSCs can act on macrophages or dendritic cells to produce IL-10, but whether or not MSCs can secret IL-10 by themselves is still controversial (Yagi et al., 2010).

In a very comprehensive and detailed comparative study, it has been demonstrated that MSC from various tissues secreted MCP-1, IL-8, VEGF, IL-6, IL-5, IFNγ, and MIP-1β influenced by the age of the culture (Croitoru-Lamoury et al., 2007). In the studies, MSCs from different tissues were tested without treatment, where it was found that fat-derived MSCs secrete the highest levels of IL-6. The pro-inflammatory cytokines TNF-α, IL-2, IL-9, and IL-17, expressed in the supernatant, were associated with myogenic differentiation (Croitoru-Lamoury et al., 2007). The collaborative application of IFN-γ and TNF-α significantly amplifies MSCs' ability to produce factor H, a pivotal molecule crucial for impeding complement activation (Tu et al., 2010; Saparov et al., 2016). Similar to our result, IL-1b induced TNF-α, IL-6, IL-8, IL-23A, CCL5, CCL20, CXCL10, CXCL11 cytokine secretion along with increased expression of adhesion molecules (VCAM-1, ICAM-1, ICAM-4) (Saparov et al., 2016). When MSC was subjected to multi-cytokine priming involving TNF-α, IL-1β, and IFN-γ, the presence of IL-1β further amplified the well-established immunoregulatory activity initiated by TNF-α/IFN-γ (Hackel et al., 2021). Prolonged treatment of TNFa resulted in similar gene expression and cytokine secretion (IL-4, IL-8, IL6, and IL10 to our findings (Lee et al., 2010; Ting et al., 2021).

However, how these treatments affect the real wound healing ability was not tested. TLR receptors are one of the most ancient components of defense against pathogens and innate immunity. Tests with LPS (TLR4) and PolyI:C (TLR3) showed that MSC lifted their IL-6 and IL-8 expression (Fuenzalida et al., 2016; Park et al., 2016; Vereb et al., 2016; Vereb et al., 2020; Szucs et al., 2023), and the TLR3 manifest a more potent immunosuppressive phenotype (Fuenzalida et al., 2016; Park et al., 2016).

In summary, AD-MSCs have emerged as formidable allies in pursuing effective treatments for non-healing, chronic, and inflamed wounds, even in prolonged inflammation. While these diverse treatments may activate distinct pathways, their cumulative potential in fostering tissue healing, remodeling the extracellular matrix, and promoting regeneration within clinical settings is undeniably remarkable (Hu and Li, 2018; Naji et al., 2019; Pittenger et al., 2019; Mazini et al., 2020; Szucs et al., 2023).

Data availability statement

The original contributions presented in the study are included in the article/Supplementary Material, further inquiries can be directed to the corresponding author.

Ethics statement

The studies involving humans were approved by National Public Health and Medical Officer Service (NPHMOS) and the National Medical Research Council (16821-6/2017/EÜIG, STEM-01/2017. The studies were conducted in accordance with the local legislation and institutional requirements. The participants provided their written informed consent to participate in this study.

Author contributions

DS: Data curation, Investigation, Methodology, Visualization, Writing–original draft, Writing–review and editing. TM: Data curation, Investigation, Methodology, Visualization, Writing–original draft. VM: Data curation, Formal Analysis, Investigation, Methodology, Software, Validation, Visualization, Writing–original draft, Writing–review and editing. ZP: Writing–original draft, Data curation. SP: Investigation, Methodology, Resources, Writing–original draft, Writing–review and editing. LK: Funding acquisition, Visualization, Writing–review and editing. ZV: Conceptualization, Funding acquisition, Investigation, Methodology, Project administration, Resources, Supervision, Writing–original draft, Writing–review and editing.

Funding

The author(s) declare that financial support was received for the research, authorship, and/or publication of this article. This work was supported by the National Research, Development, and Innovation Office (NKFI PD 132570 to ZV) and GINOP_PLUSZ-2.1.1-21-2022-00043 project (co-financed by the European Union and the European Regional Development Fund) ZV was supported by the Bolyai János Postdoctoral Fellowship (BO/00190/20/5). Project no. TKP2021-EGA-28 has been implemented with support from the Ministry of Innovation and Technology of Hungary from the National Research, Development and Innovation Fund, financed under the TKP2021-EGA funding scheme. LK has received funding from the EU's Horizon 2020 research and innovation program under grant agreement No. 739593. The Biobank Competence Centre of the Life Sciences Cluster of the Centre of Excellence for Interdisciplinary Research, Development, and Innovation of the University of Szeged supported the research. SP was supported by Project no. TKP2021-NKTA-34 has been implemented with the support provided by the Ministry of Culture and Innovation of Hungary from the National Research, Development and Innovation Fund, financed under the TKP2021-NKTA funding scheme.

Acknowledgments

We would like to express our very great appreciation to Katalin Boldog for her administrative and technical support during our research work.

Conflict of interest

The authors declare that the research was conducted in the absence of any commercial or financial relationships that could be construed as a potential conflict of interest.

Publisher's note

All claims expressed in this article are solely those of the authors and do not necessarily represent those of their affiliated organizations, or those of the publisher, the editors and the reviewers. Any product that may be evaluated in this article, or claim that may be made by its manufacturer, is not guaranteed or endorsed by the publisher.

Supplementary material

The Supplementary Material for this article can be found online at: https://www.frontiersin.org/articles/10.3389/fcell.2024.1367242/full#supplementary-material

SUPPLEMENTARY FIGURE S1
Successful tri-lineage differentiation of AD-MSCs is demonstrated, with microscopic images illustrating the characteristic features of each tissue type.

SUPPLEMENTARY TABLE S1
The result of Functional Gene Ontology enrichment performed by ViSEAGO.

References

Aggarwal Sp, M. F., and Pittenger, M. F. (2005). Human mesenchymal stem cells modulate allogeneic immune cell responses. *Blood* 1054, 1815–1822. doi:10.1182/blood-2004-04-1559

Al-Ghadban, S., and Bunnell, B. A. (2020). Adipose tissue-derived stem cells: immunomodulatory effects and therapeutic potential. *Physiology* 352, 125–133. doi:10.1152/physiol.00021.2019

Anton, K., Banerjee, D., and Glod, J. (2012). Macrophage-associated mesenchymal stem cells assume an activated, migratory, pro-inflammatory phenotype with increased IL-6 and CXCL10 secretion. *Plos One* 74, e35036. doi:10.1371/journal.pone.0035036

Bartholomew, A., Sturgeon, C., Siatskas, M., Ferrer, K., McIntosh, K., Patil, S., et al. (2002). Mesenchymal stem cells suppress lymphocyte proliferation *in vitro* and prolong skin graft survival *in vivo*. *Exp. Hematol.* 301, 42–48. doi:10.1016/s0301-472x(01)00769-x

Brembilla, N. C., Vuagnat, H., Boehncke, W. H., Krause, K. H., and Preynat-Seauve, O. (2023). Adipose-derived stromal cells for chronic wounds: scientific evidence and roadmap toward clinical practice. *Stem Cell Transl. Med.* 121, 17–25. doi:10.1093/stcltm/szac081

Brionne, A., Juanchich, A., and Hennequet-Antier, C. (2019). ViSEAGO: a Bioconductor package for clustering biological functions using Gene Ontology and semantic similarity. *BioData Min.* 12, 16. doi:10.1186/s13040-019-0204-1

Bunnell Ba, (2021). Adipose tissue-derived mesenchymal stem cells. *Cells* 10, 3433. doi:10.3390/cells10123433

Cao, W., Cao, K., Cao, J., Wang, Y., and Shi, Y. (2015). Mesenchymal stem cells and adaptive immune responses. *Immunol. Lett.* 1682, 147–153. doi:10.1016/j.imlet.2015.06.003

Carelli, S., Colli, M., Vinci, V., Caviggioli, F., Klinger, M., and Gorio, A. (2018). Mechanical activation of adipose tissue and derived mesenchymal stem cells: novel anti-inflammatory properties. *Int. J. Mol. Sci.* 191, 267. doi:10.3390/ijms19010267

Carvalho, A. E. S., Sousa, M. R. R., Alencar-Silva, T., Carvalho, J. L., and Saldanha-Araujo, F. (2019). Mesenchymal stem cells immunomodulation: the road to IFN-gamma licensing and the path ahead. *Cytokine and growth factor Rev.* 47, 32–42. doi:10.1016/j.cytogfr.2019.05.006

Chang, M., and Nguyen, T. T. (2021). Strategy for treatment of infected diabetic foot ulcers. *Accounts Chem. Res.* 545, 1080–1093. doi:10.1021/acs.accounts.0c00864

Chen, Z., Qiu, X., and Gu, J. (2009). Immunoglobulin expression in non-lymphoid lineage and neoplastic cells. *Am. J. pathology* 1744, 1139–1148. doi:10.2353/ajpath.2009.080879

Cheng, H. Y., Anggelia, M. R., Lin, C. H., and Wei, F. C. (2023). Toward transplantation tolerance with adipose tissue-derived therapeutics. *Front. Immunol.* 14, 1111813. doi:10.3389/fimmu.2023.1111813

Chinnadurai, R., Rajan, D., Ng, S., McCullough, K., Arafat, D., Waller, E. K., et al. (2017). Immune dysfunctionality of replicative senescent mesenchymal stromal cells is corrected by IFNγ priming. *Blood Adv.* 111, 628–643. doi:10.1182/bloodadvances.2017006205

Croitoru-Lamoury, J., Lamoury, F. M., Zaunders, J. J., Veas, L. A., and Brew, B. J. (2007). Human mesenchymal stem cells constitutively express chemokines and chemokine receptors that can be upregulated by cytokines, IFN-beta, and Copaxone. *J. Interferon Cytokine Res.* 271, 53–64. doi:10.1089/jir.2006.0037

Crop, M. J. B., Korevaar, C. C., Ijzermans, S. S., Pescatori, J. N., et al. (2010). Inflammatory conditions affect gene expression and function of human adipose tissue-derived mesenchymal stem cells. *Clin. Exp. Immunol.* 1623, 474–486. doi:10.1111/j.1365-2249.2010.04256.x

DelaRosa, O., and Lombardo, E. (2010). Modulation of adult mesenchymal stem cells activity by toll-like receptors: implications on therapeutic potential. *Mediat. Inflamm.* 2010, 865601. doi:10.1155/2010/865601

Feldbrin, Z., Omelchenko, E., Lipkin, A., and Shargorodsky, M. (2018). Osteopontin levels in plasma, muscles, and bone in patient with non-healing diabetic foot ulcers: a new player in wound healing process? *J. Diabetes Complicat* 328, 795–798. doi:10.1016/j.jdiacomp.2018.05.009

François, M., Romieu-Mourez, R., Li, M. Y., and Galipeau, J. (2012). Human MSC suppression correlates with cytokine induction of indoleamine 2,3-dioxygenase and bystander M2 macrophage differentiation. *Mol. Ther.* 201, 187–195. doi:10.1038/mt.2011.189

Fu, X., Han, B., Cai, S., Lei, Y., Sun, T., and Sheng, Z. (2009). Migration of bone marrow-derived mesenchymal stem cells induced by tumor necrosis factor-alpha and its possible role in wound healing. *Wound repair Regen.* 172, 185–191. doi:10.1111/j.1524-475X.2009.00454.x

Fuenzalida, P., Kurte, M., Fernandez-O'ryan, C., Ibanez, C., Gauthier-Abeliuk, M., Vega-Letter, A. M., et al. (2016). Toll-like receptor 3 pre-conditioning increases the therapeutic efficacy of umbilical cord mesenchymal stromal cells in a dextran sulfate sodium-induced colitis model. *Cytotherapy* 185, 630–641. doi:10.1016/j.jcyt.2016.02.002

Furuta, T., Miyaki, S., Ishitobi, H., Ogura, T., Kato, Y., Kamei, N., et al. (2016). Mesenchymal stem cell-derived exosomes promote fracture healing in a mouse model. *Stem Cell Transl. Med.* 512, 1620–1630. doi:10.5966/sctm.2015-0285

Ghannam, S., Bouffi, C., Djouad, F., Jorgensen, C., and Noel, D. (2010). Immunosuppression by mesenchymal stem cells: mechanisms and clinical applications. *Stem Cell Res. Ther.* 11, 2. doi:10.1186/scrt2

Gu, Z., Eils, R., and Schlesner, M. (2016). Complex heatmaps reveal patterns and correlations in multidimensional genomic data. *Bioinformatics* 3218, 2847–2849. doi:10.1093/bioinformatics/btw313

Guasti, L., New, S. E., Hadjidemetriou, I., Palmiero, M., and Ferretti, P. (2018). Plasticity of human adipose-derived stem cells - relevance to tissue repair. *Int. J. Dev. Biol.* 62, 431–439. doi:10.1387/ijdb.180074pf

Hackel, A., Aksamit, A., Bruderek, K., Lang, S., and Brandau, S. (2021). TNF-α and IL-1β sensitize human MSC for IFN-γ signaling and enhance neutrophil recruitment. *Eur. J. Immunol.* 512, 319–330. doi:10.1002/eji.201948336

Heo, S. C., Jeon, E. S., Lee, I. H., Kim, H. S., Kim, M. B., and Kim, J. H. (2011). Tumor necrosis factor-alpha-activated human adipose tissue-derived mesenchymal stem cells accelerate cutaneous wound healing through paracrine mechanisms. *J. investigative dermatology* 1317, 1559–1567. doi:10.1038/jid.2011.64

Hu, C., and Li, L. (2018). Preconditioning influences mesenchymal stem cell properties *in vitro* and *in vivo*. *J. Cell. Mol. Med.* 223, 1428–1442. doi:10.1111/jcmm.13492

Huerta, C. T., Voza, F. A., Ortiz, Y. Y., Liu, Z. J., and Velazquez, O. C. (2023). Mesenchymal stem cell-based therapy for non-healing wounds due to chronic limb-threatening ischemia: a review of preclinical and clinical studies. *Front. Cardiovasc. Med.* 10, 1113982. doi:10.3389/fcvm.2023.1113982

Konno, M., Hamabe, A., Hasegawa, S., Ogawa, H., Fukusumi, T., Nishikawa, S., et al. (2013). Adipose-derived mesenchymal stem cells and regenerative medicine. *Dev. Growth Differ.* 553, 309–318. doi:10.1111/dgd.12049

Korotkevich, G., Sukhov, V., Budin, N., Shpak, B., Artyomov, M. N., and Sergushichev, A. (2021). Fast gene set enrichment analysis. *bioRxiv*. doi:10.1101/060012

Krampera, M., Cosmi, L., Angeli, R., Pasini, A., Liotta, F., Andreini, A., et al. (2006). Role for interferon-gamma in the immunomodulatory activity of human bone marrow mesenchymal stem cells. *Stem Cells* 242, 386–398. doi:10.1634/stemcells.2005-0008

Krampera, M., and Le Blanc, K. (2021). Mesenchymal stromal cells: putative microenvironmental modulators become cell therapy. *Cell stem Cell* 2810, 1708–1725. doi:10.1016/j.stem.2021.09.006

Krawczenko, A., and Klimczak, A. (2022). Adipose tissue-derived mesenchymal stem/stromal cells and their contribution to angiogenic processes in tissue regeneration. *Int. J. Mol. Sci.* 23, 2425. doi:10.3390/Ijms23052425

Kuca-Warnawin, E., Janicka, I., Szczesny, P., Olesinska, M., Bonek, K., Gluszko, P., et al. (2020). Modulation of T-cell activation markers expression by the adipose tissue-derived mesenchymal stem cells of patients with rheumatic diseases. *Cell Transplant.* 29, 963689720945682. doi:10.1177/0963689720945682

Kurte, M., Vega-Letter, A. M., Luz-Crawford, P., Djouad, F., Noël, D., Khoury, M., et al. (2020). Time-dependent LPS exposure commands MSC immunoplasticity through TLR4 activation leading to opposite therapeutic outcome in EAE. *Stem Cell Res. Ther.* 111, 416. doi:10.1186/s13287-020-01840-2

Lee, M. J., Kim, J., Kim, M. Y., Bae, Y. S., Ryu, S. H., Lee, T. G., et al. (2010). Proteomic analysis of tumor necrosis factor-alpha-induced secretome of human adipose tissue-derived mesenchymal stem cells. *J. Proteome Res.* 94, 1754–1762. doi:10.1021/pr900898n

Li, N., and Hua, J. L. (2017). Interactions between mesenchymal stem cells and the immune system. *Cell Mol. Life Sci.* 7413, 2345–2360. doi:10.1007/s00018-017-2473-5

Li, W., Ren, G., Huang, Y., Su, J., Han, Y., Li, J., et al. (2012). Mesenchymal stem cells: a double-edged sword in regulating immune responses. *Cell death Differ.* 199, 1505–1513. doi:10.1038/cdd.2012.26

Lu, S., and Qiao, X. (2021). Single-cell profiles of human bone marrow-derived mesenchymal stromal cells after IFN-γ and TNF-α licensing. *Gene* 771, 145347. doi:10.1016/j.gene.2020.145347

Mazini, L., Rochette, L., Admou, B., Amal, S., and Malka, G. (2020). Hopes and limits of adipose-derived stem cells (ADSCs) and mesenchymal stem cells (MSCs) in wound healing. *Int. J. Mol. Sci.* 214, 1306. doi:10.3390/Ijms21041306

Meisel, R., Zibert, A., Laryea, M., Gobel, U., Daubener, W., and Dilloo, D. (2004). Human bone marrow stromal cells inhibit allogeneic T-cell responses by indoleamine 2,3-dioxygenase-mediated tryptophan degradation. *Blood* 10312, 4619–4621. doi:10.1182/blood-2003-11-3909

Munir, S., Basu, A., Maity, P., Krug, L., Haas, P., Jiang, D. S., et al. (2020). TLR4-dependent shaping of the wound site by MSCs accelerates wound healing. *Embo Rep.* 215, e48777. doi:10.15252/embr.201948777

Mushahary, D., Spittler, A., Kasper, C., Weber, V., and Charwat, V. (2018). Isolation, cultivation, and characterization of human mesenchymal stem cells. *Cytom. Part A* 93A1, 19–31. doi:10.1002/cyto.a.23242

Naji, A., Eitoku, M., Favier, B., Deschaseaux, F., Rouas-Freiss, N., and Suganuma, N. (2019). Biological functions of mesenchymal stem cells and clinical implications. *Cell Mol. Life Sci.* 7617, 3323–3348. doi:10.1007/s00018-019-03125-1

Neuss, S., Becher, E., Wöltje, M., Tietze, L., and Jahnen-Dechent, W. (2004). Functional expression of HGF and HGF receptor/c-met in adult human mesenchymal stem cells suggests a role in cell mobilization, tissue repair, and wound healing. *Stem Cells* 223, 405–414. doi:10.1634/stemcells.22-3-405

Nieto-Nicolau, N., Martinez-Conesa, E. M., Fuentes-Julian, S., Arnalich-Montiel, F., Garcia-Tunon, I., De Miguel, M. P., et al. (2021). Priming human adipose-derived mesenchymal stem cells for corneal surface regeneration. *J. Cell. Mol. Med.* 2511, 5124–5137. doi:10.1111/jcmm.16501

Park, K. S., Kim, S. H., Das, A., Yang, S. N., Jung, K. H., Kim, M. K., et al. (2016). TLR3-/4-Priming differentially promotes Ca(2+) signaling and cytokine expression and Ca(2+)-dependently augments cytokine release in hMSCs. *Sci. Rep.* 6, 23103. doi:10.1038/srep23103

Pittenger, M. F., Discher, D. E., Peault, B. M., Phinney, D. G., Hare, J. M., and Caplan, A. I. (2019). Mesenchymal stem cell perspective: cell biology to clinical progress. *NPJ Regen. Med.* 4, 22. doi:10.1038/s41536-019-0083-6

Qi, K., Li, N., Zhang, Z., and Melino, G. (2018). Tissue regeneration: the crosstalk between mesenchymal stem cells and immune response. *Cell. Immunol.* 326, 86–93. doi:10.1016/j.cellimm.2017.11.010

Renner, P., Eggenhofer, E., Rosenauer, A., Popp, F. C., Steinmann, J. F., Slowik, P., et al. (2009). Mesenchymal stem cells require a sufficient, ongoing immune response to exert their immunosuppressive function. *Transplant. Proc.* 416, 2607–2611. doi:10.1016/j.transproceed.2009.06.119

Ridiandries, A., Tan, J. T. M., and Bursill, C. A. (2018). The role of chemokines in wound healing. *Int. J. Mol. Sci.* 1910, 3217. doi:10.3390/Ijms19103217

Sahu, A., Foulsham, W., Amouzegar, A., Mittal, S. K., and Chauhan, S. K. (2019). The therapeutic application of mesenchymal stem cells at the ocular surface. *ocular Surf.* 172, 198–207. doi:10.1016/j.jtos.2019.01.006

Saparov, A., Ogay, V., Nurgozhin, T., Jumabay, M., and Chen, W. C. (2016). Preconditioning of human mesenchymal stem cells to enhance their regulation of the immune response. *Stem Cells Int.* 2016, 3924858. doi:10.1155/2016/3924858

Shin, T. H., Lee, B. C., Choi, S. W., Shin, J. H., Kang, I., Lee, J. Y., et al. (2017). Human adipose tissue-derived mesenchymal stem cells alleviate atopic dermatitis via regulation of B lymphocyte maturation. *Oncotarget* 81, 512–522. doi:10.18632/oncotarget.13473

Shohara, R., Yamamoto, A., Takikawa, S., Iwase, A., Hibi, H., Kikkawa, F., et al. (2012). Mesenchymal stromal cells of human umbilical cord Wharton's jelly accelerate wound healing by paracrine mechanisms. *Cytotherapy* 1410, 1171–1181. doi:10.3109/14653249.2012.706705

Skibber, M. A., Olson, S. D., Prabhakara, K. S., Gill, B. S., and Cox, C. S. (2022). Enhancing mesenchymal stromal cell potency: inflammatory licensing *via* mechanotransduction. *Front. Immunol.* 13, 874698. doi:10.3389/Fimmu.2022.874698

Song, N., Scholtemeijer, M., and Shah, K. (2020). Mesenchymal stem cell immunomodulation: mechanisms and therapeutic potential. *Trends Pharmacol. Sci.* 419, 653–664. doi:10.1016/j.tips.2020.06.009

Szucs, D., Miklos, V., Monostori, T., Guba, M., Kun-Varga, A., Poliska, S., et al. (2023). Effect of inflammatory microenvironment on the regenerative capacity of adipose-derived mesenchymal stem cells. *Cells* 1215, 1966. doi:10.3390/cells12151966

Ti, D., Hao, H., Tong, C., Liu, J., Dong, L., Zheng, J., et al. (2015). LPS-preconditioned mesenchymal stromal cells modify macrophage polarization for resolution of chronic inflammation via exosome-shuttled let-7b. *J. Transl. Med.* 13, 308. doi:10.1186/s12967-015-0642-6

Ting, H. K., Chen, C. L., Meng, E., Cherng, J. H., Chang, S. J., Kao, C. C., et al. (2021). Inflammatory regulation by TNF-alpha-activated adipose-derived stem cells in the human bladder cancer microenvironment. *Int. J. Mol. Sci.* 228. doi:10.3390/ijms22083987

Trayhurn, P., Drevon, C. A., and Eckel, J. (2011). Secreted proteins from adipose tissue and skeletal muscle - adipokines, myokines and adipose/muscle cross-talk. *Archives physiology Biochem.* 1172, 47–56. doi:10.3109/13813455.2010.535835

Tu, Z., Li, Q., Bu, H., and Lin, F. (2010). Mesenchymal stem cells inhibit complement activation by secreting factor H. *Stem Cells Dev.* 1911, 1803–1809. doi:10.1089/scd.2009.0418

Vereb, Z., Mazlo, A., Szabo, A., Poliska, S., Kiss, A., Litauszky, K., et al. (2020). Vessel wall-derived mesenchymal stromal cells share similar differentiation potential and immunomodulatory properties with bone marrow-derived stromal cells. *Stem Cells Int.* 2020, 8847038. doi:10.1155/2020/8847038

Vereb, Z., Poliska, S., Albert, R., Olstad, O. K., Boratko, A., Csortos, C., et al. (2016). Role of human corneal stroma-derived mesenchymal-like stem cells in corneal immunity and wound healing. *Sci. Rep.* 6, 26227. doi:10.1038/srep26227

Wang, K. X., Chen, Z. Y., Jin, L., Zhao, L. L., Meng, L. B., Kong, F. T., et al. (2022). LPS-pretreatment adipose-derived mesenchymal stromal cells promote wound healing in diabetic rats by improving angiogenesis. *Injury* 53 (5312), 3920–3929. doi:10.1016/j.injury.2022.09.041

Wang, Y., Chen, X., Cao, W., and Shi, Y. (2014). Plasticity of mesenchymal stem cells in immunomodulation: pathological and therapeutic implications. *Nat. Immunol.* 1511, 1009–1016. doi:10.1038/ni.3002

Waterman, R. S., Tomchuck, S. L., Henkle, S. L., and Betancourt, A. M. (2010). A new mesenchymal stem cell (MSC) paradigm: polarization into a pro-inflammatory MSC1 or an Immunosuppressive MSC2 phenotype. *Plos One* 54, e10088. doi:10.1371/journal.pone.0010088

Wiese, D. M., Wood, C. A., Ford, B. N., and Braid, L. R. (2022). Cytokine activation reveals tissue-imprinted gene profiles of mesenchymal stromal cells. *Front. Immunol.* 13, 917790. doi:10.3389/fimmu.2022.917790

Wu, L., Cai, X., Zhang, S., Karperien, M., and Lin, Y. (2013). Regeneration of articular cartilage by adipose tissue derived mesenchymal stem cells: perspectives from stem cell biology and molecular medicine. *J. Cell. physiology* 2285, 938–944. doi:10.1002/jcp.24255

Xiao, K., He, W., Guan, W., Hou, F., Yan, P., Xu, J., et al. (2020). Mesenchymal stem cells reverse EMT process through blocking the activation of NF-kappaB and Hedgehog pathways in LPS-induced acute lung injury. *Cell death Dis.* 1110, 863. doi:10.1038/s41419-020-03034-3

Yagi, H., Soto-Gutierrez, A., Kitagawa, Y., Tilles, A. W., Tompkins, R. G., and Yarmush, M. L. (2010). Bone marrow mesenchymal stromal cells attenuate organ injury induced by LPS and burn. *Cell Transplant.* 196, 823–830. doi:10.3727/096368910X508942

Yu, G., Li, F., Qin, Y., Bo, X., Wu, Y., and Wang, S. (2010). GOSemSim: an R package for measuring semantic similarity among GO terms and gene products. *Bioinformatics* 267, 976–978. doi:10.1093/bioinformatics/btq064

Zhao, J., Peng, H., Gao, J., Nong, A., Hua, H. M., Yang, S. L., et al. (2021). Current insights into the expression and functions of tumor-derived immunoglobulins. *Cell Death Discov.* 7, 148. doi:10.1038/s41420-021-00550-9

Zwick, R. K., Guerrero-Juarez, C. F., Horsley, V., and Plikus, M. V. (2018). Anatomical, physiological, and functional diversity of adipose tissue. *Cell metab.* 271, 68–83. doi:10.1016/j.cmet.2017.12.002

frontiers | Frontiers in Cell and Developmental Biology

TYPE Original Research
PUBLISHED 31 May 2024
DOI 10.3389/fcell.2024.1385712

OPEN ACCESS

EDITED BY
Tokiko Nagamura-Inoue,
The University of Tokyo, Japan

REVIEWED BY
Pawan Kumar Raghav,
University of California, San Francisco, United States
Kshitiz Raj Shrestha,
Independent Researcher, Kathmandu, Nepal

*CORRESPONDENCE
Vitale Miceli,
vmiceli@ismett.edu

†These authors have contributed equally to this work and share first authorship

RECEIVED 13 February 2024
ACCEPTED 13 May 2024
PUBLISHED 31 May 2024

CITATION
Calligaris M, Zito G, Busà R, Bulati M, Iannolo G, Gallo A, Carreca AP, Cuscino N, Castelbuono S, Carcione C, Centi C, Amico G, Bertani A, Chinnici CM, Conaldi PG, Scilabra SD and Miceli V (2024), Proteomic analysis and functional validation reveal distinct therapeutic capabilities related to priming of mesenchymal stromal/stem cells with IFN-γ and hypoxia: potential implications for their clinical use. *Front. Cell Dev. Biol.* 12:1385712. doi: 10.3389/fcell.2024.1385712

Proteomic analysis and functional validation reveal distinct therapeutic capabilities related to priming of mesenchymal stromal/stem cells with IFN-γ and hypoxia: potential implications for their clinical use

Matteo Calligaris[1†], Giovanni Zito[2†], Rosalia Busà[2†], Matteo Bulati[2], Gioacchin Iannolo[2], Alessia Gallo[2], Anna Paola Carreca[1], Nicola Cuscino[2], Salvatore Castelbuono[2], Claudia Carcione[3], Claudio Centi[2], Giandomenico Amico[3], Alessandro Bertani[4], Cinzia Maria Chinnici[5], Pier Giulio Conaldi[2], Simone Dario Scilabra[1] and Vitale Miceli[2*]

[1]Proteomics Group, Ri.MED Foundation c/o IRCCS ISMETT, Palermo, Italy, [2]Research Department, IRCCS ISMETT (Istituto Mediterraneo per i Trapianti e Terapie ad alta Specializzazione), Palermo, Italy, [3]Ri.MED Foundation c/o IRCCS ISMETT, Palermo, Italy, [4]Thoracic Surgery and Lung Transplantation Unit, IRCCS ISMETT (Istituto Mediterraneo per i Trapianti e Terapie ad alta Specializzazione), Palermo, Italy, [5]Regenerative Medicine and Immunotherapy Area, Ri.MED Foundation c/o IRCCS ISMETT, Palermo, Italy

Mesenchymal stromal/stem cells (MSCs) are a heterogeneous population of multipotent cells that can be obtained from various tissues, such as dental pulp, adipose tissue, bone marrow and placenta. MSCs have gained importance in the field of regenerative medicine because of their promising role in cell therapy and their regulatory abilities in tissue repair and regeneration. However, a better characterization of these cells and their products is necessary to further potentiate their clinical application. In this study, we used unbiased high-resolution mass spectrometry-based proteomic analysis to investigate the impact of distinct priming strategies, such as hypoxia and IFN-γ treatment, on the composition and therapeutic functionality of the secretome produced by MSCs derived from the amniotic membrane of the human placenta (hAMSCs). Our investigation revealed that both types of priming improved the therapeutic efficacy of hAMSCs, and these improvements were related to the secretion of functional factors present in the conditioned medium (CM) and exosomes (EXOs), which play crucial roles in mediating the paracrine effects of MSCs. In particular, hypoxia was able to induce a pro-angiogenic, innate immune response-activating, and tissue-regenerative hAMSC phenotype, as highlighted by the elevated production of regulatory factors such as VEGFA, PDGFRB, ANGPTL4, ENG, GRO-γ, IL8, and GRO-α. IFN-γ priming, instead, led to an immunosuppressive profile in hAMSCs, as indicated by increased levels of TGFB1, ANXA1, THBS1, HOMER2, GRN, TOLLIP and MCP-1. Functional assays validated the increased angiogenic properties of hypoxic hAMSCs and the enhanced immunosuppressive activity of IFN-γ-treated hAMSCs. This study

extends beyond the direct priming effects on hAMSCs, demonstrating that hypoxia and IFN-γ can influence the functional characteristics of hAMSC-derived secretomes, which, in turn, orchestrate the production of functional factors by peripheral blood cells. This research provides valuable insights into the optimization of MSC-based therapies by systematically assessing and comparing the priming type-specific functional features of hAMSCs. These findings highlight new strategies for enhancing the therapeutic efficacy of MSCs, particularly in the context of multifactorial diseases, paving the way for the use of hAMSC-derived products in clinical practice.

KEYWORDS

placenta-derived mesenchymal stromal/stem cells, MSC priming, IFN-γ priming, hypoxia priming, proteomic analysis, MSC therapeutic properties, MSC paracrine effects

1 Introduction

Mesenchymal stromal/stem cells (MSCs) are a heterogeneous population of multipotent cells that can be isolated from various adult or neonatal tissues, including dental pulp, adipose tissue, bone marrow, umbilical cord and placenta, among others (Parolini et al., 2008; Hass et al., 2011; Burja et al., 2020). These cells play a physiological role in tissue repair and regeneration due to their inherent regulatory abilities (Jackson et al., 2012; Morrison and Scadden, 2014; Wosczyna et al., 2019; Miceli et al., 2020; Schmelzer et al., 2020; Lo Nigro et al., 2021), and therefore have been widely explored as promising candidates for therapeutic applications within the field of regenerative medicine (Iijima et al., 2018; Chinnici et al., 2021; Cittadini et al., 2022; Margiana et al., 2022; Miceli and Bertani, 2022; Miceli et al., 2023a; Miceli et al., 2023b; Russo et al., 2023b). Over the years, scientific evidence has highlighted that the therapeutic effects of MSCs are, at least in part, mediated by the secretion of paracrine functional factors and/or biovesicles, including cytokines, chemokines, growth factors, and extracellular vesicles (EVs) such as exosomes (EXOs) (Caplan and Dennis, 2006; Miceli et al., 2021b; Papait et al., 2022; Miceli et al., 2023b; Cui et al., 2023). Consequently, considering the role of paracrine activity in the beneficial effects of MSCs, there is growing interest in elucidating the molecular mechanisms underlying MSC secretion, as this process is crucial for their therapeutic efficacy. Notably, EXOs represent a fundamental functional component of the secretome that is responsible for mediating the paracrine effects of MSCs (Takeuchi et al., 2021; Alberti et al., 2022; Russo et al., 2023a; Bulati et al., 2023). In this case, it is very important to analyze the EXO fraction to characterize its contents and establish its functional role in the context of the MSC secretome.

The examination of MSC secretome features has become fundamental, especially considering the variability in therapeutic outcomes observed in clinical trials where MSCs were used to treat a wide range of diseases, including orthopedic, neurodegenerative, cardiovascular, lung, liver, and kidney diseases (Chen et al., 2023) (as evidenced by 1613 registered clinical trials on clinicaltrials.gov; 03 February 2024). In fact, many studies have previously shown that although MSC-based therapies have demonstrated good safety and tolerability profiles (Wang Y. et al., 2021; Uccelli et al., 2021), their effectiveness varies significantly, often resulting in minimal or no discernible effects (Squillaro et al., 2016; Lukomska et al., 2019; Fricova et al., 2020; Zhou et al., 2021). The different therapeutic outcomes have been linked to the high degree of heterogeneity that characterizes MSCs. In recent years, many findings have associated this observed MSC heterogeneity with both intrinsic biological aspects, such as differences in tissue origin and donor-to-donor variation in MSC function (McLeod and Mauck, 2017; Zha et al., 2021), and technical aspects, such as differences in the harvesting and culturing laboratory methods required for MSC expansion before clinical application (Stroncek et al., 2020; Wang Y. H. et al., 2021). Both cell sources and surface markers have proven to be unreliable as indicators of MSC therapeutic success (Robey, 2017). In this regard, however, the International Society for Cell and Gene Therapy (ISCT) recommend that the definition of MSCs be integrated with their tissue origin to underscore the tissue-specific properties of MSCs, which might be linked to expected therapeutic actions (Viswanathan et al., 2019). Several studies have suggested that MSCs isolated from different tissues exhibit distinct phenotypes and functional properties (Melief et al., 2013; Phinney and Sensebe, 2013). This heterogeneity has led some research groups to carefully characterize the MSC secretome in terms of trophic (Hofer and Tuan, 2016), immunomodulatory (Munoz-Perez et al., 2021), and pro-angiogenic factors (Maacha et al., 2020). In particular, quantitative proteomic analyses have revealed functional disparities between the secretomes of MSCs derived from fetal and adult skin (Gaetani et al., 2018). Additionally, using liquid chromatography-tandem mass spectrometry, variable angiogenic potential has been demonstrated between the secretomes of MSCs derived from adipose tissue, bone marrow, and Wharton's jelly (Kehl et al., 2019). These recent findings reveal that MSCs isolated from diverse tissue sources possess distinct proteomic and functional traits and underscore the challenge of establishing consistent conclusions regarding the true therapeutic efficacy of MSCs.

To address these issues, many studies have focused on the concept of preconditioning MSCs (MSC priming) before their clinical use as a possible strategy to enhance and modulate the beneficial therapeutic properties of MSCs. In this regard, different stimuli and culture conditions, such as hypoxia exposure, cytokine treatments and 3D culture conditions have been used to direct MSCs toward specific immunomodulatory or trophic effects, thereby augmenting their regenerative potential (Ferreira et al., 2018; Miceli et al., 2019; Gallo et al., 2022). Several studies have shown that specific priming strategies at different stages of MSC production can modify the MSC secretome (Miceli et al., 2020; Miceli et al.,

2021a; Zito et al., 2022; Bulati et al., 2023; Chouaib et al., 2023), emphasizing the potential role of the preconditioning strategy in the standardization of this approach (Dunn et al., 2021; Miceli et al., 2023b; Chouaib et al., 2023). For instance, IFN-γ has been employed as a crucial activator of MSC-mediated immunosuppression by upregulating the production of indoleamine 2,3-dioxygenase 1 (IDO), prostaglandin E synthase 2 (PGE2), interleukin 10 (IL10), and CCL4 (MIP1B) (Kim et al., 2018; Bulati et al., 2020). Preclinical studies have also demonstrated that IFN-γ-primed MSCs exhibit greater efficacy than naïve cells in various immune-related disease models (Duijvestein et al., 2011; Kanai et al., 2021). As anticipated, the composition of the MSC secretome can also be modulated by preconditioning MSCs under hypoxia. In this regard, in both *in vitro* and *in vivo* models, it has been revealed that when MSCs are exposed to temporary hypoxia, mimicking the stem cell niche microenvironment, they undergo genetic transcription changes that lead to an increase in cytoprotective and regenerative abilities, along with improved angiogenic properties (Leroux et al., 2010; Wei et al., 2012; Hu et al., 2016).

In this study, using MSCs derived from the amniotic membrane of the human placenta (hAMSCs), we aim to characterize the hAMSC secretome by evaluating both secreted and exosomal proteins. Our goals are to comprehensively investigate the impact of IFN-γ or hypoxia priming on hAMSCs and to systematically assess and compare priming type-specific functional features.

2 Materials and methods

2.1 Isolation, culture and phenotypic characterization of amnion-derived mesenchymal stromal/stem cells

To obtain MSCs, written informed consent was obtained from each donor, and the procedure was approved by IRCCS ISMETT's Institutional Research Review Board (IRRB, code: IRRB/39/20). MSCs were isolated from the amniotic membrane of the human term placenta (38–40 weeks of gestation) of healthy donors within 6 h of birth. The amnion was mechanically separated from the chorion and washed several times in phosphate-buffered saline (PBS). The amniotic membrane was then cut into pieces of 3 × 3 cm^2 and each piece was decontaminated via incubation in PBS supplemented with 2.5% iodopovidone (Esoform, Italy) for a few seconds, followed by incubation in PBS containing 500 U/mL penicillin, 500 mg/mL streptomycin, 12.5 mg/mL amphotericin B, and 1.87 mg/mL cefamezin (Pfizer, Italy) for 3 min and subsequent incubation in PBS containing 100 U/mL penicillin and 100 mg/mL streptomycin for 5 min. Decontaminated fragments were treated for 9 min at 37°C in hanks' balanced salt solution (HBSS) (Lonza, CH) containing 2.5 U/mL dispase (Corning, NY, United States). To neutralize the dispase, the fragments were incubated for 5 min at room temperature in roswell park memorial institute (RPMI) 1640 complete medium (Invitrogen, United States) supplemented with 10% fetal bovine serum (FBS) (HyClone, United States) and then digested with 0.94 mg/mL collagenase A (Roche, Germany) and 20 mg/mL DNase (Roche, Germany) for 2.5 h at 37°C. The digest was successively filtered through 100 µm and 70 µm cell strainers (BD Falcon, United States), pelleted by centrifugation at 150–300 g for 10 min, and resuspended in RPMI 1640 complete medium (Invitrogen, United States) supplemented with 10% FBS for cell counting. The cells obtained were cultured in polystyrene culture dishes (Corning, NY, United States) at 37°C and 5% CO_2 in Chang medium (Irvine Scientific, United States) for the first step and expansion. For phenotypic characterization, hAMSCs were first washed twice with FACS buffer (PBS containing 0.3% BSA and 0.1% NaN_3) and then incubated on ice for 30 min with specific antibodies against CD90, CD73, CD13, CD45, and HLA-DR (BD Biosciences, United States). Finally. the cells were washed twice with FACS buffer and analyzed using the FACSCelesta™ cytometer (BD Life Sciences, United Kingdom).

2.2 Priming and conditioned medium preparation

For conditioned medium (CM) collection from cultures with or without priming, hAMSCs at the second step were cultured in Chang medium until 90% confluence. Then the medium was replaced with serum-free dulbecco's modified eagle medium (DMEM) medium supplemented with or without 200 IU/mL IFN-γ (Human IFN-g1b premium grade, Miltenyi Biotec, Germany) and the cells were grown at 37°C, 20% O_2 and 5% CO_2. For CM collection from hypoxic priming, the cells were cultured with serum-free DMEM medium at 37°C, 1% O_2 and 5% CO_2. The supernatants from all the cultures were harvested after 48 h and frozen at −80°C until use.

2.3 Isolation and characterization of exosomes

EXOs were isolated from each primed and unprimed CM through ultracentrifugation. The CM was centrifuged at 300 *g* for 10 min to remove the debris. To further remove both cells and debris, the CM was centrifuged for 20 min at 16500 × g and then ultracentrifuged at 120000 × g for 90 min at 4°C to pellet the EXOs. The total protein content of the EXO preparations was determined using the Micro BCA Protein Assay Reagent Kit following the manufacturer's instructions (Thermo Scientific, United States). To characterize the EXOs, their size, distribution, and concentration (Figure 1C) were determined via nanoparticle tracking analysis (NTA) in a NanoSight NS3000 (Malvern Instruments Ltd., United Kingdom). The samples were diluted 1: 500 with PBS to reach an optimal concentration for instrument linearity. Readings were taken in quintuplicate of 60 s at 25 frames per second, and the data obtained were then analyzed with NTA software version 3.1 (Build 3.1.54, Analytik Ltd, United Kingdom).

2.4 Mass spectrometry analysis

2 mL of conditioned medium or 10 µg of isolated exosomes from differentially stimulated MSCs underwent filter aided sample preparation (FASP) with 10 kDa Vivacon 500 spin filters (Wisniewski et al., 2009). Briefly, proteins were reduced with 20 mM dithiothreitol for 30 min at 37°C and free cysteine residues

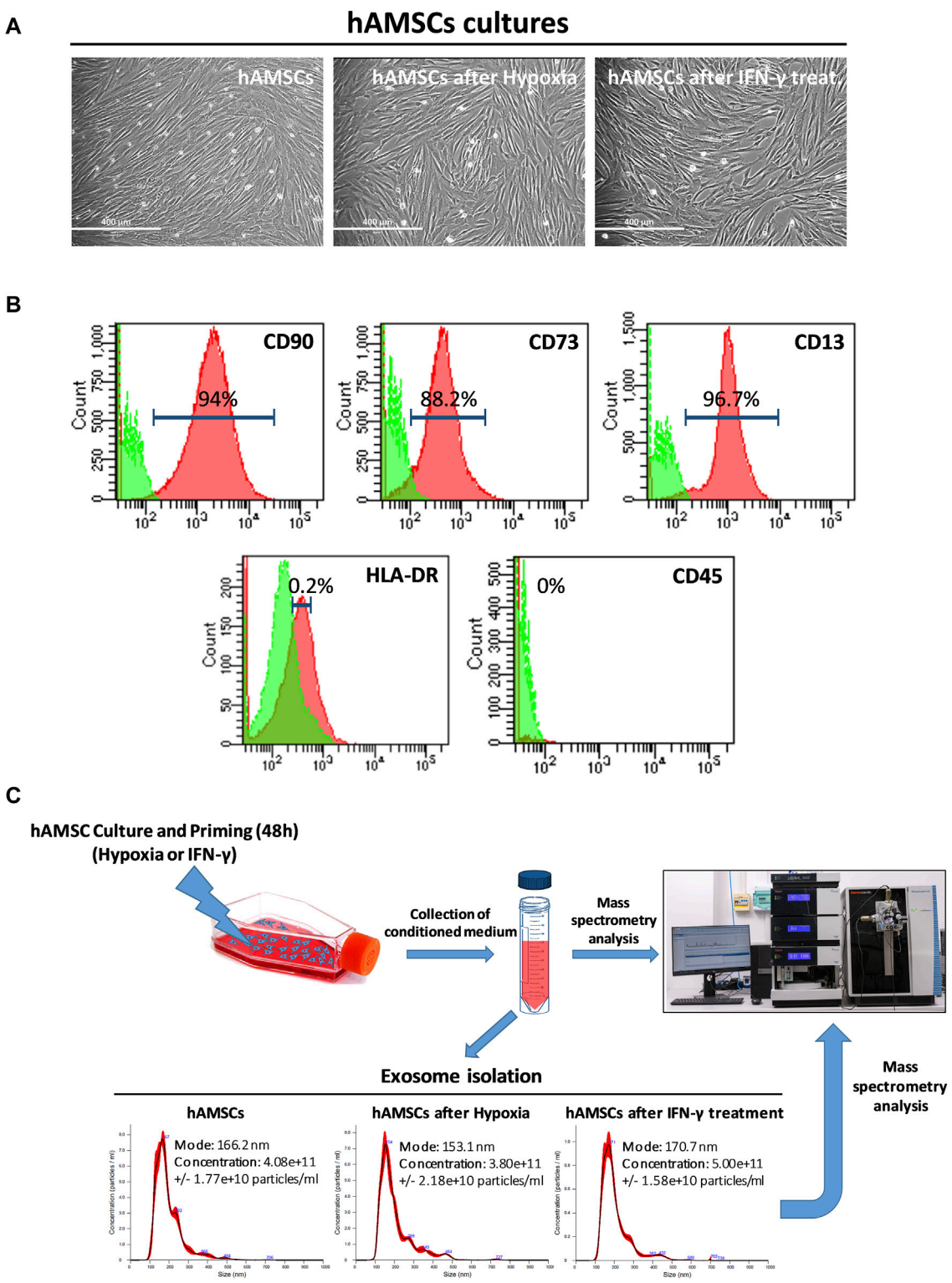

FIGURE 1
Human amnion-derived mesenchymal stromal/stem cells (hAMSCs) were grown as monolayers with or without priming. **(A)** Representative DIC images of hAMSCs grown as monolayers without priming (hAMSCs), cultured under hypoxic conditions (hAMSCs after hypoxia), or treated with IFN-γ (hAMSCs after IFN-γ treatment). **(B)** Representative images of flow cytometry analysis for quantification of hAMSCs at step 2 for both positive (CD90, CD73 and CD13) and negative surface markers (HLA-DR and CD45). Green represents the isotype control, and red represents stained cells. **(C)** Experimental plan and exosome characterization (size and concentration). DIC, differential interference contrast.

were alkylated with 50 mM iodoacetamide for 5 min at 37°C in the dark in UA (100 mM Tris/HCl 8 M urea pH 8.5) (Sigma Aldrich). After six washing steps with UB (100 mM Tris/HCl 8 M urea pH 8), proteins were digested with 0.3 µg LysC (Promega) in UC (25 mM Tris/HCl 2 M urea pH 8) for 16 h at 37°C followed by a second digestion step with 0.15 µg trypsin in 50 mM ammonium bicarbonate (Promega) for 4 h at 37°C as previously described (Saveliev et al., 2013). The peptides were eluted into collection tubes and acidified with formic acid (Sigma Aldrich) at a final concentration of 0.1%. Afterward, proteolytic peptides were desalted by stop-and-go extraction (STAGE) with self-packed C18 tips (Empore) (Rappsilber et al., 2003). Peptides were eluted using 60% acetonitrile (Sigma Aldrich) and 0.1% formic acid. After vacuum centrifugation, peptides were concentrated and dissolved in 20 µL 0.1% formic acid. At this point, peptide concentrations were analyzed by a Nanodrop 2000 (Thermo Scientific). A total amount of 1.2 µg was loaded per sample onto a Dionex UltiMate 3000 RSLCnano LC system (Thermo Scientific) which was coupled online via a Nanospray Flex Ion Source (Thermo Scientific) to a Q Exactive mass spectrometer (Thermo Scientific). Peptides were separated on an Acclaim PepMap C18 column (50 cm × 75 µm ID, Thermo Scientific) with 250 Nl/min flow using a binary gradient of water (A) and acetonitrile (B) supplemented with 0.1% formic acid (2% B 0 min, 5% B 5 min, 25% B 185 min, 35% B 230 min, 60% B 250 min, 95% B 255 min, 95% B 265 min, 2% B 265 min, 2% B 350 min). Data-dependent acquisition (DDA) was used for label-free quantification (LFQ). Full MS scans were acquired at a resolution of 70,000 (m/z range: 300–1400; automatic gain control (AGC) target: 1E+6; max injection time 50 ms). The DDA was used on the 10 most intense peptide ions per full MS scan for peptide fragmentation (resolution: 17,500; isolation width: 2 m/z; AGC target: 10^5; normalized collision energy (NCE): 25%, max injection time: 120 ms). A dynamic exclusion of 120 s was used for peptide fragmentation.

The raw data were analyzed with the software MaxQuant, version 2.0.1.0 (maxquant.org, Max Planck Institute, Munich). The MS data were searched against a reviewed canonical FASTA database of *Homo sapiens* including isoforms from UniProt (download: November the 5th 2020). Trypsin/P was defined as a protease. Two missed cleavages were allowed for the database search. The option in the first search was used to recalibrate the peptide masses within a window of 20 ppm. For the main search peptide and peptide fragment mass tolerances were set to 4.5 and 20 ppm, respectively. Carbamidomethylation of cysteine was defined as static modification. Protein N-terminal acetylation as well as oxidation of methionine were set as variable modifications. The false discovery rate for both peptides and proteins was adjusted to less than 1%. The "match between runs" option was enabled. LFQ of proteins required at least one ratio count of unique peptides. Unique and razor peptides were used for quantification. Data normalization was enabled. The protein LFQ reports from MaxQuant were further processed in Perseus (Tyanova et al., 2016).

2.5 Cluster and gene ontology (GO) analysis

Hierarchical cluster analysis of protein expression (expressed as the z-score) was used to group treatments with similar expression patterns. Protein expression data were grouped using a hierarchical clustering algorithm in the Cluster 3.0 program. A heatmap was generated using the Java TreeView program. To find GO terms enriched in the significantly deregulated proteins, we analyzed our data with the STRING web tool (Szklarczyk et al., 2019).

2.6 Endothelial cell cultures and tube formation assay

Human umbilical vein endothelial cells (HUVECs) were obtained from ATCC (United States). HUVECs were maintained in an endothelial cell basal medium (Lonza/Clonetics Corporation, United States) supplemented with a BulletKit (EBM-2) (Lonza/Clonetics Corporation, United States) in a culture flask coated with 0.1% gelatin (STEMCELL Technologies, United States) and maintained at 37°C with 5% CO_2.

A tubulogenesis assay was performed with basement membrane extract (BME) type 2 (AMSBIO, United Kingdom). HUVECs were dispensed at 1 × 10^4 cells/well (96-well microplates, Nunc, Germany) on top of the BME in serum-free DMEM (negative control), serum-free DMEM supplemented with 30 or 60 µg/mL EXOs derived from primed MSCs, or each conditioned medium (with or without EXOs) (100 µL). Following incubation at 37°C and 5% CO_2 for 6 h, the cells were visualized and images were taken using an EVOS™ FL digital inverted fluorescence microscope (Fisher Scientific, United Kingdom). The number of nodes, branches and meshes, along with the length of the master segments, branches and tubes were measured with ImageJ software (National Institutes of Health, USA). For statistical significance, six images/replicate were analyzed and quantified (n = 3).

2.7 Endothelial migration assay (xCELLigence)

Real-time monitoring of HUVECs was performed with an xCELLigence system (ACEA, United States) using CIM-Plate 16. The upper chamber was seeded with 30,000 HUVECs in serum-free DMEM medium. When endothelial cells migrated through the membrane into the bottom chamber in response to attractants (160 µL of complete DMEM as a positive control; 160 µL of serum-free DMEM without treatments (not treated, NT), or conditioned medium by each treatment, or serum-free DMEM with EXOs), they adhered to the electronic sensors resulting in increased impedance. The cell index (CI) values reflecting impedance changes were automatically recorded every 15 min. All culture conditions were carried out in quadruplicate and the analysis was performed with RTCA Software 1.2 from the xCELLigence system.

2.8 Neutrophil isolation and cell migration assay (xCELLigence)

Neutrophils were magnetically isolated from the whole blood of 3 healthy donors (two males and one female aged between 36 and 50 years) contained in a Vacutainer K2-EDTA tube (Becton

Dickinson, San Jose, CA, United States) using StraightFrom Whole Blood CD66b MicroBeads (Miltenyi Biotec, Germany). The magnetically retained CD66b$^+$ neutrophils were used for cell migration assay performed with the xCELLigence system (ACEA, United States). The upper chamber was seeded with 100,000 neutrophils in DMEM serum-free medium. When neutrophil cells migrated into the bottom chamber in response to attractants (160 µL of serum-free DMEM without treatments, NT, or conditioned medium by each treatment, or serum-free DMEM with EXOs), they adhered to the electronic sensors resulting in increased impedance. Cell index was registered every 15 min reflecting impedance changes. We used N-Formyl-Met-Leu-Phe (N-fMLP) (Sigma-Aldrich, Germany) at 1 µM as a positive control for neutrophil migration. Each culture condition was carried out in quadruplicate and the analysis was performed by RTCA Software 1.2 from the xCELLigence system.

2.9 Phagocytosis assay

The phagocytosis assay was performed by exposing heparinized blood samples (three different donors, two males and one female aged between 36 and 50 years) to pHrodo Green *E. coli* BioParticles (catalog no. P35366, Invitrogen) according to the manufacturer's instructions. The bioparticles were reconstituted in uptake buffer (20 mM HEPES in HBSS, pH 7.4) to a concentration of 1 mg/mL. The blood was pre-incubated for 1 h with 30 µL of each CM with or without EXOs (NO PRIM CM, IFN-γ CM and HYP CM) or two concentrations (30 or 60 µg/mL) of the three different EXOs (NO PRIM, IFN-γ, HYP) followed by 2 h of incubation with pHrodo *E. coli* BioParticles. At the end of the incubation time, the blood samples were lysed at room temperature for 10 min, washed and stained with CD45 APC-Conjugated antibody (Miltenyi Biotec) and 7AAD (Miltenyi Biotec), and immediately acquired by a FACSCelesta™ cytometer and analyzed with FlowJo™ v10.8.1 software (BD Life Sciences, United Kingdom).

2.10 Simultaneous quantification of secreted cytokines

Venous blood (three different donors, two males and one female aged between 36 and 50 years) was collected in K3EDTA tubes (Greiner Bio-One GmbH, Austria) and diluted 4-fold in RPMI 1640 medium supplemented with 1% penicillin/streptomycin, 10 mM HEPES (Euroclone, Pero, Italy), and 1 mM L-glutamine (Lonza Group Ltd, Switzerland). The blood was pre-incubated for 1 h with 30 µL of each CM with or without EXOs (NO PRIM CM, IFN-γ CM and HYP CM) or 30 µg/mL of three different exosomes (EXOs, IFN-γ EXOs, HYP EXOs) followed by 4 and 24 h of stimulation with *E. coli* LPS 1 µg/mL (*E. coli* O127:B8 Sigma-Aldrich). The samples were incubated at 37°C and 5% CO_2. After the incubation time with LPS, the levels of selected functional factors were assessed in the supernatants using Luminex magnetic bead technology with the ProcartaPlex Multiplex Immunoassay according to the manufacturer's instructions (Affymetrix, Austria).

2.11 Statistics

All the results were expressed as the mean ± standard deviation (SD). Statistical analysis was performed using GraphPad Prism 6.0 (GraphPad Software, United States). For statistical comparison, the one-way ANOVA with Tukey multiple comparison test was used. p-values <0.05 were considered to indicate statistical significance ($^*p < 0.05$, $^{**}p < 0.01$, $^{***}p < 0.001$, $^{****}p < 0.0001$).

3 Results

3.1 Isolation, cultivation, and characterization of hAMSCs and collection of both CM and EXOs

MSCs from human amniotic membranes were isolated from the placentas of distinct donors ($n = 4$) and cultured in the appropriate Chang medium. Primary cultures of hAMSCs were expanded *in vitro* until step 2 and then grown in conventional culture (hAMSCs), in hypoxia (hAMSCs after hypoxic treatment), or in the presence of IFN-γ (hAMSCs after IFN-γ treatment). All the cultures exhibited an elongated and fibroblastic-like morphology typical of MSCs (Figure 1A). The hAMSCs were analyzed by flow cytometry and were found to be positive for CD90 (94%), CD73 (88.2%), and CD13 (96.7%), and negative for HLA-DR (0.2%) and CD45 (0%) (Figure 1B). After hAMSC priming, no differences in mortality were found between the treatments (data not shown). As depicted in Figure 1C, following 48 h of culture, we harvested the CM generated from the hAMSCs and isolated EXOs from each CM. We obtained EXOs with an average diameter of 163 nm from hAMSCs and hypoxia-treated hAMSCs at similar concentrations (4.08×10^{11} and 3.80×10^{11} particles/mL, respectively), while a higher EXO concentration was produced by IFN-γ-treated hAMSCs (5.00×10^{11} particles/mL). We also confirmed differences in EXO concentrations through the analysis of EXO protein levels, which were similar in EXOs produced from hAMSCs and hypoxia-treated hAMSCs (18.545 µg/mL and 17.272 µg/mL, respectively) and greater in EXOs produced from IFN-γ-treated hAMSCs (22.727 µg/mL).

3.2 Proteomic analysis of hAMSC CM and EXOs reveals distinct patterns of protein secretion associated with specific priming methods impacting different biological processes

We used unbiased high-resolution mass spectrometry-based proteomics to compare the proteome of both CM and EXOs after hypoxic or IFN-γ priming of hAMSCs. A total of 1476 and 1441 different proteins were identified in CM and EXOs, respectively (for the list of all proteins, see Supplementary Table S1 for CM and S2 for EXOs). Only the proteins that were detected in CM samples from at least three out of four donors or in EXO samples from at least two out of three donors were taken into consideration.

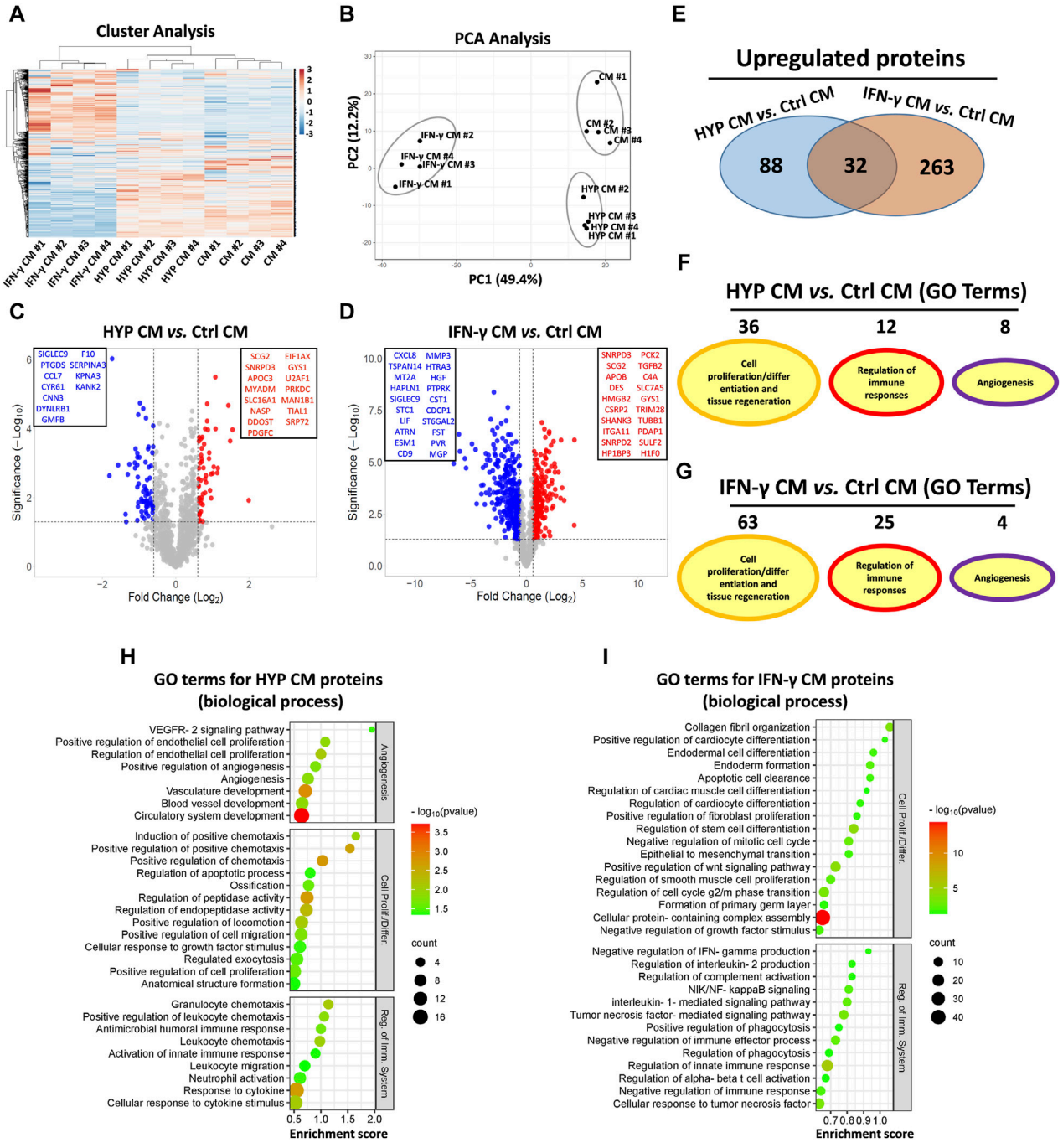

FIGURE 2
Protein secretion profiles in conditioned medium (CM) derived from unprimed hAMSCs (ctrl) and primed hAMSCs under hypoxia (HYP) or IFN-γ. **(A)** Secretion clusters (z-scores) of both up- and downregulated proteins in CM derived from hAMSCs (CM), hypoxic hAMSCs (HYP CM) and IFN-γ-treated hAMSCs (IFN-γ CM). **(B)** Principal component analysis (PCA). **(C)** Volcano plot analysis (fold change >1.5 and $p < 0.05$) of secreted proteins in HYP CM vs. ctrl CM and **(D)** IFN-γ CM vs. ctrl CM. **(E)** Venn diagram showing the number of upregulated proteins in HYP CM and IFN-γ CM. **(F)** Number of GO-enriched terms associated with upregulated HYP CM and **(G)** IFN-γ CM proteins grouped by category. **(H)** GO enrichment terms of HYP CM- and **(I)** IFN-γ CM-upregulated proteins; partial list of the 30 most significantly enriched terms.

In the CM samples, the normalized heatmap revealed a distinct proteomic profile between primed and unprimed hAMSCs, as well as between hypoxic or IFN-γ priming (Figure 2A). These data were confirmed by principal component analysis (PCA) (Figure 2B). We statistically analyzed deregulated proteins across groups by volcano plot analysis (fold change >1.5 and *p*-value <0.05) and detected significant changes in protein secretion under the different priming conditions. Specifically, compared to those in the conventional

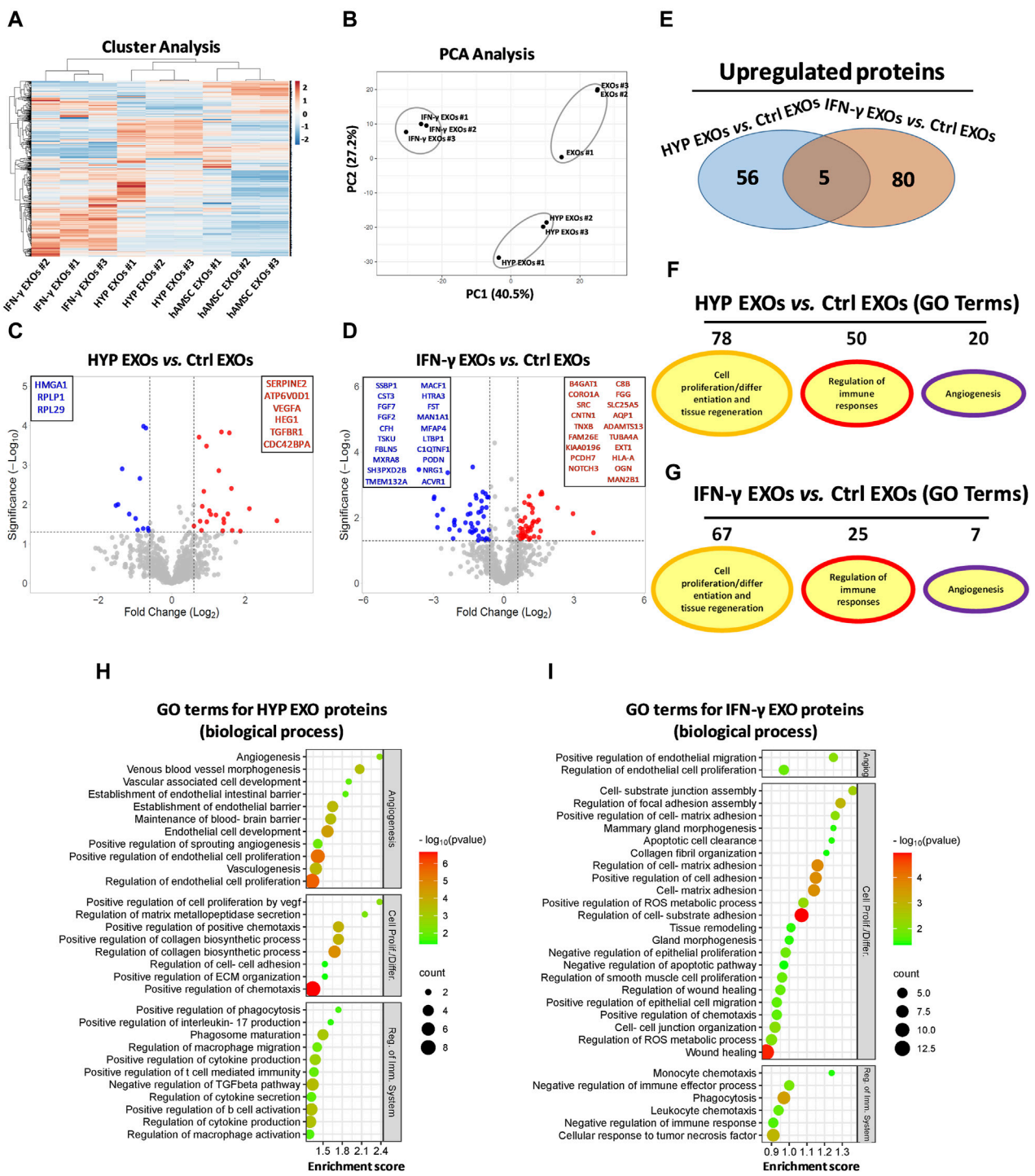

FIGURE 3
Protein secretion profiles of exosomes (EXOs) derived from unprimed hAMSC ctrl and primed hAMSCs under hypoxia (HYP) or IFN-γ. **(A)** Secretion clusters (z-scores) of both up- and downregulated proteins in EXOs derived from hAMSCs (hAMSC EXOs), hypoxic hAMSCs (HYP EXOs) and IFN-γ-treated hAMSCs (IFN-γ EXOs). **(B)** Principal component analysis (PCA). **(C)** Volcano plot analysis (fold change >1.5 and $p < 0.05$) of secreted protein in HYP EXOs vs. ctrl EXOs and **(D)** IFN-γ EXOs vs. ctrl EXOs. **(E)** Venn diagram showing the number of upregulated proteins in HYP EXOs and IFN-γ EXOs. **(F)** Number of GO-enriched terms associated with upregulated HYP EXO and **(G)** IFN-γ EXO proteins grouped by category. **(H)** GO enrichment terms of HYP EXO- and **(I)** IFN-γ EXO-upregulated proteins; partial list of the 30 most significantly enriched terms.

hAMSC CM (control CM), 88 proteins were significantly upregulated and 69 were lost in the hypoxic hAMSC CM (HYP CM) (Figures 2C–E), while 263 proteins were upregulated and 477 were downregulated in the IFN-γ CM (Figures 2D,E). We then performed a GO analysis to investigate whether deregulated proteins affect biological processes related to tissue repair/regeneration, immune system regulation and angiogenesis, which are of particular interest in the field of regenerative medicine. Notably, compared to IFN-γ priming, hypoxic priming appears to be more effective at inducing the overexpression of CM functional proteins that regulate angiogenic pathways, while more GO terms related to tissue repair/regeneration and immune system regulation were targeted by overexpressed proteins detected in IFN-γ CM (Figures 2F,G). A list of the top 30 GO terms related to HYP- and IFN-γ-upregulated proteins is shown for CM in Figures 2H,I, and the complete list of GO-enriched terms is displayed in Supplementary Table S3. A similar trend was observed for the EXO samples. In particular, both heatmap and PCA analyses revealed differences in proteomic profiles between EXOs produced from unprimed hAMSCs, hypoxic hAMSCs and IFN-γ-treated hAMSCs (Figures 3A,B). Regarding the protein content in the EXO samples, compared with unprimed hAMSC EXOs, hypoxic priming (HYP EXOs) resulted in the upregulation of 56 proteins and the disappearance of 15 proteins (Figures 3C–E). In addition, IFN-γ treatment (IFN-γ EXOs) led to the upregulation of 80 proteins and the downregulation of 66 proteins (Figures 3D,E). In contrast to the upregulated proteins in CM, when we analyzed overexpressed proteins in EXOs, compared to those in IFN-γ EXOs, we observed that the overproduced factors obtained in hypoxic priming (HYP EXOs) targeted more GO terms related to tissue repair/regeneration, the immune system and angiogenesis regulation (Figures 3F,G). The top 30 GO terms related to proteins contained in HYP EXOs and IFN-γ EXOs are shown in Figures 3H,I, and the complete list is presented in Supplementary Table S4. A total of 32 (Figure 2E) and 5 (Figure 3E) proteins exhibited increased expression with hypoxic and IFN-γ priming in CM and EXOs, respectively.

3.3 Conditioned medium and exosomes produced through hypoxic priming contain the highest angiogenic proteome

The functional angiogenic effects of both CM and EXOs produced with or without priming were examined by analyzing *in vitro* two important aspects of the angiogenesis process: endothelial cell migration and the formation of capillary-like structures (tube formation). As expected, the highest amount of capillary structures was observed in the positive control group (DMEM with FBS, positive ctrl), and the smallest was observed in the negative control group (DMEM without FBS and treatments, NT). Compared with those on the NT, we found that HUVECs plated on basement membrane extracts (BMEs) were able to form capillary-like structures mainly when cultivated with complete CM from conventional hAMSC culture or CM and EXOs from hypoxic hAMSC cultures (Figures 4A,B). We quantified the differences across the treatments and found that all capillary parameters increased significantly in response to complete hypoxic CM (HYP CM) but not in response to HYP CM without EXOs (Figures 4C–H). Moreover, both the number of nodes and the tube length increased significantly with complete conventional CM (Figures 4C,H). Interestingly, treatment with hypoxic exosomes (HYP EXOs) at a concentration of 60 μg/mL also increased the amount of specific capillary parameters, such as the number of nodes, master segment length, and tube length (Figures 4C, F, H). Very few or no effects on capillary-like structure formation were observed when cells were treated with CM or EXOs derived from IFN-γ priming (Figure 4). Interestingly, we observed that the migration-related behavior of HUVECs was similar to that of tube formation. We observed a marked increase in HUVEC migration in the presence of conventional CM, HYP CM or HYP CM without EXOs (in contrast to the tube formation assay) (Figure 5).

3.4 Conditioned medium and exosomes produced through the priming of hAMSCs induce recruitment of neutrophils and activation of phagocytosis

Using a real-time transwell migration assay, we analyzed the ability of both CM and EXOs to recruit neutrophils. We observed that CM produced by both hypoxia and IFN-γ priming stimulates intense chemotaxis in neutrophils (approximately 2-fold increase) compared to CM produced by conventional hAMSCs, which induces moderate chemotaxis. Relevant chemotaxis was also induced by HYP EXOs at a concentration of 60 μg/mL (comparable to that of complete IFN-γ CM), IFN-γ CM without EXOs, and IFN-γ EXOs at a concentration of 60 μg/mL (comparable to that of complete conventional CM) (Figures 6A,B).

A phagocytosis assay was performed using peripheral blood from healthy adult volunteers. We preliminarily optimized the analysis in terms of time, dose and minimum blood volume requirement. As expected, nonphagocytic cells did not fluoresce (Figure 6D, negative control), whereas the positive control caused a significant increase in phagocytic cells (approximately 17%) (Figures 6C,D, positive control: blood samples exposed to pHrodo Green *E. coli* BioParticles). Interestingly, incubation of whole blood with pHrodo-labeled bacteria in the presence of CM, IFN-γ CM or HYP CM (with or without EXOs), resulted in a marked and significant shift in the fluorescence of phagocytic cells (approximately 39% for both CM and IFN-γ CM and 43% for HYP CM) compared to that of the positive control. Although we observed an increase in phagocytic cells after treatment with all types of EXOs at both 30 and 60 μg/mL (approximately 28%, 24%, and 25% with EXOs, IFN-γ EXOs and HYP EXOs, respectively), we did not find significant differences compared to the positive control (Figures 6C,D). The gating strategy for obtaining viable cells is shown in Supplementary Figure S1.

3.5 Dynamic analysis of immune responses to LPS in the presence or absence of hAMSC-derived CM or EXOs through simultaneous quantification of secreted cytokines in whole blood

We evaluated the immune functional effects of both primed and unprimed hAMSC-derived products through a sequential analysis (at both 4 and 24 h) of the secretion of different factors in whole

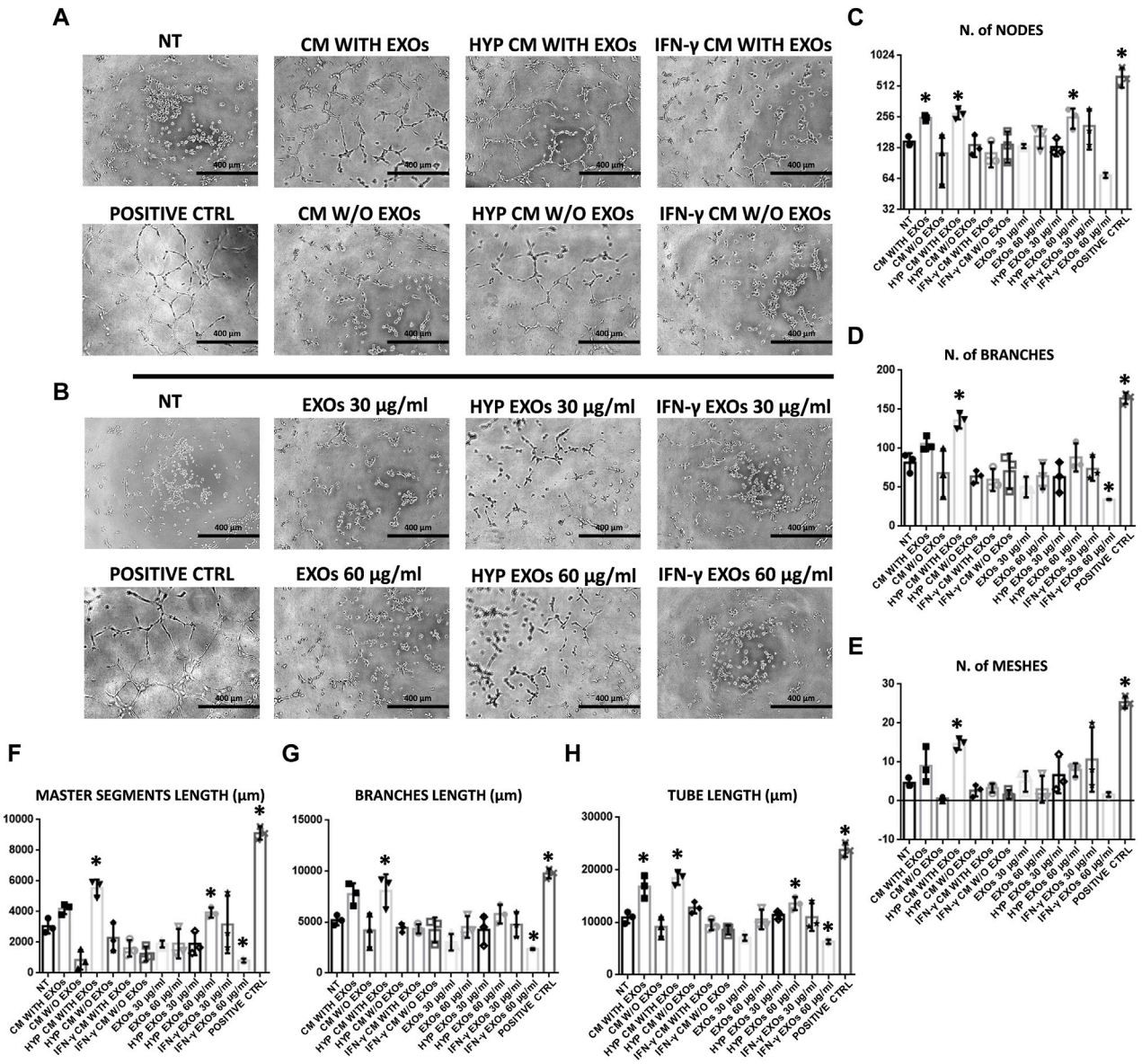

FIGURE 4
HUVEC capillary-like formation assay. **(A)** Representative images of HUVECs on BME treated with conditioned medium (CM) or **(B)** exosomes (EXOs). **(C–H)**- Graphs represent a quantitative analysis of the **(C)** number of nodes, **(D)** number of branches, **(E)** number of meshes, **(F)** master segment length, **(G)** branch length, and **(H)** tube length. Untreated serum-free DMEM (NT); Untreated DMEM with serum (positive ctrl); Serum-free DMEM conditioned by hAMSCs (CM with EXOs); Serum-free DMEM conditioned by hAMSCs depleted of EXOs (CM w/o EXOs); Serum-free DMEM conditioned by hypoxic hAMSCs (HYP CM with EXOs); Serum-free DMEM conditioned by hypoxic hAMSCs depleted of EXOs (HYP CM w/o EXOs); Serum-free DMEM conditioned by IFN-γ-treated hAMSCs (IFN-γ CM with EXOs); Serum-free DMEM conditioned by IFN-γ-treated hAMSCs depleted of EXOs (IFN-γ CM w/o EXOs); 30 µg/mL EXOs secreted by hAMSCs (EXOs 30 µg/mL); 60 µg/mL EXOs secreted by hAMSCs (EXOs 60 µg/mL); 30 µg/mL EXOs secreted by hypoxic hAMSCs (HYP EXOs 30 µg/mL); 60 µg/mL EXOs secreted by hypoxic hAMSCs (HYP EXOs 60 µg/mL); 30 µg/mL EXOs secreted by IFN-γ-treated hAMSCs (IFN-γ EXOs 30 µg/mL); 60 µg/mL EXOs secreted by IFN-γ-treated hAMSCs (IFN-γ EXOs 60 µg/mL). Data are presented as the means ± SD of triplicate in two independent experiments. *$p < 0.05$ vs. NT.

blood stimulated with LPS. We analyzed angiogenic factors as well as pro- and anti-inflammatory factors, such as tumor necrosis factor alpha (TNFα), interleukin 1 beta (IL1β), CCL11 (Eotaxin), hepatocyte growth factor (HGF), vascular endothelial growth factor A (VEGFA), CXCL10 (IP10), CCL2 (MCP1), interleukin 1 receptor antagonist (IL1RA), interleukin 6 (IL6), colony stimulating factor 3 (G-CSF), and IL10, and observed different expression patterns when blood was stimulated or not with LPS for both 4 and 24 h (Figures 7A,B). Treatment with LPS effectively induced an increase in pro-inflammatory cytokines such as TNFα and IL1β in control samples (whole blood without hAMSC-derived CM or EXOs stimulated with LPS, ctrl) after both 4 and 24 h, whereas a reduction in the same cytokines was observed in the presence of both primed and unprimed hAMSC-derived CM and EXOs (Figures 7A,B). Interestingly, after both 4 and 24 h, a significant increase in crucial angiogenic factors such as Eotaxin and VEGFA was observed in response to HYP CM treatment, and a slightly less intense effect was also observed in response to HYP CM

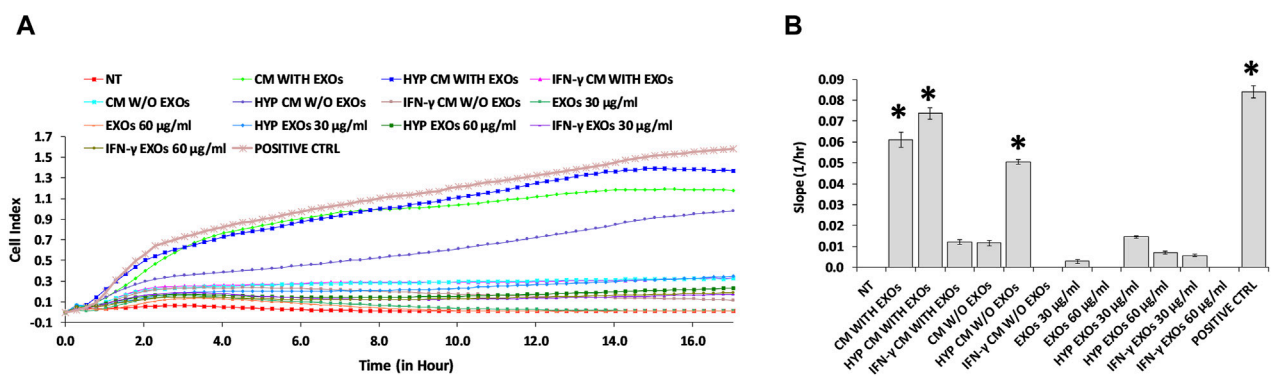

FIGURE 5
HUVEC migration assay. **(A)** Real-time migration monitoring of HUVECs with the xCELLigence system. **(B)** Slopes of migration curves. Untreated serum-free DMEM (NT); Untreated DMEM with serum (positive ctrl); Serum-free DMEM conditioned by hAMSCs (CM with EXOs); Serum-free DMEM conditioned by hAMSCs depleted of EXOs (CM w/o EXOs); Serum-free DMEM conditioned by hypoxic hAMSCs (HYP CM with EXOs); Serum-free DMEM conditioned by hypoxic hAMSCs depleted of EXOs (HYP CM w/o EXOs); Serum-free DMEM conditioned by IFN-γ-treated hAMSCs (IFN-γ CM with EXOs); Serum-free DMEM conditioned by IFN-γ-treated hAMSCs depleted of EXOs (IFN-γ CM w/o EXOs); 30 µg/mL EXOs secreted by hAMSCs (EXOs 30 µg/mL); 60 µg/mL EXOs secreted by hAMSCs (EXOs 60 µg/mL); 30 µg/mL EXOs secreted by hypoxic hAMSCs (HYP EXOs 30 µg/mL); 60 µg/mL EXOs secreted by hypoxic hAMSCs (HYP EXOs 60 µg/mL); 30 µg/mL EXOs secreted by IFN-γ-treated hAMSCs (IFN-γ EXOs 30 µg/mL); 60 µg/mL EXOs secreted by IFN-γ-treated hAMSCs (IFN-γ EXOs 60 µg/mL). Data are presented as the means ± SD of quadruplicate in two independent experiments. $*p < 0.05$ vs. NT.

w/o EXOs. Additionally, in the same treatment groups, the production of the pro-angiogenic factor HGF was higher only at 4 h (Figure 7A). In contrast, 4 h of treatment with IFN-γ CM increased the production of crucial immunomodulatory factors, such as IP10, MCP1, IL1RA, IL6, and G-CSF, whereas the production of only IP10, MCP1, IL1RA, and IL6 increased after 24 h of treatment. Weak effects at both 4 and 24 h were observed following treatment with IFN-γ CM w/o EXOs. Notably, treatment with IFN-γ CM for 24 h induced a significant increase in IL10 production (Figure 7B). Furthermore, although treatment with all types of EXOs inhibited the overproduction of pro-inflammatory cytokines, such as TNFα and IL1β, it did not affect the production of any of the other factors analyzed (Figures 7A,B). To investigate the dynamic variations in the aforementioned functional factors, we also evaluated the differences in concentrations between 4 and 24 h. As shown in Figure 7C, significant increases in Eotaxin and VEGFA were detected with HYP CM treatment (with or without EXOs), whereas no significant variation was observed for HGF. The same treatment also induced a variation in the production of IL1RA, G-CSF and IL10. Moreover, treatment with IFN-γ CM induced a significant overproduction of IL1RA, IL10 and MCP1. Using correlation analysis, we found that the pro-angiogenic factor VEGFA significantly correlated with other pro-angiogenic factors, such as Eotaxin and HGF, after both 4 and 24 h of treatment. Significant correlations were also observed among the immunomodulatory factors after both 4 and 24 h of treatment (Figure 7D).

4 Discussion

MSCs exhibit robust immunoregulatory, angiogenic and regenerative characteristics (Iijima et al., 2018; Miceli et al., 2019; Pittenger et al., 2019; Bulati et al., 2020; Lo Nigro et al., 2021; Bulati et al., 2023). Consequently, they have been investigated extensively in the field of regenerative medicine for the treatment of various diseases (Cittadini et al., 2022; Miceli and Bertani, 2022; Miceli et al., 2023a; Russo et al., 2023b). Recent scientific findings have elucidated that products derived from MSCs, such as CM and EXOs, may contribute, at least partially, to the therapeutic effects of MSCs (Miceli et al., 2021a; Chinnici et al., 2021; Takeuchi et al., 2021; Alberti et al., 2022; Russo et al., 2023a). Intriguingly, diverse priming strategies can enhance the therapeutic properties of both MSCs and their derived products (Noronha et al., 2019; Miceli et al., 2021b; Gallo et al., 2022; Miceli et al., 2023b).

Our study explored the impact of distinct priming strategies, specifically hypoxia and IFN-γ treatment, on the proteomic profile of the hAMSC-derived secretome. We used amnion-derived MSCs for their numerous advantages, including their abundance, non-invasive procurement, and ease of cultivation to a transplantable quantity, thereby avoiding ethical concerns associated with allografting (Parolini et al., 2009). Our findings indicate that both hypoxia and IFN-γ priming effectively enhanced the paracrine regenerative properties of hAMSC-derived CM and EXOs by promoting the production of functional factors associated with angiogenesis, immune system regulation, and tissue regeneration (Figures 2, 3). In particular, as revealed by our GO analysis, we observed that biological processes related to the regulation of angiogenesis were mainly targeted by CM and EXOs derived from hAMSCs primed with hypoxia. Hypoxic hAMSCs were also capable of producing functional factors that activate specific processes, such as neutrophil/macrophage activation, leukocyte chemotaxis and phagocytosis, ultimately activating innate immune responses. On the other hand, treatment with IFN-γ induced hAMSCs inhibited immune system activation by stimulating processes such as negative regulation of IFN-γ

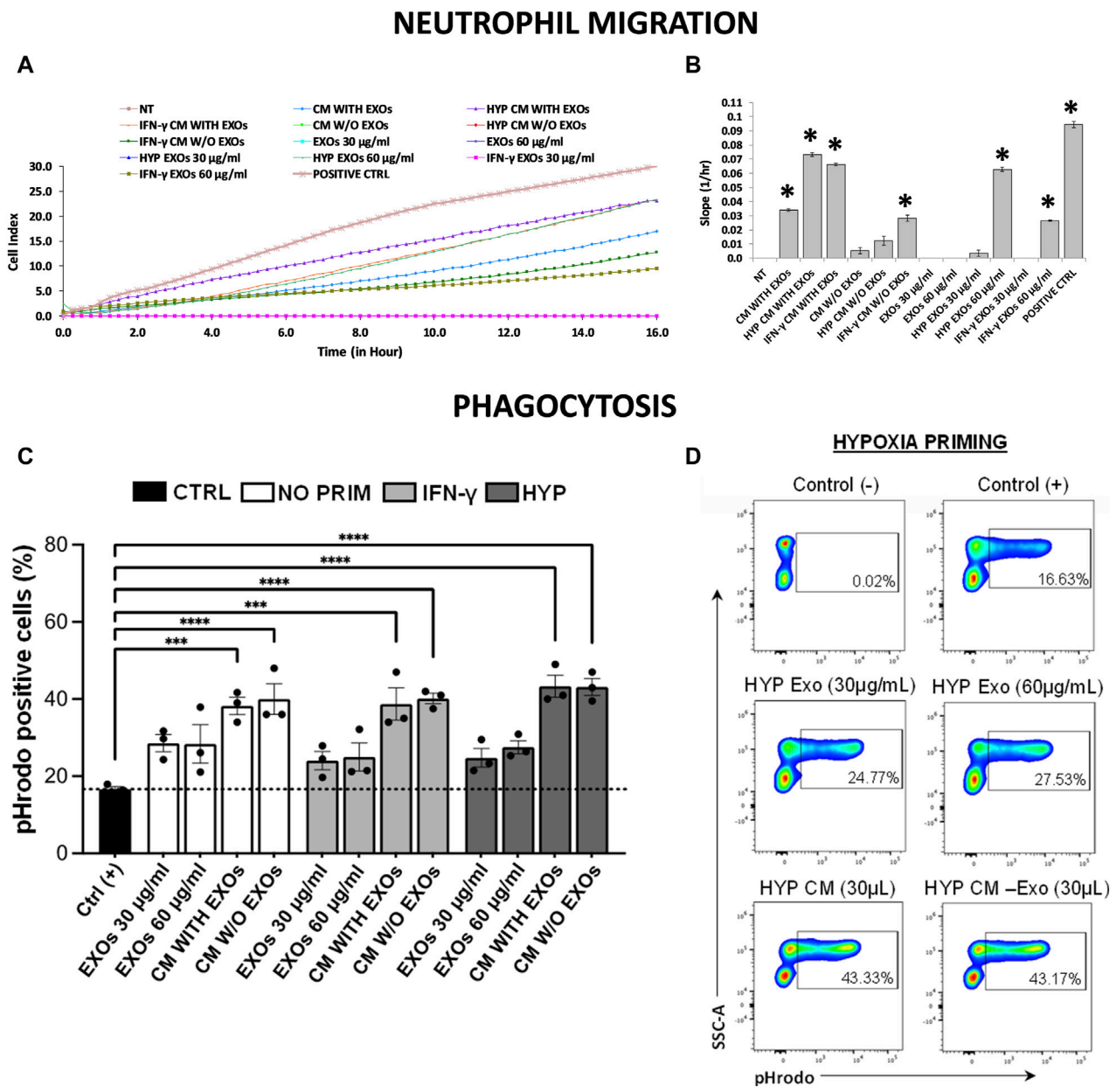

FIGURE 6
Neutrophil migration and phagocytosis assays. **(A)** Real-time migration monitoring of neutrophils with the xCELLigence system. **(B)** Slopes of migration curves. **(C, D)** Analysis of phagocytosis in blood samples using pHrodo-labeled particles. **(C)** The histogram shows the percentages of pHrodo + cells analyzed by flow cytometry after each treatment. **(D)** Representative plots showing the percentages of pHrodo-labeled cells after treatment of blood samples with both CM and EXOs derived from hypoxic hAMSCs. Untreated serum-free DMEM (NT); Untreated DMEM with serum (positive ctrl); Serum-free DMEM conditioned by hAMSCs (CM with EXOs); Serum-free DMEM conditioned by hAMSCs depleted of EXOs (CM w/o EXOs); Serum-free DMEM conditioned by hypoxic hAMSCs (HYP CM with EXOs); Serum-free DMEM conditioned by hypoxic hAMSCs depleted of EXOs (HYP CM w/o EXOs); Serum-free DMEM conditioned by IFN-γ-treated hAMSCs (IFN-γ CM with EXOs); Serum-free DMEM conditioned by IFN-γ-treated hAMSCs depleted of EXOs (IFN-γ CM w/o EXOs); 30 µg/mL EXOs secreted by hAMSCs (EXOs 30 µg/mL); 60 µg/mL EXOs secreted by hAMSCs (EXOs 60 µg/mL); 30 µg/mL EXOs secreted by hypoxic hAMSCs (HYP EXOs 30 µg/mL); 60 µg/mL EXOs secreted by hypoxic hAMSCs (HYP EXOs 60 µg/mL); 30 µg/mL EXOs secreted by IFN-γ-treated hAMSCs (IFN-γ EXOs 30 µg/mL); 60 µg/mL EXOs secreted by IFN-γ-treated hAMSCs (IFN-γ EXOs 60 µg/mL). Data are presented as the means ± SD of quadruplicate in a and b and triplicate in c and **(D)** $*p < 0.05$ vs. NT in **(B)**. $***p < 0.001$ and $****p < 0.0001$ vs. positive control in **(C)**.

production, negative regulation of the immune effector process and negative regulation of the immune response (Figures 2F–I and 3F-I). Our data revealed that hypoxic priming induced an increase in the production of crucial angiogenic factors, including VEGFA and angiopoietin-like 4 (ANGPTL4), in both CM and EXOs and the in the production of endoglin (ENG) and platelet-derived growth factor receptor beta (PDGFRB), but only in EXOs (Supplementary Tables S3, S4). VEGFA, PDGFRB, ANGPTL4 and ENG have been shown to play major roles in angiogenesis and vascular homeostasis, not only in physiological regeneration but also in most pathological angiogenic processes such as cancer (Raica and Cimpean, 2010; Nassiri et al., 2011; Shibuya,

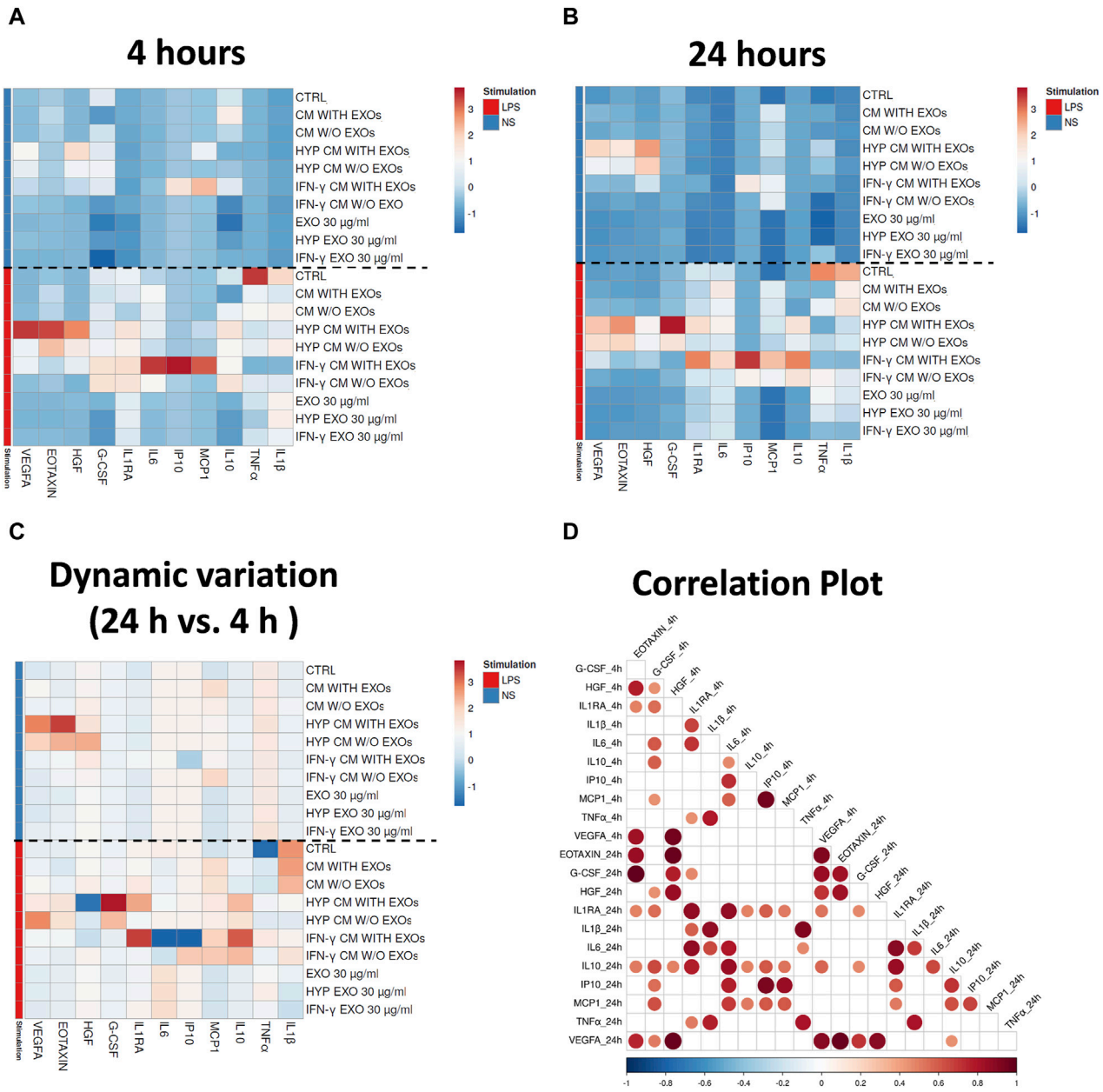

FIGURE 7
Secretion clusters (z-scores) of both up- and downregulated proteins in peripheral blood. Quantification of soluble factors secreted by peripheral blood cells stimulated or unstimulated with LPS in the presence or absence of each treatment after **(A)** four and **(B)** 24 h of culture. **(C)** Dynamic variations of factors between 4 and 24 h. **(D)** Correlation matrix of the factors. The degree of correlation between the two factors is shown through color intensity and the diameter of the circles. Significance was analyzed using a Spearman rank test, and the level of significance was set at $p < 0.05$. Whole blood without treatments (ctrl); Whole blood with serum-free DMEM conditioned by hAMSCs (CM with EXOs); Whole blood with serum-free DMEM conditioned by hAMSCs depleted of EXOs (CM w/o EXOs); Whole blood with serum-free DMEM conditioned by hypoxic hAMSCs (HYP CM with EXOs); Whole blood with serum-free DMEM conditioned by hypoxic hAMSCs depleted of EXOs (HYP CM w/o EXOs); Whole blood with serum-free DMEM conditioned by IFN-γ-treated hAMSCs (IFN-γ CM with EXOs); Whole blood with serum-free DMEM conditioned by IFN-γ-treated hAMSCs depleted of EXOs (IFN-γ CM w/o EXOs); Whole blood with 30 µg/mL EXOs secreted by hAMSCs (EXOs 30 µg/mL); Whole blood with 60 µg/mL EXOs secreted by hAMSCs (EXOs 60 µg/mL); Whole blood with 30 µg/mL EXOs secreted by hypoxic hAMSCs (HYP EXOs 30 µg/mL); Whole blood with 60 µg/mL EXOs secreted by hypoxic hAMSCs (HYP EXOs 60 µg/mL); Whole blood with 30 µg/mL EXOs secreted by IFN-γ-treated hAMSCs (IFN-γ EXOs 30 µg/mL); Whole blood with 60 µg/mL EXOs secreted by IFN-γ-treated hAMSCs (IFN-γ EXOs 60 µg/mL).

2011; Uccelli et al., 2019; Fernandez-Hernando and Suarez, 2020). Additionally, hypoxic hAMSCs produced functional factors such as CXCL3 (GRO-γ), CXCL8 (IL8) and CXCL1 (GRO-α) (Supplementary Tables S3, S4), which play roles in angiogenesis as well as in chemotaxis/activation of crucial cell components of the innate immune system, such as neutrophils and macrophages (Lukaszewicz-Zajac et al., 2020; Sokulsky et al., 2020; Cambier et al., 2023). In contrast, IFN-γ priming led to the overproduction of immunosuppressive factors, such as transforming growth factor beta 1 (TGFB1) and annexin A1

(ANXA1), both in CM and EXOs; thrombospondin 1 (THBS1), only in EXOs; and homer scaffold protein 2 (HOMER2), granulin precursor (GRN), toll interacting protein (TOLLIP) and CCL2 (MCP-1), only in CM (Supplementary Tables S3, S4). TGFB1 and ANXA1 have been shown to be very effective at limiting inflammation in several experimental models (Gavins and Hickey, 2012; Sanjabi et al., 2017). THBS1 has immunosuppressive effects that regulate the function/activation of multiple immune cells (Kaur and Roberts, 2024). HOMER2 can negatively regulate both IL-2 expression and T cell activation through competition with calcineurin and through binding with nuclear factor of activated T cells (NFAT) (Huang et al., 2008). In various immune-related diseases, the GRN protein has been shown to have anti-inflammatory effects by inhibiting TNFα activity (Tian et al., 2014). TOLLIP has been implicated in the control of inflammatory cytokine production and is crucial as a negative regulator of IL-1-activated NF-κB signaling (Didierlaurent et al., 2006). MCP-1 is a monocyte chemoattractant that can have immunosuppressive effects inducing the generation of immunoregulatory dendritic cells (DCreg) (Kudo-Saito et al., 2013). Therefore, our data showed that the composition of functional factors in CM and EXOs varies with the specific priming strategy, leading to distinct functional responses. Hypoxia priming appears to polarize naïve hAMSCs to stimulate angiogenesis, and activate innate immune responses and tissue regeneration. In contrast, IFN-γ treatment induces an anti-inflammatory and pro-trophic phenotype in hAMSCs, regulating inflammatory responses and facilitating tissue remodeling.

In accordance with the observed proteomic profiles, we confirmed the greater angiogenic properties of the hypoxic hAMSC products through *in vitro* functional assays. In particular, hypoxia-induced CM significantly enhanced the formation of capillary-like structures and the migration of endothelial cells (Figures 4, 5). Notably, recruitment of endothelial cells has been shown to be essential for vascular growth (Carmeliet and Jain, 2011). Moreover, we demonstrated that both CM and EXOs derived from hypoxic priming conditions might also induce both neutrophil recruitment (Figures 6A,B) and phagocytosis (Figures 6C,D), crucial processes during the activation of innate immune responses (Selders et al., 2017).

Interestingly, our study goes beyond the direct effects of priming on hAMSCs, demonstrating that hypoxia and IFN-γ can influence the functional characteristics of the hAMSC-derived secretome, which, in turn, orchestrates the production of functional factors by peripheral blood cells (PBCs). In fact, we performed a whole blood assay in which the CM produced through distinct priming stimuli elicited the production of different functional factors by PBCs (Figure 7). Indeed, our data showed that while hypoxia priming induced the production and release of angiogenic factors such as VEGFA, HGF and EOTAXIN (Salcedo et al., 2001; Sulpice et al., 2009), IFN-γ priming was shown to stimulate the production of anti-inflammatory factors such as IP10, MCP1, the interleukin 1 receptor antagonist (IL1RA), IL6, G-CSF and IL10 (Grutz, 2005; Martins et al., 2010; Gupta et al., 2011; Hunter and Jones, 2015; Gschwandtner et al., 2019; Fan et al., 2023). This experiment also revealed that the treatment of PBCs with CM and EXOs primed with both hypoxia and IFN-γ inhibited the production of pro-inflammatory factors such as IL1β and TNFα (Ott et al., 2007) induced by LPS stimulation of PBCs (Figure 7). Notably, treatment with IFN-γ CM was able to stimulate IL10 production after 24 h of treatment (Figure 7B). IL10 is a crucial anti-inflammatory cytokine capable of inhibiting the production of both IL1β and TNFα (Cassatella et al., 1993). In a mouse model of septic shock, IL10 was shown to inhibit the *in vivo* production of TNFα protecting it from mortality (Gerard et al., 1993). In addition, considering the functional role of IL10 in the progression of inflammation (Iyer and Cheng, 2012), our findings revealed an important time-dependent effect of IFN-γ CM in regulating the resolution of inflammation.

Our comprehensive protein characterization and functional analyses collectively indicate that hypoxia-primed hAMSCs exhibited a greater propensity to stimulate angiogenesis, while IFN-γ priming demonstrated a heightened capacity to induce immunosuppressive effects. As illustrated in Figure 6, both priming strategies also effectively stimulate innate immune response activation. The paracrine effects observed in this study seem to be mostly linked to the presence of the CM and not to the presence of EXOs, as suggested by the minimal effects observed upon EXO treatment in the tube formation assay and neutrophil migration (Figures 4, 5). Additionally, no significant differences were detected between whole CM and EXO-depleted CM, emphasizing the pivotal role of CM in mediating the paracrine effects of hAMSCs (Figure 5; 7). Based on our findings, we speculate that angiogenesis promotion induced by hypoxia-primed hAMSCs is a promising strategy for addressing pathological conditions characterized by inadequate or abnormal vessel formation. This potential role can also be applied to the wound healing process (Tonnesen et al., 2000), vascular growth during tissue regeneration (Saberianpour et al., 2018), and the context of ischemia (Hayashi et al., 2006). Furthermore, the activation of innate immune responses by hypoxic hAMSCs may play a crucial role in orchestrating the resolution of such pathologies (Julier et al., 2017). In contrast, the use of hAMSCs primed with IFN-γ, which has major immunosuppressive effects, might be therapeutically useful for the treatment of diseases characterized by an exacerbation of immune system activity (Chen and Brosnan, 2006; Leite et al., 2021; Kadri et al., 2023) (Figure 8).

In this study, we highlight a potential way to optimize MSC-based therapies, with the overall goal of improving their efficacy and mitigating the suboptimal outcomes observed in numerous clinical trials (Squillaro et al., 2016; Lukomska et al., 2019; Fricova et al., 2020; Zhou et al., 2021). As demonstrated in physiological contexts, MSCs undergo functional activation during stress conditions such as hypoxia and inflammatory environments (Miceli et al., 2021b; Miceli et al., 2023b). Consequently, employing priming strategies may prove decisive in directing MSC therapeutic properties toward specific disease classes (Figure 8) and in facilitating the use of MSC-derived products, such as CM and EXOs, rather than the cells themselves (Miceli et al., 2021b; Miceli et al., 2023b). Notably, the utilization of hAMSC products presents numerous advantages for clinical translation, encompassing considerations related to manufacturing, logistics, safety, and regulatory aspects.

Another important aspect highlighted in this study concerns EXOs. In the last decade, the role of MSC-derived EXOs in regulating inflammatory responses and tissue regeneration remained unclear. However, these functional vesicles have

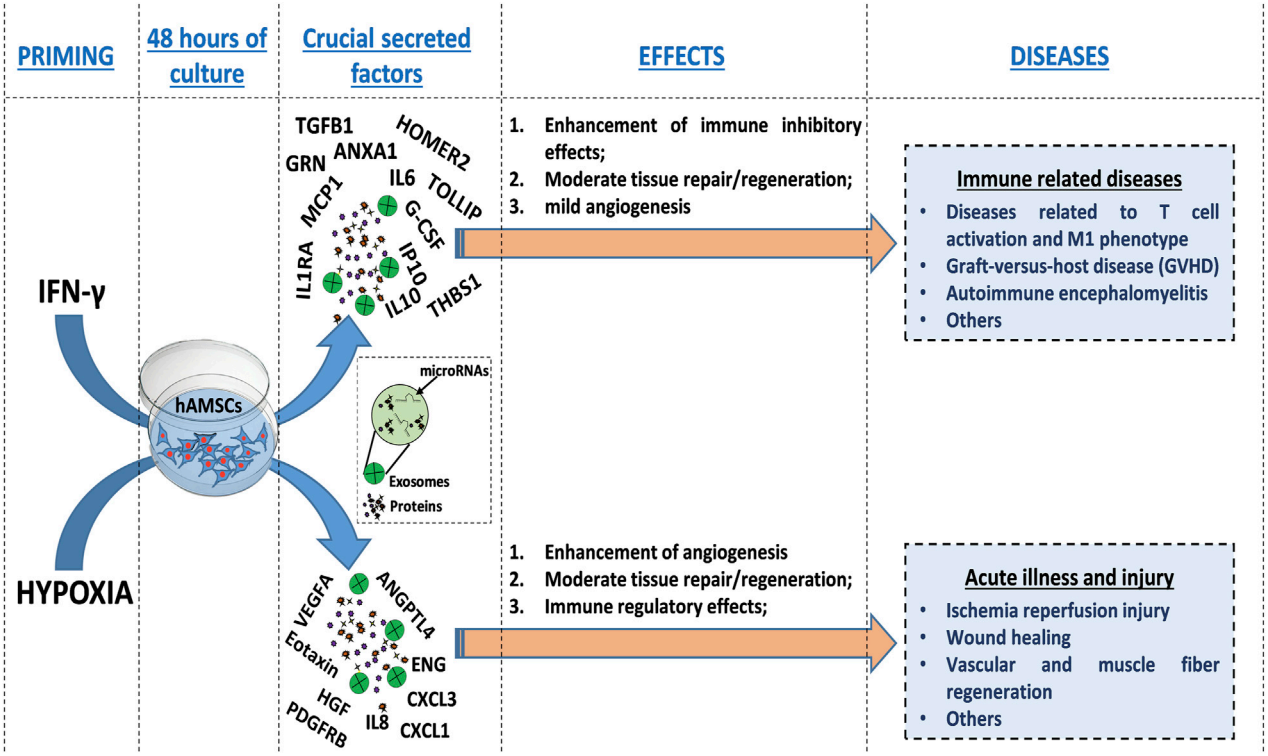

FIGURE 8
Schematic representation of the molecular effects and therapeutic potential of hAMSCs after priming. HAMSCs were preconditioned through hypoxia or IFN-γ treatment and each priming strategy differentially induced the production of specific factors (soluble factors or EXO-containing factors), which affected the activation of biological processes involved in angiogenesis, tissue repair/regeneration and the modulation of inflammation. Additionally, the priming strategies mentioned above also led to the preconditioning of hAMSCs, which in turn influenced the production of functional factors by peripheral blood cells (as shown in the whole blood assay results). Different priming strategies might be used to direct the therapeutic effects of hAMSCs toward specific diseases.

demonstrated similar beneficial effects to their parent cells in suppressing various autoreactive immune cells or inducing cutaneous wound healing (Baharlooi et al., 2020; Hu et al., 2022). Furthermore, there is the possibility to enhance EXO-therapeutic potential by tissue-engineered MSCs or by direct engineering of EXOs. In these cases, specific molecules and/or receptors can enable EXOs to target specific pathways of interest (Baharlooi et al., 2020; Hu et al., 2022; Raghav et al., 2022). In line with that, although our study emphasizes that the functional effects of MSCs are primarily associated with the use of CM, our data reveal that the EXO protein composition is also influenced by priming. It is well established that EXOs, to some extent, play a role in mediating the therapeutic effects of MSCs (Alberti et al., 2022; Russo et al., 2023a; Bulati et al., 2023). Therefore, further studies are needed to determine the role of EXOs in mediating the paracrine effects of MSCs, and how priming might be used to improve their therapeutic properties.

5 Conclusion

Our data suggest that distinct priming strategies significantly alter the protein composition of hAMSC-derived CM and EXOs leading to enhanced therapeutic effects. Hypoxic priming emphasizes angiogenesis, while IFN-γ priming has immunosuppressive effects. We have confirmed these results through functional studies and reveal the potential of fine-tuning the therapeutic properties of hAMSCs in a priming-dependent manner. This strategy provides new perspectives for enhancing the therapeutic efficacy of MSCs and guiding their therapeutic effects towards targeted pathologies. These cells are able to release a plethora of regulatory bioactive factors that, if opportunely modulated by specific priming strategies, might be capable of acting simultaneously on multiple targets and sustaining the therapeutic effects of MSCs, mainly in certain so-called multifactorial diseases (for which multiple molecular targets are involved in the pathogenesis), including Alzheimer's, Parkinson's disease (Youdim et al., 2014; Kumar et al., 2022), cancer (Petrelli and Giordano, 2008) and ischemia-reperfusion injury (Davidson et al., 2019). These insights offer ways to optimize MSC-based therapies, potentially improving their effectiveness and addressing challenges faced in clinical trials. Our study underscores the potential of hAMSC-derived products, particularly CM, in clinical translations, considering the numerous advantages that this approach entails. Moreover, our findings pave the way for further studies to understand the role of EXOs in mediating MSC paracrine effects and optimize their therapeutic use in multifactorial pathologies. This study highlights that MSC-based therapeutic products could be effective therapies for several diseases in the field of regenerative medicine.

While our study provides valuable insights into the impact of distinct priming strategies on the therapeutic properties of MSCs, there are several limitations that should be acknowledged. Our research primarily relies on *in vitro* experiments to assess the effects of hypoxia and IFN-γ priming on hAMSC-derived secretome. While these experiments offer controlled environments to study cellular responses, they may not fully replicate the complexities of *in vivo* conditions, potentially limiting the translational relevance of our findings. Moreover, we focused exclusively on placenta as a cell source for our study for its advantages. However, this narrow focus limits the generalizability of our findings, as different cell sources may respond differently to priming strategies. Future studies should explore the effects of priming on MSCs derived from other tissues to provide a more comprehensive understanding.

Data availability statement

The data presented in the study are deposited in the ProteomeXchange repository accession number PDX052445, via the link http://www.ebi.ac.uk/pride/archive/projects/PXD052445.

Ethics statement

The studies involving humans were approved by the IRCCS ISMETT's Institutional Research Review Board. The studies were conducted in accordance with the local legislation and institutional requirements. The participants provided their written informed consent to participate in this study.

Author contributions

MC: Conceptualization, Data curation, Formal Analysis, Investigation, Methodology, Software, Writing–review and editing. GZ: Conceptualization, Data curation, Formal Analysis, Investigation, Methodology, Writing–review and editing. RB: Conceptualization, Data curation, Formal Analysis, Investigation, Methodology, Software, Writing–review and editing. MB: Investigation, Methodology, Writing–review and editing. GI: Formal Analysis, Investigation, Methodology, Writing–review and editing. AG: Investigation, Methodology, Writing–review and editing. AC: Investigation, Methodology, Writing–review and editing. NC: Formal Analysis, Investigation, Methodology, Writing–review and editing. SC: Data curation, Formal Analysis, Investigation, Methodology, Writing–review and editing. CCa: Investigation, Methodology, Writing–review and editing. CCe: Investigation, Methodology, Writing–review and editing. GA: Investigation, Methodology, Writing–review and editing. AB: Conceptualization, Resources, Writing–review and editing. CMC: Data curation, Investigation, Methodology, Writing–review and editing. PC: Writing–eview and editing, Conceptualization, Resources, Supervision. SS: Conceptualization, Data curation, Formal Analysis, Investigation, Methodology, Writing–review and editing. VM: Conceptualization, Data curation, Formal Analysis, Investigation, Methodology, Project administration, Resources, Software, Supervision, Validation, Writing–original draft, Writing–review and editing.

Funding

The author(s) declare that no financial support was received for the research, authorship, and/or publication of this article. This research was funded by the Italian Ministry of Health, Ricerca Corrente.

Conflict of interest

The authors declare that the research was conducted in the absence of any commercial or financial relationships that could be construed as a potential conflict of interest.

Publisher's note

Supplementary material

The Supplementary Material for this article can be found online at: https://www.frontiersin.org/articles/10.3389/fcell.2024.1385712/full#supplementary-material

References

Alberti, G., Russo, E., Corrao, S., Anzalone, R., Kruzliak, P., Miceli, V., et al. (2022). Current perspectives on adult mesenchymal stromal cell-derived extracellular vesicles: biological features and clinical indications. *Biomedicines* 10 (11), 2822. doi:10.3390/biomedicines10112822

Baharlooi, H., Azimi, M., Salehi, Z., and Izad, M. (2020). Mesenchymal stem cell-derived exosomes: a promising therapeutic ace card to address autoimmune diseases. *Int. J. Stem Cells* 13 (1), 13–23. doi:10.15283/ijsc19108

Bulati, M., Gallo, A., Zito, G., Busa, R., Iannolo, G., Cuscino, N., et al. (2023). 3D culture and interferon-gamma priming modulates characteristics of mesenchymal stromal/stem cells by modifying the expression of both intracellular and exosomal microRNAs. *Biol. (Basel)* 12 (8), 1063. doi:10.3390/biology12081063

Bulati, M., Miceli, V., Gallo, A., Amico, G., Carcione, C., Pampalone, M., et al. (2020). The immunomodulatory properties of the human amnion-derived mesenchymal stromal/stem cells are induced by INF-gamma produced by activated lymphomonocytes and are mediated by cell-to-cell contact and soluble factors. *Front. Immunol.* 11, 54. doi:10.3389/fimmu.2020.00054

Burja, B., Barlic, A., Erman, A., Mrak-Poljsak, K., Tomsic, M., Sodin-Semrl, S., et al. (2020). Human mesenchymal stromal cells from different tissues exhibit unique responses to different inflammatory stimuli. *Curr. Res. Transl. Med.* 68 (4), 217–224. doi:10.1016/j.retram.2020.05.006

Cambier, S., Gouwy, M., and Proost, P. (2023). The chemokines CXCL8 and CXCL12: molecular and functional properties, role in disease and efforts towards

pharmacological intervention. *Cell Mol. Immunol.* 20 (3), 217–251. doi:10.1038/s41423-023-00974-6

Caplan, A. I., and Dennis, J. E. (2006). Mesenchymal stem cells as trophic mediators. *J. Cell Biochem.* 98 (5), 1076–1084. doi:10.1002/jcb.20886

Carmeliet, P., and Jain, R. K. (2011). Molecular mechanisms and clinical applications of angiogenesis. *Nature* 473 (7347), 298–307. doi:10.1038/nature10144

Cassatella, M. A., Meda, L., Bonora, S., Ceska, M., and Constantin, G. (1993). Interleukin 10 (IL-10) inhibits the release of proinflammatory cytokines from human polymorphonuclear leukocytes. Evidence for an autocrine role of tumor necrosis factor and IL-1 beta in mediating the production of IL-8 triggered by lipopolysaccharide. *J. Exp. Med.* 178 (6), 2207–2211. doi:10.1084/jem.178.6.2207

Chen, F., Chen, N., Xia, C., Wang, H., Shao, L., Zhou, C., et al. (2023). Mesenchymal stem cell therapy in kidney diseases: potential and challenges. *Cell Transpl.* 32, 9636897231164251. doi:10.1177/09636897231164251

Chen, L., and Brosnan, C. F. (2006). Exacerbation of experimental autoimmune encephalomyelitis in P2X7R-/- mice: evidence for loss of apoptotic activity in lymphocytes. *J. Immunol.* 176 (5), 3115–3126. doi:10.4049/jimmunol.176.5.3115

Chinnici, C. M., Russelli, G., Bulati, M., Miceli, V., Gallo, A., Busa, R., et al. (2021). Mesenchymal stromal cell secretome in liver failure: perspectives on COVID-19 infection treatment. *World J. Gastroenterol.* 27 (17), 1905–1919. doi:10.3748/wjg.v27.i17.1905

Chouaib, B., Haack-Sorensen, M., Chaubron, F., Cuisinier, F., and Collart-Dutilleul, P. Y. (2023). Towards the standardization of mesenchymal stem cell secretome-derived product manufacturing for tissue regeneration. *Int. J. Mol. Sci.* 24 (16), 12594. doi:10.3390/ijms241612594

Cittadini, E., Brucculeri, A. M., Quartararo, F., Vaglica, R., Miceli, V., and Conaldi, P. G. (2022). Stem cell therapy in the treatment of organic and dysfunctional endometrial pathology. *Minerva Obstet. Gynecol.* 74 (6), 504–515. doi:10.23736/S2724-606X.21.04919-8

Cui, E., Lv, L., Chen, W., Chen, N., and Pan, R. (2023). Mesenchymal stem/stromal cell-based cell-free therapy for the treatment of acute lung injury. *J. Cell Biochem.* 124 (9), 1241–1248. doi:10.1002/jcb.30469

Davidson, S. M., Ferdinandy, P., Andreadou, I., Botker, H. E., Heusch, G., Ibanez, B., et al. (2019). Multitarget strategies to reduce myocardial ischemia/reperfusion injury: JACC review topic of the week. *J. Am. Coll. Cardiol.* 73 (1), 89–99. doi:10.1016/j.jacc.2018.09.086

Didierlaurent, A., Brissoni, B., Velin, D., Aebi, N., Tardivel, A., Kaslin, E., et al. (2006). Tollip regulates proinflammatory responses to interleukin-1 and lipopolysaccharide. *Mol. Cell Biol.* 26 (3), 735–742. doi:10.1128/MCB.26.3.735-742.2006

Duijvestein, M., Wildenberg, M. E., Welling, M. M., Hennink, S., Molendijk, I., van Zuylen, V. L., et al. (2011). Pretreatment with interferon-gamma enhances the therapeutic activity of mesenchymal stromal cells in animal models of colitis. *Stem Cells* 29 (10), 1549–1558. doi:10.1002/stem.698

Dunn, C. M., Kameishi, S., Grainger, D. W., and Okano, T. (2021). Strategies to address mesenchymal stem/stromal cell heterogeneity in immunomodulatory profiles to improve cell-based therapies. *Acta Biomater.* 133, 114–125. doi:10.1016/j.actbio.2021.03.069

Fan, Y. C., Fong, Y. C., Kuo, C. T., Li, C. W., Chen, W. Y., Lin, J. D., et al. (2023). Tumor-derived interleukin-1 receptor antagonist exhibits immunosuppressive functions and promotes pancreatic cancer. *Cell Biosci.* 13 (1), 147. doi:10.1186/s13578-023-01090-8

Fernandez-Hernando, C., and Suarez, Y. (2020). ANGPTL4: a multifunctional protein involved in metabolism and vascular homeostasis. *Curr. Opin. Hematol.* 27 (3), 206–213. doi:10.1097/MOH.0000000000000580

Ferreira, J. R., Teixeira, G. Q., Santos, S. G., Barbosa, M. A., Almeida-Porada, G., and Goncalves, R. M. (2018). Mesenchymal stromal cell secretome: influencing therapeutic potential by cellular pre-conditioning. *Front. Immunol.* 9, 2837. doi:10.3389/fimmu.2018.02837

Fricova, D., Korchak, J. A., and Zubair, A. C. (2020). Challenges and translational considerations of mesenchymal stem/stromal cell therapy for Parkinson's disease. *NPJ Regen. Med.* 5 (1), 20. doi:10.1038/s41536-020-00106-y

Gaetani, M., Chinnici, C. M., Carreca, A. P., Di Pasquale, C., Amico, G., and Conaldi, P. G. (2018). Unbiased and quantitative proteomics reveals highly increased angiogenesis induction by the secretome of mesenchymal stromal cells isolated from fetal rather than adult skin. *J. Tissue Eng. Regen. Med.* 12 (2), e949–e961. doi:10.1002/term.2417

Gallo, A., Cuscino, N., Contino, F., Bulati, M., Pampalone, M., Amico, G., et al. (2022). Changes in the transcriptome profiles of human amnion-derived mesenchymal stromal/stem cells induced by three-dimensional culture: a potential priming strategy to improve their properties. *Int. J. Mol. Sci.* 23 (2), 863. doi:10.3390/ijms23020863

Gavins, F. N., and Hickey, M. J. (2012). Annexin A1 and the regulation of innate and adaptive immunity. *Front. Immunol.* 3, 354. doi:10.3389/fimmu.2012.00354

Gerard, C., Bruyns, C., Marchant, A., Abramowicz, D., Vandenabeele, P., Delvaux, A., et al. (1993). Interleukin 10 reduces the release of tumor necrosis factor and prevents lethality in experimental endotoxemia. *J. Exp. Med.* 177 (2), 547–550. doi:10.1084/jem.177.2.547

Grutz, G. (2005). New insights into the molecular mechanism of interleukin-10-mediated immunosuppression. *J. Leukoc. Biol.* 77 (1), 3–15. doi:10.1189/jlb.0904484

Gschwandtner, M., Derler, R., and Midwood, K. S. (2019). More than just attractive: how CCL2 influences myeloid cell behavior beyond chemotaxis. *Front. Immunol.* 10, 2759. doi:10.3389/fimmu.2019.02759

Gupta, G., Majumdar, S., Adhikari, A., Bhattacharya, P., Mukherjee, A. K., Majumdar, S. B., et al. (2011). Treatment with IP-10 induces host-protective immune response by regulating the T regulatory cell functioning in Leishmania donovani-infected mice. *Med. Microbiol. Immunol.* 200 (4), 241–253. doi:10.1007/s00430-011-0197-y

Hass, R., Kasper, C., Bohm, S., and Jacobs, R. (2011). Different populations and sources of human mesenchymal stem cells (MSC): a comparison of adult and neonatal tissue-derived MSC. *Cell Commun. Signal* 9, 12. doi:10.1186/1478-811X-9-12

Hayashi, T., Deguchi, K., Nagotani, S., Zhang, H., Sehara, Y., Tsuchiya, A., et al. (2006). Cerebral ischemia and angiogenesis. *Curr. Neurovasc Res.* 3 (2), 119–129. doi:10.2174/156720206776875902

Hofer, H. R., and Tuan, R. S. (2016). Secreted trophic factors of mesenchymal stem cells support neurovascular and musculoskeletal therapies. *Stem Cell Res. Ther.* 7 (1), 131. doi:10.1186/s13287-016-0394-0

Hu, J. C., Zheng, C. X., Sui, B. D., Liu, W. J., and Jin, Y. (2022). Mesenchymal stem cell-derived exosomes: a novel and potential remedy for cutaneous wound healing and regeneration. *World J. Stem Cells* 14 (5), 318–329. doi:10.4252/wjsc.v14.i5.318

Hu, X., Xu, Y., Zhong, Z., Wu, Y., Zhao, J., Wang, Y., et al. (2016). A large-scale investigation of hypoxia-preconditioned allogeneic mesenchymal stem cells for myocardial repair in nonhuman primates: paracrine activity without remuscularization. *Circ. Res.* 118 (6), 970–983. doi:10.1161/CIRCRESAHA.115.307516

Huang, G. N., Huso, D. L., Bouyain, S., Tu, J., McCorkell, K. A., May, M. J., et al. (2008). NFAT binding and regulation of T cell activation by the cytoplasmic scaffolding Homer proteins. *Science* 319 (5862), 476–481. doi:10.1126/science.1151227

Hunter, C. A., and Jones, S. A. (2015). IL-6 as a keystone cytokine in health and disease. *Nat. Immunol.* 16 (5), 448–457. doi:10.1038/ni.3153

Iijima, H., Isho, T., Kuroki, H., Takahashi, M., and Aoyama, T. (2018). Effectiveness of mesenchymal stem cells for treating patients with knee osteoarthritis: a meta-analysis toward the establishment of effective regenerative rehabilitation. *NPJ Regen. Med.* 3, 15. doi:10.1038/s41536-018-0041-8

Iyer, S. S., and Cheng, G. (2012). Role of interleukin 10 transcriptional regulation in inflammation and autoimmune disease. *Crit. Rev. Immunol.* 32 (1), 23–63. doi:10.1615/critrevimmunol.v32.i1.30

Jackson, W. M., Nesti, L. J., and Tuan, R. S. (2012). Concise review: clinical translation of wound healing therapies based on mesenchymal stem cells. *Stem Cells Transl. Med.* 1 (1), 44–50. doi:10.5966/sctm.2011-0024

Julier, Z., Park, A. J., Briquez, P. S., and Martino, M. M. (2017). Promoting tissue regeneration by modulating the immune system. *Acta Biomater.* 53, 13–28. doi:10.1016/j.actbio.2017.01.056

Kadri, N., Amu, S., Iacobaeus, E., Boberg, E., and Le Blanc, K. (2023). Current perspectives on mesenchymal stromal cell therapy for graft versus host disease. *Cell Mol. Immunol.* 20 (6), 613–625. doi:10.1038/s41423-023-01022-z

Kanai, R., Nakashima, A., Doi, S., Kimura, T., Yoshida, K., Maeda, S., et al. (2021). Interferon-gamma enhances the therapeutic effect of mesenchymal stem cells on experimental renal fibrosis. *Sci. Rep.* 11 (1), 850. doi:10.1038/s41598-020-79664-6

Kaur, S., and Roberts, D. D. (2024). Emerging functions of thrombospondin-1 in immunity. *Semin. Cell Dev. Biol.* 155 (Pt B), 22–31. doi:10.1016/j.semcdb.2023.05.008

Kehl, D., Generali, M., Mallone, A., Heller, M., Uldry, A. C., Cheng, P., et al. (2019). Proteomic analysis of human mesenchymal stromal cell secretomes: a systematic comparison of the angiogenic potential. *NPJ Regen. Med.* 4, 8. doi:10.1038/s41536-019-0070-y

Kim, D. S., Jang, I. K., Lee, M. W., Ko, Y. J., Lee, D. H., Lee, J. W., et al. (2018). Enhanced immunosuppressive properties of human mesenchymal stem cells primed by interferon-γ. *EBioMedicine* 28, 261–273. doi:10.1016/j.ebiom.2018.01.002

Kudo-Saito, C., Shirako, H., Ohike, M., Tsukamoto, N., and Kawakami, Y. (2013). CCL2 is critical for immunosuppression to promote cancer metastasis. *Clin. Exp. Metastasis* 30 (4), 393–405. doi:10.1007/s10585-012-9545-6

Kumar, B., Thakur, A., Dwivedi, A. R., Kumar, R., and Kumar, V. (2022). Multi-target-directed ligands as an effective strategy for the treatment of Alzheimer's disease. *Curr. Med. Chem.* 29 (10), 1757–1803. doi:10.2174/0929867328666210512005508

Leite, A. O. F., Bento Torres Neto, J., Dos Reis, R. R., Sobral, L. L., de Souza, A. C. P., Trevia, N., et al. (2021). Unwanted exacerbation of the immune response in neurodegenerative disease: a time to review the impact. *Front. Cell Neurosci.* 15, 749595. doi:10.3389/fncel.2021.749595

Leroux, L., Descamps, B., Tojais, N. F., Seguy, B., Oses, P., Moreau, C., et al. (2010). Hypoxia preconditioned mesenchymal stem cells improve vascular and skeletal muscle fiber regeneration after ischemia through a Wnt4-dependent pathway. *Mol. Ther.* 18 (8), 1545–1552. doi:10.1038/mt.2010.108

Lo Nigro, A., Gallo, A., Bulati, M., Vitale, G., Paini, D. S., Pampalone, M., et al. (2021). Amnion-derived mesenchymal stromal/stem cell paracrine signals potentiate human liver organoid differentiation: translational implications for liver regeneration. *Front. Med. (Lausanne)* 8, 746298. doi:10.3389/fmed.2021.746298

Lukaszewicz-Zajac, M., Paczek, S., Mroczko, P., and Kulczynska-Przybik, A. (2020). The significance of CXCL1 and CXCL8 as well as their specific receptors in colorectal cancer. *Cancer Manag. Res.* 12, 8435–8443. doi:10.2147/CMAR.S267176

Lukomska, B., Stanaszek, L., Zuba-Surma, E., Legosz, P., Sarzynska, S., and Drela, K. (2019). Challenges and controversies in human mesenchymal stem cell therapy. *Stem Cells Int.* 2019, 9628536. doi:10.1155/2019/9628536

Maacha, S., Sidahmed, H., Jacob, S., Gentilcore, G., Calzone, R., Grivel, J. C., et al. (2020). Paracrine mechanisms of mesenchymal stromal cells in angiogenesis. *Stem Cells Int.* 2020, 4356359. doi:10.1155/2020/4356359

Margiana, R., Markov, A., Zekiy, A. O., Hamza, M. U., Al-Dabbagh, K. A., Al-Zubaidi, S. H., et al. (2022). Clinical application of mesenchymal stem cell in regenerative medicine: a narrative review. *Stem Cell Res. Ther.* 13 (1), 366. doi:10.1186/s13287-022-03054-0

Martins, A., Han, J., and Kim, S. O. (2010). The multifaceted effects of granulocyte colony-stimulating factor in immunomodulation and potential roles in intestinal immune homeostasis. *IUBMB Life* 62 (8), 611–617. doi:10.1002/iub.361

McLeod, C. M., and Mauck, R. L. (2017). On the origin and impact of mesenchymal stem cell heterogeneity: new insights and emerging tools for single cell analysis. *Eur. Cell Mater* 34, 217–231. doi:10.22203/eCM.v034a14

Melief, S. M., Zwaginga, J. J., Fibbe, W. E., and Roelofs, H. (2013). Adipose tissue-derived multipotent stromal cells have a higher immunomodulatory capacity than their bone marrow-derived counterparts. *Stem Cells Transl. Med.* 2 (6), 455–463. doi:10.5966/sctm.2012-0184

Miceli, V., and Bertani, A. (2022). Mesenchymal stromal/stem cells and their products as a therapeutic tool to advance lung transplantation. *Cells* 11 (5), 826. doi:10.3390/cells11050826

Miceli, V., Bertani, A., Chinnici, C. M., Bulati, M., Pampalone, M., Amico, G., et al. (2021a). Conditioned medium from human amnion-derived mesenchymal stromal/stem cells attenuating the effects of cold ischemia-reperfusion injury in an *in vitro* model using human alveolar epithelial cells. *Int. J. Mol. Sci.* 22 (2), 510. doi:10.3390/ijms22020510

Miceli, V., Bulati, M., Gallo, A., Iannolo, G., Busa, R., Conaldi, P. G., et al. (2023a). Role of mesenchymal stem/stromal cells in modulating ischemia/reperfusion injury: current state of the art and future perspectives. *Biomedicines* 11 (3), 689. doi:10.3390/biomedicines11030689

Miceli, V., Bulati, M., Iannolo, G., Zito, G., Gallo, A., and Conaldi, P. G. (2021b). Therapeutic properties of mesenchymal stromal/stem cells: the need of cell priming for cell-free therapies in regenerative medicine. *Int. J. Mol. Sci.* 22 (2), 763. doi:10.3390/ijms22020763

Miceli, V., Chinnici, C. M., Bulati, M., Pampalone, M., Amico, G., Schmelzer, E., et al. (2020). Comparative study of the production of soluble factors in human placenta-derived mesenchymal stromal/stem cells grown in adherent conditions or as aggregates in a catheter-like device. *Biochem. Biophys. Res. Commun.* 522 (1), 171–176. doi:10.1016/j.bbrc.2019.11.069

Miceli, V., Pampalone, M., Vella, S., Carreca, A. P., Amico, G., and Conaldi, P. G. (2019). Comparison of immunosuppressive and angiogenic properties of human amnion-derived mesenchymal stem cells between 2D and 3D culture systems. *Stem Cells Int.* 2019, 7486279. doi:10.1155/2019/7486279

Miceli, V., Zito, G., Bulati, M., Gallo, A., Busa, R., Iannolo, G., et al. (2023b). Different priming strategies improve distinct therapeutic capabilities of mesenchymal stromal/stem cells: potential implications for their clinical use. *World J. Stem Cells* 15 (5), 400–420. doi:10.4252/wjsc.v15.i5.400

Morrison, S. J., and Scadden, D. T. (2014). The bone marrow niche for haematopoietic stem cells. *Nature* 505 (7483), 327–334. doi:10.1038/nature12984

Munoz-Perez, E., Gonzalez-Pujana, A., Igartua, M., Santos-Vizcaino, E., and Hernandez, R. M. (2021). Mesenchymal stromal cell secretome for the treatment of immune-mediated inflammatory diseases: latest trends in isolation, content optimization and delivery avenues. *Pharmaceutics* 13 (11), 1802. doi:10.3390/pharmaceutics13111802

Nassiri, F., Cusimano, M. D., Scheithauer, B. W., Rotondo, F., Fazio, A., Yousef, G. M., et al. (2011). Endoglin (CD105): a review of its role in angiogenesis and tumor diagnosis, progression and therapy. *Anticancer Res.* 31 (6), 2283–2290.

Noronha, N. C., Mizukami, A., Caliari-Oliveira, C., Cominal, J. G., Rocha, J. L. M., Covas, D. T., et al. (2019). Correction to: priming approaches to improve the efficacy of mesenchymal stromal cell-based therapies. *Stem Cell Res. Ther.* 10 (1), 132. doi:10.1186/s13287-019-1259-0

Ott, L. W., Resing, K. A., Sizemore, A. W., Heyen, J. W., Cocklin, R. R., Pedrick, N. M., et al. (2007). Tumor Necrosis Factor-alpha- and interleukin-1-induced cellular responses: coupling proteomic and genomic information. *J. Proteome Res.* 6 (6), 2176–2185. doi:10.1021/pr060665l

Papait, A., Ragni, E., Cargnoni, A., Vertua, E., Romele, P., Masserdotti, A., et al. (2022). Comparison of EV-free fraction, EVs, and total secretome of amniotic mesenchymal stromal cells for their immunomodulatory potential: a translational perspective. *Front. Immunol.* 13, 960909. doi:10.3389/fimmu.2022.960909

Parolini, O., Alviano, F., Bagnara, G. P., Bilic, G., Buhring, H. J., Evangelista, M., et al. (2008). Concise review: isolation and characterization of cells from human term placenta: outcome of the first international Workshop on Placenta Derived Stem Cells. *Stem Cells* 26 (2), 300–311. doi:10.1634/stemcells.2007-0594

Parolini, O., Soncini, M., Evangelista, M., and Schmidt, D. (2009). Amniotic membrane and amniotic fluid-derived cells: potential tools for regenerative medicine? *Regen. Med.* 4 (2), 275–291. doi:10.2217/17460751.4.2.275

Petrelli, A., and Giordano, S. (2008). From single-to multi-target drugs in cancer therapy: when aspecificity becomes an advantage. *Curr. Med. Chem.* 15 (5), 422–432. doi:10.2174/092986708783503212

Phinney, D. G., and Sensebe, L. (2013). Mesenchymal stromal cells: misconceptions and evolving concepts. *Cytotherapy* 15 (2), 140–145. doi:10.1016/j.jcyt.2012.11.005

Pittenger, M. F., Discher, D. E., Peault, B. M., Phinney, D. G., Hare, J. M., and Caplan, A. I. (2019). Mesenchymal stem cell perspective: cell biology to clinical progress. *NPJ Regen. Med.* 4, 22. doi:10.1038/s41536-019-0083-6

Raghav, P. K., Mann, Z., Ahlawat, S., and Mohanty, S. (2022). Mesenchymal stem cell-based nanoparticles and scaffolds in regenerative medicine. *Eur. J. Pharmacol.* 918, 174657. doi:10.1016/j.ejphar.2021.174657

Raica, M., and Cimpean, A. M. (2010). Platelet-derived growth factor (PDGF)/PDGF receptors (PDGFR) Axis as target for antitumor and antiangiogenic therapy. *Pharm. (Basel)* 3 (3), 572–599. doi:10.3390/ph3030572

Rappsilber, J., Ishihama, Y., and Mann, M. (2003). Stop and go extraction tips for matrix-assisted laser desorption/ionization, nanoelectrospray, and LC/MS sample pretreatment in proteomics. *Anal. Chem.* 75 (3), 663–670. doi:10.1021/ac026117i

Robey, P. (2017). Mesenchymal stem cells": fact or fiction, and implications in their therapeutic use. *F1000Res* 6, 524. doi:10.12688/f1000research.10955.1

Russo, E., Alberti, G., Corrao, S., Borlongan, C. V., Miceli, V., Conaldi, P. G., et al. (2023a). The truth is out there: biological features and clinical indications of extracellular vesicles from human perinatal stem cells. *Cells* 12 (19), 2347. doi:10.3390/cells12192347

Russo, E., Corrao, S., Di Gaudio, F., Alberti, G., Caprnda, M., Kubatka, P., et al. (2023b). Facing the challenges in the COVID-19 pandemic era: from standard treatments to the umbilical cord-derived mesenchymal stromal cells as a new therapeutic strategy. *Cells* 12 (12), 1664. doi:10.3390/cells12121664

Saberianpour, S., Heidarzadeh, M., Geranmayeh, M. H., Hosseinkhani, H., Rahbarghazi, R., and Nouri, M. (2018). Tissue engineering strategies for the induction of angiogenesis using biomaterials. *J. Biol. Eng.* 12, 36. doi:10.1186/s13036-018-0133-4

Salcedo, R., Young, H. A., Ponce, M. L., Ward, J. M., Kleinman, H. K., Murphy, W. J., et al. (2001). Eotaxin (CCL11) induces *in vivo* angiogenic responses by human CCR3+ endothelial cells. *J. Immunol.* 166 (12), 7571–7578. doi:10.4049/jimmunol.166.12.7571

Sanjabi, S., Oh, S. A., and Li, M. O. (2017). Regulation of the immune response by TGF-β: from conception to autoimmunity and infection. *Cold Spring Harb. Perspect. Biol.* 9 (6), a022236. doi:10.1101/cshperspect.a022236

Saveliev, S. V., Woodroofe, C. C., Sabat, G., Adams, C. M., Klaubert, D., Wood, K., et al. (2013). Mass spectrometry compatible surfactant for optimized in-gel protein digestion. *Anal. Chem.* 85 (2), 907–914. doi:10.1021/ac302423t

Schmelzer, E., Miceli, V., Chinnici, C. M., Bertani, A., and Gerlach, J. C. (2020). Effects of mesenchymal stem cell coculture on human lung small airway epithelial cells. *Biomed. Res. Int.* 2020, 9847579. doi:10.1155/2020/9847579

Selders, G. S., Fetz, A. E., Radic, M. Z., and Bowlin, G. L. (2017). An overview of the role of neutrophils in innate immunity, inflammation and host-biomaterial integration. *Regen. Biomater.* 4 (1), 55–68. doi:10.1093/rb/rbw041

Shibuya, M. (2011). Vascular endothelial growth factor (vegf) and its receptor (vegfr) signaling in angiogenesis: a crucial target for anti- and pro-angiogenic therapies. *Genes Cancer* 2 (12), 1097–1105. doi:10.1177/1947601911423031

Sokulsky, L. A., Garcia-Netto, K., Nguyen, T. H., Girkin, J. L. N., Collison, A., Mattes, J., et al. (2020). A critical role for the CXCL3/CXCL5/CXCR2 neutrophilic chemotactic Axis in the regulation of type 2 responses in a model of rhinoviral-induced asthma exacerbation. *J. Immunol.* 205 (9), 2468–2478. doi:10.4049/jimmunol.1901350

Squillaro, T., Peluso, G., and Galderisi, U. (2016). Clinical trials with mesenchymal stem cells: an update. *Cell Transpl.* 25 (5), 829–848. doi:10.3727/096368915X689622

Stroncek, D. F., Jin, P., McKenna, D. H., Takanashi, M., Fontaine, M. J., Pati, S., et al. (2020). Human mesenchymal stromal cell (MSC) characteristics vary among laboratories when manufactured from the same source material: a report by the cellular therapy team of the biomedical excellence for safer transfusion (best) collaborative. *Front. Cell Dev. Biol.* 8, 458. doi:10.3389/fcell.2020.00458

Sulpice, E., Ding, S., Muscatelli-Groux, B., Berge, M., Han, Z. C., Plouet, J., et al. (2009). Cross-talk between the VEGF-A and HGF signalling pathways in endothelial cells. *Biol. Cell* 101 (9), 525–539. doi:10.1042/BC20080221

Szklarczyk, D., Gable, A. L., Lyon, D., Junge, A., Wyder, S., Huerta-Cepas, J., et al. (2019). STRING v11: protein-protein association networks with increased coverage, supporting functional discovery in genome-wide experimental datasets. *Nucleic Acids Res.* 47 (D1), D607–D613. doi:10.1093/nar/gky1131

Takeuchi, S., Tsuchiya, A., Iwasawa, T., Nojiri, S., Watanabe, T., Ogawa, M., et al. (2021). Small extracellular vesicles derived from interferon-gamma pre-conditioned mesenchymal stromal cells effectively treat liver fibrosis. *NPJ Regen. Med.* 6 (1), 19. doi:10.1038/s41536-021-00132-4

Tian, Q., Zhao, Y., Mundra, J. J., Gonzalez-Gugel, E., Jian, J., Uddin, S. M., et al. (2014). Three TNFR-binding domains of PGRN act independently in inhibition of TNF-alpha binding and activity. *Front. Biosci. Landmark Ed.* 19 (7), 1176–1185. doi:10.2741/4274

Tonnesen, M. G., Feng, X., and Clark, R. A. (2000). Angiogenesis in wound healing. *J. Investig. Dermatol Symp. Proc.* 5 (1), 40–46. doi:10.1046/j.1087-0024.2000.00014.x

Tyanova, S., Temu, T., Sinitcyn, P., Carlson, A., Hein, M. Y., Geiger, T., et al. (2016). The Perseus computational platform for comprehensive analysis of (prote)omics data. *Nat. Methods* 13 (9), 731–740. doi:10.1038/nmeth.3901

Uccelli, A., Laroni, A., Ali, R., Battaglia, M. A., Blinkenberg, M., Brundin, L., et al. (2021). Safety, tolerability, and activity of mesenchymal stem cells versus placebo in multiple sclerosis (MESEMS): a phase 2, randomised, double-blind crossover trial. *Lancet Neurol.* 20 (11), 917–929. doi:10.1016/S1474-4422(21)00301-X

Uccelli, A., Wolff, T., Valente, P., Di Maggio, N., Pellegrino, M., Gurke, L., et al. (2019). Vascular endothelial growth factor biology for regenerative angiogenesis. *Swiss Med. Wkly.* 149, w20011. doi:10.4414/smw.2019.20011

Viswanathan, S., Shi, Y., Galipeau, J., Krampera, M., Leblanc, K., Martin, I., et al. (2019). Mesenchymal stem versus stromal cells: international society for cell & Gene therapy (ISCT®) mesenchymal stromal cell committee position statement on nomenclature. *Cytotherapy* 21 (10), 1019–1024. doi:10.1016/j.jcyt.2019.08.002

Wang, Y., Yi, H., and Song, Y. (2021a). The safety of MSC therapy over the past 15 years: a meta-analysis. *Stem Cell Res. Ther.* 12 (1), 545. doi:10.1186/s13287-021-02609-x

Wang, Y. H., Tao, Y. C., Wu, D. B., Wang, M. L., Tang, H., and Chen, E. Q. (2021b). Cell heterogeneity, rather than the cell storage solution, affects the behavior of mesenchymal stem cells *in vitro* and *in vivo*. *Stem Cell Res. Ther.* 12 (1), 391. doi:10.1186/s13287-021-02450-2

Wei, L., Fraser, J. L., Lu, Z. Y., Hu, X., and Yu, S. P. (2012). Transplantation of hypoxia preconditioned bone marrow mesenchymal stem cells enhances angiogenesis and neurogenesis after cerebral ischemia in rats. *Neurobiol. Dis.* 46 (3), 635–645. doi:10.1016/j.nbd.2012.03.002

Wisniewski, J. R., Zougman, A., Nagaraj, N., and Mann, M. (2009). Universal sample preparation method for proteome analysis. *Nat. Methods* 6 (5), 359–362. doi:10.1038/nmeth.1322

Wosczyna, M. N., Konishi, C. T., Perez Carbajal, E. E., Wang, T. T., Walsh, R. A., Gan, Q., et al. (2019). Mesenchymal stromal cells are required for regeneration and homeostatic maintenance of skeletal muscle. *Cell Rep.* 27 (7), 2029–2035. doi:10.1016/j.celrep.2019.04.074

Youdim, M. B., Kupershmidt, L., Amit, T., and Weinreb, O. (2014). Promises of novel multi-target neuroprotective and neurorestorative drugs for Parkinson's disease. *Park. Relat. Disord.* 20 (Suppl. 1), S132–S136. doi:10.1016/S1353-8020(13)70032-4

Zha, K., Li, X., Yang, Z., Tian, G., Sun, Z., Sui, X., et al. (2021). Heterogeneity of mesenchymal stem cells in cartilage regeneration: from characterization to application. *NPJ Regen. Med.* 6 (1), 14. doi:10.1038/s41536-021-00122-6

Zhou, T., Yuan, Z., Weng, J., Pei, D., Du, X., He, C., et al. (2021). Challenges and advances in clinical applications of mesenchymal stromal cells. *J. Hematol. Oncol.* 14 (1), 24. doi:10.1186/s13045-021-01037-x

Zito, G., Miceli, V., Carcione, C., Busa, R., Bulati, M., Gallo, A., et al. (2022). Human amnion-derived mesenchymal stromal/stem cells pre-conditioning inhibits inflammation and apoptosis of immune and parenchymal cells in an *in vitro* model of liver ischemia/reperfusion. *Cells* 11 (4), 709. doi:10.3390/cells11040709

Glossary

ANXA1	Annexin A1
AGC	Automatic gain control
ANGPTL4	Angiopoietin-like 4
BMEs	Basement membrane extracts
CI	Cell index
CM	Conditioned medium
DCreg	Dendritic cells
DDA	Data-dependent acquisition
ENG	Endoglin
EVs	Extracellular vesicles
EXOs	Exosomes
FASP	Filter aided sample preparation
FBS	Fetal bovine serum
GO	Gene ontology
G-CSF	Colony stimulating factor 3
GRN	Granulin precursor
hAMSCs	Human amnion-derived mesenchymal stromal/stem cells
HGF	Hepatocyte growth factor
HUVECs	Human umbilical vein endothelial cells
IDO	Indoleamine 2,3-dioxygenase 1
IL1β	Interleukin 1 beta
IL6	Interleukin 6
IL10	Interleukin 10
IL1RA	Interleukin 1 receptor antagonist
ISCT	International Society for Cell and Gene Therapy
LFQ	Label-free quantification
MSCs	Mesenchymal stromal/stem cells
NCE	Normalized collision energy
NFAT	Nuclear factor of activated T cells
NTA	Nanoparticle tracking analysis
PBCs	Peripheral blood cells
PBS	Phosphate-buffered saline
PGE2	Prostaglandin E synthase 2
PCA	Principal component analysis
SD	Standard deviation
STAGE	Stop-and-go extraction
TGFB1	Transforming growth factor beta 1
THBS1	Thrombospondin 1
TNFα	Tumor necrosis factor alpha
TOLLIP	Toll interacting protein
VEGFA	Vascular endothelial growth factor A

frontiers | Frontiers in Cell and Developmental Biology

TYPE Original Research
PUBLISHED 14 June 2024
DOI 10.3389/fcell.2024.1363541

OPEN ACCESS

EDITED BY
Willem Fibbe,
Leiden University Medical Center (LUMC), Netherlands

REVIEWED BY
Naseem Ahamad,
The University of Texas Health Science Center at San Antonio, United States
Yuyao Tian,
Massachusetts General Hospital and Harvard Medical School, United States

*CORRESPONDENCE
Takashi Okada,
t-okada@ims.u-tokyo.ac.jp
Yuko Nitahara-Kasahara,
y-kasahara@ims.u-tokyo.ac.jp

RECEIVED 30 December 2023
ACCEPTED 22 April 2024
PUBLISHED 14 June 2024

CITATION
Nitahara-Kasahara Y, Posadas-Herrera G, Hirai K, Oda Y, Snagu-Miyamoto N, Yamanashi Y and Okada T (2024), Characterization of disease-specific alterations in metabolites and effects of mesenchymal stromal cells on dystrophic muscles.
Front. Cell Dev. Biol. 12:1363541.
doi: 10.3389/fcell.2024.1363541

Characterization of disease-specific alterations in metabolites and effects of mesenchymal stromal cells on dystrophic muscles

Yuko Nitahara-Kasahara[1]*, Guillermo Posadas-Herrera[1], Kunio Hirai[2], Yuki Oda[2], Noriko Snagu-Miyamoto[2,3], Yuji Yamanashi[4] and Takashi Okada[1]*

[1]Division of Molecular and Medical Genetics, Center for Gene and Cell Therapy, The Institute of Medical Science, The University of Tokyo, Tokyo, Japan, [2]Division of Cell and Gene Therapy, Nippon Medical School, Tokyo, Japan, [3]Division of Oral and Maxillofacial Surgical, Tokyo Women's Medical School, Tokyo, Japan, [4]Division of Genetics, The Institute of Medical Science, The University of Tokyo, Tokyo, Japan

Introduction: Duchenne muscular dystrophy (DMD) is a genetic disorder caused by mutations in the dystrophin-encoding gene that leads to muscle necrosis and degeneration with chronic inflammation during growth, resulting in progressive generalized weakness of the skeletal and cardiac muscles. We previously demonstrated the therapeutic effects of systemic administration of dental pulp mesenchymal stromal cells (DPSCs) in a DMD animal model. We showed preservation of long-term muscle function and slowing of disease progression. However, little is known regarding the effects of cell therapy on the metabolic abnormalities in DMD. Therefore, here, we aimed to investigate the mechanisms underlying the immunosuppressive effects of DPSCs and their influence on DMD metabolism.

Methods: A comprehensive metabolomics-based approach was employed, and an ingenuity pathway analysis was performed to identify dystrophy-specific metabolomic impairments in the *mdx* mice to assess the therapeutic response to our established systemic DPSC-mediated cell therapy approach.

Results and Discussion: We identified DMD-specific impairments in metabolites and their responses to systemic DPSC treatment. Our results demonstrate the feasibility of the metabolomics-based approach and provide insights into the therapeutic effects of DPSCs in DMD. Our findings could help to identify molecular marker targets for therapeutic intervention and predict long-term therapeutic efficacy.

KEYWORDS

Duchenne muscular dystrophy, mesenchymal stromal cells, metabolomics, cell therapy, *mdx* mouse

1 Introduction

Duchenne muscular dystrophy (DMD) is an X-linked disorder triggered by primary abnormalities in the *DMD* gene that causes degenerative myopathy with secondary inflammation and necrotizing phase. Mutations in the dystrophin-encoding gene lead to dystrophin–glycoprotein complex deficiency in the sarcolemma, which leads to progressive degeneration/regeneration cycles in the striated muscle, manifesting as muscle weakness and eventual skeletal muscle atrophy (Ervasti et al., 1990; Campbell, 1995). In addition to the main symptoms of myopathy, patients often experience complications, such as endocrine metabolic disorders. As metabolic alterations also play a dominating influential role in the initiation and progression of various inherited or acquired diseases, abnormal metabolic function has been described as a part of the physiological challenges of DMD. Loss of dystrophin, the large membrane cytoskeletal protein, results in multiple systemic alterations, including extensive changes in energy production, in both patients (Boca et al., 2016; Srivastava et al., 2016; Spitali et al., 2018) and genetic animal models of DMD (Guiraud et al., 2015; Joseph et al., 2018; Lee-McMullen et al., 2019). Classically, creatine kinase (CK) released from leaked muscle tissue membranes, which is elevated in patients and animal models, is widely used as a clinical blood biomarker of DMD. However, its levels are highly variable and do not reflect the degree of muscle atrophy because they gradually decline and are no longer correlated with the severity of the disease.

Various studies have focused on metabolic alterations in the skeletal muscles (Dabaj et al., 2021; Merckx et al., 2022), cardiac muscles (Khairallah et al., 2007), brain (Tracey et al., 1996), and serum or plasma (Spitali et al., 2018; Xu et al., 2023) derived from patients with DMD, animal models, animals with Golden retriever muscular dystrophy (GRMD) (Abdullah et al., 2017), and *mdx* mice (Tsonaka et al., 2020).

MSCs are isolated from several organs, such as bone-marrow (Friedenstein et al., 1968), adipose tissue (Zannettino et al., 2008), amnion (Tsai et al., 2004), dental pulp (Zhang et al., 2008), peripheral blood (He et al., 2007), and cord blood (Oh et al., 2008) express several common cell surface antigenic markers, e.g., CD44, CD73, CD90, and CD105, and low levels of major histocompatibility complex class I molecules. They do not express hematopoietic markers CD34 or CD45 (Friedenstein et al., 1968). Dental pulp stem cells (DPSCs) obtained from decidual tooth tissue are a less invasive cell source, and demonstrated multipotency (Zhang et al., 2008) as well as high proliferative and immunosuppressive activities (Jo et al., 2007). DPSCs can also modulate immune effectors, thereby affecting crucial processes such as cell development, maturation, and function, as well as reactive T-cell responses (Ozdemir et al., 2016). Because regulating severe inflammation in dystrophic muscles could prolong the duration of therapeutic effects, DPSCs are also attractive candidates for cell-based strategies that target diseases with chronic inflammation, including DMD (Ichim et al., 2010). We previously demonstrated the therapeutic effects of systemic administration of DPSCs in model dogs and mice, i.e., preservation of long-term muscle function and slowing of disease progression (Nitahara-Kasahara et al., 2021). However, the mechanisms underlying the immunosuppressive effects of DPSCs, including abnormal skeletal muscle metabolism, have not been sufficiently characterized.

Currently, little is known regarding the effects of cell therapy on the metabolic abnormalities in DMD. In this study, we aimed to identify dystrophy-specific metabolomic impairments and assess therapeutic responsiveness to systemic DPSC administration via a comprehensive metabolomics-based approach using CE and liquid chromatography-mass spectrometry (LC–MS/MS). We also aimed to investigate whether metabolite monitoring is an appropriate component of the therapeutic evaluation of DMD.

2 Materials and methods

2.1 Animals

Mdx mice have a premature stop mutation in the exon 23 of the murine *Dmd* gene, which results in failure to translate dystrophin. These mice mimic various aspects of the human disease (Bulfield et al., 1984; Sicinski et al., 1989). C57BL/6-background *mdx* mice were developed by Dr. T. Sasaoka (National Institute for Basic Biology, Aichi, Japan) and were maintained in our animal facility. Age-matched and untreated male *mdx* littermates (P30 and P90, n = 3; P60, n = 6) and wild-type C57BL/6 mice (P30 and P90, n = 3; P60, n = 6) were used as controls in these metabolic studies. All mice remained healthy in appearance, activity, and body weight throughout the observation period. All experiments were conducted in accordance with the protocols described in the experimental protocols approved by the Ethics Committee for the Treatment of Laboratory Animals at the Nippon Medical School and Institute of Medical Science. The same male littermates were housed together in individually ventilated cages, with four to six mice per cage. Each group of mice was randomly assigned to a cage. All mice were maintained under a regular 12-h light/12-h dark diurnal lighting cycle with *ad libitum* access to food and water.

2.2 Culture and transplantation of DPSCs into mice and sampling

DPSCs were provided by JCR Pharmaceuticals (Hyogo, Japan). The cells were cultured in DMEM (Thermo Fisher Scientific) supplemented with 10% fetal bovine serum (Thermo Fisher Scientific) and 1% antibiotic-antimycotic solution (Wako Pure Chemical Industries) at 37°C in a 5% CO_2 atmosphere. The animals *were* randomly divided into two groups: control and MSC-treated groups. Systemic delivery of DPSCs (8.0×10^5 cells/100 μL of PBS) into *mdx* mice via the tail vein was conducted using four injections (treated-*mdx*, n = 3, each) administered at an interval of 1 week, beginning at 4–5 weeks of age (body weight [BW] > 10 g), as previously reported (Nitahara-Kasahara et al., 2021). Age-matched male WT and *mdx* mice (n = 3 each) were used as controls. At the ages of 30-, 60-, and 90 days (P30, P60, and P90), the animals were euthanized by cervical cord dislocation, and tissues were excised for histological and molecular analysis.

2.3 Histopathological analysis

Muscle samples were collected from the DPSC-treated mice and immediately frozen in liquid nitrogen-cooled isopentane. Subsequently, 8-μm-thick transverse cryosections were prepared from the skeletal muscles and stained with hematoxylin and eosin (H&E) using standard procedures. Tissue sections were visualized using the IX71 or IX83 microscope (Olympus, Tokyo, Japan). Quantification of nuclear infiltration and collagen-stained areas was performed using the HALO image analysis software (Indica Labs, Corrales, MN, USA). The nucleic area (%) was calculated by dividing the nuclear infiltration area by the total area.

2.4 Enzyme-linked immunosorbent assay (ELISA)

Serum CK levels were determined using an ELISA mouse kit (Cloud-Clone, Corp., TX, USA) according to the manufacturer's recommendations.

2.5 Metabolomic analysis

Plasma and skeletal muscle samples were collected from young (P30) and adult (P60 and P90) *mdx* mice and age-matched WT mice (three male mice each group). The collected tissue samples (30 mg) were stored at −80°C until the assay was performed. Blood collected from the heart was centrifuged at 1,500 *g* for 15 min at 4°C. Plasma was isolated from the resulting supernatant.

Mouse plasma (50 μL) was added to a 450 μL methanol solution prepared to achieve a concentration of 10 μM of the pretreatment internal standard for capillary electrophoresis-time-of-flight mass spectrometry (CE-TOFMS). This mixture was added to 500 μL of chloroform and 200 μL of Milli-Q water and centrifuged at 2,300 *g* and 4°C for 5 min. After centrifugation, 400 μL of the aqueous layer was transferred to an ultrafiltration tube (Ultrafree MC PLHCC, HMT, centrifugal filter unit 5 kDa) and centrifuged (9,100 ×*g*, 4°C, 120 min) followed by ultrafiltration. The filtrate was dried and dissolved again in 50 μL of Milli-Q water for measurement. For liquid chromatography-time-of-flight mass spectrometry (LC-TOFMS) analysis, 300 μL of mouse plasma was added to 900 μL of formic acid-acetonitrile solution (1%) prepared as the internal standard (6 μM) and was centrifuged (2,300 ×*g*, 4°C, 5 min). Phospholipids were removed from the supernatant by solid-phase extraction and dried. For measurement, the dried sample was dissolved in 100 μL of 50% isopropanol solution (v/v).

The skeletal muscle sample (30 mg) added to 750 μL of 50% acetonitrile solution (v/v) was crushed using a crusher under cooling (1,500 rpm, 120 s × 3 times). The same volume of 50% acetonitrile solution (v/v) was added, and the sample was centrifuged at 2,300 *g* at 4°C for 5 min. The upper layer (400 μL) was transferred to an ultrafiltration tube (Ultra-free MC PLHCC, HMT, centrifugal filter unit 5 kDa) and was centrifuged (9,100 ×*g*, 4°C, 120 min), followed by ultrafiltration. The filtrated sample was dried and dissolved again in 50 μL of Milli-Q water for CE-TOFMS. For LC-TOFMS analysis, the skeletal muscle sample from the lower legs (30 mg) added in 500 μL of 1% formic acid-acetonitrile solution was crushed (1,500 rpm, 120 s × three times, and 1,500 rpm, 120 s × one time after addition of 167 μL Milli-Q water) using a crusher under cooling conditions and then centrifuged (2,300 × *g*, 4°C, 5 min). The supernatant was added to 500 μL of 1% formic acid-acetonitrile AMEOR-HMT-0096 and 167 μL of Milli-Q water to precipitate and stirred. Three tubes with a volume of 350 μL (NANOSEP 3 K Ω, PALL) were transferred to an ultrafiltration unit. The samples in the tubes were subjected to centrifugation (9,100 ×*g*, 4°C, 120 min) and ultrafiltration. After phospholipids in the mixture were removed using solid-phase extraction, the sample was dried and dissolved in 100 μL of 50% isopropanol solution (v/v) for analysis.

The mass spectrometers of the CE-TOFMS system (Agilent; Santa Clara, CA, USA) (Capillary: Fused silica capillary i.d. 50 μm × 80 cm, CE voltage: Positive, 27 kV; MS ionization: ESI Positive or ESI Negative; MS capillary voltage: 4,000 V, and MS scan range: m/z 50–1,000) and Agilent 1,200 series RRLC system SL (Column: ODS column, 2 × 50 mm, 2 μm; Column temp.: 40°C, Flow rate: 0.3 mL/min, Run time: 20 min, Post time: 7.5 min, Gradient condition: 0–0.5 min: B 1%, 0.5–13.5 min: B 1%–100%, 13.5–20 min: B 100%, MS ionization mode: ESI Positive, MS Nebulizer pressure: 40 psi, MS dry gas flow: 10 L/min, MS dry gas temp: 350°C, MS capillary voltage: 3500 V, MS scan range: m/z 100–1700) were operated in positive and negative electrospray ionization conditions. Three independent measurements were performed for each group.

Candidate compounds were assigned to 451 peaks in the plasma sample and 336 peaks in the skeletal muscle using the mass-to-charge ratio (*m/z*), migration time (MT), and retention time (RT) values of the substances in the HMT metabolite library (Human Metabolome Technologies Inc.) and the Kyoto Encyclopedia of Genes and Genomes (KEGG). For group comparisons, relative area ratios were calculated for each of the peaks corresponding to skeletal muscles and plasma, facilitating the identification of candidate compounds. Quantitative analysis was performed for the candidate compounds. To this end, the calibration curves incorporated peak areas corrected by internal standards, and concentrations were calculated via single-point calibration of 100 μM of substance (internal standard of 200 μM). Ingenuity pathway analysis (IPA; QIAGEN, CA, USA) was performed based on the quantified data from the plasma of each mouse group.

2.6 Statistical analyses

For each group, data were excluded when data acquisition was difficult due to weight loss, debilitation, or death or when there were concerns regarding peculiar values, mechanical errors in measurement, or external environmental influences because motor function and tissue structure could not be correctly assessed. Data are presented as the mean ± standard deviation (SD). Differences between the two groups were assessed using unpaired two-tailed t-tests. Multiple comparisons between three or more groups were performed using analysis of variance (ANOVA, n = 3, Tukey's *post hoc* test). Statistical significance was defined as $^{*}p < 0.05$, $^{**}p < 0.01$, $^{***}p < 0.001$, and $^{****}p < 0.0001$ and was calculated using GraphPad Prism eight or 9 (GraphPad, La Jolla, CA, USA).

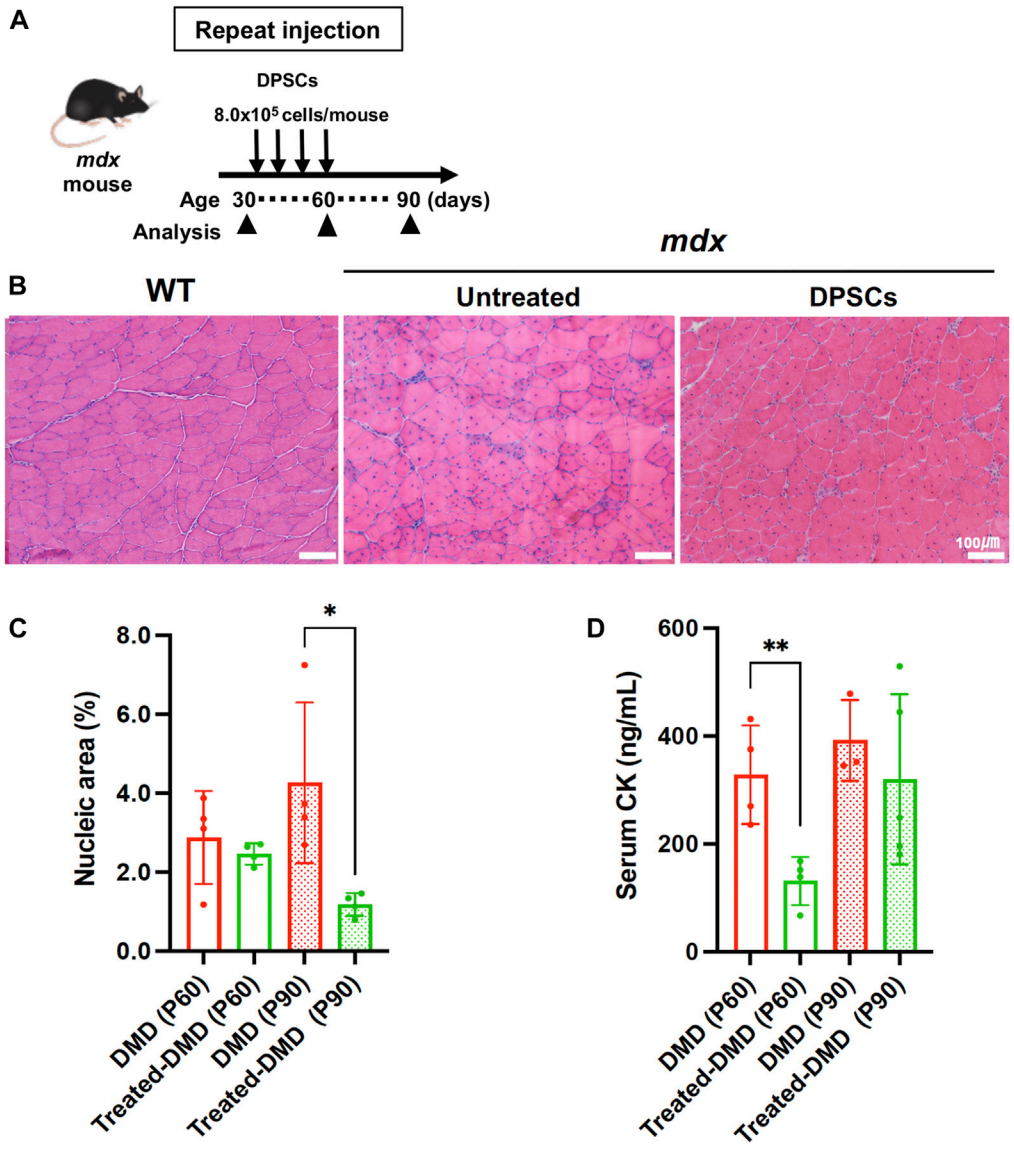

FIGURE 1
Systemic treatment of the *mdx* mice with DPSCs **(A)** Schematic representation of the repeated DPSC treatments of the *mdx* mice. **(B)** Hematoxylin and eosin (H&E) staining of the tibialis anterior (TA) muscle (original magnification, ×40, each) of untreated *mdx* mice and *mdx* mice treated four times with DPSC. Scale bars, 100 μm. **(C)** Quantification of the hematoxylin-positive area in the cross-section (% of total area) of the TA muscle of control *mdx* (DMD) mice and *mdx* mice treated four times DPSCs (Treated-DMD) at the age of 60 and 90 days (P60, P90, n = 4, each). Statistical differences between WT vs. DMD (*$p < 0.05$, and **$p < 0.01$) are indicated; two-way ANOVA or multiple *t*-tests. **(D)** Serum creatine kinase (CK) levels in each group of mice; at the age of 60 and 90 days (P60, and P90) of control *mdx* (n = 4, and 3), and hDPSC-*mdx* (Treated-DMD; n = 4, each), using ELISA.

3 Results

3.1 *Mdx* mice repeatedly treated with DPSCs showed milder DMD disease phenotypes

Mdx mice were repeatedly administered DPSCs via the tail vein (Figure 1A). The cross-section of the tibialis anterior (TA) muscle of the untreated *mdx* mice showed fibers with smaller (regenerating) and larger (hypertrophic) diameters, centrally nucleated fibers (CNFs), spread muscle interstitium, and cell infiltration interspersed in the muscle interstitium (Figure 1B). Histopathological findings observed in the repeatedly DPSC treated mdx mice included limited interstitial muscle area and nuclear infiltration. Quantitative analysis revealed a reduction in the nuclear inflammation area in the DPSC-treated TA muscle compared with that in untreated *mdx* mice (Figure 1C). In addition, high concentrations of circulating CK decreased temporarily after DPSC treatment in *mdx* mice (Figure 1D).

3.2 Metabolite variation on the dystrophic muscle with or without DPSC-treatment

We investigated the therapeutic effects of DPSC-treatment on the DMD pathology-specific metabolic abnormalities. To understand the biological responses to DPSC treatment or

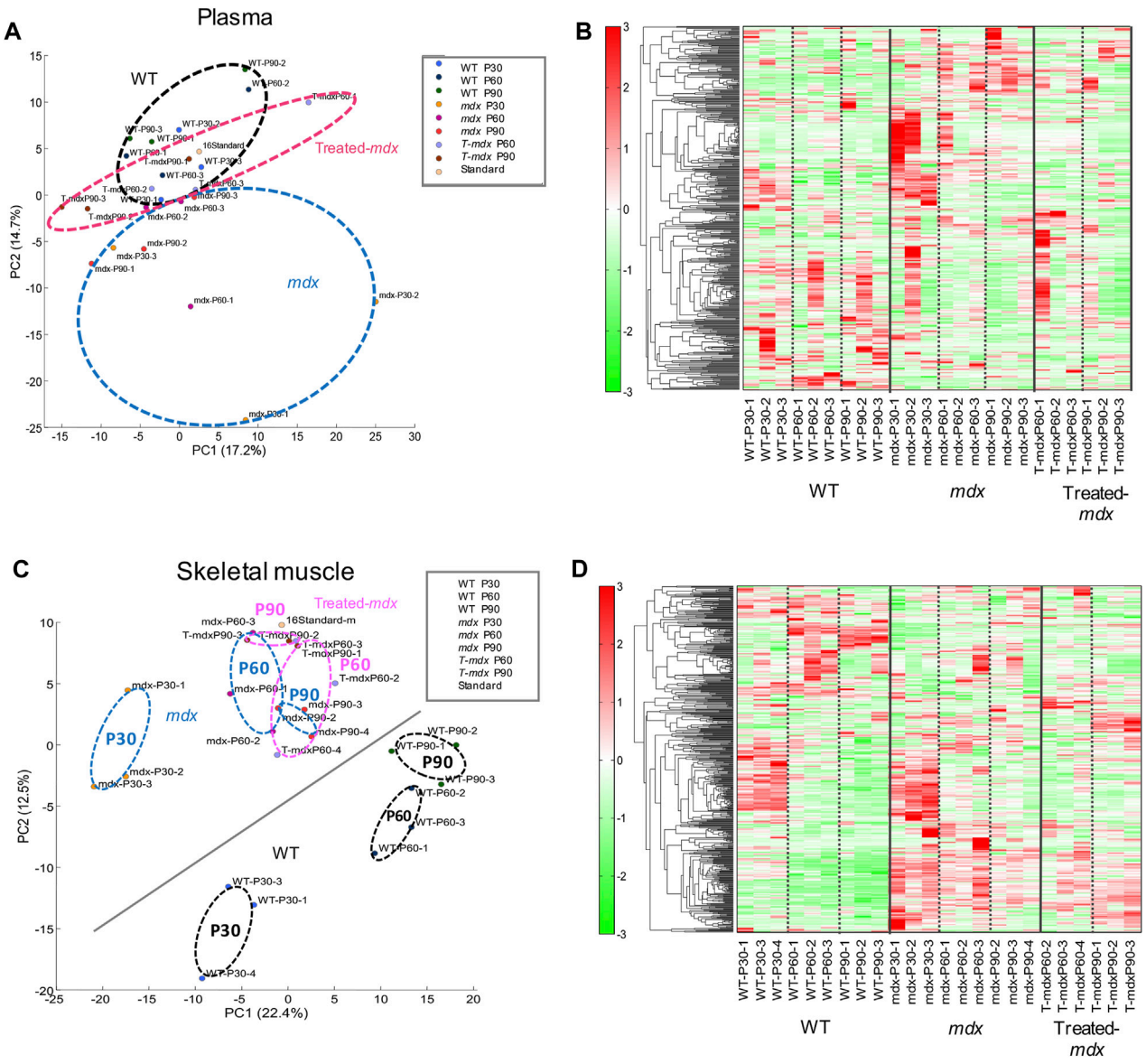

FIGURE 2
Principal component analysis (PCA) and differential concentration of metabolites A principal component analysis (PCA) plot **(A,C)** and heat map depicting hierarchical clustering analysis **(B,D)** of plasma **(A,B)** and the tibialis anterior (TA) muscles **(C,D)** derived from 30-, 60-, and 90-day-old (P30, P60, and P90) C57BL/6 mice (wild type, WT), untreated *mdx* mice (DMD), and DPSC-treated *mdx* mice (Treated-*mdx*). The PCA plot revealed significant separation among the mouse groups (n = 3). High and low concentrations of the metabolites are shown on a continuum from red to green.

environmental changes in disease-specific features, we analyzed metabolic disturbances in plasma and TA muscles from WT (healthy), dystrophic *mdx*, and DPSC-treated *mdx* mice. Metabolic analysis by CE-TOFMS and LC-TOFMS revealed several substances in the plasma samples (451 metabolites; CE-TOFMS, cation: 195, anion: 95; LC-TOFMS, positive: 72, negative: 89, Supplementary Table S1) and skeletal muscle samples (460 metabolites; CE-TOFMS, cation: 212, anion: 126; LC-TOF-MS, positive: 85, negative: 37, Supplementary Table S2).

In the case of plasma samples, we used metabolic profiling to identify and quantitate a total of 165 metabolites, which revealed that changes in a total of 85 metabolites were statistically significant ($p \leq 0.05$). The levels were either elevated or decreased in the comparison of untreated *mdx* mice versus WT (P30, 21 metabolites; P60, 26 metabolites; P90, 37 metabolites). Significant alterations were observed in 25 metabolites upon comparison of DPSC-treated *mdx* mice versus untreated *mdx* mice (P60, 11 metabolites; P90, 22 metabolites), and 31 metabolites were significantly changed upon the comparison of DPSC-treated *mdx* versus WT (P60, 27 metabolites; P90, 9 metabolites) (Supplementary Table S3).

Using global metabolic profiling, we identified and quantitated metabolites in the skeletal muscles. We found that changes in 62 metabolites were statistically significant ($p \leq 0.05$), which either increased or reduced in the comparison of untreated *mdx* mice versus WT (P30, 23 metabolites; P60, 30 metabolites; P90, 37 metabolites). A total of 33 metabolites were significantly altered in the comparison of DPSC-treated *mdx* mice versus untreated *mdx*

TABLE 1 Top and bottom 30 loading factors based on the principal component analysis (PCA) of plasma samples Based on the quantitative metabolic differences annotated in the Human Metabolome Database (HMBD), PCA was performed on plasma samples derived from each group, namely, wild-type, untreated *mdx* mice and DPSC-treated *mdx* mice. Factor loading top and bottom 30 metabolites sorted by PC1 (top, R > 0.727, p < 5.74E-05; bottom, R < −0.307, p < 1.45E-01) are listed in the upper two tables, whereas the corresponding top and bottom 30 metabolites sorted by PC2 (top, R > 0.678, p < 2.72E-04; bottom, R < −0.498, p < 1.33E-02) are listed in the bottom two tables.

Factor loadings (top 30)			PC1	
Rank	ID	Compound name	R	*p*
1	C_0128	*N*-Acetyllysine	0.920	1.94E-10
2	C_0024	GABA	0.884	9.98E-09
3	A_0075	6-Phosphogluconic acid	0.862	6.20E-08
4	A_0081	3′-CMP	0.851	1.36E-07
		2′-CMP		
5	C_0191	Glutathione (GSSG)_divalent	0.846	1.88E-07
6	A_0109	UDP-glucose	0.836	3.54E-07
		UDP-galactose		
7	C_0171	Malonylcarnitine	0.826	6.70E-07
8	A_0112	UDP-*N*-acetylgalactosamine	0.818	1.05E-06
		UDP-*N*-acetylglucosamine		
9	C_0022	3-Aminoisobutyric acid	0.813	1.41E-06
10	A_0049	3-Phosphoglyceric acid	0.811	1.52E-06
11	C_0198	*S*-Adenosylmethionine	0.802	2.48E-06
12	C_0093	Glu	0.794	3.71E-06
13	A_0048	2-Phosphoglyceric acid	0.778	7.70E-06
14	C_0195	NMN	0.776	8.48E-06
15	C_0049	Nicotinamide	0.772	1.00E-05
16	C_0046	Betaine aldehyde_+H_2O	0.772	1.00E-05
17	C_0148	Kynurenine	0.763	1.42E-05
18	N_0046	*cis*-11-Eicosenoic acid	0.763	1.44E-05
19	C_0014	β-Ala	0.761	1.56E-05
20	P_0033	Ethyl arachidonate	0.759	1.73E-05
21	C_0190	Arg-Glu	0.755	1.99E-05
22	A_0083	UMP	0.752	2.27E-05
23	C_0085	4-Guanidinobutyric acid	0.747	2.74E-05
24	P_0016	Sphingosine	0.744	3.02E-05
25	C_0109	*S*-Methylmethionine	0.740	3.59E-05
26	C_0172	Pyridoxamine 5′-phosphate	0.739	3.75E-05
27	A_0090	GMP	0.734	4.49E-05
28	P_0068	α-Tocopherol acetate	0.731	4.98E-05
29	C_0197	*S*-Adenosylhomocysteine	0.729	5.33E-05
30	C_0088	Spermidine	0.727	5.74E-05

(Continued on following page)

TABLE 1 (*Continued*) Top and bottom 30 loading factors based on the principal component analysis (PCA) of plasma samples Based on the quantitative metabolic differences annotated in the Human Metabolome Database (HMBD), PCA was performed on plasma samples derived from each group, namely, wild-type, untreated *mdx* mice and DPSC-treated *mdx* mice. Factor loading top and bottom 30 metabolites sorted by PC1 (top, R > 0.727, p < 5.74E-05; bottom, R < −0.307, p < 1.45E-01) are listed in the upper two tables, whereas the corresponding top and bottom 30 metabolites sorted by PC2 (top, R > 0.678, p < 2.72E-04; bottom, R < −0.498, p < 1.33E-02) are listed in the bottom two tables.

Factor loadings (bottom 30)			PC1	
Rank	ID	Compound name	R	*p*
30	P_0026	Deoxycorticosterone	−0.307	1.45E-01
		17α-Hydroxyprogesterone		
29	C_0005	Methylguanidine	−0.307	1.44E-01
28	C_0041	Val	−0.310	1.40E-01
27	P_0023	Linoleyl ethanolamide	−0.312	1.37E-01
26	N_0002	FA(13:0)	−0.315	1.33E-01
25	P_0072	1,2-Distearoyl-glycero-3-phosphocholine	−0.319	1.28E-01
23	N_0020	FA(16:3)-2	−0.326	1.20E-01
22	N_0015	FA(15:0)-2	−0.369	7.60E-02
21	P_0031	21-Deoxycortisol-1	−0.377	6.94E-02
20	N_0059	Leukotriene B4-1	−0.387	6.16E-02
19	C_0156	3-Hydroxykynurenine	−0.388	6.11E-02
18	P_0052	AC(16:2)-1	−0.389	6.04E-02
17	C_0050	Picolinic acid	−0.402	5.14E-02
16	A_0055	Phenaceturic acid	−0.423	3.96E-02
15	C_0118	Arg	−0.424	3.90E-02
14	P_0018	Estriol-1	−0.462	2.31E-02
13	N_0081	1-Palmitoyl-glycero-3-phosphoethanolamine	−0.470	2.06E-02
12	A_0013	2-Oxoisovaleric acid	−0.474	1.94E-02
11	A_0030	2-Oxoglutaric acid	−0.484	1.67E-02
10	C_0145	Trp	−0.500	1.29E-02
9	N_0067	FA(24:2)	−0.503	1.22E-02
8	A_0021	4-Methyl-2-oxovaleric acid	−0.540	6.51E-03
		3-Methyl-2-oxovaleric acid		
7	N_0039	FA(19:0)	−0.564	4.12E-03
6	P_0020	Progesterone	−0.575	3.31E-03
5	C_0165	Cystine	−0.577	3.13E-03
4	C_0121	Serotonin	−0.598	2.00E-03
3	N_0016	3-Hydroxytetradecanoic acid-1	−0.605	1.73E-03
		2-Hydroxytetradecanoic acid		
2	A_0060	*S*-Sulfocysteine	−0.643	7.09E-04
1	A_0003	Pyruvic acid	−0.742	3.28E-05

(Continued on following page)

TABLE 1 (*Continued*) Top and bottom 30 loading factors based on the principal component analysis (PCA) of plasma samples Based on the quantitative metabolic differences annotated in the Human Metabolome Database (HMBD), PCA was performed on plasma samples derived from each group, namely, wild-type, untreated *mdx* mice and DPSC-treated *mdx* mice. Factor loading top and bottom 30 metabolites sorted by PC1 (top, R > 0.727, p < 5.74E-05; bottom, R < −0.307, p < 1.45E-01) are listed in the upper two tables, whereas the corresponding top and bottom 30 metabolites sorted by PC2 (top, R > 0.678, p < 2.72E-04; bottom, R < −0.498, p < 1.33E-02) are listed in the bottom two tables.

Factor loadings (top 30)			PC2	
Rank	ID	Compound name	R	*p*
1	P_0065	Hecogenin-2	0.809	1.72E-06
2	N_0066	FA(24:4)	0.808	1.80E-06
3	N_0057	FA(22:3)-1	0.791	4.19E-06
4	N_0056	FA(22:4)-2	0.773	9.57E-06
5	N_0051	*cis*-4,7,10,13,16,19-Docosahexaenoic acid	0.771	1.05E-05
6	N_0052	FA(22:5)-1	0.769	1.13E-05
7	N_0053	FA(22:5)-2	0.768	1.17E-05
8	N_0044	cis-11,14-Eicosadienoic acid-1	0.766	1.26E-05
9	N_0058	FA(22:3)-2	0.766	1.26E-05
10	N_0026	FA(17:2)	0.766	1.27E-05
11	P_0050	Stigmasterol-1	0.765	1.35E-05
12	N_0054	FA(22:5)-3	0.760	1.62E-05
13	N_0042	FA(20:3)	0.755	2.04E-05
14	N_0001	FA(12:0)	0.751	2.31E-05
15	N_0065	FA(24:5)	0.749	2.52E-05
16	N_0032	Linolenic acid	0.748	2.62E-05
17	N_0045	cis-11,14-Eicosadienoic acid-2	0.739	3.69E-05
18	N_0021	FA(16:2)-1	0.729	5.34E-05
19	N_0030	FA(17:0)-2	0.729	5.37E-05
		Heptadecanoic acid-2		
20	N_0031	Stearidonic acid	0.725	6.20E-05
21	P_0026	Deoxycorticosterone	0.717	8.06E-05
		17α-Hydroxyprogesterone		
22	N_0034	Oleic acid	0.716	8.37E-05
23	N_0027	FA(17:1)	0.706	1.14E-04
24	N_0022	FA(16:2)-2	0.705	1.18E-04
25	A_0024	2-Hydroxy-4-methylvaleric acid	0.702	1.31E-04
26	N_0033	Linoleic acid	0.700	1.41E-04
27	N_0055	FA(22:4)-1	0.696	1.61E-04
29	P_0048	5α-Cholestan-3-one-1	0.681	2.51E-04
30	N_0040	*cis*-5,8,11,14,17-Eicosapentaenoic acid	0.678	2.72E-04
		Abietic acid		

(Continued on following page)

10.3389/fcell.2024.1363541

TABLE 1 (*Continued*) Top and bottom 30 loading factors based on the principal component analysis (PCA) of plasma samples Based on the quantitative metabolic differences annotated in the Human Metabolome Database (HMBD), PCA was performed on plasma samples derived from each group, namely, wild-type, untreated *mdx* mice and DPSC-treated *mdx* mice. Factor loading top and bottom 30 metabolites sorted by PC1 (top, R > 0.727, p < 5.74E-05; bottom, R < −0.307, p < 1.45E-01) are listed in the upper two tables, whereas the corresponding top and bottom 30 metabolites sorted by PC2 (top, R > 0.678, p < 2.72E-04; bottom, R < −0.498, p < 1.33E-02) are listed in the bottom two tables.

Factor loadings (bottom 30)			PC2	
Rank	ID	Compound name	R	*p*
30	C_0082	*N*-Ethylmaleimide_+H_2O	−0.498	1.33E-02
29	A_0112	UDP-*N*-acetylgalactosamine	−0.498	1.33E-02
		UDP-*N*-acetylglucosamine		
28	A_0010	Glyceric acid	−0.499	1.31E-02
27	A_0025	Malic acid	−0.502	1.25E-02
26	A_0110	UDP-glucuronic acid	−0.506	1.16E-02
25	C_0061	6-Aminohexanoic acid	−0.522	8.83E-03
24	C_0027	Choline	−0.539	6.58E-03
23	C_0177	Thiamine	−0.541	6.35E-03
22	A_0090	GMP	−0.541	6.32E-03
21	C_0049	Nicotinamide	−0.542	6.26E-03
20	A_0104	UTP	−0.544	5.97E-03
19	A_0108	ADP-ribose	−0.545	5.87E-03
18	C_0160	Ergothioneine	−0.550	5.41E-03
17	A_0012	Fumaric acid	−0.550	5.36E-03
15	P_0071	Sphingomyelin(d18:1/16:0)	−0.563	4.15E-03
14	C_0081	Ectoine	−0.569	3.71E-03
13	C_0036	3-Amino-2-piperidone	−0.583	2.81E-03
12	A_0020	5-Oxoproline	−0.585	2.68E-03
11	A_0083	UMP	−0.587	2.55E-03
10	C_0122	Gluconolactone	−0.608	1.63E-03
9	C_0126	Phosphorylcholine	−0.608	1.62E-03
8	C_0143	Spermine	−0.610	1.54E-03
7	A_0016	Succinic acid	−0.632	9.21E-04
6	C_0090	*threo*-β-Methylaspartic acid	−0.635	8.55E-04
5	A_0095	UDP	−0.637	8.07E-04
4	A_0029	4-Acetamidobutanoic acid	−0.638	7.91E-04
3	C_0103	Imidazolelactic acid	−0.643	7.00E-04
2	C_0119	Guanidinosuccinic acid	−0.668	3.58E-04
1	C_0176	Glycerophosphocholine	−0.709	1.05E-04

mice (P60, 11 metabolites; P90, 25 metabolites), and 50 metabolites were significantly changed in the comparison of DPSC-treated *mdx* mice versus WT (P60, 21 metabolites; P90, 41 metabolites) (Supplementary Table S4).

Based on quantitative metabolite differences, principal component analysis (PCA) showed a clear separation between WT and dystrophic muscles (Figures 2A, B). The first and second PCA components explained 17.2% and 14.7% of the variation in plasma (Figure 2A) and 22.4% and 12.5% of the variation in the TA muscles (Figure 2B), respectively. In addition, DPSC-treated *mdx* mice showed an intermediate distribution between these groups in the PCA graph. While plasma samples showed negligible change with respect to the time course among mouse groups in the PCA results, we

TABLE 2 Top and bottom 30 loading factors based on the principal component analysis (PCA) of the skeletal muscles Based on the quantitative metabolic differences annotated in the Human Metabolome Database (HMBD), PCA was performed on the skeletal muscle derived from each group, namely, wild-type, untreated *mdx* mice, and DPSC-treated *mdx* mice. Factor loading top and bottom 30 metabolites sorted by PC1 (top, R > 0.512, $p < 1.05E-02$; bottom, R < −0.814, $p < 1.30E-06$) are listed in the upper two tables, whereas the corresponding top and bottom 30 metabolites sorted by PC2 (top, R > 0.636, $p < 8.28E-04$; bottom, R < −0.552, $p < 5.16E-03$) are listed in the bottom two tables.

Factor loadings (top 30)			PC1	
Rank	ID	Compound name	R	*p*
1	C_0181	Homocarnosine	0.903	1.56E-09
14	C_0220	Adenosine	0.740	3.60E-05
17	C_0167	Carnosine	0.719	7.66E-05
21	A_0135	NAD^+	0.675	2.99E-04
25	P_0040	Campesterol	0.543	6.15E-03
27	A_0124	ATP	0.535	7.12E-03
28	C_0117	Serotonin	0.533	7.34E-03
30	A_0137	$NADP^+$	0.512	1.05E-02
Factor loadings (bottom 30)			**PC1**	
Rank	ID	Compound name	R	*p*
30	C_0139	Ser-Ser	−0.814	1.30E-06
29	A_0052	Ribulose 5-phosphate	−0.816	1.18E-06
27	C_0076	Spermidine	−0.820	9.16E-07
26	C_0105	Taurocyamine	−0.824	7.66E-07
24	C_0032	Homoserine	−0.825	6.88E-07
23	A_0134	CMP-*N*-acetylneuraminate	−0.826	6.81E-07
22	C_0231	Glu-Lys	−0.826	6.51E-07
		Lys-Glu		
21	A_0043	Gluconic acid	−0.828	6.09E-07
19	P_0012	Sphinganine	−0.833	4.41E-07
18	A_0073	6-Phosphogluconic acid	−0.846	1.89E-07
17	C_0074	4-Guanidinobutyric acid	−0.850	1.47E-07
15	C_0135	Gly-Asp	−0.860	7.36E-08
13	A_0016	Ethanolamine phosphate	−0.862	6.00E-08
12	C_0097	*O*-Acetylhomoserine	−0.866	4.41E-08
		2-Aminoadipic acid		
10	C_0050	3-Guanidinopropionic acid	−0.872	2.93E-08
8	C_0130	*N*-Acetyllysine	−0.882	1.23E-08
		Ala-Val		
		Ile-Gly		
		Leu-Gly		
		Val-Ala		

(Continued on following page)

TABLE 2 (*Continued*) Top and bottom 30 loading factors based on the principal component analysis (PCA) of the skeletal muscles Based on the quantitative metabolic differences annotated in the Human Metabolome Database (HMBD), PCA was performed on the skeletal muscle derived from each group, namely, wild-type, untreated *mdx* mice, and DPSC-treated *mdx* mice. Factor loading top and bottom 30 metabolites sorted by PC1 (top, R > 0.512, p < 1.05E-02; bottom, R < −0.814, p < 1.30E-06) are listed in the upper two tables, whereas the corresponding top and bottom 30 metabolites sorted by PC2 (top, R > 0.636, p < 8.28E-04; bottom, R < −0.552, p < 5.16E-03) are listed in the bottom two tables.

Factor loadings (bottom 30)			PC1	
Rank	ID	Compound name	R	*p*
7	A_0133	UDP-*N*-acetylgalactosamine	−0.892	4.91E-09
		UDP-*N*-acetylglucosamine		
6	A_0129	UDP-glucuronic acid	−0.896	3.39E-09
Factor loadings (top 30)			**PC2**	
Rank	ID	Compound name	R	*p*
1	C_0090	His	0.796	3.36E-06
2	C_0096	N^6-Methyllysine	0.788	4.87E-06
3	P_0072	Trilaurin-1	0.777	7.98E-06
4	C_0101	5-Hydroxylysine	0.763	1.47E-05
7	A_0039	Citric acid	0.738	3.87E-05
8	A_0037	3-Phosphoglyceric acid	0.734	4.42E-05
9	P_0073	Trilaurin-2	0.729	5.41E-05
11	C_0027	Pro	0.723	6.68E-05
12	C_0132	N^6,N^6,N^6-Trimethyllysine	0.720	7.31E-05
14	C_0008	Sarcosine	0.708	1.07E-04
15	C_0168	2′-Deoxycytidine	0.706	1.14E-04
16	C_0049	Hydroxyproline	0.706	1.15E-04
17	P_0074	Trilaurin-3	0.702	1.31E-04
18	C_0114	Citrulline	0.702	1.33E-04
19	C_0017	2-Aminoisobutyric acid	0.701	1.37E-04
		2-Aminobutyric acid		
20	A_0003	Pyruvic acid	0.697	1.54E-04
21	A_0018	2-Hydroxyglutaric acid	0.694	1.71E-04
22	C_0020	Ser	0.688	2.02E-04
23	C_0064	Trigonelline	0.688	2.04E-04
25	A_0047	Phosphocreatine	0.685	2.23E-04
28	C_0131	N_{ω}-Methylarginine	0.639	7.73E-04
30	C_0144	ADMA	0.636	8.28E-04
Factor loadings (bottom 30)			**PC2**	
Rank	ID	Compound name	R	*p*
30	C_0289	Cysteine glutathione disulfide	−0.552	5.16E-03
29	C_0208	Ile-Gln	−0.554	4.95E-03
		Leu-Gln		
28	C_0216	Ile-Met	−0.559	4.54E-03

(Continued on following page)

TABLE 2 (*Continued*) Top and bottom 30 loading factors based on the principal component analysis (PCA) of the skeletal muscles Based on the quantitative metabolic differences annotated in the Human Metabolome Database (HMBD), PCA was performed on the skeletal muscle derived from each group, namely, wild-type, untreated *mdx* mice, and DPSC-treated *mdx* mice. Factor loading top and bottom 30 metabolites sorted by PC1 (top, R > 0.512, p < 1.05E-02; bottom, R < −0.814, p < 1.30E-06) are listed in the upper two tables, whereas the corresponding top and bottom 30 metabolites sorted by PC2 (top, R > 0.636, p < 8.28E-04; bottom, R < −0.552, p < 5.16E-03) are listed in the bottom two tables.

Factor loadings (bottom 30)			PC2	
Rank	ID	Compound name	R	*p*
		Leu-Met		
		Met-Ile		
		Met-Leu		
26	C_0173	Ile-Val	−0.569	3.70E-03
22	A_0011	Isethionic acid	−0.585	2.68E-03
17	C_0087	Xanthine	−0.610	1.55E-03
13	C_0217	Phe-Val	−0.634	8.90E-04
12	C_0143	Ile-Ala	−0.644	6.83E-04
		Leu-Ala		
11	C_0073	Ile-Arg_divalent	−0.646	6.44E-04
10	C_0207	Glycerophosphocholine	−0.651	5.78E-04
8	A_0026	Uric acid	−0.671	3.33E-04
6	C_0111	Val-Gly	−0.691	1.87E-04
		N-Acetylornithine		
1	A_0010	2-Hydroxyvaleric acid	−0.808	1.81E-06

observed time-series variation in the analysis of data derived using the partial least-squares method (PLS) (Supplementary Figure S1). In the skeletal muscles, PCA analysis described clear time-series changes between 30 and 60–90 days for both WT and *mdx* mice. These data suggest that DPSC-treated *mdx* mice demonstrated a PCA distribution closer to that of WT mice than to that of untreated *mdx* mice in both plasma and skeletal muscle samples.

Considering the observed changes in metabolite levels, we next investigated how *mdx* and DPSC-treated mice exhibited metabolite imbalances compared to WT mice in the plasma and skeletal muscle. The heat map in Figures 2B, D shows the results of hierarchical clustering analysis (HCA). In HCA of skeletal muscle, WT and *mdx* mice showed notable differentiation consistent with PCA findings (Figure 2C), especially evident between the 30- and 60–90-day groups (Figure 2D). While less prominent than the differentiation between WT and *mdx* mice, we also detected some alterations in HCA patterns in DPSC-treated *mdx* mice compared to those in the untreated *mdx* mice, particularly at 60–90 days of age.

3.3 Metabolites that varied markedly in the dystrophic muscles with or without DPSC-treatment

The top and bottom 30 factor loadings annotated in the Human Metabolome Database (HMBD) containing PC1 and PC2 using PCA for the plasma samples (Table 1) as well as PC1 and PC2 for the skeletal muscle samples are listed in Table 2.

When we focused on the regions of the HCA map where a marked difference between WT and *mdx* mice was observed, we noticed that several amino acid metabolites were present in addition to HMBD. In terms of concentration, amino acid metabolites, such as Asn (asparagine), Asp, Lys, and Met, were accumulated in plasma samples (Supplementary Table S3), and Asn and Gln were abundant in the skeletal muscles of the *mdx* mice compared to those in the WT mice (Supplementary Table S4). Ser in plasma and Ile and Tyr in the skeletal muscle were lower than those in the WT. Accumulated amino acid metabolites in the *mdx* mice were downregulated in the DPSC-treated group, including Asn (ratio of *mdx* ver. WT P60, 1.5, p = 0.021; treated-*mdx* ver. *mdx*, 0.7; p = 0.046) and Met (ratio of *mdx* ver. WT P60, 1.27, p = 0.015; treated-*mdx* ver. *mdx*, 0.83, p = 0.035) in the plasma samples and Asn (ratio of *mdx* ver. WT P90, 1.49, p = 0.012; treated-*mdx* ver. *mdx*, 0.72; p = 0.023) in the skeletal muscles.

3.4 Identification of DMD and DPSC-treatment specifically altered metabolites

To compare the exact metabolite amounts, we focused on the quantification of their areas, as reported by the peaks of the mass spectrum. We found that some metabolites, such as phosphocreatine, homocarnosine, *S*-methylcysteine, guanidinosuccinic acid, and thiamine, were altered in the plasma samples of the 60–90-day-old *mdx* mice compared to those in the WT. Among these metabolites, statistical analysis confirmed that *S*-methylcysteine in the DPSC-treated mice at P90 showed significant differences compared to that in the *mdx* mice

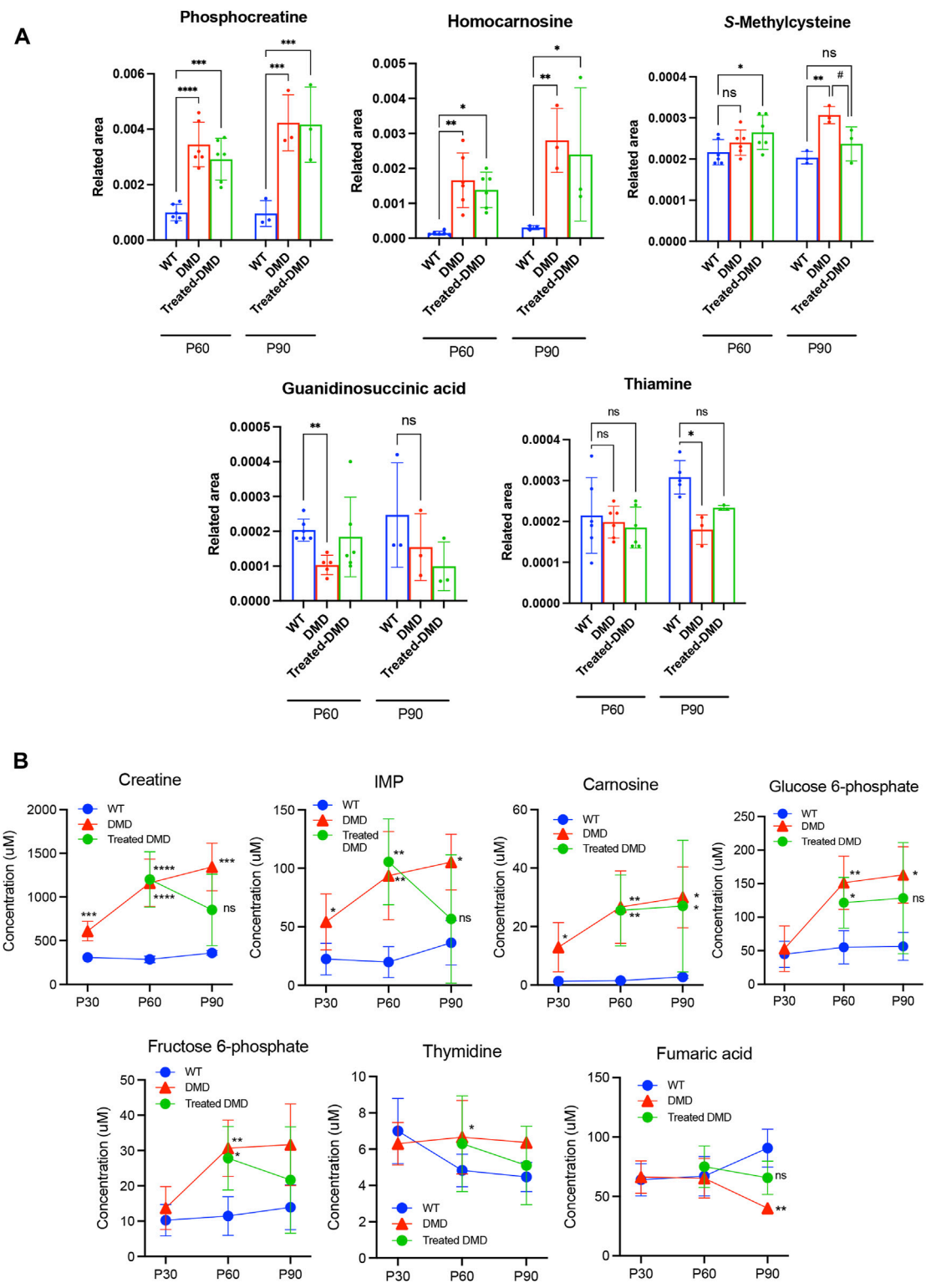

FIGURE 3
Altered metabolites in the plasma of dystrophic mice and effects of DPSC treatment **(A)** Quantitative analysis of metabolites altered in the plasma samples derived from 60- and 90-day-old (P60 and P90) C57BL/6 mice (wild type, WT), untreated *mdx* mice (DMD), and DPSC-treated *mdx* mice (Treated-*mdx*). Relative values of differentially expressed metabolites were described as fold changes compared to standard peaks. **(B)** Plasma levels of metabolite concentrations are described in 30–90-day-old mice (P30, P60, and P90). Statistical differences between WT vs. DMD (*$p < 0.05$, **$p < 0.01$, ***$p < 0.001$, and ****$p < 0.0001$) and DMD vs. Treated-DMD ($^{\#}p < 0.05$) are indicated; ns, not significant, two-way ANOVA or multiple *t*-tests. n = 3 for each group. Data are presented as the mean ± SD.

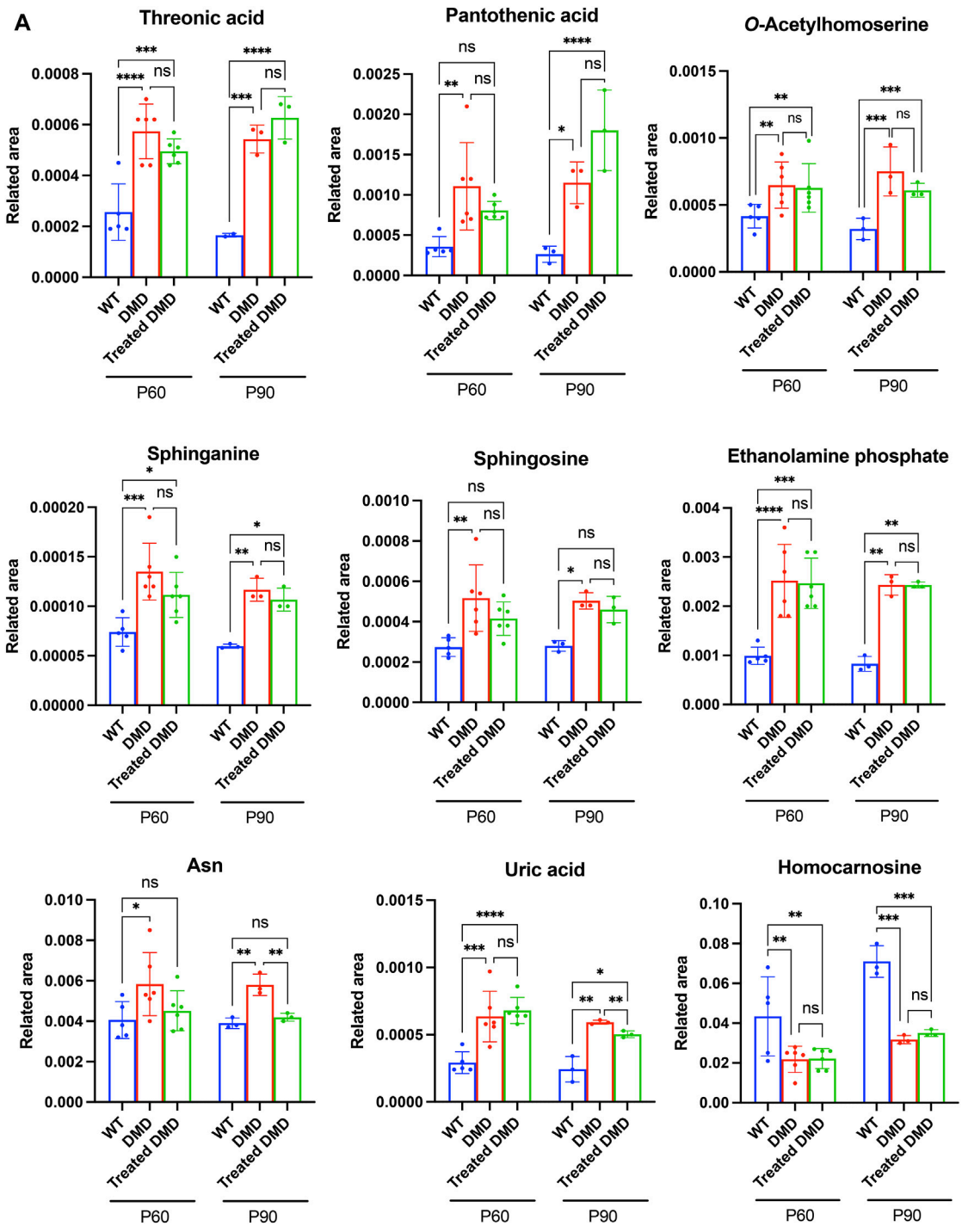

FIGURE 4
(Continued).

(Figure 3A). Analysis of plasma samples from 30 to 90-day-old mice among the three groups showed that the metabolites creatine, inosine monophosphate (IMP), and carnosine accumulated in the early phase of the *mdx* mice at the age of 30–90 days (Figure 3B). Additionally, glucose 6-phosphate (G-6-P), fructose 6-phosphate, and thymidine levels were higher in the *mdx* mice than in WT mice after the age of 60 days. In contrast, fumaric acid was reduced in the *mdx* mice after the age of 60 days than in WT mice. Creatine, IMP, G-6-P, and fumaric acid levels in DPSC-treated *mdx* mice were not significantly different from those in WT mice at 90 days of age. Furthermore, in the quantification data of the skeletal muscle, the metabolites, threonic acid, pantothenic acid, *O*-acetylhomoserine, sphinganine, sphingosine, ethanolamine phosphate, and uric acid accumulated in the *mdx* mice at the age of 60–90 days, whereas homocarnosine levels decreased compared to those in WT mice (Figure 4A). Especially, the elevation of Ans and uric acid in the *mdx* mice after DPSC treatment showed a reduction at P90,

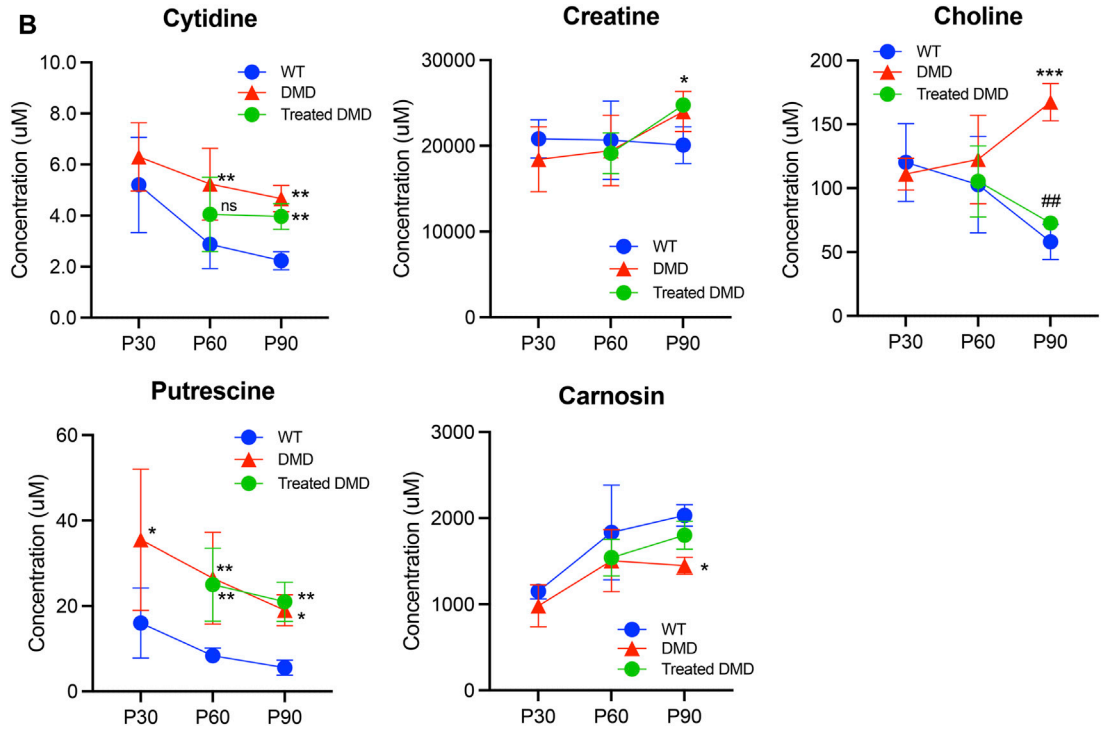

FIGURE 4
(Continued). Altered metabolites in the skeletal muscle of dystrophic mice and effects of DPSC-treatment **(A)** Quantitative analysis of metabolites altered in the skeletal muscles derived from 60- and 90-day old (P60, and P90) C57BL/6 mice (wild type, WT), untreated *mdx* mice (DMD), and DPSC-treated *mdx* mice (Treated-*mdx*). Relative values of differentially expressed metabolites described as fold changes to standard peaks. **(B)** Metabolite concentrations in the skeletal muscles are described for 30–90-day-old mice (P30, P60, and P90). Statistical differences between WT vs. DMD (*p < 0.05, **p < 0.01, ***p < 0.001, and ****p < 0.0001) and DMD vs. Treated-DMD ($^{\#\#}p$ < 0.01) are indicated; ns, not significant, two-way ANOVA or multiple t-test. n = 3 for each group. Data are presented as the mean ± SD.

indicating significant differences when compared to the untreated *mdx* mice (DMD vs. treated-med, Ans, $p = 0.008$; uric acid, $p = 0.006$). Next, we examined the changes in metabolites in the skeletal muscles of mice at the ages of 30–90 days by comparing the three groups of mice (Figure 4B). Choline, creatine, and putrescine levels in the *mdx* mice increased at 60 and 90 days of age. The metabolites choline and Asn were downregulated in DPSC-treated *mdx* mice (Figures 4A, B). While the levels of carnosine in the *mdx* mice were lower than those in WT mice, the differences were not significant when compared with the levels in WT mice after DPSC treatment. In addition, we found that cis-5,8,11,14,17-eicosapentaenoic acid, nicotinamide, and ornitin were transiently elevated in the skeletal muscles of DPSC-treated mice compared with those in the WT and *mdx* mice (Supplementary Table S4; Supplementary Figure S4).

3.5 Characterization of disease-specific modified features and the effects of DPSC treatment on the metabolite pathway determined using ingenuity pathway analysis

To understand the significance of the metabolites that underwent disease-specific changes or that varied after DPSC administration, we carried out "diseases and biological functions" analysis using IPA. To detect early changes, we performed the IPA analysis at P60, immediately following DPSC administration. The results revealed canonical pathways that were altered in the plasma samples of mice in the DPSC-treatment group. A total of 21 pathways with predicted upper or lower activation states were detected when untreated *mdx* mice and DPSC-treated *mdx* mice were compared (Table 3). As predicted by the activation z-score, the top pathways activated in *mdx* mice included "transport of amino acids, mobilization of Ca^{2+}, uptake of D-glucose, release of nitric oxide, synthesis of prostaglandin E2". Hence, the relevant factors were reduced in DPSC-treated mice. The top pathways in the *mdx* mice included "uptake of amino acids, storage or concentration of triacylglycerol, uptake of glutamine family amino acid, and conversion of lipid." Next, we confirmed the differences in these parameters between WT and *mdx* mice along with variability ratios in the untreated and DPSC-treated *mdx* mice (Table 4). We found that the "transport of L-amino acid" and "uptake of L-amino acid" were enriched in the *mdx* mice compared with those in the WT. In contrast, "conversion of lipid" and "uptake of amino acids" were decreased in *mdx* mice. The pathways that were altered in the untreated *mdx* mice compared with those in the WT were increased by approximately two-fold in *mdx* mice compared to those in the DPSC-treated group, except for the "uptake of L-amino acid." These results imply that the enriched pathways in the *mdx* mice were

TABLE 3 Disease or function annotation using ingenuity pathway analysis (IPA) The plasma samples derived from 60-day-old (P60) untreated *mdx* mice (DMD) and DPSC-treated *mdx* mice (treated-*mdx*) mice were compared by "Disease or function annotation analysis" using IPA and listed as predicted by the activation z-score (>2.0, or < −2.0).

Disease or function annotation	*p*-value	Predicted activation state	Activation z-score	# Molecules
Transport of alpha-amino acid	1.71E-04	Increased	2.902	12
Mobilization of $Ca2^{+}$	8.78E-06	Increased	2.891	24
Transport of neutral amino acid	9.49E-05	Increased	2.772	9
Transport of L-amino acid	6.44E-04	Increased	2.737	11
Efflux of L-amino acid	1.81E-04	Increased	2.588	10
Stimulation of neurons	7.96E-04	Increased	2.538	11
Excitation of neurons	1.03E-03	Increased	2.526	10
Stimulation of cells	3.09E-04	Increased	2.424	18
Export of molecule	1.81E-08	Increased	2.377	31
Synthesis of prostaglandin	1.96E-04	Increased	2.279	17
Proliferation of pancreatic cells	1.78E-03	Increased	2.219	6
Uptake of D-glucose	6.10E-03	Increased	2.208	15
Release of nitric oxide	3.12E-03	Increased	2.184	13
Synthesis of prostaglandin E2	1.04E-03	Increased	2.095	14
Cell viability of tumor cell lines	8.43E-05	Increased	2.059	23
Uptake of amino acids	8.77E-07	Decreased	−3.172	23
Uptake of L-amino acid	1.29E-06	Decreased	−3.069	20
Storage of triacylglycerol	3.62E-04	Decreased	−2.222	5
Concentration of triacylglycerol	1.17E-05	Decreased	−2.194	21
Uptake of glutamine family amino acid	1.38E-05	Decreased	−2.177	14
Conversion of lipid	7.94E-09	Decreased	−2.08	36

downregulated in DPSC-treated *mdx* mice, resembling WT mice closely. In contrast, pathways such as the "uptake of amino acids," "concentration of triacylglycerol," "uptake of glutamine family amino acid," and "conversion of lipid," which were downregulated in the *mdx* mice compared with those in the WT, were upregulated in the DPSC-treated group, indicating a trend toward similarity with WT mice in the DPSC-treated group.

IPA was used to identify the upstream regulators that explained the observed changes in the metabolites because upstream regulators were activated early and subsequently contributed to downstream metabolic changes (Figure 5; Supplementary Table S5). This suggests that several upstream regulators are critical for DMD and MSC treatment. The most activated upstream regulators in WT vs. *mdx* mice included disease-specific factors, LEP, NOS3, and 3-nitropropionic acid, while the inhibited state targeted 6–8 molecules such as creatinine, D-sphingosine, glutathione, and L-arginine. LDL and BHMT in the activated state targeted 5–6 molecules such as cholesterol, D-sphingosine, and glutathione.

In the case of DPSC-treated *mdx* mice, the top activated upstream regulators included methamphetamine in an inhibitory state targeting molecules such as 4-hydroxy-3-methoxyphenylacetic acid, 5-hydroxytryptamine, creatinine, GABA, and glutathione as predicted, and upstream regulators BHMT, UCP1, NOS1, and GNRH1 in the activated state, targeting molecules such as creatinine, GABA, L-arginine, L-glutamic acid, oleic acid, phosphorylcholine, and glycero-3-phosphocholine. These results demonstrated that disease-specific or DPSC-treated DMD-specific pathways, including upstream regulators, could be identified using IPA.

4 Discussion

We investigated the metabolic signatures of previously identified and newly characterized factors associated with the effects of DPSC treatment on the metabolic status of dystrophic mice. Although a previous study reported metabolic disturbances in DMD using mouse and dog models (Nitahara-Kasahara et al., 2021), this study is the first to report the therapeutic evaluation of cell therapy focused on metabolic abnormalities in DMD. We identified DMD-specific impairments in metabolites and their responses to systemic DPSC treatment. Our results demonstrate that metabolomics-based pathological assessment is expected to help understand the histopathological mechanisms associated with the anti-inflammatory effects of DPSC treatment and can help identify the therapeutic targets and pathways.

TABLE 4 Disease and bio function determined using IPA The plasma samples derived from 60-day-old wild type (WT), untreated *mdx* mice, and DPSC-treated *mdx* (treated-*mdx*) mice were compared by "Disease and bio function" using IPA, and the items were listed according to the ratio of the results of *mdx* vs. treated-*mdx* mice (>2.0, or < −2.0). Corresponding values obtained after a comparison between *mdx* vs. WT were also included.

Disease and bio function	Ratio	
	mdx vs. WT	*mdx vs.* Treated *mdx*
Transport of alpha-amino acid	−3.74	2.90
Mobilization of Ca^{2+}	0.73	2.89
Transport of neutral amino acid	−1.17	2.77
Transport of L-amino acid	41.29	2.74
Efflux of L-amino acid	−1.78	2.59
Stimulation of neurons	0.90	2.54
Excitation of neurons	1.24	2.53
Stimulation of cells	0.55	2.42
Export of molecule	2.92	2.38
Synthesis of prostaglandin	0.47	2.28
Proliferation of pancreatic cells	1.80	2.22
Uptake of D-glucose	0.00	2.21
Release of nitric oxide	1.40	2.18
Synthesis of prostaglandin E2	0.62	2.10
Cell viability of tumor cell lines	19.32	2.06
Uptake of amino acids	−7.60	−3.17
Uptake of L-amino acid	18.24	−3.07
Storage of triacylglycerol	0.82	−2.22
Concentration of triacylglycerol	−4.20	−2.19
Uptake of glutamine family amino acid	−2.60	−2.18
Conversion of lipid	−50.03	−2.08

Early systemic DPSC administration in *mdx* mice ameliorated the progressive phenotypes and retained milder histological phenotypes (Figure 1). DPSC-treated mice retained motor function, resulting in the long-term improvement of skeletal muscles, as in our previous study (Nitahara-Kasahara et al., 2021). However, the therapeutic mechanisms, target molecules, and environmental changes in the skeletal muscle after systemic administration of DPSCs were unclear. As chronic inflammation is followed by the controlled degeneration and necrosis of muscle fibers, it was considered that the treated mice might have efficient energy production, metabolism, and structural stability, which may be closely related to muscle function.

PCA and heat maps showed that the overall variants of metabolites depended on the time course in *mdx* mice and DPSC-treated *mdx* mice compared to those in WT mice (Figure 2). Quantitative analysis provided a list of metabolites with disease-specific variations, and groups of factors that were further altered by cell therapy were obtained (Tables 1, 2). Furthermore, we focused on the marked differences between normal and disease conditions during the growth process (Figures 3, 4) and suggested that the metabolite variety was affected by DPSC treatment during disease progression.

In dystrophic muscles, disruption of the dystrophin-glycoprotein complex initiates complex pathogenesis, including membrane microrupturing, Ca^{2+}-induced proteolytic degradation, and fiber degeneration, followed by chronic inflammation (Allen et al., 2016; Smith, and Barton, 2018; Tidball et al., 2018). In addition to progressive muscle wasting, metabolic abnormalities have been reported previously. For instance, changes in plasma metabolites have been observed in patients with DMD, including alterations in unsaturated fatty acids, carnitine, and lipids. Moreover, metabolites associated with amino acid metabolism, such as elevated levels of Gln and Glu, as well as decreased levels of Val, have been noted compared to healthy controls. (Xu et al., 2023). In an animal model, the metabolites Ala, Met, Gly, and Glu showed different variants in dystrophic *mdx* mice (Lorena et al., 2023) compared to those in the WT. Glu accumulates in GRMD (Kornegay, 2017); however, this alteration may be specific to certain animal models. Our study revealed that DPSC treatments may influence variations in amino acid metabolites, particularly those that are disease-specific and altered in *mdx* mice. This effect is possibly attributed to elevated levels of Asn and Glu (Figure 4A; Supplementary Tables S3, S4).

We found that elevated uric acid and reduced carnosine levels in the skeletal muscle of *mdx* mice showed a trend similar to that of WT mice after DPSC treatment (Figures 4A, B). Similarly, patients with DMD had much higher muscle concentrations of uric acid than healthy individuals, which is associated with purine metabolism (Camina et al., 1995). The hypothesis that DMD involves alterations leading to the blockage of the IMP-purine pathway was supported. Therefore, inhibition of xanthine oxidase is expected to delay the loss of hypoxanthine in the form of uric acid, thus favoring the restoration of nucleotide levels via IMP and guanine (Camina et al., 1995). Considering this pathway, the IMP levels in plasma after the treatment of dystrophic mice with DPSCs were comparable to those in the untreated controls and were not sufficient to restore purine levels in our study (Figure 3B).

Carnosine is a dipeptide that is highly concentrated in the skeletal muscles (Kohen et al., 1988). A previous study showed that significantly decreased carnosine in GRMD could set the stage for eventual muscle damage (e.g., due to lactic acid or oxidative damage). This decline may lead to limited myosin ATPase activity, as highlighted in a previous study (Rayment, 1996), and may contribute to muscle fatigue (Parker, and Ring, 1970). Patients also have significantly lower muscle concentrations of ATP, ADP, GTP, GDP, IMP, S-AMP, hypoxanthine, and guanine (Camina et al., 1995). Our results showed that carnosine levels in the skeletal muscle of DPSC-treated mice were similar to those in WT mice (Figure 4B). We also demonstrated that the locomotor function of *mdx* mice was maintained for a long time after DPSC treatment (Nitahara-Kasahara et al., 2021). These results suggest that energy production and metabolic efficiency may also contribute to the maintenance of muscle function, followed by decreased muscle damage by downregulating inflammation via DPSCs. Future investigations of the relationship between changes in muscle fiber type and metabolic variation may provide clues to

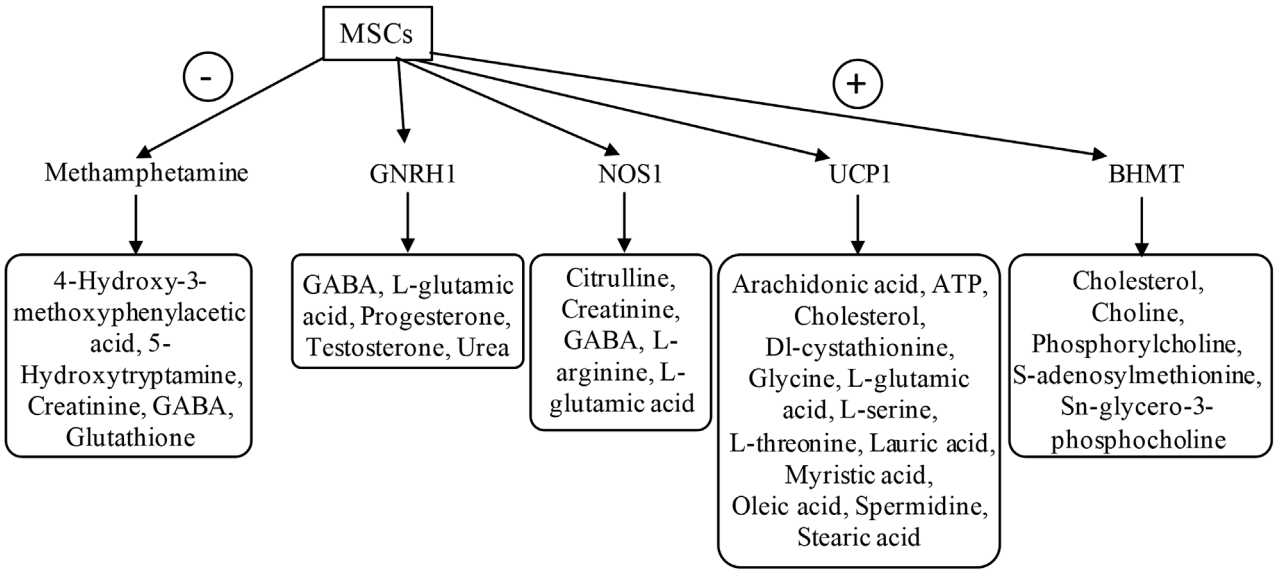

FIGURE 5
Upstream regulator analysis using IPA The plasma samples derived from 60-day-old untreated *mdx* mice and DPSC-treated *mdx* mice (treated-*mdx*) were compared using "Upstream regulator" analysis by IPA and were listed by activated upstream regulators for both downregulated factors (-; Inhibited, activation z-score; < −2.0), and upregulated factors (+; Activated, activation z-score; >2.0). The target molecules listed based on each upstream factor are surrounded by a square.

explain the mechanisms of the therapeutic effects by DPSC-treatment. Furthermore, higher levels of metabolites involved in glycolysis, including 6-phosphoglycerate, fructose-6-phosphate, and glucose-6-phosphate have been previously reported in *mdx* mice (Xu et al., 2023). Similar results were obtained in this study, and the abnormal metabolism of amino acids, energy, and lipids in DMD was consistent with pathological features, such as recurrent muscle necrosis and regeneration and inflammation, which also partially reflect therapeutic effects.

Choline-containing compounds were approximately three times higher than those in healthy individuals and patients with other myopathies, whereas creatine levels were within the normal range, indicating that abnormal cell membrane function may be correlated with abnormal dystrophin or lack of dystrophin in the brains of patients with DMD (Kato et al., 1997). We found that increased choline in the skeletal muscle of *mdx* mice was similar to that in patients with DMD and was downregulated after DPSC-treatment (Figure 4B). These findings are consistent with the protective cell membrane function in DPSC-treated dystrophic muscle compared with that in the untreated control. Lower levels of circulating CK in the treated mice imply the retention of cellular fragility, albeit temporarily, associated with an improved histological appearance of the skeletal muscle. Therefore, these measurements imply that tissue damage was decreased by DPSC-treatments, reflecting protection against physical damage. In contrast, sphingolipid biosynthesis is known to be upregulated in dystrophic muscles (Laurila et al., 2022), but was not significantly influenced by DPSC treatment.

The IPA pathway is disease-specific and influences various signaling pathways. We found that the main differences between disease and treatment groups included the variation related to increased "transport of amino acid and mobilization of Ca^{2+}" and decreased "uptake of amino acids and storage of triacylglycerol" in the analysis of "Diseases or functions annotation" (Table 3). Choline was included as a factor in the "triacylglycerol enrichment or storage" category with a reduced predicted activation state. Carnosine and Glu were also in the "lipid metabolism" Pathway. Creatine and uric acid were in "release of nitric oxide, stimulation of cells, and mobilization of Ca^{2+}." As nitric oxide and Ca^{2+} are known to be involved in the pathogenesis of muscle dystrophy, DPSCs are expected to have the potential to maintain tissue structure. Furthermore, BHMT was identified as an upstream molecule that regulates factors, including choline and its analogs (Figure 5; Supplementary Table S5). There are many upstream factors that regulate Glu; here, we identified UCP1, GNRH1, and NOS1. The dystrophic muscle membrane induces the secondary loss of neuronal nitric oxide synthase. Because nitric oxide is a potent regulator of skeletal muscle metabolism, the loss of NO bioavailability is likely a key contributor to chronic pathology (Timpani et al., 2017). Considering the above findings and our results using IPA based on metabolite variation, we successfully characterized pathways that reflect disease pathology and suggest that treatment may ameliorate disease progression.

There are a few reports on metabolites resulting from MSC administration, for example, MSC-triggered metabolomic alterations in liver-resident immune cells from acute liver injury model mice (Shi et al., 2019), and key metabolic pathways in MSC-mediated immunomodulation for GVHD (Burnham et al., 2020). This is the first report of metabolic improvements following DPSC administration in relation to muscular dystrophy. Whether the supply of DPSCs has a significant impact on the metabolic network and crosstalk with the immune response to alter the disease progression of DMD needs to be further investigated. Metabolite analysis may be useful for understanding the molecular targets and mechanisms underlying cellular therapies.

Data availability statement

The original contributions presented in the study are included in the article/Supplementary Material, further inquiries can be directed to the corresponding authors.

Ethics statement

Ethical approval was not required for the studies on humans in accordance with the local legislation and institutional requirements because only commercially available established cell lines were used. The animal study was approved by the Ethics Committee for the Treatment of Laboratory Animals at the Nippon Medical School and Institute of Medical Science. The study was conducted in accordance with the local legislation and institutional requirements.

Author contributions

YN-K: Data curation, Formal Analysis, Investigation, Methodology, Software, Writing–original draft, Writing–review and editing. GP-H: Methodology, Writing–review and editing. KH: Methodology, Writing–original draft. YO: Methodology, Writing–original draft. NS-M: Methodology, Writing–original draft. YY: Conceptualization, Funding acquisition, Project administration, Supervision, Writing–review and editing. TO: Conceptualization, Funding acquisition, Project administration, Supervision, Writing–review and editing.

Funding

The author(s) declare that financial support was received for the research, authorship, and/or publication of this article. This work was supported by the Japan Agency for Medical Research and Development (AMED) under grant number DNW-15006 and and Grant-in-Aid for Scientific Research (B), and (C) from the Japan Society for the Promotion of Science (#20H03788, #23K20328, #22K06921).

Acknowledgments

The authors express their gratitude to Jun Tanihata, Tomoko Mori, and Chiaki Masuda for technical advice, support, and helpful discussions. We also thank Sonoko Shimazu, Tomomi Fukatsu, Maya Kawamura, and Yuko Aizen for their technical assistance. The authors thank Editage (www.editage.jp) for editing the manuscript draft.

Conflict of interest

YN-K and TO were members of the Division of Cell and Gene Therapy, Nippon Medical School, which is an endowment department supported by a grant from JCR Pharmaceuticals Co., Ltd.

Publisher's note

Supplementary material

The Supplementary Material for this article can be found online at: https://www.frontiersin.org/articles/10.3389/fcell.2024.1363541/full#supplementary-material

References

Abdullah, M., Kornegay, J. N., Honcoop, A., Parry, T. L., Balog-Alvarez, C. J., O'Neal, S. K., et al. (2017). Non-targeted metabolomics analysis of golden retriever muscular dystrophy-affected muscles reveals alterations in arginine and proline metabolism, and elevations in glutamic and oleic acid *in vivo*. *Metabolites* 7, 38. doi:10.3390/metabo7030038

Allen, D. G., Whitehead, N. P., and Froehner, S. C. (2016). Absence of dystrophin disrupts skeletal muscle signaling: roles of Ca2+, reactive oxygen species, and nitric oxide in the development of muscular dystrophy. *Physiol. Rev.* 96, 253–305. doi:10.1152/physrev.00007.2015

Boca, S. M., Nishida, M., Harris, M., Rao, S., Cheema, A. K., Gill, K., et al. (2016). Discovery of metabolic biomarkers for Duchenne muscular dystrophy within a natural history study. *PLoS One* 11, e0153461. doi:10.1371/journal.pone.0153461

Bulfield, G., Siller, W. G., Wight, P. A., and Moore, K. J. (1984). X chromosome-linked muscular dystrophy (mdx) in the mouse. *Proc. Natl. Acad. Sci. U. S. A.* 81, 1189–1192. doi:10.1073/pnas.81.4.1189

Burnham, A. J., Foppiani, E. M., and Horwitz, E. M. (2020). Key metabolic pathways in MSC-mediated immunomodulation: implications for the prophylaxis and treatment of graft versus host disease. *Front. Immunol.* 11, 609277. doi:10.3389/fimmu.2020.609277

Camina, F., Novo-Rodriguez, M. I., Rodriguez-Segade, S., and Castro-Gago, M. (1995). Purine and carnitine metabolism in muscle of patients with Duchenne muscular dystrophy. *Clin. Chim. Acta* 243, 151–164. doi:10.1016/0009-8981(95)06164-9

Campbell, K. P. (1995). Three muscular dystrophies: loss of cytoskeleton-extracellular matrix linkage. *Cell* 80, 675–679. doi:10.1016/0092-8674(95)90344-5

Dabaj, I., Ferey, J., Marguet, F., Gilard, V., Basset, C., Bahri, Y., et al. (2021). Muscle metabolic remodelling patterns in Duchenne muscular dystrophy revealed by ultra-high-resolution mass spectrometry imaging. *Sci. Rep.* 11, 1906. doi:10.1038/s41598-021-81090-1

Ervasti, J. M., Ohlendieck, K., Kahl, S. D., Gaver, M. G., and Campbell, K. P. (1990). Deficiency of a glycoprotein component of the dystrophin complex in dystrophic muscle. *Nature* 345, 315–319. doi:10.1038/345315a0

Friedenstein, A. J., Petrakova, K. V., Kurolesova, A. I., and Frolova, G. P. (1968). Heterotopic of bone marrow. Analysis of precursor cells for osteogenic and hematopoietic tissues. *Transplantation* 6, 230–247. doi:10.1097/00007890-196803000-00009

Guiraud, S., Squire, S. E., Edwards, B., Chen, H., Burns, D. T., Shah, N., et al. (2015). Second-generation compound for the modulation of utrophin in the therapy of DMD. *Hum. Mol. Genet.* 24, 4212–4224. doi:10.1093/hmg/ddv154

He, Q., Wan, C., and Li, G. (2007). Concise review: multipotent mesenchymal stromal cells in blood. *Stem Cells* 25, 69–77. doi:10.1634/stemcells.2006-0335

Ichim, T. E., Alexandrescu, D. T., Solano, F., Lara, F., Campion Rde, N., Paris, E., et al. (2010). Mesenchymal stem cells as anti-inflammatories: implications for treatment of Duchenne muscular dystrophy. *Cell Immunol.* 260, 75–82. doi:10.1016/j.cellimm.2009.10.006

Jo, Y. Y., Lee, H. J., Kook, S. Y., Choung, H. W., Park, J. Y., Chung, J. H., et al. (2007). Isolation and characterization of postnatal stem cells from human dental tissues. *Tissue Eng.* 13, 767–773. doi:10.1089/ten.2006.0192

Joseph, J., Cho, D. S., and Doles, J. D. (2018). Metabolomic analyses reveal extensive progenitor cell deficiencies in a mouse model of Duchenne muscular dystrophy. *Metabolites* 8, 61. doi:10.3390/metabo8040061

Kato, T., Nishina, M., Matsushita, K., Hori, E., Akaboshi, S., and Takashima, S. (1997). Increased cerebral choline-compounds in Duchenne muscular dystrophy. *Neuroreport* 8, 1435–1437. doi:10.1097/00001756-199704140-00022

Khairallah, M., Khairallah, R., Young, M. E., Dyck, J. R., Petrof, B. J., and Des Rosiers, C. (2007). Metabolic and signaling alterations in dystrophin-deficient hearts precede overt cardiomyopathy. *J. Mol. Cell Cardiol.* 43, 119–129. doi:10.1016/j.yjmcc.2007.05.015

Kohen, R., Yamamoto, Y., Cundy, K. C., and Ames, B. N. (1988). Antioxidant activity of carnosine, homocarnosine, and anserine present in muscle and brain. *Proc. Natl. Acad. Sci. U. S. A.* 85, 3175–3179. doi:10.1073/pnas.85.9.3175

Kornegay, J. N. (2017). The golden retriever model of Duchenne muscular dystrophy. *Skelet. Muscle* 7, 9. doi:10.1186/s13395-017-0124-z

Laurila, P. P., Luan, P., Wohlwend, M., Zanou, N., Crisol, B., Imamura de Lima, T., et al. (2022). Inhibition of sphingolipid *de novo* synthesis counteracts muscular dystrophy. *Sci. Adv.* 8, eabh4423. doi:10.1126/sciadv.abh4423

Lee-McMullen, B., Chrzanowski, S. M., Vohra, R., Forbes, S. C., Vandenborne, K., Edison, A. S., et al. (2019). Age-dependent changes in metabolite profile and lipid saturation in dystrophic mice. *NMR Biomed.* 32, e4075. doi:10.1002/nbm.4075

Lorena, M., Santos, E. K. D., Ferretti, R., Nagana Gowda, G. A., Odom, G. L., Chamberlain, J. S., et al. (2023). Biomarkers for Duchenne muscular dystrophy progression: impact of age in the mdx tongue spared muscle. *Skelet. Muscle* 13, 16. doi:10.1186/s13395-023-00325-z

Merckx, C., and De Paepe, B. (2022). The role of taurine in skeletal muscle functioning and its potential as a supportive treatment for Duchenne muscular dystrophy. *Metabolites* 12, 193. doi:10.3390/metabo12020193

Nitahara-Kasahara, Y., Kuraoka, M., Guillermo, P. H., Hayashita-Kinoh, H., Maruoka, Y., Nakamura-Takahasi, A., et al. (2021). Dental pulp stem cells can improve muscle dysfunction in animal models of Duchenne muscular dystrophy. *Stem Cell Res. Ther.* 12, 78. doi:10.1186/s13287-020-02099-3

Oh, W., Kim, D. S., Yang, Y. S., and Lee, J. K. (2008). Immunological properties of umbilical cord blood-derived mesenchymal stromal cells. *Cell Immunol.* 251, 116–123. doi:10.1016/j.cellimm.2008.04.003

Ozdemir, A. T., Ozgul Ozdemir, R. B., Kirmaz, C., Sariboyaci, A. E., Unal Halbutogllari, Z. S., Ozel, C., et al. (2016). The paracrine immunomodulatory interactions between the human dental pulp derived mesenchymal stem cells and CD4 T cell subsets. *Cell Immunol.* 310, 108–115. doi:10.1016/j.cellimm.2016.08.008

Parker, C. J., Jr., and Ring, E. (1970). A comparative study of the effect of carnosine on myofibrillar-ATPase activity of vertebrate and invertebrate muscles. *Comp. Biochem. Physiol.* 37, 413–419. doi:10.1016/0010-406X(70)90569-4

Rayment, I. (1996). The structural basis of the myosin ATPase activity. *J. Biol. Chem.* 271, 15850–15853. doi:10.1074/jbc.271.27.15850

Shi, X., Liu, J., Chen, D., Zhu, M., Yu, J., Xie, H., et al. (2019). MSC-triggered metabolomic alterations in liver-resident immune cells isolated from CCl(4)-induced mouse ALI model. *Exp. Cell Res.* 383, 111511. doi:10.1016/j.yexcr.2019.111511

Sicinski, P., Geng, Y., Ryder-Cook, A. S., Barnard, E. A., Darlison, M. G., and Barnard, P. J. (1989). The molecular basis of muscular dystrophy in the mdx mouse: a point mutation. *Science* 244, 1578–1580. doi:10.1126/science.2662404

Smith, L. R., and Barton, E. R. (2018). Regulation of fibrosis in muscular dystrophy. *Matrix Biol.* 68-69, 602–615. doi:10.1016/j.matbio.2018.01.014

Spitali, P., Hettne, K., Tsonaka, R., Sabir, E., Seyer, A., Hemerik, J. B. A., et al. (2018). Cross-sectional serum metabolomic study of multiple forms of muscular dystrophy. *J. Cell Mol. Med.* 22, 2442–2448. doi:10.1111/jcmm.13543

Srivastava, N. K., Annarao, S., and Sinha, N. (2016). Metabolic status of patients with muscular dystrophy in early phase of the disease: *in vitro*, high resolution NMR spectroscopy based metabolomics analysis of serum. *Life Sci.* 151, 122–129. doi:10.1016/j.lfs.2016.01.032

Tidball, J. G., Welc, S. S., and Wehling-Henricks, M. (2018). Immunobiology of inherited muscular dystrophies. *Compr. Physiol.* 8, 1313–1356. doi:10.1002/cphy.c170052

Timpani, C. A., Hayes, A., and Rybalka, E. (2017). Therapeutic strategies to address neuronal nitric oxide synthase deficiency and the loss of nitric oxide bioavailability in Duchenne Muscular Dystrophy. *Orphanet J. Rare Dis.* 12, 100. doi:10.1186/s13023-017-0652-y

Tracey, I., Dunn, J. F., and Radda, G. K. (1996). Brain metabolism is abnormal in the mdx model of Duchenne muscular dystrophy. *Brain* 119 (Pt 3), 1039–1044. doi:10.1093/brain/119.3.1039

Tsai, M. S., Lee, J. L., Chang, Y. J., and Hwang, S. M. (2004). Isolation of human multipotent mesenchymal stem cells from second-trimester amniotic fluid using a novel two-stage culture protocol. *Hum. Reprod.* 19, 1450–1456. doi:10.1093/humrep/deh279

Tsonaka, R., Signorelli, M., Sabir, E., Seyer, A., Hettne, K., Aartsma-Rus, A., et al. (2020). Longitudinal metabolomic analysis of plasma enables modeling disease progression in Duchenne muscular dystrophy mouse models. *Hum. Mol. Genet.* 29, 745–755. doi:10.1093/hmg/ddz309

Xu, H., Cai, X., Xu, K., Wu, Q., and Xu, B. (2023). The metabolomic plasma profile of patients with Duchenne muscular dystrophy: providing new evidence for its pathogenesis. *Orphanet J. Rare Dis.* 18, 273. doi:10.1186/s13023-023-02885-1

Zannettino, A. C., Paton, S., Arthur, A., Khor, F., Itescu, S., Gimble, J. M., et al. (2008). Multipotential human adipose-derived stromal stem cells exhibit a perivascular phenotype *in vitro* and *in vivo*. *J. Cell Physiol.* 214, 413–421. doi:10.1002/jcp.21210

Zhang, W., Walboomers, X. F., Van Kuppevelt, T. H., Daamen, W. F., Van Damme, P. A., Bian, Z., et al. (2008). *In vivo* evaluation of human dental pulp stem cells differentiated towards multiple lineages. *J. Tissue Eng. Regen. Med.* 2, 117–125. doi:10.1002/term.71

frontiers | Frontiers in Cell and Developmental Biology

TYPE Original Research
PUBLISHED 25 July 2024
DOI 10.3389/fcell.2024.1286815

OPEN ACCESS

EDITED BY
Tokiko Nagamura-Inoue,
The University of Tokyo, Japan

REVIEWED BY
Pedro Prata,
Hôpital Saint-Louis, France
Anastasia Conti,
San Raffaele Telethon Institute for Gene Therapy (SR-Tiget), Italy

*CORRESPONDENCE
Josune Zubicaray,
josune.zubicaray@salud.madrid.org

RECEIVED 31 August 2023
ACCEPTED 13 May 2024
PUBLISHED 25 July 2024

CITATION
Zubicaray J, Ivanova M, Iriondo J, García Martínez J, Muñoz-Viana R, Abad L, García-García L, González de Pablo J, Gálvez E, Sebastián E, Ramírez M, Madero L, Díaz MÁ, González-Murillo Á and Sevilla J (2024), Role of the mesenchymal stromal cells in bone marrow failure of Fanconi Anemia patients. *Front. Cell Dev. Biol.* 12:1286815. doi: 10.3389/fcell.2024.1286815

Role of the mesenchymal stromal cells in bone marrow failure of Fanconi Anemia patients

Josune Zubicaray [1]*, Maria Ivanova [1,2], June Iriondo[1], Jorge García Martínez[3,4], Rafael Muñoz-Viana[4], Lorea Abad[4], Lorena García-García[2,4], Jesús González de Pablo[1], Eva Gálvez[1], Elena Sebastián[1], Manuel Ramírez[1,2,3,4], Luis Madero[1,4], Miguel Ángel Díaz[5], África González-Murillo[2,4] and Julián Sevilla [1]

[1]Hematology and Hemotherapy Unit, Pediatric Onco-hematology Department, Hospital Infantil Universitario Niño Jesús, Madrid, Spain, [2]Advanced Therapy Unit, Oncology, Fundación para la Investigación Biomédica Hospital Infantil Universitario Niño Jesús, Madrid, Spain, [3]Instituto de Investigación Sanitaria Hospital Universitario de La Princesa (IIS-Princesa), Madrid, Spain, [4]Department of Pediatric Hematology and Oncology, Hospital Infantil Universitario Niño Jesús, Madrid, Spain, [5]Hematopoietic Stem Cell Transplant Unit, Hospital Infantil Universitario Niño Jesús, Madrid, Spain

Introduction: Fanconi anemia (FA) is an inherited disorder characterized by bone marrow failure, congenital malformations, and predisposition to malignancies. Alterations in hematopoietic stem cells (HSC) have been reported, but little is known regarding the bone marrow (BM) stroma. Thus, the characterization of Mesenchymal Stromal Cells (MSC) would help to elucidate their involvement in the BM failure.

Methods: We characterized MSCs of 28 FA patients (FA-MSC) before and after treatment (hematopoietic stem cell transplantation, HSCT; or gene therapy, GT). Phenotypic and functional properties were analyzed and compared with MSCs expanded from 26 healthy donors (HD-MSCs). FA-MSCs were genetically characterized through, mitomycin C-test and chimerism analysis. Furthermore, RNA-seq profiling was used to identify dysregulated metabolic pathways.

Results: Overall, FA-MSC had the same phenotypic and functional characteristics as HD-MSC. Of note, MSC-GT had a lower clonogenic efficiency. These findings were not confirmed in the whole FA patients' cohort. Transcriptomic profiling identified dysregulation in HSC self-maintenance pathways in FA-MSC (HOX), and was confirmed by real-time quantitative polymerase chain reaction (RT-qPCR).

Discussion: Our study provides a comprehensive characterization of FA-MSCs, including for the first time MSC-GT and constitutes the largest series published to date. Interestingly, transcript profiling revealed dysregulation of metabolic pathways related to HSC self-maintenance. Taken together, our results or findings provide new insights into the pathophysiology of the disease, although whether these niche defects are involved in the hematopoietic defects seen of FA deserves further investigation.

KEYWORDS

mesenchymal stromal cells, bone marrow microenvironment, bone marrow failure, gene therapy, Fanconi anemia

1 Introduction

Fanconi anemia (FA) is a rare genetic disorder that results from DNA repair defects arising from pathogenic variants (PVs) in at least 22 genes (*FANCA*, *FANCB*, *FANCC*, *FANCD1/BRCA2*, *FANCD2*, *FANCE*, *FANCF*, *FANCG*, *FANCI*, *FANCJ/BRIP1*, *FANCL*, *FANCM*, *FANCN/PALB2*, *FANCO/RAD51C*, *FANCP/SLX4*, *FANCQ/ERCC4/XPF*, *FANCR/RAD51*, *FANCS/BRCA1*, FANCT/UBE2T, *FANCU/XRCC2*, *FANCV/REV7/MAD2L2*, and *FANCW/RFWD3*) discovered to play a role in the FA DNA repair pathway. All PVs in these genes are inherited in an autosomal recessive manner except those in *FANCB* and *FANCR/RAD51*, which are X-linked and autosomal dominant, respectively (Ceccaldi et al., 2016; Wegman-Ostrosky and Savage, 2017). Most patients with FA are characterized by bone marrow failure (BMF), somatic malformations, cancer predisposition and sensitivity to proinflammatory cytokines and alkylating agents (Svahn et al., 2016; Dufour and Pierri, 2022).

Mesenchymal stromal cells (MSCs) represent one of the key components of the bone marrow (BM) microenvironment, where they contribute to the creation of the hematopoietic stem cell (HSC) niche and play a crucial role in sustaining the development and differentiation of the hematopoietic system (Zhang et al., 2003). There is growing evidence suggesting that the microenvironment plays a role in several hematopoietic disorders, such as myeloproliferative and myelodysplastic neoplasms (Raaijmakers, 2012; Cogle et al., 2015; Li and Calvi, 2017; Curto-Garcia et al., 2020). However, the impact in the pathogenesis of BMF in FA remains unclear.

Few studies have described the role of the stroma in the hematological alterations of FA. It has been reported that the microenvironment could be involved in the pathogenesis of FA-related BMF in mice (Li et al., 2009). Also in mice, Zhou et al. have shown that MSCs have increased senescence, reduced proliferation and impaired differentiation, leading to skeletal alterations and a diminished ability to support hematopoiesis (Zhou et al., 2017). These data suggest that the pathogenesis of hematopoietic defects in FA is complex and likely depends, at least in part, on the interaction between abnormal hematopoietic cells and a dysfunctional niche. This hypothesis has only been analyzed in three studies with human samples. These studies described different alterations, some of them in a consistent manner, and others with controversial findings.

In this study we characterized BM-derived MSCs from pediatric patients affected by FA. We compared FA-MSCs with those expanded from healthy donors (HD-MSCs) to outline the differences that could elucidate the importance of the microenvironment on the exhaustion of HSC. Moreover, in patients that received a hematopoietic stem cell transplantation (HSCT) or gene therapy (GT), we studied MSCs before and after each treatment, in order to evaluate their potential impact on the BM niche.

2 Materials and methods

2.1 FA patients and healthy donors

Regarding inclusion criteria, pediatric patients with confirmed genetic diagnosis of FA assessed at the Hospital Infantil Universitario Niño Jesús between September 2018 and June 2021 could be included in the study. All patients with FA below 18 years that had undergone a bone marrow aspiration study to monitor their disease and had signed the informed consent were eligible for enrollment.

Some of the included patients did not receive treatment for bone marrow failure, while others were treated with HSCT or GT during their evolution. In those who received treatment, MSCs were isolated from BM aspirates obtained before and after treatment for the bone marrow failure.

As controls, we used MSCs isolated from HDs who underwent orthopedic surgery in which a bone marrow sample was obtained during the procedure.

This study was approved by the ethics committee of the Hospital Infantil Universitario Niño Jesus. Parents or legal guardians and HDs gave their written informed consent/assent.

2.2 Isolation and culture of BM-derived FA- and HD-MSCs

Mononuclear cells (MNCs) were isolated from BM aspirates (three to five mL) of FA patients and HDs by density gradient centrifugation and plated in non-coated 75–175 cm^2 tissue culture flasks at a density of 500,000/cm^2 in complete culture medium. MSCs were harvested, after reaching ≥80% confluence, using Trypsin, and were propagated at 5,000 cells/cm^2.

2.3 Characterization of *ex-vivo* expanded FA- and HD- MSCs

2.3.1 Immune-phenotype

Mesenchymal stromal cells were phenotypically characterized by flow-cytometry at P4 to evaluate the presence of the surface markers CD90, CD73 and CD29 and the absence of CD14, CD45 and CD19, using fluorescein isothiocyanate (FITC) or phycoerythrin (PE)-conjugated monoclonal antibodies (all from BioLegend and BD Biosciences). The sample was acquired on a FACSCanto II (BD) flow cytometer, and data were analyzed using the FACSDiva and Flowjo (BD) software.

2.3.2 Proliferative capacity

Cell growth was analyzed by direct cell counts and population doublings (PDs) were determined at each passage. The number of PDs was calculated for each MSC sample by using the formula $\log_{10}(N)/\log_{10}$ (Wegman-Ostrosky and Savage, 2017) where N represents cells harvested/cells seeded; results were expressed as cumulative PD from passage (P) 1 to P5 (Zuk et al., 2001).

2.3.3 Differentiation capacity

Adipogenic differentiation, osteogenic differentiation and the capacity to differentiate to cartilage tissue was evaluated as previously described (Mantelli et al., 2015). Differentiation was evaluated at P4–P6 by seeding MSCs at a density of 3.8×10^4 in p12 plates for 6–7 days until 90% confluence. At that time, the medium was changed to the specific differentiation medium. After 15 days of culture differentiation was evaluated through the specific

methodology in each case as reported in section 1.1 of the Supplementary Material.

2.3.4 Fibroblast colony-forming unit (CFU-F) ability

CFU-F formation was assessed by examining the cultures at day +15; the clonogenic efficiency was calculated as the number of colonies per 6×10^3MNCs initially seeded.

2.3.5 Senescence assay

FA-MSCs and HD-MSCs were maintained in culture until reaching replicative senescence. MSCs were closely monitored during senescence for up to 20 passages before interrupting the cultures, in order to identify any change in morphology and/or proliferation rate. Senescence of MSCs was assessed by staining with β-galactosidase. Furthermore, senescence was also characterized among the samples included in the RNA-seq analysis by evaluating the transcriptomic data sets for genes and pathways associated with senescence.

2.4 MSC-mediated support of long-term hematopoiesis

The capacity of FA-MSC to support normal hematopoiesis *in vitro* was assessed as follows. Early passage (P4–P6) MSCs were irradiated (25 Gy by a Cesium irradiator) and plated into a 96-well plate at a concentration of 3×10^4/well. One day later, $CD34^+$ cells obtained by immunomagnetic selection of mobilized hematopoietic progenitors from HDs, were plated onto the MSC feeder at a concentration of 1×10^4/well in the presence of Myelocult medium (StemCells Inc, Vancouver, BA, Canada) and 10^6 mol/L hydrocortisone. The cultures were incubated for 5 weeks at 37°C, 5% CO_2. Then, cultures were trypsinized and a classical methylcellulose assay was performed. The total number of colonies (colony-forming cells, CFCs) was scored after 14 days by an inverted microscope. Parallel experiments were performed using HD-MSCs as controls. Each experiment was performed in triplicates.

2.5 *In vitro* peripheral blood mononuclear cells (PBMNC) proliferation assay with phytohaemagglutinin

PBMNCs were obtained from peripheral blood samples from adult HDs. The proliferation of HD-PBMNCs in RPMI 1640 medium (Gibco, Life Technologies Ltd) supplemented with 10% FBS, in response to phytohaemagglutinin (PHA-P; Sigma-Aldrich), either in the presence or absence of MSCs, was performed in triplicate in flat-bottomed 96-well tissue culture plates (BD Falcon). Briefly, FA- and HD-MSCs were seeded at MSC:PBMNC ratios of 1:10 (10.000 MSC/100.000 PBMC) per well and allowed to adhere overnight before adding 1×10^5 PBMNCs per well with or without PHA (4 lg/mL). After a 5-day incubation, the supernatant was collected for analysis by flow cytometry using CFSE (carboxyfluorescein succinimidyl ester) labeling. Lymphocyte proliferation (without MSC and stimulated by PHA) was considered as 100% proliferation and this percentage was used as a reference value to normalize or correlate lymphocyte proliferation in the presence of MSC.

2.6 Genetic characterization of FA-MSCs

2.6.1 Mitomycin C (MMC) test

Due to the role of FA pathway proteins in DNA repair mechanisms, patient cells are extremely sensitive to DNA cross-linking agents such as MMC. MMC resistance testing was performed as previously described (González-Murillo et al., 2010; Diez et al., 2017). To assess this sensitivity, cells were exposed to increasing concentrations of MMC (0–333 nM; Sigma-Aldrich). The MSCs were seeded at a concentration of 5×10^3 cells/cm^2 in 24-well plates. 10–15 days afterwards cell viability was determined by flow cytometry with 7AAD.

2.6.2 Chimerism studies

The chimerism study was carried out on MSC of patients with FA who were transplanted, to confirm whether the origin of these cells came from the donor or the recipient. This analysis was performed on DNA extracted from a MSC population at passage P4-P7 to avoid contamination with hematopoietic cells that could remain residual in the culture. The chimerism study was performed by microsatellite analysis, Short Tandem Repeats (STR), by PCR and fragment analysis. To quantify the levels of chimerism in the samples, the DNA profiles of the donor and recipient were previously characterized.

2.7 RNA-seq studies

2.7.1 Ribonucleic acid preparation

For the study of the transcriptome, the cell fraction of the MSC cultures from P6-P8 was used. Total ribonucleic acid (RNA) from MSCs was extracted using Qiagen's RNeasy Mini Kit, according to the manufacturer's instructions. The total RNA that had a standard concentration of ≥200 ng/mL, mass ≥10 mg and RNA integrity number (RIN) ≥8.0 was subjected to RNA-Seq. Sequencing was performed at the Massive Sequencing Unit of the Madrid Science Park (NIMgenetics). The analysis was carried out by the Bioinformatics department of the Hospital Infantil Universitario Niño Jesús (section 1.2 of the Supplementary Material).

2.7.2 Validation of gene expression by real time quantitative polymerase chain reaction (RT-qPCR)

To validate the results, the expression levels of seven selected transcripts were determined by RT-qPCR with the housekeeping gene GAPDH and RNA 18S as an endogenous reference. Relative quantification of the gene expression was determined normalizing the data of the gene to GAPDH and RNA 18S housekeeping gene and using the $2^{-\Delta\Delta CT}$ method.

2.8 Statistical analysis

Quantitative variables were presented as the mean ± standard deviation (SD) or as the median ± range or interquartile range (IQR), as appropriate. All experiments were performed in triplicates.

TABLE 1 Patient characteristics. FA: Fanconi Anemia. HSCT: hematopoietic stem cell transplant. GT: Gene therapy. NA: not available.

	FA patients
N	28
Sex	
- Male, n (%)	13 (46.43)
- Female, n (%)	15 (53.57)
Age, years	
- At diagnosis, median (range)	4 (1–12)
- At treatment, median (range)	6 (2–14)
Diagnosis-treatment time	
- Years, median (range)	1 (0–6)
Complementation group	
- FANCA, n (%)	24 (85.71)
- FANCG, n (%)	3 (10.71)
- FANCD2, n (%)	1 (3.57)
Bone marrow failure severity	
- Severe, n (%)	3 (10.71)
- Moderate, n (%)	13 (46.42)
- Mild, n (%)	7 (25)
- NA, n (%)	5 (17.85)
Curative intent treatment for bone marrow failure	
- None, n (%)	7 (25)
- HSCT, n (%)	10 (35.71)
- GT, n (%)	11 (39.28)
Transfusion independent	
- Yes, n (%)	23 (82.14)
Patients alive	
- Yes, n (%)	27 (96.42)

The normal distribution was checked through the Saphiro-Wilk normality test. In cases where the samples did not demonstrate a normal distribution, comparisons were made using non-parametric tests. Thus, the Kruskal–Wallis's test was used to compare means of >2 groups, while the Mann-Whitney test was used to compare means of two groups. When the results of normality test allowed it, parametric tests such as t-student or ANOVA were used to compare means. For comparisons of repeated measures, the Wilcoxon test was used in the case of two comparison groups. On the contrary, the Friedman test was used to compare repeated measures of >2 study groups. p values lower than 0.05 were considered to be statistically significant ($^{*}p < 0.05$; $^{**}p < 0.01$; $^{***}p < 0.001$). Statistical analysis was performed using SPSS Statistical Software version 22 and Graph Pad Prism 5.0 (Graph Pad Software, CA, EEUU).

3 Results

3.1 Patients and characteristics of the series

Twenty-eight FA pediatric patients assessed at the Hospital Infantil Universitario Niño Jesús between September 2018 and June 2021 were included in the study.

The median age at diagnosis was 4 years (range 1–12) and the median age at treatment was 6 years (range 2–14). 46.43% of the patients were male and 53.57% female. Diagnosis was confirmed by molecular studies in all cases. The vast majority of patients belonged to the complementation group A (*FANCA* 85.71%). Table 1 details patient characteristics.

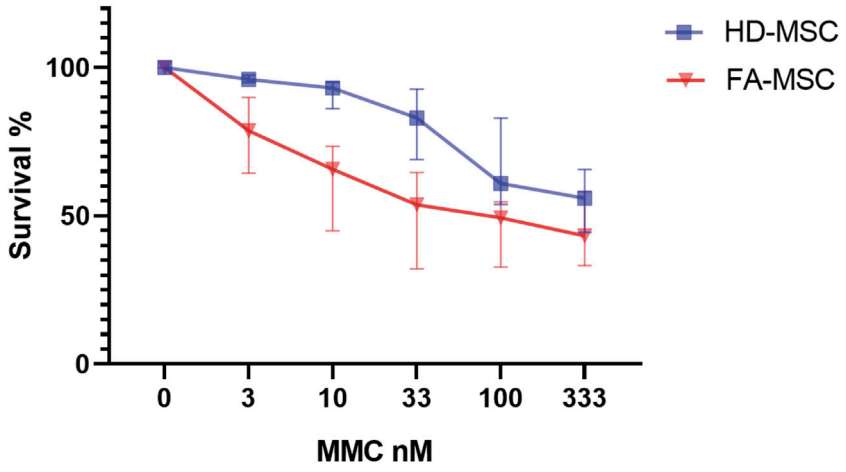

FIGURE 1
Mitomycin C (MMC) resistance testing. Cell viability and survival determined by flow cytometry with 7AAD at different MMC concentrations. Healthy donor's mesenchymal stromal cells (HD-MSCs), Fanconi Anemia MSCs (FA-MSC).

We analyzed samples from twenty-one patients that received either HSCT or GT as curative intention treatment. HSCT was performed in 10 patients and 11 were treated within the GT trials (NCT03157804, NCT04248439). Eight patients underwent a non-related human leucocyte antigen (HLA)- matched donor transplant, whereas the remaining two children received an haploidentical T cell-depleted family donor HSCT and a matched related donor HSCT (embryo selection), respectively. In addition, we also analyzed samples from seven patients not receiving any treatment.

When feasible, MSCs were isolated from BM aspirates before and after treatment. The paired sequence of the same patient with a sample both prior and after treatment was achieved in 10 patients. Seven of them were treated with GT and three underwent HSCT. Within the follow-up of the patients in the gene therapy trial, marrow samples were obtained at the following time-points according to the trial protocol: at 6 months (n: 10), at 1 year (n:8) and beyond 1 year (n:8) from the infusion. However, no more than one replicate from the same patient was included in the same analysis.

As controls, we used MSCs isolated from 26 HDs with a median age of 17 years (range 13–21). Their peripheral blood cell counts were reviewed, confirming normality of the cell blood counts in all the cases.

Therefore, the total number of samples included in the study was 64, corresponding to 26 healthy donors, 28 FA patients and 10 paired samples of 10 of the FA patients.

3.2 Characterization of BM-derived FA-MSCs

MSCs were successfully expanded in all samples. Both FA-MSCs and HD-MSCs displayed the characteristic spindle-shaped morphology. All of them met the criteria established by the International Society for Cellular Therapy (ISCT) consortium, demonstrating >95% positivity for positive markers, and <2% for negative markers. HD-MSCs and FA-MSC prior and after treatment presented similar differentiation capacity.

MSC survival assays to DNA cross-linking agents confirmed that FA-MSCs cells were significantly more sensitive to MMC than HD-MSCs ($p < 0.05$) (Figure 1, and Supplementary Table S1). When performing the sub-analysis of the samples according to the study subgroups no differences were observed in survival (Supplementary Table S2). MSC chimerism was analyzed in nine of the patients who had received HSCT, demonstrating that the cellularity was 100% of the receptor, thus confirming the autologous origin of the stroma.

In terms of proliferative capacity, there were no significant differences between FA-MSCs and HD-MSCs in early passages (Figure 2A, $p = 0.38$), nor among the different FA subgroups (Figure 2B, $p = 0.38$). Likewise, in seven paired samples of GT-MSC group no differences were observed before or after treatment (Supplementary Table S3). Interestingly, the same trend was confirmed in late cell culture passages where FA-MSCs presented a proliferative capacity similar to that of HD-MSCs (Supplementary Table S4). Thus, senescence was observed between P12-P19 for FA-MSC and between P11-P19 for HD-MSC (Supplementary Figure S1). These differences were not statistically significant ($p = 0.85$ in P19).

The clonogenic efficiency of FA-MSCs was comparable to that of HD-MSCs (6.45 vs. 8.35, $p = 0.23$). Of note, CFU-F ability of GT-MSCs was significantly lower than that of both HD- and FA-MSCs obtained at baseline or after HSCT (3.60 vs. 8.35 vs. 7.58 vs. 11.41, $p = 0.015$) (Figure 2C). Six paired samples from three patients undergoing gene therapy were then analyzed. The three post-treatment samples demonstrated a trend towards a reduced capacity to generate CFU-F compared to the pre-treatment samples (10.00 vs. 2.50) (Supplementary Table S5).

3.3 Ability of FA-MSCs to support long-term hematopoiesis

The capacity to support hematopoiesis was evaluated in 14 FA patients and 3 HDs at early passages. Our results showed that the CFC output of long-term culture-initiating cell (LTC-IC) assays did

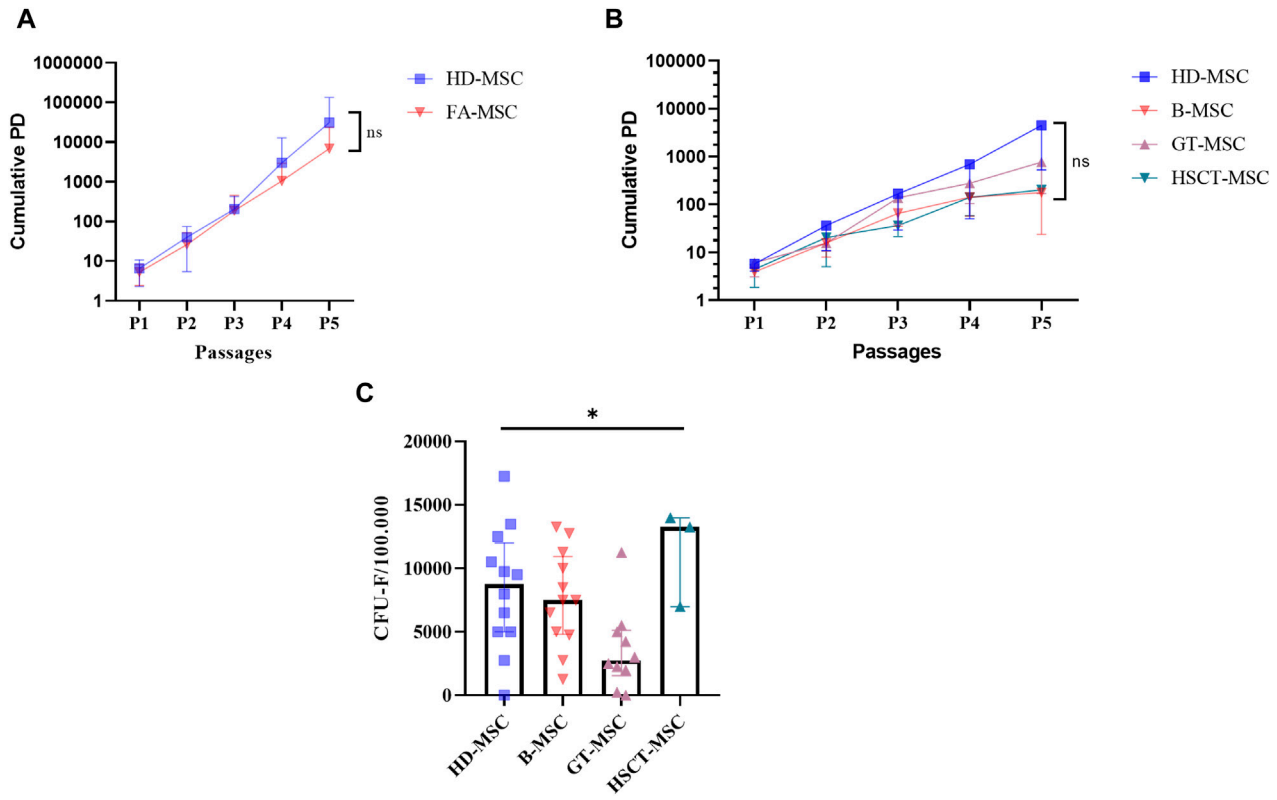

FIGURE 2
Proliferative capacity of mesenchymal stromal cells (MSCs). **(A)** Cumulative population doublings (PDs) from passage (P)1 to P5 of MSCs isolated from healthy donors (HDs) and from Fanconi Anemia (FA) patients. **(B)** Cumulative PDs from passage P1 to P5 of MSCs isolated from HDs and from FA patients divided into different subgroups: untreated or baseline-MSC (B-MSC), gene therapy-MSC (GT-MSC) and hematopoietic stem cell transplantation MSC (HSCT-MSC). **(C)** Fibroblast-colony forming unit (CFU-F) ability of FA-MSCs obtained before and after treatment (gene-therapy, GT-MSC or hematopoietic stem cell transplantation, HSCT-MSC) as compared with HD-MSCs.

not significantly differ between MSCs derived from HDs and those from FA patients (Figure 3A).

Nonetheless, the ability to maintain hematopoiesis was not equal when comparing the four study subgroups (HD-MSC, B-MSC, GT-MSC, and HSCT-MSC, $p = 0.016$) suggesting that the generation of CFC was lower in the GT-MSC group (Figure 3B and Supplementary Table S6). When analyzing four of the patients belonging to the GT group in a paired manner, the ability to support hematopoiesis did not seem to be determined by treatment, since CFC generation was similar before and after GT (6.35 vs. 6.88, respectively) (Supplementary Table S7).

3.4 Effect of FA-MSCs on PHA-induced PBMNC proliferation

We measured PBMNC proliferation induced by PHA either in the presence or in the absence of MSCs. 37 samples were analyzed: five of them corresponding to HD-MSC, 15 MSC from patients without treatment (B-MSC), and 17 MSC samples from patients treated for their BMF (11 GT-MSC and 6 HSCT-MSC).

FA-MSC exerted an inhibitory effect on PHA-induced PBMNC proliferation similar to HD-MSC in the 1:10 ratio, showing a median proliferation percentage of 27.65% (IQR 17.23–42.32) *versus* 26.19% (IQR 15.14–35.94), respectively ($p = 0.27$) (Figure 3C). Of note, HSCT-MSC showed a trend towards a greater residual proliferation in comparison to the other study groups, but this difference was not statistically significant (B-MSC 25.84% [IQR 16.82–39.30], GT-MSC 25.84% [IQR 16.82–39.30], and HSCT-MSC 42.23 [20.54–53.13], $p = 0.13$) (Figure 3D). Overall, these results indicate that MSCs isolated from the BM of FA patients have a similar immunomodulatory effect as MSCs from HDs, and that it is not significantly affected by treatment.

3.5 Transcriptomic profiling of FA patients (FANCA −/−) *versus* healthy donors MSCs

We compared the transcriptomic profiling of seven untreated FA-MSC samples and 3 HD-MSCs. All seven patients had a pathogenic variant in the *FANCA* gene.

RNA-seq expression profiling of FA-MSC *versus* HD-MSC segregated populations based on hierarchical clustering (Figure 4). Principal-component analysis revealed two differentiated groups, according to the FA pathway, three samples of healthy donors on the one hand, and the group of patients on the other.

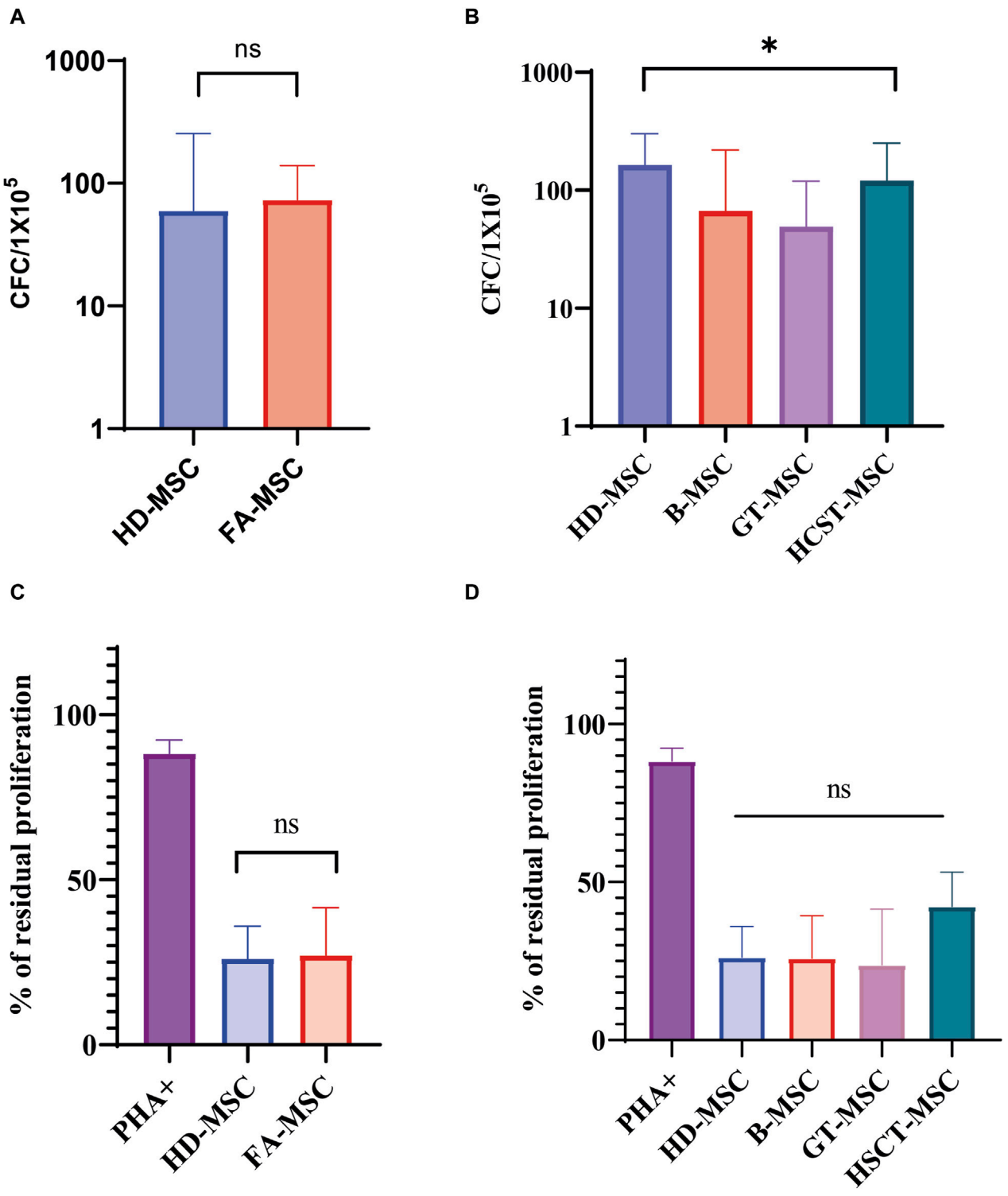

FIGURE 3
Functional characterization of mesenchymal stromal cells (MSCs). **(A)** Ability of Fanconi Anemia (FA) MSCs (FA-MSCs) and healthy donors MSC (HD-MSC) to support long-term hematopoiesis. Results are expressed as the median number of colony-forming-cells (CFCs) and represent the median of triplicate experiments. Ns: non-significant. **(B)** Ability to support long-term hematopoiesis of the different study subgroups: HD-MSCs, baseline or untreated FA patients (B-MSCs), and FA patients that received gene therapy (GT-MSCs) or hematopoietic stem cell transplant (HSCT-MSCs). Results are expressed as the median number of CFCs and represent the median of triplicate experiments. **(C)** *In vitro* immunomodulatory effect of HD-MSCs and FA-MSCs on peripheral blood mononuclear cells (PBMNCs) in an allogeneic setting. The graph shows the percentage of residual proliferation of PBMNCs stimulated with phytohaemagglutinin (PHA) in the presence of HD-MSCs or FA-MSCs. Each bar represents the percentage of residual proliferation of 10^5 PBMNCs, in the presence of MSC:PBMNC at a ratio of 1:10. **(D)** *In vitro* immunomodulatory effect of the different study subgroups on PBMCs in an allogeneic setting. The graph shows the percentage of residual proliferation of PBMCs stimulated with phytohaemagglutinin (PHA) in the presence of HD-MSCs, B-MSC, GT-MSC or HSCT-MSC. Each bar represents the percentage of residual proliferation of 10^5 PBMCs, in the presence of MSC:PBMC at a ratio of 1:10.

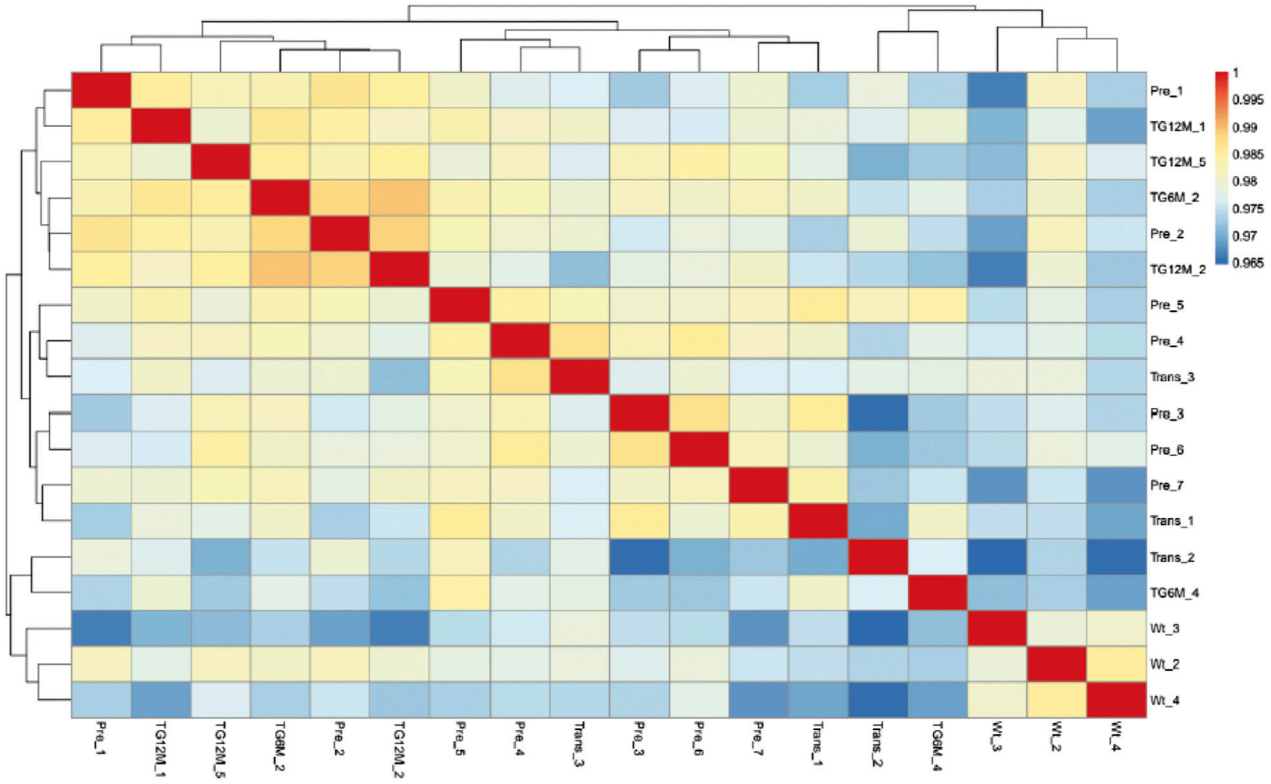

FIGURE 4
Transcript profiling of Fanconi Anemia (FA) patients *versus* healthy donors (HD) mesenchymal stromal cells (MSCs). Heat-map illustration of gene expression FA-MSCs from FA patients (n = 7) and HD-MSCs (n = 3).

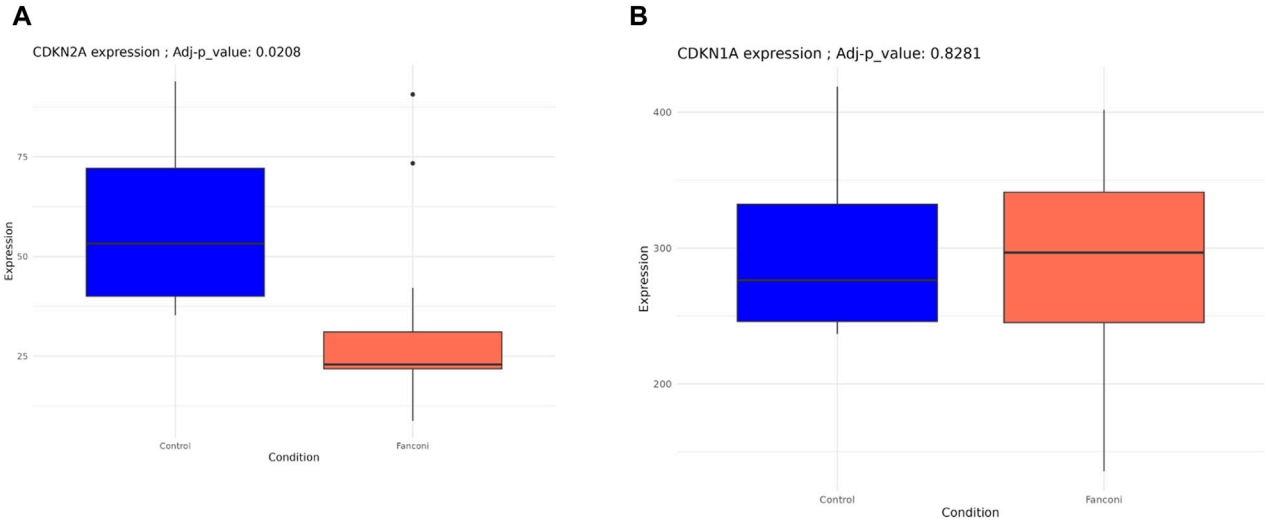

FIGURE 5
Transcript profiling of senescence-associated pathways from FA-MSCs (n = 7) and HD-MSCs (n = 3). **(A)** CDKN2A/p16 gene expression FA-MSCs from FA patients (n = 7) and HD- MSC (n = 3). **(B)** CDKN1A/p21 gene expression FA-MSCs from FA patients (n = 7) and HD- MSC (n = 3).

To evaluate whether the exhaustion of HSCs is related to the chronic activation of stress signaling pathways and to conclude about its effect in cell-aging or senescence process, we conducted a targeted analysis to evaluate some of the master regulators of senescence, as well as senescence-associated secretory phenotype (SASP). Among these senescence hallmarks, only CDKN2A/

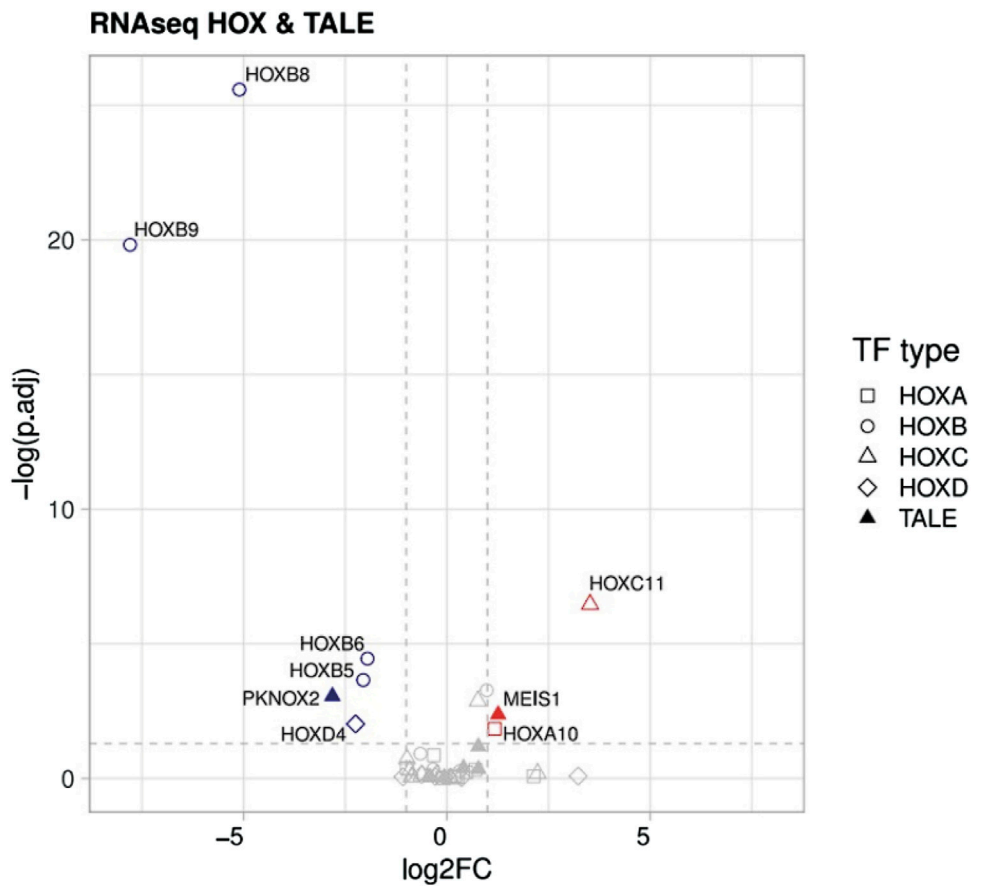

FIGURE 6
Transcriptomic studies. Differences between downregulated vs. upregulated pathways in HOX and TALE members.

p16 differed significantly between FA-MSC and HD-MSC, so that HD-MSCs showed an overexpression CDKN2A/p16 (p 0.02, Figure 5A). However, FA-MSCs showed a trend to a higher repression in pathways such as CDKN1A/p21 (Figure 5B) or SASP complex (IL6, IL1-α, IGF-BP3), without reaching statistical significance in any of the cases.

Besides, as it is known that MSC-derived secretomes contribute to activating an inflammatory transcriptome, we also evaluated other pathways related to inflammation. Indeed, no significant dysregulations were observed between groups regarding other inflammation-related pathways such as NF-KB, SMAD2/3, TGF-β or TNF-α.

Finally, we performed a targeted analysis to investigate the expression of HOX and TALE transcription factors as noted by a previous group in the FA-MSC setting. (Cagnan et al., 2019). It is worth mentioning that our analysis identified repression of *HOXB 5-6-eight to nine* and *HOXD4*, with overexpression of *HOXA10* and *HOXC11* (Figure 6). Moreover, due to the fact that the HOX pathway is one of the driving mechanisms of cancer development such as leukemia we evaluated the genes related to its evolution. However, no alterations were identified in FA-MSC in the genes related to myelodysplasia/acute leukemia.

Validation of the sequencing results by RT-qPCR. To confirm the reliability of the expression profiles generated using the RNA-Seq and DEGs analysis, RT-qPCR was applied in seven up/downregulated candidate genes (*HOXC 11, HOXA 10, HOXD 4, HOXB 5, HOXB 6, HOXB 8*, and *HOXB 9*). As expected, the RT-qPCR results matched the RNA-seq results in the majority, except in *HOXA 10* gene, in which its overexpression was not confirmed in more than half of the samples.

4 Discussion

Despite the genetic heterogeneity of patients with FA, many of them share a common phenotype characterized by the development of BMF. It is estimated that the risk of BMF is 50% at the age of 40, and in 75% of the cases it occurs during the first decade of life (Alter, 2014; Alter et al., 2022). Thus, most of the therapies for these patients are focused on treating BMF.

Nonetheless, the pathophysiology of the exhaustion of HSCs remains unclear. There is increasing evidence suggesting a potential role of the microenvironment as a contributing component in other hematopoietic disorders (Cogle et al., 2015; Curto-Garcia et al., 2020). In the present study, we expanded *ex vivo* MSCs derived from BM of children with FA, both before and after receiving treatment and compared with those obtained from HDs, in order to address whether the niche plays a role in the BMF of these patients.

Prior to our study, the first group that explored the involvement of the niche in the BMF of human FA patients included only samples

from untreated subjects. They found functional deficits in MSC after long-term cultures, concluding that FA-MSC could be involved in the development of BMF (Lecourt et al., 2010). Later, Mantelli et al. expanded this information with the characterization of FA-MSC of patients treated with HSCT (Mantelli et al., 2015). They pointed out that FA-MSC were defective in their ability to proliferate, but they maintained their functionality as HD-MSC. Hence, they could not conclude that these phenotypic defects impacted on the pathophysiology of BMF. To the best of our knowledge, the present work is the largest series published to date with MSCs from FA patients. Furthermore, we characterized the stroma of patients treated with GT for the first time, not only in FA but also in other monogenic diseases where gene therapy is being used.

Our data showed that FA-MSCs exhibit similar morphology, immunophenotype and differentiation potential to HD-MSCs as in the previous studies (Lecourt et al., 2010; Mantelli et al., 2015).

MMC survival assays demonstrated that FA-MSCs cells were significantly more sensitive to DNA cross-linking agents in comparison to HD-MSCs confirming that the FA pathway is not functional in stromal cells either. Moreover, according to other groups, when comparing MSCs after transplant we confirmed the autologous origin of the stroma. In HSCT recipients, MSCs remain of recipient origin, indicating that these cells are not fully eradicated by a non-myeloablative conditioning.

In accordance with Mantelli et al, the proliferative capacity of FA-MSCs obtained before treatment was comparable to that of HD-MSCs. However, in contrast to what was observed by Mantelli`s group, in our study FA-MSC obtained after HSCT did not display a significantly lower proliferative capacity compared to HD-MSCs. As we will discuss later on, the time of collection of the samples after transplant could influence these results.

When evaluating the proliferative capacity at high passages of cell cultures (P5-P19) and the *in vitro* life-span of FA-MSCs, we found that these cells obtained before and after HSCT or GT did not develop signs of senescence earlier than HD-MSCs, as opposed to the previously reported data (Lecourt et al., 2010; Mantelli et al., 2015). This difference may be due to the duration of the cultures, since Lecourt et al. reported a median culture time of 11–12 weeks, Mantelli et al. pointed out a duration between 8 and 12 weeks, and in our series the majority were between 7 and 8 weeks.

Regarding clonogenic efficiency, in line with previously reported data, we did not find any major differences in fibroblast colony-forming unit ability between B-MSC and HD-MSC. However, in contrast to what was observed by Mantelli et al(Mantelli et al., 2015), in our series FA-MSC obtained after HSCT did not display a significantly lower clonogenic efficiency compared to HD-MSCs. They suggested that the differences they observed might indicate either an intrinsic defect of FA-MSCs or a toxic effect of the conditioning regimens (Mantelli et al., 2015). In our opinion, the disparity of our results in this respect, and those related to the early proliferative capacity, compared to those of Mantelli´s can be explained by the time elapsed from the treatment to the obtaining of the sample for the clonogenic efficiency analysis. Mantelli's group evaluates the cohort of post-HSCT samples 100 days after treatment, whereas in our series the median time was greater than 12 months. It has been previously described that these differences in the time of collection of the samples could be critical in order to interpret the results. Ding et al, showed that the amount of MSC was drastically reduced in the early phase after HSCT and returned to a normal level 9 months after transplantation. Thus, the number of CFU-F increases in a time-dependent manner from the first month and reaches approximately 90% in the ninth month after HSCT (Ding et al., 2014). Also of note was our observation that the MSCs obtained after GT showed a trend to a lower clonogenic capacity. Nevertheless, the limited number of samples prevents us from clearly concluding on its functional inferiority.

It is worth to note that, the subgroup of MSC-GT showed a tendency to generate less CFU-F than the other subgroups. However, these data should be evaluated with caution due to the scarce number of samples. Moreover, the abscense of this type of studies in the GT setting does not allow us to support our results with the experience of other groups.

On the question of whether there were differences in the functionality of the MSCs, in line with previously reported data, we did not find any major differences in the ability to support long-term hematopoiesis between FA-MSCs and HD-MSCs, suggesting that FA- MSCs do not display, *in vitro* and at early passages, an impaired capacity to sustain the proliferation and expansion of HD-HSCs (Mantelli et al., 2015). We also investigated the ability of FA-MSC to inhibit *in vitro* mitogen-induced PBMNC proliferation, both before and after treatment, not observing statistically significant differences between groups. In summary, in accordance with Mantelli et al's work, these data indicate that the main functions of the MSCs are globally preserved in FA patients (Mantelli et al., 2015).

In addition, we performed a thorough analysis of molecular pathways related to different processes in the niche. Bone marrow failure in FA is multifactorial and largely results from the death of HSCs due to genomic instability. Following DNA damage, proteins of the FA pathway act in a complex cascade to repair interstrand crosslinks, which are caused by reactive oxygen species or exposure to reactive aldehydes. Moreover, the elevation of inflammatory markers and hypersusceptibility to proinflammatory cytokines that induce cell death is a phenotype associated with FA gene mutations. In this respect, Oppezzo et al demonstrated the association between bone marrow failure and the constitutive expression of Microphthalmia Transcription Factor (MiTF) in mouse FA HSCs, through the cooperative, unscheduled activation of several stress-signaling pathways, including the SMAD2/3, p38 MAPK, NF-κB, and AKT cascades (Oppezzo et al., 2020). A growing amount of evidence has demonstrated that the activation of these pathways leads to a state of quiescence in HSCs, and therefore to the accumulation of DNA damage and a reduction in their repopulation capacity (De Haan and Lazare, 2018; Di Micco et al., 2021). This supports the hypothesis that the exhaustion of HSCs in FA is the consequence of defects in the response to DNA damage combined with the chronic activation of stress signaling pathways that in a normal situation should be activated only transiently.

However, as the mentioned studies reflect, this inflammatory background in FA has been previously studied in HSCs, hence the impact of the niche is still not clear. We studied pathways related to inflammation in our MSC samples, such as NF-κB, SMAD 2/3, IL-6, TGF-β or TNF-α, and have not found dysregulation in any of them.

Therefore, this suggests that the constitutive expression is intrinsic to the HSCs but not to the stroma cells.

As demonstrated by others, inflammation is tightly related to cellular aging or senescence. Even though the processes behind MSC senescence remain unclear, several studies have made progress in elucidating the aspects of the age-related changes (Weng et al., 2022). Stenderup et al found out that MSCs from older donors exhibited accelerated senescense comparing with MSCs from younger donors (aged 18–29 years *versus* aged 68–81 years) (Stenderup et al., 2003). Unfortunately, no similar studies have been published with pediatric cohorts to our knowledge.

When we expanded the characterization of MSC senescence in our samples by reviewing several hallmarks or master regulators of a senescent phenotype, CDKN2A/p16 was the only one that was differentially expressed among the two study groups, showing an overexpression in HD-MSCs. This finding suggests that MSCs from our FA patients are less senescent than the HD-MSCs included in the study. Nevertheless, we did not observe differences in other genes or pathways such as CDKN1A/p21 or senescense-associated secretory phenotype (SASP) complex, nor in long-term cultures or in β-galactosidase staining assay either, suggesting that there are no major differences in the cellular ageing between both groups.

Finally, we performed a targeted analysis to investigate the expression of HOX and TALE transcription factors in FA-MSC. It is thought that these are important regulators of development and homeostasis, determining cellular identity and predisposing to cancer progression if dysregulated (Cagnan et al., 2019). Cagnan et al, compared the expression levels of those genes in bone marrow MSCs obtained from FA patients and HDs. In general, they observed highly conserved expression levels between patient and donor cells, except in PKNOX2 which was downregulated. In contrast, our transcriptomic studies did not find differences in PKNOX2 expression between FA-MSC patients and HDs. Conversely, we found differences among several HOX members, which were not observed by Cagnan et al. (Cagnan et al., 2019) Nevertheless, methodological differences should be kept in mind. It would be intringuing to compare expression changes of these genes upon cell passing, since Cagnan et al used MSCs at the third culture passage to analyze the differential expression whereas we used MSCs at passage six.

It is worth mentioning that our study has several limitations. First, age was not homogeneous between the two main study groups (FA-MSC and HD-MSC). The median age in HD was significantly higher since usually the patients that undergo orthopedic surgery are teenagers, whereas the diagnose of FA is usually made before age 10 years. Despite this, we decided to use this population as a control group, given the difficulty of accessing BM samples from younger HD. In our opinion, the age difference between both groups should not affect the phenotype and functionality of the MSCs in a pediatric cohort. For instance, in the senescence studies, we found no major differences between both groups, although differences had been previously reported related with age (Stenderup et al., 2003). However, the age range between both cohorts of that study (18–21 *versus* 68–81) is much wider than the difference between the patients and HDs included in ours, which together with the fact that no other data were found analyzing samples from pediatric patients in this or other diseases, does not allow us to establish an age threshold related to the MSC features.

Second, the absence of similar studies in GT settings makes the interpretation of some of the particularities of that MSC subgroup more challenging. Third, transcriptomic studies have been carried out on a small number of samples. In fact, samples from treated patients were not included. However, these results must be evaluated considering the scenario of a pediatric rare disease in which obtaining a sufficient sample for several studies is not always feasible.

In conclusion, our study provides a comprehensive characterization of BM-derived MSCs obtained from FA patients, including for the first time MSCs from patients treated with gene therapy. Our findings suggest that FA-MSCs maintain their main functional properties, making their direct implication in BMF development less likely. Interestingly, a suppressed metabolic pathway has been identified in FA-MSC (HOX). In this sense, more studies will be needed to further explore the possible involvement of the niche in the evolution of bone marrow failure of FA patients.

Data availability statement

The data presented in the study are deposited in a public repository: https://www.ncbi.nlm.nih.gov/bioproject/1114677. Submission ID: SUB14594881, BioProject ID: PRJNA1114677.

Ethics statement

The studies involving humans were approved by ethics committee of the Niño Jesús University Children's Hospital, with the following board members: Mª Ángeles García Teresa, president, Eva Escribano Ceruelo, vice president, Hospital Infantil Universitario Niño Jesús Maitane Andión Catalán, secretary, Hospital Infantil Universitario Niño Jesús, and 14 other committee members. The studies were conducted in accordance with the local legislation and institutional requirements. Written informed consent for participation in this study was provided by the participants' legal guardians/next of kin.

Author contributions

JZ: Conceptualization, Data curation, Formal Analysis, Funding acquisition, Investigation, Methodology, Project administration, Resources, Validation, Writing–original draft, Writing–review and editing. MI: Data curation, Investigation, Methodology, Writing–review and editing. JGM: Software, Writing–review and editing. RM-V: Software, Writing–review and editing. LA: Investigation, Writing–review and editing. JI: Writing–review and editing. LG-G: Investigation, Methodology, Writing–review and editing. JGP: Writing–review and editing. EG: Writing–review and editing. ES: Writing–review and editing. MR: Writing–review and editing. LM: Writing–review and editing. MAD: Writing–review and editing. AG-M: Supervision, Writing–review and editing. JS: Supervision, Writing–review and editing.

Funding

The author(s) declare that financial support was received for the research, authorship, and/or publication of this article. This work was funded by the Spanish Society of Hematology and Hemotherapy and the Carlos III Health Institute of the Ministry of Science and Innovation of the Spanish government, and co-funded by the European Union (projects PI19/00782, PI22/00603 and AC20/00066).

Acknowledgments

The authors thank the Fundación para la Investigation Biomédica del Hospital Infantil Universitario Niño Jesús. The authors are also indebted to the patients with FA, their families, and clinicians from the Fundación Anemia de Fanconi.

Conflict of interest

JS reports financial support outside the submitted work for educational lectures by Novartis, Miltenyi, and Amgen; advisory board member for Rocket Pharma, Novartis, Sobi, Agios, and Amgen. JZ reports financial support outside the submitted work for educational lectures by Novartis.

The remaining authors declare that the research was conducted in the absence of any commercial or financial relationships that could be construed as a potential conflict of interest.

Publisher's note

Supplementary material

The Supplementary Material for this article can be found online at: https://www.frontiersin.org/articles/10.3389/fcell.2024.1286815/full#supplementary-material

References

Alter, B. P. (2014). Fanconi anemia and the development of leukemia. *Best. Pract. Res. Clin. Haematol.* 27 (3–4), 214–221. doi:10.1016/j.beha.2014.10.002

Alter, B. P., Giri, N., McReynolds, L. J., and Altintas, B. (2022). Fanconi anaemia: a syndrome with distinct subgroups. *Br. J. Haematol.* 197 (4), 467–474. doi:10.1111/bjh.18091

Cagnan, I., Cosgun, E., Konu, O., Uckan, D., and Gunel-Ozcan, A. (2019). PKNOX2 expression and regulation in the bone marrow mesenchymal stem cells of Fanconi anemia patients and healthy donors. *Mol. Biol. Rep.* 46 (1), 669–678. doi:10.1007/s11033-018-4522-z

Ceccaldi, R., Sarangi, P., and D'Andrea, A. D. (2016). The Fanconi anaemia pathway: new players and new functions. *Nat. Rev. Mol. Cell. Biol.* 17 (6), 337–349. doi:10.1038/nrm.2016.48

Cogle, C. R., Saki, N., Khodadi, E., Li, J., Shahjahani, M., and Azizidoost, S. (2015). Bone marrow niche in the myelodysplastic syndromes. *Leuk. Res.* 39 (10), 1020–1027. doi:10.1016/j.leukres.2015.06.017

Curto-Garcia, N., Harrison, C., and McLornan, D. P. (2020). Bone marrow niche dysregulation in myeloproliferative neoplasms. *Haematologica* 105 (5), 1189–1200. doi:10.3324/haematol.2019.243121

De Haan, G., and Lazare, S. S. (2018). Aging of hematopoietic stem cells. *Blood* 131 (5), 479–487. doi:10.1182/blood-2017-06-746412

Diez, B., Genovese, P., Roman-Rodriguez, F. J., Alvarez, L., Schiroli, G., Ugalde, L., et al. (2017). Therapeutic gene editing in CD34(+) hematopoietic progenitors from Fanconi anemia patients. *EMBO Mol. Med.* 9 (11), 1574–1588. doi:10.15252/emmm.201707540

Di Micco, R., Krizhanovsky, V., Baker, D., and d'Adda Di Fagagna, F. (2021). Cellular senescence in ageing: from mechanisms to therapeutic opportunities. *Nat. Rev. Mol. Cell. Biol.* 22 (2), 75–95. doi:10.1038/s41580-020-00314-w

Ding, L., Zhu, H., Yang, Y., Wang, Z. D., Zheng, X. L., Yan, H. M., et al. (2014). Functional mesenchymal stem cells remain present in bone marrow microenvironment of patients with leukemia post-allogeneic hematopoietic stem cell transplant. *Leuk. Lymphoma* 55 (7), 1635–1644. doi:10.3109/10428194.2013.858815

Dufour, C., and Pierri, F. (2022). Modern management of Fanconi anemia. *Hematol. Am. Soc. Hematol. Educ. Program* 2022 (1), 649–657. doi:10.1182/hematology.2022000393

González-Murillo, Á., Lozano, M. L., Álvarez, L., Jacome, A., Almarza, E., Navarro, S., et al. (2010). Development of lentiviral vectors with optimized transcriptional activity for the gene therapy of patients with Fanconi anemia. *Hum. Gene Ther.* 21 (5), 623–630. doi:10.1089/hum.2009.141

Lecourt, S., Vanneaux, V., Leblanc, T., Leroux, G., Ternaux, B., Benbunan, M., et al. (2010). Bone marrow microenvironment in Fanconi anemia: a prospective functional study in a cohort of Fanconi anemia patients. *Stem Cells Dev.* 19 (2), 203–208. doi:10.1089/scd.2009.0062

Li, A. J., and Calvi, L. M. (2017). The microenvironment in myelodysplastic syndromes: niche-mediated disease initiation and progression. *Exp. Hematol.* 55, 3–18. doi:10.1016/j.exphem.2017.08.003

Li, Y., Chen, S., Yuan, J., Yang, Y., Li, J., Ma, J., et al. (2009). Mesenchymal stem/progenitor cells promote the reconstitution of exogenous hematopoietic stem cells in Fancg−/− mice *in vivo*. *Blood* 113 (10), 2342–2351. doi:10.1182/blood-2008-07-168138

Mantelli, M., Avanzini, M. A., Rosti, V., Ingo, D. M., Conforti, A., Novara, F., et al. (2015). Comprehensive characterization of mesenchymal stromal cells from patients with Fanconi anaemia. *Br. J. Haematol.* 170 (6), 826–836. doi:10.1111/bjh.13504

Oppezzo, A., Bourseguin, J., Renaud, E., Pawlikowska, P., and Rosselli, F. (2020). Microphthalmia transcription factor expression contributes to bone marrow failure in Fanconi anemia. *J. Clin. Investig.* 130 (3), 1377–1391. doi:10.1172/JCI131540

Raaijmakers, MHGP (2012). Myelodysplastic syndromes: revisiting the role of the bone marrow microenvironment in disease pathogenesis. *Int. J. Hematol.* 95 (1), 17–25. doi:10.1007/s12185-011-1001-x

Stenderup, K., Justesen, J., Clausen, C., and Kassem, M. (2003). Aging is associated with decreased maximal life span and accelerated senescence of bone marrow stromal cells. *Bone* 33 (6), 919–926. doi:10.1016/j.bone.2003.07.005

Svahn, J., Bagnasco, F., Cappelli, E., Onofrillo, D., Caruso, S., Corsolini, F., et al. (2016). Somatic, hematologic phenotype, long-term outcome, and effect of hematopoietic stem cell transplantation. An analysis of 97 Fanconi anemia patients from the Italian national database on behalf of the Marrow Failure Study Group of the AIEOP (Italian Association of Pediatric Hematology-Oncology). *Am. J. Hematol.* 91 (7), 666–671. doi:10.1002/ajh.24373

Wegman-Ostrosky, T., and Savage, S. A. (2017). The genomics of inherited bone marrow failure: from mechanism to the clinic. *Br. J. Haematol.* 177 (4), 526–542. doi:10.1111/bjh.14535

Weng, Z., Wang, Y., Ouchi, T., Liu, H., Qiao, X., Wu, C., et al. (2022). Mesenchymal stem/stromal cell senescence: hallmarks, mechanisms, and combating strategies. *Stem Cells Transl. Med.* 11 (4), 356–371. doi:10.1093/stcltm/szac004

Zhang, J., Niu, C., Ye, L., Huang, H., He, X., Tong, W. G., et al. (2003). Identification of the haematopoietic stem cell niche and control of the niche size. *Nature* 425 (6960), 836–841. doi:10.1038/nature02041

Zhou, Y., He, Y., Xing, W., Zhang, P., Shi, H., Chen, S., et al. (2017). An abnormal bone marrow microenvironment contributes to hematopoietic dysfunction in Fanconi anemia. *Haematologica* 102 (6), 1017–1027. doi:10.3324/haematol.2016.158717

Zuk, P. A., Zhu, M., Mizuno, H., Huang, J., Futrell, J. W., Katz, A. J., et al. (2001). Multilineage cells from human adipose tissue: implications for cell-based therapies. *Tissue Eng.* 7 (2), 211–228. doi:10.1089/107632701300062859

frontiers | Frontiers in Cell and Developmental Biology

TYPE Review
PUBLISHED 26 July 2024
DOI 10.3389/fcell.2024.1400347

OPEN ACCESS

EDITED BY
Keiya Ozawa,
Jichi Medical University, Japan

REVIEWED BY
Xiaolei Li,
University of Pennsylvania, United States
Takeo Mukai,
The University of Tokyo, Japan

*CORRESPONDENCE
Urban Švajger,
urban.svajger@ztm.si

RECEIVED 13 March 2024
ACCEPTED 15 July 2024
PUBLISHED 26 July 2024

CITATION
Česnik AB and Švajger U (2024), The issue of heterogeneity of MSC-based advanced therapy medicinal products–a review.
Front. Cell Dev. Biol. 12:1400347.
doi: 10.3389/fcell.2024.1400347

The issue of heterogeneity of MSC-based advanced therapy medicinal products–a review

Ana Bajc Česnik[1] and Urban Švajger[1,2]*

[1]Slovenian Institute for Transfusion Medicine, Department for Therapeutic Services, Ljubljana, Slovenia, [2]Faculty of Pharmacy, University of Ljubljana, Ljubljana, Slovenia

Mesenchymal stromal stem cells (MSCs) possess a remarkable potential for numerous clinical applications due to their unique properties including self-renewal, immunomodulation, paracrine actions and multilineage differentiation. However, the translation of MSC-based Advanced Therapy Medicinal Products (ATMPs) into the clinic has frequently met with inconsistent outcomes. One of the suspected reasons for this issue is the inherent and extensive variability that exists among such ATMPs, which makes the interpretation of their clinical efficacy difficult to assess, as well as to compare the results of various studies. This variability stems from numerous reasons including differences in tissue sources, donor attributes, variances in manufacturing protocols, as well as modes of administration. MSCs can be isolated from various tissues including bone marrow, umbilical cord, adipose tissue and others, each with its unique phenotypic and functional characteristics. While MSCs from different sources do share common features, they also exhibit distinct gene expression profiles and functional properites. Donor-specific factors such as age, sex, body mass index, and underlying health conditions can influence MSC phenotype, morphology, differentiation potential and function. Moreover, variations in preparation of MSC products introduces additional heterogeneity as a result of cell culture media composition, presence or absence of added growth factors, use of different serum supplements and culturing techniques. Once MSC products are formulated, storage protocols play a pivotal role in its efficacy. Factors that affect cell viability include cell concentration, delivery solution and importantly, post-thawing protocols where applicable. Ensuing, differences in administration protocols can critically affect the distribution and functionallity of administered cells. As MSC-based therapies continue to advance through numerous clinical trials, implication of strategies to reduce product heterogeneity is imperative. Central to addressing these challenges is the need for precise prediction of clinical responses, which require well-defined MSC populations and harmonized assessment of their specific functions. By addressing these issues by meaningful approaches, such as, e.g., MSC pooling, the field can overcome barriers to advance towards more consistent and effective MSC-based therapies.

KEYWORDS

mesenchymal stromal (stem) cell, heterogeneity, pooling, equipotency, advanced therapy medicinal product (ATMP), cell therapy

1 Introduction

Mesenchymal stromal cells (MSCs) are a heterogeneous population of somatic stem cells with a capacity for self-renewal, multilineage differentiation, and immunomodulation (Figure 1). They are considered a promising therapeutic tool to control aberrant inflammatory responses and assist in regenerative medicine applications as Advanced Therapy Medicinal Products (ATMPs) (Cheung et al., 2020; Maldonado et al., 2023). Very briefly, according to EU legislation and classification, ATMPs are defined as medicines for human use that are based on genes, tissues or cells. The have been classified into three main types, namely, gene therapy medicinces, somatic-cell therapy medicines and tissue-engineered medicines. According to this classification, MSC-based ATMPs are somatic-cell therapy medicines, and their therapeutic use has been studied for a broad range of diseases. Some of the conditions proposed to benefit from MSC treatment are graft-versus-host-disease (GvHD) (Kelly and Rasko, 2021; Kadri et al., 2023), Crohn's disease (Wang et al., 2023), critical limb ischemia (Lozano Navarro et al., 2022), osteoarthritis (Thoene et al., 2023), type 1 diabetes (Koehler et al., 2022), type 2 diabetes (Gao et al., 2022), endometrial injury (Cen et al., 2022), multiple sclerosis (Liu et al., 2022), lupus (Li et al., 2013), cardiovascular diseases (Mabotuwana et al., 2022), liver disorders (Han et al., 2022), respiratory disorders (Raza and Khan, 2022), spinal cord injury (Montoto-Meijide et al., 2023), kidney failure (Morello et al., 2022), skin diseases (Chang et al., 2021; Lwin et al., 2021), Alzheimer's disease (Regmi et al., 2022), and Parkinson's disease (Kouchakian et al., 2021). Administration of MSCs continuously proves to be safe with very little evidence of serious adverse events such as infusion-related toxicity, infection, malignancy and development of thrombotic or thrombo-embolic events (Thompson et al., 2020; Wang Y. et al., 2021), athough exceptions have been observed (Veceric-Haler et al., 2022).

A plethora of investigations involving MSC products shows their preclinical and early clinical efficacy can be inconsistent and remains frequently unconfirmed in late-phase trials. It can also be challenging to anticipate, as most of the *in vitro* assays have failed to reproducibly and reliably predict the clinical potency of transplanted MSCs (Krampera and Le Blanc, 2021). At least in part, the inconsistencies of these outcomes could be attributed to the heterogeneity of transplanted MSC batches. The first important step toward greater harmonization was made in 2006, when basic criteria for MSC characterization have been proposed by the International Society for Cell and Gene Therapy (ISCT), and are as follows:

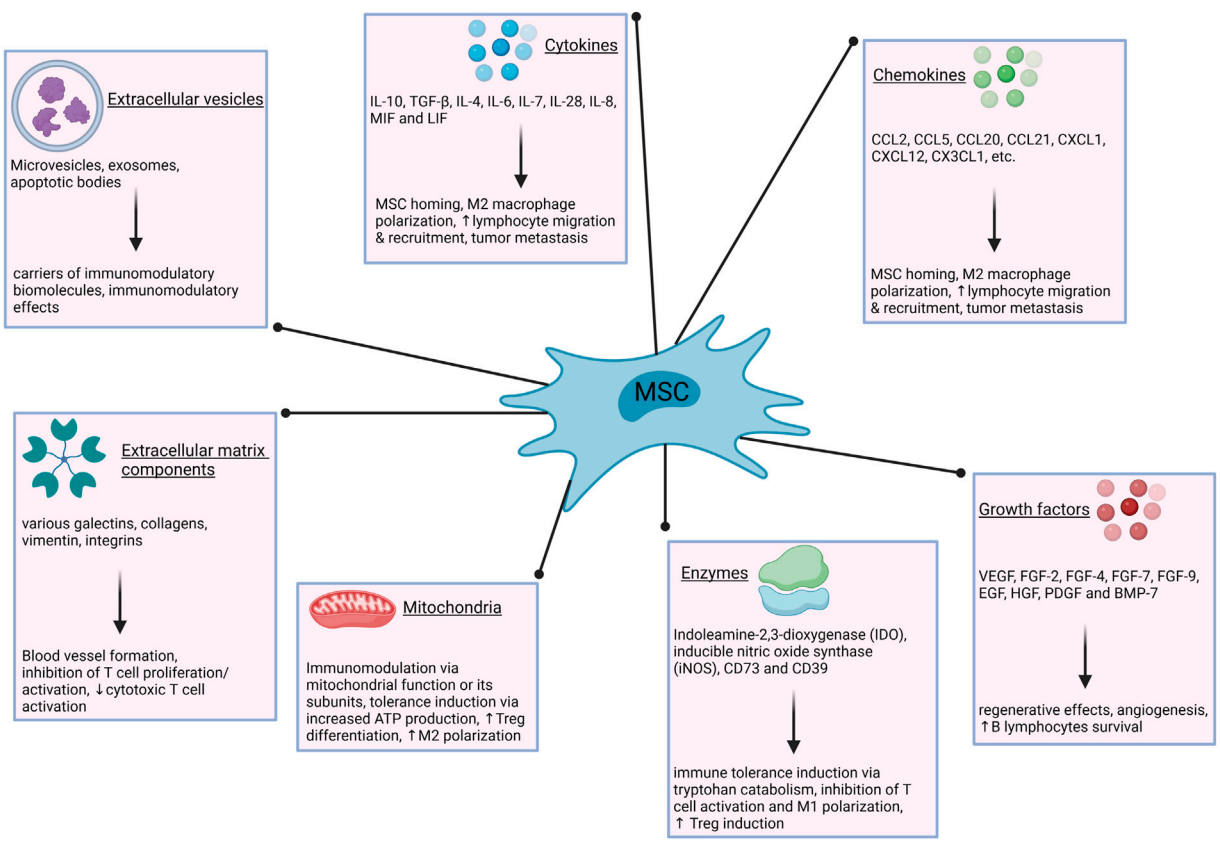

FIGURE 1
Immunomodulatory mechanisms of MSCs. The modulation of immune responses by MSCs is exerted via numerous secreted factors and entities, such as cytokines, growth factors, extracellular vesicles and others. ATP–adenosine triphosphate; BMP–bone morphogenetic protein; CCL–chemokine (C-C motif) ligand; CX3CL–chemokine (C-X3-C motif) ligand; CXCL–chemokine (C-X-C motif) ligand; EGF–epidermal growth factor; FGF–fibroblast growth factor; HGF–hepatocyte growth factor; IL–interleukin; LIF–leukemia inhibitory factor; M1–type one macrophages; M2–type two macrophages; MIF–macrophage migration inhibitory factor; PDGF–platelet derived growth factor; TGF–transforming growth factor; VEGF–vascular endothelial growth factor.

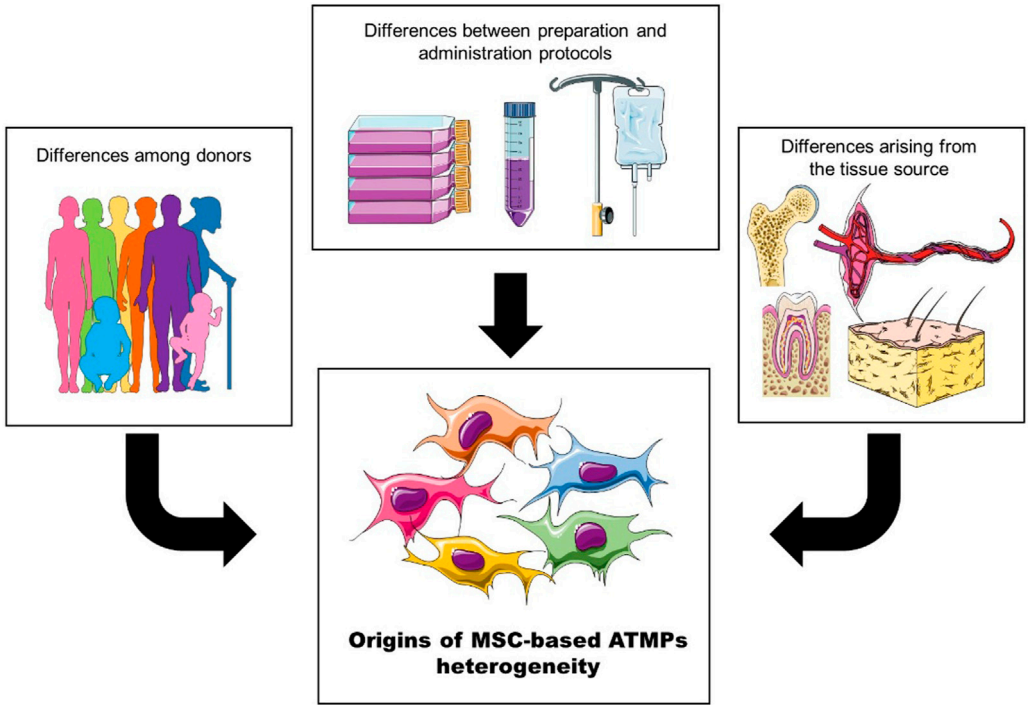

FIGURE 2
The heterogeneity of MSC-based ATMPs can be broadly categorized into three groups: differences among donors, variations arising from the tissue source, and differences introduced by preparation and administration protocols.

- adherence to plastic in standard culture conditions,
- specific surface antigen expression (≥95% of the MSC population must express CD105, CD73 and CD90, and lack expression (≤2% positive) of CD45, CD34, CD14 or CD11b, CD79a or CD19 and HLA class II as measured by flow cytometry),
- multipotent differentiation potential–they must be able to differentiate into osteoblasts, adipocytes and chondroblasts under standard *in vitro* differentiating conditions. (Dominici et al., 2006).

However, a scoping review by Renesme et al. reports that only 18% of randomly analyzed studies involving MSC explicitly referred to the ISCT criteria. More precisely, only 36% of the studies reported plastic adherence, 40% reported any kind of *in vitro* differentiation assay and 53% of the studies performed analysis of cell markers (Renesme et al., 2022). Since MSC-based products are regarded as medicinal products according to EU legislation, it is of further importance particularly for future studies, that uniformity of their characteristics and efficacy is comprehensible and unambigous to the greatest possible extent. In this review, we take a closer look at the origins of MSC variability, their impact on clinical and preclinical studies, and propose potential solutions to address these issues.

2 Origins of MSC heterogeneity

ISCT acknowledges that MSCs encompass a heterogeneous population pool, which includes fibroblasts, myofibroblasts, and a small proportion of stem/progenitor cells, while lacking hematopoietic or endothelial cells (Viswanathan et al., 2019). Single-cell RNA sequencing (scRNA-seq) of MSCs has identified several candidate subpopulations with different functional characteristics - some exhibit greater proliferation ability while others show higher osteogenic, chondrogenic or adipogenic differentiation potency and maintenance of stemness (Sun et al., 2020; Wang et al., 2021b; Hou et al., 2021; Chen et al., 2022; Xie et al., 2022). It has been shown that extracellular matrix highly contributes to the heterogeneity of MSC populations in a tissue-type-dependent pattern (Wang et al., 2021c). The secretory and immunomodulatory functions linked to clinical benefits in MSC-based therapies are believed to arise from the bulk, heterogeneous stromal cell fraction (Viswanathan et al., 2019). However, others argue that different MSC populations should be separated immediately after isolation, individually expanded *in vitro* and selected according to their characteristics to treat different diseases (Wang et al., 2017; Zhang S. et al., 2021). Still, research shows that even colonies originating from a single cell will in time become functionally heterogeneous (Rennerfeldt et al., 2019).

Due to the variations in multiple factors across studies, pinpointing key aspects that influence clinical outcomes can be challenging. However, they can be broadly categorized into three groups (Figure 2):

- Differences arising from the tissue source,
- Donor attributes,
- Preparation and administration protocols.

2.1 Heterogeneity arising from tissue source

Throughout the years, the acronym MSC has accumulated quite a bit of controversy, starting with Caplan, who in 1991 coined the term adult "mesenchymal stem cells", referring to a small number of cells involved in repair and turnover of skeletal tissues (Caplan, 1991). Later, similar cells have been found in most anatomical locations and researchers called for a name change from mesenchymal stem cells to mesenchymal stromal cells, reflecting their stromal residence (Dominici et al., 2006). However, disputes continue, as some would change the term to multipotent stromal cells, while others go as far as to argue for complete abolition of the acronym MSC (Sipp et al., 2018; Soliman et al., 2021). Currently, the official position of the International Society for Cell and Gene Therapy (ISCT) Mesenchymal Stromal Cell committee is that the acronym "MSC" should remain in use, however, information about the tissue source should always be provided (Viswanathan et al., 2019).

MSCs reside and can be isolated from various tissues, including bone marrow (BM-MSCs) (Li et al., 2016), umbilical cord blood (CB-MSCs) (Um et al., 2020), umbilical cord tissue (UC-MSCs), Wharton's jelly (WJ-MSC) and fetal placenta (Beeravolu et al., 2017), adipose tissue (AD-MSCs) (Ong et al., 2021), dental tissue and dental pulp (DT-MSCs and DP-MSCs) (Li et al., 2023), fetal liver (Gridelli et al., 2012), endometrial tissue and menstrual blood (Meng et al., 2007; Allickson et al., 2011; Schüring et al., 2011; Bozorgmehr et al., 2020). Although the majority of research focuses on BM-MSCs, AD-MSCs and UC-MSCs (as well as WJ-MSCs), MSCs from other tissues have noticeable therapeutic benefits. For instance, DP-MSCs also possess the capacity to differentiate into different cell types and are quite extensively used in regenerative medicine, although mainly in preclinical research. Thus, they have been used for tissue repair in context of periodontal diseases, tooth reconstruction, dental pulp regeneration, as well as for distant anatomical tissues, e.g., for regeneration of neuronal and skeletal tissue damage (Graziano et al., 2008; Ledesma-Martinez et al., 2016). Nevertheless, the most commonly used sources are bone marrow, followed by umbilical cord and adipose tissue (Naji et al., 2019).

MSCs isolated from different sources share many common characteristics, but they also show particular phenotypic and functional differences (Patel et al., 2016; Wu et al., 2018; Rady et al., 2020a; Shin et al., 2021; Li Y. et al., 2022; Li S. et al., 2022; Laloze et al., 2023). Comparison of scRNA-seq of BM-MSC and UC-MSC has revealed more differences in gene expression between tissue sources than between individual donors (Medrano-Trochez et al., 2021). Moreover, a massive parallel multiplexing scRNA-seq performed across multiple tissues and donors has revealed a tissue-type-dependent pattern of MSC subpopulations, indicating that MSCs from different tissues have prominent transcriptomic heterogeneity (Wang et al., 2021c). This also gave rise to the rationale that patients burdened with certain pathologies could benefit from MSCs sourced from a specific tissue, which could be functionally relevant for their clinical efficacy.

Still, MSC capabilities (and identity) from different tissues are not fully characterized, leading to contradictory results. For example, under the same culturing conditions, AD-MSCs displayed the highest immunosuppressive potency, followed by BM-MSCs and UC-MSCs (Calcat-i-Cervera et al., 2023). Others report BM-MSCs to have the lowest immunosuppressive abilities compared to AD- and UC-MSCs (Ketterl et al., 2015a). On the other hand, BM-MSCs showed a superior capacity to support angiogenesis and induce endothelial cell migration in comparison to AD-MSCs or UC-MSCs (Calcat-i-Cervera et al., 2023). Similarly, comparing gene expressions of BM-MSCs and AD-MSCs from the same pool of donors has revealed distinct transcriptomic profiles that directly translate into MSC capacity to interact with immune cells (Ménard et al., 2019). For example, the study showed that BM-MSCs were better at suppressing NK cell proliferation, while AD-MSCs were better at suppressing T cell proliferation.

2.2 Donor heterogeneity

Another factor contributing to the difficulties in standardization of MSC products is the high variability between donors, which includes a multitude of factors, such as donor age, sex, BMI, as well as systemic and autoimmune diseases (Sun et al., 2007; Siegel et al., 2013; Patel et al., 2016; Rady et al., 2020b). Such variabilities can manifest as differences in MSC phenotype, morphology, doubling time, immunosuppressive potential, gene expression, proliferation, differentiation, and colony-forming capacity (CFU) (Siegel et al., 2013; Ganguly et al., 2019; Li S. et al., 2022). For instance, AD-MSCs from older donors have shown increased cellular senescence, reduced viability and proliferation, as well as reduced differentiation potential in comparison to younger donors (Choudhery et al., 2014). Similarly, BM-MSCs from infant donors doubled more quickly, differentiated into bone and fat cells more efficiently and formed more and denser CFUs. They were also better at suppressing T cell proliferation at lower concentrations than BM-MSCs from adult donors (Myneni et al., 2019). Furthermore, single-cell multiomic analysis profiling the transcriptome and epigenome of BM-MSCs from four healthy donors allowed for classification of cells into four clusters, indicating that BM-MSCs from different donors possess distinct chromatin accessible regulatory elements, which was reflected as variations in their differentiation potential into osteoblasts (Chen et al., 2023). Interestingly, it has been shown that MSCs' immunomodulatory and angiogenic fitness are inversely correlated and can predict inter-donor differences in proangiogenic *versus* anti-inflammatory/immune suppressive activities in cell-based assays (Robb et al., 2022a; Lee et al., 2023).

It would be rational to assume that deriving MSCs from umbilical cords would eliminate certain heterogeneity originating from donors' age, lifestyle, and pathophysiological conditions. Remarkably, an opposing trend has been observed. A study examining the cellular heterogeneity in single-cell transcriptomes of MSCs discovered higher inter-donor variability in WJ-MSC samples compared to BM-MSC samples (Zhang C. et al., 2022). In another scRNA-seq study, UC-MSCs exhibited significantly higher heterogeneity in their subpopulations across different donors when compared to MSCs from adult donors (Wang et al., 2021d).

Moreover, in a study comparing MSCs derived from umbilical cords of 12 donors, doubling time and population doubling varied by a factor of two between donors (Mebarki et al., 2021). A comparison of UC-MSCs from 32 donors revealed a substantial

variability in both their proliferation rates and immunomodulatory properties (Zhang C. et al., 2021). Interestingly, while no correlation was found between their proliferation rates and immunosuppressive capacity, the latter exhibited a close alignment with their therapeutic effects observed in a mouse spinal cord injury model (Zhang C. et al., 2021; Zhu et al., 2022). In a study aimed at standardizing isolation and expansion methods, MSCs derived from umbilical cords of 90 donors were examined. Interestingly, lower gestational age was associated with a shorter time to P0 harvest, suggesting that even minor variables, such as time of delivery, could potentially exert a significant influence on MSC characteristics (Todtenhaupt et al., 2023).

A comparison of CB-MSCs from seven donors identified two distinct groups based on angiogenic capacity under hypoxic conditions: one with low and another with high angiogenic potential. These distinctions correlated with the differential expression of four specific genes—ANGPTL4, ADM, CDON, and GLUT3—which were chosen based on prior research highlighting their roles in angiogenesis and sensitivity to hypoxic conditions (Kang et al., 2018a).

The discussed donor variability stands as a significant barrier in the development of consistent protocols and cellular medicinal products. Despite efforts to control for variables with substantial impacts on the clinical quality of MSCs by using more primitive MSCs, such as UC- and less often CB-MSCs, heterogeneity between batches clearly persists. Exploring strategies like, e.g., pooling cells from different donors might perhaps mitigate these effects and ensure more comparable products, leading to more consistent results.

2.3 Heterogeneity introduced by variations in preparation and administration protocols

Clinical efficacy of MSC products can vary considerably, depending not only on tissue source and donor characteristics but also on preparation and administration protocols. Given the regularly irreproducible effectiveness of MSCs in clinical trials, the optimization of cell manufacturing protocols is still a work in progress. However, this pursuit also holds the potential to further introduce heterogeneity into preparation conditions. Despite advancements towards standardization of the production procedures and accurate characterization of the MSC products, variabilities among manufacturing centers are very much present (Bieback et al., 2019). Understanding these differences and their impact on product quality would allow for a better comparison of the clinical outcomes across various institutions.

2.3.1 Media supplements

Efficient MSC expansion in culture requires basal medium supplemented with growth factors, proteins, and enzymes to support attachment, growth, and proliferation. The most commonly used supplement in cell culture media in general is fetal bovine serum (FBS), due to its rich supply of growth factors, cytokines, and chemokines (Bieback, 2013).

However, the utilization of FBS in cell culture poses scientific, economic and moral issues (Subbiahanadar Chelladurai et al., 2021). The most critical concern in using FBS for clinical applications is its potential contamination with xenogeneic elements, including prion proteins, endotoxins, various types of microbes, immunoglobulins, and viruses. Another issue pertains to the uncertainty surrounding the precise composition of FBS and its batch-to-batch variability, both of which can impact the biological properties of cultured cells. Thirdly, the growing demand and limited production capacity can result in unpredictable shortages and higher prices of FBS. Last but not least, the increasing number of fetuses slaughtered specifically for FBS production and the potential fetal distress during blood collection give rise to significant ethical concerns regarding animal welfare (Subbiahanadar Chelladurai et al., 2021).

To address these issues, alternatives to FBS are being developed and integrated into MSC manufacturing protocols. Among the most widely adopted alternatives are human platelet lysate (Cañas-Arboleda et al., 2020), pooled human AB-serum (Savelli et al., 2018), human umbilical cord serum (Afzal et al., 2023), and serum-free media (Caneparo et al., 2022). Nevertheless, similar to FBS, these alternatives struggle with certain challenges. For example, platelet lysate-plasma contains fibrinogen and other coagulation factors. To prevent gelation, commercially available platelet lysate usually contains animally-sourced heparin, making it no longer xeno-free (Altrock et al., 2023). Supplements derived from human blood also share some concerns with FBS, particularly regarding the potential transmission of infectious agents and the variability in their composition (Bieback, 2013).

Culturing MSCs in variously supplemented media can lead to alterations in their fundamental characteristics, including changes in proliferation rate, morphology, gene expression patterns, senescence, immunomodulatory properties, and differentiation capacity (Dam et al., 2021; Takao et al., 2021; Jakl et al., 2023). It has been shown that growing MSCs in serum-free media leads to smaller cells with increased proliferation rate that are better at forming colonies than those grown in FBS-supplemented media (Aussel et al., 2022; Caneparo et al., 2022). However, they exhibited lower osteogenic and chondrogenic differentiation capacity (Caneparo et al., 2022).

Similarly, BM-MSCs grown in medium with human platelet lysate showed faster proliferation rates and lower differentiation capacity compared to those in FBS-supplemented medium (Anerillas et al., 2023). Additionally, BM-MSCs expanded in medium with human AB-serum exhibited round cell enrichment, better adhesion, and faster proliferation rates compared to those in medium with human platelet lysate (Savelli et al., 2018). In a study comparing human platelet lysate, fetal bovine serum, and human AB-serum, platelet lysate emerged as the superior choice for supporting AD-MSC proliferation, differentiation, and growth in 3D cultures (Kirsch et al., 2021).

Considering the collective body of research, determining the ideal supplement for MSC manufacturing remains a challenging task. However, although MSCs cultured in media supplemented with platelet lysate exhibit notably accelerated proliferation and marked variations in cellular morphology compared to those cultured in FBS, no discernible alterations in DNA-methylation patterns have been observed, and only modest differences in gene expression profiles were detected. Moreover, the changes in proliferation and morphology proved to be reversible (Fernandez-Rebollo et al., 2017).

2.3.2 Culturing techniques

While one of the defining criteria for MSCs has been *in vitro* plastic adherence, conventional methods of their extensive 2D *in vitro* expansion are not representative of the *in vivo* environment. Instead, MSCs exist within their niches as a part of heterogeneous cell population, where they tightly adhere to each other and exhibit complex cell-cell and cell-extracellular matrix interactions (Yen et al., 2023).

Conventional MSC manufacturing techniques, selected for their convenience and low cost of implementation, are aimed at generating a clinically relevant number of cells. However, they can negatively impact MSC characteristics and functions, which could be responsible for their limited therapeutic efficacy. In an effort to preserve or enhance MSC phenotypes and consequently improve their *in vivo* performance, 3D culturing techniques have been developed (Kouroupis and Correa, 2021). When grown suspended in culture, MSCs spontaneously coalesce and form spherical multicellular aggregates, termed spheroids (Fuentes et al., 2022). These are thought to better recapitulate *in vivo* interactions, promote secretion of paracrine factors, improve cell survival, increase MSC differentiation potential, and delay their replicative senescence (Cesarz and Tamama, 2016; Yen et al., 2023).

The methods used to generate MSC spheroids can be generally classified as scaffold-free and scaffold-based culture platforms (Kouroupis and Correa, 2021). Scaffold-free methods can be further divided into static and dynamic approaches. The most trivial static technique is growing cells in a non- or low-adherent environment that allows self-organization of cells into suspended spheroids (Redondo-Castro et al., 2018). More complex methods encompass hanging-drop method (Bartosh and Ylostalo, 2014; Au - Ylostalo et al., 2017), forced aggregation (Rettinger et al., 2014) and magnetic levitation (Lewis et al., 2017; Gaitán-Salvatella et al., 2023). Among the most investigated dynamic approaches are spinner flask culture and rotating wall vessel techniques (Marques et al., 2023). Additionally, various scaffold-based MSC spheroid generation methods have been proposed using both natural and synthetic biomaterials. Biomaterial selection should be based on the therapeutic application in mind, as physical-chemical characteristics of scaffolds such as porosity and biodegradation can dramatically affect MSC stemness and differentiation capacities (Kouroupis and Correa, 2021).

Studies show that mild hypoxia present within the inner zones of MSC spheroids may positively affect MSC survival and secretory capacity. 3D culture conditions significantly increase the relative expression of stemness-related transcriptional factors in MSCs and promote their anti-inflammatory profile (Bartosh et al., 2010a; Rybkowska et al., 2023). RNA-seq data obtained from human amnion-derived MSCs following 3D culture revealed increased expression of pleiotropic factors important in tissue regeneration, such as CXCL12, LIF, VEGF-A, HGF, BDNF, IL6, EGF, PGE2, CCL20, BMP2, TGFB1, CXCL1, CCL2, GDF15, IL11, and CCL7 (Gallo et al., 2022). Growing MSCs under hypoxic conditions does not change their specific surface antigen expression (Kang et al., 2018a; Tomecka et al., 2021). Nevertheless, they exhibit improved abilities for multi-lineage differentiation, survival, migration and proliferation, better support of angiogenesis and increased expression of stemness-related genes (Kang et al., 2018b; Meng et al., 2018; Wang et al., 2022). They were also shown to spontaneously generate 3D niche-like structures of undifferentiated, small, round Oct4 and HIF-2a positive fast growing cells (Drela et al., 2014).

As of today, no clinical trials have been conducted to evaluate the therapeutic potential of MSC spheroids. Consequently, there are no specific criteria in place to define conditions where MSC spheroids might be preferred over MSCs expanded in a monolayer. Still, it has become more and more evident that conventional culturing methods cannot ensure the preservation of MSC characteristics and their associated functionality to the same extent. The adoption of reproducible, high-throughput methods that meet regulatory requirements for MSC spheroid production could facilitate their clinical use and potentially lead to MSC products with improved therapeutic efficacy.

2.3.3 Expansion level

MSC-based therapies require a substantial number of cells, as individual doses are measured in millions of cells per kilogram of body mass, particularly for systemic treatments like in GvHD (Kelly and Rasko, 2021). Consequently, to obtain the necessary cell quantity for clinical applications, extensive MSC expansion is inevitable. Unfortunately, such expansion can significantly alter MSC characteristics and has been proposed as a possible cause for poor performance in certain clinical trials (Galipeau, 2013; Hoch and Leach, 2014). These changes can impact phenotypic, morphological, genetic and functional attributes of MSCs, along with their regenerative and immunomodulatory secretome profile (Yang et al., 2018; Miclau et al., 2023).

Indeed, population doubling has been reported to inversely correlate with MSC potency, with early-passage cells being more potent than batches of extensively expanded cells, possibly due to cell senescence (von Bahr et al., 2012). Conversely, there is a theory that rapidly dividing clones with less favorable characteristics may outcompete slower proliferating cells during each passage, gradually increasing the ratio of poorly performing cells. An interesting study by Selich et al. has demonstrated, that when MSCs are first introduced into culture, they constitute a heterogeneous cell population. However, with successive passaging, this initial diversity diminishes, leading to the selection of a limited number of clones in later passages (Selich et al., 2016).

It appears as though expansion of MSCs with optimal function is limited to a few passages, increasing the cost and reducing the feasibility of mass production for MSC therapeutics. Nevertheless, some argue that a brief period of culturing in a 3D format prior to administration could induce extensively expanded MSCs to express and secrete anti-inflammatory and immunomodulatory factors, thereby enhancing their ability to generate a larger cell population (Bartosh et al., 2010b). Further research is required to fully confirm this hypothesis.

2.3.4 Administration protocols

MSCs can be introduced through either systemic or local delivery methods. However, following intravenous infusion, most MSCs get entrapped in pulmonary vasculature, where they form emboli. In about 24h, the vast majority of cells are cleared from the lungs and only a minor fraction home to different organs such as heart, brain, liver and kidney (Lee et al., 2009; Eggenhofer et al., 2014; Luk et al., 2016). To prevent their entrapment in the lungs,

MSCs can be administered directly to the site of the lesion or inflammation (Moon et al., 2019; Lamo-Espinosa et al., 2020; Czarnecka et al., 2021; Ouboter et al., 2023). Nevertheless, local administration can be invasive, more complex, and requires additional training for medical practitioners. Moreover, in certain conditions such as GvHD and solid organ transplantation, MSCs cannot be administered locally and instead require systemic delivery (Franquesa et al., 2013; Podesta et al., 2020).

Multiple factors can affect viability and key functional characteristics of MSCs at the time of administration, including cell concentration, the choice of solution in which the cells are delivered and post-thawing protocols (Zhang et al., 2017; Aabling et al., 2023). A droplet-based scRNA-seq comparing pre-freeze and post-freeze BM-MSC samples has identified numerous differentially expressed genes associated with a wide range of cellular functions, such as cytokine signaling, cell proliferation, cell adhesion, cholesterol/steroid biosynthesis, and regulation of apoptosis (Medrano-Trochez et al., 2021). Indeed, in the first 24 h after thawing, cryopreservation reduces cell viability, increases apoptosis level and impairs MSC metabolic activity, immunosuppressive potency and adhesion potential (Ketterl et al., 2015b; Bahsoun et al., 2020; Giri and Galipeau, 2020).

Prior to infusion, cells are usually formulated with a saline solution, human albumin solution or even administered directly in their cryopreservant solution (Trento et al., 2018). It is worth noting that only a limited number of clinical trials specify the handling of MSC products, from dose preparation to cell administration (Wiese et al., 2022).

3 Strategies for MSC standardization

Given the numerous ongoing clinical trials involving MSCs and the growing need for large-scale manufacturing protocols, it is imperative to establish consensus assays for MSC processing and the release of MSC products. Reference materials and validated, uniformly applied tests for quality control of MSC products are required (Robb et al., 2019). However, some stakeholders in the MSC field advocate for caution when establishing definitive cell standards, since there are still gaps in our current understanding of MSC biology that could potentially distort or inhibit the adoption of MSC-based therapies (Wilson et al., 2023). Central to this challenge is the need for precise clinical response prediction, which requires well-defined MSC populations and, contingent upon the therapeutic goal, an assessment of their desired specific activities such as differentiation potential, proliferation rate, secretory profile, and angiogenesis capacity.

3.1 Defining MSC subpopulations via specifically expressed surface antigens

It has been shown that ISCT criteria for phenotypic MSC identification can be insufficient for distinction between MSCs and certain other cell types, such as fibroblasts (Denu et al., 2016; Brinkhof et al., 2020; Budeus et al., 2023a). In fact, MSCs are morphologically indistinguishable from fibroblasts (Soundararajan and Kannan, 2018). What is more, Denu and colleagues have demonstrated that none of the ISCT criteria can reliably discern MSCs from fibroblasts, even arguing that they could represent the same cell type (Denu et al., 2016). Some suggest that fibroblasts could in certain instances be used as a more practical alternative to MSCs, while others maintain that they have complementary roles, especially in cell homeostasis and tissue development and injury (Ichim et al., 2018; Janja et al., 2021). Soundararajan and Kannan propose that the resemblance in characteristics between fibroblasts and aged MSCs, such as diminished differentiation potential, proliferation, immunomodulatory capacity, and specific cell surface markers, could mean that MSCs are in fact immature fibroblasts (Soundararajan and Kannan, 2018). Indeed, single-cell transcriptome sequencing has revealed that MSCs could constitute a subclass of fibroblasts (Fan et al., 2022).

On the other hand, gene expression and epigenetic studies have been successful in discerning MSC and fibroblast populations based on molecular signatures of homeobox genes and transcriptional factors (Taskiran and Karaosmanoglu, 2019; Budeus et al., 2023b). Likewise, comparative microarray transcriptome profiling of three fibroblast populations and MSCs from five different sources demonstrated a marked distinction between the “fibroblast” and “MSC” group, particularly in transcripts associated with structuration of the tissue skeleton (Haydont et al., 2020). Wiese and Braid propose a panel of 24 signature genes to support standardized and accessible MSC characterization, including five that have been shown to be upregulated in MSCs *versus* fibroblasts (Wiese and Braid, 2020).

So while RNA sequencing and microarrays could possibly discern between MSCs and fibroblasts, protocols for clinical application should be as straightforward and affordable as possible. Therefore the use of cell surface antigens would be preferable, however, to this date, they have proven insufficient to indisputably identify MSCs. Brinkhof et al. propose CD166 as a marker to differentiate MSCs from fibroblasts, as it is the only marker they have found to be upregulated in MSCs compared to fibroblasts. Notably, its expression levels positively correlated with those of CD105, although CD166 exhibited greater specificity for MSCs (Brinkhof et al., 2020). Nevertheless, Sober et al. did not detect significant difference in CD166 expression between MSCs derived from various tissues and fibroblasts. However, they put forward a panel of markers that could distinguish between MSCs originating from a specific tissue and fibroblasts; for instance, CD79a, CD105, CD106, CD146, and CD271 could be used to differentiate AD-MSCs from fibroblasts (Sober et al., 2023).

Adding to the complexity, a study on changes in MSC-related surface antigen expression during *in vitro* culture revealed that after 7 days, synovial fibroblasts began displaying MSC characteristics, further blurring the distinction between the 2 cell types (Isono et al., 2022).

Moreover, due to a multitude of discouraging clinical outcomes, there is a growing demand to identify additional surface markers capable of defining MSCs while capturing their biological and manufacturing variability, as well as clinical performance (Camilleri et al., 2016; Samsonraj et al., 2017). Consequently, various markers have been proposed to better define distinct subpopulations within MSCs (Smolinska et al., 2023).

Lately, CD146 has been frequently mentioned as a surface antigen that could serve as a marker for MSC potency evaluation

(Bowles et al., 2020; Ma et al., 2021a). It is a transmembrane glycoprotein involved in adhesion, cellular signaling and numerous other physiological and pathological processes (Wang et al., 2020). It is expressed in MSCs derived from a wide range of tissue sources, both fetal and adult (Barilani et al., 2018). CD146 positive MSCs exhibit stronger proliferation, differentiation, migration and immunomodulatory abilities, however, prolonged passaging can result in progressive loss of CD146 on the cell surface (Yang et al., 2018; Al Bahrawy, 2021; Ma et al., 2021b; Zhang L. et al., 2022). Indeed, MSCs expressing high levels of CD146 display a more pronounced therapeutic effect compared to MSCs with low levels of CD146, as evident by increased survival rate in a mouse GvHD model (Bikorimana et al., 2022).

Another surface antigen implicated in MSC function is CD271, present on MSCs derived from adult but not fetal tissues. The reported abundance of CD271 varies widely, ranging from 4% to nearly 100%. Nevertheless, the majority of studies converge on an approximate 20% fraction of CD271+ positive cells within the bulk MSC population (Quirici et al., 2010; Watson et al., 2013; Beckenkamp et al., 2018; Smith et al., 2021). MSCs positive for CD271 display enhanced capacity for differentiation, proliferation, and colony formation when compared to their CD271− counterparts or mixed-population. However, the CD271 antigen diminishes rapidly with cell passaging, highlighting the importance of using cells subjected to minimal expansion procedures for therapeutic applications (Smith et al., 2021).

Moreover, CD271-depleted BM-MSCs have altered morphology, poor proliferation capacity, increased expression of hematopoietic markers, nearly no multi-lineage potential and are unable to form colonies, therefore failing to meet ISCT criteria for MSCs (Kuci et al., 2010; Petters et al., 2018). Notably, RNA sequencing analysis has revealed that there is a larger difference in gene expression between CD271+ and CD271− populations in AD-MSCs than between donors. Among genes with altered expression levels are those associated with inflammation and angiogenesis (Smith et al., 2021). MSC that are CD271 positive show superior promotion of cartilage repair to MSCs consisting of heterogeneous populations (Kohli et al., 2019). Nevertheless, when seeded on 3D osteoconductive biomaterial scaffold for bone regeneration, CD271+ MSCs proved inferior to heterogeneous MSCs, underscoring the need for caution when transferring results from monolayer to 3D cultures (Muller et al., 2019).

Several other surface antigens have been proposed as markers for MSCs and their specific subpopulations, such as STRO-1 as a marker for dental/gingival MSCs (Yu et al., 2010; Perczel-Kovách et al., 2021). Through advancements in methodologies, novel antigens are continually unveiled, prompting further investigations into their distribution and potential as phenotype markers. For example, based on single-cell RNA sequencing data, CD167b, CD91, CD130, and CD118 were proposed as novel surface markers for BM-MSC enrichment or purification. However, further molecular validations are needed (Wang et al., 2021b).

3.2 Functional assays

Contributing to the challenges in predicting clinical outcomes following MSC administration are the uncertainties surrounding mechanisms through which they drive tissue regeneration and exert immunoregulatory functions. Regulatory authorities require the development of tests to measure potency as part of release criteria of advanced clinical trials designed to support marketing approval and registration. Still, they allow for a considerable flexibility in determining the appropriate measurements of potency for each product and the adequacy of these tests is evaluated on a case-by-case basis (Galipeau et al., 2016). Ideally, the potency assay should reflect the *in vivo* mechanisms of action. However, since MSCs act through a complex range of mechanisms with unknown key steps, there are currently no definitive and unambiguous tests available that could accurately measure their clinical efficacy (Galipeau et al., 2016; Hematti, 2016; Robb et al., 2019).

Consequently, ISCT suggests an alternative approach. Rather than relying on a single potency assay, a collection of complementary assays should be conducted to evaluate relevant biological and therapeutic properties of the cells including quantitative analysis of mRNA expression, measurement of functionally relevant surface markers by flow cytometry, and protein-based assays to detect secreted factors (Galipeau et al., 2016).

3.2.1 Differentiation potential of MSCs

One of the most intriguing and therapeutically promising MSC characteristics is their differentiation potential. Under both *in vivo* and *in vitro* stimulation, they can differentiate into several mesodermal-derived lineages, in particular chondrogenic, osteogenic, and adipogenic cells. Various studies suggest that they can also differentiate into non-mesodermal lineages like hepatocytes, neurons and pancreatic cells (Shibu et al., 2023). It is therefore important to distinguish MSC "potency" in a manufacturing context from their capacity to differentiate toward multiple cell lineages.

While tri-lineage differentiation potential is not typically assessed in MSC potency assays, it is still considered a key criterion for routine MSC characterization (Dominici et al., 2006; Montesinos et al., 2009). Therefore it is somewhat surprising, that most of the time researchers omit these assays, especially when conducting clinical studies (Wilson et al., 2021; Renesme et al., 2022). Furthermore, despite decades of undertaking MSC differentiation assays, there is still lack of consensus regarding the optimal media composition, detection reagents, and quantification methods to determine the extent of *in vitro* differentiation (Kakkar et al., 2020; Mollentze et al., 2021). Additionally, recent trends indicate a growing reliance on commercially available differentiation media, which are often elusive regarding their composition, thus exacerbating the heterogeneity among protocols (Eggerschwiler et al., 2019; Labedz-Maslowska et al., 2021; Bajetto et al., 2023).

When characterizing MSCs through tri-lineage differentiation in clinical and preclinical trials, researchers commonly present representative images of differentiated MSCs, confirmed through specific staining reagents (Aghayan et al., 2022; Shimizu et al., 2022; Krakenes et al., 2023). Following adipogenic differentiation, staining with Oil Red O or Nile Red is used to visualize intracellular lipid vacuoles. Osteogenic differentiation is confirmed by the detection of calcium deposits in the extracellular matrix via Von Kossa or Alizarin Red S staining. Chondrogenic differentiation is

confirmed through the staining of cartilage deposits by Safranin-O/Fast Green or Alcian Blue (Ciuffreda et al., 2016).

However, when aiming to determine the extent of differentiation, colorimetric methods offer only semi-quantitative analysis options. Specifically, osteogenic differentiation can be evaluated by assessing extracellular calcium deposits through Alizarin Red S staining or by quantification of alkaline phosphatase activity (Widholz et al., 2019). Adipogenic differentiation can be estimated by staining intracellular lipid droplets with Oil Red O and chondrogenic differentiation by staining glycosaminoglycans, proteoglycans and collagen content with Safranin O. The extent of differentiation is then evaluated by semi-quantitative measurement of absorbance levels (Du et al., 2023).

Therefore, most of the studies that set to quantify the extent of MSC differentiation, have to analyze gene expression profile specific for the desired differentiation through real-time polymerase chain reaction (RT-PCR). Briefly, RNA extracted from cells that are undergoing chondrogenic, osteogenic, or adipogenic differentiation, is reversely transcribed, resulting in the generation of first-strand complementary DNA. This cDNA then serves as a template for amplification by RT-PCR using sequence-specific primers, followed by relative quantitation of gene expression (Kim et al., 2023). Certain changes in gene expression following MSC differentiation are well established, while others are still being discovered and could potentially serve as basis for quantification of differentiated MSCs (Hou et al., 2021; Stefanska et al., 2023).

In recent years, new methods for quantification of MSC differentiation are emerging. One of more compelling approaches is digital image analysis of histological staining. It aims to simplify the laboratory procedures to objectively quantify and classify the degree of differentiation as well as the differentiation potential among different MSC cell lines or cell subpopulations (Avercenc-Leger et al., 2017; Eggerschwiler et al., 2019). Another recently proposed strategy for determining the extent of osteogenic differentiation utilizes 18F. This radioactive tracer binds with a high affinity to newly synthesized hydroxyapatite and can then be evaluated by 18F μ-positron emission tomography scanning and activimeter analysis (Grossner et al., 2020). All in all, methods are continually being developed, in an effort to simplify and refine quantification of MSC differentiation and by extension, their therapeutic efficacy.

3.2.2 Lymphocyte proliferation assay

While MSC ability to suppress lymphocyte proliferation is well documented, assays to quantify this process lack standardization and vary between groups and methodologies (Juhl et al., 2022). Still, *in vitro* inhibition of lymphocyte proliferation is considered a gold standard in predicting MSC functionality (Galipeau et al., 2016; Nicotra et al., 2020). Lymphocyte proliferation can be induced either by unspecific mitogens such as phytohaemagglutinin (PHA) and Staphylococcal enterotoxin B or by specific antibody-mediated activation of CD3 associated with the T cell receptor and CD28 for co-stimulatory signaling (Chinnadurai et al., 2018; Hammink et al., 2021). Alternatively, in mixed lymphocyte reactions (MLR) proliferation of T cells is activated by allorecognition, in which T cells are directly activated by allogeneic antigen-presenting cells (DeWolf et al., 2016). Lymphocyte proliferation can be quantified by several methods. Firstly, the amount of newly synthesized DNA can be measured by incorporation of thymidine analogs such as bromodeoxyuridine or 3H-thymidine (Svajger et al., 2021; Piede et al., 2023). Alternatively, total DNA content can be assessed by fluorescent dye binding using Hoechst or CyQUANT® NF reagents (Suzdaltseva et al., 2022). One of the most widely accepted methods is tracking generations of cell division by dilution of covalently binding proliferation dyes such as CFSE (carboxyfluorescein succinimidyl ester) or CellTrace Violet (Kashef et al., 2022; Lemieszek et al., 2022).

However, these dyes can be toxic to a certain extent, prompting an exploration of alternative approaches. One such alternative is the assessment of cell proliferation by measuring the rate of metabolic activity. This can be achieved by utilizing colorimetric assays with tetrazolium salts or by quantifying the ATP levels with bioluminescent reagents that detect increases in healthy proliferating cells (Herzig et al., 2021; Herzig et al., 2023). Additionally, some researchers assess cell proliferation by measuring accumulation of cell cycle-associated proteins such as intracellular Ki67 or simply by counting cells, using, for example, CountBright Absolute Counting Beads (Cruz-Barrera et al., 2020).

In an effort to minimize the impact of donor variation, researchers pool peripheral blood mononuclear cells (PBMCs) from up to 10 different donors in MLR and mitogen induced lymphocyte proliferation (Christy et al., 2020). However, recent report indicates that optimal lymphocyte proliferation in MLR experiments can be achieved with as few as four donors (Hansen et al., 2022). Furthermore, two studies have identified PHA as the most suitable mitogen among tested components in their panels (Hansen et al., 2022; Kashef et al., 2022). It is noteworthy that, despite the conventional duration of 4–5 days for most lymphocyte proliferation assays, the peak of PBMC proliferation suppression occurs within 48 h following co-culture with MSCs, and extending the incubation window does not elicit significant changes (DeWolf et al., 2016; Suzdaltseva et al., 2022).

3.2.3 Other assays

One of the assays to evaluate MSC potency, not required by ISCT but still frequently employed, is the endothelial cell tube formation assay. It evaluates MSC ability to support angiogenesis *in vitro* (Arnaoutova et al., 2009). Briefly, endothelial cells, whether primary or immortalized, are combined with MSC conditioned media and then seeded onto a basement membrane matrix. In response to angiogenic signals present in the media, cells start to rapidly form capillary-like structures. Within 1 hour, they align themselves, and by the second hour, tubules containing lumens begin to emerge. *In vitro* angiogenesis is then quantified as the number of branch sites/nodes, loops/meshes, or the number and length of tubes formed (DeCicco-Skinner et al., 2014; Carpentier et al., 2020). As the probable mechanism of action by which MSCs elicit an angiogenic response is through their paracrine activity, a quantification of expression of angiogenic factors and cytokines such as VEGF can be used to assess their angiogenic potency (Thej et al., 2017).

In accordance with ISCT guidelines, recent studies focus on developing assay matrix approach in order to predict MSC potency (Figure 3). One of the more commonly employed strategies involves utilizing secretory soluble factors, specifically chemokines and

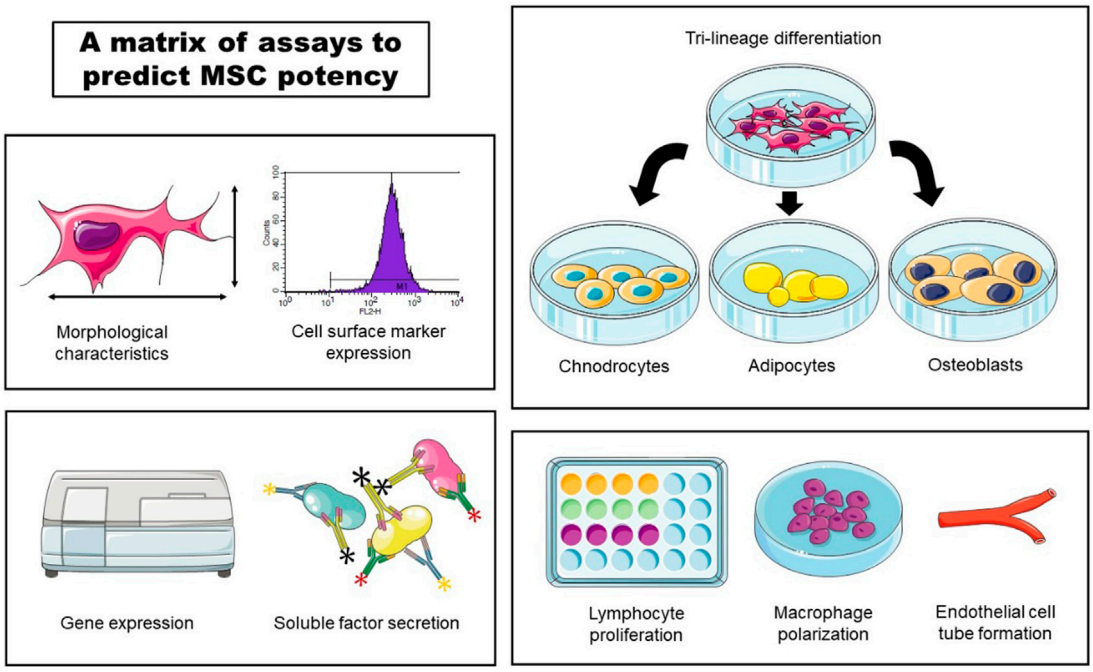

FIGURE 3
An example of a matrix of assays to predict MSC potency. Morphological characteristics, cell surface marker expression, gene expression, soluble factor secretion, tri-lineage differentiation, lymphocyte proliferation, macrophage polarization and endothelial cell tube formation could be used to assess potency of MSC cell product lots.

cytokines, through a multiplex analytical method (Lipat et al., 2022; Porter et al., 2022). Additionally, Kowal et al. claim that they could predict BM-MSCs proliferative capacity and the differentiation potential by assessing their morphological characteristics (Kowal et al., 2020).

In line with these efforts, Robb et al. developed an *in vitro* matrix of multivariate readouts, specifically, cell morphology, gene expression, soluble factor expression, macrophage polarization and angiogenesis (Robb et al., 2022b). Quantification of these critical quality attributes would serve to prospectively screen potent MSC donors or cell culture conditions to optimize for the desired basal MSC immunomodulatory or angiogenic fitness.

3.3 Autologous vs. allogeneic origin of MSCs

While autologous MSCs were historically favored for their lower risk of immune rejection, in recent years, the medical community has increasingly embraced allogeneic sources owing to immunological » invisibility« of MSCs in general. This shift can be ascribed to several factors, including their convenience, optimal donor and tissue selection, cost-effectiveness, as well as a compelling body of clinical evidence supporting their efficacy and safety. Still, some warn that the discrepancies between outcomes of murine preclinical models and human clinical trials could be attributed to the pre-clinical mouse data overwhelming use of syngeneic, major histocompatibility complex (MHC)-matched cells when examining efficacy endpoints (Galipeau and Sensebe, 2018; Giri and Galipeau, 2020). Indeed, repeated intra-articular injection of allogeneic mesenchymal stem cells in equine model resulted in an adverse clinical response, suggesting there is a potential for immune recognition of allogeneic MSCs upon repetitive exposures (Joswig et al., 2017).

Unfortunately, clinical trials directly comparing the application of allogeneic and autologous MSCs are rare and often inconclusive, primarily due to small sample sizes (Hare et al., 2012a). However, a study comparing safety and efficacy of autologous and allogeneic BM-MSCs in patients with non-ischemic dilated cardiomyopathy reported superior efficacy for allogeneic MSCs (Hare et al., 2012b)). A recent study comparing transplantation of autologous BM-MNCs (bone marrow mononuclear cells) to allogeneic WJ-MSCs into diabetic patients with chronic limb-threatening ischemia confirmed that both treatments are safe and effective. However, the therapeutic benefit was more pronounced when treating patients with allogeneic WJ-MSCs (Arango-Rodriguez et al., 2023). Furthermore, in a study investigating the potential of MSCs to alleviate GVHD following hematopoietic stem cell transplantation, there was no observed correlation between donor HLA-match and response rate (Le Blanc et al., 2008).

A recent review evaluating the outcomes of clinical trials using culture-expanded MSCs to treat osteoarthritis could not definitively distinguish between autologous and allogeneic MSCs in terms of efficacy (Copp et al., 2023). Similarly, *in vitro* study comparing immunomodulating effects of autologous and full HLA mismatched donor MSCs relative to the responder cells did not detect any significant difference in inhibition of PBMC proliferation (Waldner et al., 2018). Conversely, in a meta-analysis of randomized controlled trials comparing the efficacy and safety of autologous and allogeneic MSCs for knee osteoarthritis management, autologous MSCs emerged as superior in providing

long-term pain relief and a lower incidence of adverse events (Jeyaraman et al., 2022).

Autologous MSCs sources can prove functionally inferior to allogeneic, especially when derived from donors with underlying systemic diseases. For example, AD-MSC derived from patients with chronic obstructive pulmonary disease exhibited decreased migration capacity than those derived from healthy donors. Still, they were equally efficient at reducing lung emphysematic damage in a mouse model (Rio et al., 2023). Importantly, autologous MSCs may exhibit suboptimal quality and fail to meet the requisite criteria for clinical utility, most often due to quality of starting material (Alves-Paiva et al., 2022). For example, a study investigating safety and feasibility of intramuscular transplantation of autologous BM-MSCs for patients with no-option critical limb ischemia reported a high rate of karyotype abnormalities in expanded cells (Mohamed et al., 2020). Moreover, MSCs derived from patients with type 2 diabetes displayed altered phenotype that most likely compromised their therapeutic efficacy (Capilla-Gonzalez et al., 2018). Similarly, MSCs derived from patients with systemic lupus erythematosus displayed dysfunctional phenotype and while patients responded to allogeneic MSC treatment, no response was seen with autologous cell transplantation (Cheng et al., 2019; El-Jawhari et al., 2021).

There is yet no clear clinical evidence to confirm whether autologous or allogeneic MSCs are superior to one another. It is plausible that specific conditions, especially those requiring tissue repair associated with MSC differentiation, may benefit more from autologous MSCs, while others, particularly may derive greater benefits from allogeneic MSCs. However, given the numerous advantages associated with allogeneic MSCs, particularly the greater ease of acquisition and production, it is probable that allogeneic MSCs will increasingly replace autologous cell sources.

4 Defining the optimal tissue source

Given the several tissues from which MSCs can be obtained, a natural question arises: which source is the most suitable? While multiple factors contribute to the decision made by institutions or medical teams, some sources offer more advantages than others. While bone marrow has traditionally served as a primary source for MSCs, the therapeutic potential of BM-MSCs is constrained by invasive harvesting techniques, suboptimal collection efficiency, age-related decline in quality, and donor-associated morbidities. On the other hand, a particularly advantageous source is the umbilical cord, primarily due to its noninvasive, low cost and ethically acceptable collection procedure.

4.1 Umbilical cord as a superior source of MSCs?

UC-MSCs can be isolated from various compartments including Wharton's jelly, veins, arteries, umbilical cord lining, subamnion, perivascular regions, or the whole umbilical cord (Nagamura-Inoue and He, 2014). In recent years, Wharton's jelly, the mucoid connective tissue surrounding the umbilical cord's arteries and vein, has emerged as the preferred compartment for MSC isolation, although some argue that whole umbilical cord offers more advantages (Subramanian et al., 2015; Semenova et al., 2021).

UC-MSCs are considered more primitive than MSCs derived from adult tissues because they share more common gene expression with embryonic stem cells and show higher expandability *in vitro* (Hsieh et al., 2010; Musiał-Wysocka et al., 2019). Additionally, studies have reported a stronger immunomodulatory potential for UC-MSC in comparison to MSCs derived from alternative tissue sources. For example, higher expression levels of immunosuppressive molecules CD152 and HLA-G have been observed in UC-MSC compared to AD-MSC and DT-MSC (Zoehler et al., 2022). Furthermore, scRNA-seq data from MSCs originating from four distinct tissues reveal UC-MSCs as possessing the highest immunoregulatory scores among the analyzed samples (Hou et al., 2021). UC-MSCs have also demonstrated superior immunosuppressive function in comparison to BM-MSC in MLR and mitogen-induced T-cell proliferation (Ketterl et al., 2015b). Importantly, the use of UC-MSCs allows for planned selection of starting materials, using perfectly healthy donors, thereby avoiding potential functional compromises of final MSC products that could arise from patient-derived, autologous products (Oliva-Olivera et al., 2015; Widholz et al., 2019). It also allows for the opportunity to avoid age-related problems, which can represent an important issue BM-or AD-MSCs derived from elderly patients. Nevertheless, special attention should be given to gestational age when harvesting umbilical cords. As shown by Iwatani et al. UC-MSC proliferation can vary significantly when comparing pre-term and term UC-MSCs, a phenomenon demonstrated to be dependent by differential expression of the WNT pathway (Iwatani et al., 2017).

In clinical settings, BM-MSCs and UC-MSCs displayed comparable therapeutic effects when transplanted into patients with type 1 diabetes, including improvements in glycemic control and the preservation of β-cells (Zhang W. et al., 2022). More importantly, a systematic review investigating the generation of donor-specific antibodies after allogeneic MSC treatment has revealed that only when MSCs were obtained from the umbilical cord, there was no allo-response in any of the treated patients (Sanabria-de la Torre et al., 2021). The especially low immunogenicity of UC-MSCs compared to other MSC types renders their use particularly relevant in repetitive administration protocols, considering the possibility of immune sensitization and subsequent allo-rejection of the cellular product. Regarding specific aspects of their clinical utility, UC-MSC could prove to be superior in regenerative medicine particularly for treatments relying on increased neoangiogenesis. Namely, Kehl et al. have performed a detailed proteomic analysis, showing that MSC derived from wharton's jelly display an enriched profile of angiogenic factors, with significantly higher concentrations of angiogenic proteins, compared to AD-MSCs and BM-MSCs (Kehl et al., 2019). Such differences between MSC types could have important implications for MSC selection in future clinical studies.

4.1.1 Differentiation potential of UC-MSCs in tissue regeneration

Most of the studies report reduced differentiation capacity of UC-MSCs compared to MSCs derived from other tissue sources (Batsali et al., 2017; Todtenhaupt et al., 2023). It was suggested that

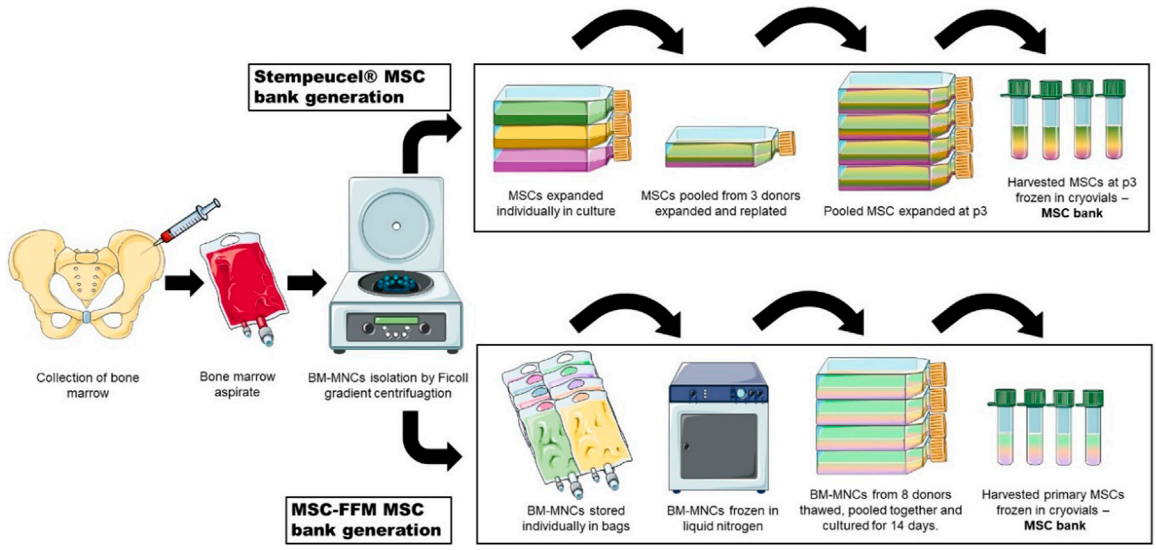

FIGURE 4
Two strategies of MSC pooling currently used in therapeutic applications. MSCs from three donors are individually expanded and then pooled together for Stempeucel® MSC bank generation. On the other hand, in MSC-FFM, MNCs from eight donors are pooled together before cells attach to the surface of tissue culture flasks. After expansion, cells are harvested and stored in cryovials to constitute a MSC bank.

the differential expression of the WNT pathway-associated molecules could have a role in the inferior osteogenic and adipogenic potential of UC-MSCs compared to BM-MSCs (Batsali et al., 2017). Interestingly, while UC-MSCs display a lower capacity for differentiation along osteogenic, adipogenic, and chondrogenic lineages compared to BM-MSCs, they outperform BM-MSCs in tenogenic differentiation. Namely, they exhibit superiority in forming a well-organized tendon-like matrix and in enhancing full-thickness tendon defect regeneration (Yea et al., 2023).

Along these lines, a meta-analysis comparing bone marrow aspirate concentrate (BM-AC) with CB-MSCs as a supporting treatment in various knee osteoarthritis patients undergoing high tibial osteotomy reported improved clinical outcomes in both groups. However, CB-MSCs allowed for a better articular cartilage regeneration than BM-AC augmentation (Park et al., 2023).

On the other hand, some studies have demonstrated higher osteogenic differentiation of UC-MSCs than BM-MSCs (Baksh et al., 2007). And a recent systematic review, centered on MSC transplantation for articular cartilage lesions in the human knee, established that UC-MSC transplants yielded superior outcomes when compared to BM-AC (Wang and Xing, 2023).

4.2 Pooled MSCs vs. MSCs from individual donors

The variability in biological properties among MSCs due to donor-to-donor heterogeneity is compromising the quality of data and hindering inter-study comparability. Pooling MSCs from several different donors has been proposed as a strategy to overcome these challenges (Zyrafete et al., 2016). The aim was to reduce the variance observed across donors. One of the first studies has shown that pooling MSCs leads to a greater increase of their ability to suppress lymphocyte proliferation than performances of MSCs derived from individual donors (Samuelsson et al., 2009). This was confirmed to some extent clinically by Ringden et al. where BM-MSCs from two different donors were pooled to treat a patient with myelofibrosis experiencing severe hemorrhage, yielding an encouraging outcome (Ringden and Leblanc, 2011).

Since then, several strategies of pooling MSCs have been tried, revealing interesting findings. More recently, we have also witnessed publications of GMP-compliant protocols for manufacture of MSCs, pooled from different donors (Padhiar et al., 2022). A study comparing the immunosuppressive potential of single batches to pooled products of MSCs prepared from iliac crest bone marrow aspirates did not show a significant difference that would favor pooled MSCs over MSCs from single donor batches. The allo-suppressive potential was comparable in both variants (Hejretova et al., 2020). Other studies comparing MSCs from various tissue sources have confirmed compensation for intra-individual variances among donors. However, there was no statistically significant difference in their immunosuppressive potential between the mean of a single MSC donor and pooled donors (Hansen et al., 2022). On the other hand, pooling BM-MNCs together before generation of BM-MSCs led to a significantly higher allosuppressive potential of the pooled cells. This phenomenon indicates that MNC pooling induces a strong alloreaction, which could positively select progenitor cell fractions for MSCs with higher allosuppressive potential, either through cell–cell interactions and/or soluble molecules (Zyrafete et al., 2016; Bieback et al., 2019). Among the published data, Waldner et al. had a surprisingly different approach–they pooled cells from the same donor but from different tissue sources, specifically bone marrow and adipose tissue. Interestingly, the pooled cells demonstrated a synergistic immunosuppressive effect on PBMC proliferation (Waldner et al., 2018).

Examining other characteristics after establishing MSC pools reveals varied reports. Some studies confirmed a correlation between mean proliferation rate of individual donors to proliferation rate of pooled MSCs (Zyrafete et al., 2016). Others, however, observed a higher population doubling for pooled cells compared to individual batches, inferring that the fast proliferating cells contribute more towards the whole cell population in the pooled setting, resulting in faster overall proliferation rate and eventually increasing the relative portion of the respective cells (Widholz et al., 2019). It has been shown that pooling BM-MSCs at different passages does not change their functional characteristics or diminish their quality (Willer et al., 2022). Additionally, introducing multiple rounds of cryopreservation of pooled cells does not induce significant changes in their fundamental characteristics (Mamidi et al., 2012). However, comparing WJ-MSCs from individual donors to cells pooled from three donors revealed lower levels of expression of pro-inflammatory cytokines in the pooled batches. This observation prompted speculation that the act of pooling MSCs could potentially create a slightly inflammatory microenvironment, consequently directing MSCs toward a more immunosuppressive phenotype. Still, the immunosuppressive potential of the pooled MSCs remained similar to that of individual donor cells (Kannan et al., 2022).

Currently, two MSC products containing pooled cells for therapeutic applications are in active use (Figure 4). Leading the way is Stempeutics, an India-based company and the first to commercialize pooled MSCs. Their advanced therapy medicinal product, Stempeucel®, consists of BM-MSCs pooled from three healthy donors and is intended to treat a variety of conditions such as limb ischemia, osteoarthritis of the knee joint, perianal fistulas and diabetic foot ulcers (Rengasamy et al., 2016; Gupta et al., 2017; Thej et al., 2017; Gupta et al., 2023a; Gupta et al., 2023b). The other is generated from pooled BM-MNCs from eight allogeneic donors, also referred to as "MSC-Frankfurt am Main" or MSC-FFM, named after the city where it was produced. This pooled product is licensed with a national hospital exemption authorization in Germany. It is applied to patients with steroid and therapy-refractory acute GvHD and was shown to be safe and effective (Zyrafete et al., 2016; Bader et al., 2018; Bonig et al., 2019).

While the use of pooled MSCs definitely represents several potential advancements toward product harmonization, as well as offering several logistical solutions, potential limitations should be addressed. One such is the potential for alloreactive immune response associated with allogeneic cell therapy treatments. Most likely, this is not an issue of great concern, since MSCs are widely recognized as hypoimmunogenic (due to low expression of HLA molecules) and their allogeneic clinical use is extensively documented, confirming safety. Nevertheless, consideration of histocompatibility barriers along with anticipation of immune rejections and immune sensitization reactions should be kept in mind. For example, certain percentage of patients have been shown to develop alloantibodies and subsequent immune rejection of administered MSCs (Sanabria-de la Torre et al., 2021). Even in case of UC-MSCs, where the formation of alloantibodies is seldom reported, this phenomenon could be potentially amplified using pooled MSC products from different donors, where HLA diversity is further increased.

5 Conclusion

The potential of MSCs to regulate the host immune system and promote tissue regeneration through paracrine signaling offers a great promise for addressing a variety of issues. However, studies that would reproducibly and reliably confirm this potential in clinical setting are still lacking. One of the culprits most frequently implicated in these discrepancies is the heterogeneity of transplanted MSC batches. It can arise from inherent biological differences among tissue sources, donors and MSC subpopulations or it can be introduced by variations in preparation protocols. Strategies to mitigate these differences could range from careful selection of tissue source, donors and specific MSC subpopulations, to harmonized growing conditions, potency assays and administration protocols. Amidst the multitude of options, we also propose an off the shelf approach of pooling UC-MSCs to increase consistency and homogeneity of the final cell product. UC-MSCs are relatively easy to obtain and have several advantageous characteristics in comparison to MSCs derived from other tissue sources. Moreover, pooling UC-MSCs from several donors would reduce inter-donor variability, improve dose-to-dose equivalence between patients, and facilitate the comparison of therapeutic efficacy across clinical studies. This approach could be relatively easily implemented in hospital GMP manufacturing centers. The main pre-requisites are established standard operating protocols in association with maternity wards for the supply of biological starting materials, and obviously for MSC manufacture. In addition, the pre-requisite that a well-managed cryobank is present for storing allogeneic MSC aliquots is key. In closing, we propose increased academic research efforts in the area of MSC pooling, to further resolve potential benefits, as well as its limitations and challenges on the path toward standardized and homogeneous MSC-based ATMPs.

Author contributions

AC: Investigation, Writing–original draft. US: Conceptualization, Investigation, Supervision, Writing–original draft, Writing–review and editing.

Funding

The author(s) declare that financial support was received for the research, authorship, and/or publication of this article. This work was partially supported by the program P3-0371 of the Slovenian Research Agency.

Conflict of interest

The authors declare that the research was conducted in the absence of any commercial or financial relationships that could be construed as a potential conflict of interest.

The author(s) declared that they were an editorial board member of Frontiers, at the time of submission. This had no impact on the peer review process and the final decision.

Publisher's note

References

Aabling, R. R., Alstrup, T., Kjær, E. M., Poulsen, K. J., Pedersen, J. O., Revenfeld, A. L., et al. (2023). Reconstitution and post-thaw storage of cryopreserved human mesenchymal stromal cells: pitfalls and optimizations for clinically compatible formulants. *Regen. Ther.* 23, 67–75. doi:10.1016/j.reth.2023.03.006

Afzal, E., Pakzad, M., Nouri, M., Moghadasali, R., and Zarrabi, M. (2023). Human umbilical cord serum as an alternative to fetal bovine serum for *in vitro* expansion of umbilical cord mesenchymal stromal cells. *Cell. Tissue Bank.* 24 (1), 59–66. doi:10.1007/s10561-022-10011-x

Aghayan, H. R., Salimian, F., Abedini, A., Fattah Ghazi, S., Yunesian, M., Alavi-Moghadam, S., et al. (2022). Human placenta-derived mesenchymal stem cells transplantation in patients with acute respiratory distress syndrome (ARDS) caused by COVID-19 (phase I clinical trial): safety profile assessment. *Stem Cell. Res. Ther.* 13 (1), 365. doi:10.1186/s13287-022-02953-6

Al Bahrawy, M. (2021). Comparison of the migration potential through microperforated membranes of CD146+ GMSC population versus heterogeneous GMSC population. *Stem Cells Int.* 2021, 5583421. doi:10.1155/2021/5583421

Allickson, J. G., Sanchez, A., Yefimenko, N., Borlongan, C. V., and Sanberg, P. R. (2011). Recent studies assessing the proliferative capability of a novel adult stem cell identified in menstrual blood. *Open Stem Cell. J.* 3, 4–10. doi:10.2174/1876893801103010004

Altrock, E., Sens-Albert, C., Hofmann, F., Riabov, V., Schmitt, N., Xu, Q., et al. (2023). Significant improvement of bone marrow-derived MSC expansion from MDS patients by defined xeno-free medium. *Stem Cell. Res. Ther.* 14 (1), 156. doi:10.1186/s13287-023-03386-5

Alves-Paiva, R. M., do Nascimento, S., De Oliveira, D., Coa, L., Alvarez, K., Hamerschlak, N., et al. (2022). Senescence state in mesenchymal stem cells at low passages: implications in clinical use. *Front. Cell. Dev. Biol.* 10, 858996. doi:10.3389/fcell.2022.858996

Anerillas, L. O., Wiberg, M., Kingham, P. J., and Kelk, P. (2023). Platelet lysate for expansion or osteogenic differentiation of bone marrow mesenchymal stem cells for 3D tissue constructs. *Regen. Ther.* 24, 298–310. doi:10.1016/j.reth.2023.07.011

Arango-Rodriguez, M. L., Mateus, L. C., Sossa, C. L., Becerra-Bayona, S. M., Solarte-David, V. A., Ochoa Vera, M. E., et al. (2023). A novel therapeutic management for diabetes patients with chronic limb-threatening ischemia: comparison of autologous bone marrow mononuclear cells versus allogenic Wharton jelly-derived mesenchymal stem cells. *Stem Cell. Res. Ther.* 14 (1), 221. doi:10.1186/s13287-023-03427-z

Arnaoutova, I., George, J., Kleinman, H. K., and Benton, G. (2009). The endothelial cell tube formation assay on basement membrane turns 20: state of the science and the art. *Angiogenesis* 12 (3), 267–274. doi:10.1007/s10456-009-9146-4

Aussel, C., Busson, E., Vantomme, H., Peltzer, J., and Martinaud, C. (2022). Quality assessment of a serum and xenofree medium for the expansion of human GMP-grade mesenchymal stromal cells. *PeerJ* 10, e13391. doi:10.7717/peerj.13391

Au - Ylostalo, J. H., Bazhanov, N., Mohammadipoor, A., and Bartosh, T. J. (2017). Production and administration of therapeutic mesenchymal stem/stromal cell (MSC) spheroids primed in 3-D cultures under xeno-free conditions. *JoVE* (121), e55126. doi:10.3791/55126

Avercenc-Leger, L., Guerci, P., Virion, J. M., Cauchois, G., Hupont, S., Rahouadj, R., et al. (2017). Umbilical cord-derived mesenchymal stromal cells: predictive obstetric factors for cell proliferation and chondrogenic differentiation. *Stem Cell. Res. Ther.* 8 (1), 161. doi:10.1186/s13287-017-0609-z

Bader, P., Kuçi, Z., Bakhtiar, S., Basu, O., Bug, G., Dennis, M., et al. (2018). Effective treatment of steroid and therapy-refractory acute graft-versus-host disease with a novel mesenchymal stromal cell product (MSC-FFM). *Bone Marrow Transpl.* 53 (7), 852–862. doi:10.1038/s41409-018-0102-z

Bahsoun, S., Coopman, K., and Akam, E. C. (2020). Quantitative assessment of the impact of cryopreservation on human bone marrow-derived mesenchymal stem cells: up to 24 h post-thaw and beyond. *Stem Cell. Res. Ther.* 11 (1), 540. doi:10.1186/s13287-020-02054-2

Bajetto, A., Pattarozzi, A., Sirito, R., Barbieri, F., and Florio, T. (2023). Metformin potentiates immunosuppressant activity and adipogenic differentiation of human umbilical cord-mesenchymal stem cells. *Int. Immunopharmacol.* 124 (Pt B), 111078. doi:10.1016/j.intimp.2023.111078

Baksh, D., Yao, R., and Tuan, R. S. (2007). Comparison of proliferative and multilineage differentiation potential of human mesenchymal stem cells derived from umbilical cord and bone marrow. *Stem Cells* 25 (6), 1384–1392. doi:10.1634/stemcells.2006-0709

Barilani, M., Banfi, F., Sironi, S., Ragni, E., Guillaumin, S., Polveraccio, F., et al. (2018). Low-affinity nerve growth factor receptor (CD271) heterogeneous expression in adult and fetal mesenchymal stromal cells. *Sci. Rep.* 8 (1), 9321. doi:10.1038/s41598-018-27587-8

Bartosh, T. J., and Ylostalo, J. H. (2014). Preparation of anti-inflammatory mesenchymal stem/precursor cells (MSCs) through sphere formation using hanging-drop culture technique. *Curr. Protoc. Stem Cell. Biol.* 28 (1), 2B.6.1–2B.6.23. doi:10.1002/9780470151808.sc02b06s28

Bartosh, T. J., Ylöstalo, J. H., Mohammadipoor, A., Bazhanov, N., Coble, K., Claypool, K., et al. (2010a). Aggregation of human mesenchymal stromal cells (MSCs) into 3D spheroids enhances their antiinflammatory properties. *Proc. Natl. Acad. Sci.* 107 (31), 13724–13729. doi:10.1073/pnas.1008117107

Bartosh, T. J., Ylöstalo, J. H., Mohammadipoor, A., Bazhanov, N., Coble, K., Claypool, K., et al. (2010b). Aggregation of human mesenchymal stromal cells (MSCs) into 3D spheroids enhances their antiinflammatory properties. *Proc. Natl. Acad. Sci. U. S. A.* 107 (31), 13724–13729. doi:10.1073/pnas.1008117107

Batsali, A. K., Pontikoglou, C., Koutroulakis, D., Pavlaki, K. I., Damianaki, A., Mavroudi, I., et al. (2017). Differential expression of cell cycle and WNT pathway-related genes accounts for differences in the growth and differentiation potential of Wharton's jelly and bone marrow-derived mesenchymal stem cells. *Stem Cell. Res. Ther.* 8 (1), 102. doi:10.1186/s13287-017-0555-9

Beckenkamp, L. R., Souza, L. E. B., Melo, F. U. F., Thomé, C. H., Magalhães, D. A. R., Palma, P. V. B., et al. (2018). Comparative characterization of CD271(+) and CD271(-) subpopulations of CD34(+) human adipose-derived stromal cells. *J. Cell. Biochem.* 119 (5), 3873–3884. doi:10.1002/jcb.26496

Beeravolu, N., McKee, C., Alamri, A., Mikhael, S., Brown, C., Perez-Cruet, M., et al. (2017). Isolation and characterization of mesenchymal stromal cells from human umbilical cord and fetal placenta. *J. Vis. Exp.* (122), 55224. doi:10.3791/55224

Bieback, K. (2013). Platelet lysate as replacement for fetal bovine serum in mesenchymal stromal cell cultures. *Transfus. Med. Hemotherapy* 40 (5), 326–335. doi:10.1159/000354061

Bieback, K., Kuçi, S., and Schäfer, R. (2019). Production and quality testing of multipotent mesenchymal stromal cell therapeutics for clinical use. *Transfusion* 59 (6), 2164–2173. doi:10.1111/trf.15252

Bikorimana, J. P., Saad, W., Abusarah, J., Lahrichi, M., Talbot, S., Shammaa, R., et al. (2022). CD146 defines a mesenchymal stromal cell subpopulation with enhanced suppressive properties. *Cells* 11 (15), 2263. doi:10.3390/cells11152263

Bonig, H., Kuçi, Z., Kuçi, S., Bakhtiar, S., Basu, O., Bug, G., et al. (2019). Children and adults with refractory acute graft-versus-host disease respond to treatment with the mesenchymal stromal cell preparation "MSC-FFM"-Outcome report of 92 patients. *Cells* 8 (12), 1577. doi:10.3390/cells8121577

Bowles, A. C., Kouroupis, D., Willman, M. A., Perucca Orfei, C., Agarwal, A., and Correa, D. (2020). Signature quality attributes of CD146(+) mesenchymal stem/stromal cells correlate with high therapeutic and secretory potency. *Stem Cells* 38 (8), 1034–1049. doi:10.1002/stem.3196

Bozorgmehr, M., Gurung, S., Darzi, S., Nikoo, S., Kazemnejad, S., Zarnani, A. H., et al. (2020). Endometrial and menstrual blood mesenchymal stem/stromal cells: biological properties and clinical application. *Front. Cell. Dev. Biol.* 8, 497. doi:10.3389/fcell.2020.00497

Brinkhof, B., Zhang, B., Cui, Z., Ye, H., and Wang, H. (2020). ALCAM (CD166) as a gene expression marker for human mesenchymal stromal cell characterisation. *Gene* 763, 100031. doi:10.1016/j.gene.2020.100031

Budeus, B., Unger, K., Hess, J., Sentek, H., and Klein, D. (2023a). Comparative computational analysis to distinguish mesenchymal stem cells from fibroblasts. *Front. Immunol.* 14, 1270493. doi:10.3389/fimmu.2023.1270493

Budeus, B., Unger, K., Hess, J., Sentek, H., and Klein, D. (2023b). Comparative computational analysis to distinguish mesenchymal stem cells from fibroblasts. *Front. Immunol.* 14, 1270493. doi:10.3389/fimmu.2023.1270493

Calcat-i-Cervera, S., Rendra, E., Scaccia, E., Amadeo, F., Hanson, V., Wilm, B., et al. (2023). Harmonised culture procedures minimise but do not eliminate mesenchymal stromal cell donor and tissue variability in a decentralised multicentre manufacturing approach. *Stem Cell. Res. Ther.* 14 (1), 120. doi:10.1186/s13287-023-03352-1

Camilleri, E. T., Gustafson, M. P., Dudakovic, A., Riester, S. M., Garces, C. G., Paradise, C. R., et al. (2016). Identification and validation of multiple cell surface markers of clinical-grade adipose-derived mesenchymal stromal cells as novel release criteria for good manufacturing practice-compliant production. *Stem Cell. Res. Ther.* 7 (1), 107. doi:10.1186/s13287-016-0370-8

Cañas-Arboleda, M., Beltrán, K., Medina, C., Camacho, B., and Salguero, G. (2020). Human platelet lysate supports efficient expansion and stability of wharton's jelly mesenchymal stromal cells via active uptake and release of soluble regenerative factors. *Int. J. Mol. Sci.* 21 (17), 6284. doi:10.3390/ijms21176284

Caneparo, C., Chabaud, S., Fradette, J., and Bolduc, S. (2022). Evaluation of a serum-free medium for human epithelial and stromal cell culture. *Int. J. Mol. Sci.* 23 (17), 10035. doi:10.3390/ijms231710035

Capilla-Gonzalez, V., López-Beas, J., Escacena, N., Aguilera, Y., de la Cuesta, A., Ruiz-Salmerón, R., et al. (2018). PDGF restores the defective phenotype of adipose-derived mesenchymal stromal cells from diabetic patients. *Mol. Ther.* 26 (11), 2696–2709. doi:10.1016/j.ymthe.2018.08.011

Caplan, A. I. (1991). Mesenchymal stem cells. *J. Orthop. Res.* 9 (5), 641–650. doi:10.1002/jor.1100090504

Carpentier, G., Berndt, S., Ferratge, S., Rasband, W., Cuendet, M., Uzan, G., et al. (2020). Angiogenesis analyzer for ImageJ - a comparative morphometric analysis of "endothelial tube formation assay" and "fibrin bead assay". *Sci. Rep.* 10 (1), 11568. doi:10.1038/s41598-020-67289-8

Cen, J., Zhang, Y., Bai, Y., Ma, S., Zhang, C., Jin, L., et al. (2022). Research progress of stem cell therapy for endometrial injury. *Mater Today Bio* 16, 100389. doi:10.1016/j.mtbio.2022.100389

Cesarz, Z., and Tamama, K. (2016). Spheroid culture of mesenchymal stem cells. *Stem Cells Int.* 2016, 9176357. doi:10.1155/2016/9176357

Chang, W. L., Lee, W. R., Kuo, Y. C., and Huang, Y. H. (2021). Vitiligo: an autoimmune skin disease and its immunomodulatory therapeutic intervention. *Front. Cell. Dev. Biol.* 9, 797026. doi:10.3389/fcell.2021.797026

Chen, D., Liu, S., Chu, X., Reiter, J., Gao, H., McGuire, P., et al. (2023). Osteogenic differentiation potential of mesenchymal stem cells using single cell multiomic analysis. *Genes.* 14 (10), 1871. doi:10.3390/genes14101871

Chen, H., Wen, X., Liu, S., Sun, T., Song, H., Wang, F., et al. (2022). Dissecting heterogeneity reveals a unique BAMBI(high) MFGE8(high) subpopulation of human UC-MSCs. *Adv. Sci. (Weinh)* 10 (1), e2202510. doi:10.1002/advs.202202510

Cheng, R. J., Xiong, A. J., Li, Y. H., Pan, S. Y., Zhang, Q. P., Zhao, Y., et al. (2019). Mesenchymal stem cells: allogeneic MSC may Be immunosuppressive but autologous MSC are dysfunctional in lupus patients. *Front. Cell. Dev. Biol.* 7, 285. doi:10.3389/fcell.2019.00285

Cheung, T. S., Bertolino, G. M., Giacomini, C., Bornhäuser, M., Dazzi, F., and Galleu, A. (2020). Mesenchymal stromal cells for graft versus host disease: mechanism-based biomarkers. *Front. Immunol.* 11, 1338. doi:10.3389/fimmu.2020.01338

Chinnadurai, R., Rajan, D., Qayed, M., Arafat, D., Garcia, M., Liu, Y., et al. (2018). Potency analysis of mesenchymal stromal cells using a combinatorial assay matrix approach. *Cell. Rep.* 22 (9), 2504–2517. doi:10.1016/j.celrep.2018.02.013

Choudhery, M. S., Badowski, M., Muise, A., Pierce, J., and Harris, D. T. (2014). Donor age negatively impacts adipose tissue-derived mesenchymal stem cell expansion and differentiation. *J. Transl. Med.* 12 (1), 8. doi:10.1186/1479-5876-12-8

Christy, B. A., Herzig, M. C., Delavan, C. P., Abaasah, I., Cantu, C., Salgado, C., et al. (2020). Use of multiple potency assays to evaluate human mesenchymal stromal cells. *J. Trauma Acute Care Surg.* 89 (2S Suppl. 2), S109-S117–S117. doi:10.1097/TA.0000000000002743

Ciuffreda, M. C., Malpasso, G., Musaro, P., Turco, V., and Gnecchi, M. (2016). "Protocols for *in vitro* differentiation of human mesenchymal stem cells into osteogenic, chondrogenic and adipogenic lineages," in *Mesenchymal stem cells: methods and protocols*. Editor M. Gnecchi (New York, NY: Springer New York), 149–158.

Copp, G., Robb, K. P., and Viswanathan, S. (2023). Culture-expanded mesenchymal stromal cell therapy: does it work in knee osteoarthritis? A pathway to clinical success. *Cell. Mol. Immunol.* 20 (6), 626–650. doi:10.1038/s41423-023-01020-1

Cruz-Barrera, M., Flórez-Zapata, N., Lemus-Diaz, N., Medina, C., Galindo, C. C., González-Acero, L. X., et al. (2020). Integrated analysis of transcriptome and secretome from umbilical cord mesenchymal stromal cells reveal new mechanisms for the modulation of inflammation and immune activation. *Front. Immunol.* 11, 575488. doi:10.3389/fimmu.2020.575488

Czarnecka, A., Odziomek, A., Murzyn, M., Dubis, J., Bagłaj-Oleszczuk, M., and Hryncewicz-Gwóźdź, A. (2021). Wharton's jelly-derived mesenchymal stem cells in the treatment of four patients with alopecia areata. *Adv. Clin. Exp. Med.* 30 (2), 211–218. doi:10.17219/acem/132069

Dam, P. T. M., Hoang, V. T., Bui, H. T. H., Hang, L. M., Hoang, D. M., Nguyen, H. P., et al. (2021). Human adipose-derived mesenchymal stromal cells exhibit high HLA-DR levels and altered cellular characteristics under a xeno-free and serum-free condition. *Stem Cell. Rev. Rep.* 17 (6), 2291–2303. doi:10.1007/s12015-021-10242-7

DeCicco-Skinner, K. L., Henry, G. H., Cataisson, C., Tabib, T., Gwilliam, J. C., Watson, N. J., et al. (2014). Endothelial cell tube formation assay for the *in vitro* study of angiogenesis. *J. Vis. Exp.* (91), e51312. doi:10.3791/51312

Denu, R. A., Nemcek, S., Bloom, D. D., Goodrich, A. D., Kim, J., Mosher, D. F., et al. (2016). Fibroblasts and mesenchymal stromal/stem cells are phenotypically indistinguishable. *Acta Haematol.* 136 (2), 85–97. doi:10.1159/000445096

DeWolf, S., Shen, Y., and Sykes, M. (2016). A new window into the human alloresponse. *Transplantation* 100 (8), 1639–1649. doi:10.1097/TP.0000000000001064

Dominici, M., Le Blanc, K., Mueller, I., Slaper-Cortenbach, I., Marini, F., Krause, D., et al. (2006). Minimal criteria for defining multipotent mesenchymal stromal cells. The International Society for Cellular Therapy position statement. *Cytotherapy* 8 (4), 315–317. doi:10.1080/14653240600855905

Drela, K., Sarnowska, A., Siedlecka, P., Szablowska-Gadomska, I., Wielgos, M., Jurga, M., et al. (2014). Low oxygen atmosphere facilitates proliferation and maintains undifferentiated state of umbilical cord mesenchymal stem cells in an hypoxia inducible factor-dependent manner. *Cytotherapy* 16 (7), 881–892. doi:10.1016/j.jcyt.2014.02.009

Du, J., Zhao, L., Kang, Q., He, Y., and Bi, Y. (2023). An optimized method for Oil Red O staining with the salicylic acid ethanol solution. *Adipocyte* 12 (1), 2179334. doi:10.1080/21623945.2023.2179334

Eggenhofer, E., Luk, F., Dahlke, M. H., and Hoogduijn, M. J. (2014). The life and fate of mesenchymal stem cells. *Front. Immunol.* 5, 148. doi:10.3389/fimmu.2014.00148

Eggerschwiler, B., Canepa, D. D., Pape, H. C., Casanova, E. A., and Cinelli, P. (2019). Automated digital image quantification of histological staining for the analysis of the trilineage differentiation potential of mesenchymal stem cells. *Stem Cell. Res. Ther.* 10 (1), 69. doi:10.1186/s13287-019-1170-8

El-Jawhari, J. J., El-Sherbiny, Y., McGonagle, D., and Jones, E. (2021). Multipotent mesenchymal stromal cells in rheumatoid arthritis and systemic lupus erythematosus; from a leading role in pathogenesis to potential therapeutic saviors? *Front. Immunol.* 12, 643170. doi:10.3389/fimmu.2021.643170

Fan, C., Liao, M., Xie, L., Huang, L., Lv, S., Cai, S., et al. (2022). Single-cell transcriptome integration analysis reveals the correlation between mesenchymal stromal cells and fibroblasts. *Front. Genet.* 13, 798331. doi:10.3389/fgene.2022.798331

Fernandez-Rebollo, E., Mentrup, B., Ebert, R., Franzen, J., Abagnale, G., Sieben, T., et al. (2017). Human platelet lysate versus fetal calf serum: these supplements do not select for different mesenchymal stromal cells. *Sci. Rep.* 7 (1), 5132. doi:10.1038/s41598-017-05207-1

Franquesa, M., Hoogduijn, M. J., Reinders, M. E., Eggenhofer, E., Engela, A. U., Mensah, F. K., et al. (2013). Mesenchymal stem cells in solid organ transplantation (MiSOT) fourth meeting: lessons learned from first clinical trials. *Transplantation* 96 (3), 234–238. doi:10.1097/TP.0b013e318298f9fa

Fuentes, P., Torres, M. J., Arancibia, R., Aulestia, F., Vergara, M., Carrión, F., et al. (2022). Dynamic culture of mesenchymal stromal/stem cell spheroids and secretion of paracrine factors. *Front. Bioeng. Biotechnol.* 10, 916229. doi:10.3389/fbioe.2022.916229

Gaitán-Salvatella, I., González-Alva, P., Montesinos, J. J., and Alvarez-Perez, M. A. (2023). *In vitro* bone differentiation of 3D microsphere from dental pulp-mesenchymal stem cells. *Bioengineering* 10 (5), 571. doi:10.3390/bioengineering10050571

Galipeau, J. (2013). The mesenchymal stromal cells dilemma--does a negative phase III trial of random donor mesenchymal stromal cells in steroid-resistant graft-versus-host disease represent a death knell or a bump in the road? *Cytotherapy* 15 (1), 2–8. doi:10.1016/j.jcyt.2012.10.002

Galipeau, J., Krampera, M., Barrett, J., Dazzi, F., Deans, R. J., DeBruijn, J., et al. (2016). International Society for Cellular Therapy perspective on immune functional assays for mesenchymal stromal cells as potency release criterion for advanced phase clinical trials. *Cytotherapy* 18 (2), 151–159. doi:10.1016/j.jcyt.2015.11.008

Galipeau, J., and Sensebe, L. (2018). Mesenchymal stromal cells: clinical challenges and therapeutic opportunities. *Cell. Stem Cell.* 22 (6), 824–833. doi:10.1016/j.stem.2018.05.004

Gallo, A., Cuscino, N., Contino, F., Bulati, M., Pampalone, M., Amico, G., et al. (2022). Changes in the transcriptome profiles of human amnion-derived mesenchymal stromal/stem cells induced by three-dimensional culture: a potential priming strategy to improve their properties. *Int. J. Mol. Sci.* 23 (2), 863. doi:10.3390/ijms23020863

Ganguly, P., El-Jawhari, J. J., Burska, A. N., Ponchel, F., Giannoudis, P. V., and Jones, E. A. (2019). *The Analysis of in vivo Aging in human bone marrow mesenchymal stromal cells using colony-forming unit-fibroblast Assay and the CD45*low*CD271+*</sup> phenotype. *Stem Cells Int.* 2019, 5197983. doi:10.1155/2019/5197983

Gao, S., Zhang, Y., Liang, K., Bi, R., and Du, Y. (2022). Mesenchymal stem cells (MSCs): a novel therapy for type 2 diabetes. *Stem Cells Int.* 2022, 8637493. doi:10.1155/2022/8637493

Giri, J., and Galipeau, J. (2020). Mesenchymal stromal cell therapeutic potency is dependent upon viability, route of delivery, and immune match. *Blood Adv.* 4 (9), 1987–1997. doi:10.1182/bloodadvances.2020001711

Graziano, A., d'Aquino, R., Laino, G., and Papaccio, G. (2008). Dental pulp stem cells: a promising tool for bone regeneration. *Stem Cell. Rev.* 4 (1), 21–26. doi:10.1007/s12015-008-9013-5

Gridelli, B., Vizzini, G., Pietrosi, G., Luca, A., Spada, M., Gruttadauria, S., et al. (2012). Efficient human fetal liver cell isolation protocol based on vascular perfusion for liver cell-based therapy and case report on cell transplantation. *Liver Transpl.* 18 (2), 226–237. doi:10.1002/lt.22322

Grossner, T., Haberkorn, U., and Gotterbarm, T. (2020). (18)F- based quantification of the osteogenic potential of hMSCs. *Int. J. Mol. Sci.* 21 (20), 7692. doi:10.3390/ijms21207692

Gupta, P. K., Krishna, M., Chullikana, A., Desai, S., Murugesan, R., Dutta, S., et al. (2017). Administration of adult human bone marrow-derived, cultured, pooled, allogeneic mesenchymal stromal cells in critical limb ischemia due to buerger's disease: phase II study report suggests clinical efficacy. *Stem Cells Transl. Med.* 6 (3), 689–699. doi:10.5966/sctm.2016-0237

Gupta, P. K., Maheshwari, S., Cherian, J. J., Goni, V., Sharma, A. K., Tripathy, S. K., et al. (2023a). Efficacy and safety of Stempeucel in osteoarthritis of the knee: a phase 3 randomized, double-blind, multicenter, placebo-controlled study. *Am. J. Sports Med.* 51 (9), 2254–2266. doi:10.1177/03635465231180323

Gupta, P. K., Maheshwari, S., Cherian, J. J., Goni, V., Sharma, A. K., Tripathy, S. K., et al. (2023b). Efficacy and safety of Stempeucel in osteoarthritis of the knee: a phase 3 randomized, double-blind, multicenter, placebo-controlled study. *Am. J. Sports Med.* 51 (9), 2254–2266. doi:10.1177/03635465231180323

Hammink, R., Weiden, J., Voerman, D., Popelier, C., Eggermont, L. J., Schluck, M., et al. (2021). Semiflexible immunobrushes induce enhanced T cell activation and expansion. *ACS Appl. Mater Interfaces* 13 (14), 16007–16018. doi:10.1021/acsami.0c21994

Han, H. T., Jin, W. L., and Li, X. (2022). Mesenchymal stem cells-based therapy in liver diseases. *Mol. Biomed.* 3 (1), 23. doi:10.1186/s43556-022-00088-x

Hansen, S. B., Højgaard, L. D., Kastrup, J., Ekblond, A., Follin, B., and Juhl, M. (2022). Optimizing an immunomodulatory potency assay for mesenchymal stromal cell. *Front. Immunol.* 13, 1085312. doi:10.3389/fimmu.2022.1085312

Hare, J. M., Fishman, J. E., Gerstenblith, G., DiFede Velazquez, D. L., Zambrano, J. P., Suncion, V. Y., et al. (2012a). Comparison of allogeneic vs autologous bone marrow-derived mesenchymal stem cells delivered by transendocardial injection in patients with ischemic cardiomyopathy: the POSEIDON randomized trial. *JAMA* 308 (22), 2369–2379. doi:10.1001/jama.2012.25321

Hare, J. M., Fishman, J. E., Gerstenblith, G., DiFede Velazquez, D. L., Zambrano, J. P., Suncion, V. Y., et al. (2012b). Comparison of allogeneic vs autologous bone marrow–derived mesenchymal stem cells delivered by transendocardial injection in patients with ischemic cardiomyopathy: the POSEIDON randomized trial. *JAMA* 308 (22), 2369–2379. doi:10.1001/jama.2012.25321

Haydont, V., Neiveyans, V., Perez, P., Busson, É., Lataillade, J., Asselineau, D., et al. (2020). Fibroblasts from the human skin dermo-hypodermal junction are distinct from dermal papillary and reticular fibroblasts and from mesenchymal stem cells and exhibit a specific molecular profile related to extracellular matrix organization and modeling. *Cells* 9 (2), 368. doi:10.3390/cells9020368

Hejretova, L., Čedíková, M., Dolejšová, M., Vlas, T., Jindra, P., Lysák, D., et al. (2020). Comparison of the immunomodulatory effect of single MSC batches versus pooled MSC products. *Cell. Tissue Bank.* 21 (1), 119–129. doi:10.1007/s10561-019-09805-3

Hematti, P. (2016). Characterization of mesenchymal stromal cells: potency assay development. *Transfusion* 56 (4), 32S-5S–5S. doi:10.1111/trf.13569

Herzig, M. C., Christy, B. A., Montgomery, R. K., Cantu-Garza, C., Barrera, G. D., Lee, J. H., et al. (2023). Short-term assays for mesenchymal stromal cell immunosuppression of T-lymphocytes. *Front. Immunol.* 14, 1225047. doi:10.3389/fimmu.2023.1225047

Herzig, M. C., Delavan, C. P., Jensen, K. J., Cantu, C., Montgomery, R. K., Christy, B. A., et al. (2021). A streamlined proliferation assay using mixed lymphocytes for evaluation of human mesenchymal stem cell immunomodulation activity. *J. Immunol. Methods* 488, 112915. doi:10.1016/j.jim.2020.112915

Hoch, A. I., and Leach, J. K. (2014). Concise review: optimizing expansion of bone marrow mesenchymal stem/stromal cells for clinical applications. *Stem Cells Transl. Med.* 3 (5), 643–652. doi:10.5966/sctm.2013-0196

Hou, W., Duan, L., Huang, C., Li, X., Xu, X., Qin, P., et al. (2021). Cross-tissue characterization of heterogeneities of mesenchymal stem cells and their differentiation potentials. *Front. Cell. Dev. Biol.* 9, 781021. doi:10.3389/fcell.2021.781021

Hsieh, J. Y., Chang, S. J., Tsuang, Y. H., and Wang, H. W. (2010). Functional module analysis reveals differential osteogenic and stemness potentials in human mesenchymal stem cells from bone marrow and Wharton's jelly of umbilical cord. *Stem Cells Dev.* 19 (12), 1895–1910. doi:10.1089/scd.2009.0485

Ichim, T. E., O'Heeron, P., and Kesari, S. (2018). Fibroblasts as a practical alternative to mesenchymal stem cells. *J. Transl. Med.* 16 (1), 212. doi:10.1186/s12967-018-1536-1

Isono, M., Takeuchi, J., Maehara, A., Nakagawa, Y., Katagiri, H., Miyatake, K., et al. (2022). Effect of CD44 signal axis in the gain of mesenchymal stem cell surface antigens from synovial fibroblasts *in vitro*. *Heliyon* 8 (10), e10739. doi:10.1016/j.heliyon.2022.e10739

Iwatani, S., Shono, A., Yoshida, M., Yamana, K., Thwin, K. K. M., Kuroda, J., et al. (2017). Involvement of WNT signaling in the regulation of gestational age-dependent umbilical cord-derived mesenchymal stem cell proliferation. *Stem Cells Int.* 2017, 8749751. doi:10.1155/2017/8749751

Jakl, V., Popp, T., Haupt, J., Port, M., Roesler, R., Wiese, S., et al. (2023). Effect of expansion media on functional characteristics of bone marrow-derived mesenchymal stromal cells. *Cells* 12 (16), 2105. doi:10.3390/cells12162105

Janja, Z. (2021). "Mesenchymal stem/stromal cells and fibroblasts: their roles in tissue injury and regeneration, and age-related degeneration," in *Fibroblasts*. Editors B. Mojca Frank and L. Katja (Rijeka: IntechOpen). Ch. 2.

Jeyaraman, M., Muthu, S., Nischith, D. S., Jeyaraman, N., Nallakumarasamy, A., and Khanna, M. (2022). PRISMA-compliant meta-analysis of randomized controlled trials on osteoarthritis of knee managed with allogeneic vs autologous MSCs: efficacy and safety analysis. *Indian J. Orthop.* 56 (12), 2042–2059. doi:10.1007/s43465-022-00751-z

Joswig, A. J., Mitchell, A., Cummings, K. J., Levine, G. J., Gregory, C. A., Smith, R., et al. (2017). Repeated intra-articular injection of allogeneic mesenchymal stem cells causes an adverse response compared to autologous cells in the equine model. *Stem Cell. Res. Ther.* 8 (1), 42. doi:10.1186/s13287-017-0503-8

Juhl, M., Follin, B., Christensen, J. P., Kastrup, J., and Ekblond, A. (2022). Functional *in vitro* models of the inhibitory effect of adipose tissue-derived stromal cells on lymphocyte proliferation: improved sensitivity and quantification through flow cytometric analysis. *J. Immunol. Methods* 510, 113360. doi:10.1016/j.jim.2022.113360

Kadri, N., Amu, S., Iacobaeus, E., Boberg, E., and Le Blanc, K. (2023). Current perspectives on mesenchymal stromal cell therapy for graft versus host disease. *Cell. Mol. Immunol.* 20 (6), 613–625. doi:10.1038/s41423-023-01022-z

Kakkar, A., Singh, A., Saraswat, S. K., Srivastava, S., Khatri, N., Nagar, R. K., et al. (2020). Cartilage repair using stem cells and biomaterials: advancement from bench to bedside. *Mol. Biol. Rep.* 47 (10), 8007–8021. doi:10.1007/s11033-020-05748-1

Kang, I., Lee, B. C., Choi, S. W., Lee, J. Y., Kim, J. J., Kim, B. E., et al. (2018a). Donor-dependent variation of human umbilical cord blood mesenchymal stem cells in response to hypoxic preconditioning and amelioration of limb ischemia. *Exp. Mol. Med.* 50 (4), 35–15. doi:10.1038/s12276-017-0014-9

Kang, I., Lee, B. C., Choi, S. W., Lee, J. Y., Kim, J. J., Kim, B. E., et al. (2018b). Donor-dependent variation of human umbilical cord blood mesenchymal stem cells in response to hypoxic preconditioning and amelioration of limb ischemia. *Exp. Mol. Med.* 50 (4), 35–15. doi:10.1038/s12276-017-0014-9

Kannan, S., Viswanathan, P., Gupta, P. K., and Kolkundkar, U. K. (2022). Characteristics of pooled wharton's jelly mesenchymal stromal cells (WJ-MSCs) and their potential role in rheumatoid arthritis treatment. *Stem Cell. Rev. Rep.* 18 (5), 1851–1864. doi:10.1007/s12015-022-10344-w

Kashef, S., Moghtaderi, M., Hatami, H. R., Kalani, M., Alyasin, S., Nabavizadeh, H., et al. (2022). Evaluation of T Cell proliferation using CFSE dilution assay: a comparison between stimulation with PHA and anti-CD3/anti-CD28 coated Beads. *Iran. J. Allergy Asthma Immunol.* 21 (4), 458–466. doi:10.18502/ijaai.v21i4.10293

Kehl, D., Generali, M., Mallone, A., Heller, M., Uldry, A. C., Cheng, P., et al. (2019). Proteomic analysis of human mesenchymal stromal cell secretomes: a systematic comparison of the angiogenic potential. *NPJ Regen. Med.* 4, 8. doi:10.1038/s41536-019-0070-y

Kelly, K., and Rasko, J. E. J. (2021). Mesenchymal stromal cells for the treatment of graft versus host disease. *Front. Immunol.* 12, 761616. doi:10.3389/fimmu.2021.761616

Ketterl, N., Brachtl, G., Schuh, C., Bieback, K., Schallmoser, K., Reinisch, A., et al. (2015a). A robust potency assay highlights significant donor variation of human mesenchymal stem/progenitor cell immune modulatory capacity and extended radio-resistance. *Stem Cell. Res. Ther.* 6 (1), 236. doi:10.1186/s13287-015-0233-8

Ketterl, N., Brachtl, G., Schuh, C., Bieback, K., Schallmoser, K., Reinisch, A., et al. (2015b). A robust potency assay highlights significant donor variation of human mesenchymal stem/progenitor cell immune modulatory capacity and extended radio-resistance. *Stem Cell. Res. Ther.* 6, 236. doi:10.1186/s13287-015-0233-8

Kim, D. H., Kim, S. H., Park, S. H., Kwon, M. Y., Lim, C. Y., Park, S. H., et al. (2023). Characteristics of human nasal turbinate stem cells under hypoxic conditions. *Cells* 12 (19), 2360. doi:10.3390/cells12192360

Kirsch, M., Rach, J., Handke, W., Seltsam, A., Pepelanova, I., Strauß, S., et al. (2021). Comparative analysis of mesenchymal stem cell cultivation in fetal calf serum, human serum, and platelet lysate in 2D and 3D systems. *Front. Bioeng. Biotechnol.* 8, 598389. doi:10.3389/fbioe.2020.598389

Koehler, N., Buhler, L., Egger, B., and Gonelle-Gispert, C. (2022). Multipotent mesenchymal stromal cells interact and support islet of langerhans viability and function. *Front. Endocrinol. (Lausanne)* 13, 822191. doi:10.3389/fendo.2022.822191

Kohli, N., Al-Delfi, I. R. T., Snow, M., Sakamoto, T., Miyazaki, T., Nakajima, H., et al. (2019). CD271-selected mesenchymal stem cells from adipose tissue enhance cartilage repair and are less angiogenic than plastic adherent mesenchymal stem cells. *Sci. Rep.* 9 (1), 3194. doi:10.1038/s41598-019-39715-z

Kouchakian, M. R., Baghban, N., Moniri, S. F., Baghban, M., Bakhshalizadeh, S., Najafzadeh, V., et al. (2021). The clinical trials of mesenchymal stromal cells therapy. *Stem Cells Int.* 2021, 1634782. doi:10.1155/2021/1634782

Kouroupis, D., and Correa, D. (2021). Increased mesenchymal stem cell functionalization in three-dimensional manufacturing settings for enhanced therapeutic applications. *Front. Bioeng. Biotechnol.* 9, 621748. doi:10.3389/fbioe.2021.621748

Kowal, J. M., Schmal, H., Halekoh, U., Hjelmborg, J. B., and Kassem, M. (2020). Single-cell high-content imaging parameters predict functional phenotype of cultured human bone marrow stromal stem cells. *Stem Cells Transl. Med.* 9 (2), 189–202. doi:10.1002/sctm.19-0171

Krakenes, T., Wergeland, S., Al-Sharabi, N., Mohamed-Ahmed, S., Fromreide, S., Costea, D. E., et al. (2023). The neuroprotective potential of mesenchymal stem cells from bone marrow and human exfoliated deciduous teeth in a murine model of demyelination. *PLoS One* 18 (11), e0293908. doi:10.1371/journal.pone.0293908

Krampera, M., and Le Blanc, K. (2021). Mesenchymal stromal cells: putative microenvironmental modulators become cell therapy. *Cell. Stem Cell.* 28 (10), 1708–1725. doi:10.1016/j.stem.2021.09.006

Kuci, S., Kuçi, Z., Kreyenberg, H., Deak, E., Pütsch, K., Huenecke, S., et al. (2010). CD271 antigen defines a subset of multipotent stromal cells with immunosuppressive and lymphohematopoietic engraftment-promoting properties. *Haematologica* 95 (4), 651–659. doi:10.3324/haematol.2009.015065

Labedz-Maslowska, A., Szkaradek, A., Mierzwinski, T., Madeja, Z., and Zuba-Surma, E. (2021). Processing and *ex vivo* expansion of adipose tissue-derived mesenchymal stem/stromal cells for the development of an advanced therapy medicinal product for use in humans. *Cells* 10 (8), 1908. doi:10.3390/cells10081908

Laloze, J., Lacoste, M., Marouf, F., Carpentier, G., Vignaud, L., Chaput, B., et al. (2023). Specific features of stromal cells isolated from the two layers of subcutaneous adipose tissue: roles of their secretion on angiogenesis and neurogenesis. *J. Clin. Med.* 12 (13), 4214. doi:10.3390/jcm12134214

Lamo-Espinosa, J. M., Blanco, J. F., Sánchez, M., Moreno, V., Granero-Moltó, F., Sánchez-Guijo, F., et al. (2020). Phase II multicenter randomized controlled clinical trial on the efficacy of intra-articular injection of autologous bone marrow mesenchymal stem cells with platelet rich plasma for the treatment of knee osteoarthritis. *J. Transl. Med.* 18 (1), 356. doi:10.1186/s12967-020-02530-6

Le Blanc, K., Frassoni, F., Ball, L., Locatelli, F., Roelofs, H., Lewis, I., et al. (2008). Mesenchymal stem cells for treatment of steroid-resistant, severe, acute graft-versus-host disease: a phase II study. *Lancet* 371 (9624), 1579–1586. doi:10.1016/S0140-6736(08)60690-X

Ledesma-Martinez, E., Mendoza-Nunez, V. M., and Santiago-Osorio, E. (2016). Mesenchymal stem cells derived from dental pulp: a review. *Stem Cells Int.* 2016, 4709572. doi:10.1155/2016/4709572

Lee, R. H., Boregowda, S. V., Shigemoto-Kuroda, T., Bae, E., Haga, C. L., Abbery, C. A., et al. (2023). TWIST1 and TSG6 are coordinately regulated and function as potency biomarkers in human MSCs. *Sci. Adv.* 9 (45), eadi2387. doi:10.1126/sciadv.adi2387

Lee, R. H., Pulin, A. A., Seo, M. J., Kota, D. J., Ylostalo, J., Larson, B. L., et al. (2009). Intravenous hMSCs improve myocardial infarction in mice because cells embolized in lung are activated to secrete the anti-inflammatory protein TSG-6. *Cell. Stem Cell.* 5 (1), 54–63. doi:10.1016/j.stem.2009.05.003

Lemieszek, M. B., Findlay, S. D., and Siegers, G. M. (2022). "CellTrace™ violet flow cytometric assay to assess cell proliferation," in *Cancer cell biology: methods and protocols*. Editor S. L. Christian (New York, NY: Springer US), 101–114.

Lewis, N. S., Lewis, E. E., Mullin, M., Wheadon, H., Dalby, M. J., and Berry, C. C. (2017). Magnetically levitated mesenchymal stem cell spheroids cultured with a collagen gel maintain phenotype and quiescence. *J. Tissue Eng.* 8, 2041731417704428. doi:10.1177/2041731417704428

Li, H., Ghazanfari, R., Zacharaki, D., Lim, H. C., and Scheding, S. (2016). Isolation and characterization of primary bone marrow mesenchymal stromal cells. *Ann. N. Y. Acad. Sci.* 1370 (1), 109–118. doi:10.1111/nyas.13102

Li, P., Ou, Q., Shi, S., and Shao, C. (2023). Immunomodulatory properties of mesenchymal stem cells/dental stem cells and their therapeutic applications. *Cell. Mol. Immunol.* 20 (6), 558–569. doi:10.1038/s41423-023-00998-y

Li, S., Wang, J., Jiang, B., Jiang, J., Luo, L., Zheng, B., et al. (2022b). Mesenchymal stem cells derived from different perinatal tissues donated by same donors manifest variant performance on the acute liver failure model in mouse. *Stem Cell. Res. Ther.* 13 (1), 231. doi:10.1186/s13287-022-02909-w

Li, X., Wang, D., Liang, J., Zhang, H., and Sun, L. (2013). Mesenchymal SCT ameliorates refractory cytopenia in patients with systemic lupus erythematosus. *Bone Marrow Transpl.* 48 (4), 544–550. doi:10.1038/bmt.2012.184

Li, Y., Hao, J., Hu, Z., Yang, Y. G., Zhou, Q., Sun, L., et al. (2022a). Current status of clinical trials assessing mesenchymal stem cell therapy for graft versus host disease: a systematic review. *Stem Cell. Res. Ther.* 13 (1), 93. doi:10.1186/s13287-022-02751-0

Lipat, A. J., Cottle, C., Pirlot, B. M., Mitchell, J., Pando, B., Helmly, B., et al. (2022). Chemokine assay matrix defines the potency of human bone marrow mesenchymal stromal cells. *Stem Cells Transl. Med.* 11 (9), 971–986. doi:10.1093/stcltm/szac050

Liu, S., Mao, X., Hou, Z., Wei, H., Gao, H., Liu, Y., et al. (2022). Multiple transplantation of mesenchymal stem cells in a patient with active progressive multiple sclerosis: long term therapeutic outcomes. *Clin. Neurol. Neurosurg.* 223, 107475. doi:10.1016/j.clineuro.2022.107475

Lozano Navarro, L. V., Chen, X., Giratá Viviescas, L. T., Ardila-Roa, A. K., Luna-Gonzalez, M. L., Sossa, C. L., et al. (2022). Mesenchymal stem cells for critical limb ischemia: their function, mechanism, and therapeutic potential. *Stem Cell. Res. Ther.* 13 (1), 345. doi:10.1186/s13287-022-03043-3

Luk, F., de Witte, S. F. H., Korevaar, S. S., Roemeling-van Rhijn, M., Franquesa, M., Strini, T., et al. (2016). Inactivated mesenchymal stem cells maintain immunomodulatory capacity. *Stem Cells Dev.* 25 (18), 1342–1354. doi:10.1089/scd.2016.0068

Lwin, S. M., Snowden, J. A., and Griffiths, C. E. M. (2021). The promise and challenges of cell therapy for psoriasis. *Br. J. Dermatol* 185 (5), 887–898. doi:10.1111/bjd.20517

Ma, L., Huang, Z., Wu, D., Kou, X., Mao, X., and Shi, S. (2021a). CD146 controls the quality of clinical grade mesenchymal stem cells from human dental pulp. *Stem Cell. Res. Ther.* 12 (1), 488. doi:10.1186/s13287-021-02559-4

Ma, L., Huang, Z., Wu, D., Kou, X., Mao, X., and Shi, S. (2021b). CD146 controls the quality of clinical grade mesenchymal stem cells from human dental pulp. *Stem Cell. Res. Ther.* 12 (1), 488. doi:10.1186/s13287-021-02559-4

Mabotuwana, N. S., Rech, L., Lim, J., Hardy, S. A., Murtha, L. A., Rainer, P. P., et al. (2022). Paracrine factors released by stem cells of mesenchymal origin and their effects in cardiovascular disease: a systematic review of pre-clinical studies. *Stem Cell. Rev. Rep.* 18 (8), 2606–2628. doi:10.1007/s12015-022-10429-6

Maldonado, V. V., Patel, N. H., Smith, E. E., Barnes, C. L., Gustafson, M. P., Rao, R. R., et al. (2023). Clinical utility of mesenchymal stem/stromal cells in regenerative medicine and cellular therapy. *J. Biol. Eng.* 17 (1), 44. doi:10.1186/s13036-023-00361-9

Mamidi, M. K., Nathan, K. G., Singh, G., Thrichelvam, S. T., Mohd Yusof, N. A. N., Fakharuzi, N. A., et al. (2012). Comparative cellular and molecular analyses of pooled bone marrow multipotent mesenchymal stromal cells during continuous passaging and after successive cryopreservation. *J. Cell. Biochem.* 113 (10), 3153–3164. doi:10.1002/jcb.24193

Marques, C. R., Fuzeta, M. d. A., Dos Santos Cunha, R. M., Pereira-Sousa, J., Silva, D., Campos, J., et al. (2023). Neurodifferentiation and neuroprotection potential of mesenchymal stromal cell-derived secretome produced in different dynamic systems. *Biomedicines* 11 (5), 1240. doi:10.3390/biomedicines11051240

Mebarki, M., Iglicki, N., Marigny, C., Abadie, C., Nicolet, C., Churlaud, G., et al. (2021). Development of a human umbilical cord-derived mesenchymal stromal cell-based advanced therapy medicinal product to treat immune and/or inflammatory diseases. *Stem Cell. Res. Ther.* 12 (1), 571. doi:10.1186/s13287-021-02637-7

Medrano-Trochez, C., Chatterjee, P., Pradhan, P., Stevens, H. Y., Ogle, M. E., Botchwey, E. A., et al. (2021). Single-cell RNA-seq of out-of-thaw mesenchymal stromal cells shows tissue-of-origin differences and inter-donor cell-cycle variations. *Stem Cell. Res. Ther.* 12 (1), 565. doi:10.1186/s13287-021-02627-9

Ménard, C., Dulong, J., Roulois, D., Hébraud, B., Verdière, L., Pangault, C., et al. (2019). Integrated transcriptomic, phenotypic, and functional study reveals tissue-specific immune properties of mesenchymal stromal cells. *Stem Cells* 38 (1), 146–159. doi:10.1002/stem.3077

Meng, S. S., Xu, X. P., Chang, W., Lu, Z. H., Huang, L. L., Xu, J. Y., et al. (2018). LincRNA-p21 promotes mesenchymal stem cell migration capacity and survival through hypoxic preconditioning. *Stem Cell. Res. Ther.* 9 (1), 280. doi:10.1186/s13287-018-1031-x

Meng, X., Ichim, T. E., Zhong, J., Rogers, A., Yin, Z., Jackson, J., et al. (2007). Endometrial regenerative cells: a novel stem cell population. *J. Transl. Med.* 5, 57. doi:10.1186/1479-5876-5-57

Miclau, K., Hambright, W. S., Huard, J., Stoddart, M. J., and Bahney, C. S. (2023). Cellular expansion of MSCs: shifting the regenerative potential. *Aging Cell.* 22 (1), e13759. doi:10.1111/acel.13759

Mohamed, S. A., Howard, L., McInerney, V., Hayat, A., Krawczyk, J., Naughton, S., et al. (2020). Autologous bone marrow mesenchymal stromal cell therapy for "no-option" critical limb ischemia is limited by karyotype abnormalities. *Cytotherapy* 22 (6), 313–321. doi:10.1016/j.jcyt.2020.02.007

Mollentze, J., Durandt, C., and Pepper, M. S. (2021). An *in vitro* and *in vivo* comparison of osteogenic differentiation of human mesenchymal stromal/stem cells. *Stem Cells Int.* 2021, 9919361. doi:10.1155/2021/9919361

Montesinos, J. J., Flores-Figueroa, E., Castillo-Medina, S., Flores-Guzmán, P., Hernández-Estévez, E., Fajardo-Orduña, G., et al. (2009). Human mesenchymal stromal cells from adult and neonatal sources: comparative analysis of their morphology, immunophenotype, differentiation patterns and neural protein expression. *Cytotherapy* 11 (2), 163–176. doi:10.1080/14653240802582075

Montoto-Meijide, R., Meijide-Faílde, R., Díaz-Prado, S. M., and Montoto-Marqués, A. (2023). Mesenchymal stem cell therapy in traumatic spinal cord injury: a systematic review. *Int. J. Mol. Sci.* 24 (14), 11719. doi:10.3390/ijms241411719

Moon, K.-C., Suh, H. S., Kim, K. B., Han, S. K., Young, K. W., Lee, J. W., et al. (2019). Potential of allogeneic adipose-derived stem cell–hydrogel complex for treating diabetic foot ulcers. *Diabetes* 68 (4), 837–846. doi:10.2337/db18-0699

Morello, W., Budelli, S., Bernstein, D. A., Montemurro, T., Montelatici, E., Lavazza, C., et al. (2022). First clinical application of cord blood mesenchymal stromal cells in children with multi-drug resistant nephrotic syndrome. *Stem Cell. Res. Ther.* 13 (1), 420. doi:10.1186/s13287-022-03112-7

Muller, S., Nicholson, L., Al Harbi, N., Mancuso, E., Jones, E., Dickinson, A., et al. (2019). Osteogenic potential of heterogeneous and CD271-enriched mesenchymal stromal cells cultured on apatite-wollastonite 3D scaffolds. *BMC Biomed. Eng.* 1, 16. doi:10.1186/s42490-019-0015-y

Musiał-Wysocka, A., Kot, M., Sułkowski, M., Badyra, B., and Majka, M. (2019). Molecular and functional verification of wharton's jelly mesenchymal stem cells (WJ-MSCs) pluripotency. *Int. J. Mol. Sci.* 20 (8), 1807. doi:10.3390/ijms20081807

Myneni, V. D., McClain-Caldwell, I., Martin, D., Vitale-Cross, L., Marko, K., Firriolo, J. M., et al. (2019). Mesenchymal stromal cells from infants with simple polydactyly modulate immune responses more efficiently than adult mesenchymal stromal cells. *Cytotherapy* 21 (2), 148–161. doi:10.1016/j.jcyt.2018.11.008

Nagamura-Inoue, T., and He, H. (2014). Umbilical cord-derived mesenchymal stem cells: their advantages and potential clinical utility. *World J. Stem Cells* 6 (2), 195–202. doi:10.4252/wjsc.v6.i2.195

Naji, A., Eitoku, M., Favier, B., Deschaseaux, F., Rouas-Freiss, N., and Suganuma, N. (2019). Biological functions of mesenchymal stem cells and clinical implications. *Cell. Mol. Life Sci.* 76 (17), 3323–3348. doi:10.1007/s00018-019-03125-1

Nicotra, T., Desnos, A., Halimi, J., Antonot, H., Reppel, L., Belmas, T., et al. (2020). Mesenchymal stem/stromal cell quality control: validation of mixed lymphocyte reaction assay using flow cytometry according to ICH Q2(R1). *Stem Cell. Res. Ther.* 11 (1), 426. doi:10.1186/s13287-020-01947-6

Oliva-Olivera, W., Leiva Gea, A., Lhamyani, S., Coín-Aragüez, L., Alcaide Torres, J., Bernal-López, M. R., et al. (2015). Differences in the osteogenic differentiation capacity of omental adipose-derived stem cells in obese patients with and without metabolic syndrome. *Endocrinology* 156 (12), 4492–4501. doi:10.1210/en.2015-1413

Ong, W. K., Chakraborty, S., and Sugii, S. (2021). Adipose tissue: understanding the heterogeneity of stem cells for regenerative medicine. *Biomolecules* 11 (7), 918. doi:10.3390/biom11070918

Ouboter, L. F., Barnhoorn, M. C., Verspaget, H. W., Plug, L., Pool, E. S., Szuhai, K., et al. (2023). Local administration of mesenchymal stromal cells is safe and modulates the immune compartment in ulcerative proctitis. *JCI Insight* 8 (9), e167402. doi:10.1172/jci.insight.167402

Padhiar, C., Aruni, A. W., Abhaya, M., Muthuchamy, M., Dhanraj, A. K., Ganesan, V., et al. (2022). GMP compliant clinical grade and xenofree manufacturing of human Wharton's jelly derived mesenchymal stem cell from pooled donors. *Biochem. Eng. J.* 184, 108470. doi:10.1016/j.bej.2022.108470

Park, D., Choi, Y. H., Kang, S. H., Koh, H. S., and In, Y. (2023). Bone marrow aspirate concentrate versus human umbilical cord blood-derived mesenchymal stem cells for combined cartilage regeneration procedure in patients undergoing high tibial osteotomy: a systematic review and meta-analysis. *Med. Kaunas.* 59 (3), 634. doi:10.3390/medicina59030634

Patel, R. S., Carter, G., El Bassit, G., Patel, A. A., Cooper, D. R., Murr, M., et al. (2016). Adipose-derived stem cells from lean and obese humans show depot specific differences in their stem cell markers, exosome contents and senescence: role of protein kinase C delta (PKCδ) in adipose stem cell niche. *Stem Cell. Investig.* 3, 2. doi:10.3978/j.issn.2306-9759.2016.01.02

Perczel-Kovách, K., Hegedűs, O., Földes, A., Sangngoen, T., Kálló, K., Steward, M. C., et al. (2021). STRO-1 positive cell expansion during osteogenic differentiation: a comparative study of three mesenchymal stem cell types of dental origin. *Archives oral Biol.* 122, 104995. doi:10.1016/j.archoralbio.2020.104995

Petters, O., Schmidt, C., Henkelmann, R., Pieroh, P., Hütter, G., Marquass, B., et al. (2018). Single-stage preparation of human cartilage grafts generated from bone marrow-derived CD271(+) mononuclear cells. *Stem Cells Dev.* 27 (8), 545–555. doi:10.1089/scd.2017.0218

Piede, N., Bremm, M., Farken, A., Pfeffermann, L. M., Cappel, C., Bonig, H., et al. (2023). Validation of an ICH Q2 compliant flow cytometry-based assay for the assessment of the inhibitory potential of mesenchymal stromal cells on T cell proliferation. *Cells* 12 (6), 850. doi:10.3390/cells12060850

Podesta, M. A., Remuzzi, G., and Casiraghi, F. (2020). Mesenchymal stromal cell therapy in solid organ transplantation. *Front. Immunol.* 11, 618243. doi:10.3389/fimmu.2020.618243

Porter, A. P., Pirlot, B. M., Dyer, K., Uwazie, C. C., Nguyen, J., Turner, C., et al. (2022). Conglomeration of T- and B-cell matrix responses determines the potency of human bone marrow mesenchymal stromal cells. *Stem Cells* 40 (12), 1134–1148. doi:10.1093/stmcls/sxac064

Quirici, N., Scavullo, C., de Girolamo, L., Lopa, S., Arrigoni, E., Deliliers, G. L., et al. (2010). Anti-L-NGFR and -CD34 monoclonal antibodies identify multipotent mesenchymal stem cells in human adipose tissue. *Stem Cells Dev.* 19 (6), 915–925. doi:10.1089/scd.2009.0408

Rady, D., Abbass, M. M. S., El-Rashidy, A. A., El Moshy, S., Radwan, I. A., Dörfer, C. E., et al. (2020a). Mesenchymal stem/progenitor cells: the prospect of human clinical translation. *Stem Cells Int.* 2020, 8837654. doi:10.1155/2020/8837654

Rady, D., Abbass, M. M. S., El-Rashidy, A. A., El Moshy, S., Radwan, I. A., Dörfer, C. E., et al. (2020b). Mesenchymal stem/progenitor cells: the prospect of human clinical translation. *Stem Cells Int.* 2020, 8837654. doi:10.1155/2020/8837654

Raza, S. S., and Khan, M. A. (2022). Mesenchymal stem cells: a new front emerges in coronavirus disease 2019 treatment. *Cytotherapy* 24 (8), 755–766. doi:10.1016/j.jcyt.2020.07.002

Redondo-Castro, E., Cunningham, C. J., Miller, J., Cain, S. A., Allan, S. M., and Pinteaux, E. (2018). Generation of human mesenchymal stem cell 3D spheroids using low-binding plates. *Bio-protocol* 8 (16), e2968. doi:10.21769/BioProtoc.2968

Regmi, S., Liu, D. D., Shen, M., Kevadiya, B. D., Ganguly, A., Primavera, R., et al. (2022). Mesenchymal stromal cells for the treatment of Alzheimer's disease: strategies and limitations. *Front. Mol. Neurosci.* 15, 1011225. doi:10.3389/fnmol.2022.1011225

Renesme, L., Pierro, M., Cobey, K. D., Mital, R., Nangle, K., Shorr, R., et al. (2022). Definition and characteristics of mesenchymal stromal cells in preclinical and clinical studies: a scoping review. *Stem Cells Transl. Med.* 11 (1), 44–54. doi:10.1093/stcltm/szab009

Rengasamy, M., Gupta, P. K., Kolkundkar, U., Singh, G., Balasubramanian, S., SundarRaj, S., et al. (2016). Preclinical safety and toxicity evaluation of pooled, allogeneic human bone marrow-derived mesenchymal stromal cells. *Indian J. Med. Res.* 144 (6), 852–864. doi:10.4103/ijmr.IJMR_1842_15

Rennerfeldt, D. A., Raminhos, J. S., Leff, S. M., Manning, P., and Van Vliet, K. J. (2019). Emergent heterogeneity in putative mesenchymal stem cell colonies: single-cell time lapsed analysis. *PLoS One* 14 (4), e0213452. doi:10.1371/journal.pone.0213452

Rettinger, C. L., Fourcaudot, A. B., Hong, S. J., Mustoe, T. A., Hale, R. G., and Leung, K. P. (2014). *In vitro* characterization of scaffold-free three-dimensional mesenchymal stem cell aggregates. *Cell. Tissue Res.* 358 (2), 395–405. doi:10.1007/s00441-014-1939-0

Ringden, O., and Leblanc, K. (2011). Pooled MSCs for treatment of severe hemorrhage. *Bone Marrow Transpl.* 46 (8), 1158–1160. doi:10.1038/bmt.2010.262

Rio, C., Jahn, A. K., Martin-Medina, A., Calvo Bota, A. M., De Francisco Casado, M. T., Pont Antona, P. J., et al. (2023). Mesenchymal stem cells from COPD patients are capable of restoring elastase-induced emphysema in a murine experimental model. *Int. J. Mol. Sci.* 24 (6), 5813. doi:10.3390/ijms24065813

Robb, K. P., Audet, J., Gandhi, R., and Viswanathan, S. (2022a). Putative critical quality attribute matrix identifies mesenchymal stromal cells with potent immunomodulatory and angiogenic "fitness" ranges in response to culture process parameters. *Front. Immunol.* 13, 972095. doi:10.3389/fimmu.2022.972095

Robb, K. P., Audet, J., Gandhi, R., and Viswanathan, S. (2022b). Putative critical quality attribute matrix identifies mesenchymal stromal cells with potent immunomodulatory and angiogenic "fitness" ranges in response to culture process parameters. *Front. Immunol.* 13, 972095. doi:10.3389/fimmu.2022.972095

Robb, K. P., Fitzgerald, J. C., Barry, F., and Viswanathan, S. (2019). Mesenchymal stromal cell therapy: progress in manufacturing and assessments of potency. *Cytotherapy* 21 (3), 289–306. doi:10.1016/j.jcyt.2018.10.014

Rybkowska, P., Radoszkiewicz, K., Kawalec, M., Dymkowska, D., Zabłocka, B., Zabłocki, K., et al. (2023). The metabolic changes between monolayer (2D) and three-dimensional (3D) culture conditions in human mesenchymal stem/stromal cells derived from adipose tissue. *Cells* 12 (1), 178. doi:10.3390/cells12010178

Samsonraj, R. M., Raghunath, M., Nurcombe, V., Hui, J. H., van Wijnen, A. J., and Cool, S. M. (2017). Concise review: multifaceted characterization of human mesenchymal stem cells for use in regenerative medicine. *Stem Cells Transl. Med.* 6 (12), 2173–2185. doi:10.1002/sctm.17-0129

Samuelsson, H., Ringdén, O., Lönnies, H., and Le Blanc, K. (2009). Optimizing *in vitro* conditions for immunomodulation and expansion of mesenchymal stromal cells. *Cytotherapy* 11 (2), 129–136. doi:10.1080/14653240802684194

Sanabria-de la Torre, R., Quiñones-Vico, M. I., Fernández-González, A., Sánchez-Díaz, M., Montero-Vílchez, T., Sierra-Sánchez, Á., et al. (2021). Alloreactive immune response associated to human mesenchymal stromal cells treatment: a systematic review. *J. Clin. Med.* 10 (13), 2991. doi:10.3390/jcm10132991

Savelli, S., Trombi, L., D'Alessandro, D., Moscato, S., Pacini, S., Giannotti, S., et al. (2018). Pooled human serum: a new culture supplement for bioreactor-based cell therapies. Preliminary results. *Cytotherapy* 20 (4), 556–563. doi:10.1016/j.jcyt.2017.12.013

Schüring, A. N., Schulte, N., Kelsch, R., Röpke, A., Kiesel, L., and Götte, M. (2011). Characterization of endometrial mesenchymal stem-like cells obtained by endometrial biopsy during routine diagnostics. *Fertil. Steril.* 95 (1), 423–426. doi:10.1016/j.fertnstert.2010.08.035

Selich, A., Daudert, J., Hass, R., Philipp, F., von Kaisenberg, C., Paul, G., et al. (2016). Massive clonal selection and transiently contributing clones during expansion of mesenchymal stem cell cultures revealed by lentiviral RGB-barcode technology. *Stem Cells Transl. Med.* 5 (5), 591–601. doi:10.5966/sctm.2015-0176

Semenova, E., Grudniak, M. P., Machaj, E. K., Bocian, K., Chroscinska-Krawczyk, M., Trochonowicz, M., et al. (2021). Mesenchymal stromal cells from different parts of umbilical cord: approach to comparison and characteristics. *Stem Cell. Rev. Rep.* 17 (5), 1780–1795. doi:10.1007/s12015-021-10157-3

Shibu, M. A., Huang, C. Y., and Ding, D. C. (2023). Comparison of two hepatocyte differentiation protocols in human umbilical cord mesenchymal stem cells: *in vitro* study. *Tissue Cell.* 83, 102153. doi:10.1016/j.tice.2023.102153

Shimizu, Y., Gumin, J., Gao, F., Hossain, A., Shpall, E. J., Kondo, A., et al. (2022). Characterization of patient-derived bone marrow human mesenchymal stem cells as oncolytic virus carriers for the treatment of glioblastoma. *J. Neurosurg.* 136 (3), 757–767. doi:10.3171/2021.3.JNS203045

Shin, S., Lee, J., Kwon, Y., Park, K. S., Jeong, J. H., Choi, S. J., et al. (2021). Comparative proteomic analysis of the mesenchymal stem cells secretome from adipose, bone marrow, placenta and Wharton's jelly. *Int. J. Mol. Sci.* 22 (2), 845. doi:10.3390/ijms22020845

Siegel, G., Kluba, T., Hermanutz-Klein, U., Bieback, K., Northoff, H., and Schäfer, R. (2013). Phenotype, donor age and gender affect function of human bone marrow-derived mesenchymal stromal cells. *BMC Med.* 11 (1), 146. doi:10.1186/1741-7015-11-146

Sipp, D., Robey, P. G., and Turner, L. (2018). Clear up this stem-cell mess. *Nature* 561 (7724), 455–457. doi:10.1038/d41586-018-06756-9

Smith, R. J. P., Faroni, A., Barrow, J. R., Soul, J., and Reid, A. J. (2021). The angiogenic potential of CD271+ human adipose tissue-derived mesenchymal stem cells. *Stem Cell. Res. Ther.* 12 (1), 160. doi:10.1186/s13287-021-02177-0

Smolinska, A., Bzinkowska, A., Rybkowska, P., Chodkowska, M., and Sarnowska, A. (2023). Promising markers in the context of mesenchymal stem/stromal cells subpopulations with unique properties. *Stem Cells Int.* 2023, 1842958. doi:10.1155/2023/1842958

Sober, S. A., Darmani, H., Alhattab, D., and Awidi, A. (2023). Flow cytometric characterization of cell surface markers to differentiate between fibroblasts and mesenchymal stem cells of different origin. *Archives Med. Sci.* 19 (5), 1487–1496. doi:10.5114/aoms/131088

Soliman, H., Theret, M., Scott, W., Hill, L., Underhill, T. M., Hinz, B., et al. (2021). Multipotent stromal cells: one name, multiple identities. *Cell. Stem Cell.* 28 (10), 1690–1707. doi:10.1016/j.stem.2021.09.001

Soundararajan, M., and Kannan, S. (2018). Fibroblasts and mesenchymal stem cells: two sides of the same coin? *J. Cell. Physiol.* 233 (12), 9099–9109. doi:10.1002/jcp.26860

Stefanska, K., Nemcova, L., Blatkiewicz, M., Żok, A., Kaczmarek, M., Pieńkowski, W., et al. (2023). Expression profile of new marker genes involved in differentiation of human Wharton's jelly-derived mesenchymal stem cells into chondrocytes, osteoblasts, adipocytes and neural-like cells. *Int. J. Mol. Sci.* 24 (16), 12939. doi:10.3390/ijms241612939

Subbiahanadar Chelladurai, K., Selvan Christyraj, J. D., Rajagopalan, K., Yesudhason, B. V., Venkatachalam, S., Mohan, M., et al. (2021). Alternative to FBS in animal cell culture - an overview and future perspective. *Heliyon* 7 (8), e07686. doi:10.1016/j.heliyon.2021.e07686

Subramanian, A., Fong, C. Y., Biswas, A., and Bongso, A. (2015). Comparative characterization of cells from the various compartments of the human umbilical cord shows that the wharton's jelly compartment provides the best source of clinically utilizable mesenchymal stem cells. *PLOS ONE* 10 (6), e0127992. doi:10.1371/journal.pone.0127992

Sun, C., Wang, L., Wang, H., Huang, T., Yao, W., Li, J., et al. (2020). Single-cell RNA-seq highlights heterogeneity in human primary Wharton's jelly mesenchymal stem/stromal cells cultured *in vitro*. *Stem Cell. Res. Ther.* 11 (1), 149. doi:10.1186/s13287-020-01660-4

Sun, L., Zhang, H. Y., Feng, X. B., Hou, Y. Y., Lu, L. W., and Fan, L. M. (2007). Abnormality of bone marrow-derived mesenchymal stem cells in patients with systemic lupus erythematosus. *Lupus* 16 (2), 121–128. doi:10.1177/0961203306075793

Suzdaltseva, Y., Goryunov, K., Silina, E., Manturova, N., Stupin, V., and Kiselev, S. L. (2022). Equilibrium among inflammatory factors determines human MSC-mediated immunosuppressive effect. *Cells* 11 (7), 1210. doi:10.3390/cells11071210

Svajger, U., Tesic, N., and Rozman, P. (2021). Programmed death ligand 1 (PD-L1) plays a vital part in DC tolerogenicity induced by IFN-γ. *Int. Immunopharmacol.* 99, 107978. doi:10.1016/j.intimp.2021.107978

Takao, S., Nakashima, T., Masuda, T., Namba, M., Sakamoto, S., Yamaguchi, K., et al. (2021). Human bone marrow-derived mesenchymal stromal cells cultured in serum-free media demonstrate enhanced antifibrotic abilities via prolonged survival and robust regulatory T cell induction in murine bleomycin-induced pulmonary fibrosis. *Stem Cell. Res. Ther.* 12 (1), 506. doi:10.1186/s13287-021-02574-5

Taskiran, E. Z., and Karaosmanoglu, B. (2019). Transcriptome analysis reveals differentially expressed genes between human primary bone marrow mesenchymal stem cells and human primary dermal fibroblasts. *Turk J. Biol.* 43 (1), 21–27. doi:10.3906/biy-1808-81

Thej, C., Ramadasse, B., Walvekar, A., Majumdar, A. S., and Balasubramanian, S. (2017). Development of a surrogate potency assay to determine the angiogenic activity of Stempeucel®, a pooled, *ex-vivo* expanded, allogeneic human bone marrow mesenchymal stromal cell product. *Stem Cell. Res. Ther.* 8 (1), 47. doi:10.1186/s13287-017-0488-3

Thoene, M., Bejer-Olenska, E., and Wojtkiewicz, J. (2023). The current state of osteoarthritis treatment options using stem cells for regenerative therapy: a review. *Int. J. Mol. Sci.* 24 (10), 8925. doi:10.3390/ijms24108925

Thompson, M., Mei, S. H. J., Wolfe, D., Champagne, J., Fergusson, D., Stewart, D. J., et al. (2020). Cell therapy with intravascular administration of mesenchymal stromal cells continues to appear safe: an updated systematic review and meta-analysis. *EClinicalMedicine* 19, 100249. doi:10.1016/j.eclinm.2019.100249

Todtenhaupt, P., Franken, L. A., Groene, S. G., van Hoolwerff, M., van der Meeren, L. E., van Klink, J. M. M., et al. (2023). A robust and standardized method to isolate and expand mesenchymal stromal cells from human umbilical cord. *Cytotherapy* 25 (10), 1057–1068. doi:10.1016/j.jcyt.2023.07.004

Tomecka, E., Lech, W., Zychowicz, M., Sarnowska, A., Murzyn, M., Oldak, T., et al. (2021). Assessment of the neuroprotective and stemness properties of human wharton's jelly-derived mesenchymal stem cells under variable (5% vs. 21%) aerobic conditions. *Cells* 10 (4), 717. doi:10.3390/cells10040717

Trento, C., Bernardo, M. E., Nagler, A., Kuçi, S., Bornhäuser, M., Köhl, U., et al. (2018). Manufacturing mesenchymal stromal cells for the treatment of graft-versus-host disease: a survey among centers affiliated with the European society for blood and marrow transplantation. *Biol. Blood Marrow Transpl.* 24 (11), 2365–2370. doi:10.1016/j.bbmt.2018.07.015

Um, S., Ha, J., Choi, S. J., Oh, W., and Jin, H. J. (2020). Prospects for the therapeutic development of umbilical cord blood-derived mesenchymal stem cells. *World J. Stem Cells* 12 (12), 1511–1528. doi:10.4252/wjsc.v12.i12.1511

Veceric-Haler, Z., Sever, M., Kojc, N., Halloran, P. F., Boštjančič, E., Mlinšek, G., et al. (2022). Autologous mesenchymal stem cells for treatment of chronic active antibody-mediated kidney graft rejection: report of the phase I/II clinical trial case series. *Transpl. Int.* 35, 10772. doi:10.3389/ti.2022.10772

Viswanathan, S., Shi, Y., Galipeau, J., Krampera, M., Leblanc, K., Martin, I., et al. (2019). Mesenchymal stem versus stromal cells: international society for cell and gene therapy (ISCT®) mesenchymal stromal cell committee position statement on nomenclature. *Cytotherapy* 21 (10), 1019–1024. doi:10.1016/j.jcyt.2019.08.002

von Bahr, L., Sundberg, B., Lönnies, L., Sander, B., Karbach, H., Hägglund, H., et al. (2012). Long-term complications, immunologic effects, and role of passage for outcome in mesenchymal stromal cell therapy. *Biol. Blood Marrow Transpl.* 18 (4), 557–564. doi:10.1016/j.bbmt.2011.07.023

Waldner, M., Zhang, W., James, I. B., Allbright, K., Havis, E., Bliley, J. M., et al. (2018). Characteristics and immunomodulating functions of adipose-derived and bone marrow-derived mesenchymal stem cells across defined human leukocyte antigen barriers. *Front. Immunol.* 9, 1642. doi:10.3389/fimmu.2018.01642

Wang, H., Jiang, H. Y., Zhang, Y. X., Jin, H. Y., Fei, B. Y., and Jiang, J. L. (2023). Mesenchymal stem cells transplantation for perianal fistulas: a systematic review and meta-analysis of clinical trials. *Stem Cell. Res. Ther.* 14 (1), 103. doi:10.1186/s13287-023-03331-6

Wang, L., Li, P., Tian, Y., Li, Z., Lian, C., Ou, Q., et al. (2017). Human umbilical cord mesenchymal stem cells: subpopulations and their difference in cell biology and effects on retinal degeneration in RCS rats. *Curr. Mol. Med.* 17 (6), 421–435. doi:10.2174/1566524018666171205140806

Wang, P., Zhu, P., Yu, C., and Wu, J. (2022). The proliferation and stemness of peripheral blood-derived mesenchymal stromal cells were enhanced by hypoxia. *Front. Endocrinol. (Lausanne)* 13, 873662. doi:10.3389/fendo.2022.873662

Wang, P. F., and Xing, J. (2023). The clinical outcomes of intra-articular injection of human umbilical cord blood-derived mesenchymal stem cells vs. bone marrow aspirate concentrate in cartilage regeneration: a systematic review. *Eur. Rev. Med. Pharmacol. Sci.* 27 (16), 7533–7543. doi:10.26355/eurrev_202308_33405

Wang, Y., Yi, H., and Song, Y. (2021a). The safety of MSC therapy over the past 15 years: a meta-analysis. *Stem Cell. Res. Ther.* 12 (1), 545. doi:10.1186/s13287-021-02609-x

Wang, Z., Chai, C., Wang, R., Feng, Y., Huang, L., Zhang, Y., et al. (2021c). Single-cell transcriptome atlas of human mesenchymal stem cells exploring cellular heterogeneity. *Clin. Transl. Med.* 11 (12), e650. doi:10.1002/ctm2.650

Wang, Z., Chai, C., Wang, R., Feng, Y., Huang, L., Zhang, Y., et al. (2021d). Single-cell transcriptome atlas of human mesenchymal stem cells exploring cellular heterogeneity. *Clin. Transl. Med.* 11 (12), e650. doi:10.1002/ctm2.650

Wang, Z., Li, X., Yang, J., Gong, Y., Zhang, H., Qiu, X., et al. (2021b). Single-cell RNA sequencing deconvolutes the *in vivo* heterogeneity of human bone marrow-derived mesenchymal stem cells. *Int. J. Biol. Sci.* 17 (15), 4192–4206. doi:10.7150/ijbs.61950

Wang, Z., Xu, Q., Zhang, N., Du, X., Xu, G., and Yan, X. (2020). CD146, from a melanoma cell adhesion molecule to a signaling receptor. *Signal Transduct. Target Ther.* 5 (1), 148. doi:10.1038/s41392-020-00259-8

Watson, J. T., Foo, T., Wu, J., Moed, B. R., Thorpe, M., Schon, L., et al. (2013). CD271 as a marker for mesenchymal stem cells in bone marrow versus umbilical cord blood. *Cells Tissues Organs* 197 (6), 496–504. doi:10.1159/000348794

Widholz, B., Tsitlakidis, S., Reible, B., Moghaddam, A., and Westhauser, F. (2019). Pooling of patient-derived mesenchymal stromal cells reduces inter-individual confounder-associated variation without negative impact on cell viability, proliferation and osteogenic differentiation. *Cells* 8 (6), 633. doi:10.3390/cells8060633

Wiese, D. M., and Braid, L. R. (2020). Transcriptome profiles acquired during cell expansion and licensing validate mesenchymal stromal cell lineage genes. *Stem Cell. Res. Ther.* 11 (1), 357. doi:10.1186/s13287-020-01873-7

Wiese, D. M., Wood, C. A., and Braid, L. R. (2022). From vial to vein: crucial gaps in mesenchymal stromal cell clinical trial reporting. *Front. Cell. Dev. Biol.* 10, 867426. doi:10.3389/fcell.2022.867426

Willer, H., Spohn, G., Morgenroth, K., Thielemann, C., Elvers-Hornung, S., Bugert, P., et al. (2022). Pooled human bone marrow-derived mesenchymal stromal cells with defined trophic factors cargo promote dermal wound healing in diabetic rats by improved vascularization and dynamic recruitment of M2-like macrophages. *Front. Immunol.* 13, 976511. doi:10.3389/fimmu.2022.976511

Wilson, A. J., Brown, N., Rand, E., and Genever, P. G. (2023). Attitudes towards standardization of mesenchymal stromal cells-A qualitative exploration of expert views. *Stem Cells Transl. Med.* 12 (11), 745–757. doi:10.1093/stcltm/szad056

Wilson, A. J., Rand, E., Webster, A. J., and Genever, P. G. (2021). Characterisation of mesenchymal stromal cells in clinical trial reports: analysis of published descriptors. *Stem Cell. Res. Ther.* 12 (1), 360. doi:10.1186/s13287-021-02435-1

Wu, M., Zhang, R., Zou, Q., Chen, Y., Zhou, M., Li, X., et al. (2018). Comparison of the biological characteristics of mesenchymal stem cells derived from the human placenta and umbilical cord. *Sci. Rep.* 8 (1), 5014. doi:10.1038/s41598-018-23396-1

Xie, Z., Yu, W., Ye, G., Li, J., Zheng, G., Liu, W., et al. (2022). Single-cell RNA sequencing analysis of human bone-marrow-derived mesenchymal stem cells and

functional subpopulation identification. *Exp. Mol. Med.* 54 (4), 483–492. doi:10.1038/s12276-022-00749-5

Yang, Y. K., Ogando, C. R., Wang See, C., and Barabino, G. A. (2018). Changes in phenotype and differentiation potential of human mesenchymal stem cells aging *in vitro*. *Stem Cell. Res. Ther.* 9 (1), 131. doi:10.1186/s13287-018-0876-3

Yea, J. H., Kim, Y., and Jo, C. H. (2023). Comparison of mesenchymal stem cells from bone marrow, umbilical cord blood, and umbilical cord tissue in regeneration of a full-thickness tendon defect *in vitro* and *in vivo*. *Biochem. Biophys. Rep.* 34, 101486. doi:10.1016/j.bbrep.2023.101486

Yen, B. L., Hsieh, C. C., Hsu, P. J., Chang, C. C., Wang, L. T., and Yen, M. L. (2023). Three-Dimensional spheroid culture of human mesenchymal stem cells: offering therapeutic advantages and *in vitro* glimpses of the *in vivo* state. *Stem Cells Transl. Med.* 12 (5), 235–244. doi:10.1093/stcltm/szad011

Yu, J., He, H., Tang, C., Zhang, G., Li, Y., Wang, R., et al. (2010). Differentiation potential of STRO-1+ dental pulp stem cells changes during cell passaging. *BMC Cell. Biol.* 11, 32–37. doi:10.1186/1471-2121-11-32

Zhang, C., Han, X., Liu, J., Chen, L., Lei, Y., Chen, K., et al. (2022a). Single-cell transcriptomic analysis reveals the cellular heterogeneity of mesenchymal stem cells. *Genomics, Proteomics Bioinforma.* 20 (1), 70–86. doi:10.1016/j.gpb.2022.01.005

Zhang, C., Zhou, L., Wang, Z., Gao, W., Chen, W., Zhang, H., et al. (2021b). Eradication of specific donor-dependent variations of mesenchymal stem cells in immunomodulation to enhance therapeutic values. *Cell. Death Dis.* 12 (4), 357. doi:10.1038/s41419-021-03644-5

Zhang, F., Ren, H., Shao, X., Zhuang, C., Chen, Y., and Qi, N. (2017). Preservation media, durations and cell concentrations of short-term storage affect key features of human adipose-derived mesenchymal stem cells for therapeutic application. *PeerJ* 5, e3301. doi:10.7717/peerj.3301

Zhang, L., Sun, Y., Zhang, X. X., Liu, Y. B., Sun, H. Y., Wu, C. T., et al. (2022b). Comparison of CD146 +/- mesenchymal stem cells in improving premature ovarian failure. *Stem Cell. Res. Ther.* 13 (1), 267. doi:10.1186/s13287-022-02916-x

Zhang, S., Wang, J. Y., Yin, F., and Liu, H. (2021a). Single-cell transcriptome analysis of uncultured human umbilical cord mesenchymal stem cells. *Stem Cell. Res. Ther.* 12 (1), 25. doi:10.1186/s13287-020-02055-1

Zhang, W., Ling, Q., Wang, B., Wang, K., Pang, J., Lu, J., et al. (2022c). Comparison of therapeutic effects of mesenchymal stem cells from umbilical cord and bone marrow in the treatment of type 1 diabetes. *Stem Cell. Res. Ther.* 13 (1), 406. doi:10.1186/s13287-022-02974-1

Zhu, X., Wang, Z., Sun, Y. E., Liu, Y., Wu, Z., Ma, B., et al. (2022). Neuroprotective effects of human umbilical cord-derived mesenchymal stem cells from different donors on spinal cord injury in mice. *Front. Cell. Neurosci.* 15, 768711. doi:10.3389/fncel.2021.768711

Zoehler, B., Fracaro, L., Boldrini-Leite, L. M., da Silva, J. S., Travers, P. J., Brofman, P. R. S., et al. (2022). HLA-G and CD152 expression levels encourage the use of umbilical cord tissue-derived mesenchymal stromal cells as an alternative for immunosuppressive therapy. *Cells* 11 (8), 1339. doi:10.3390/cells11081339

Zyrafete, K., Bönig, H., Kreyenberg, H., Bunos, M., Jauch, A., Janssen, J. W. G., et al. (2016). Mesenchymal stromal cells from pooled mononuclear cells of multiple bone marrow donors as rescue therapy in pediatric severe steroid-refractory graft-versus-host disease: a multicenter survey. *Haematologica* 101 (8), 985–994. doi:10.3324/haematol.2015.140368

frontiers | Frontiers in Medicine

TYPE Review
PUBLISHED 30 July 2024
DOI 10.3389/fmed.2024.1406547

OPEN ACCESS

EDITED BY
Willem Fibbe,
Leiden University Medical Center (LUMC), Netherlands

REVIEWED BY
Eiji Kawamoto,
Mie University, Japan
Marcel I. Ramirez,
Oswaldo Cruz Foundation, Brazil

*CORRESPONDENCE
Yongmin Yan
✉ yym@wjrmyy.cn
Zhiliang Xu
✉ clinlab@wjrmyy.cn

†These authors have contributed equally to this work

RECEIVED 25 March 2024
ACCEPTED 18 July 2024
PUBLISHED 30 July 2024

CITATION
Din MAU, Wan A, Chu Y, Zhou J, Yan Y and Xu Z (2024) Therapeutic role of extracellular vesicles from human umbilical cord mesenchymal stem cells and their wide therapeutic implications in inflammatory bowel disease and other inflammatory disorder.
Front. Med. 11:1406547.
doi: 10.3389/fmed.2024.1406547

Therapeutic role of extracellular vesicles from human umbilical cord mesenchymal stem cells and their wide therapeutic implications in inflammatory bowel disease and other inflammatory disorder

Muhammad Azhar Ud Din[1,2†], Aijun Wan[3†], Ying Chu[1], Jing Zhou[1], Yongmin Yan[1*] and Zhiliang Xu[1*]

[1]Changzhou Key Laboratory of Molecular Diagnostics and Precision Cancer Medicine, Wujin Hospital Affiliated with Jiangsu University, Jiangsu University, Changzhou, China, [2]Key Laboratory of Medical Science and Laboratory Medicine of Jiangsu Province, School of Medicine Jiangsu University, Zhenjiang, China, [3]Zhenjiang College, Zhenjiang, China

The chronic immune-mediated inflammatory condition known as inflammatory bowel disease (IBD) significantly affects the gastrointestinal system. While the precise etiology of IBD remains elusive, extensive research suggests that a range of pathophysiological pathways and immunopathological mechanisms may significantly contribute as potential factors. Mesenchymal stem cells (MSCs) have shown significant potential in the development of novel therapeutic approaches for various medical conditions. However, some MSCs have been found to exhibit tumorigenic characteristics, which limit their potential for medical treatments. The extracellular vesicles (EVs), paracrine factors play a crucial role in the therapeutic benefits conferred by MSCs. The EVs consist of proteins, microRNAs, and lipids, and are instrumental in facilitating intercellular communication. Due to the ease of maintenance, and decreased immunogenicity, tumorigenicity the EVs have become a new and exciting option for whole cell treatment. This review comprehensively assesses recent preclinical research on human umbilical cord mesenchymal stem cell (hUC-MSC)-derived EVs as a potential IBD therapy. It comprehensively addresses key aspects of various conditions, including diabetes, cancer, dermal injuries, neurological disorders, cardiovascular issues, liver and kidney diseases, and bone-related afflictions.

KEYWORDS

inflammatory bowel disease, human umbilical mesenchymal stem cells, exosomes, genes, extracellular vesicles

1 Introduction

Inflammatory bowel disease (IBD) refers to a group of chronic inflammatory disorders of the gastrointestinal tract, with two primary subtypes: Crohn's disease (CD) and ulcerative colitis (UC) (1). These disorders result from an abnormal immune response in genetically susceptible individuals, triggered by environmental factors. The characteristic symptoms

include abdominal pain, diarrhea, rectal bleeding, weight loss, and fatigue (2). The chronic and relapsing nature of IBD often leads to a diminished quality of life and a higher risk of complications such as bowel strictures, abscesses, and even colorectal cancer. Over the years, various treatment modalities have been developed to treat patient with IBD including anti-inflammatory medications, immunosuppressant, biological therapies, and surgical interventions (3). While these treatments have been effective for many patients, they are not without limitations. Long-term use of immunosuppressive drugs can lead to increased susceptibility to infections, and biologic therapies often come with a high financial burden. Moreover, a significant proportion of IBD patients do not respond adequately to existing treatments, highlighting the urgent need for novel therapeutic strategies (4).

The complexities of IBD, including its multifactorial etiology and heterogeneity in disease presentation, pose a challenge for clinicians seeking to tailor treatment approaches to individual patients (5). Currently, a significant proportion of the etiology and pathology underlying this condition remains elusive to the scientific community. Nevertheless, it is widely acknowledged that the condition is characterized by a polygenic and multifactorial nature (6). Incorporating the insights obtained from numerous recent studies, the fundamental elements contributing to the onset of IBD involve genetic interactions, dysregulated mucosal immune responses prompted by environmental factors, and disruptions in the regulation of the gut microbiota (6). Currently, several treatment protocols, including immunomodulatory, thiopurine agents, and monoclonal antibodies targeting tumor necrosis factor (anti-TNF), are employed for the management of IBD. However, these treatments have been found to lack the attainment of sufficiently favorable therapeutic outcomes (7). Consequently, researchers are actively exploring the development of advanced clinical techniques and strategies for the treatment of IBD. In this context, the search for safer and more effective therapies has led researchers to explore the regenerative potential of mesenchymal stem cells (MSCs) and their extracellular vesicles (EVs) (8, 9). MSCs are multipotent, adult stem cells found in various tissues, including bone marrow, adipose tissue, and the umbilical cord (10). These cells have garnered immense interest in the field of regenerative medicine due to their remarkable self-renewal capabilities and their ability to differentiate into multiple cell lineages, including osteocytes, adipocytes, and chondrocytes (11, 12). Moreover, the quantity of stem cells and their capacity for proliferation and differentiation exhibited a marked decline with advancing age (13), thereby imposing limitations on the application of these cells in clinical trials (14). The morphological characteristics, immunophenotype, proliferation rate, multi-directional differentiation capacity, and their potential to induce hematopoietic stem cell (HSC) differentiation in umbilical cord-derived mesenchymal stem cells (UC-MSCs) closely resemble those observed in bone marrow-derived mesenchymal stem cells (BM-MSCs) (15), but, it is noteworthy that UC-MSCs display a heightened proliferative capacity and lower levels of human leukocyte antigen (HLA)-ABC and HLA-DR expression in comparison to BM-MSCs (16). Furthermore, it is worth noting that UC-MSCs exhibit a diverse array of stem cell types, making them readily available and easily collectable resource that can be efficiently preserved (17, 18). Consequently, UC-MSCs assume a distinctive role in diminishing both the frequency and severity of graft-versus-host disease (GVHD), a complication that affects over 50% of patients undergoing hematopoietic stem cell transplantation (HSCT) (18). Moreover, owing to their inherent migratory potential towards cancer cells, numerous studies have suggested the utilization of UC-MSCs in cell-based therapies aimed at targeting tumors and facilitating the localized delivery of anti-cancer agents (19). Nonetheless, several facets of research concerning UC-MSCs are still in their early stages of development. UC-MSCs are considered optimal candidate cells for cell replacement therapy, primarily due to their minimal immunogenicity, robust proliferative potential, and capacity for differentiation (20).

The therapeutic effectiveness of MSCs do not exclusively hinge on their ability to differentiate into various cell types. Instead, their paracrine effects, which involve the release of trophic factors and EVs, assume a central role in promoting tissue repair and modulating the immune response (21). MSCs can orchestrate a coordinated response by influencing local cell populations, reducing inflammation, and promoting tissue regeneration (22). The secretion of EVs, in particular, has gained significant attention for their role in intercellular communication and their potential as therapeutic agents (23). EVs are small membranous vesicles released by virtually all cell types, including MSCs. They are involved in cell-to-cell communication and serve as vehicles for the transfer of bioactive molecules, including proteins, lipids, and nucleic acids, between cells (24, 25). EVs are classified into several subtypes, including exosomes, macrovesicles, and apoptotic bodies, based on their biogenesis and size. Among these, exosomes, typically ranging from 30 to 150 nanometers in diameter, have garnered significant interest for the therapeutic potential (26). Exosomes are released into the extracellular space through the fusion of multivesicular bodies with the plasma membrane (27). Extensive investigations have revealed the secretion of exosomes by a wide range of cell types, including mast cells, dendritic cells (27), B cells (28), T cells (29), tumor cells (30), and epithelial cells. Exosomes have also been found in numerous kinds of body fluids, such as saliva, urine, breast milk, and plasma (31, 32) urine (33, 34). Exosomes, like their parent cells, carry a cargo of bioactive molecules that can modulate various cellular processes (35, 36). These molecules include growth factors, cytokines, microRNAs, and lipids, all of which can influence recipient cells' behavior (37, 38). This cargo is carefully packaged within the exosome's lipid bilayer, protecting it from degradation and ensuring its efficient delivery to target cells (39). This unique characteristic makes exosomes ideal candidates for therapeutic interventions, as they can harness the regenerative power of their parent cells in a more controlled and targeted manner (40, 41). Exosomes originating from diverse sources exert an influence on the etiology of IBD (42). The significance of intercellular communication in maintaining homeostasis in multicellular organisms has been well-documented previously. Consequently, exosomes, which are secreted by a majority of cells, play a critical role in forming a network and actively participating in intracellular signaling (43). They facilitate the transfer of bioactive components including, lipids, nucleic acids, and proteins from one cell to another, thereby initiating biological responses in the recipient cells (44). Exosomes have demonstrated a greater efficacy than their parent cells and can be stored without compromising their functionality, making them an appealing focus of research. Recently, there has been an increasing interest in utilizing exosome administration as a novel therapeutic strategy to expedite preclinical research endeavors (45, 46). Furthermore, exosome-delivered miRNAs contribute to lymphangiogenesis and play a role in

IBD. Exosomes derived from adipose tissue-derived MSCs modulate the miRNA-132/TGF-β pathway, thereby promoting VEGF-C-dependent lymphangiogenesis (47). MSC-derived exosomes have been substantiated to augment angiogenesis in endothelial cells by transporting miR-125a (48). Conversely, BM-MSCs promote lymphangiogenesis through the secretion of VEGF-A, which stimulates lymphatic endothelial cells (LECs) to activate the VEGFR-2 pathway (49).

The therapeutic potential of EVs, including those derived from MSCs, extends beyond their immunomodulatory effects (50, 51). Studies have demonstrated that MSC-derived EVs can promote tissue repair and regeneration in various disease models, including myocardial infarction, stroke, and cartilage injury (52). The cargo carried by these vesicles plays a pivotal role in modulating the recipient cell's behavior, promoting angiogenesis, reducing fibrosis, and enhancing tissue remodeling (52). The isolation and characterization of human umbilical cord mesenchymal stem cell (hUC-MSC)-derived EVs represent a critical step in harnessing their therapeutic potential (53). Researchers have developed various methods to isolate and purify these vesicles, including ultracentrifugation, size exclusion chromatography, and immunoaffinity-based techniques (54).

These methods ensure the enrichment of exosomes and other EV subtypes from hUC-MSC culture supernatants, allowing for their subsequent analysis and utilization (55). One of the most striking features of hUC-MSC-derived EVs is their ability to modulate the immune response (56). These vesicles can suppress the activation of pro-inflammatory immune cells while promoting the expansion of regulatory T cells and M2 macrophages, thus shifting the immune milieu towards an anti-inflammatory and tissue-healing phenotype (57). This immunomodulatory capacity has profound implications for the treatment of immune-mediated disorders like IBD (58). Recent preclinical studies and early-phase clinical trials have provided compelling evidence of the therapeutic potential of hUC-MSC-derived EVs in the management of IBD (59). These studies have shown that the administration of hUC-MSC-derived EVs can ameliorate disease symptoms, reduce inflammation, and promote mucosal healing in animal models and human patients with IBD. The mechanisms underlying these effects involve the immunomodulatory properties of the vesicles, as well as their ability to enhance epithelial barrier function and promote tissue repair (60, 61). The therapeutic potential of hUC-MSC-derived EVs extends beyond gastrointestinal disorders. Researchers are exploring their use in various neurological disorders, such as Parkinson's disease, Alzheimer's disease, and spinal cord injury (SCI) (62, 63). These vesicles have shown promise in promoting neuroprotection, reducing inflammation, and enhancing neural tissue repair in preclinical models (64). Cardiovascular diseases, including myocardial infarction and heart failure, are leading causes of morbidity and mortality worldwide. The hUC-MSC-derived EVs have emerged as potential candidates for cardiac regeneration and repair. Their ability to stimulate angiogenesis, reduce oxidative stress, and modulate immune responses has made them attractive for the treatment of cardiovascular disorders (65, 66). Musculoskeletal disorders, such as osteoarthritis and bone fractures, present significant challenges in the field of regenerative medicine. The hUC-MSC-derived EVs have shown promise in promoting bone and cartilage regeneration by enhancing the proliferation and differentiation of osteoblasts and chondrocytes. These vesicles may offer a minimally invasive and cell-free alternative to traditional treatments (67).

While the therapeutic potential of hUC-MSC-derived EVs is promising, several challenges must be addressed before their widespread clinical adoption. Standardization of isolation and characterization methods, determination of optimal dosing regimens, and long-term safety assessments are crucial steps in the path to clinical translation (54). Moreover, regulatory approvals and manufacturing scalability need to be addressed to ensure the accessibility of these therapies to a broader patient population. The heterogeneity of diseases like IBD underscores the importance of personalized medicine. Identifying biomarkers that can predict patient responses to hUC-MSC-derived EV therapy is a critical research area. Biomarker discovery will enable clinicians to select the most appropriate patients for treatment and tailor therapy regimens accordingly, maximizing therapeutic outcomes (68). As the field of regenerative medicine advances, ethical and regulatory considerations become increasingly important (69). Ensuring the ethical sourcing of umbilical cord tissue and transparent reporting of research findings is essential. Regulatory agencies must also develop clear guidelines to govern the production and clinical use of hUC-MSC-derived EVs, balancing innovation with patient safety (61). The therapeutic role of hUC-MSC-derived EVs represent a promising frontier in the treatment of IBD and a wide array of other disorders (70). With their ability to modulate the immune response, promote tissue repair, and enhance regenerative processes, hUC-MSC-derived EVs hold the potential to revolutionize the way we approach the management of chronic and debilitating conditions (71).

This study has undertaken an exploration of the complexities surrounding IBD, delving into the regenerative capabilities of MSCs, revealing the therapeutic potential inherent in EVs, and engaging in a discussion concerning the promising prospects of hUC-MSC-EVs within the context of IBD. The journey towards fully harnessing the therapeutic potential of these minuscule communicators is an ongoing endeavor, replete with a myriad of challenges and opportunities that await both researchers and clinicians. As we continue to venture deeper into the realm of regenerative medicine, we stand at the precipice of uncovering innovative solutions that have the potential to transform the lives of individuals grappling with chronic and presently incurable diseases. This review underscores the paramount importance of sustained research and clinical progress within this promising field, emphasizing the potential of hUC-MSC-EVs as an exceptional therapeutic avenue not only for IBD but also for a spectrum of inflammatory conditions.

2 Extracellular vesicles

The release of EVs is a fundamental biological process in both prokaryotic and eukaryotic cells, occurring under normal physiological conditions as well as in aberrant situations. Despite being written off in the past as little more than biological waste with little significance, recent studies have highlighted their crucial function as bioactive transporters. These vesicles mediate a wide range of biological processes and act as transporters of many cellular components, enabling complex cellular communications (72). Proteins such as cell surface receptors, signaling proteins, transcription factors, enzymes, and extracellular matrix proteins are among the diverse cargo carried by EVs (73). Additionally, they have lipids and nucleic acids (DNA, mRNA, and miRNA) that can be transferred

from donor to recipient cells to facilitate molecular transfer and intercellular communication (74). It has been discovered that EVs are linked to pathological conditions like cancer, heart disease, and neurological illnesses (75). EVs comprise a range of subtypes that are categorized based on their mechanisms of synthesis and release, such as exosomes, apoptotic blebs, and other EV subgroups (76). Additionally, they can be categorized according to the type of cell from which they originated, such as endothelium or platelet-derived cells, or according to the physiological state of the cells, such as "prostasomes" coming from the prostate and "oncosomes" originating from cancer cells. The primary components of EVs include apoptotic bodies, exosomes, and microvesicles (77). However, other forms have been discovered recently, including membrane particles, large oncosomes, migrasomes (78), ectosomes (78), exomeres (79) and supermeres (Table 1).

Recently, EVs have emerged as a promising therapeutic option for a range of diseases and conditions, including BD (91). In animal models of IBD, studies have provided evidence showing that EVs derived from various sources, including MSCs, possess the ability to mitigate inflammation and facilitate tissue healing (92). Using EVs as a therapeutic alternative presents several challenges that need to be addressed. In the preparation of EVs, standardization of isolation and characterization is a significant challenge in maintaining the purity and quality of EVs (93). The immunogenicity potential and pro-coagulant effects are two additional safety concerns associated with EV-based medicines (94). Despite these obstacles, EV-based medicines are still being clinically researched and developed, demonstrating significant potential for the treatment of various inflammatory illnesses including IBD. Herein, the MSC-derived-exosomes are the main focus of the study to provide comprehensive use, specifically in the treatment of IDB and other pathological inflammatory conditions in general.

3 Exosomes

Exosomes, a type of EVs, which originate from endosomes, typically exhibit an average diameter of approximately 50–100 nm (95). The plasma membrane undergoes a sequential process of invagination, leading to the eventual formation of multivesicular bodies (MVBs). These MVBs have the ability to interact with other intracellular vesicles and organelles, thereby contributing to the diversity of components found in exosomes. Depending on the specific cell they originate from, exosomes, can encompass a wide range of cellular constituents, such as DNA, RNA, lipids, metabolites, as well as cytosolic and cell-surface proteins (96).

Exosomes, in particular, have emerged as crucial mediators of cellular communication, playing significant roles in both normal physiological processes, such as lactation (97), immune response (34) and neuronal function (97), and also in the development and progression of diseases, such as liver disease (97), neurodegenerative diseases (98) and cancer. Exosomes are increasingly recognized as promising therapeutic agents for gastrointestinal conditions, IBD, using a cell-free therapeutic strategy (98, 99).

TABLE 1 Extracellular vesicles as therapeutic tools and targets for diseases.

Subtype	Size	Origin of EV	Density	Biomarkers	Mechanism	References
Exosomes	50–150	Multivesicle body	1.13–1.19	CD9, CD63, CD81, Tsg101, ALIX, HSP70	Endosomes develop into late endosomes, which have intraluminal vesicles that fuse with the plasma membrane to release MVBs (dependent or independent of ESCRT)	(80, 81)
Microvesicles	100–1,000	Plasma membrane	1.032–1.068	Integrins, Selectins, CD40, tissue factor	Direct plasma membrane budding and cleavage are caused by calcium influx and remodelling of the cortical cytoskeleton	(81, 82)
Migrasomes	500–3,000	Retraction fibers	Unknown	Tspan4, CD63, Annexin A1	Actin polarisation and cell migration cause migratory cells to migrate and create migratory granules at the tip or by bifurcating the retraction fibres	(83)
Apoptotic Bodies	100–5,000	Plasma membrane	1.16–1.28	Annexin V, C3b, thrombospondin, Annexin A1, histone coagulation factor	Programed cell death involves the fragmentation of cytoplasm	(81, 84, 85)
Exomeres	Secreting from cells	≤50	1.1–1.19	TGFBI, ENO1 and GPC1	Large cytoplasmic extensions are cleaved off the cell body	(86)
Oncosomes	1,000–10,000	The shedding of non-apoptotic plasma membrane blebbing	1.10–1.15	Cav-1 or ADP ribosylation factor 6	Released by cancerous cells with amoeboid movement	(87, 88)
Supermeres	~35 (<50)	Unknown	Unknown	TGFBI, ACE2, PCSK9, miR-1246, MET, GPC1 and AGO2, exRNA; miR-1246	Unknown	(89, 90)

Numerous diseases associated with IBD, characterized by disruptions in mucosal immune responses, compromised intestinal barrier integrity, and alterations in the balance of intestinal microbial populations, are orchestrated through pathways involving exosomal intercellular communication (100). Exosomes, being complex molecules, are discharged into human serum and other bodily fluids, and their functional contents exhibit variations between IBD patients and healthy individuals (101). Consequently, exosomes may have the potential to serve as diagnostic biomarkers that reflect the current state of IBD (101, 102).

3.1 Characteristics and properties of exosomes

3.1.1 Characteristics of exosomes

Exosomes originate from endosomal vesicles within the cell and exhibit distinctive characteristics that set them apart from other cell-secreted microvesicles (103). They are enclosed by a phospholipid bilayer architecture, with a size ranging from 30 to 150 nanometers and a density falling within the range of 1.13 to 1.19 grams per milliliter (104, 105). When observed through transmission electron microscopy (TEM), exosomes present a cup-shaped morphology, further confirming their identity. Moreover, the presence of specific proteins, including tetraspanins (e.g., CD63, CD9, and CD81) and β-actin, serves as additional markers to differentiate exosomes from other vesicular structures (101, 104). To emphasize their prevalence, it is noteworthy that approximately 1×10^{12} exosomes can be found in just 1 milliliter of blood (105). These distinct characteristics and abundance make exosomes a subject of significant interest in various fields of research and clinical applications (106).

3.1.2 Biogenesis of exosomes

Exosome biogenesis is a highly regulated process that occurs in various cell types under both pathological and physiological conditions. The secretion of exosomes is governed by the modulation of Rab27a and Rab27b expression (107). A diverse array of cell types, including lymphocytes, dendritic cells, fibroblasts, erythrocytes, platelets, mast cells, tumor cells, stem cells, monocytes, macrophages, natural killer (NK) cells, B lymphocytes, and T lymphocytes, are known to synthesize exosomes (108).

The process of exosome biogenesis commences with the internalization of the cell membrane, leading to the formation of small intracellular structures referred to as early endosomes (103–107). Early endosome development involves a progressive maturation process that culminates in the generation of intraluminal vesicles (ILVs). On the other hand, late endosomes, known as multivesicular bodies (MVBs), are formed through the inward folding of segments of the endosomal membrane (106). The fusion of MVBs with the plasma membrane results in the exocytotic release of ILVs into the extracellular space, where they ultimately undergo transformation into exosomes (99–102, 105). This intricate process is visually depicted in Figure 1.

Notably, exosomes are present in a variety of physiological fluids, including serum, as well as in saliva, amniotic fluid, and breast milk (106). Their presence in these fluids underscores the ubiquity of exosomes in biological systems and their potential significance in various biological and clinical contexts.

3.1.3 Composition of exosomes

Exosomes, which are minuscule in size and invisible to the naked eye and standard light microscopes, can only be observed using electron microscopy. Their morphology is characterized by flattened spheres, which can result from the dehydration process required for electron microscopy preparation, leading to their collapse (108, 109). Exosomes are complex structures composed of proteins, particularly those derived from the plasma or endosomal membrane, lipids, and various cytosolic components (Figure 2). It's important to note that exosomes lack proteins originating from the Golgi apparatus, nuclear pore complex, mitochondria, and endoplasmic reticulum (Figure 2). Exosomes lack proteins of the Golgi apparatus, nuclear pore complex, mitochondria and endoplasmic reticulum (110). Data on exosomal content are systematically curated and updated in databases such as ExoCarta, Vesiclepedia, and EVpedia (111). Although initial investigations suggest the presence of proteins from the cytosol, endosomes, and plasma membrane in exosomes, it is essential to acknowledge that cellular organelles such as mitochondria, the Golgi apparatus, or the nucleus do not exclusively consist of proteins. The establishment of exosomal protein databases has been a collaborative effort among multiple research teams. Exosome repositories like ExoCarta[1] and Vesiclepedia[2] have cataloged a total of 9,769 proteins, 1,116 lipids, 3,408 mRNAs, and 2,838 miRNAs within exosomes originating from various cellular sources and organisms up to the present day (110). Exosome protein sorting, a newly explored field of study, relies, at least in part, on the endosomal sorting complex required for transport (ESCRT) machinery and protein ubiquitylation (112). During exosome biogenesis, ESCRT orchestrates the formation of intricate structures on the plasma membrane, resembling membranous necks. These structures encompass conical funnels, tubular arrangements, planar spirals, and filaments, which are hypothesized to regulate membrane remodeling processes.

Exosomes encompass a substantial number of transport proteins, including tubulin, actin, and actin-binding molecules (110), in addition to various proteins intricately involved in specific roles within secretory cells (113). Exosomal proteins are categorized into diverse groups based on their family, function, and subcellular localization (114). The most frequently encountered protein categories in exosomes include those related to (i) the formation of multivesicular bodies (MVBs), (ii) transmembrane proteins acting as targeting or adhesion molecules, such as tetraspanins like CD9, CD63, and CD81, which play roles in membrane fusion, (iii) signal transduction proteins such as annexin and 14-3-3 proteins, (iv) cytoskeletal proteins including actin, syntenin, and myosin, (v) chaperones like HSPA8 and HSP90, and (vi) metabolic enzymes, such as GAPDH, LDHA, PGK1, aldolase, and PKM (111, 113). Each individual exosome also contains MHC class I molecules, among distinct components (114), and heat shock proteins (112). These proteins participate in antigen presentation and antigenic peptide attachment to MHC class I molecules (113). Tetraspanin family members CD9, CD63, CD81, and CD82 interact with other transmembrane proteins to facilitate antigen presentation and adhesion. The interaction of CD9 and CD82 with integrins can inhibit the migration and invasion of tumor cells (111). Exosomes exhibit distinctive lipid compositions in addition to their protein

1 www.exocarta.org
2 www.microvesicles.org

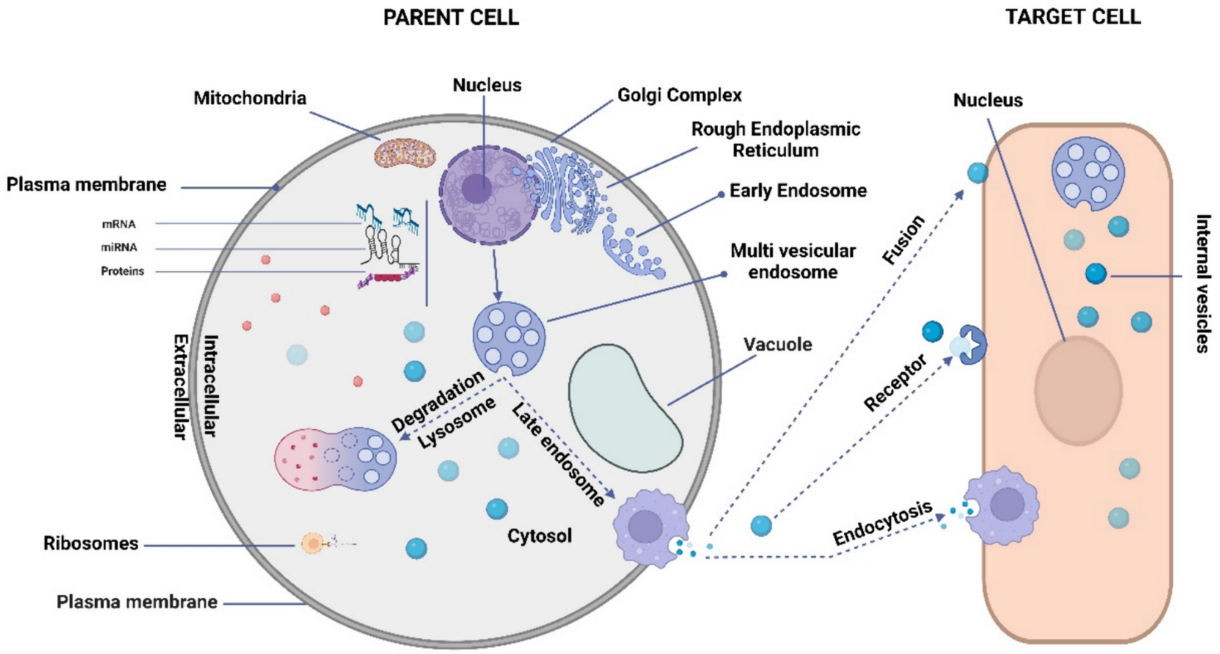

FIGURE 1
Schematic representation of exosome biogenesis. The process of exosome biogenesis is illustrated schematically in this figure. During exosome biogenesis, multivesicular endosomes (MVEs) initially undergo invagination, resulting in the formation of small intracellular vesicles. These vesicles encapsulate a diverse array of cytoplasmic cargo molecules, including proteins, messenger RNAs (mRNAs), and microRNAs (miRNAs). Notably, MVEs demonstrate two distinct fusion pathways: one involves fusion with the cellular membrane, facilitating the exocytosis of the enclosed exosomes (referred to as intravesicular vesicles). The other pathway entails fusion with lysosomes, leading to the degradation of the contents within MVEs. Consequently, exosomes gain entry into recipient cells through two distinct mechanisms: initially, they traverse the endocytic route, followed by internalization by the recipient cell. Secondly, they can merge directly with the recipient cell's plasma membrane, subsequently releasing their cargo into the cytoplasm. It's important to note that cells possess the capacity to generate membrane-derived vesicles that bud directly from the plasma membrane. These vesicles serve as vehicles for transporting functional proteins, RNAs, and other bioactive molecules.

content (113). Intriguingly, they are deficient in lysobisphosphatidic acid and intraluminal vesicle (ILV) lipids (115) but contain high levels of sphingomyelin, phosphatidylserine, ceramide, and cholesterol.

Exosomes are recognized for their substantial content of DNA and RNA, alongside lipids and proteins. The term "EV-DNA" refers to DNA enclosed within EVs, spanning a size range of 100 base pairs to 2.5 kilobases (115). Analysis of complete RNA sequencing data from EVs isolated from serum suggests that RNA repeats constitute approximately 50% of the total EV-RNA content. Additionally, miRNAs and tRNAs are estimated to account for up to 15% of the EV-RNA content (115, 116). Certain RNAs are found in higher concentrations in exosomes than in the originating cells, particularly in exosomes from MSCs (116). Numerous studies have provided evidence that RNA can indeed be transferred between cells via exosomes (117). However, the extent to which transferred RNA retains its functionality in recipient cells, as well as the proportion that undergoes fragmentation and subsequent transport, remains an area of ongoing investigation.

4 Human umbilical cord mesenchymal stem cells origin and biological characteristics

MSCs have gained significant prominence in experimental cell-based therapeutic approaches for a variety of human ailments. They are widely employed due to their proven efficacy in numerous disease-related animal models and their excellent safety record in clinical settings. MSCs offer great potential for treating human illnesses because of their ability to differentiate, self-renew, and modulate the immune response (118). While MSCs have garnered attention as a potential cellular treatment for various medical conditions, emerging evidence suggests that their therapeutic benefits are primarily mediated through EVs produced via paracrine processes (119). These EVs play a crucial role in conveying the therapeutic advantages of MSCs. The hUC-MSCs have been the subject of numerous research projects that have explored their potential use for the treatments of various medical problems, including diabetes (120), cancer (121), liver (122), bone (123), cartilage (124), brain (125), cardiovascular issues (126), and IBD (127), and Figure 3 illustrates the therapeutic effects of hUC-MSC, both in *in vivo* and *in vitro* environments. The administration of hUC-MSCs demonstrates marked amelioration in pivotal parameters, encompassing the disease activity index, fluctuations in body weight, alterations in colonic length, and histopathological assessments of colitis, predominantly through the mitigation of inflammation. A discernible correlation exists between the dosage of hUC-MSCs and the extent of therapeutic response as these parameters serve as standard indicators in IBD evaluations, reflecting both disease severity and the effectiveness of therapeutic interventions (126–128).

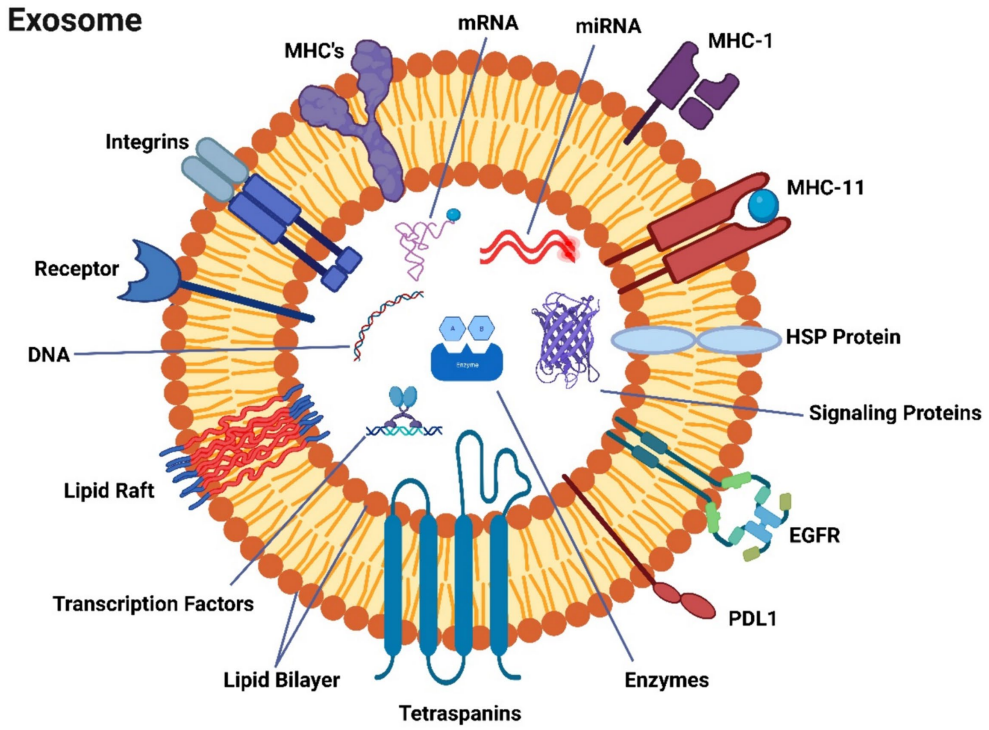

FIGURE 2
A description of exosomes' molecular make-up.

4.1 Biological characteristics

4.1.1 The UC-MSC's (hUC-MSC) immunological characteristics

The subcortical endothelium of the umbilical cord, Wharton's jelly (WJ), and the perivascular area are the primary locations where UC-MSCs are commonly found. Wharton's Jelly has a structure primarily resembling a sponge, with collagen fibers, proteoglycans, and stromal cells intertwined within it (20). When analyzing UC-MSCs from Wharton's Jelly using flow cytometry, it was discovered that CD24 and CD108 were abundantly expressed, while the dermal fibroblast marker CD40 and fibroblast-specific markers (FAP and FSP) were not discernible, which highlights the abundance of MSCs in the Wharton's Jelly region (128, 129). UC-MSCs can exhibit distinctive markers corresponding to various cell lineages, exemplifying their pluripotent nature (130). In contrast to hematopoietic stem cells, UC-MSCs exhibit the expression of MSC-specific markers such as CD105, CD90, and CD73, along with adhesion molecule markers including CD54, CD13, CD29, and CD44. Conversely, UC-MSCs shows reduced or absent expression of surface antigens CD31, CD14, CD34, and CD45 (131). Additionally, these cells are deficient in immune response-related antigens necessary for T lymphocyte activation, including CD80, CD86, CD40, and CD40L, as well as the MHC class II antigen HLA-DR. (132) UC-MSCs exhibit reduced immunogenicity compared to BM-derived cells due to their considerably lower expression levels of CD106 and HLA-ABC (133).

4.1.2 UC-MSCs' capability to proliferate and differentiate

WJ-MSCs, which exhibited the highest proliferation rate, outperformed adipose tissue and BM-MSCs by a factor of three to four in terms of proliferation (134). Based on the inquiry conducted by the Mennan research team, no significant disparity in the rate of proliferation was observed. The population of UC-MSCs exhibited an average twofold increase between passages P0 and P3 within a span of 2–3 days. This rate of expansion significantly exceeds the duration observed for BM-MSCs (135). UC-MSCs have the capacity for multidirectional differentiation, enabling them to differentiate into various tissues such as bone, fat, cartilage, and others (136). Therefore, in the field of regenerative medicine, these cells are considered ideal seed cells due to their potential to facilitate the healing of various tissues and organs (137). According to studies, chemokines are produced by biological tissues that undergo damage due to ischemia-anoxia or persistent inflammation (138). These chemokines aid in recruiting MSCs to the injury site and subsequently regulate their migration to facilitate their differentiation into various cell lineages (139). Under specific conditions in an *in vitro* setting, UC-MSCs have been observed to exhibit the ability to undergo "trans-differentiation," resulting in their differentiation into osteoblast-like mesodermal cell types (140), endothelial cells (141), cardiomyocytes (142), as well as ectoderm-derived hepatocytes with potential for neuronal transformation (143), and pancreatic cells (144), bridging the germinal layers within the endoderm.

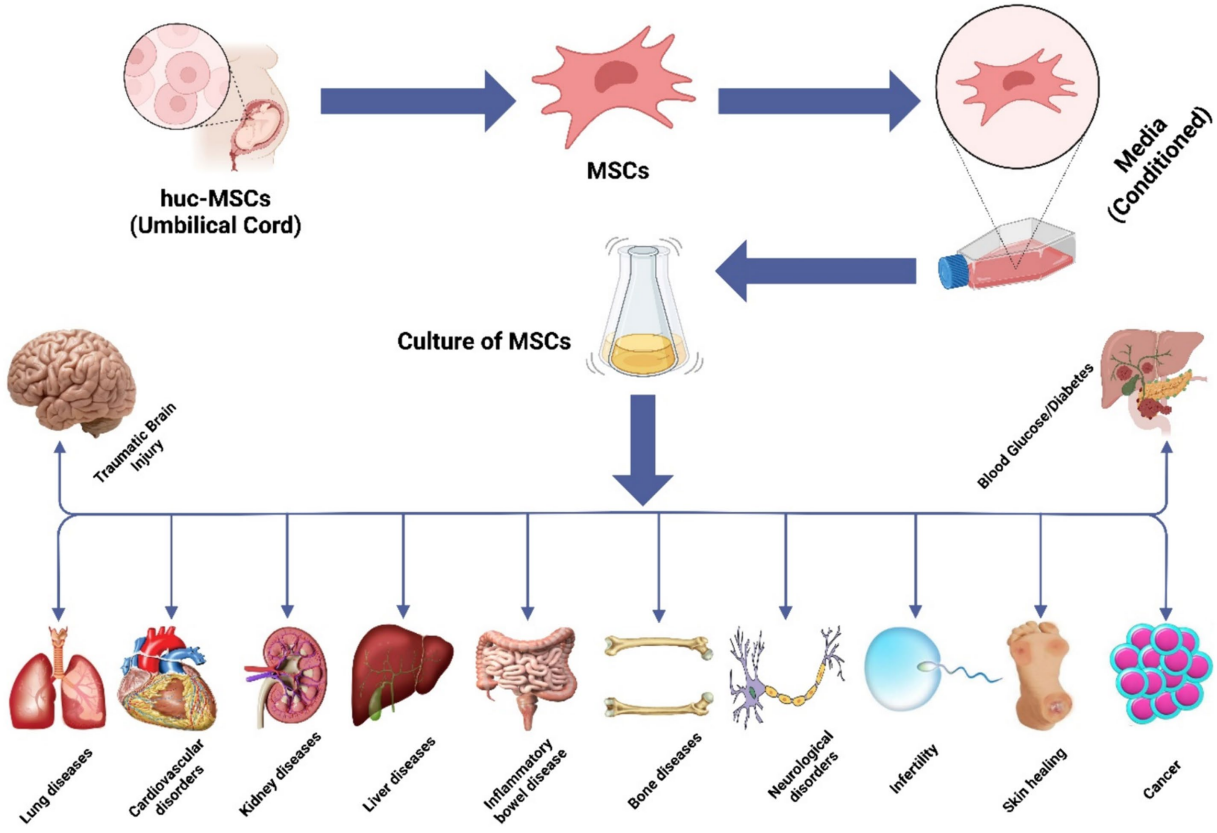

FIGURE 3
Illustration of the hUC-MSC in various abnormalities.

4.1.3 hUC-MSC-EVs (exosomes) isolation and characterization

To maximize the therapeutic effects of EVs, it is essential for researchers to isolate and characterize them. The isolation and characterization of hUC-MSC-EVs hold great importance for their potential therapeutic use in IBD and other associated illnesses (145). However, the extraction of EVs from biological fluids, such as serum or conditioned media, can be challenging due to the heterogeneity of EV populations and the presence of impurities (93). In response to this challenge, various methodologies have been developed to achieve optimal purity and cost-effectiveness of EVs. These techniques include ultracentrifugation, density gradient centrifugation, and size-exclusion chromatography, all aiming to achieve high levels of purity (146). Ultracentrifugation, are commonly used technique for EV extraction, involves differential centrifugation at high speeds, reaching up to 100,000 x g, to pellet EVs (147). This method can be further optimized by utilizing sucrose or iodixanol gradients to separate EVs from other subcellular components (148). Another technique, density gradient centrifugation, employs a continuous gradient to separate EVs based on their buoyant density. This method is often used for isolating specific EV subpopulations, such as exosomes (149). Size-exclusion chromatography (SEC) is another method used for EV isolation, where EVs are separated based on their size characteristics. This technology is useful for removing unwanted contaminants, such as proteins and lipoproteins, which may be present during the isolation process (150). Once the isolation process is complete, hUC-MSC-EVs can be characterized by analyzing their physical and biochemical properties. Physical characterization includes assessing various attributes of EVs, such as their dimensions, structure, and abundance. Techniques such as dynamic light scattering (DLS), transmission electron microscopy (TEM), and nanoparticle tracking analysis (NTA) are commonly employed for this purpose (151). Biochemical characterization involves the detection and analysis of specific EV markers, including CD9, CD63, and CD81, using techniques like western blotting, flow cytometry, or immunogold labeling (152). Furthermore, the cargo of hUC-MSC-EVs can be characterized through proteomics, RNA sequencing, and lipidomics, providing insights into their functional properties and potential therapeutic targets (153).

It is important to acknowledge the inherent challenges associated with the extraction and characterization of EVs, which stem from the diverse nature of EV populations and the potential risk of contamination (154). Therefore, it is crucial to employ a range of isolation and characterization methodologies to ensure the integrity and homogeneity of hUC-MSC-EVs for their potential clinical application. By improving separation and characterization techniques and tailoring the cargo of EVs to therapeutic targets, researchers can develop novel IBD medications that are more effective and exhibit fewer side effects than current treatments. For a comprehensive overview of different techniques for exosome isolation and characterization, please refer to Table 2.

TABLE 2 A comparative analysis of various techniques for isolating exosomes.

Technique used	Principle	Dimension	Advantages	Drawbacks	References
Ultrafiltration	Immune affinity	Large	Convenient, efficient and logical	Impure, exosomes with reduced purity may exhibit a tendency to partially adhere to the cellular membrane	(155)
Immune-affinity capture	Shape and molecular size	Small	Pureness/increased purity	Expensive and yielding is very low	(156)
Ultracentrifugation	Antigen and antibody specific binding	Large	Inexpensive reagent cost, the likelihood of pollution is minimal	Costly apparatus and significant amount of time along with the biological activity and integrity of exosomes are compromised due to their poor quality	(157)
Size exclusion chromatography	Density, molecular size, and shape	Medium	Assurance of exosome yield, purity, integrity, and biological activity can be achieved	Utilization of specialized equipment	(158)
Microfluidic	Molecular size	Small	Affordability, convenience, and automation	Verification of selectivity and specificity is required	(159)

5 Role of UC-MSC/hUC-MSC-derived EVs in IBD

MSC-derived EVs have been shown in numerous studies to be an effective treatment for experimentally induced colitis in mice. One study documented and examined the weight loss, stool viscosity, and hematochezia in mice with DSS-induced colitis treated with MSCs, MSC-Exs, and placebo in distinct groups. The findings demonstrated that MSCs and MSC-Exs both had an equal anti-inflammatory impact and could treat colitis in mice (160). Additionally, studies on MSCs' immediate and long-term protective effects on experimental colitis have shown that MSCs produced from human adipose tissue not only temporarily relieve colitis but also have positive long-term regulatory effects on IBD (161) (Table 3).

5.1 Mechanism of MSC-derived EVs in the treatment of IBD

It has been documented that the MSC-Exos have the ability to home in on areas of intestinal inflammation, interact with immune cells like macrophages, T lymphocytes, and DCs, and modulate the characteristics and activities of immune cells by releasing bioactive substances, such as cytokines, to regulate irregular immune responses and suppress inflammatory reactions (153), as outlined in Figure 4.

Furthermore, MSC-Exos possess the capability to influence intestinal epithelial cells (IECs), facilitate the restoration of the intestinal epithelial barrier (IEB), mitigate oxidative stress, and alleviate colon fibrosis. Therefore, exhibit potential in the treatment of IBD (171). The therapeutic utilization of MSC-derived EVs in the treatment of IBD are given in Table 4.

5.2 Macrophages

It has been determined that macrophages are the primary cells responsible for causing colon inflammation (184, 185), as depicted in Figure 5. Upon activation by pro-inflammatory stimuli, macrophages are mobilized to inflamed areas and undergo differentiation into macrophages with distinct polarities under the influence of chemokines and inflammatory factors. M1 macrophages release proinflammatory cytokines (IL-1β, IL-6, TNF-α, and IL-12) as well as Th1 chemokines (CXCL9, CXCL10, and CXCL11), which are involved in antigen presentation, T cell activation, and the initiation of an adaptive immune response. M2 macrophages release suppressive cytokines like IL-10 and TGF-β, which serve to dampen immune reactions and counteract inflammatory responses (186, 187). Anomalous polarization of macrophages contributes to immune irregularities within the intestinal mucosa and mediates the onset of intestinal inflammation, a key triggering factor in the development of IBD (188). Research indicates that the regulation of macrophage polarization and the balance between M1 and M2 macrophages is crucial in the immunotherapeutic approach to IBD (187–190). Both laboratory studies and animal trials have demonstrated that when lipopolysaccharide (LPS)-activated macrophages are co-cultured with BM-derived MSC-Exos, fluorescently labeled MSC-Exos are observed within the macrophages after 24 h. This interaction leads to the modulation of macrophage polarization towards the M2 phenotype, resulting in a decreased M1/M2 ratio and reduced expression of IL-6, IL-7, TNF-α, and IL-12, along with diminished macrophage infiltration in colon tissue (165, 173). Additionally, further research has indicated that adipose-derived MSC-Exos harbor an anti-inflammatory agent, TNF-α stimulated gene-6 (TSG-6), plays a pivotal role in orchestrating the polarization of M2 macrophages (191). The potential pathways through which MSC-Exos regulate macrophages include:

5.2.1 Transfer of miRNA

At the site of intestinal inflammation, MSC-Exos bind to macrophages and release encapsulated miRNA, which in turn selectively modulates the mRNA within macrophages and influences the polarization of M2 macrophages. Research has demonstrated that the ExomiRNAs of MSCs, including miR-146a, can downregulate the expression of TNF receptor-related factor 6 (TRAF-6) and IL-1 receptor-related kinase 1 (IRAK-1), thereby suppressing the release of proinflammatory cytokines and promoting the expression of the anti-inflammatory factor IL-10 (192).

TABLE 3 Unveiling the role of MSCs and MSC-Exo in IBD treatment.

Disease	Administration route	Therapy	Model/Sample	Results	References
IBD	Intraperitoneal injection	HucMSC-Exs	*In vivo* (mice)	MSC-Exs reduced IBD in mice by means of TSG-6-mediated mucosal barrier repair and intestinal immunological homeostasis restoration	(162)
IBD	Intraperitoneal injection	cAT-MSCs	*In vivo* (mice)	TSG-6 secreted by cAT-MSCs induced a shift in the macrophage phenotype from M1 to M2 in mice, alleviating IBD symptoms and regulating the expression of pro-and anti-inflammatory cytokines in the colon	(163)
IBD	Intraperitoneal injections	BM-MSCs	*In vivo* (mice)	In the peritoneum, BM-MSCs accumulated and produced the immunomodulatory factor TSG-6, which reduced intestinal inflammation	(164)
UC	Peritoneal injection	BMSC-Exs	*In vivo* (mice)/*in vitro* (LPS-treated macrophages)	BMSC-Exs reduced the inflammatory response by down-regulating pro-inflammatory proteins, up-regulating anti-inflammatory proteins, and promoting the conversion of macrophages into the M2 phenotype	(165)
IBD	Intraperitoneal injection	ADMSC-Exs	*In vivo* (mice)	AdMSC-Exs may alleviate the clinical signs of IBD by modulating Treg populations and cytokines	(166)
IBD	Intraperitoneal injections	MSCs	*In vivo* (mice)	In patients with colitis, hUCMSCs enhanced the proportion of Tr1 cells in the spleen and mesenteric lymph nodes, decreased the percentage of helper T cells (Th1 and Th17 cells), promoted the expansion of Tr1 cells, and inhibited apoptosis, effectively alleviating IBD	(167)
IBD	Intravenous infusion	MSC-Exs (miR-378a-3p)	*In vivo* (mice)/*in vitro* (IEC-6)	MSCs-Exs suppress IBD by reducing GATA2 expression and downregulating AQP4, thereby inhibiting the PPAR signaling pathway	(168)
IBD T	Intravenous infusion	-MSCs	*In vivo* (mice)	Intravenous infusion of T-MSCs increased circulating IGF-1 levels and ameliorated colitis in mice	(169)
IBD	Enemas	MSCs	*In vivo* (mice)	Activating the Nrf2/Keap1/ARE pathway could be an effective strategy for MSCs to promote intestinal mucosal healing in experimental colitis	(170)

5.2.2 Anti-inflammatory proteins delivery

MSC-Exo contains a multitude of proteins, notably metallothionein-2 (MT-2), renowned for its capacity to suppress colitis activity. This protein plays a pivotal role in mitigating the intestinal inflammatory response by upholding the integrity of the intestinal barrier and fostering the polarization of M2b macrophages (179).

5.2.3 Induction of Toll-like receptors

MSC-Exos penetrate macrophages, potentially triggering the myeloid differentiation primary response gene 88 (MyD88)-dependent signaling pathway in macrophages upon recognition of TLR3 by the enclosed dsRNA. This activation leads to the induction of M2 polarization in macrophages, the release of anti-inflammatory factors, and the inhibition of the inflammatory response (193).

5.2.4 Competitive inhibition of CC chemokine receptor 2

In the presence of inflammatory stimuli, the interaction between CC chemokine receptor 2 (CCR2) expressed on the surface of monocytes and CC chemokine ligand 2 expressed on the surface of macrophages triggers the migration of monocytes to inflammatory sites, where they transform into macrophages, thereby intensifying the inflammatory response and exacerbating tissue damage. Notably, MSC-Exos exhibit high expression of CCR2, which competitively binds to the chemokine ligand 2 on the surface of macrophages. This competitive binding inhibits the recruitment and activation of monocytes, prevents the polarization of M1 macrophages, and reduces the expression of proinflammatory cytokines, such as IL-1β, IL-6, and TNF-α, thereby effectively restraining inflammatory responses (194).

5.2.5 Regulation of inflammatory cytokines releases

Firstly, MSC-Exos derived from MSCs, induced by specific inflammatory factors, encapsulate numerous anti-inflammatory cytokines and chemokines. Upon uptake by macrophages, these components are released into the surrounding environment. Secondly, the aforementioned pathways, once activated, govern or initiate the polarization of M2 macrophages, leading to the upregulation of

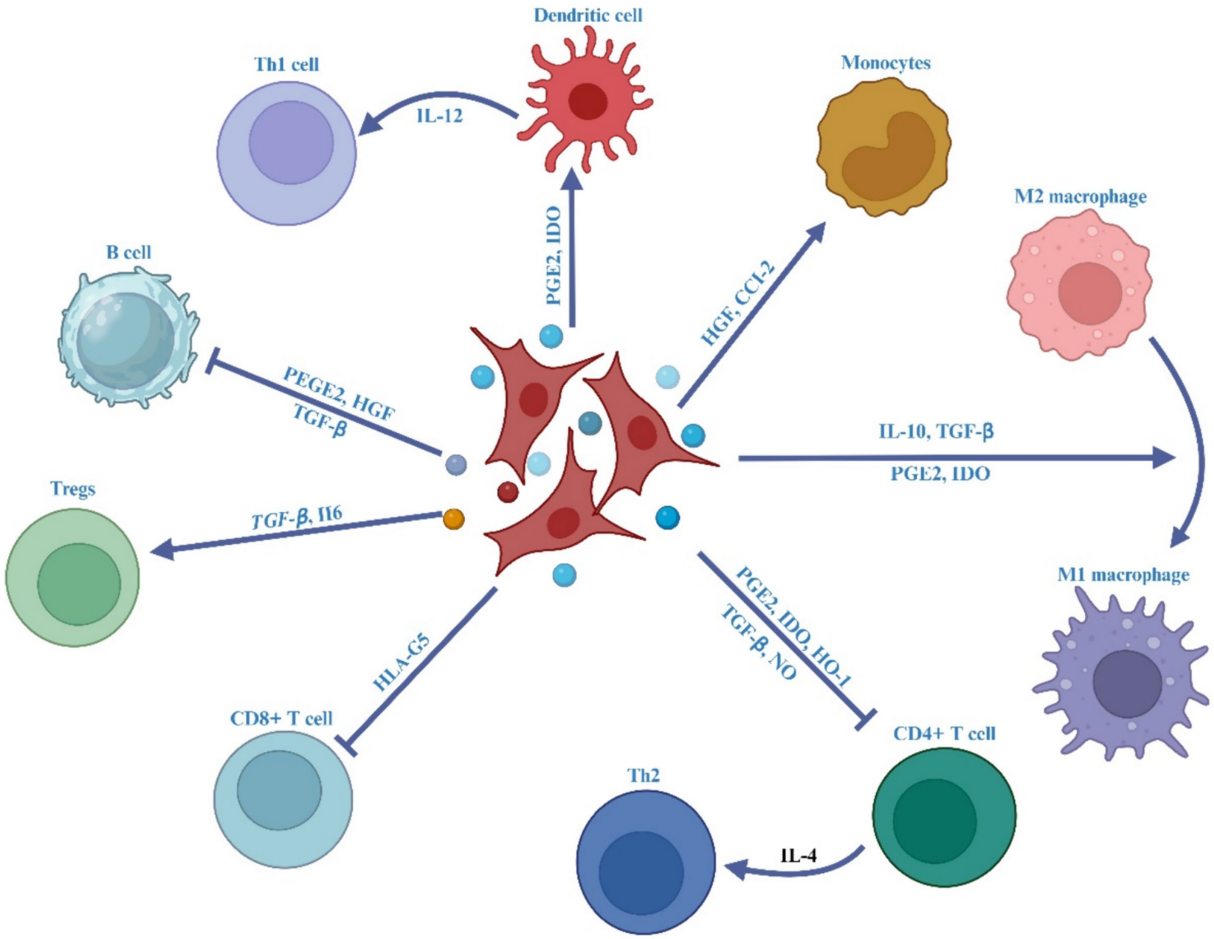

FIGURE 4
The impact of MSC-EVs on immune effector cells in IBD.

anti-inflammatory cytokines and the downregulation of proinflammatory cytokines. This orchestration serves to sustain the equilibrium of anti-inflammatory factors at inflammatory sites and effectively suppress excessive inflammatory responses (195).

5.3 T lymphocytes

The continual exposure of antigens to $CD4^+$ T cells by immune cells in the intestinal mucosa prompts the differentiation of primitive $CD4^+$ T cells (Th0) into various helper T cell subtypes (predominantly Th1, Th2, and Th17) and regulatory T (Treg) cells, under the influence of antigen presentation and cytokine regulation. The trajectory of their differentiation plays a crucial role in preserving intestinal immune equilibrium and modulating inflammatory responses within the intestine (196). Research indicates that the co-cultivation of T lymphocytes with MSC-Exos results in the downregulation of cyclinD-2 and the upregulation of P27KIP-1, thereby impeding T lymphocytes from entering the S phase and inhibiting their growth and proliferation. This suggests that MSC-Exos have the capacity to modulate the proliferation and differentiation of T lymphocytes. Notably, MSC-Exos primarily regulate the equilibrium between Th1 and Th2, as well as Treg and Th17 cells (196).

5.3.1 The regulation of the transformation balance between Th1 and Th2

Th1 and Th2 cells represent the two primary subtypes of Th0 differentiation. Th1 cells primarily express IFN-γ and IL-12, while Th2 cells predominantly express IL-4 (196, 197). The dysregulation of Th1/Th2 subsets is intricately linked to the chronic inflammation observed in IBD (197, 198). The direction of differentiation is largely influenced by the concentration of IL-12 in the environment and the activation status of antigen-presenting cells. Through the regulation of DCs and macrophages, MSC-Exos induce the polarization of M2 macrophages, impede the antigen presentation of DCs, and diminish the release of proinflammatory cytokines, such as IL-12. This environment is conducive to the transition of T cells into Th2 cells. Studies have demonstrated that MSC-Exos can markedly diminish the expression of IL-12, hinder the differentiation and proliferation of Th1 cells, and facilitate the transition of T cells into Th2 cells following co-cultivation with T cells activated by phytohemagglutinin (199, 200). Furthermore, research has revealed that the TSG-6 protein detected in hUC-MSC-exo regulates the immune response of Th2 and Th17 cells in mesenteric lymph nodes (MLN), downregulates proinflammatory cytokines in colon tissue, and upregulates anti-inflammatory cytokines, thereby safeguarding the integrity of the intestinal barrier (162).

TABLE 4 Therapeutic application of MSC-derived EVs for treating IBD.

Sources	Effector molecules	Mechanism	Effect	References
hUC-MSCs	miRNA-326	NF-κB signaling pathway and enzymes associated to neddylation	Preventing neddylation and reducing colitis	(172)
hUC-MSCs	miRNA-378a-5p	IL-1β, IL-18, the NLRP3 axis, and caspase-1	Reducing colitis by controlling the pyroptosis of macrophages	(173)
hUC-MSCs	miRNA-378a-5p	NLRP3 axis	Suppressing colitis brought on by DSS and controlling macrophage pyroptosis	(174)
AD-MSCs	miRNA-132	TGF-β/Smad signaling and Smad-7	Facilitating lymphangiogenesis reliant on VEGF-C	(175)
hUC-MSCs	miRNA-146a	SUMO1 axis	Preventing colitis	(172)
hUC-MSCs	lnc78583-miRNA-3202	HOXB13 axis	Alleviate bowel inflammation	(176)
BM-MSCs	MiRNA-200b	HMGB3 axis	Reduce the inflammatory damage that IECs have caused	(177)
BM-MSCs	miR-125a miR-125b	Stat3 axis; prevent the development of Th17 cells	Reduce the severity of colitis brought on by DSS	(178)
hUC-MSCs	TSG-6	TJ repair by upregulating TJ protein expression. Th2 and Th17 cell immune responses have been altered	Reestablishing intestinal immunological homeostasis and mucosal barrier restoration	(162)
hBM-MSCs	MT-2	M2b macrophages polarized	Lessen irritation of the mucosa	(179)
AD-MSCs	N/A	Immunomodulatory properties; control the number of Tregs	Reduce inflammation in acute colitis caused by DSS	(166)
Olfactory Ecto-MSCs	N/A	Controls Th1/Th17 subpopulations and differentiation	Reduce the intensity of IBD disease	(180)
hUC-MSCs	N/A	Suppress the production of IL-7 and iNOS	Reduce IBD and relieve inflammatory reactions	(173)
hUC-MSCs	N/A	Control the ubiquitination modification	hUC-MSCs lessen the colitis's intensity	(181)
BM-MSCs	N/A	Reduce apoptosis, oxidative stress, and intestinal inflammation	Reduce IBD's intensity	(182)
AD-MSCs	N/A	Process including inflammation, apoptosis, and immunity	Reduce the harm to the intestinal epithelium	(183)

5.3.2 The regulation of the transformation balance between Treg and Th17

Treg cells play a pivotal role in inhibiting the transformation of effector T cells and adaptive mucosal immunity in the intestine, thereby reducing immune-related tissue damage in IBD. A study has revealed that MSC-Exos induce T lymphocyte apoptosis and modulate the differentiation and proliferation of Treg cells through programmed death ligand and galactosin-1 (201). Treg cells express anti-inflammatory cytokines, such as IL-10 and TGF-β, to achieve immunosuppressive effects (193, 202, 203). In contrast, Th17 cells express proinflammatory cytokines that contribute to the inflammatory activity in IBD. Notably, the ratio of Th17/Treg in the peripheral blood of IBD patients has been found to be significantly increased, as demonstrated (204). Furthermore, Chen et al. (133) discovered a significant increase in the ratio of Th17/Treg cells in the mesenteric lymphoid tissue of colitis rats. Conversely, the ratio of Th17/Treg cells was markedly decreased, leading to a notable amelioration of colitis after the injection of MSC-Exos via the caudal vein (180, 205). Additionally, it was found that adipose-MSC-Exos (AD-MSC-Exos) can restore the proportion of Treg cells in the spleen of the IBD mouse model to the baseline level, akin to that of normal mice, and also improve the inflammation of dextran sulfate sodium (DSS)-induced colitis (166).

5.4 DCs

In the intestinal mucosa, DC are the main antigen-presenting cells. They produce and secrete proinflammatory cytokines including IL-6 and IL-12, which exacerbate the inflammatory response in IBD (refer to Figure 4) (206). Additionally, their production of reactive oxygen species (ROS) contributes to the destruction of the intestinal mucosal barrier and participates in the tissue damage observed in IBD (1). The potential mechanisms through which MSC-Exos regulate DCs encompass the following: (1) MSC-Exo-treated DCs result in the downregulation of IL-4 and IL-12, coupled with the upregulation of

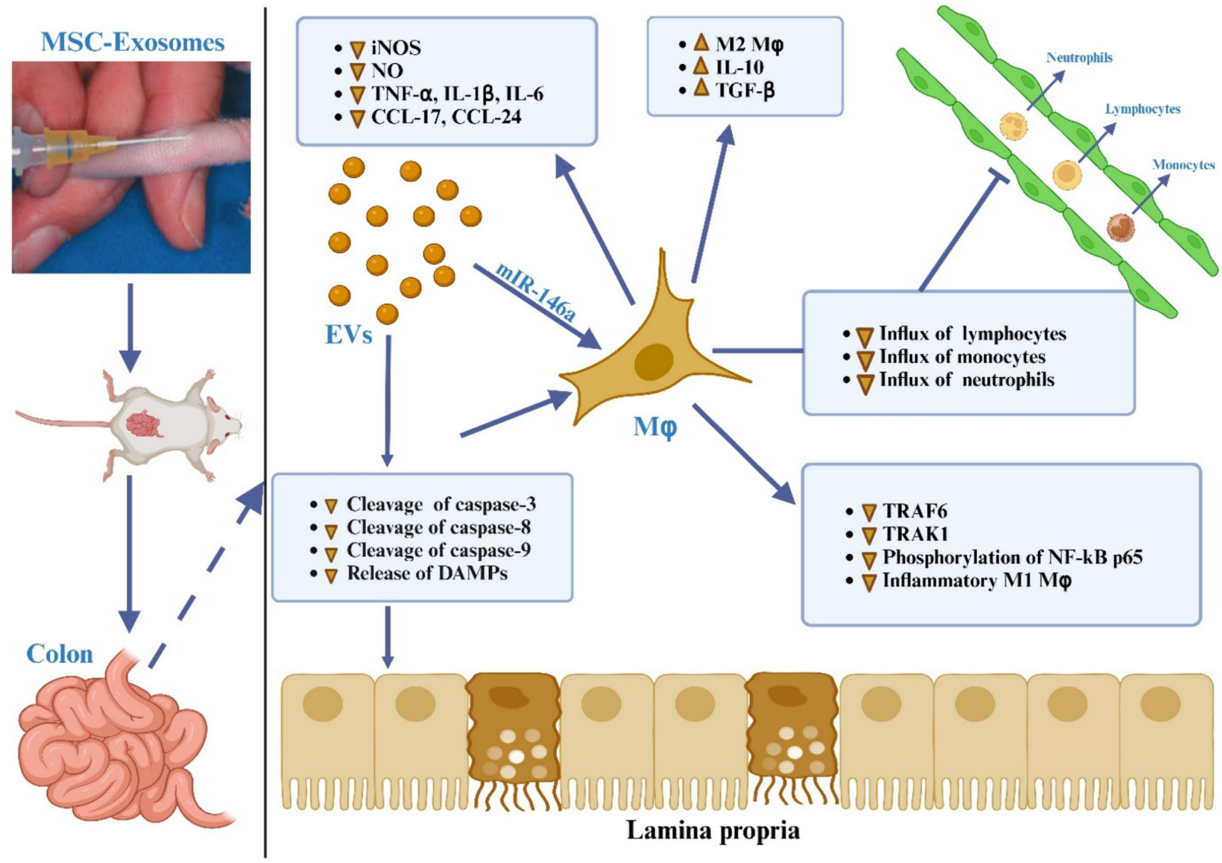

FIGURE 5
The MSC-EVs mitigate ulcerative colitis is through modulating the phenotype and function of colonic macrophages. MSC-EVs reduce the cleavage of caspase-3, -8, and -9 and lessen the release of damage-associated molecular patterns (DAMPs) from damaged gut epithelial cells, leading to decreased activation of the NF-κB signaling pathway in colon macrophages. MSC-EVs deliver miR-146a, which inhibits the expression of TNF receptor-associated factor 6 (TRAF6) and IL-1 receptor-associated kinase 1 (IRAK1), reduces phosphorylation of NF-κB p65, and suppresses the generation of inflammatory M1 macrophages. This is evidenced by decreased inducible nitric oxide synthase (iNOS) expression, significantly lower production of nitric oxide (NO), inflammatory cytokines (TNF-α, IL-1β, IL-6), and chemokines (CCL-17, CCL-24), resulting in reduced recruitment of neutrophils, monocytes, and lymphocytes to the inflamed gut. Additionally, MSC-EVs promote the polarization of colon macrophages to an anti-inflammatory M2 phenotype, marked by increased secretion of immunosuppressive cytokines TGF-β and IL-10, thus alleviating colitis.

TGF-β, thus inhibiting the maturation and differentiation of DCs (200, 207, 208). This process also induces the differentiation of T cells, affects the balance of Th1/Th2 transformation (209), and inhibits the intestinal inflammatory response (210). Furthermore, (2) MSC-Exos suppress the differentiation and maturation of DCs by modulating the TLR-NF-κB signaling pathway. In summary, MSC-Exos exert a potent immunomodulatory effect (211). In the context of IBD treatment, MSC-Exos carrying immunosuppressive factors influence M2 macrophage polarization, inhibit the proliferation of Th1 and Th17 cells, promote the differentiation of Treg cells, and induce antigen-presenting cells (212).

5.5 IECs

5.5.1 Repair of the IEB

The intestinal barrier encompasses the IEB, mucosal innate immune system, intestinal mucus, and intestinal microbiota. The IEB, constituted by the tight junctions of IECs, forms a crucial mechanical barrier and represents the most pivotal component of the intestinal barrier. Dysregulation and disturbances in various aspects, including mucosal immunity, surface mucus, intestinal microbiota, and oxidative stress, can compromise the integrity of the IEB, leading to the necrosis and apoptosis of IECs and an escalation in wall permeability. These changes underlie the pathological alterations observed in IBD (213–216). MSC-Exos exhibit the capacity to repair IEC injury, inhibit IEC apoptosis, preserve the equilibrium of oxidative stress, and diminish intestinal wall permeability, thereby facilitating the restoration of the IEB, refer to Figure 6.

5.5.1.1 Repair the injury of IECs

Mao et al. (173) observed a significant reduction in immune-mediated damage to IECs in colitis mice at 12 h post-intravenous injection of hUC-MSC-exo, indicating the therapeutic potential of exosomes in immune regulation. Additionally, Wang et al. (47) demonstrated that ADSCs-Exos treated with vascular endothelial growth factor C (VEGF-C) upregulate miR-132 and modulate the Smad-7 gene and TGF-β/Smad signaling pathways, thereby promoting the proliferation, migration, and lymphangiogenesis of lymphatic endothelial cells (LECs). Furthermore, in a DSS-induced colitis model,

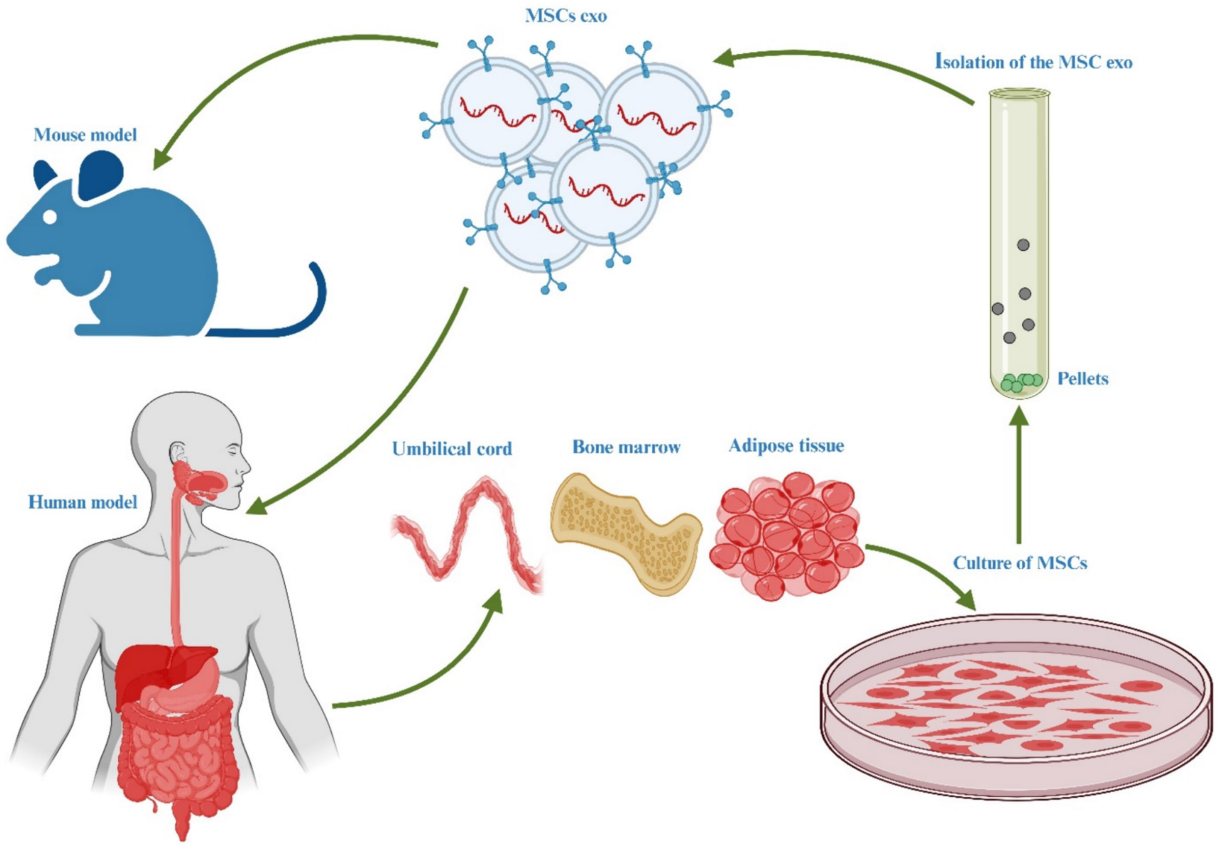

FIGURE 6
Diagrammatic illustration of the treatment of IBD by MSC-derived EVs.

hUC-MSC-exo were found to regulate the balance between ubiquitination and deubiquitination of functional proteins through miR-326, facilitating the repair of IEC damage and maintenance of IEB integrity by inhibiting neddylation (181). Although the specific regulatory process and molecular mechanism require further elucidation.

5.5.1.2 Regarding the inhibition of IEC apoptosis

It has been identified in numerous apoptotic bodies in the colon mucosa of UC patients (214). Subsequent studies revealed that the lack of NF-κB in IECs is a critical factor leading to their entry into the apoptosis program (215). Yang et al. (182) observed a high expression of caspase 3, caspase 8, and caspase 9 in the cysteinyl aspartate-specific protein (caspase) family in the colon tissue of rats with colitis. Following the injection of MSC-derived EVs into the tail vein, the expressions of these caspases were altered, indicating the potential of MSC-EVs to inhibit IEC apoptosis and repair the IEB. Similarly, Yang et al. (182) obtained similar results, further affirming the ability of MSC-EVs to mitigate the apoptosis of IECs and contribute to IEB repair.

5.5.1.3 Inhibition of oxidative stress

Oxidative stress plays a crucial role in the onset and progression of IBD. Typically, colonic tissue cells maintain a dynamic equilibrium between oxidation and antioxidation. However, chronic colonic inflammation disrupts this balance, leading to excessive production of reactive ROS by IEC and macrophages, which results in colonic tissue damage (217, 218). Elevated levels of ROS have been detected in the colonic mucosa of IBD patients and animal models, with a positive correlation to disease severity and increased peroxidation products, such as peroxidized lipid molecules and proteins (218–221). Overproduction of ROS directly damages nucleic acids, lipids, and proteins in colon epithelial cells, inducing necrosis or apoptosis of IECs and compromising the integrity of the IEB (222). While oxidative stress aids the immune system in pathogen clearance, excessive oxidative stress stimulates macrophages to produce proinflammatory cytokines, exacerbating intestinal inflammation. Research indicates that mesenchymal stem cell-derived exosomes (MSC-Exos) can repair various injuries caused by oxidative stress (223–225).

However, most studies have focused on tissues such as the heart, lungs, liver, and kidneys, with limited research on MSC-Exos in treating colitis (48). Nevertheless, MSC-Exos might repair oxidative stress-damaged IECs and help maintain the intestinal mucosal barrier. Additionally, MSC-Exos could mitigate oxidative stress injuries through immune regulation. Further research is needed to determine whether MSC-Exos can reduce intestinal ROS production and restore the balance between oxidation and antioxidation in the intestine.

5.5.1.4 Reduction of intestinal wall permeability

It was discovered that the incidence of necrotizing enterocolitis (NEC) and intestinal wall permeability significantly decreased in NEC model rats treated with intraperitoneal injections of BM MSCs or BM MSC-Exos (226). Furthermore, McCulloh et al. (227) verified that

MSC-Exos can reduce intestinal wall permeability, though the precise molecular mechanisms underlying this effect remain unclear.

5.5.2 Anticolonic fibrosis

Colonic fibrosis is a chronic complication of IBD, with more than 30% of CDpatients developing fibrosis, which rapidly leads to intestinal stenosis and adversely impacts patient prognosis (228, 229). Pathological stimuli such as chronic intestinal inflammation, oxidative stress, damage to and repair of the IEB, promote epithelial-mesenchymal transition (EMT). This transition involves the loss of epithelial cell polarity and intercellular connections, morphological and functional transformation, and significant extracellular matrix (ECM) accumulation, culminating in intestinal fibrosis (230). During tissue repair or response, fibroblast activation is crucial for fibrosis development (230). The TGF-β signaling pathway has been identified as a key activator of fibroblasts, inducing their differentiation into myofibroblasts, which is central to the pathogenesis of intestinal fibrosis (231). Yang et al. (232) demonstrated that BM-MSC-Exos can significantly reverse EMT in TGF-β1-treated (IEC-6) through miR-200b, thereby mitigating intestinal fibrosis. Various studies have shown that MSCs from different sources regulate EMT by activating TGF-β and Wnt signaling pathways, reducing ECM aggregation, and exerting antifibrotic effects (233). While MSCs have been shown to reduce fibrosis in the heart, lungs, liver, and kidneys, research on their effects on intestinal fibrosis remains limited (234). Choi et al. (234) hUCMSC-Exos suppress TGF-β1-induced fibroblast activation by inhibiting the Rho/MRTF/SRF pathway, thereby reducing intestinal fibrosis. Additionally, Duan and Cao (235) discovered that human placental MSC-Exos can decrease collagen deposition in the intestinal wall by reducing collagen production and promoting its degradation through inhibition of TGF-β1 protein expression.

5.6 hUC-MSC-derived EVs role in other inflammatory diseases

Instead of being solely associated with IBD, hUC-MSC derived EVs have demonstrated promising potential in the treatment and management of diverse pathological conditions.

5.6.1 hUC-MSC derived EVs promote functional recovery in spinal cord injury

The induction of M1 to M2 phenotypic transition in bone marrow-derived macrophages (BM-DM) can be effectively achieved through the utilization of hUC-MSC-derived exosomes, which are characterized by an average particle size of 70 nm. *In vivo* studies have provided compelling evidence that hUC-MSC-derived exosomes facilitate the process of functional recuperation subsequent to SCI through the downregulation of inflammatory cytokines, including TNF-α, MIP-1, IL-6, and IFN-γ (61). The role of hUC-MSC-exo in the transformation of macrophages from the M1 to the M2 phenotype has been established (236). Intravenous administration of these exosomes shows promise as a therapeutic approach for mitigating inflammation and facilitating the restoration of locomotor function following SCI. These findings highlight the potential of exosomes to significantly contribute to the future of SCI therapy (237).

In the treatment of SCI mice, hUC-MSC transplantation has been shown to greatly enhance the survival and regeneration of myelin and nerve cells in the injured area of the spinal cord (238). This transplantation approach also leads to a significant improvement in the motor function of the animals. These positive therapeutic outcomes may be attributed, at least in part, to the effects of hUC-MSC transplantation, which include reducing the production of IL-7 at the site of injury, enhancing the activation of M2 macrophages, and preventing inflammatory infiltration (239). A study conducted in 2022 suggests that the ability of hUC-MSCs to modulate the inflammatory response following nerve injury plays a critical role in their effectiveness in treating acute SCI. This information may guide future applications of hUC-MSCs and enhance the effectiveness of their clinical translation (240). Moreover, hUC-MSC-EVs, acting through the miR-29b-3p/PTEN/Akt/mTOR axis, have demonstrated the ability to reduce pathological alterations, enhance motor function, and promote nerve function repair in SCI rats (241).

5.6.2 hUC-MSC derived EVs suppresses programmed cell death in traumatic brain injury

Globally, traumatic brain injury (TBI) is a leading cause of fatalities and long-term impairment (242). TBI treatments have recently gained significant attention. However, the therapeutic application of hUC-MSC transplantation in TBI has been limited by challenges such as immunological rejection, ethical considerations, and the potential for tumorigenicity. Notably, hUC-MSC-exo have demonstrated the ability to enhance neurological performance, reduce cerebral edema, and decrease lesion volume following TBI (243). According to a study, hUC-MSC-exo may provide neuroprotection against TBI by exerting inhibitory effects on cell death processes, including apoptosis, pyroptosis, and ferroptosis, through the PINK1/Parkin-mediated mitophagy pathway (238). Recent studies have shed light on the emerging significance of pyroptosis in the context of brain damage. It has been demonstrated that pyroptosis plays a significant role in the development of neonatal cerebral ischemia-reperfusion (I/R) injury, exerting a substantial influence on the pathological processes involved (244). hUC-MSC-exo possesses the potential to mitigate apoptosis following TBI, reduce neuroinflammation, and promote neurogenesis (245). In order to evaluate the efficacy of exosome therapy in facilitating neurological recovery, a rat model of TBI was established. Subsequent analysis revealed a significant improvement in sensorimotor function and spatial learning in rats upon administration of hUC-MSC-exo (246). Moreover, through the inhibition of the NF-kB signaling pathway, hUC-MSC-exo exhibited a substantial reduction in the synthesis of proinflammatory cytokines. Furthermore, noteworthy observations were made regarding the neuroprotective effects of hUC-MSC-exos, including the prevention of neuronal apoptosis, attenuation of inflammation, and facilitation of neuronal regeneration within the injured cortex of rats subjected to TBI (247).

5.6.3 hUC-MSC derived EVs In myocardial infarction

A myocardial infarction (MI) is a significant inflammatory disorder triggered by an imbalance in substrate and oxygen supply versus demand, leading to ischemia or cellular demise (248, 249). Despite the frequent utilization of early revascularization and the widespread implementation of quality measures, notable variations exist at the local and regional levels regarding the management and outcomes of MI (250, 251). The therapeutic effectiveness of stem

cell-based therapy in MI for the purposes of heart repair and regeneration has been substantiated through preclinical investigations as well as clinical trials (252). A potential therapeutic approach for MI involves the utilization of MSC-EVs. To investigate the effects of hUC-MSC-EVs loaded with miR-223 in the context of MI, experiments were conducted employing both an *in vitro* cellular model of oxidative stress and cardiac fibrosis, as well as *in vivo* rat models of MI. The transfer of miR-223 via EVs demonstrated improved cardiac function in MI rat models, along with reduced fibrosis and inflammation (253). The pathogenesis of MI is primarily attributed to the presence of inflammation, wherein the detrimental effects of MI are intricately associated with the orchestrated activation of multiple inflammatory cascades and the recruitment of inflammatory cells (254). Before the widespread implementation of cardiomyocyte regeneration in clinical trials, substantial further research and development are required. In the realm of cell therapy, extensive investigations have been conducted to explore the differentiating capabilities of (hUC-MSCs). It is widely recognized that the utilization of 5-Azacytidine (5-Aza) effectively triggers the differentiation of hUC-MSCs into cardiomyocytes, resulting in morphological changes and the expression of cardiac-specific proteins, irrespective of the presence of basic fibroblast growth factor (bFGF) (255). An additional investigation has revealed that 5-Azacytidine (5-Aza) may facilitate the *in vitro* differentiation of hUC-MSCs into cardiomyocytes through the sustained phosphorylation of extracellular signal-regulated kinase (ERK) (256). Recent scientific investigations have demonstrated that the administration of injected hUC-MSCs exerts beneficial effects on cardiac function in rats with dilated cardiomyopathy (DCM) through the attenuation of myocardial fibrosis and dysfunction. These effects are achieved by the downregulation of Transforming Growth Factor-β1 (TGF-β1) and TNF-α production (257). Furthermore, emerging scientific evidence suggests that exosomes possess potential protective properties in the context of acute myocardial infarction. These exosomes have been shown to potentially facilitate cell repair mechanisms by modulating the expression of Smad7 in cardiomyocytes (257).

5.6.4 hUC-MSC derived EVs role in kidney injury repair

Depending on the concentration of serum creatinine (Scr) or glomerular filtration rate (GFR), nephrologists have classified kidney failure into two distinct syndromes: acute renal failure and chronic renal failure (258). Currently, clinical treatments for kidney injury primarily involve medication, surgery, and renal transplantation (259). As stem cell research has advanced, the preventive effects of hUC-MSCs and hUC-MSC-exo on renal tissue injury have been demonstrated (260). Acute kidney injury (AKI) refers to the clinical condition that arises from a rapid loss of renal function caused by various factors (260). Pre-renal acute kidney injury commonly arises from diminished blood volume caused by fluid loss and bleeding from various etiologies, as well as a decrease in effective arterial blood volume and alterations in intrarenal hemodynamics. Recent research has focused on the role of sepsis in causing AKI. To investigate this, a sepsis model was induced using cecal ligation and puncture (CLP), followed by treatment with hUC-MSCs (261). The data presented in the study provided evidence that the administration of hUC-MSCs resulted in substantial improvement in renal function, reduction in tissue damage, and significant enhancement of overall health in mice with sepsis (262, 263). According to the data reported, pre-treatment of hUC-MSCs with IL-1 exhibited a statistically significant augmentation in their capacity to modulate the immune system (264). In response to IL-1 stimulation, exosomes selectively encapsulated a widely recognized anti-inflammatory microRNA, MiR-146a. Subsequent delivery of exosomal MiR-146a to macrophages induced M2 polarization, leading to a reduction in kidney damage in septic mice (265). According to a study, the administration of hUC-MSCs have been demonstrated to effectively ameliorate renal ischemia-reperfusion injury (IRI) in mice. This beneficial effect is achieved through a dual mechanism involving a reduction in the infiltration of macrophages into the injured kidneys and a concomitant increase in the population of M2-like macrophages during the healing process (265). Through the modulation of inflammatory cytokine production and promotion of renal tubular cell proliferation, hUC-MSCs have been observed to expedite the recovery of renal function. Additionally, it was discovered that hUC-MSC transplantation resulted in a reduction in the levels of malondialdehyde (MDA) in renal tissues, indicating a potential protective effect of hUC-MSCs against oxidative damage and mitochondrial dysfunction in renal cells (266). Subsequent investigations revealed that the underlying mechanism responsible for cisplatin-induced nephrotoxicity was primarily attributed to the induction of oxidative stress. However, this detrimental effect can be mitigated by the administration of hUC-MSC-exo, which exert their protective effects by suppressing the activation of the p38 mitogen-activated protein kinase (MAPK) pathway (267). Renal fibrosis is a common pathway in the progression of chronic kidney disease (CKD) that often culminates in end-stage renal failure. Huang et al. provided insights into the potential therapeutic role of MSCs in mitigating obstructive chronic progressive renal interstitial fibrosis (RIF) in the context of kidney failure. Their study demonstrated that infused MSCs could effectively reach the damaged kidney tissues, offering a promising approach for addressing the underlying mechanisms involved in renal fibrosis (268).

5.6.5 hUC-MSC derived EVs role in cutaneous wounds healing

Inflammatory, proliferative, and remodeling stages are just a few of the many phases that make up the complex process of cutaneous wound healing (268). Recent years have witnessed extensive exploration into benefits of direct stem cell infusion for tissue regeneration (269, 270). A degradable, dual-sensitive hydrogel incorporating exosomes extracted from hUC-MSC was synthesized. Afterwards, the *in vivo* wound healing potential, exosome identification and material properties of the hydrogel were assessed. The exosome-loaded hydrogel demonstrated substantial improvements in wound closure rates, re-epithelialization rates and collagen deposition at the wound sites, as evidenced by the *in vivo* results (269). The administration of exosomes-loaded hydrogel to the wounded sites resulted in a higher density of skin appendages, indicating a potential for achieving full skin regeneration (271).

Clinicians persistently encounter challenges in managing diabetic wounds due to the prevalence of multiple bacterial infections and oxidative damage (272). Exosomes have been widely employed as a promising nanodrug delivery strategy for the treatment of diabetic (273). To ascertain their participation in the modulation of diabetic wound healing, a co-culture of human umbilical vein endothelial cells (HU-VECs) and hUC-MSCs was established, and hUC-MSC-exo

were subsequently utilized in both *in vitro* and *in vivo* experiments (274). The findings demonstrated that hUC-MSCs possess the ability to mitigate oxidative stress-induced damage to endothelial cells via exosomal mechanisms, thereby accelerating the healing process of diabetic cutaneous wounds in an *in vitro* setting (273). *In vivo* setting, it was observed that wounds treated with hUC-MSC-exo exhibited significantly accelerated re-epithelialization and elevated expression levels of CK19, PCNA, and collagen I (in contrast to collagen III) (274).

5.6.6 hUC-MSC cells derived EVs role in lung injury repair

Acute lung injury (ALI) leads to the early onset of lung inflammation, capillary rupture, destruction of endothelial and epithelial cells, and breakdown of tight epithelial junctions. These factors increase alveolar epithelial permeability, causing significant pulmonary edema and, in severe cases, even death (275). In animal models, transplantation of MSCs effectively enhances the recovery from ALI (276). In the LPS-induced ALI rat model, hUC-MSCs can enhance the activity of antioxidant enzymes in lung tissue (277). Based on this, photobiomodulation (PBM) was utilized to modulate the release of pro-inflammatory chemicals, reduce their levels to a certain extent, and enhance the balance of oxidative stress at the site of injury (278). Bronchopulmonary dysplasia (BPD) is a dangerous chronic lung condition characterized by a high rate of morbidity and mortality in premature neonates (279). Transplantation of MSCs is a promising strategy for treating BPD. In a rat model of BPD, the transplantation of hUC-MSC-EVs resulted in the improvement of pulmonary hypertension, restoration of lung function, and alveolar structure (280). In a BPD model treated with hUC-MSC-EVs, the proportion of Ki-67-positive lung cells increased, indicating an upregulation of cell proliferation, whereas the proportion of TUNEL-positive lung cells decreased, suggesting a downregulation of cell apoptosis (263). Furthermore, in a hyperoxia-induced BPD model treated with hUC-MSC-EVs, there was an increase in SP-C staining, a marker of type II alveolar epithelial cells (TIIAECs), as well as CD31 staining, a marker of pulmonary vascular endothelial cells (PVECs) (281). Another study has demonstrated that intervention with PBM in hUC-MSCs naturally reduces the thickness of the alveolar septum, suppresses excessive secretion of inflammatory factors, and alleviates *in vivo* conditions of bleeding, edema, and fibrosis (278). PBM is a physical intervention that enhances the therapeutic effect of hUC-MSCs and shows promise as a therapy for the treatment of ALI. Furthermore, the use of hUC-MSCs may potentially reduce bleomycin-induced mouse mortality and attenuate lung collagen buildup (282). The transplantation of hUC-MSCs induced the proliferation of alveolar type 2 (AT2) cells, while concurrently suppressing the proliferation of lung fibroblasts (283). After the transplantation of hUC-MSCs, there is an induction of AT2 cell proliferation, concomitant with the suppression of lung fibroblast proliferation. Additionally, this transplantation leads to increased release of CXCL9 and CXCL10 by interferon-stimulated cells (IFNSMs), thereby attracting additional Treg cells to the injured lung (284). In a study, hUC-MSCs were administered, and lung morphometry was successfully enhanced (285). Further research has revealed the crucial role of exosome-resident miR-377-3p in controlling autophagy, thereby preventing LPS-induced ALI (286).

5.6.7 hUC-MSC cells derived EVs role in hepatic injury repair

The liver, which is widely considered to be the most critical organ in the body, plays a pivotal role in the detoxification, secretion, and metabolism of medications and toxins (287). Acute liver failure (ALF), a pathological condition resulting from rapid deterioration in hepatic function, and is clinically characterized by jaundice, coagulopathy, and encephalopathy (288). In recent years, increasing scientific research has indicated that the transplantation of MSCs holds promise as a potential therapeutic strategy for the treatment of ALF (289, 290). Findings of ta study revealed that the administration of hUC-MSC-exo via a single tail vein injection resulted in a significant improvement in the survival rate, prevention of hepatocyte death, and enhancement of liver function in an experimental mouse model of ALF induced by APAP (291). Furthermore, the administration of hUC-MSCs effectively mitigated APAP-induced hepatocyte apoptosis by modulating oxidative stress markers (292). This was evident through the downregulation of glutathione (GSH) and superoxide dismutase (SOD) levels, as well as the attenuation of MDA production. Additionally, the excessive expression of cytochrome P450 E1 (CYP2E1) and 4-hydroxynonenal (4-HNE), which are known contributors to oxidative stress, was significantly suppressed. These findings highlight the ability of hUC-MSC-exo to regulate oxidative stress pathways, thereby conferring protection against APAP-induced hepatocyte death in the context of acute liver failure (293). In a study, mouse models of acute and chronic liver damage, as well as liver tumors, were generated by intraperitoneal injection of carbon tetrachloride (CCl4) followed by the intravenous infusion of hUC-MSC-exo. The results of the study demonstrated the hepatoprotective effect of hUC-MSC-exo, as evidenced by a significant reduction in liver damage (294). hUC-MSC-exo treatment has been shown to mitigate the expression of the NLRP3 inflammasome and associated inflammatory factors (295), offering a potential therapeutic approach for the management of acute liver failure. Furthermore, in lipopolysaccharide (LPS)-stimulated RAW 264.7 macrophages, hUC-MSC-exo demonstrated inhibitory effects on the expression of NLRP3, caspase-1, IL-1β, and IL-6. These findings highlight the immunomodulatory properties of hUC-MSC-exo, which could contribute to the attenuation of inflammatory responses in various pathological conditions (296). The proteolytic activation of pro-IL-1β is facilitated by activated caspase-1. Caspase-1, IL-1β, and NLRP3 play pivotal roles in the development of acute pancreatic and hepatic injury, inflammation, and subsequent organ damage. These factors are crucial in the pathophysiological processes associated with inflammatory responses and tissue injury in the pancreas and liver (297). The primary outcome of a recent study revealed that T-Exo treatment effectively reduces circulating levels of alanine aminotransferase (ALT), aspartate aminotransferase (AST), and proinflammatory cytokines. Additionally, T-Exo therapy attenuates the activation of proteins involved in the NLRP3 inflammation-associated pathway, thereby mitigating the pathological liver damage associated with acute ALF (298). Notably, TNF stimulation of MSCs leads to the selective packaging of anti-inflammatory microRNA-299-3p into exosomes, which can be utilized for exosomal therapy purposes (299).

5.6.8 hUC-MSC cells derived EVs role in controlling blood sugar/diabetes

Diabetes mellitus (DM), a collective term referring to a group of metabolic disorders, is distinguished by the presence of elevated blood glucose levels, commonly known as hyperglycemia (300). Over the preceding half-century, the dynamics of lifestyles and the process of globalization have imparted profound ramifications on political, environmental, societal, and human behavioral domains. DM represents a complex disorder influenced by a combination of genetic predisposition and environmental factors, leading to compromised insulin secretion or insulin resistance (IR). These physiological aberrations contribute to the characteristic pathophysiology of DM and its associated metabolic dysregulation (300, 301). In recent years, obesity and physical inactivity have become more common, and rapid population expansion, aging, and urbanization have all contributed to the worldwide health issue that is DM (302). To maintain physiological equilibrium within the body's ecosystem, it is imperative to regulate the homeostasis of blood glucose, which is contingent upon the management of vital life processes (303). In the year 2018, a team of researchers conducted an investigation into the correlation between hUC-MSC-exo and hyperglycemia induced by type 2 diabetes mellitus (T2DM) (304). The findings unequivocally indicate that hUC-MSC-exo consistently mitigated blood glucose levels in T2DM-afflicted rats subjected to a high-fat diet (HFD) and streptozotocin (STZ). Notably, hUC-MSC-exo enhanced the uptake of the fluorescent glucose analogue 2-NBDG in myotubes and hepatocytes, thereby substantiating their role in facilitating glucose absorption. Additionally, hUC-MSC-exo promoted glucose uptake in the muscles, upregulated the expression of the glucose-responsive transporter (GLUT4) in T2DM rats, and reinstated hepatic glucose homeostasis through the activation of insulin signaling. The activation of the insulin/AKT signaling pathway further corroborated the potential of hUC-MSC-exo to enhance insulin sensitivity in both *in vivo* and *in vitro* settings. Moreover, an evidence demonstrated that hUC-MSC-exo facilitated insulin secretion and islet regeneration by preventing STZ-induced caspase-3 alterations that lead to cellular apoptosis (305).

6 Safety and efficacy in clinical trials

Clinical trials are currently underway to evaluate the safety and efficacy of MSC-EVs in the management of IBD and its related conditions (306). Significantly, a series of phase I and II trials have been conducted, resulting in promising results. Significantly, the administration of hUC-MSC-exosomes demonstrated protective effects against weight loss, without eliciting adverse effects on liver or renal functions (307, 308). Furthermore, the versatility of hUC-MSC-exosomes was highlighted through diverse evaluations, encompassing assessments for hemolysis, activation of vascular and muscular systems, systemic anaphylaxis, pyrogenicity, and hematological markers (309). In another phase I clinical trial, four individuals exhibited a response to therapy 6 months after the initiation of treatment. Three out of the patients who underwent exosome injections achieved full recovery, while one patient reported no improvement and had active discharge from the fistula site. Furthermore, all five patients (100%) reported no occurrence of local or systemic side effects (310). In a similar vein, a team of scientists has developed a comprehensive systemic quality control system and robust testing methods to ensure the safety and efficacy of hUC-MSCs, based on a minimal set of requirements for MSC-based products. The validity of this system for quality control and assessment of hUC-MSCs as a cell-based product has been verified, as none of the qualified hUC-MSCs demonstrated any serious adverse reactions during the 1-year follow-up period, even after testing for multiple indications (311). However, to ascertain the safety and effectiveness of hUC-MSC-EVs in treating IBD and related illnesses, larger, multicenter clinical trials are necessary. Furthermore, long-term follow-up research is required to assess the durability of treatment response and the presence of any potential side effects.

6.1 Regulatory and manufacturing considerations

Given the variation of MSC-based therapies across countries and regions, adherence to regulations is crucial. The development of hUC-MSC-EVs as a therapeutic option for IBD and related disorders necessitates meticulous consideration of regulatory and manufacturing aspects. Considering the scalability and cost-effectiveness of production procedures is imperative to enable the widespread clinical utilization of hUC-MSCs. To successfully integrate EV-based therapies into clinical practice, it is crucial to address multiple challenges associated with scalability, standardization, and characterization of EV products. Establishing standardized manufacturing processes is essential to guarantee the reproducibility, safety, and quality of the ultimate therapeutic product (312, 313). Current efforts focus on developing strategies, such as the utilization of bioreactors and microfluidic systems, for the large-scale production of EVs (314, 315). To effectively integrate the use of hUC-MSC-EVs into clinical applications, adherence to regulatory and manufacturing factors is imperative.

The European Medicines Agency (EMA) has issued guidelines regarding the utilization of MSCs in clinical studies (316). To comply with regulatory standards, it is necessary to ensure adherence to Good Manufacturing Practices (GMP) during the production of MSC-based products. In accordance with regulatory requirements, it is mandatory to submit a Clinical Trial Application (CTA) prior to the initiation of any clinical trials.

Similarly, In the United States, the Food and Drug Administration (FDA) has established recommendations for the utilization of MSCs in clinical trials. Based on the stipulations outlined in these rules, MSCs are categorized as biological entities and, as a result, are subject to regulatory oversight by the Food and Drug Administration (FDA). In accordance with the established protocols, it is necessary to complete and submit an Investigational New Drug (IND) application prior to initiating clinical trials (317). Additionally, for the production of MSC-based products, strict adherence to Good Manufacturing Practices (GMP) is mandatory.

7 Conclusion

Various characteristics of hUC-MSCs, including their anti-inflammatory, immunomodulatory, and regenerative properties, have been extensively investigated both *in-vivo* and *in-vitro*. These findings suggest that hUC-MSCs hold promise for mitigating inflammation and promoting the healing of damaged tissues in individuals affected

by IBD and related conditions. Consequently, hUC-MSCs may serve as a potential therapeutic intervention in the treatment of IBD and its associated ailments. The development of standardized protocols for the isolation and purification of EVs will be essential to ensure their quality, safety, and efficacy in clinical applications. Further research is needed to optimize the isolation, characterization, and administration of hUC-MSC-EVs. Furthermore, further studies are required to elucidate the molecular mechanisms and signaling pathways that underlie the therapeutic effects of hUC-MSC-EVs. This will enhance our comprehension of their mode of action and guide the development of more precise therapies. To fully realize the potential of this innovative therapy, it will be crucial to address the regulatory and manufacturing challenges as clinical trials progress. Ensuring the safety and effectiveness of hUC-MSC-EVs in human patients will be crucial, and carefully planned clinical trials will be essential in determining the therapeutic usefulness of these vesicles. Furthermore, the development of scalable manufacturing processes that can produce large quantities of high-quality hUC-MSC-EVs will be essential for meeting the demands of clinical use. There are also several challenges associated with the administration of hUC-MSC-EVs, such as determining the optimal dosage, route of administration, and frequency of treatment. Future studies should explore these parameters in order to maximize the therapeutic potential of hUC-MSC-EVs and minimize potential side effects. In addition, the development of biomarkers for patient stratification and monitoring treatment response could help to personalize and optimize hUC-MSC-EV-based therapies for individual patients.

In conclusion, hUC-MSC-EVs represent a promising and novel therapeutic approach for IBD and other related disorders. The growing body of preclinical evidence supporting their therapeutic potential, coupled with advancements in our understanding of their biogenesis, molecular mechanisms, and clinical translation, offers hope for more effective and targeted treatments for patients suffering from these debilitating conditions. By addressing the current challenges and building upon the existing knowledge, researchers and clinicians can work together to harness the full potential of hUC-MSC-EVs and bring this innovative therapy to the forefront of IBD treatment.

Author contributions

MD: Conceptualization, Writing – original draft. AW: Conceptualization, Writing – original draft. YC: Writing – review & editing, Funding acquisition. JZ: Writing – original draft, Conceptualization. YY: Conceptualization, Writing – review & editing. ZX: Visualization, Writing – review & editing.

Funding

The author(s) declare that financial support was received for the research, authorship, and/or publication of this article. This work was supported by the Grant of the Scientific Project of Jiangsu Health Commission (Z2020038); the Grant of the Open Project of Jiangsu Key Laboratory of New Drug Research and Clinical Pharmacy (XZSYSKF2020032); Jiangsu 333 High-Level Talents Training Project, Changzhou High-Level Medical Talents Training Project (2022CZBJ111) and Zhenjiang Key Research and Development Plan (Social Development) (Grant No. SH2022062).

Acknowledgments

We extend our sincere appreciation to Professor Mao Fei for his invaluable and comprehensive guidance throughout the entire manuscript writing process. Additionally, we would like to express our sincere appreciation and recognition to Dr. Arif Rashid, School of Food and Biological Engineering, Jiangsu University, for his diligent and meticulous review of this article.

Conflict of interest

The authors declare that the research was conducted in the absence of any commercial or financial relationships that could be construed as a potential conflict of interest.

Publisher's note

References

1. Prakash S, Tanaka T, Ashat D. A nationwide study of patients hospitalized with indeterminate colitis: a comparison with Crohn's disease and ulcerative colitis. *Int J Color Dis*. (2023) 38:223. doi: 10.1007/s00384-023-04515-5

2. Hemmer A, Forest K, Rath J, Bowman J. Inflammatory bowel disease: a concise review. *S D Med*. (2023) 76:416–23.

3. Roda G, Chien Ng S, Kotze PG, Argollo M, Panaccione R, Spinelli A, et al. Crohn's disease. *Nat Rev Dis Primers*. (2020) 6:22. doi: 10.1038/s41572-020-0156-2

4. Li Y, Chen J, Bolinger AA, Chen H, Liu Z, Cong Y, et al. Target-based small molecule drug discovery towards novel therapeutics for inflammatory bowel diseases. *Inflamm Bowel Dis*. (2021) 27:S38–62. doi: 10.1093/ibd/izab190

5. Gajendran M, Loganathan P, Catinella AP, Hashash JG. A comprehensive review and update on Crohn's disease. *Dis Mon*. (2018) 64:20–57. doi: 10.1016/j.disamonth.2017.07.001

6. Loddo I, Romano C. Inflammatory bowel disease: genetics, epigenetics, and pathogenesis. *Front Immunol*. (2015) 6:551. doi: 10.3389/fimmu.2015.00551

7. Uranga JA, López-Miranda V, Lombó F, Abalo R. Food, nutrients and nutraceuticals affecting the course of inflammatory bowel disease. *Pharmacol Rep*. (2016) 68:816–26. doi: 10.1016/j.pharep.2016.05.002

8. Danese S, Allez M, van Bodegraven AA, Dotan I, Gisbert JP, Hart A, et al. Unmet medical needs in ulcerative colitis: an expert group consensus. *Dig Dis*. (2019) 37:266–83. doi: 10.1159/000496739

9. Armuzzi A, Liguori G. Quality of life in patients with moderate to severe ulcerative colitis and the impact of treatment: a narrative review. *Dig Liver Dis*. (2021) 53:803–8. doi: 10.1016/j.dld.2021.03.002

10. Ding D-C, Shyu W-C, Lin S-Z. Mesenchymal stem cells. *Cell Transplant*. (2011) 20:5–14. doi: 10.3727/096368910X

11. Najera J, Hao J. Recent advance in mesenchymal stem cells therapy for atopic dermatitis. *J Cell Biochem*. (2023) 124:181–7. doi: 10.1002/jcb.30365

12. Zhu X, Xu X, Shen M, Wang Y, Zheng T, Li H, et al. Transcriptomic heterogeneity of human mesenchymal stem cells derived from bone marrow, dental pulp, adipose tissue, and umbilical cord. *Cell Reprogram*. (2023) 25:162–70. doi: 10.1089/cell.2023.0019

13. Marędziak M, Marycz K, Tomaszewski KA, Kornicka K, Henry BM. The influence of aging on the regenerative potential of human adipose derived mesenchymal stem cells. *Stem Cells Int*. (2016) 2016:2152435. doi: 10.1155/2016/2152435

14. Kern S, Eichler H, Stoeve J, Klüter H, Bieback K. Comparative analysis of mesenchymal stem cells from bone marrow, umbilical cord blood, or adipose tissue. *Stem Cells*. (2006) 24:1294–301. doi: 10.1634/stemcells.2005-0342

15. Thaweesapphithak S, Tantrawatpan C, Kheolamai P, Tantikanlayaporn D, Roytrakul S, Manochantr S. Human serum enhances the proliferative capacity and immunomodulatory property of MSCs derived from human placenta and umbilical cord. *Stem Cell Res Ther*. (2019) 10:79. doi: 10.1186/s13287-019-1175-3

16. Shang Y, Guan H, Zhou F. Biological characteristics of umbilical cord mesenchymal stem cells and its therapeutic potential for hematological disorders. *Front Cell Dev Biol*. (2021) 9:570179. doi: 10.3389/fcell.2021.570179

17. Jovic D, Yu Y, Wang D, Wang K, Li H, Xu F, et al. A brief overview of global trends in MSC-based cell therapy. *Stem Cell Rev Rep*. (2022) 18:1525–45. doi: 10.1007/s12015-022-10369-1

18. Zhao L, Chen S, Yang P, Cao H, Li L. The role of mesenchymal stem cells in hematopoietic stem cell transplantation: prevention and treatment of graft-versus-host disease. *Stem Cell Res Ther*. (2019) 10:723–9. doi: 10.3727/096368912X655217

19. Bajetto A, Pattarozzi A, Corsaro A, Barbieri F, Daga A, Bosio A, et al. Different effects of human umbilical cord mesenchymal stem cells on glioblastoma stem cells by direct cell interaction or via released soluble factors. *Front Cell Neurosci*. (2017) 11:312. doi: 10.3389/fncel.2017.00312

20. Watson N, Divers R, Kedar R, Mehindru A, Mehindru A, Borlongan MC, et al. Discarded Wharton jelly of the human umbilical cord: a viable source for mesenchymal stromal cells. *Cytotherapy*. (2015) 17:18–24. doi: 10.1016/j.jcyt.2014.08.009

21. Katsuda T, Kosaka N, Takeshita F, Ochiya T. The therapeutic potential of mesenchymal stem cell-derived extracellular vesicles. *Proteomics*. (2013) 13:1637–53. doi: 10.1002/pmic.201200373

22. Balaji S, Keswani SG, Crombleholme TM. The role of mesenchymal stem cells in the regenerative wound healing phenotype. *Adv Wound Care*. (2012) 1:159–65.

23. van Niel G, Carter DRF, Clayton A, Lambert DW, Raposo G, Vader P. Challenges and directions in studying cell–cell communication by extracellular vesicles. *Nat Rev Mol Cell Biol*. (2022) 23:369–82. doi: 10.1038/s41580-022-00460-3

24. Mentkowski KI, Snitzer JD, Rusnak S, Lang JK. Therapeutic potential of engineered extracellular vesicles. *AAPS J*. (2018) 20:50. doi: 10.1208/s12248-018-0211-z

25. Lazar S, Mor S, Chen J, Hao D, Wang A. Bioengineered extracellular vesicle-loaded bioscaffolds for therapeutic applications in regenerative medicine. *Extracell Vesicles Circ Nucl Acids*. (2021) 2:175. doi: 10.20517/evcna.2021.10

26. Alzhrani GN, Alanazi ST, Alsharif SY, Albalawi AM, Alsharif AA, Abdel-Maksoud MS, et al. Exosomes: isolation, characterization, and biomedical applications. *Cell Biol Int*. (2021) 45:1807–31. doi: 10.1002/cbin.11620

27. Chaput N, Taïeb J, Schartz NEC, André F, Angevin E, Zitvogel L. Exosome-based immunotherapy. *Cancer Immunol Immunother*. (2004) 53:234–9. doi: 10.1007/s00262-003-0472-x

28. Raposo G, Nijman HW, Stoorvogel W, Liejendekker R, Harding CV, Melief CJ, et al. B lymphocytes secrete antigen-presenting vesicles. *J Exp Med*. (1996) 183:1161–72. doi: 10.1084/jem.183.3.1161

29. Zhang B, Shen L, Shi H, Pan Z, Wu L, Yan Y, et al. Exosomes from human umbilical cord mesenchymal stem cells: identification, purification, and biological characteristics. *Stem Cells Int*. (2016) 2016:1929536. doi: 10.1155/2016/1929536

30. Andre F, Schartz NEC, Movassagh M, Flament C, Pautier P, Morice P, et al. Malignant effusions and immunogenic tumour-derived exosomes. *Lancet*. (2002) 360:295–305. doi: 10.1016/S0140-6736(02)09552-1

31. Admyre C, Grunewald J, Thyberg J, Gripenbäck S, Tornling G, Eklund A, et al. Exosomes with major histocompatibility complex class II and co-stimulatory molecules are present in human BAL fluid. *Eur Respir J*. (2003) 22:578–83. doi: 10.1183/09031936.03.00041703

32. Caby M-P, Lankar D, Vincendeau-Scherrer C, Raposo G, Bonnerot C. Exosomal-like vesicles are present in human blood plasma. *Int Immunol*. (2005) 17:879–87. doi: 10.1093/intimm/dxh267

33. Palanisamy V, Sharma S, Deshpande A, Zhou H, Gimzewski J, Wong DT. Nanostructural and transcriptomic analyses of human saliva derived exosomes. *PLoS One*. (2010) 5:e8577. doi: 10.1371/journal.pone.0008577

34. Admyre C, Johansson SM, Qazi KR, Filén J-J, Lahesmaa R, Norman M, et al. Exosomes with immune modulatory features are present in human breast milk. *J Immunol*. (2007) 179:1969–78. doi: 10.4049/jimmunol.179.3.1969

35. Lee TH, D'Asti E, Magnus N, Al-Nedawi K, Meehan B, Rak J. Microvesicles as mediators of intercellular communication in cancer—the emerging science of cellular 'debris'. *Semin Immunopathol*. (2011) 33:455–67. doi: 10.1007/s00281-011-0250-3

36. Tai Y, Chen K, Hsieh J, Shen T. Exosomes in cancer development and clinical applications. *Cancer Sci*. (2018) 109:2364–74. doi: 10.1111/cas.13697

37. Ohyashiki JH, Umezu T, Ohyashiki K. Extracellular vesicle-mediated cell–cell communication in haematological neoplasms. *Philos Trans R Soc B*. (2018) 373:20160484. doi: 10.1098/rstb.2016.0484

38. Safdar A, Tarnopolsky MA. Exosomes as mediators of the systemic adaptations to endurance exercise. *Cold Spring Harb Perspect Med*. (2018) 8:a029827. doi: 10.1101/cshperspect.a029827

39. Tenchov R, Sasso JM, Wang X, Liaw W-S, Chen C-A, Zhou QA. Exosomes—nature's lipid nanoparticles, a rising star in drug delivery and diagnostics. *ACS Nano*. (2022) 16:17802–46. doi: 10.1021/acsnano.2c08774

40. Kooijmans SAA, Schiffelers RM, Zarovni N, Vago R. Modulation of tissue tropism and biological activity of exosomes and other extracellular vesicles: new nanotools for cancer treatment. *Pharmacol Res*. (2016) 111:487–500. doi: 10.1016/j.phrs.2016.07.006

41. Liu H, Deng S, Han L, Ren Y, Gu J, He L, et al. Mesenchymal stem cells, exosomes and exosome-mimics as smart drug carriers for targeted cancer therapy. *Colloids Surf B*. (2022) 209:112163. doi: 10.1016/j.colsurfb.2021.112163

42. Wang X, Zhou G, Zhou W, Wang X, Wang X, Miao C. Exosomes as a new delivery vehicle in inflammatory bowel disease. *Pharmaceutics*. (2021) 13:1644. doi: 10.3390/pharmaceutics13101644

43. Carrière J, Barnich N, Nguyen HTT. Exosomes: from functions in host-pathogen interactions and immunity to diagnostic and therapeutic opportunities. *Rev Physiol Biochem Pharmacol*. (2016) 172:39–75. doi: 10.1007/112_2016_7

44. Toh WS, Lai RC, Hui JHP, Lim SK. MSC exosome as a cell-free MSC therapy for cartilage regeneration: implications for osteoarthritis treatment. *Semin Cell Dev Biol*. (2017) 67:56–64. doi: 10.1016/j.semcdb.2016.11.008

45. Guo S, Perets N, Betzer O, Ben-Shaul S, Sheinin A, Michaelevski I, et al. Intranasal delivery of mesenchymal stem cell derived exosomes loaded with phosphatase and tensin homolog si RNA repairs complete spinal cord injury. *ACS Nano*. (2019) 13:10015–28. doi: 10.1021/acsnano.9b01892

46. Elahi FM, Farwell DG, Nolta JA, Anderson JD. Preclinical translation of exosomes derived from mesenchymal stem/stromal cells. *Stem Cells*. (2020) 38:15–21. doi: 10.1002/stem.3061

47. Wang X, Wang H, Cao J, Ye C. Exosomes from adipose-derived stem cells promotes VEGF-C-dependent lymphangiogenesis by regulating miRNA-132/TGF-β pathway. *Cell Physiol Biochem*. (2018) 49:160–71. doi: 10.1159/000492851

48. Liang X, Zhang L, Wang S, Han Q, Zhao RC. Exosomes secreted by mesenchymal stem cells promote endothelial cell angiogenesis by transferring miR-125a. *J Cell Sci*. (2016) 129:2182–9. doi: 10.1242/jcs.170373

49. Maertens L, Erpicum C, Detry B, Blacher S, Lenoir B, Carnet O, et al. Bone marrow-derived mesenchymal stem cells drive lymphangiogenesis. *PLoS One*. (2014) 9:e106976. doi: 10.1371/journal.pone.0106976

50. Ferreira JR, Teixeira GQ, Santos SG, Barbosa MA, Almeida-Porada G, Gonçalves RM. Mesenchymal stromal cell secretome: influencing therapeutic potential by cellular pre-conditioning. *Front Immunol*. (2018) 9:2837. doi: 10.3389/fimmu.2018.02837

51. Kronstadt SM, Pottash AE, Levy D, Wang S, Chao W, Jay SM. Therapeutic potential of extracellular vesicles for sepsis treatment. *Adv Ther*. (2021) 4:2000259. doi: 10.1002/adtp.202000259

52. Keshtkar S, Azarpira N, Ghahremani MH. Mesenchymal stem cell-derived extracellular vesicles: novel frontiers in regenerative medicine. *Stem Cell Res Ther*. (2018) 9:63. doi: 10.1186/s13287-018-0791-7

53. Hassanzadeh A, Rahman HS, Markov A, Endjun JJ, Zekiy AO, Chartrand MS, et al. Mesenchymal stem/stromal cell-derived exosomes in regenerative medicine and cancer; overview of development, challenges, and opportunities. *Stem Cell Res Ther*. (2021) 12:297. doi: 10.1186/s13287-021-02378-7

54. Guo Y, Hu D, Lian L, Zhao L, Li M, Bao H, et al. Stem cell-derived extracellular vesicles: a promising nano delivery platform to the brain? *Stem Cell Rev Rep*. (2023) 19:285–308. doi: 10.1007/s12015-022-10455-4

55. Gimona M, Pachler K, Laner-Plamberger S, Schallmoser K, Rohde E. Manufacturing of human extracellular vesicle-based therapeutics for clinical use. *Int J Mol Sci*. (2017) 18:1190. doi: 10.3390/ijms18061190

56. Cargnoni A, Papait A, Masserdotti A, Pasotti A, Stefani FR, Silini AR, et al. Extracellular vesicles from perinatal cells for anti-inflammatory therapy. *Front Bioeng Biotechnol*. (2021) 9:637737. doi: 10.3389/fbioe.2021.637737

57. Sun W, Yan S, Yang C, Yang J, Wang H, Li C, et al. Mesenchymal stem cells-derived exosomes ameliorate lupus by inducing M2 macrophage polarization and regulatory T cell expansion in MRL/lpr mice. *Immunol Investig*. (2022) 51:1785–803. doi: 10.1080/08820139.2022.2055478

58. Dias IE, Pinto PO, Barros LC, Viegas CA, Dias IR, Carvalho PP. Mesenchymal stem cells therapy in companion animals: useful for immune-mediated diseases? *BMC Vet Res*. (2019) 15:358. doi: 10.1186/s12917-019-2087-2

59. Valade G, Libert N, Martinaud C, Vicaut E, Banzet S, Peltzer J. Therapeutic potential of mesenchymal stromal cell-derived extracellular vesicles in the prevention of organ injuries induced by traumatic hemorrhagic shock. *Front Immunol*. (2021) 12:749659. doi: 10.3389/fimmu.2021.749659

60. Phan J, Kumar P, Hao D, Gao K, Farmer D, Wang A. Engineering mesenchymal stem cells to improve their exosome efficacy and yield for cell-free therapy. *J Extracell Vesicles*. (2018) 7:1522236. doi: 10.1080/20013078.2018.1522236

61. Fang Y, Lao P, Tang L, Chen J, Chen Y, Sun L, et al. Mechanisms of potential therapeutic utilization of mesenchymal stem cells in COVID-19 treatment. *Cell Transplant*. (2023) 32:09636897231184611. doi: 10.1177/09636897231184611

62. Lazar SV, Mor S, Wang D, Goldbloom-Helzner L, Clark K, Hao D, et al. Engineering extracellular vesicles for Alzheimer's disease: an emerging cell-free approach for earlier diagnosis and treatment. *WIREs Mech Dis*. (2022) 14:e1541. doi: 10.1002/wsbm.1541

63. You B, Jin C, Zhang J, Xu M, Xu W, Sun Z, et al. MSC-derived extracellular vesicle-delivered L-PGDS inhibit gastric cancer progression by suppressing cancer cell stemness and STAT3 phosphorylation. *Stem Cells Int*. (2022) 2022:9668239. doi: 10.1155/2022/9668239

64. Heris RM, Shirvaliloo M, Abbaspour-Aghdam S, Hazrati A, Shariati A, Youshanlouei HR, et al. The potential use of mesenchymal stem cells and their exosomes in Parkinson's disease treatment. *Stem Cell Res Ther*. (2022) 13:371. doi: 10.1186/s13287-022-03050-4

65. Ramasubramanian L, Du S, Gidda S, Bahatyrevich N, Hao D, Kumar P, et al. Bioengineering extracellular vesicles for the treatment of cardiovascular diseases. *Adv Biol*. (2022) 6:e2200087. doi: 10.1002/adbi.202200087

66. Wang X, Tang Y, Liu Z, Yin Y, Li Q, Liu G, et al. The application potential and advance of mesenchymal stem cell-derived exosomes in myocardial infarction. *Stem Cells Int*. (2021) 2021:5579904. doi: 10.1155/2021/5579904

67. Zhang Y, Zhuang H, Ren X, Jiang F, Zhou P. Therapeutic effects of different intervention forms of human umbilical cord mesenchymal stem cells in the treatment of osteoarthritis. *Front Cell Dev Biol*. (2023) 11:1246504. doi: 10.3389/fcell.2023.1246504

68. Kang Y, Song Y, Luo Y, Song J, Li C, Yang S, et al. Exosomes derived from human umbilical cord mesenchymal stem cells ameliorate experimental non-alcoholic steatohepatitis via Nrf 2/NQO-1 pathway. *Free Radic Biol Med*. (2022) 192:25–36. doi: 10.1016/j.freeradbiomed.2022.08.037

69. Mason C, Dunnill P. A brief definition of regenerative medicine. *Reg Med*. (2008) 3:1–5. doi: 10.2217/17460751.3.1.1

70. Merino-González C, Zuñiga FA, Escudero C, Ormazabal V, Reyes C, Nova-Lamperti E, et al. Mesenchymal stem cell-derived extracellular vesicles promote angiogenesis: potencial clinical application. *Front Physiol*. (2016) 7:24. doi: 10.3389/fphys.2016.00024

71. Lu J, Zhang Y, Yang X, Zhao H. Harnessing exosomes as cutting-edge drug delivery systems for revolutionary osteoarthritis therapy. *Biomed Pharmacother*. (2023) 165:115135. doi: 10.1016/j.biopha.2023.115135

72. Johnstone RM, Adam M, Hammond JR, Orr L, Turbide C. Vesicle formation during reticulocyte maturation. Association of plasma membrane activities with released vesicles (exosomes). *J Biol Chem*. (1987) 262:9412–20. doi: 10.1016/S0021-9258(18)48095-7

73. Chang W-H, Cerione RA, Antonyak MA. Extracellular vesicles and their roles in cancer progression. *Methods Mol Biol*. (2021) 2174:143–70. doi: 10.1007/978-1-0716-0759-6_10

74. Xie F, Zhou X, Fang M, Li H, Su P, Tu Y, et al. Extracellular vesicles in cancer immune microenvironment and cancer immunotherapy. *Adv Sci*. (2019) 6:1901779. doi: 10.1002/advs.201901779

75. Abhange K, Makler A, Wen Y, Ramnauth N, Mao W, Asghar W, et al. Small extracellular vesicles in cancer. *Bioact Mater*. (2021) 6:3705–43. doi: 10.1016/j.bioactmat.2021.03.015

76. Shah R, Patel T, Freedman JE. Circulating extracellular vesicles in human disease. *N Engl J Med*. (2018) 379:958–66. doi: 10.1056/NEJMra1704286

77. Ono R, Yoshioka Y, Furukawa Y, Naruse M, Kuwagata M, Ochiya T, et al. Novel hepatotoxicity biomarkers of extracellular vesicle (EV)-associated miRNAs induced by CCl4. *Toxicol Rep*. (2020) 7:685–92. doi: 10.1016/j.toxrep.2020.05.002

78. Anand S, Samuel M, Mathivanan S. Exomeres: a new member of extracellular vesicles family. *Subcell Biochem*. (2021) 97:89–97. doi: 10.1007/978-3-030-67171-6_5

79. Lötvall J, Hill AF, Hochberg F, Buzás EI, Di Vizio D, Gardiner C, et al. Minimal experimental requirements for definition of extracellular vesicles and their functions: a position statement from the International Society for Extracellular Vesicles. *J Extracell Vesicles*. (2014) 3:26913. doi: 10.3402/jev.v3.26913

80. Yáñez-Mó M, Siljander PR-M, Andreu Z, Bedina Zavec A, Borràs FE, Buzas EI, et al. Biological properties of extracellular vesicles and their physiological functions. *J Extracell Vesicles*. (2015) 4:27066. doi: 10.3402/jev.v4.27066

81. Mathieu M, Martin-Jaular L, Lavieu G, Théry C. Specificities of secretion and uptake of exosomes and other extracellular vesicles for cell-to-cell communication. *Nat Cell Biol*. (2019) 21:9–17. doi: 10.1038/s41556-018-0250-9

82. Yang Y, Li C-W, Chan L-C, Wei Y, Hsu J-M, Xia W, et al. Exosomal PD-L1 harbors active defense function to suppress T cell killing of breast cancer cells and promote tumor growth. *Cell Res*. (2018) 28:862–4. doi: 10.1038/s41422-018-0060-4

83. Ma L, Li Y, Peng J, Wu D, Zhao X, Cui Y, et al. Discovery of the migrasome, an organelle mediating release of cytoplasmic contents during cell migration. *Cell Res*. (2015) 25:24–38. doi: 10.1038/cr.2014.135

84. Akers JC, Gonda D, Kim R, Carter BS, Chen CC. Biogenesis of extracellular vesicles (EV): exosomes, microvesicles, retrovirus-like vesicles, and apoptotic bodies. *J Neuro-Oncol*. (2013) 113:1–11. doi: 10.1007/s11060-013-1084-8

85. Hristov M, Erl W, Linder S, Weber PC. Apoptotic bodies from endothelial cells enhance the number and initiate the differentiation of human endothelial progenitor cells *in vitro*. *Blood*. (2004) 104:2761–6. doi: 10.1182/blood-2003-10-3614

86. Zhang H, Freitas D, Kim HS, Fabijanic K, Li Z, Chen H, et al. Identification of distinct nanoparticles and subsets of extracellular vesicles by asymmetric flow field-flow fractionation. *Nat Cell Biol*. (2018) 20:332–43. doi: 10.1038/s41556-018-0040-4

87. Meehan B, Rak J, Di Vizio D. Oncosomes—large and small: what are they, where they came from? *J Extracell Vesicles*. (2016) 5:33109. doi: 10.3402/jev.v5.33109

88. Minciacchi VR, Freeman MR, Di Vizio D. Extracellular vesicles in cancer: exosomes, microvesicles and the emerging role of large oncosomes. *Semin Cell Dev Biol*. (2015) 40:41–51. doi: 10.1016/j.semcdb.2015.02.010

89. Zhang Q, Jeppesen DK, Higginbotham JN, Graves-Deal R, Trinh VQ, Ramirez MA, et al. Supermeres are functional extracellular nanoparticles replete with disease biomarkers and therapeutic targets. *Nat Cell Biol*. (2021) 23:1240–54. doi: 10.1038/s41556-021-00805-8

90. Tosar JP, Cayota A, Witwer K. Exomeres and supermeres: monolithic or diverse? *J Extracell Biol*. (2022) 1:e45. doi: 10.1002/jex2.45

91. Pallio G. Novel therapeutic approaches in inflammatory bowel diseases. *Biomedicines*. (2023) 11:2466. doi: 10.3390/biomedicines11092466

92. Varderidou-Minasian S, Lorenowicz MJ. Mesenchymal stromal/stem cell-derived extracellular vesicles in tissue repair: challenges and opportunities. *Theranostics*. (2020) 10:5979. doi: 10.7150/thno.40122

93. Witwer KW, Buzás EI, Bemis LT, Bora A, Lässer C, Lötvall J, et al. Standardization of sample collection, isolation and analysis methods in extracellular vesicle research. *J Extracell Vesicles*. (2013) 2:20360. doi: 10.3402/jev.v2i0.20360

94. Buzas EI, György B, Nagy G, Falus A, Gay S. Emerging role of extracellular vesicles in inflammatory diseases. *Nat Rev Rheumatol*. (2014) 10:356–64. doi: 10.1038/nrrheum.2014.19

95. Gibbings DJ, Ciaudo C, Erhardt M, Voinnet O. Multivesicular bodies associate with components of miRNA effector complexes and modulate miRNA activity. *Nat Cell Biol*. (2009) 11:1143–9. doi: 10.1038/ncb1929

96. Kalluri R, LeBleu VS. The biology, function, and biomedical applications of exosomes. *Science*. (2020) 367:eaau6977. doi: 10.1126/science.aau6977

97. Harding C, Heuser J, Stahl P. Receptor-mediated endocytosis of transferrin and recycling of the transferrin receptor in rat reticulocytes. *J Cell Biol*. (1983) 97:329–39. doi: 10.1083/jcb.97.2.329

98. Vella LJ, Sharples RA, Nisbet RM, Cappai R, Hill AF. The role of exosomes in the processing of proteins associated with neurodegenerative diseases. *Eur Biophys J*. (2008) 37:323–32. doi: 10.1007/s00249-007-0246-z

99. Baghaei K, Tokhanbigli S, Asadzadeh H, Nmaki S, Reza Zali M, Hashemi SM. Exosomes as a novel cell-free therapeutic approach in gastrointestinal diseases. *J Cell Physiol*. (2019) 234:9910–26. doi: 10.1002/jcp.27934

100. Carrière J, Bretin A, Darfeuille-Michaud A, Barnich N, Nguyen HTT. Exosomes released from cells infected with Crohn's disease-associated adherent-invasive *Escherichia coli* activate host innate immune responses and enhance bacterial intracellular replication. *Inflamm Bowel Dis*. (2016) 22:516–28. doi: 10.1097/MIB.0000000000000635

101. Mitsuhashi S, Feldbrügge L, Csizmadia E, Mitsuhashi M, Robson SC, Moss AC. Luminal extracellular vesicles (EVs) in inflammatory bowel disease (IBD) exhibit proinflammatory effects on epithelial cells and macrophages. *Inflamm Bowel Dis*. (2016) 22:1587–95. doi: 10.1097/MIB.0000000000000840

102. Zheng X, Chen F, Zhang Q, Liu Y, You P, Sun S, et al. Salivary exosomal PSMA7: a promising biomarker of inflammatory bowel disease. *Protein Cell*. (2017) 8:686–95. doi: 10.1007/s13238-017-0413-7

103. Hovhannisyan L, Czechowska E, Gutowska-Owsiak D. The role of non-immune cell-derived extracellular vesicles in allergy. *Front Immunol*. (2021) 12:702381. doi: 10.3389/fimmu.2021.702381

104. Gross JC, Chaudhary V, Bartscherer K, Boutros M. Active Wnt proteins are secreted on exosomes. *Nat Cell Biol*. (2012) 14:1036–45. doi: 10.1038/ncb2574

105. Natasha G, Gundogan B, Tan A, Farhatnia Y, Wu W, Rajadas J, et al. Exosomes as immunotheranostic nanoparticles. *Clin Ther*. (2014) 36:820–9. doi: 10.1016/j.clinthera.2014.04.019

106. Tran T-H, Mattheolabakis G, Aldawsari H, Amiji M. Exosomes as nanocarriers for immunotherapy of cancer and inflammatory diseases. *Clin Immunol*. (2015) 160:46–58. doi: 10.1016/j.clim.2015.03.021

107. Boukouris S, Mathivanan S. Exosomes in bodily fluids are a highly stable resource of disease biomarkers. *Proteomics Clin Appl*. (2015) 9:358–67. doi: 10.1002/prca.201400114

108. Ostrowski M, Carmo NB, Krumeich S, Fanget I, Raposo G, Savina A, et al. Rab 27a and Rab 27b control different steps of the exosome secretion pathway. *Nat Cell Biol*. (2010) 12:19–30. doi: 10.1038/ncb2000

109. Greening DW, Gopal SK, Xu R, Simpson RJ, Chen W. Exosomes and their roles in immune regulation and cancer. *Semin Cell Dev Biol*. (2015) 40:72–81. doi: 10.1016/j.semcdb.2015.02.009

110. Théry C, Boussac M, Véron P, Ricciardi-Castagnoli P, Raposo G, Garin J, et al. Proteomic analysis of dendritic cell-derived exosomes: a secreted subcellular compartment distinct from apoptotic vesicles. *J Immunol*. (2001) 166:7309–18. doi: 10.4049/jimmunol.166.12.7309

111. Mathivanan S, Fahner CJ, Reid GE, Simpson RJ. ExoCarta 2012: database of exosomal proteins, RNA and lipids. *Nucleic Acids Res*. (2012) 40:D1241–4. doi: 10.1093/nar/gkr828

112. Li P, Kaslan M, Lee SH, Yao J, Gao Z. Progress in exosome isolation techniques. *Theranostics*. (2017) 7:789. doi: 10.7150/thno.18133

113. Théry C, Zitvogel L, Amigorena S. Exosomes: composition, biogenesis and function. *Nat Rev Immunol*. (2002) 2:569–79. doi: 10.1038/nri855

114. Gebert LFR, Mac Rae IJ. Regulation of microRNA function in animals. *Nat Rev Mol Cell Biol*. (2019) 20:21–37. doi: 10.1038/s41580-018-0045-7

115. Matsuo H, Chevallier J, Mayran N, Le Blanc I, Ferguson C, Fauré J, et al. Role of LBPA and Alix in multivesicular liposome formation and endosome organization. *Science*. (2004) 303:531–4. doi: 10.1126/science.1092425

116. Bellingham SA, Coleman BM, Hill AF. Small RNA deep sequencing reveals a distinct miRNA signature released in exosomes from prion-infected neuronal cells. *Nucleic Acids Res*. (2012) 40:10937–49. doi: 10.1093/nar/gks832

117. Eirin A, Riester SM, Zhu X-Y, Tang H, Evans JM, O'Brien D, et al. MicroRNA and mRNA cargo of extracellular vesicles from porcine adipose tissue-derived mesenchymal stem cells. *Gene*. (2014) 551:55–64. doi: 10.1016/j.gene.2014.08.041

118. Ren H, Sang Y, Zhang F, Liu Z, Qi N, Chen Y. Comparative analysis of human mesenchymal stem cells from umbilical cord, dental pulp, and menstrual blood as sources for cell therapy. *Stem Cells Int*. (2016) 2016:3516574. doi: 10.1155/2016/3516574

119. Zhou J, Benito-Martin A, Mighty J, Chang L, Ghoroghi S, Wu H, et al. Retinal progenitor cells release extracellular vesicles containing developmental transcription factors, microRNA and membrane proteins. *Sci Rep*. (2018) 8:2823. doi: 10.1038/s41598-018-20421-1

120. Bi S, Nie Q, Wang W, Zhu Y, Ma X, Wang C, et al. Human umbilical cord mesenchymal stem cells therapy for insulin resistance: a novel strategy in clinical implication. *Curr Stem Cell Res Ther*. (2018) 13:658–64. doi: 10.2174/1574888X13666180810154048

121. Xiong Z-H, Wei J, Lu M-Q, Jin M-Y, Geng H-L. Protective effect of human umbilical cord mesenchymal stem cell exosomes on preserving the morphology and angiogenesis of placenta in rats with preeclampsia. *Biomed Pharmacother*. (2018) 105:1240–7. doi: 10.1016/j.biopha.2018.06.032

122. Guo G, Zhuang X, Xu Q, Wu Z, Zhu Y, Zhou Y, et al. Peripheral infusion of human umbilical cord mesenchymal stem cells rescues acute liver failure lethality in monkeys. *Stem Cell Res Ther*. (2019) 10:84. doi: 10.1186/s13287-019-1184-2

123. Day AGE, Francis WR, Fu K, Pieper IL, Guy O, Xia Z. Osteogenic potential of human umbilical cord mesenchymal stem cells on coralline hydroxyapatite/calcium carbonate microparticles. *Stem Cells Int*. (2018) 2018:4258613. doi: 10.1155/2018/4258613

124. Wu K-C, Chang Y-H, Liu H-W, Ding D-C. Transplanting human umbilical cord mesenchymal stem cells and hyaluronate hydrogel repairs cartilage of osteoarthritis in the minipig model. *Tzu Chi Med J*. (2019) 31:11–9. doi: 10.4103/tcmj.tcmj_87_18

125. Tanaka E, Ogawa Y, Mukai T, Sato Y, Hamazaki T, Nagamura-Inoue T, et al. Dose-dependent effect of intravenous administration of human umbilical cord-derived mesenchymal stem cells in neonatal stroke mice. *Front Neurol*. (2018) 9:133. doi: 10.3389/fneur.2018.00133

126. Mirza A, Khan I, Salim A, Husain M, Herzig JW. Role of Wnt/β-catenin pathway in cardiac lineage commitment of human umbilical cord mesenchymal stem cells by zebularine and 2′-deoxycytidine. *Tissue Cell*. (2022) 77:101850. doi: 10.1016/j.tice.2022.101850

127. Mao F, Wu Y, Tang X, Wang J, Pan Z, Zhang P, et al. Human umbilical cord mesenchymal stem cells alleviate inflammatory bowel disease through the regulation of 15-LOX-1 in macrophages. *Biotechnol Lett*. (2017) 39:929–38. doi: 10.1007/s10529-017-2315-4

128. Li Y, Ma K, Zhang L, Xu H, Zhang N. Human umbilical cord blood derived-mesenchymal stem cells alleviate dextran sulfate sodium-induced colitis by increasing regulatory T cells in mice. *Front Cell Dev Biol*. (2020) 8:604021. doi: 10.3389/fcell.2020.604021

129. Subramanian A, Fong C-Y, Biswas A, Bongso A. Comparative characterization of cells from the various compartments of the human umbilical cord shows that the Wharton's jelly compartment provides the best source of clinically utilizable mesenchymal stem cells. *PLoS One*. (2015) 10:e0127992. doi: 10.1371/journal.pone.0127992

130. Rizano A, Margiana R, Supardi S, Narulita P. Exploring the future potential of mesenchymal stem/stromal cells and their derivatives to support assisted reproductive technology for female infertility applications. *Hum Cell*. (2023) 36:1604–19. doi: 10.1007/s13577-023-00941-3

131. Bárcia RN. What makes umbilical cord tissue-derived mesenchymal stromal cells superior immunomodulators when compared to bone marrow derived mesenchymal stromal cells? *Stem Cells Intern*. (2015) 1:583984.

132. Stefańska K, Ożegowska K, Hutchings G, Popis M, Moncrieff L, Dompe C, et al. Human Wharton's jelly—cellular specificity, stemness potency, animal models, and current application in human clinical trials. *J Clin Med*. (2020) 9:1102. doi: 10.3390/jcm9041102

133. Chen K, Wang D, Du WT, Han Z-B, Ren H, Chi Y, et al. Human umbilical cord mesenchymal stem cells hUC-MSCs exert immunosuppressive activities through a PGE2-dependent mechanism. *Clin Immunol*. (2010) 135:448–58. doi: 10.1016/j.clim.2010.01.015

134. Kim J-H, Jo CH, Kim H-R, Hwang Y. Comparison of immunological characteristics of mesenchymal stem cells from the periodontal ligament, umbilical cord, and adipose tissue. *Stem Cells Int*. (2018) 2018:8429042. doi: 10.1155/2018/8429042

135. Mennan C, Wright K, Bhattacharjee A, Balain B, Richardson J, Roberts S. Isolation and characterisation of mesenchymal stem cells from different regions of the human umbilical cord. *Biomed Res Int*. (2013) 2013:916136. doi: 10.1155/2013/916136

136. Jo CH, Lim H-J, Yoon KS. Characterization of tendon-specific markers in various human tissues, tenocytes and mesenchymal stem cells. *Tissue Eng Regen Med*. (2019) 16:151–9. doi: 10.1007/s13770-019-00182-2

137. Wang Z, He Z, Liang S, Yang Q, Cheng P, Chen A. Comprehensive proteomic analysis of exosomes derived from human bone marrow, adipose tissue, and umbilical cord mesenchymal stem cells. *Stem Cell Res Ther*. (2020) 11:511. doi: 10.1186/s13287-020-02032-8

138. Monov D, Pashanova O. Experimental substantiation of the use of phenibut combinations with salicylic, nicotinic, and glutamic acids in cerebral ischemia. *Neurocrit Care*. (2023) 39:464–77. doi: 10.1007/s12028-023-01719-z

139. Kidd S, Spaeth E, Dembinski JL, Dietrich M, Watson K, Klopp A, et al. Direct evidence of mesenchymal stem cell tropism for tumor and wounding microenvironments using *in vivo* bioluminescent imaging. *Stem Cells*. (2009) 27:2614–23. doi: 10.1002/stem.187

140. Xue Z-L, Meng Y-L, Ge J-H. Upregulation of miR-132 attenuates osteoblast differentiation of UC-MSCs. *Eur Rev Med Pharmacol Sci*. (2018) 22:1580–7. doi: 10.26355/eurrev_201808_15643

141. Motawea SM, Noreldin RI, Naguib YM. Potential therapeutic effects of endothelial cells trans-differentiated from Wharton's jelly-derived mesenchymal stem cells on altered vascular functions in aged diabetic rat model. *Diabetol Metab Syndr*. (2020) 12:40. doi: 10.1186/s13098-020-00546-y

142. Wu KH, Wang SY, Xiao QR, Yang Y, Huang NP, Mo XM, et al. Efficient generation of functional cardiomyocytes from human umbilical cord-derived virus-free induced pluripotent stem cells. *Cell Tissue Res*. (2018) 374:275–83. doi: 10.1007/s00441-018-2875-1

143. Zhou X, Cui L, Zhou X, Yang Q, Wang L, Guo G, et al. Induction of hepatocyte-like cells from human umbilical cord-derived mesenchymal stem cells by defined microRNAs. *J Cell Mol Med*. (2017) 21:881–93. doi: 10.1111/jcmm.13027

144. Van Pham P, Nguyen PT-M, Nguyen AT-Q, Pham VM, Bui AN-T, Dang LT-T, et al. Improved differentiation of umbilical cord blood-derived mesenchymal stem cells into insulin-producing cells by PDX-1 mRNA transfection. *Differentiation*. (2014) 87:200–8. doi: 10.1016/j.diff.2014.08.001

145. Ortiz GGR, Zaidi NH, Saini RS, Coronel AAR, Alsandook T, Lafta MH, et al. The developing role of extracellular vesicles in autoimmune diseases: special attention to mesenchymal stem cell-derived extracellular vesicles. *Int Immunopharmacol*. (2023) 122:110531. doi: 10.1016/j.intimp.2023.110531

146. Lener T, Gimona M, Aigner L, Börger V, Buzas E, Camussi G, et al. Applying extracellular vesicles based therapeutics in clinical trials—an ISEV position paper. *J Extracell Vesicles*. (2015) 4:30087. doi: 10.3402/jev.v4.30087

147. Théry C, Amigorena S, Raposo G, Clayton A. Isolation and characterization of exosomes from cell culture supernatants and biological fluids. *Curr Protoc Cell Biol*. (2006) 30:3–22. doi: 10.1002/0471143030.cb0322s30

148. Lobb RJ, Becker M, Wen Wen S, Wong CSF, Wiegmans AP, Leimgruber A, et al. Optimized exosome isolation protocol for cell culture supernatant and human plasma. *J Extracell Vesicles*. (2015) 4:27031. doi: 10.3402/jev.v4.27031

149. Gardiner C, Di Vizio D, Sahoo S, Théry C, Witwer KW, Wauben M, et al. Techniques used for the isolation and characterization of extracellular vesicles: results of a worldwide survey. *J Extracell Vesicles*. (2016) 5:32945. doi: 10.3402/jev.v5.32945

150. Lozano-Ramos I, Bancu I, Oliveira-Tercero A, Armengol MP, Menezes-Neto A, Del Portillo HA, et al. Size-exclusion chromatography-based enrichment of extracellular vesicles from urine samples. *J Extracell Vesicles*. (2015) 4:27369. doi: 10.3402/jev.v4.27369

151. Arraud N, Gounou C, Turpin D, Brisson AR. Fluorescence triggering: a general strategy for enumerating and phenotyping extracellular vesicles by flow cytometry. *Cytometry A*. (2016) 89:184–95. doi: 10.1002/cyto.a.22669

152. Chen C, Luo Y, He W, Zhao Y, Kong Y, Liu H, et al. Exosomal long noncoding RNA LNMAT2 promotes lymphatic metastasis in bladder cancer. *J Clin Invest*. (2020) 130:404–21. doi: 10.1172/JCI130892

153. Kusuma GD, Barabadi M, Tan JL, Morton DA V, Frith JE, Lim R. To protect and to preserve: novel preservation strategies for extracellular vesicles. *Front Pharmacol*. (2018) 9:1199. doi: 10.3389/fphar.2018.01199

154. Llorente A, van Deurs B, Sandvig K. Cholesterol regulates prostasome release from secretory lysosomes in PC-3 human prostate cancer cells. *Eur J Cell Biol*. (2007) 86:405–15. doi: 10.1016/j.ejcb.2007.05.001

155. Diaz G, Bridges C, Lucas M, Cheng Y, Schorey JS, Dobos KM, et al. Protein digestion, ultrafiltration, and size exclusion chromatography to optimize the isolation of exosomes from human blood plasma and serum. *J Vis Exp*. (2018):e57467. doi: 10.3791/57467-v

156. Shtam T, Evtushenko V, Samsonov R, Zabrodskaya Y, Kamyshinsky R, Zabegina L, et al. Evaluation of immune and chemical precipitation methods for plasma exosome isolation. *PLoS One*. (2020) 15:e0242732. doi: 10.1371/journal.pone.0242732

157. Li K, Wong DK, Hong KY, Raffai RL. Cushioned-density gradient ultracentrifugation (C-DGUC): a refined and high performance method for the isolation, characterization, and use of exosomes. *Methods Mol Biol*. (2018) 1740:69–83. doi: 10.1007/978-1-4939-7652-2_7

158. Sidhom K, Obi PO, Saleem A. A review of exosomal isolation methods: is size exclusion chromatography the best option? *Int J Mol Sci*. (2020) 21:6466. doi: 10.3390/ijms21186466

159. Wang J, Ma P, Kim DH, Liu B-F, Demirci U. Towards microfluidic-based exosome isolation and detection for tumor therapy. *Nano Today*. (2021) 37:101066. doi: 10.1016/j.nantod.2020.101066

160. Li Y, Altemus J, Lightner AL. Mesenchymal stem cells and acellular products attenuate murine induced colitis. *Stem Cell Res Ther*. (2020) 11:515. doi: 10.1186/s13287-020-02025-7

161. Alves VBF, de Sousa BC, Fonseca MTC, Ogata H, Caliari-Oliveira C, Yaochite JNU, et al. A single administration of human adipose tissue-derived mesenchymal stromal cells (MSC) induces durable and sustained long-term regulation of inflammatory response in experimental colitis. *Clin Exp Immunol*. (2019) 196:139–54. doi: 10.1111/cei.13262

162. Yang S, Liang X, Song J, Li C, Liu A, Luo Y, et al. A novel therapeutic approach for inflammatory bowel disease by exosomes derived from human umbilical cord mesenchymal stem cells to repair intestinal barrier via TSG-6. *Stem Cell Res Ther*. (2021) 12:315. doi: 10.1186/s13287-021-02404-8

163. Song W-J, Li Q, Ryu M-O, Ahn J-O, Bhang DH, Jung YC, et al. TSG-6 released from intraperitoneally injected canine adipose tissue-derived mesenchymal stem cells ameliorate inflammatory bowel disease by inducing M2 macrophage switch in mice. *Stem Cell Res Ther*. (2018) 9:91. doi: 10.1186/s13287-018-0841-1

164. Sala E, Genua M, Petti L, Anselmo A, Arena V, Cibella J, et al. Mesenchymal stem cells reduce colitis in mice via release of TSG6, independently of their localization to the intestine. *Gastroenterology*. (2015) 149:163–76. doi: 10.1053/j.gastro.2015.03.013

165. Cao L, Xu H, Wang G, Liu M, Tian D, Yuan Z. Extracellular vesicles derived from bone marrow mesenchymal stem cells attenuate dextran sodium sulfate-induced ulcerative colitis by promoting M2 macrophage polarization. *Int Immunopharmacol*. (2019) 72:264–74. doi: 10.1016/j.intimp.2019.04.020

166. Heidari N, Abbasi-Kenarsari H, Namaki S, Baghaei K, Zali MR, Ghaffari Khaligh S, et al. Adipose-derived mesenchymal stem cell-secreted exosome alleviates dextran sulfate sodium-induced acute colitis by Treg cell induction and inflammatory cytokine reduction. *J Cell Physiol*. (2021) 236:5906–20. doi: 10.1002/jcp.30275

167. Qi L, Wu J, Zhu S, Wang X, Lv X, Liu C, et al. Mesenchymal stem cells alleviate inflammatory bowel disease via Tr1 cells. *Stem Cell Rev Rep*. (2022) 18:2444–57. doi: 10.1007/s12015-022-10353-9

168. Li P, Zhang H, Gao J, Du W, Tang D, Wang W, et al. Mesenchymal stem cells-derived extracellular vesicles containing miR-378a-3p inhibit the occurrence of inflammatory bowel disease by targeting GATA2. *J Cell Mol Med*. (2022) 26:3133–46. doi: 10.1111/jcmm.17176

169. Xu J, Wang X, Chen J, Chen S, Li Z, Liu H, et al. Embryonic stem cell-derived mesenchymal stem cells promote colon epithelial integrity and regeneration by elevating circulating IGF-1 in colitis mice. *Theranostics*. (2020) 10:12204. doi: 10.7150/thno.47683

170. Liu P, Xie X, Wu H, Li H, Chi J, Liu X, et al. Mesenchymal stem cells promote intestinal mucosal repair by positively regulating the Nrf 2/Keap 1/ARE signaling pathway in acute experimental colitis. *Dig Dis Sci*. (2023) 68:1835–46. doi: 10.1007/s10620-022-07722-2

171. Lou G, Chen Z, Zheng M, Liu Y. Mesenchymal stem cell-derived exosomes as a new therapeutic strategy for liver diseases. *Exp Mol Med*. (2017) 49:e346–6. doi: 10.1038/emm.2017.63

172. Shen Z, Huang W, Liu J, Tian J, Wang S, Rui K. Effects of mesenchymal stem cell-derived exosomes on autoimmune diseases. *Front Immunol*. (2021) 12:749192. doi: 10.3389/fimmu.2021.749192

173. Mao F, Wu Y, Tang X, Kang J, Zhang B, Yan Y, et al. Exosomes derived from human umbilical cord mesenchymal stem cells relieve inflammatory bowel disease in mice. *Biomed Res Int*. (2017) 2017:5356760. doi: 10.1155/2017/5356760

174. Cai X, Zhang Z, Yuan J, Ocansey DKW, Tu Q, Zhang X, et al. hucMSC-derived-derived exosomes attenuate colitis by regulating macrophage pyroptosis via the miR-378a-5p/NLRP3 axis. *Stem Cell Res Ther*. (2021) 12:416. doi: 10.1186/s13287-021-02492-6

175. Yu H, Yang X, Xiao X, Xu M, Yang Y, Xue C, et al. Human adipose mesenchymal stem cell-derived exosomes protect mice from DSS-induced inflammatory bowel disease by promoting intestinal-stem-cell and epithelial regeneration. *Aging Dis*. (2021) 12:1423. doi: 10.14336/AD.2021.0601

176. Xu Y, Zhang L, Ocansey DKW, Wang B, Hou Y, Mei R, et al. HucMSC-Ex alleviates inflammatory bowel disease via the lnc78583-mediated miR3202/HOXB13 pathway. *J Zhejiang Univ Sci B*. (2022) 23:423–31. doi: 10.1631/jzus.B2100793

177. Sun D, Cao H, Yang L, Lin L, Hou B, Zheng W, et al. MiR-200b in heme oxygenase-1-modified bone marrow mesenchymal stem cell-derived exosomes alleviates inflammatory injury of intestinal epithelial cells by targeting high mobility group box 3. *Cell Death Dis*. (2020) 11:480. doi: 10.1038/s41419-020-2685-8

178. Yang R, Huang H, Cui S, Zhou Y, Zhang T, Zhou Y. IFN-γ promoted exosomes from mesenchymal stem cells to attenuate colitis via miR-125a and miR-125b. *Cell Death Dis*. (2020) 11:603. doi: 10.1038/s41419-020-02788-0

179. Liu H, Liang Z, Wang F, Zhou C, Zheng X, Hu T, et al. Exosomes from mesenchymal stromal cells reduce murine colonic inflammation via a macrophage-dependent mechanism. *JCI Insight*. (2019) 4:e131273. doi: 10.1172/jci.insight.131273

180. Tian J, Zhu Q, Zhang Y, Bian Q, Hong Y, Shen Z, et al. Olfactory ecto-mesenchymal stem cell-derived exosomes ameliorate experimental colitis via modulating Th1/Th17 and Treg cell responses. *Front Immunol*. (2020) 11:598322. doi: 10.3389/fimmu.2020.598322

181. Wu Y, Qiu W, Xu X, Kang J, Wang J, Wen Y, et al. Exosomes derived from human umbilical cord mesenchymal stem cells alleviate inflammatory bowel disease in mice through ubiquitination. *Am J Transl Res*. (2018) 10:2026.

182. Yang J, Liu X-X, Fan H, Tang Q, Shou Z-X, Zuo D-M, et al. Extracellular vesicles derived from bone marrow mesenchymal stem cells protect against experimental colitis via attenuating colon inflammation, oxidative stress and apoptosis. *PLoS One*. (2015) 10:e0140551. doi: 10.1371/journal.pone.0145800

183. Zhang N, Chen Y, Huang C, Wei M, Li T, Lv Y, et al. Adipose-derived mesenchymal stem cells may reduce intestinal epithelial damage in ulcerative colitis by communicating with macrophages and blocking inflammatory pathways: an analysis *in silico*. *Aging*. (2022) 14:2665. doi: 10.18632/aging.203964

184. Baumgart DC, Carding SR. Inflammatory bowel disease: cause and immunobiology. *Lancet*. (2007) 369:1627–40. doi: 10.1016/S0140-6736(07)60750-8

185. Lee SH, Eun Kwon J, Cho M-L. Immunological pathogenesis of inflammatory bowel disease. *Intest Res*. (2018) 16:26–42. doi: 10.5217/ir.2018.16.1.26

186. Mosser DM, Edwards JP. Exploring the full spectrum of macrophage activation. *Nat Rev Immunol*. (2008) 8:958–69. doi: 10.1038/nri2448

187. Atri C, Guerfali FZ, Laouini D. Role of human macrophage polarization in inflammation during infectious diseases. *Int J Mol Sci*. (2018) 19:1801. doi: 10.3390/ijms19061801

188. Na YR, Stakenborg M, Seok SH, Matteoli G. Macrophages in intestinal inflammation and resolution: a potential therapeutic target in IBD. *Nat Rev Gastroenterol Hepatol*. (2019) 16:531–43. doi: 10.1038/s41575-019-0172-4

189. Vergadi E, Ieronymaki E, Lyroni K, Vaporidi K, Tsatsanis C. Akt signaling pathway in macrophage activation and M1/M2 polarization. *J Immunol*. (2017) 198:1006–14. doi: 10.4049/jimmunol.1601515

190. Laskin DL, Sunil VR, Gardner CR, Laskin JD. Macrophages and tissue injury: agents of defense or destruction? *Annu Rev Pharmacol Toxicol*. (2011) 51:267–88. doi: 10.1146/annurev.pharmtox.010909.105812

191. An J-H, Li Q, Ryu M-O, Nam A-R, Bhang D-H, Jung Y-C, et al. TSG-6 in extracellular vesicles from canine mesenchymal stem/stromal is a major factor in relieving DSS-induced colitis. *PLoS One*. (2020) 15:e0220756. doi: 10.1371/journal.pone.0220756

192. Wang J, Pei B, Yan J, Xu X, Fang A-N, Ocansey DKW, et al. hucMSC-derived exosomes alleviate the deterioration of colitis via the miR-146a/SUMO1 axis. *Mol Pharm*. (2022) 19:484–93. doi: 10.1021/acs.molpharmaceut.1c00450

193. Zhang B, Yin Y, Lai RC, Tan SS, Choo ABH, Lim SK. Mesenchymal stem cells secrete immunologically active exosomes. *Stem Cells Dev*. (2014) 23:1233–44. doi: 10.1089/scd.2013.0479

194. Shen B, Liu J, Zhang F, Wang Y, Qin Y, Zhou Z, et al. CCR2 positive exosome released by mesenchymal stem cells suppresses macrophage functions and alleviates ischemia/reperfusion-induced renal injury. *Stem Cells Int*. (2016) 2016:1240301. doi: 10.1155/2016/1240301

195. Willis GR, Fernandez-Gonzalez A, Anastas J, Vitali SH, Liu X, Ericsson M, et al. Mesenchymal stromal cell exosomes ameliorate experimental bronchopulmonary dysplasia and restore lung function through macrophage immunomodulation. *Am J Respir Crit Care Med*. (2018) 197:104–16. doi: 10.1164/rccm.201705-0925OC

196. Kane S, Lemieux N. The role of breastfeeding in postpartum disease activity in women with inflammatory bowel disease. *Am J Gastroenterol*. (2005) 100:102–5. doi: 10.1111/j.1572-0241.2005.40785.x

197. Fuss IJ, Heller F, Boirivant M, Leon F, Yoshida M, Fichtner-Feigl S, et al. Nonclassical CD1d-restricted NK T cells that produce IL-13 characterize an atypical Th2 response in ulcerative colitis. *J Clin Invest*. (2004) 113:1490–7. doi: 10.1172/JCI19836

198. Kanai T, Kawamura T, Dohi T, Makita S, Nemoto Y, Totsuka T, et al. TH1/TH2-mediated colitis induced by adoptive transfer of $CD4^+$ CD45RBhigh T lymphocytes into nude mice. *Inflamm Bowel Dis*. (2006) 12:89–99. doi: 10.1097/01.MIB.0000197237.21387.mL

199. Lotfinejad P, Shamsasenjan K, Baradaran B, Safarzadeh E, Kazemi T, Movassaghpour AA. Immunomodulatory effect of human umbilical cord blood-derived mesenchymal stem cells on activated T-lymphocyte. *Iran J Allergy Asthma Immunol*. (2021) 20:711–20. doi: 10.18502/ijaai.v20i6.8022

200. Jiang X-X, Zhang YI, Liu B, Zhang S-X, Wu Y, Yu X-D, et al. Human mesenchymal stem cells inhibit differentiation and function of monocyte-derived dendritic cells. *Blood*. (2005) 105:4120–6. doi: 10.1182/blood-2004-02-0586

201. Rabinovich GA, Alonso CR, Sotomayor CE, Durand S, Bocco JL, Riera CM. Molecular mechanisms implicated in galectin-1-induced apoptosis: activation of the AP-1 transcription factor and downregulation of Bcl-2. *Cell Death Differ*. (2000) 7:747–53. doi: 10.1038/sj.cdd.4400708

202. Francisco LM, Salinas VH, Brown KE, Vanguri VK, Freeman GJ, Kuchroo VK, et al. PD-L1 regulates the development, maintenance, and function of induced regulatory T cells. *J Exp Med*. (2009) 206:3015–29. doi: 10.1084/jem.20090847

203. Del Fattore A, Luciano R, Pascucci L, Goffredo BM, Giorda E, Scapaticci M, et al. Immunoregulatory effects of mesenchymal stem cell-derived extracellular vesicles on T lymphocytes. *Cell Transplant*. (2015) 24:2615–27. doi: 10.3727/096368915X687543

204. Eastaff-Leung N, Mabarrack N, Barbour A, Cummins A, Barry S. Foxp 3^+ regulatory T cells, Th17 effector cells, and cytokine environment in inflammatory bowel disease. *J Clin Immunol*. (2010) 30:80–9. doi: 10.1007/s10875-009-9345-1

205. Galley JD, Parry NM, Ahmer BMM, Fox JG, Bailey MT. The commensal microbiota exacerbate infectious colitis in stressor-exposed mice. *Brain Behav Immun*. (2017) 60:44–50. doi: 10.1016/j.bbi.2016.09.010

206. Morel PA, Butterfield LH. Dendritic cell control of immune responses. *Front Immunol*. (2015) 6:42. doi: 10.3389/fimmu.2015.00042

207. Nakamura Y, Miyaki S, Ishitobi H, Matsuyama S, Nakasa T, Kamei N, et al. Mesenchymal-stem-cell-derived exosomes accelerate skeletal muscle regeneration. *FEBS Lett*. (2015) 589:1257–65. doi: 10.1016/j.febslet.2015.03.031

208. La Rocca G, Anzalone R, Corrao S, Magno F, Loria T, Lo Iacono M, et al. Isolation and characterization of Oct-4^+/HLA-G^+ mesenchymal stem cells from human umbilical cord matrix: differentiation potential and detection of new markers. *Histochem Cell Biol*. (2009) 131:267–82. doi: 10.1007/s00418-008-0519-3

209. Bang OY, Kim EH. Mesenchymal stem cell-derived extracellular vesicle therapy for stroke: challenges and progress. *Front Neurol*. (2019) 10:211. doi: 10.3389/fneur.2019.00211

210. Zhao Q, Yang W-R, Wang X-H, Li G-Q, Xu L-Q, Cui X, et al. *Clostridium butyricum* alleviates intestinal low-grade inflammation in TNBS-induced irritable bowel syndrome in mice by regulating functional status of lamina propria dendritic cells. *World J Gastroenterol*. (2019) 25:5469. doi: 10.3748/wjg.v25.i36.5469

211. Qian X, An N, Ren Y, Yang C, Zhang X, Li L. Immunosuppressive effects of mesenchymal stem cells-derived exosomes. *Stem Cell Rev Rep*. (2021) 17:411–27. doi: 10.1007/s12015-020-10040-7

212. Grégoire C, Lechanteur C, Briquet A, Baudoux É, Baron F, Louis E, et al. Mesenchymal stromal cell therapy for inflammatory bowel diseases. *Aliment Pharmacol Ther*. (2017) 45:205–21. doi: 10.1111/apt.13864

213. Chi L, Khan I, Lin Z, Zhang J, Lee MYS, Leong W, et al. Fructo-oligosaccharides from *Morinda officinalis* remodeled gut microbiota and alleviated depression features in a stress rat model. *Phytomedicine*. (2020) 67:153157. doi: 10.1016/j.phymed.2019.153157

214. He Z, Cui B-T, Zhang T, Li P, Long C-Y, Ji G-Z, et al. Fecal microbiota transplantation cured epilepsy in a case with Crohn's disease: the first report. *World J Gastroenterol*. (2017) 23:3565. doi: 10.3748/wjg.v23.i19.3565

215. Llewellyn SR, Britton GJ, Contijoch EJ, Vennaro OH, Mortha A, Colombel J-F, et al. Interactions between diet and the intestinal microbiota alter intestinal permeability and colitis severity in mice. *Gastroenterology*. (2018) 154:1037–46. doi: 10.1053/j.gastro.2017.11.030

216. Holmberg FEO, Pedersen J, Jørgensen P, Soendergaard C, Jensen KB, Nielsen OH. Intestinal barrier integrity and inflammatory bowel disease: stem cell-based approaches to regenerate the barrier. *J Tissue Eng Regen Med*. (2018) 12:923–35. doi: 10.1002/term.2506

217. Bhattacharyya A, Chattopadhyay R, Mitra S, Crowe SE. Oxidative stress: an essential factor in the pathogenesis of gastrointestinal mucosal diseases. *Physiol Rev*. (2014) 94:329–54. doi: 10.1152/physrev.00040.2012

218. Tanida S, Mizoshita T, Mizushima T, Sasaki M, Shimura T, Kamiya T, et al. Involvement of oxidative stress and mucosal addressin cell adhesion molecule-1 (MAdCAM-1) in inflammatory bowel disease. *J Clin Biochem Nutr*. (2011) 48:112–6. doi: 10.3164/jcbn.10-41

219. Pravda J. Radical induction theory of ulcerative colitis. *World J Gastroenterol*. (2005) 11:2371. doi: 10.3748/wjg.v11.i16.2371

220. Pavlick KP, Laroux FS, Fuseler J, Wolf RE, Gray L, Hoffman J, et al. Role of reactive metabolites of oxygen and nitrogen in inflammatory bowel disease. *Free Radic Biol Med*. (2002) 33:311–22. doi: 10.1016/S0891-5849(02)00853-5

221. Hatsugai M, Kurokawa MS, Kouro T, Nagai K, Arito M, Masuko K, et al. Protein profiles of peripheral blood mononuclear cells are useful for differential diagnosis of ulcerative colitis and Crohn's disease. *J Gastroenterol*. (2010) 45:488–500. doi: 10.1007/s00535-009-0183-y

222. Rachmilewitz D, Stamler JS, Karmeli F, Mullins ME, Singel DJ, Loscalzo J, et al. Peroxynitrite-induced rat colitis—a new model of colonic inflammation. *Gastroenterology*. (1993) 105:1681–8. doi: 10.1016/0016-5085(93)91063-N

223. Li X, Fang P, Mai J, Choi ET, Wang H, Yang X. Targeting mitochondrial reactive oxygen species as novel therapy for inflammatory diseases and cancers. *J Hematol Oncol*. (2013) 6:19. doi: 10.1186/1756-8722-6-19

224. Lawlor KE, Vince JE. Ambiguities in NLRP3 inflammasome regulation: Is there a role for mitochondria? *Biochim Biophys Acta*. (2014) 1840:1433–40. doi: 10.1016/j.bbagen.2013.08.014

225. Cristani M, Speciale A, Saija A, Gangemi S, Lucia Minciullo P, Cimino F. Circulating advanced oxidation protein products as oxidative stress biomarkers and progression mediators in pathological conditions related to inflammation and immune dysregulation. *Curr Med Chem*. (2016) 23:3862–82. doi: 10.2174/0929867323666160902154748

226. Rager TM, Olson JK, Zhou Y, Wang Y, Besner GE. Exosomes secreted from bone marrow-derived mesenchymal stem cells protect the intestines from experimental necrotizing enterocolitis. *J Pediatr Surg*. (2016) 51:942–7. doi: 10.1016/j.jpedsurg.2016.02.061

227. McCulloh CJ, Olson JK, Wang Y, Zhou Y, Tengberg NH, Deshpande S, et al. Treatment of experimental necrotizing enterocolitis with stem cell-derived exosomes. *J Pediatr Surg*. (2018) 53:1215–20. doi: 10.1016/j.jpedsurg.2018.02.086

228. Rieder F, Fiocchi C, Rogler G. Mechanisms, management, and treatment of fibrosis in patients with inflammatory bowel diseases. *Gastroenterology*. (2017) 152:340–50. doi: 10.1053/j.gastro.2016.09.047

229. Hayashi Y, Nakase H. The molecular mechanisms of intestinal inflammation and fibrosis in Crohn's disease. *Front Physiol*. (2022) 13:845078. doi: 10.3389/fphys.2022.845078

230. Frangogiannis NG. Fibroblast—extracellular matrix interactions in tissue fibrosis. *Curr Pathobiol Rep*. (2016) 4:11–8. doi: 10.1007/s40139-016-0099-1

231. Lamouille S, Xu J, Derynck R. Molecular mechanisms of epithelial–mesenchymal transition. *Nat Rev Mol Cell Biol*. (2014) 15:178–96. doi: 10.1038/nrm3758

232. Yang J, Zhou C, Zhu R, Fan H, Liu X, Duan X, et al. miR-200b-containing microvesicles attenuate experimental colitis associated intestinal fibrosis by inhibiting epithelial-mesenchymal transition. *J Gastroenterol Hepatol*. (2017) 32:1966–74. doi: 10.1111/jgh.13797

233. Yao Y, Chen R, Wang G, Zhang Y, Liu F. Exosomes derived from mesenchymal stem cells reverse EMT via TGF-β1/Smad pathway and promote repair of damaged endometrium. *Stem Cell Res Ther*. (2019) 10:225. doi: 10.1186/s13287-019-1332-8

234. Choi YJ, Koo JB, Kim HY, Seo JW, Lee EJ, Kim WR, et al. Umbilical cord/placenta-derived mesenchymal stem cells inhibit fibrogenic activation in human intestinal myofibroblasts via inhibition of myocardin-related transcription factor A. *Stem Cell Res Ther*. (2019) 10:291. doi: 10.1186/s13287-019-1385-8

235. Duan L, Cao X. Human placenta mesenchymal stem cells-derived extracellular vesicles regulate collagen deposition in intestinal mucosa of mice with colitis. *Chin J Tissue Eng Res*. (2021) 25:1026.

236. Pan Y, Wu W, Jiang X, Liu Y. Mesenchymal stem cell-derived exosomes in cardiovascular and cerebrovascular diseases: from mechanisms to therapy. *Biomed Pharmacother*. (2023) 163:114817. doi: 10.1016/j.biopha.2023.114817

237. Sun G, Li G, Li D, Huang W, Zhang R, Zhang H, et al. hucMSC derived exosomes promote functional recovery in spinal cord injury mice via attenuating inflammation. *Mater Sci Eng C*. (2018) 89:194–204. doi: 10.1016/j.msec.2018.04.006

238. Pang Q-M, Deng K-Q, Zhang M, Wu X-C, Yang R-L, Fu S-P, et al. Multiple strategies enhance the efficacy of MSCs transplantation for spinal cord injury. *Biomed Pharmacother*. (2023) 157:114011. doi: 10.1016/j.biopha.2022.114011

239. Bao CS, Li XL, Liu L, Wang B, Yang FB, Chen LG. Transplantation of human umbilical cord mesenchymal stem cells promotes functional recovery after spinal cord injury by blocking the expression of IL-7. *Eur Rev Med Pharmacol Sci*. (2018) 22:6436–47. doi: 10.26355/eurrev_201810_16056

240. Zhu X, Wang Z, Sun YE, Liu Y, Wu Z, Ma B, et al. Neuroprotective effects of human umbilical cord-derived mesenchymal stem cells from different donors on spinal cord injury in mice. *Front Cell Neurosci*. (2022) 15:768711. doi: 10.3389/fncel.2021.768711

241. Xiao X, Li W, Rong D, Xu Z, Zhang Z, Ye H, et al. Human umbilical cord mesenchymal stem cells-derived extracellular vesicles facilitate the repair of spinal cord injury via the miR-29b-3p/PTEN/Akt/mTOR axis. *Cell Death Discov*. (2021) 7:212. doi: 10.1038/s41420-021-00572-3

242. GBD 2016 Traumatic Brain Injury and Spinal Cord Injury Collaborators. Global, regional, and national burden of traumatic brain injury and spinal cord injury,

1990-2016: a systematic analysis for the Global Burden of Disease Study 2016. *Lancet Neurol.* (2019) 18:56–87. doi: 10.1016/S1474-4422(18)30415-0

243. Zhang L, Lin Y, Bai W, Sun L, Tian M. Human umbilical cord mesenchymal stem cell-derived exosome suppresses programmed cell death in traumatic brain injury via PINK1/Parkin-mediated mitophagy. *CNS Neurosci Ther*. (2023) 29:2236–58. doi: 10.1111/cns.14159

244. Xia P, Marjan M, Liu Z, Zhou W, Zhang Q, Cheng C, et al. Chrysophanol postconditioning attenuated cerebral ischemia-reperfusion injury induced NLRP3-related pyroptosis in a TRAF6-dependent manner. *Exp Neurol*. (2022) 357:114197. doi: 10.1016/j.expneurol.2022.114197

245. Nazari S, Pourmand SM, Motevaseli E, Hassanzadeh G. Mesenchymal stem cells (MSCs) and MSC-derived exosomes in animal models of central nervous system diseases: targeting the NLRP3 inflammasome. *IUBMB Life*. (2023) 75:794–810. doi: 10.1002/iub.2759

246. Yang H-C, Zhang M, Wu R, Zheng H-Q, Zhang L-Y, Luo J, et al. CC chemokine receptor type 2-overexpressing exosomes alleviated experimental post-stroke cognitive impairment by enhancing microglia/macrophage M2 polarization. *World J Stem Cells*. (2020) 12:152. doi: 10.4252/wjsc.v12.i2.152

247. Zhang Z-W, Wei P, Zhang G-J, Yan J-X, Zhang S, Liang J, et al. Intravenous infusion of the exosomes derived from human umbilical cord mesenchymal stem cells enhance neurological recovery after traumatic brain injury via suppressing the NF-κB pathway. *Open Life Sci*. (2022) 17:189–201. doi: 10.1515/biol-2022-0022

248. Hofmann R, James SK, Jernberg T, Lindahl B, Erlinge D, Witt N, et al. Oxygen therapy in suspected acute myocardial infarction. *N Engl J Med*. (2017) 377:1240–9. doi: 10.1056/NEJMoa1706222

249. Diebold S, Moellmann J, Kahles F, Haj-Yehia E, Liehn EA, Nickel A, et al. Myocardial infarction is sufficient to increase GLP-1 secretion, leading to improved left ventricular contractility and mitochondrial respiratory capacity. *Diabetes Obes Metab*. (2018) 20:2911–8. doi: 10.1111/dom.13472

250. Vallabhajosyula S, Patlolla SH, Dunlay SM, Prasad A, Bell MR, Jaffe AS, et al. Regional variation in the management and outcomes of acute myocardial infarction with cardiogenic shock in the United States. *Circ Heart Fail*. (2020) 13:e006661. doi: 10.1161/CIRCHEARTFAILURE.120.007154

251. Hao D, Swindell HS, Ramasubramanian L, Liu R, Lam KS, Farmer DL, et al. Extracellular matrix mimicking nanofibrous scaffolds modified with mesenchymal stem cell-derived extracellular vesicles for improved vascularization. *Front Bioeng Biotechnol*. (2020) 8:633. doi: 10.3389/fbioe.2020.00633

252. Chen J, Zhan Y, Wang Y, Han D, Tao B, Luo Z, et al. Chitosan/silk fibroin modified nanofibrous patches with mesenchymal stem cells prevent heart remodeling post-myocardial infarction in rats. *Acta Biomater*. (2018) 80:154–68. doi: 10.1016/j.actbio.2018.09.013

253. Yang M, Liao M, Liu R, Zhang Q, Zhang S, He Y, et al. Human umbilical cord mesenchymal stem cell-derived extracellular vesicles loaded with miR-223 ameliorate myocardial infarction through P53/S100A9 axis. *Genomics*. (2022) 114:110319. doi: 10.1016/j.ygeno.2022.110319

254. Zhou R, Gao J, Xiang C, Liu Z, Zhang Y, Zhang J, et al. Salvianolic acid A attenuated myocardial infarction-induced apoptosis and inflammation by activating Trx. *Naunyn Schmiedeberg's Arch Pharmacol*. (2020) 393:991–1002. doi: 10.1007/s00210-019-01766-4

255. Hollweck T, Hartmann I, Eblenkamp M, Wintermantel E, Reichart B, Uberfuhr P, et al. Cardiac differentiation of human Wharton's jelly stem cells–experimental comparison of protocols. *Open Tissue Eng Regen Med J*. (2011) 4:95–102. doi: 10.2174/1875043501104010095

256. Qian Q, Qian H, Zhang X, Zhu W, Yan Y, Ye S, et al. 5-Azacytidine induces cardiac differentiation of human umbilical cord-derived mesenchymal stem cells by activating extracellular regulated kinase. *Stem Cells Dev*. (2012) 21:67–75. doi: 10.1089/scd.2010.0519

257. Zhang C, Zhou G, Chen Y, Liu S, Chen F, Xie L, et al. Human umbilical cord mesenchymal stem cells alleviate interstitial fibrosis and cardiac dysfunction in a dilated cardiomyopathy rat model by inhibiting TNF-α and TGF-β1/ERK1/2 signaling pathways. *Mol Med Rep*. (2018) 17:71–8. doi: 10.3892/mmr.2017.7882

258. Chao C-T, Lin Y-F, Tsai H-B, Wu V-C, Ko W-J. Acute kidney injury network staging in geriatric postoperative acute kidney injury patients: shortcomings and improvements. *J Am Coll Surg*. (2013) 217:240–50. doi: 10.1016/j.jamcollsurg.2013.03.024

259. Barbano B, Sardo L, Gigante A, Ludovica Gasperini M, Liberatori M, Di Lazzaro Giraldi G, et al. Pathophysiology, diagnosis and clinical management of hepatorenal syndrome: from classic to new drugs. *Curr Vasc Pharmacol*. (2014) 12:125–35. doi: 10.2174/15701611120114032716393O

260. Yaghoubi Y, Movassaghpour A, Zamani M, Talebi M, Mehdizadeh A, Yousefi M. Human umbilical cord mesenchymal stem cells derived-exosomes in diseases treatment. *Life Sci*. (2019) 233:116733. doi: 10.1016/j.lfs.2019.116733

261. Muiru AN, Hsu JY, Zhang X, Appel LJ, Chen J, Cohen DL, et al. Risk for chronic kidney disease progression after acute kidney injury: findings from the chronic renal insufficiency cohort study. *Ann Intern Med*. (2023) 176:961–8. doi: 10.7326/M22-3617

262. Al-Dhalimy AMB, Salim HM, Shather AH, Naser IH, Hizam MM, Alshujery MK. The pathological and therapeutically role of mesenchymal stem cell (MSC)-derived exosome in degenerative diseases; particular focus on LncRNA and microRNA. *Pathol Res Pract*. (2023):154778. doi: 10.1016/j.prp.2023.154778

263. Huang F, He Y, Zhang M, Luo K, Li J, Li J, et al. Progress in research on stem cells in neonatal refractory diseases. *J Pers Med*. (2023) 13:1281. doi: 10.3390/jpm13081281

264. Wang Y, Li H, Li X, Su X, Xiao H, Yang J. Hypoxic preconditioning of human umbilical cord mesenchymal stem cells is an effective strategy for treating acute lung injury. *Stem Cells Dev*. (2021) 30:128–34. doi: 10.1089/scd.2020.0174

265. Li W, Zhang Q, Wang M, Wu H, Mao F, Zhang B, et al. Macrophages are involved in the protective role of human umbilical cord-derived stromal cells in renal ischemia–reperfusion injury. *Stem Cell Res*. (2013) 10:405–16. doi: 10.1016/j.scr.2013.01.005

266. Peng X, Xu H, Zhou Y, Wang B, Yan Y, Zhang X, et al. Human umbilical cord mesenchymal stem cells attenuate cisplatin-induced acute and chronic renal injury. *Exp Biol Med*. (2013) 238:960–70. doi: 10.1177/1477153513497176

267. Zhou Y, Xu H, Xu W, Wang B, Wu H, Tao Y, et al. Exosomes released by human umbilical cord mesenchymal stem cells protect against cisplatin-induced renal oxidative stress and apoptosis *in vivo* and *in vitro*. *Stem Cell Res Ther*. (2013) 4:34. doi: 10.1186/scrt194

268. Huang D, Yi Z, He X, Mo S, Dang X, Wu X. Distribution of infused umbilical cord mesenchymal stem cells in a rat model of renal interstitial fibrosis. *Ren Fail*. (2013) 35:1146–50. doi: 10.3109/0886022X.2013.815109

269. Hsu L, Peng B, Chen M, Thalib B, Ruslin M, Tung TDX, et al. The potential of the stem cells composite hydrogel wound dressings for promoting wound healing and skin regeneration: *in vitro* and *in vivo* evaluation. *J Biomed Mater Res B*. (2019) 107:278–85. doi: 10.1002/jbm.b.34118

270. Ju Z, Ma J, Wang C, Yu J, Qiao Y, Hei F. Exosomes from iPSCs delivering siRNA attenuate intracellular adhesion molecule-1 expression and neutrophils adhesion in pulmonary microvascular endothelial cells. *Inflammation*. (2017) 40:486–96. doi: 10.1007/s10753-016-0494-0

271. Li Q, Gong S, Yao W, Yang Z, Wang R, Yu Z, et al. Exosome loaded genipin crosslinked hydrogel facilitates full thickness cutaneous wound healing in rat animal model. *Drug Deliv*. (2021) 28:884–93. doi: 10.1080/10717544.2021.1912210

272. Greenhalgh DG. Wound healing and diabetes mellitus. *Clin Plast Surg*. (2003) 30:37–45. doi: 10.1016/S0094-1298(02)00066-4

273. Yan C, Xv Y, Lin Z, Endo Y, Xue H, Hu Y, et al. Human umbilical cord mesenchymal stem cell-derived exosomes accelerate diabetic wound healing via ameliorating oxidative stress and promoting angiogenesis. *Front Bioeng Biotechnol*. (2022) 10:829868. doi: 10.3389/fbioe.2022.829868

274. Conese M, Portincasa A. Mesenchymal stem cells, secretome and biomaterials in *in-vivo* animal models: regenerative medicine application in cutaneous wound healing. *Biocell*. (2022) 46:1815–26. doi: 10.32604/biocell.2022.019448

275. Jiang Y, Huang Z. Ulinastatin alleviates pulmonary edema by reducing pulmonary permeability and stimulating alveolar fluid clearance in a rat model of acute lung injury. *Iran J Basic Med Sci*. (2022) 25:1002. doi: 10.22038/IJBMS.2022.64655.14230

276. McIntyre LA, Moher D, Fergusson DA, Sullivan KJ, Mei SHJ, Lalu M, et al. Efficacy of mesenchymal stromal cell therapy for acute lung injury in preclinical animal models: a systematic review. *PLoS One*. (2016) 11:e0147170. doi: 10.1371/journal.pone.0147170

277. Chen J, Li C, Liang Z, Li C, Li Y, Zhao Z, et al. Human mesenchymal stromal cells small extracellular vesicles attenuate sepsis-induced acute lung injury in a mouse model: the role of oxidative stress and the mitogen-activated protein kinase/nuclear factor kappa B pathway. *Cytotherapy*. (2021) 23:918–30. doi: 10.1016/j.jcyt.2021.05.009

278. Chen H, Cai Y, Sun S, Pan Z, Han Z, Liu P, et al. Repair effect of photobiomodulation combined with human umbilical cord mesenchymal stem cells on rats with acute lung injury. *J Photochem Photobiol B*. (2022) 234:112541. doi: 10.1016/j.jphotobiol.2022.112541

279. Levy PT, Levin J, Leeman KT, Mullen MP, Hansmann G, Kourembanas S. Diagnosis and management of pulmonary hypertension in infants with bronchopulmonary dysplasia. *Semin Fetal Neonatal Med*. (2022):101351. doi: 10.1016/j.siny.2022.101351

280. Ai D, Shen J, Sun J, Zhu Z, Gao R, Du Y, et al. Mesenchymal stem cell-derived extracellular vesicles suppress hyperoxia-induced transdifferentiation of rat alveolar type 2 epithelial cells. *Stem Cells Dev*. (2022) 31:53–66. doi: 10.1089/scd.2021.0256

281. You J, Zhou O, Liu J, Zou W, Zhang L, Tian D, et al. Human umbilical cord mesenchymal stem cell-derived small extracellular vesicles alleviate lung injury in rat model of bronchopulmonary dysplasia by affecting cell survival and angiogenesis. *Stem Cells Dev*. (2020) 29:1520–32. doi: 10.1089/scd.2020.0156

282. Guo Z, Zhang Y, Yan F. Potential of mesenchymal stem cell-based therapies for pulmonary fibrosis. *DNA Cell Biol*. (2022) 41:951–65. doi: 10.1089/dna.2022.0327

283. Ahani-Nahayati M, Niazi V, Moradi A, Pourjabbar B, Roozafzoon R, Keshel SH, et al. Umbilical cord mesenchymal stem/stromal cells potential to treat organ disorders; an emerging strategy. *Curr Stem Cell Res Ther*. (2022) 17:126–46. doi: 10.2174/1574888X16666210907164046

284. Tang Z, Gao J, Wu J, Zeng G, Liao Y, Song Z, et al. Human umbilical cord mesenchymal stromal cells attenuate pulmonary fibrosis via regulatory T cell through interaction with macrophage. *Stem Cell Res Ther*. (2021) 12:397. doi: 10.1186/s13287-021-02469-5

285. Liu J, Xing F, Fu Q, He B, Jia Z, Du J, et al. hUC-MSCs exosomal miR-451 alleviated acute lung injury by modulating macrophage M2 polarization via regulating MIF-PI3K-AKT signaling pathway. *Environ Toxicol*. (2022) 37:2819–31. doi: 10.1002/tox.23639

286. Wei X, Yi X, Lv H, Sui X, Lu P, Li L, et al. MicroRNA-377-3p released by mesenchymal stem cell exosomes ameliorates lipopolysaccharide-induced acute lung injury by targeting RPTOR to induce autophagy. *Cell Death Dis*. (2020) 11:657. doi: 10.1038/s41419-020-02857-4

287. Wu C-T, Deng J-S, Huang W-C, Shieh P-C, Chung M-I, Huang G-J. Salvianolic acid C against acetaminophen-induced acute liver injury by attenuating inflammation, oxidative stress, and apoptosis through inhibition of the Keap 1/Nrf2/HO-1 signaling. *Oxid Med Cell Longev*. (2019) 2019:9056845. doi: 10.1155/2019/9056845

288. Lin M, Li S, Yang L, Ye D, Xu L, Zhang X, et al. Plasma membrane vesicles of human umbilical cord mesenchymal stem cells ameliorate acetaminophen-induced damage in HepG2 cells: a novel stem cell therapy. *Stem Cell Res Ther*. (2020) 11:225. doi: 10.1186/s13287-020-01738-z

289. Hua D, Ju Z, Gan X, Wang Q, Luo C, Gu J, et al. Human amniotic mesenchymal stromal cells alleviate acute liver injury by inhibiting the pro-inflammatory response of liver resident macrophage through autophagy. *Ann Transl Med*. (2019) 7:392. doi: 10.21037/atm.2019.08.83

290. Liu Z, Meng F, Li C, Zhou X, Zeng X, He Y, et al. Human umbilical cord mesenchymal stromal cells rescue mice from acetaminophen-induced acute liver failure. *Cytotherapy*. (2014) 16:1207–19. doi: 10.1016/j.jcyt.2014.05.018

291. Guo G, Tan Z, Liu Y, Shi F, She J. The therapeutic potential of stem cell-derived exosomes in the ulcerative colitis and colorectal cancer. *Stem Cell Res Ther*. (2022) 13:138. doi: 10.1186/s13287-022-02811-5

292. Chen P, Yao L, Yuan M, Wang Z, Zhang Q, Jiang Y, et al. Mitochondrial dysfunction: a promising therapeutic target for liver diseases. *Genes Dis*. (2023) 11:101115. doi: 10.1016/j.gendis.2023.101115

293. Wu H-Y, Zhang X-C, Jia B-B, Cao Y, Yan K, Li J-Y, et al. Exosomes derived from human umbilical cord mesenchymal stem cells alleviate acetaminophen-induced acute liver failure through activating ERK and IGF-1R/PI3K/AKT signaling pathway. *J Pharmacol Sci*. (2021) 147:143–55. doi: 10.1016/j.jphs.2021.06.008

294. Jiang W, Tan Y, Cai M, Zhao T, Mao F, Zhang X, et al. Human umbilical cord MSC-derived exosomes suppress the development of CCl4-induced liver injury through antioxidant effect. *Stem Cells Int*. (2018) 2018:6079642. doi: 10.1155/2018/6079642

295. Che J, Wang H, Dong J, Wu Y, Zhang H, Fu L, et al. Human umbilical cord mesenchymal stem cell-derived exosomes attenuate neuroinflammation and oxidative stress through the NRF2/NF-κB/NLRP3 pathway. *CNS Neurosci Ther*. (2024) 30:e14454. doi: 10.1111/cns.14454

296. Jiang L, Zhang S, Hu H, Yang J, Wang X, Ma Y, et al. Exosomes derived from human umbilical cord mesenchymal stem cells alleviate acute liver failure by reducing the activity of the NLRP3 inflammasome in macrophages. *Biochem Biophys Res Commun*. (2019) 508:735–41. doi: 10.1016/j.bbrc.2018.11.189

297. Hoque R, Farooq A, Ghani A, Gorelick F, Mehal WZ. Lactate reduces liver and pancreatic injury in toll-like receptor-and inflammasome-mediated inflammation via GPR81-mediated suppression of innate immunity. *Gastroenterology*. (2014) 146:1763–74. doi: 10.1053/j.gastro.2014.03.014

298. Wang Z, Yao L, Hu X, Yuan M, Chen P, Liu P, et al. Advancements in mesenchymal stem cell therapy for liver cirrhosis: unveiling origins, treatment mechanisms, and current research frontiers. *Tissue Cell*. (2023) 84:102198. doi: 10.1016/j.tice.2023.102198

299. Zhang S, Jiang L, Hu H, Wang H, Wang X, Jiang J, et al. Pretreatment of exosomes derived from hUCMSCs with TNF-α ameliorates acute liver failure by inhibiting the activation of NLRP3 in macrophage. *Life Sci*. (2020) 246:117401. doi: 10.1016/j.lfs.2020.117401

300. He L-Y, Li Y, Niu S-Q, Bai J, Liu S-J, Guo J-L. Polysaccharides from natural resource: ameliorate type 2 diabetes mellitus via regulation of oxidative stress network. *Front Pharmacol*. (2023) 14:1184572. doi: 10.3389/fphar.2023.1184572

301. He X, Ou C, Xiao Y, Han Q, Li H, Zhou S. LncRNAs: key players and novel insights into diabetes mellitus. *Oncotarget*. (2017) 8:71325. doi: 10.18632/oncotarget.19921

302. Li X, Liu R, Chen Y, Han Y, Wang Q, Xu Y, et al. Patterns and trends in mortality associated with and due to diabetes mellitus in a transitioning region with 3.17 million people: observational study. *JMIR Public Health Surveill*. (2023) 9:e43687. doi: 10.2196/43687

303. Suh S-H, Paik I-Y, Jacobs KA. Regulation of blood glucose homeostasis during prolonged exercise. *Mol Cells*. (2007) 23:272–9. doi: 10.1016/S1016-8478(23)10717-5

304. Yang M, Chen J, Chen L. The roles of mesenchymal stem cell-derived exosomes in diabetes mellitus and its related complications. *Front Endocrinol*. (2022) 13:1027686. doi: 10.3389/fendo.2022.1027686

305. Sun Y, Shi H, Yin S, Ji C, Zhang X, Zhang B, et al. Human mesenchymal stem cell derived exosomes alleviate type 2 diabetes mellitus by reversing peripheral insulin resistance and relieving β-cell destruction. *ACS Nano*. (2018) 12:7613–28. doi: 10.1021/acsnano.7b07643

306. Lee B-C, Kang I, Yu K-R. Therapeutic features and updated clinical trials of mesenchymal stem cell (MSC)-derived exosomes. *J Clin Med*. (2021) 10:711. doi: 10.3390/jcm10040711

307. Marcheque J, Bussolati B, Csete M, Perin L. Concise reviews: stem cells and kidney regeneration: an update. *Stem Cells Transl Med*. (2019) 8:82–92. doi: 10.1002/sctm.18-0115

308. Bruno S, Kholia S, Deregibus MC, Camussi G. The role of extracellular vesicles as paracrine effectors in stem cell-based therapies. *Adv Exp Med Biol*. (2019) 1201:175–93. doi: 10.1007/978-3-030-31206-0_9

309. Sun LI, Xu R, Sun X, Duan Y, Han Y, Zhao Y, et al. Safety evaluation of exosomes derived from human umbilical cord mesenchymal stromal cell. *Cytotherapy*. (2016) 18:413–22. doi: 10.1016/j.jcyt.2015.11.018

310. Nazari H, Alborzi F, Heirani-Tabasi A, Hadizadeh A, Asbagh RA, Behboudi B, et al. Evaluating the safety and efficacy of mesenchymal stem cell-derived exosomes for treatment of refractory perianal fistula in IBD patients: clinical trial phase I. *Gastroenterol Rep*. (2022) 10:goac075. doi: 10.1093/gastro/goac075

311. Xie Y, Liu W, Liu S, Wang L, Mu D, Cui Y, et al. The quality evaluation system establishment of mesenchymal stromal cells for cell-based therapy products. *Stem Cell Res Ther*. (2020) 11:176. doi: 10.1186/s13287-020-01696-6

312. Agrahari V, Agrahari V, Burnouf P-A, Chew CH, Burnouf T. Extracellular microvesicles as new industrial therapeutic frontiers. *Trends Biotechnol*. (2019) 37:707–29. doi: 10.1016/j.tibtech.2018.11.012

313. Liguori GL, Kisslinger A. Standardization and reproducibility in EV research: the support of a Quality Management System. *Adv Biomembr Lipid Self-Assem*. (2021) 33:175–206. doi: 10.1016/bs.abl.2020.05.005

314. Grangier A, Branchu J, Volatron J, Piffoux M, Gazeau F, Wilhelm C, et al. Technological advances towards extracellular vesicles mass production. *Adv Drug Deliv Rev*. (2021) 176:113843. doi: 10.1016/j.addr.2021.113843

315. Giancaterino S, Boi C. Alternative biological sources for extracellular vesicles production and purification strategies for process scale-up. *Biotechnol Adv*. (2023) 63:108092. doi: 10.1016/j.biotechadv.2022.108092

316. Ghanem B, Seoane-Vazquez E, Brown L, Rodriguez-Monguio R. Analysis of the gene therapies authorized by the United States Food and Drug Administration and the European Medicines Agency. *Med Care*. (2023) 61:438–47. doi: 10.1097/MLR.0000000000001840

317. LoRusso PM, Boerner SA, Seymour L. An overview of the optimal planning, design, and conduct of phase I studies of new therapeutics. *Clin Cancer Res*. (2010) 16:1710–1718.

Frontiers in
Cell and Developmental Biology

Explores the fundamental biological processes of life, covering intracellular and extracellular dynamics.

The world's most cited developmental biology journal, advancing our understanding of the fundamental processes of life. It explores a wide spectrum of cell and developmental biology, covering intracellular and extracellular dynamics.

Discover the latest Research Topics

See more →

Frontiers

Avenue du Tribunal-Fédéral 34
1005 Lausanne, Switzerland
frontiersin.org

Contact us

+41 (0)21 510 17 00
frontiersin.org/about/contact